

Development of New Methods Involving Strained Heterocycles

by

Marc R. Becker

A dissertation submitted in partial fulfillment
of the requirements for the degree of
Doctor of Philosophy
(Chemistry)
in the University of Michigan
2021

Doctoral Committee:

Professor Corinna S. Schindler, Chair
Professor Anna K. Mapp
Professor Alison R. H. Narayan
Professor Corey R. J. Stephenson

Marc R. Becker

marcrb@umich.edu

ORCID iD: [0000-0003-4259-6992](https://orcid.org/0000-0003-4259-6992)

© Marc R. Becker 2021

DEDICATION

To Katie, Marion and Thomas

ACKNOWLEDGEMENTS

The completion of this dissertation is a direct product of the mentorship and support of many people, who helped me succeed and develop into the scientist that I am today. First and foremost, I am deeply grateful to my advisor, Prof. Corinna Schindler. Even before starting my graduate studies, I had the incredible privilege to work in Corinna's laboratory as a visiting student and meet the amazing and inspiring young research group of hers. This experience solidified my ambitions to pursue a graduate career in chemistry, and I am very appreciative of the trust Corinna had to accept me as a visiting student, and later as a graduate student in her laboratory. After starting my graduate studies, Corinna has been a driving force for my development as a young scientist. Her dedication to work ethic, scientific curiosity and enthusiasm about research had a profound impact on me and let me grow into an independent researcher. The support and freedom I received to visit multiple national conferences, to work on exciting projects and explore my own scientific ideas truly set me up for a successful and productive graduate career, and I am very grateful for this opportunity. I would also like to thank Prof. Alison Narayan for advising me during my first year at the University of Michigan, and joining my thesis committee. It was a great privilege to work in her incredibly talented group for a semester and be exposed to a new, evolving research area. I am also thankful for my other committee members, Prof. Anna Mapp and Prof. Corey Stephenson. Your time, support and feedback at various points of my graduate career has always been appreciated, and has greatly contributed to my development as a scientist.

Over the past five years, I had the opportunity to work with many talented and highly motivated people. Out of those, Dr. Jacob Ludwig is deserving of a special mention. It is important to say that I owe a lot of my scientific success to his advice and mentorship. Since my first day in the Schindler lab, Jake has always pushed and challenged me to work towards the most difficult and intriguing scientific questions. Although we rarely had the chance to work together on the same project, we always knew exactly about our most recent scientific successes and failures, and I always appreciated the many discussions about chemistry. Jake is one of the most creative and knowledgeable scientists I have met, and I am fortunate to have worked next to him for most of my graduate career and, most importantly, for the great friendship that we built during that time. I am also thankful for all the people from my lab that I directly worked with on various scientific endeavors. These include Alistair Richardson, Emily Wearing, Katie Rykaczewski, Scott Kim, Dr. Rebecca Watson, Dr. Haley Albright and Hannah Vonesh. I would also like to thank Prof. Jolene Reid from the University of British Columbia, who has been a tremendous collaborator. I greatly appreciated her expertise in statistical analysis and computational chemistry, and I gained many valuable insights from this collaboration. Also, thanks to everybody else from the Schindler lab, who have been coworkers, friends and family to me over the last five to six years: Dr. Jonathon Ryan, Dr. Lara Cala Alvarez, Ashlee Davis, Mario Gaviria, Troy Zehnder, Dr. Christopher McAtee, Dr. Daniel Nasrallah, Dr. Paul Riehl, Dr. James Annand, Dr. Ahlam Armaly, Dr. Alexander Golonka, Dr. Emilia Groso, Dr. Yvonne DePorre, Brandon Alexander, Ryan Harding, Lindsey Karp, Dr. J. Lizeth Gomez Lopez, Dr. Xu Zhu, Dr. Sukanta Bar and Dr. Joseph Gianino. You are an incredible group of scientists, and have filled my time in the laboratory with many memorable moments. I would also like to thank all the present and past members from the

Stephenson lab, especially my “year-mates” Ted McClain and Matt Galliher. Finally, thanks to my two former roommates John Orlet and Joseph Meadows for the enjoyable time living together.

My time at the University of Michigan would have not been as successful without the training and mentorship I received at the University of Münster, and I owe a lot to my former Master thesis advisor Prof. Ryan Gilmour. Thank you for the opportunity to do exciting research in your laboratory, getting to work with such enthusiastic scientists and the valuable advice throughout that time. I would also like to thank my former mentor in the Gilmour lab, Dr. Jan Metternich. His work ethic, motivation and curiosity had a lasting impact on me, and I am fortunate to have worked with him.

Graduate school is a long journey with many ups and downs, so having friends and family behind you with never-ending love and support has been invaluable to me. Moving to a different country for your PhD, although an extraordinary experience, comes at the cost of sacrificing time with your loved ones. I am indebted to my parents, Marion and Thomas Becker, for their unconditional support for my decision to move so far away from home. You have taught me to be humble, work hard and be my best self – thank you for helping me to become the person I am today. I would also like to thank my siblings Verena, Frederic, Lennart, my sister-in-law Alina, and everybody else from my family. Finally, I have to thank Katie Rykaczewski – meeting you has certainly been the best thing to have happened to me during graduate school. Your endless amounts of love and support never stop to amaze me and have kept me sane even at the most challenging parts of graduate school. There has not been a single accomplishment along the way that you haven’t helped me achieve. Thank you for your patience and encouragement, for being such an important part in my life and for being my biggest supporter – I am excited to see what our future together holds.

Table of Contents

DEDICATION	ii
ACKNOWLEDGEMENTS	iii
LIST OF FIGURES	viii
LIST OF TABLES	xiv
LIST OF ABBREVIATIONS	xvii
ABSTRACT	xx
Chapter 1: Divergent Reactivity in Lewis Acid-Catalyzed Transformations Between Carbonyls and Olefins	1
1.1. Introduction.....	1
1.1.1. Traditional Reactivity Between Carbonyls and Olefins	1
1.1.2. Previous Models Developed to Describe Lewis Acid Reactivity.....	4
1.2. Statistical Tools to Characterize Lewis Acid Reactivity	7
1.3. Lewis Acid Evaluation and Scope	9
1.4. Mechanistic Investigations.....	14
1.5. Reaction Profiling and Model Development	16
1.6. Conclusion	23
1.7. Experimental Section	25
1.7.1. General Information.....	25
1.7.2. Reaction Optimization	26
1.7.3. Experimental Procedures	27
1.7.4. Computational Details	65
Chapter 2: Development of Intramolecular Visible Light-Mediated [2+2] Cycloaddition Reactions for the Synthesis of Functionalized Azetidines	82
2.1. Introduction.....	82
2.1.1. Azetidines in Pharmaceuticals	82
2.1.2. Traditional Methods for the Synthesis of Azetidines	84
2.1.3. Synthesis of Azetidines via Photochemical [2+2] Cycloaddition Reactions.....	88

2.1.4.	Triplet Energy Transfer Catalysis	93
2.2.	Reaction Design and Optimization	96
2.3.	Substrate Scope	98
2.4.	Mechanistic Studies	101
2.5.	Synthetic Applications	105
2.6.	Conclusion	106
2.7.	Experimental Section	107
2.7.1.	General Information	107
2.7.2.	Reaction Optimization	109
2.7.3.	Mechanistic Experiments	110
2.7.4.	Experimental Procedures	115
Chapter 3:	Synthesis of Azetidines via Intermolecular Visible Light-Mediated [2+2]	
	Cycloaddition Reactions	183
3.1.	Introduction	183
3.1.1.	Photochemistry of Oximes	183
3.1.2.	Triplet State Oximes via Visible Light Energy Transfer Catalysis	187
3.2.	Reaction Design and Optimization	192
3.3.	Substrate Scope	197
3.4.	Synthetic Applications	201
3.5.	Mechanistic Studies	204
3.6.	Conclusion and Outlook	209
3.7.	Experimental Section	211
3.7.1.	General Information	211
3.7.2.	Reaction Optimization	213
3.7.3.	Mechanistic Investigations	219
3.7.4.	Experimental Procedures	229
	Bibliography	309

LIST OF FIGURES

Figure 1.1: Different modes of reactivity between carbonyls and olefins via (A) the carbonyl-ene reaction, (B) the Prins reaction, (C) the carbonyl-olefin metathesis reaction, and (D) the interrupted carbonyl-olefin metathesis reaction.	2
Figure 1.2: Competing carbonyl-olefin metathesis and carbonyl-ene reactions discovered during the synthesis of polycyclic aromatic hydrocarbons.	3
Figure 1.3: The carbonyl-ene reaction is in competition with the intermolecular ring-opening carbonyl-olefin metathesis reaction.	4
Figure 1.4: Select examples of methods to quantitatively assess Lewis acidity.....	5
Figure 1.5: Statistical analysis by Prochazka and coworkers.	8
Figure 1.6: Substrate scope of the Me ₂ AlCl- and SnCl ₄ -catalyzed carbonyl-ene reaction.	13
Figure 1.7: Quantum chemical investigation into the carbonyl-ene and carbonyl-olefin metathesis reaction paths catalyzed by FeCl ₃ and Me ₂ AlCl.....	15
Figure 1.8: Workflow for model development.	18
Figure 1.9: Developed statistical models.	20
Figure 1.10: Evaluating the prediction capabilities of the developed statistical models with a control substrate not included in the training set.	21
Figure 1.11: Evaluating the prediction capabilities of the developed statistical models with a Lewis acid not included in the training set.	22

Figure 1.12: Development of a secondary model that accurately predicts the activation energy for carbonyl–olefin metathesis of an aryl ketone substrate.	23
Figure 1.13: Overview of collected parameters for the statistical analysis.	66
Figure 1.14: Developed statistical model for the carbonyl–olefin metathesis pathway.	76
Figure 1.15: Developed statistical model for the carbonyl–ene reaction pathway.	78
Figure 1.16: Developed secondary model for carbonyl–olefin metathesis relying on a more broadly applicable descriptor set.	80
Figure 2.1: Overview of the most commonly used nitrogen heterocycles in FDA-approved small-molecule drugs (2014).	82
Figure 2.2: FDA-approved drugs containing an azetidine ring.	83
Figure 2.3: Examples of azetidines in lead compounds.	84
Figure 2.4: Synthesis of azetidines.	85
Figure 2.5: Alternative methods for azetidine synthesis.	86
Figure 2.6: Azetidine synthesis via a thermal [2+2] cycloaddition reaction.	87
Figure 2.7: Overview of imine photochemistry.	89
Figure 2.8: Overview of imines that participate in intermolecular aza Paternò-Büchi reactions.	90
Figure 2.9: Enantioselective [2+2] cycloaddition between quinoxalinones and styrenes mediated by a chiral photosensitizer.	90
Figure 2.10: Intramolecular aza Paternò-Büchi reaction reported by Prinzbach and coworkers.	91
Figure 2.11: Transposed aza Paternò-Büchi reaction relying on a triplet state enamide.	91
Figure 2.12: Dearomatization reaction of indoles via an energy transfer-mediated [2+2] cycloaddition reaction with oximes.	92
Figure 2.13. Distinguishing energy transfer and electron transfer (photoredox) catalysis.	93

Figure 2.14: Photophysical principles for triplet energy transfer (top) and selected commercially available photosensitizers (bottom).	94
Figure 2.15: Reaction design for the intramolecular aza Paternò-Büchi reaction.	96
Figure 2.16: Scope of the developed intramolecular aza Paternò-Büchi reaction.	100
Figure 2.17: Modification of herbicide safener isoxadifen ethyl via an intramolecular aza Paternò-Büchi reaction.	100
Figure 2.18: Intramolecular aza Paternò-Büchi reaction with dienes.	101
Figure 2.19: Stern-Volmer quenching study.	102
Figure 2.20: Control reactions demonstrating (A) the lack of reactivity of terminal alkenes, (B) the stereoconvergence of the developed [2+2] cycloaddition reaction.	102
Figure 2.21: Monitoring <i>in situ</i> styrene <i>E/Z</i> isomerization by ¹ H NMR.	103
Figure 2.22: Monitoring <i>in situ</i> oxime <i>E/Z</i> isomerization by ¹ H NMR.	104
Figure 2.23: Proposed mechanism for the intramolecular aza Paternò-Büchi reaction.	105
Figure 2.24: Synthetic modification of the accessible azetidine products.	106
Figure 2.25: Cyclic voltammogram of compound (<i>E</i>)- 2.68	110
Figure 2.26: UV/Vis spectra of a representative reaction mixture.	111
Figure 2.27: NMR signals utilized for the time study.	114
Figure 2.28: Reaction setup used for the [2+2] cycloaddition reactions.	157
Figure 2.29: Selected NOE data for the synthesized azetidine products.	179
Figure 3.1: Photosensitized isomerization of oxime <i>O</i> -methyl acetophenone oxime.	183
Figure 3.2: Photo-Beckmann rearrangement and ketone formation as photoproducts via irradiation of an oxime.	184

Figure 3.3: Nitrogen-oxygen bond cleavage as relaxation pathway for the alkylation and arylation of (hetero)aromatics.	185
Figure 3.4: Photochemical [2+2] cycloaddition reactions of oximes.	186
Figure 3.5: Visible light-sensitized decarboxylative functionalization reactions.	188
Figure 3.6: Photosensitized intermolecular carboimination of alkenes.	189
Figure 3.7: Radical-radical cross coupling via photocatalytic energy transfer.	189
Figure 3.8: Synthesis of sterically hindered primary amines via tandem energy transfer and photoredox catalysis.	190
Figure 3.9: Enantioselective radical C–H amination via triplet energy transfer for the synthesis of chiral β -amino alcohols.	191
Figure 3.10: Probing the feasibility of an intermolecular aza Paternò-Büchi reaction relying on styrene sensitization.	193
Figure 3.11: Development of an intermolecular aza Paternò-Büchi reaction.	194
Figure 3.12: Control reactions probing the stability of both azetidine diastereomers.	196
Figure 3.13: Scope of the oxime component in the developed intermolecular aza Paternò-Büchi reaction.	197
Figure 3.14: Alkene scope of the developed intermolecular aza Paternò-Büchi reaction.	199
Figure 3.15: Synthesis of free azetidines via <i>N–O</i> bond cleavage through palladium-mediated hydrogenolysis reactions.	203
Figure 3.16: Synthesis modification of the obtained azetidine products.	203
Figure 3.17: Stern-Volmer quenching studies with iridium catalyst <i>fac</i> -[Ir(dF(ppy) ₃].	205
Figure 3.18: Control reactions using an organic photosensitizer (top) and different light sources without a catalyst (bottom).	206

Figure 3.19: Investigations into the structure-activity relationships of oximes in the intermolecular cycloaddition reaction.....	206
Figure 3.20: Probing the impact of alkene properties in the intermolecular cycloaddition reaction.	207
Figure 3.21: Proposed mechanism for the developed intermolecular aza Paternò-Büchi reaction.	207
Figure 3.22: Stereochemical model developed based on the observed stereoselectivity preferences of the evaluated substrates.	208
Figure 3.23: Photochemical setup used for intermolecular [2+2] photocycloaddition.....	212
Figure 3.24: UV/Vis absorption spectra of <i>fac</i> -[Ir(dFppy) ₃] and compound 3.83	219
Figure 3.25: Cyclic voltammogram of compound 3.83	221
Figure 3.26: Cyclic voltammograms of azetidines <i>exo</i> - 3.85 , 3.115 and <i>endo</i> - 3.85	221
Figure 3.27: NMR time study.	224
Figure 3.28: Control reactions testing the requirements of light and a catalyst for the cycloaddition reaction.....	226
Figure 3.29: Control reaction to demonstrate the stability of the 2-isoxazoline substrates under the reaction conditions.	226
Figure 3.30: Control reactions to test the stability of both azetidine diastereomers under the reaction conditions.....	226
Figure 3.31: Control reaction demonstrating the requirement of a cyclic backbone.....	227
Figure 3.32: Control reaction demonstrating the requirement of an electron-withdrawing group.	227
Figure 3.33: Control reaction with xanthone as an organic triplet sensitizer.	227

Figure 3.34: Overview of unsuccessful substrates in the intermolecular [2+2] cycloaddition reaction..... 228

Figure 3.35: Stereo- and regiochemistry of the azetidine products. 298

LIST OF TABLES

Table 1.1: Evaluation of Lewis acids with a biaryl substrate.	10
Table 1.2: Overview of traditional Lewis acid parameters and experimental results for the selectivity of Lewis acids towards the carbonyl–olefin metathesis (COM) and carbonyl–ene (CE) pathway.	17
Table 1.3: Collected carbonyl vibration parameters.	67
Table 1.4: Collected carbonyl lengths and angles.	68
Table 1.5: Collected key NBO charges.....	69
Table 1.6: Collected average angles and NBO charges.....	70
Table 1.7: Collected Lewis acid Sterimol descriptors.	71
Table 1.8: Collected NBO charges on the first aromatic ring.....	72
Table 1.9: Collected NBO charges on the second aromatic ring.....	73
Table 1.10: Collected Sterimol parameters from the C4 position on the first aromatic ring.....	74
Table 1.11: Collected Sterimol parameters from the C4–C6 position on the second aromatic ring.	75
Table 1.12: Training set used for the development of the carbonyl–olefin metathesis model.	77
Table 1.13: Validation set used for the development of the carbonyl–olefin metathesis model. .	77
Table 1.14: Training set used for the development of the carbonyl–ene reaction model.	79
Table 1.15: Validation set used for the development of the carbonyl–ene reaction model.....	79

Table 1.16: Training set used for the development of the secondary model for carbonyl–olefin metathesis.....	81
Table 1.17: Validation set used for the development of the secondary model for carbonyl–olefin metathesis.....	81
Table 2.1: Reaction optimization of the intramolecular aza Paternò-Büchi reaction.	97
Table 2.2: Evaluation of oxime and hydrazone substrates.	99
Table 2.3: Reaction optimization of the intramolecular aza Paternò-Büchi reaction.	109
Table 2.4: Quenching data from the Stern-Volmer quenching study.	112
Table 2.5: Data from the NMR time study.	113
Table 2.6: Crystallographic parameters and structure refinement for compound 2.77	182
Table 3.1: Photocatalyst evaluation of the developed intermolecular aza Paternò-Büchi reaction.	195
Table 3.2: Catalyst evaluation for the <i>N–O</i> bond cleavage reaction.....	201
Table 3.3: Reaction optimization of the palladium-mediated <i>N–O</i> bond cleavage reaction.	202
Table 3.4: Evaluation of substrates for photochemical [2+2] photocycloaddition.	213
Table 3.5: Photocatalyst evaluation.	215
Table 3.6: Solvent evaluation.	216
Table 3.7: Reaction concentration evaluation.....	216
Table 3.8: Alkene equivalents evaluation.	216
Table 3.9: Catalyst loading evaluation.....	216
Table 3.10: Reaction optimization of <i>N–O</i> bond cleavage reaction.	218
Table 3.11: Stern-Volmer quenching data.	222
Table 3.12: Data from the NMR time study.	225

Table 3.13: Crystallographic parameters and structure refinement for compound 3.119	302
Table 3.14: Crystallographic parameters and structure refinement for compound 3.121	305
Table 3.15: Crystallographic parameters and structure refinement for compound 3.140	308

LIST OF ABBREVIATIONS

aq.	aqueous
BAr ^F ₄	tetrakis(3,5-bis(trifluoromethyl)phenyl)borate
Bn	benzyl
Boc	<i>tert</i> -butyloxycarbonyl
bpz	2,2'-bipyrazine
bpy	2,2'-bipyridine
brsm	based on remaining starting material
Bz	benzoyl
BzOH	benzoic acid
CAM	cerium ammonium molybdate
Cbz	benzyloxycarbonyl
CE	carbonyl-ene
CFL	compact fluorescent lamp
4'-CF ₃ -ppy	2-(4-(trifluoromethyl)phenyl)pyridine
COM	carbonyl-olefin metathesis
CPCM	(for solvent model)
d.r.	diastereomer ratio
dF(CF ₃)ppy	2-(2,4-difluorophenyl)-5-(trifluoromethyl)pyridine
dF(Me)ppy	2-(2,4-difluorophenyl)-5-methylpyridine
dFppy	2-(2,4-difluorophenyl)pyridine
DFT	density-functional theory
DIBAL-H	diisobutylaluminium hydride
DMF	dimethylformamide
DMSO	dimethyl sulfoxide

dtbbpy	4,4'-di- <i>tert</i> -butyl-2,2'-bipyridine
EC ₅₀	half maximal effective concentration
EDC	1-ethyl-3-(3-dimethylaminopropyl)carbodiimide
ee	enantiomeric excess
EI	electron ionization
EN	electronegativity
ESI	electrospray ionization
Et	ethyl
<i>E</i> _T	triplet energy
ET	energy transfer
EWG	electron-withdrawing group
FDA	Food and Drug Administration
Fppy	2-(2,4-difluorophenyl)pyridine
GP	general procedure
HAT	hydrogen atom abstraction
HOMO	highest occupied molecular orbital
IBX	2-iodoxybenzoic acid
IR	infrared
ISC	intersystem crossing
LA	Lewis acid
LDA	lithium diisopropylamide
LiHMDS	lithium bis(trimethylsilyl)amide
LUMO	lowest unoccupied molecular orbital
Me	methyl
MM	molecular mechanics
MS	mass spectrometry
<i>n</i> -BuLi	<i>n</i> -butyllithium
NBO	natural bond orbital
NMR	nuclear magnetic resonance

<i>p</i> -TsCl	<i>p</i> -toluenesulfonyl chloride
Pd/C	palladium on carbon
Ph	phenyl
phen	1,10-phenanthroline
ppy	2-phenylpyridine
r.r.	regioisomer ratio
Ru/C	ruthenium on carbon
S ₀	singlet ground state
S ₁	first excited singlet state
SAR	structure–activity relationship
sat.	saturated
SCE	saturated calomel electrode
T ₁	first triplet excited state
TBS	<i>tert</i> -butyldimethylsilyl
TFA	trifluoroacetic acid
THF	tetrahydrofuran
TLC	thin-layer chromatography
Ts	tosyl
TS	transition state
UV	ultraviolet
vs.	versus
xs	excess

ABSTRACT

Four-membered heterocycles such as oxetanes and azetidines represent a unique class of small, strained rings. These scaffolds are found in a variety of biologically active natural products and also function as important structural building blocks in pharmaceutical products due to their desirable pharmacokinetic properties. However, from a synthetic standpoint, four-membered heterocycles are often considered the most difficult to access in comparison to their smaller, three-membered, as well as their larger, five- and six-membered analogs. Thus, there is a strong demand for the development of new synthetic methods that allow for the synthesis of four-membered heterocycles in an efficient and practical fashion. The synthetic challenges in accessing four-membered rings are commonly associated with their high ring-strain, yet this inherent property provides these scaffolds with unique reactivity that can also be harvested in catalytic transformations. This dissertation discusses the development of new methods for the synthesis of azetidines relying on visible light photocatalysis, as well as investigations into the Lewis acid-catalyzed carbonyl–olefin metathesis reaction that utilizes oxetanes as reactive intermediates.

The first chapter of this dissertation studies the divergent reactivity in Lewis acid-mediated transformations between carbonyls and olefins. Herein, it is demonstrated that relatively simple metal salts can achieve remarkable selectivity, resulting in either carbonyl–olefin metathesis or carbonyl–ene reaction products. Furthermore, parametrization of relevant reaction intermediates through DFT calculations allowed for the development of predictive statistical models that provide important insights into the observed divergent reactivity.

The second and third chapter of this dissertation discuss the development of new methods for the synthesis of azetidines via visible light-mediated [2+2] cycloadditions. This strategy is advantageous over traditional approaches as it utilizes readily available oxime and alkene precursors that are reacted in a single, highly atom-economic transformation. A method for the synthesis of azetidines via an intramolecular [2+2] cycloaddition is reported herein that proceeds via triplet energy transfer from a commercially available iridium photocatalyst. This reaction utilizes substrates containing styrenes, which possess low triplet energies and are amenable to activation via energy transfer. This intramolecular strategy readily affords highly functionalized azetidine products, yet it cannot be translated into an intermolecular variant due to the limited excited state lifetime of styrenes. Therefore, a new method is presented that relies on 2-isoxazoline-3-carboxylates as a previously unexplored imine reagent. This class of compound can be activated via triplet energy transfer from an iridium photocatalyst to react with unactivated alkenes with high efficiency. This new intermolecular strategy complements the limitations of previous methods for the synthesis of azetidines, and provides facile access to previously inaccessible azetidine scaffolds.

Chapter 1: Divergent Reactivity in Lewis Acid-Catalyzed Transformations Between Carbonyls and Olefins

Portions of this chapter have been published in Becker, M. R.; Reid, J. P.; Rykaczewski, K. A.; Schindler, C. S. Models for Understanding Divergent Reactivity in Lewis Acid-Catalyzed Transformations of Carbonyls and Olefins. *ACS Catal.* **2020**, *10*, 4387–4397.

1.1. Introduction

1.1.1. Traditional Reactivity Between Carbonyls and Olefins

Lewis acid-catalyzed carbon–carbon bond-forming reactions between carbonyls and olefins represent highly important processes in organic synthesis that rely on ubiquitous starting materials.¹ Coordination of a Lewis acid (LA) complex to a Lewis basic carbonyl functionality achieves lowering of the lowest unoccupied molecular orbital (LUMO) resulting in activation of the carbonyl to undergo subsequent reactions.² In the presence of an alkene, carbonyls (**1.1**) commonly undergo carbonyl–ene^{3–7} or Prins reaction^{8–11} pathways upon activation with a Lewis acid. The carbonyl-ene reaction produces a homoallylic alcohol product (**1.4**) after transfer of an allylic hydrogen, proceeding either via a concerted (**1.2**) or stepwise mechanistic scenario involving a carbocation intermediate (**1.3**) (Figure 1.1A). A similar carbocationic intermediate **1.3** is produced in the Prins reaction, which, however, is subsequently trapped by an exogenous nucleophile (**1.5**) to generate the corresponding alcohol **1.6** (Figure 1.1B). More recently, two additional reaction pathways between carbonyls and olefins have been established by our group: namely the carbonyl–olefin metathesis^{12–15} and the interrupted carbonyl–olefin metathesis reaction.¹⁶ In the carbonyl–olefin metathesis reaction, activation of the carbonyl results in an initial

asynchronous, concerted [2+2] cycloaddition with the olefin moiety, and the resulting oxetane intermediate (**1.7**) subsequently fragments via a [2+2] cycloreversion to provide an olefin-containing product (**1.9**) as well as a carbonyl by-product (**1.8**) (Figure 1.1C).¹⁷ This mode of reactivity has recently been applied to a broad scope of metathesis transformations, including ring-closing metathesis,^{13,18,27–30,19–26} ring-opening metathesis,³¹ intermolecular cross metathesis^{32,33} and transannular carbonyl–olefin metathesis.³⁴ Finally, the interrupted carbonyl–olefin metathesis reaction converts carbonyl- and olefin-containing substrates to the corresponding tetrahydrofluorenes (**1.11**) in the presence of catalytic amounts of Brønsted acid.¹⁶ Analysis of possible reaction pathways using DFT calculations support a distinct mechanistic scenario involving an oxygen atom transfer step (**1.10**), which directly provides a benzylic carbocation that subsequently undergoes dehydration and Friedel-Crafts alkylation (Figure 1.1D).

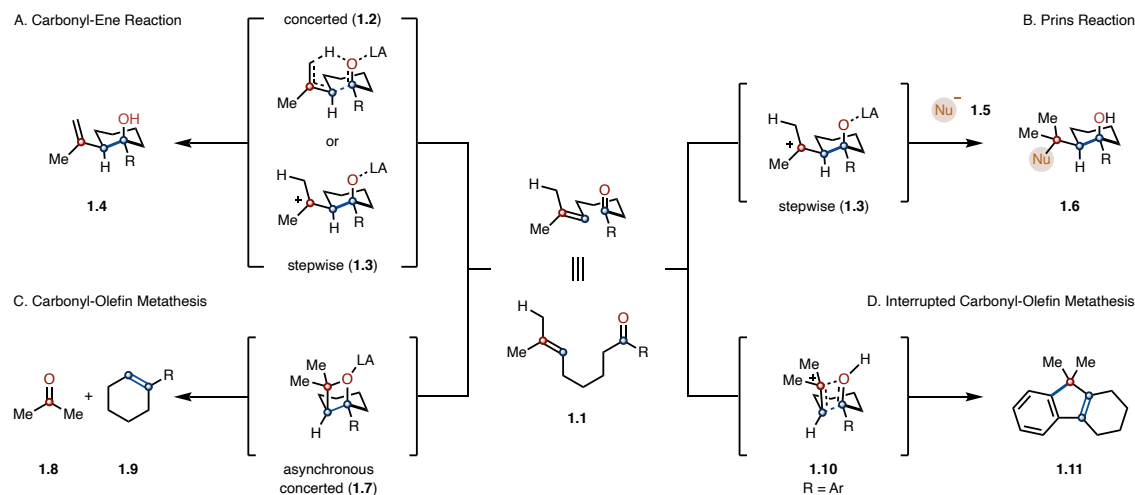


Figure 1.1: Different modes of reactivity between carbonyls and olefins via (A) the carbonyl-ene reaction, (B) the Prins reaction, (C) the carbonyl–olefin metathesis reaction, and (D) the interrupted carbonyl–olefin metathesis reaction.

Studies on the carbonyl–olefin metathesis by our group revealed that the carbonyl–ene reaction can occur as a competing pathway, oftentimes kinetically favored over the desired carbonyl–olefin metathesis pathway. Although in competition, the carbonyl–ene pathway is typically reversible, and carbonyl–ene intermediates ultimately funnel to the irreversibly formed

carbonyl–olefin metathesis product.^{16,25,34} However, in some cases the homoallylic alcohols formed in the carbonyl–ene reaction can be prone to dehydration, rendering the carbonyl–ene pathway irreversible for these types of substrates. This was found to be a synthetic challenge during the development of a carbonyl–olefin metathesis reaction for the synthesis of polycyclic aromatic hydrocarbons.³⁰ In the presence of catalytic amounts of iron(III) chloride biaryl **1.12** containing an alkene with allylic hydrogens, carbonyl–ene product **1.14** was formed as the major product in 47% yield (Figure 1.2). The undesired carbonyl–ene pathway could be suppressed by instead using a stilbenyl alkene (**1.13**) that lacks the allylic hydrogen required for the carbonyl–ene reaction.

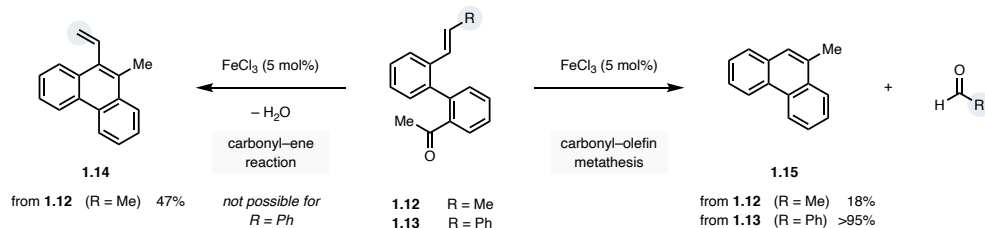


Figure 1.2: Competing carbonyl–olefin metathesis and carbonyl–ene reactions discovered during the synthesis of polycyclic aromatic hydrocarbons.

Unfortunately, this strategy was not applicable to prevent undesired carbonyl–ene reactivity for the development of a gallium(III) chloride-catalyzed ring-opening carbonyl–olefin metathesis as it required cyclic, aliphatic alkenes such as 1-methylcyclopentene (**1.17**).³¹ This reaction produced the desired ring-opening metathesis products (**1.19**) in only modest yields of up to 47% due to the formation of carbonyl–ene reaction-derived products **1.21** and **1.22** (Figure 1.3). These two products are proposed to arise from an initial carbonyl–ene reaction between the two starting materials **1.16** and **1.17** to form diene **1.20** after dehydration of the corresponding homoallylic alcohol. Intermediate **1.20** was never observed during the reaction, likely due to the fact that it rapidly reacts with an equivalent of alkene **1.17** or aldehyde **1.16** to the observed byproducts **1.21** or **1.22**.

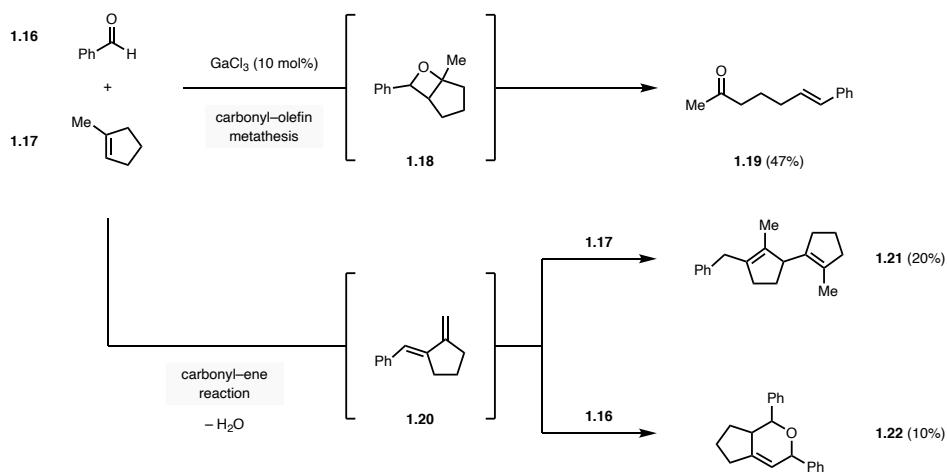


Figure 1.3: The carbonyl-ene reaction is in competition with the intermolecular ring-opening carbonyl-olefin metathesis reaction.

While carbonyl-olefin metathesis can be efficiently achieved with relatively simple Lewis acids such as FeCl₃ or GaCl₃, these catalyst systems discriminate only poorly between multiple reaction pathways for at least some substrate classes. In this case only limited options are available to improve the selectivity, most often relying on synthetic modifications to the substrate. Therefore, the design of new catalyst systems with an improved selectivity for one pathway over the other is required. This would hold great promise to advance existing protocols for carbonyl-olefin metathesis, specifically those that currently suffer from competing carbonyl-ene reaction pathways.

1.1.2. Previous Models Developed to Describe Lewis Acid Reactivity

Lewis acidity describes the strength with which a Lewis acid binds to a corresponding Lewis base, and it is a commonly used metric to define the efficiency of a Lewis acid towards bond activation or in catalysis.^{1,35-37} Considering the importance to rationally select a catalyst based on its expected reactivity, it might be surprising that there exists no broadly accepted scale for Lewis acidity. Unlike Brønsted acidity, which is strictly defined via the pK_a scale, a number of scales for Lewis acidity exist that typically differ in the physical method used to measure Lewis acid strength (Figure 1.4).³⁸

Historically, the Gutmann-Beckett method has been widely used to determine Lewis acidity based on triethylphosphine oxide as a ^{31}P NMR probe. With this method, the change in ^{31}P NMR resonance upon coordination of a Lewis acid can be correlated to the respective Lewis acidity.^{39–41} This approach was later extended by Childs in which crotonaldehyde serves as the NMR probe, often referred to as the Childs method. In this case, stoichiometric adducts of substrate and Lewis acid are analyzed by both ^1H and ^{13}C NMR spectroscopy and the change in resonance of certain signals is measured in reference to the free probe.^{42,43} While NMR-based methods allow for a relatively straightforward assessment of Lewis acid strength, those methods are limited to non-paramagnetic Lewis acids to avoid NMR disturbances. As a result, commonly used iron-based Lewis acids are typically not included in NMR-derived Lewis acid scales. Furthermore, the solubility of Lewis acids, their sensitivity to moisture or oxygen as well as achieving precise solution concentrations provide additional challenges with this approach.⁴³

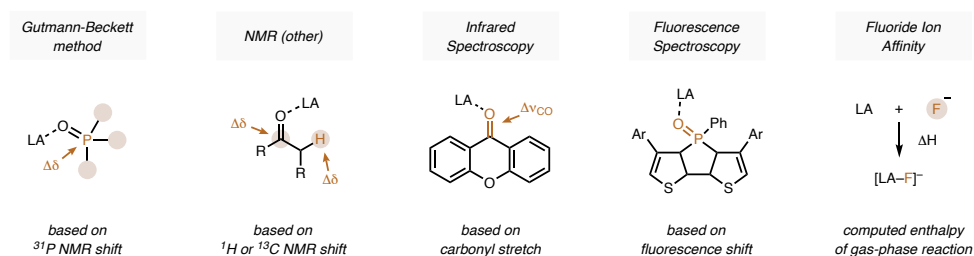


Figure 1.4: Select examples of methods to quantitatively assess Lewis acidity.

Consequently, alternative methods have been developed to quantify Lewis acidity. Considering that Lewis acids are oftentimes used in organic synthesis to activate carbonyl compounds, infrared spectroscopy (IR) of Lewis acid–carbonyl complexes has become a practical method to determine Lewis acidity. In that regard, carbonyl-containing IR probes such as xanthone,^{44,45} ethyl acetate⁴⁶ or phenalen-1-one⁴⁷ have been investigated for which the change in carbonyl stretching frequency is correlated with the strength of a Lewis acid. Although relatively comprehensive Lewis acidity scales including both paramagnetic and redox-active Lewis acids

have been reported, this approach typically requires the isolation of the stoichiometric Lewis acid-carbonyl complexes, therefore requiring rigorous air and moisture free conditions.⁴⁵ Notably, infrared spectroscopy is not only useful to quantify Lewis acidity, but has also recently been utilized to study solution interactions of carbonyls and Lewis acids in Lewis acid-catalyzed carbonyl-olefin metathesis reactions.^{48,49}

Fluorescence spectroscopy is another way to study the interaction of Lewis acids with organic substrates. For example, 10-methylacridone has been utilized as a probe to rank a broad range of Lewis acids based on the change in the fluorescence maxima.⁵⁰ Specifically, stronger Lewis acids caused a more pronounced red-shift in the fluorescence emission of the stoichiometric complex with the organic probe. Recently, this approach was further improved by Baumgartner, Caputo and coworkers, who developed a robust Lewis acidity scale for a broad range of Lewis acid classes, which included main group, cationic and transition metal-based Lewis acids.⁵¹ In contrast to previous reports, the authors utilized multiple dithienophosphole oxide probes instead of just one. In addition, the chromaticity of the resulting fluorescent Lewis adduct was measured rather than the red-shift in fluorescence emission. Methods based on the emission of Lewis acid adducts have been shown to provide Lewis acidity data that is closer in line with experimental observations.⁵¹ This is likely due to the fact that the Lewis acidity is determined in solution, thus allowing to consider effects such as coordinative flexibility, aggregation as well as other solution effects.⁵²

Computational methods have become popular to determine Lewis acidity as they negate the need for any direct experimental efforts.^{43,53,54} Specifically, fluoride ion affinity, which is classified as the enthalpy released through binding of a fluoride ion, has emerged as a frequently used technique to estimate Lewis acidities computationally.⁵⁵⁻⁵⁷ More recently, related hydride or

methyl anion affinity methods have been developed.⁵⁸ Although these computational techniques allow to rapidly generate Lewis acidity values through computations, parameters such as the fluoride ion affinity might more closely resemble fluoridophilicity as opposed to a more general Lewis acidity. In addition, computational methods typically only consider a single molecular species, thus disregarding the possibility of aggregation or solution interactions, which both have been reported to contribute to the strength of a Lewis acid.^{48,49}

1.2. Statistical Tools to Characterize Lewis Acid Reactivity

Understanding the strength of a Lewis acid is an important task in developing an efficient catalytic transformation.¹ As discussed in the previous chapter, there exists a plethora of different methods to estimate Lewis acidity, yet these approaches typically suffer from various drawbacks that limit their application in the development of new Lewis acid-catalyzed reactions. Specifically, the majority of reported Lewis acidity scales were developed using a single Lewis base, thus, Lewis acidity trends cannot be directly translated to a substrate of choice. Similarly, most methods are incompatible with certain classes of Lewis acids, which limits their general applicability, while others are unable to reflect solution effects, which have been shown to play an important role in some Lewis acid-catalyzed transformations.⁴⁹ Furthermore, most approaches to date are rarely tied to experimentally observed reactivity, which limits their use as a predictive tool.

Prochazka and coworkers utilized a computer-assisted strategy that relied on a set of 10 Lewis acid descriptors including various physical-organic and thermodynamic parameters, for example dipole moments, enthalpies and Gibbs energies of formation, bond lengths and bond energies (Figure 1.5A).⁵⁹ Based on this data the authors developed a statistically significant two-component model that was capable of aiding the reaction optimization process of three Lewis acid-catalyzed transformations, specifically an enol ether alkylation, Diels-Alder reaction and Friedel-Crafts acylation (Figure 1.5B–D).

A. Development of a statistical model using literature parameters

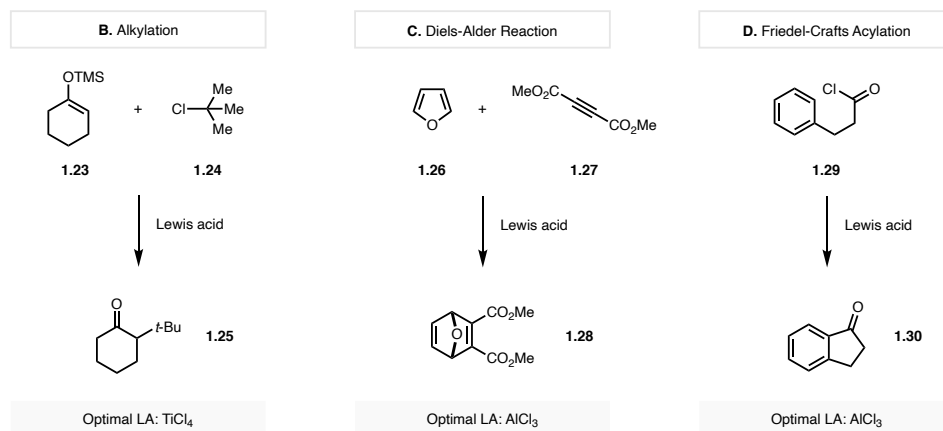
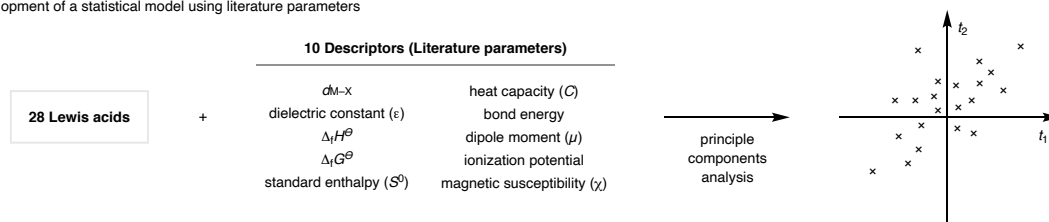


Figure 1.5: Statistical analysis by Prochazka and coworkers (A) Development of a two-component model based on a set of Lewis acids and descriptors utilized for the optimization of (B) an alkylation (C) a Diels-Alder reaction and (D) a Friedel-Crafts acylation. d_{M-X} = mean bond length; $\Delta_f H^\ominus$ = standard enthalpy of formation; $\Delta_f G^\ominus$ = standard Gibbs energy of formation. LA = Lewis acid.

The authors used the two-component model to choose Lewis acids with a maximum spread in regard to their properties as an initial starting point for the reaction optimization. Subsequently, the corresponding results were further refined through a simplex search in which the Lewis acid with the poorest performance out of a set of three was replaced with one that was oriented away from the poorest candidate in the two-component model. Ultimately, this led to the identification of optimal catalysts for all three reactions, specifically TiCl_4 for the alkylation reaction and AlCl_3 for both the Diels-Alder reaction and the Friedel-Crafts acylation. Although this report represents one of the first examples in which multivariate analysis was used for the optimization of a Lewis acid-catalyzed reaction, this approach has only found limited application since the original report in 1986.⁶⁰ In this context it is noteworthy that the descriptor set from Prochazka and coworkers was entirely based on literature values. Consequently, most Lewis acids were not described by a full set of descriptors, simply because the respective parameters had not been reported for all Lewis

acids. In addition, no reactivity data was used directly for the statistical model development, limiting its predicting capabilities. As a result, the two-component model mostly functioned as a guide for the selection of Lewis acid candidates during the reaction optimization.

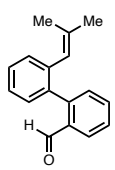
To gain further insight into the controlling features of Lewis acid-catalyzed reactions we envisioned utilizing a combination of both computational and experimental methods for the development of statistical models. Specifically, we hypothesized that generating a library of physical-organic descriptors through computational analysis of relevant Lewis acid-base complexes would hold several advantages over previous methods that aimed at analyzing and predicting Lewis acid reactivity. For example, this approach would be in principle applicable to any Lewis acid, as it foregoes the requirement of preexisting literature parameters and does not rely on a physical method to determine Lewis acidity that is likely to be limited in scope. Our initial interest was focused on the carbonyl–olefin metathesis and carbonyl–ene reaction, considering that these two pathways are closely related and oftentimes occur competitively, while the underlying Lewis acid features are only poorly understood. Successful development of a predictive statistical model for these reactions would advance our mechanistic understanding and hold the potential for the development of improved Lewis acid catalysts.

1.3. Lewis Acid Evaluation and Scope

At the outset of our studies, we sought to establish a training set of substrates and Lewis acids that could be subsequently investigated through computational and statistical methods. We hypothesized that biaryl compound **1.31** represented a suitable model substrate. This type of compound has previously been demonstrated to undergo both the carbonyl–ene or carbonyl–olefin metathesis reaction in the presence of a Lewis acid, providing either phenanthrene (**1.32**) or carbonyl–ene products **1.33** and **1.34**, the latter arising from the elimination of water from **1.33** (Table 1.1).³⁰ As the next step, we evaluated the reactivity of **1.31** with more than 30 commercially

available metal salts. For the majority of the tested Lewis acids, full conversion of **1.31** to carbonyl–olefin metathesis (**1.32**) or carbonyl–ene products (**1.33** and **1.34**) was achieved within 30 minutes at room temperature utilizing 10 mol% of Lewis acid catalyst in 1,2-dichloroethane as the reaction solvent.

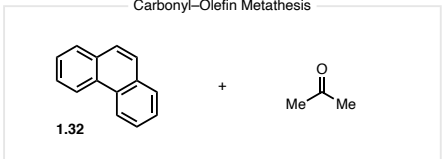
Table 1.1: Evaluation of Lewis acids with a biaryl substrate.



1.31

Lewis acid
(X mol%)
dichloroethane (0.1 M)
rt, 0.5 h

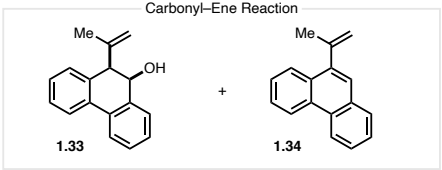
Carbonyl–Olefin Metathesis



1.32

– or –

Carbonyl–Ene Reaction



1.33 **1.34**

entry	Lewis acid (mol%)	yield 1.32 (%)	yield 1.33 (%)	yield 1.34 (%)	conv. (%)
1	FeCl ₃ (10)	33	–	19	99
2	FeBr ₃ (10)	15	–	56	99
3	Fe(OTf) ₃ (10)	15	–	82	99
4	AlCl ₃ (10)	6	61	15	99
5	AlBr ₃ (10)	7	32	60	99
6	Et ₂ AlCl (10)	1	63	17	99
7	EtAlCl ₂ (10)	8	53	29	99
8	Me ₂ AlCl (10)	1	80	20	99
9 ^a	Me ₂ AlCl (5)	–	94	5	99
10	GaCl ₃ (10)	8	–	79	99
11	GaBr ₃ (10)	14	–	58	99
12	Al ₃ (10)	5	–	82	99
13	BF ₃ ·OEt ₂ (10)	9	6	80	99
14	BCl ₃ (10)	3	13	39	99
15	TiCl ₄ (10)	6	11	59	99
16	SnCl ₂ (10)	–	29	–	39
17	Sn(OTf) ₂ (10)	10	–	63	99
18	SnCl ₄ (10)	11	–	83	99
19 ^a	SnCl ₄ (10)	3	35	61	99
20 ^{a,b}	SnCl ₄ (20)	3	–	95	99
21	InCl ₃ (10)	29	9	39	99
22	InBr ₃ (10)	22	–	44	99
23	InI ₃ (10)	22	–	58	99
24	In(OTf) ₃ (10)	16	–	84	99
25	Sc(OTf) ₃ (10)	21	26	44	99
26	ScCl ₃ (10)	1	99	–	99
27	YCl ₃ (10)	1	17	–	28

Conditions: Reactions were performed with biaryl **1.31** (0.1 mmol) in dichloroethane (0.1 M) at rt for 0.5 h. ^ain toluene (0.1 M); ^bat 50 °C. Evaluated Lewis acids with low conversion (< 20%): FeCl₂, CrCl₃, ZnCl₂, Zn(OTf)₃, RuCl₃. All yields and conversions were determined by ¹H NMR analysis of the crude reaction mixture using an internal standard.

With FeCl₃ as the Lewis acid, biaryl substrate **1.31** preferentially formed carbonyl–olefin metathesis product **1.32** in 33% yield (Table 1.1, entry 1), while other iron-based Lewis acids such as FeBr₃ and Fe(OTf)₃ provided carbonyl–ene product **1.34** as the major product in 56% and 82%, respectively, while **1.32** was only formed in 15% yield (Table 1.1, entries 2+3). These results are in agreement with previous observations from our laboratory in which FeCl₃ was identified as the optimal catalyst for carbonyl–olefin metathesis.¹³ Next, a series of aluminum Lewis acids was

investigated. AlCl_3 and AlBr_3 displayed a strong preference for the carbonyl–ene reaction pathway and resulted in a mixture of products **1.33** and **1.34** with only trace amounts of carbonyl–olefin metathesis product **1.32** (Table 1.1, entries 4+5). Similarly, alkyl aluminum Lewis acids Et_2AlCl , EtAlCl_2 and Me_2AlCl afforded high yields for the carbonyl–ene reaction pathway with an overall preference for alcohol **1.33** (Table 1.1, entries 6–8). The yield of Me_2AlCl for alcohol **1.33** could be further improved to 94% by utilizing toluene as the solvent with lowered catalyst loadings of 5 mol% (Table 1.1, entry 9). Notably, these conditions resulted in complete suppression of the carbonyl–olefin metathesis pathway. In contrast, gallium-based Lewis acids provided vinyl phenanthrene **1.34** as the major product in 79–82% yield (Table 1.1, entries 10–12). This class of Lewis acids was previously found as the optimal catalyst for intermolecular ring-opening carbonyl–olefin metathesis reactions, in which a carbonyl–ene reaction occurred as an undesired reaction pathway.³¹ In contrast, only small amounts (5–14%) of carbonyl–olefin metathesis product **1.32** were formed with biaryl substrate **1.31**. Lewis acids $\text{BF}_3\cdot\text{OEt}_2$ and BCl_3 preferentially formed vinyl phenanthrene **1.34** in 80% and 39% yield, respectively (Table 1.1, entries 13+14), while TiCl_4 provided a mixture of carbonyl–olefin metathesis and carbonyl–ene products with vinyl phenanthrene **1.34** as the major product in 59% yield (Table 1.1, entry 15). Interestingly, the Lewis acid SnCl_2 afforded alcohol **1.33** as the exclusive product, albeit in low overall conversion (Table 1.1, entry 16). In contrast, the more electrophilic $\text{Sn}(\text{OTf})_2$ provided high conversion and resulted in vinyl phenanthrene **1.34** as the major product in 63% yield (Table 1.1, entry 17). Utilizing SnCl_4 as the Lewis acid catalyst further improved the yield of **1.34** to 83% (Table 1.1, entry 18). In this case, switching the solvent to toluene dramatically reduced but not fully suppressed the carbonyl–olefin metathesis pathway from 10% to 3% (Table 1.1, entry 19). Slightly increasing the catalyst loading as well as the reaction temperature ultimately afforded **1.34** in 95%

(Table 1.1, entry 20). Evaluation of a series of indium-based Lewis acids resulted in mixtures of carbonyl–olefin metathesis and carbonyl–ene products with In(OTf)₃ exhibiting a particularly high selectivity for vinyl phenanthrene **1.34** (Table 1.1, entries 21–24). In contrast to most other tested Lewis acids, InCl₃, InBr₃ and InI₃ provided relatively high amounts of carbonyl–olefin metathesis product **1.32** with yields of 22–29%. Similarly, utilizing Sc(OTf)₃ as the catalyst resulted in 21% yield of phenanthrene (**1.32**), while carbonyl–ene products **1.33** and **1.34** were formed in 26% and 44% yield, respectively (Table 1.1, entry 25). In contrast, ScCl₃ was highly selective for alcohol **1.33** in 99% yield, highlighting how small modifications to these relatively simple metal salts can have dramatic impacts onto their selectivity (Table 1.1, entry 26). Finally, YCl₃ was found to be selective for alcohol **1.33**, but provided overall only low conversion (Table 1.1, entry 27). Other Lewis acids that resulted in poor reactivity as highlighted by conversions below 20% were FeCl₂, CrCl₃, ZnCl₂, Zn(OTf)₃ and RuCl₃.

Next, we sought to investigate the effect of substrate modifications onto the established selectivity. Specifically, we were interested in probing the generality of the carbonyl–ene reaction with Me₂AlCl and SnCl₄ as the Lewis acid catalyst, which provided either alcohol **1.33** or vinyl phenanthrene **1.34** in high yield (Figure 1.6). Biaryl substrates containing silyl protecting groups, as well as electron-donating and -withdrawing substituents and halides were tolerated by both Me₂AlCl and SnCl₄ in 86–99% yield (**1.35+1.36**, **1.37–1.47**). Interestingly, electron-rich aldehydes were prone to undergo dehydration upon cyclization and required the use of stoichiometric amounts of Me₂AlCl to achieve full consumption of starting material, which resulted in the formation of **1.42** in 66% yield. In contrast, SnCl₄ converted the same biaryl substrate in 80% yield. Furthermore, the reaction tolerated tosyl and triflate groups, resulting in products **1.48–1.50** and **1.53** in excellent yields. Notably, substrates containing acetate groups as

well as unprotected phenols could not be successfully converted with Me_2AlCl , but reacted smoothly with SnCl_4 as the Lewis acid catalyst to afford vinyl phenanthrenes **1.51** and **1.52** in 97% and 74% yield, respectively. Similarly, substrate containing heterocycles such as thiophenes, benzothiophenes or indoles were not tolerated by Me_2AlCl , but could be converted with SnCl_4 , although in slightly reduced yields of 59–89% yields (**1.56–1.58**). Finally, substrates containing an aryl ketone moiety instead of an aldehyde provided substantial amounts of carbonyl–olefin metathesis products with SnCl_4 , but selectively underwent the carbonyl–ene reaction with Me_2AlCl in 68% and 51% yield (**1.54+1.55**).

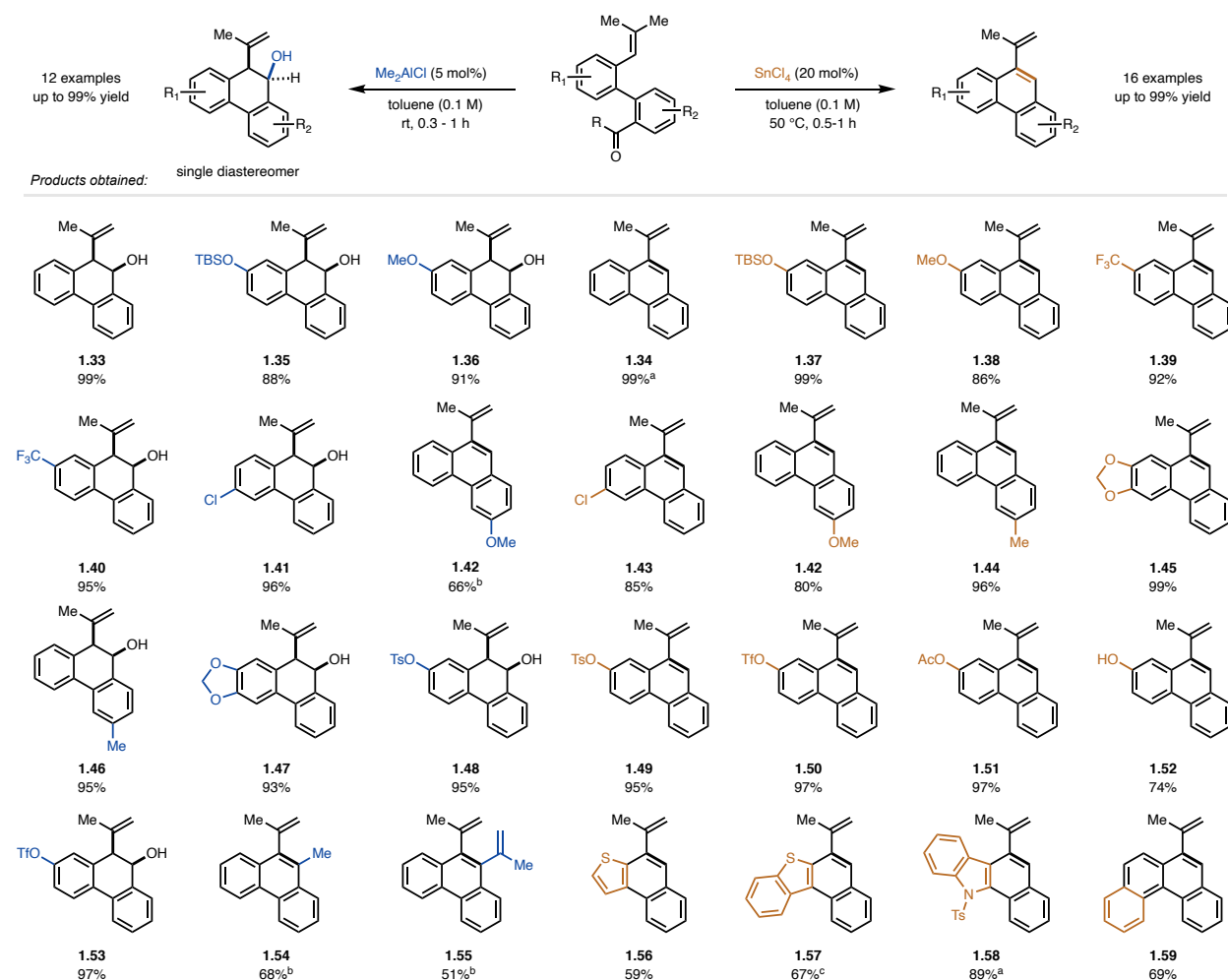


Figure 1.6: Substrate scope of the Me_2AlCl - and SnCl_4 -catalyzed carbonyl–ene reaction. Reactions were performed with biaryl substrate (0.2 mmol), Lewis acid (5 or 20 mol%) in toluene (0.1 M) at rt or 50 °C for 0.3–1 h unless noted; for Me_2AlCl , isolated yields are given; for SnCl_4 , yields were determined by ^1H NMR analysis of the crude reaction mixture; ^aisolated yield; ^bwith 100 mol% Me_2AlCl at -20 °C; ^cwith 30 mol% SnCl_4 .

These substrates required stoichiometric amounts of Lewis acid catalyst to achieve full consumption of starting material as the tertiary alcohol formed upon cyclization was prone to dehydration. Overall, evaluation of the substrate scope of the Me_2AlCl - and SnCl_4 -mediated carbonyl–ene reaction demonstrated that substrate effects only have minimal effects on the selectivity. Typically, only trace amounts of carbonyl–olefin metathesis products were observed with both catalysts, highlighting the selectivity of these two Lewis acids for the carbonyl–ene reaction pathway.

1.4. Mechanistic Investigations

To this end, we collected reactivity data that demonstrated the selectivities for carbonyl–olefin metathesis and carbonyl–ene reaction pathways for a broad range of commercially available Lewis acids. As the next step, we sought to understand the role of each reaction component to gain valuable mechanistic insights. We hypothesized that a detailed understanding of the two divergent mechanisms would assist the subsequent statistical analysis of the reaction. Therefore, the mechanism of the Lewis acid-catalyzed carbonyl–olefin metathesis and carbonyl–ene reaction was probed computationally. Me_2AlCl and FeCl_3 were chosen as the Lewis acids for this study as they were selective catalysts for either the carbonyl–ene or the carbonyl–olefin metathesis pathway. Free energies in solution were obtained from structures optimized at the B97-D/6-31G(d) level of theory, and solvent effects were added as energy corrections using the CPCM implicit solvent model for 1,2-dichloroethane. Previously conducted mechanistic investigations from our lab revealed a mechanism for carbonyl–olefin metathesis that commences with coordination of the Lewis acid catalyst to the carbonyl moiety of the substrate, followed by a concerted, asynchronous [2+2] cycloaddition reaction with the alkene. The resulting oxetane subsequently undergoes a Lewis acid-mediated concerted, asynchronous retro-[2+2] cycloaddition to provide the product.^{13,17}

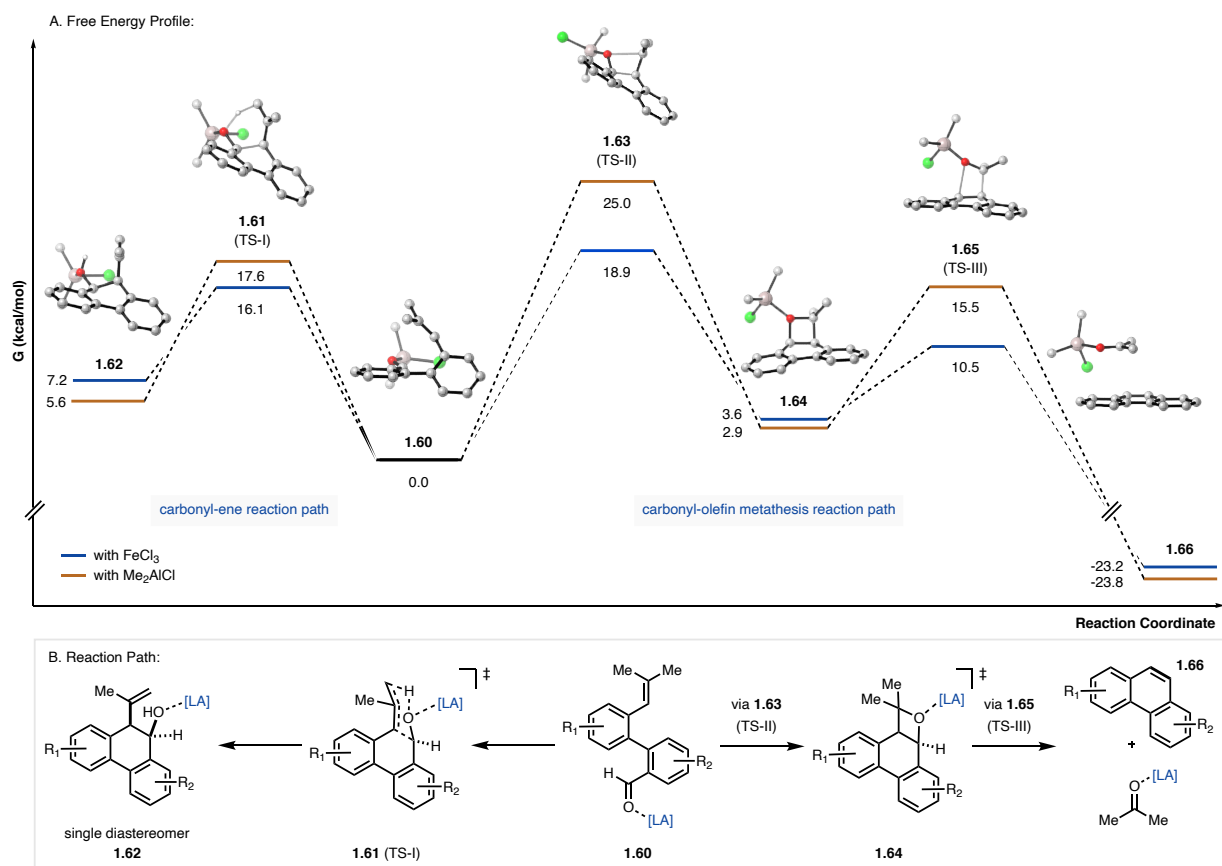


Figure 1.7: Quantum chemical investigation into the carbonyl–ene and carbonyl–olefin metathesis reaction paths catalyzed by FeCl₃ and Me₂AlCl. (A) Free energy Profile (B) Reaction Path.

Similarly, the carbonyl–olefin metathesis reaction of biaryl intermediate **1.60** was calculated to proceed via a concerted, asynchronous [2+2] cycloaddition (**1.63**) with an activation barrier of 18.9 kcal mol⁻¹ for FeCl₃ (Figure 1.7). In contrast, the same step was found to be 6.1 kcal mol⁻¹ higher in energy for Me₂AlCl. Relative to intermediate **1.60** the resulting Lewis acid-coordinated oxetane (**1.64**) is 3.6 and 2.9 kcal mol⁻¹ higher in energy for FeCl₃ and Me₂AlCl, respectively. The subsequent concerted, asynchronous retro-[2+2] cycloaddition step (**1.65**) that provides phenanthrene **1.66** and acetone as the two metathesis products was calculated to occur with an activation barrier of 10.5 kcal mol⁻¹ for FeCl₃, while the Me₂AlCl-catalyzed step was found to be 5.5 kcal mol⁻¹ higher in energy. In comparison, the calculations revealed substantially higher energy barriers for the uncatalyzed pathway with 49.9 kcal mol⁻¹ for the [2+2] cycloaddition and

42.1 kcal mol⁻¹ for the cycloreversion step. Activation barriers for the carbonyl–ene reaction pathway proceeding via transition state **1.61** were found to be lower relatively to the carbonyl–olefin metathesis pathway. Specifically, energy barriers of 16.1 kcal mol⁻¹ and 17.6 kcal mol⁻¹ were calculated for FeCl₃ and Me₂AlCl, while the uncatalyzed step would proceed with a substantially increased activation barrier of 32.4 kcal mol⁻¹. The calculations suggest that the carbonyl–ene pathway is kinetically favored over the carbonyl–olefin metathesis pathway. Yet, the carbonyl–ene reaction is likely reversible with activation barriers of 8.9 kcal mol⁻¹ and 12 kcal mol⁻¹ for the reverse reaction. Under FeCl₃-catalyzed conditions, both the carbonyl–olefin metathesis and the carbonyl–ene reaction pathway proceed with relatively similar activation barriers, but the metathesis product **1.66** is ultimately formed irreversibly under these conditions. This result is in agreement with the experimental data, in which phenanthrene (**1.32**) was the major product obtained from the reaction of biaryl **1.31** with FeCl₃. In contrast, the barrier for carbonyl–olefin metathesis for Me₂AlCl with 25.0 kcal mol⁻¹ is prohibitively high at room temperature, providing a rationale for the observed high selectivity of this catalyst for the carbonyl–ene reaction pathway.

1.5. Reaction Profiling and Model Development

Multivariate linear regression models relying on both computationally and empirically derived physical organic molecular descriptors have recently been employed as a valuable tool for the optimization of chemical reactions and the interrogation of their underlying mechanisms.^{61–63} These models are generated based on a mathematical relationship between a set of molecular descriptors and an experimental outcome, for example enantio-, regio- or chemoselectivities, reaction rates or yields.^{64–68} The resulting mathematical equation can subsequently be deployed to inform mechanistic understanding as well as predict reaction outcomes. Over the last years, this methodology has found frequent application in the optimization of catalytic systems for

stereoselective transformations.^{61–63} To this end, we hypothesized that this approach would be similarly suited to improve our understanding of the underlying characteristics of Lewis acids for their selectivity in catalytic transformations, specifically the carbonyl–olefin metathesis and carbonyl–ene reaction.

Table 1.2: Overview of traditional Lewis acid parameters and experimental results for the selectivity of Lewis acids towards the carbonyl–olefin metathesis (COM) and carbonyl–ene (CE) pathway.

entry	Lewis acid	COM/CE ratio	yield (%) (COM)	yield (%) (CE)	Lewis acidity (Brown) ^a	Lewis acidity (Cook) ^b	oxophilicity (Kepp) ^c	electronegativity ^d	ionic radius (Å) ^e
1	FeCl ₃	1.74	33	19	0.68	141	0.4	1.69	0.55–0.65
2	InCl ₃	0.60	29	48	0.54	59	0.4	1.45	0.8
3	Fe(OTf) ₃	0.18	15	82	0.53	–	0.4	1.69	0.55–0.65
4	SnCl ₄	0.13	11	83	0.79	133	0.4	1.58	0.69
5	GaCl ₃	0.10	8	79	0.75	–	–	1.56	0.62
6	BF ₃ ·OEt ₂	0.10	9	86	0.87	138	1.0	1.97	0.27
7	TiCl ₄	0.09	6	70	0.68	175	1.0	1.58	0.61
8	AlCl ₃	0.08	6	76	0.73	–	0.8	1.50	0.54
9	Me ₂ AlCl	0.01	1	99	–	–	0.8	1.50	0.54
10	ScCl ₃	0.01	1	99	0.50	–	0.8	1.32	0.75

COM/CE ratios were determined by dividing the yield of carbonyl–olefin metathesis (COM) product **1.32** and the combined yields of carbonyl–ene products **1.33** and **1.34**; yield (CE) represents the combined yield of products **1.33** and **1.34**; ^aliterature values reported by Brown⁶⁹; ^bliterature values reported by Cook⁴⁵; ^cliterature values reported by Kepp⁷⁰; ^dliterature values reported by Zhang⁷¹; ^eliterature values reported by Shannon⁷².

At the outset of our investigations, we questioned whether the observed divergent reactivity could be rationalized with previously reported Lewis acid parameters. Therefore, we selected a small number of Lewis acids and compared the observed selectivity against benchmark Lewis acid parameters (Table 1.2). In that context, we selected literature values from two different Lewis acidity scales as well as oxophilicity, electronegativity and ionic radii as additional Lewis acidity parameters.^{45,69–72} Within this subset of Lewis acids, FeCl₃ provided the highest selectivity for carbonyl–olefin metathesis (Table 1.2, entry 1). Yet, both weaker and stronger Lewis acids such as SnCl₄ and TiCl₄ were found substantially more selective for the carbonyl–ene pathway, indicating that Lewis acidity alone is insufficient to rationalize the observed reactivity (Table 1.2, entries 4+7). Similarly, no clear correlation between the other parameters and the obtained experimental data could be observed, highlighting the need for a more comprehensive study to

inform our understanding of Lewis acid reactivity. At the same time, these findings emphasize the limitations of existing Lewis acid parameters, which in most cases are not reported for all Lewis acids of interest or do not take the counterion of a Lewis acid into considerations.

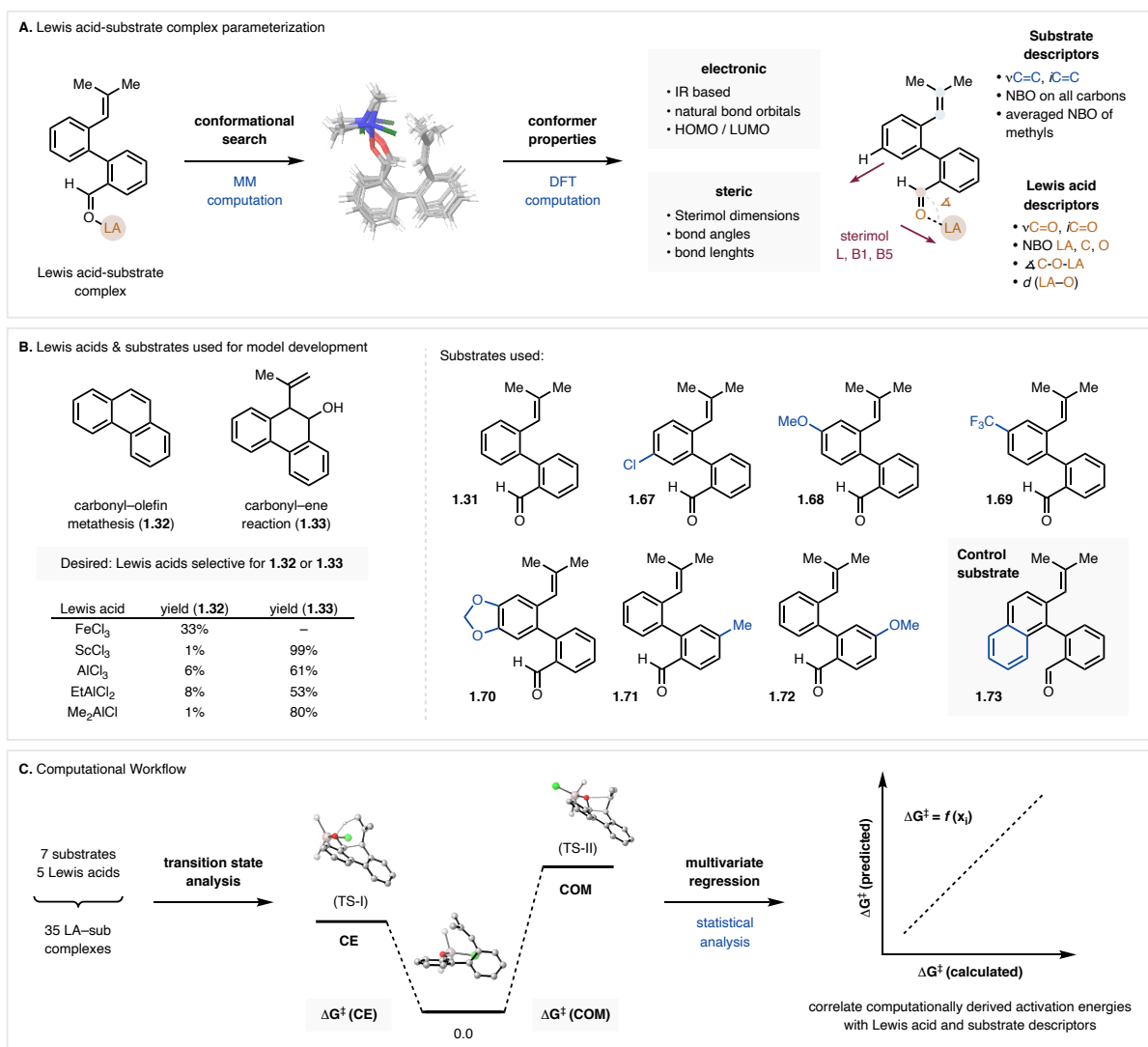


Figure 1.8: Workflow for model development. (A) Lewis acid-substrate complex parameterization (B) Lewis acids & substrates used for model development (C) computational workflow. CE = carbonyl-ene reaction; COM = carbonyl-olefin metathesis.

Therefore, we sought to adapt a workflow for our model development that would solely rely on a computationally derived library of physical organic molecular descriptors. Considering that pathway divergence originates upon coordination of a Lewis acid to a substrate, the resulting Lewis acid-carbonyl complex was used to build the parameter set. After performing a molecular

mechanics (MM) conformational search, which provided representative low-energy conformers, geometry optimization was carried out via density-functional theory (DFT) (Figure 1.8A). Relevant parameters were then collected at the M06-2X/def2-TZVP level of theory. The generated library contained more than 45 descriptors consisting of bond lengths and angles, IR vibrational parameters,⁷³ Sterimol values^{74,75} and natural bond orbital (NBO) charges.^{76,77} Notably, the collected parameters can be divided into two main groups as they contain information that either correspond to substrate or Lewis acid characteristics (Figure 1.8A).

To maintain the number of calculations to be completed at a tractable level, we selected five Lewis acids, namely FeCl₃, ScCl₃, AlCl₃, EtAlCl₂ and Me₂AlCl, for our further analysis. These Lewis acids were chosen based on their high selectivity for either the carbonyl–olefin metathesis or the carbonyl–ene pathway, while only forming minimal amounts of dehydration product (**1.34**). The elimination step provided difficulties to be investigated computationally, as the calculations suggested that different leaving groups are likely involved. Therefore, this step was omitted from our further analysis. Reaction profiling via multivariate linear regression typically requires a robust experimental output.⁶² Unfortunately, standard outputs such as reaction rates or product yields and distributions were found to be unsuitable in this case due to the rapid conversion of starting material and incomplete mass balance for some Lewis acids. Therefore, we hypothesized whether accurate predictive models could also be developed relying on computationally derived energy barriers as an alternative output. As this approach would forego the requirement for collection of experimental data, it could potentially allow to rapidly generate robust output data considering the recent advances in computational methods and resources. To test this hypothesis, we selected seven substrates (**1.31**, **1.67–1.72**) that, combined with the previously selected five Lewis acids, would provide a theoretical matrix for the subsequent

statistical analysis (Figure 1.8B). Importantly, these substrate contained a broad range of substitution patterns, but also provided sufficient overlap in the molecular space. The resulting data set, which is diversified in both the substrate as well as the catalyst dimension, contained a total of 35 unique Lewis acid-substrate combinations (Figure 1.8C). For each of these combinations we subsequently calculated the activation barriers (ΔG^\ddagger) for the carbonyl–ene pathway, proceeding via transition state **1.61**, as well the barrier for the [2+2] cycloaddition step of the carbonyl–olefin metathesis pathway, proceeding via transition state **1.63**.

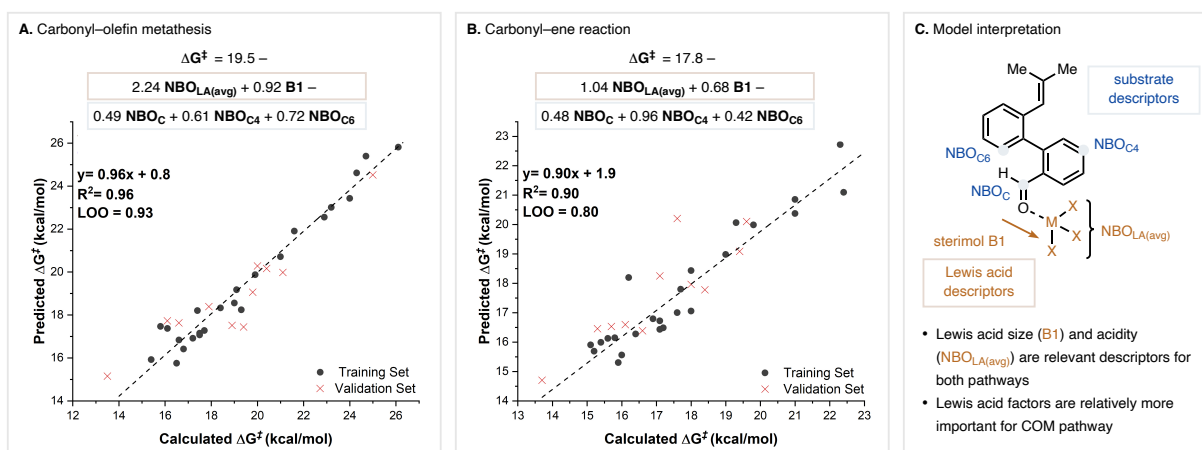
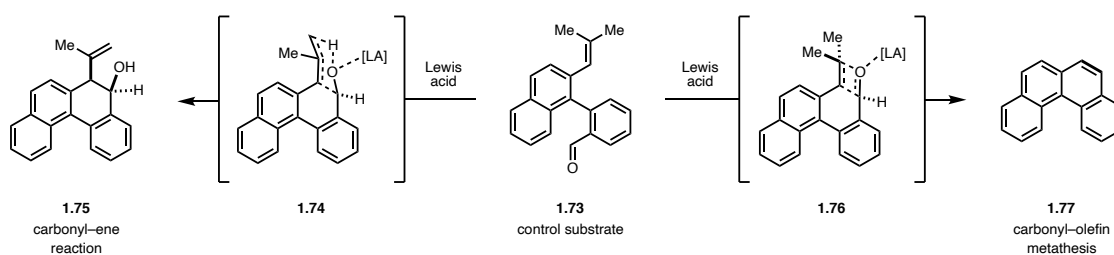


Figure 1.9: Developed statistical models for (A) the carbonyl–olefin metathesis pathway and (B) the carbonyl–ene reaction pathway (C) Model interpretation.

Next, multivariate linear regression was performed, which found that most of the output (ΔG^\ddagger) for both the carbonyl–olefin metathesis and the carbonyl–ene pathway can be expressed in five terms (Figure 1.9A+B). The averaged natural bond orbitals energies of the Lewis acid ($\text{NBO}_{\text{LA}(\text{avg})}$) as well the Lewis acid size (B1) describe Lewis acid properties, while the natural bond orbitals at the carbonyl carbon (NBO_{C}), C4 (NBO_{C4}) and C6 (NBO_{C6}) represent substrate effects (Figure 1.9C). This outcome suggests that not only the Lewis acid but also the substrate influences the selectivity between the two pathways. Furthermore, the magnitude of the coefficient for each parameter corresponds to the contribution of each term to the overall activation barrier. Interestingly, Lewis acid effects seemingly dominate for the carbonyl–olefin metathesis pathway,

and a lower barrier for this pathway is expected for Lewis acids with a small steric profile (B1) and an increased positive charge ($NBO_{LA(avg)}$). While the terms for the carbonyl–ene pathway are overall conserved, both Lewis acid and substrate parameters contribute similarly to the overall activation barrier. Thus, relative to the carbonyl–olefin metathesis pathway, substrate effects can be expected to play a larger role in determining the barrier height for the carbonyl–ene pathway. Specifically, NBO_C corresponds to the electrophilicity of the carbonyl carbon and rather intuitively suggests that a more electrophilic carbonyl will have a lower activation barrier. Interestingly, the opposite can be observed for C4 and C6 for which increasing the positive charge (NBO_{C4} or NBO_{C6}) in these positions results in a higher barrier. This may be interpreted as that substrates with substituents in this position require more energy to distort the Lewis acid–carbonyl complex to the required transition state. Ultimately, the conclusions of these models are in line with our experimental observations, in which a strong Lewis acid dependency was observed for carbonyl–olefin metathesis, while the carbonyl–ene reaction was favored across a broad range of Lewis acids as well as substrates.



	$AlCl_3$	$ScCl_3$	$FeCl_3$	$AlMe_2Cl$	$AlEtCl_2$
carbonyl–olefin metathesis pathway					
calculated ΔG^\ddagger	20.3	21.0	20.6	28.7	22.7
predicted ΔG^\ddagger	21.5	21.7	22.0	30.2	24.0
carbonyl–ene reaction pathway					
calculated ΔG^\ddagger	19.7	19.0	18.7	24.1	19.5
predicted ΔG^\ddagger	17.6	18.0	18.3	22.4	19.0

Figure 1.10: Evaluating the prediction capabilities of the developed statistical models with a control substrate not included in the training set. Activation barriers are given in $kcal\ mol^{-1}$.

Next, we sought to test the model's ability to predict both in the substrate as well as the Lewis acid space. Specifically, we chose **1.73** as a control substrate that was not included in the initial training set and contained distinct substrate features. The developed model accurately predicted the activation barriers for both pathways for all five Lewis acids, highlighting that the models can serve as a robust prediction platform for new substrates (Figure 1.10). Similarly, we were able to utilize the developed models to make predictions for Lewis acids not included in the initial model. We selected Et_2AlCl as the Lewis acid, which had provided a reactivity pattern with minimal amounts of dehydration product, similar to the five previously selected Lewis acids. Utilizing the two models, we were able to predict the activation barriers for both pathways with high precision (Figure 1.11). In agreement with our experimental observations in which Et_2AlCl was identified as a selective catalyst for the carbonyl-ene pathway, the barrier for this pathway was substantially lower than that for the carbonyl-olefin metathesis pathway.

Although the successful development of these models provided proof-of-principle that multivariate analysis can be employed to glean key mechanistic insights and predict in both the substrate as well as the Lewis acid dimension, we recognized that these models are limited to substrates containing the molecular features required for all five key descriptors. Especially substrate descriptors $\text{NBO}_{\text{C}4}$ or $\text{NBO}_{\text{C}6}$ limit the model to biaryl substrates. Thus, we evaluated whether the generated parameter set could also be employed for the development of a more broadly applicable model.

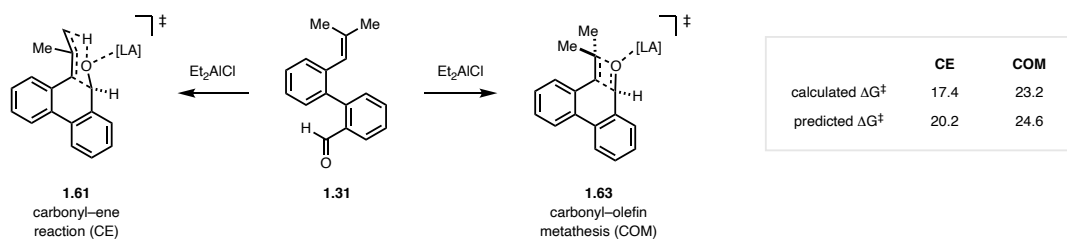


Figure 1.11: Evaluating the prediction capabilities of the developed statistical models with a Lewis acid not included in the training set. Activation barriers are given in kcal mol^{-1} .

Indeed, multivariate linear regression identified a secondary model that consisted of only three terms: the distance between Lewis acid and carbonyl ($d_{\text{LA-O}}$), the averaged natural bond orbitals energies of the Lewis acid ($\text{NBO}_{\text{LA}(\text{avg})}$) and the intensity of the carbonyl stretch ($\nu_{\text{C=O}}$) (Figure 1.12). Similar to our previous findings, a Lewis acid with a more positive charge ($\text{NBO}_{\text{LA}(\text{avg})}$) results in a lower activation barrier, while an increased distance between Lewis acid and carbonyl ($d_{\text{LA-O}}$) results in a higher barrier for this pathway. The parameter $d_{\text{LA-O}}$ can likely be interpreted as a readout for the strength of Lewis acid binding and the corresponding activation of the carbonyl.

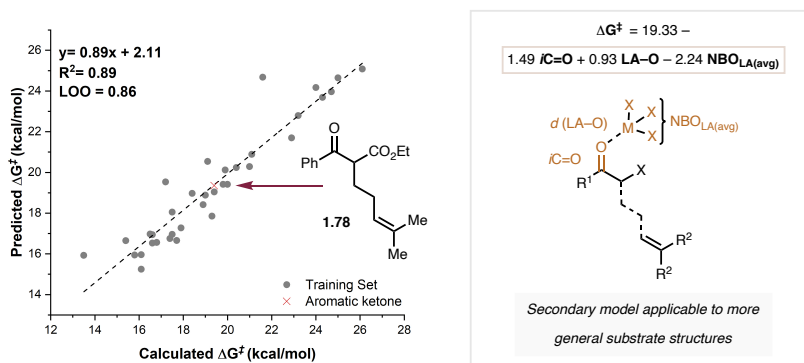


Figure 1.12: Development of a secondary model that accurately predicts the activation energy for carbonyl–olefin metathesis of an aryl ketone substrate.

Although compromised in its ability to predict in the biaryl substrate space, the model could accurately predict the carbonyl–olefin metathesis activation barrier for aryl ketone **1.78**, a substrate previously reported by our lab to be suitable for this reaction.¹³ These results highlight that the established parameter library holds the potential to be used for the development of new models that can be highly useful for the development of Lewis acid-catalyzed reactions involving new substrate classes.

1.6. Conclusion

In summary, we have evaluated a broad range of simple Lewis acid catalysts for their selectivity towards carbonyl–olefin metathesis and carbonyl–ene reaction pathways. Substrate

effects were subsequently probed using Me_2AlCl and SnCl_4 as selective catalysts. To gain mechanistic insight into the underlying controlling features of these reactions, we established an extensive library of parameters through computational analysis of Lewis acid-carbonyl complexes. Multivariate linear regression models for the two competing pathways were subsequently developed based on the correlation of computationally derived activation barriers with a set of five molecular descriptors that consisted of both Lewis acid and substrate parameters. These models proved to be robust, provided valuable mechanistic insight and allowed prediction in both the Lewis acid and substrate space. These results demonstrate that computationally derived activation barriers can function as an alternative output for the development of statistical models, particularly for reactions for which experimental data is difficult to obtain. Furthermore, we expect that the library of parameters established herein will be highly valuable to further our mechanistic understanding of Lewis acid reactivity and advance the use of statistical models as a tool for the development of new Lewis acid-catalyzed reactions.

1.7. Experimental Section

1.7.1. General Information

General Laboratory Procedures. All air- or moisture-sensitive reaction were carried out in flame-dried glassware under an atmosphere of nitrogen. Thin-layer chromatography (TLC) was performed on Merck silica gel 60 F₂₅₄ plates using UV light (254 or 366 nm), KMnO₄ or CAM stain for visualization. Flash chromatography was performed using silica gel Silia Flash[®] 40-63 micron (230-400 mesh) from Silicycle unless noted.

Materials and Instrumentation. All chemicals were purchased from Sigma-Aldrich, Alfa Aesar, Acros Organics, Oakwood, TCI America, Frontier Scientific, Matrix Scientific, Ark Pharm, and Chem Impex International, and were used as received unless otherwise stated. THF, CH₂Cl₂, toluene, DMF and DMSO were dried by being passed through a column of activated alumina under argon using a JC-Meyer Solvent Systems. Triethylamine and diisopropylamine were freshly distilled prior to use over calcium hydride and potassium hydroxide, respectively. 2-bromo-5-((*tert*-butyldimethylsilyl)oxy)benzaldehyde⁷⁸ and 1-(2'-(2-methylprop-1-en-1-yl)-[1,1'-biphenyl]-2-yl)ethan-1-one³⁰ were prepared according to literature procedures. Proton nuclear magnetic resonance (¹H NMR) spectra were recorded on Varian MR400, Varian vnmrs 500, Varian Inova 500, and Varian vnmrs 700 spectrometers and are referenced to residual protic NMR solvent (CDCl₃: δ 7.26 ppm, CD₃OD: δ 3.31 ppm, CD₂Cl₂: δ 5.32 ppm). Data for ¹H NMR are reported as follows: chemical shift (δ ppm), multiplicity (s = singlet, d = doublet, t = triplet, q = quartet, m = multiplet, br = broad), coupling constant (Hz), integration. Carbon nuclear magnetic resonance (¹³C NMR) spectra were recorded on Varian vnmrs 500 and Varian vnmrs 700 spectrometers and are referenced to the carbon resonances of the NMR solvent (CDCl₃: δ 77.16 ppm, CD₃OD: δ 49.00 ppm, CD₂Cl₂: δ 54.00 ppm). Fluorine nuclear magnetic resonance

(¹⁹F NMR) spectra were recorded on Varian vnmrs 500 and Varian vnmrs 700 spectrometers. High-resolution mass spectroscopic (MS) data was recorded at the Mass Spectrometry Facility at the Department of Chemistry of the University of Michigan in Ann Arbor, MI on an Agilent 6230 TOF HPLC-MS (ESI) or Micromass AutoSpec Ultima Magnetic Sector mass spectrometer (ESI, EI). Infrared (IR) spectra were obtained using a Thermo-Nicolet IS-50 spectrometer. IR data are represented as frequency of absorption (cm⁻¹).

1.7.2. Reaction Optimization

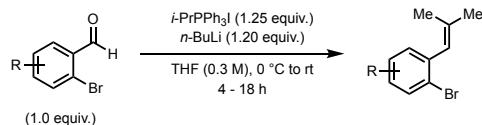
For solid Lewis acids: In a glovebox, a flame-dried 1-dram glass vial equipped with a magnetic stir bar was charged with the Lewis acid (x mol%) and the vial sealed with a rubber septum. The vial was transferred out of the glovebox and a solution of aryl aldehyde **1.31** (24 mg, 0.1 mmol, 1.0 equiv.) in 1,2-dichloroethane (0.1 M; 0.1 mmol, 1 mL) was added via syringe. The mixture was stirred for 0.5 h at rt, then passed through a short silica plug eluting with CH₂Cl₂ (5–10 mL). The filtrate was concentrated and dried *in vacuo*. The yield and conversion were subsequently determined by quantitative ¹H NMR using dimethyl terephthalate as the internal standard.

For liquid Lewis acids or solutions: A flame-dried 1-dram glass vial equipped with a magnetic stir bar was sealed under an atmosphere of nitrogen. A solution of aryl aldehyde **1.31** (24 mg, 0.1 mmol, 1.0 equiv.) in 1,2-dichloroethane (0.1 M; 0.1 mmol, 1 mL) was added to the vial via syringe followed by a solution of the respective Lewis acid (x mol%; entries 6–9: 1 M in hexanes; entry 13: neat; entry 15: 1 M in DCE; entries 18–20: 1 M solution in DCE or toluene). The mixture was stirred for 0.5 h at rt and passed through a short silica plug eluting with CH₂Cl₂ (5–10 mL). The filtrate was concentrated and dried *in vacuo*. The yield and conversion were subsequently determined by quantitative ¹H NMR using dimethyl terephthalate as internal standard.

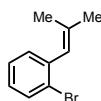
1.7.3. Experimental Procedures

Synthesis of Starting Materials and Characterization

General Procedure for Suzuki-Coupling (GP-1.1)

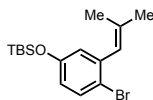


A flame-dried round-bottom flask equipped with a magnetic stir bar was charged with isopropyltriphenylphosphonium iodide (1.25 equiv.) and sealed under a nitrogen atmosphere. Dry THF (0.3 M) was added via syringe and the heterogeneous mixture cooled to 0 °C with an ice bath, followed by dropwise addition of *n*-BuLi (2.5 M in hexanes; 1.2 equiv.). After stirring for 30 min at 0 °C, the respective aryl aldehyde (1.0 equiv.) was added slowly and the reaction mixture allowed to gradually warm up to rt and stirred until complete as determined by TLC analysis (4–18 h). The reaction was quenched by the addition of a NH₄Cl solution (aq., sat.) and the biphasic mixture partitioned between water and EtOAc. The organic layer was separated and the aqueous layer extracted with EtOAc (3x). The combined organic extracts were dried over Na₂SO₄, filtered and concentrated *in vacuo*. The crude product was purified by flash column chromatography (0–5% EtOAc/hexanes) to afford the pure olefin product.



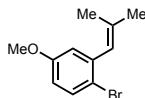
1-Bromo-2-(2-methylprop-1-en-1-yl)benzene (A1.1): Prepared according to GP-1.1 from 2-bromobenzaldehyde (24.9 mmol). Purification by flash column chromatography (100% hexanes) afforded the title compound (4.80 g, 92%) as a colorless oil. Spectroscopic data were consistent with those reported in the literature.³⁰

¹H NMR (400 MHz, CDCl₃): δ 7.56 (d, *J* = 7.7 Hz, 1H), 7.29 – 7.20 (m, 2H), 7.10 – 7.02 (m, 1H), 6.24 (s, 1H), 1.94 (s, 3H), 1.75 (s, 3H).



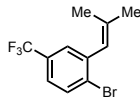
(4-Bromo-3-(2-methylprop-1-en-1-yl)phenoxy)(tert-butyl)dimethylsilane (A1.2): Prepared according to GP-1.1 from 2-bromo-5-((tert-butyl)dimethylsilyloxy)benzaldehyde (15.9 mmol). Purification by flash column chromatography (100% hexanes) afforded the title compound as a colorless oil (4.96 g, 92%).

¹H NMR (400 MHz, CDCl₃): δ 7.38 (d, *J* = 8.6 Hz, 1H), 6.72 (s, 1H), 6.58 (d, *J* = 8.5 Hz, 1H), 6.19 (s, 1H), 1.92 (s, 3H), 1.76 (s, 3H), 0.98 (s, 9H), 0.19 (s, 6H); **¹³C NMR** (176 MHz, CDCl₃): δ 154.6, 139.6, 136.8, 133.0, 124.9, 122.7, 119.9, 115.7, 26.3, 25.8, 19.6, 18.4, -4.3; **IR** (cm⁻¹): 2956, 2929, 2857, 1582, 1562, 1462, 1396, 1290, 1252, 1176, 984, 888, 860, 836, 779, 671; **HRMS**: *m/z* calculated for C₁₆H₂₆BrOSi⁺ [M+H]⁺: 341.0931; found: 341.0931.



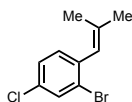
1-Bromo-4-methoxy-2-(2-methylprop-1-en-1-yl)benzene (A1.3): Prepared according to GP-1.1 from 2-bromo-5-methoxybenzaldehyde (4.65 mmol). Purification by flash column chromatography (5% EtOAc/hexanes) afforded the title compound as a colorless oil (982 mg, 88%).

¹H NMR (700 MHz, CDCl₃): δ 7.44 (d, *J* = 8.7 Hz, 1H), 6.79 (d, *J* = 3.0 Hz, 1H), 6.65 (dd, *J* = 8.7, 3.0 Hz, 1H), 6.22 (s, 1H), 3.78 (s, 3H), 1.93 (s, 3H), 1.77 (s, 3H); **¹³C NMR** (176 MHz, CDCl₃): δ 158.5, 139.5, 137.1, 133.0, 124.9, 116.7, 115.0, 113.5, 55.6, 26.3, 19.6; **IR** (cm⁻¹): 2933, 2909, 1589, 1565, 1461, 1290, 1237, 1197, 1166, 1047, 1015, 867, 798, 700, 644; **HRMS**: *m/z* calculated for C₁₁H₁₃BrO⁺ [M]⁺: 240.0150; found: 240.0143.



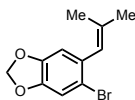
1-Bromo-2-(2-methylprop-1-en-1-yl)-4-(trifluoromethyl)benzene (A1.4): Prepared according to GP-1.1 from 2-bromo-5-(trifluoromethyl)benzaldehyde (2.69 mmol). Purification by flash column chromatography (100% hexanes) afforded the title compound as a colorless oil (640 mg, 85%).

¹H NMR (500 MHz, CDCl₃): δ 7.68 (d, *J* = 8.3 Hz, 1H), 7.47 (d, *J* = 1.7 Hz, 1H), 7.31 (dd, *J* = 8.3, 2.0 Hz, 1H), 6.24 (s, 1H), 1.96 (s, 3H), 1.76 (s, 3H); **¹³C NMR** (176 MHz, CDCl₃): δ 139.6, 138.7, 133.1, 129.5 (q, *J* = 32.6 Hz), 128.2 (q, *J* = 1.7 Hz), 127.7 (q, *J* = 3.8 Hz), 124.3 (q, *J* = 3.7 Hz), 124.1 (q, *J* = 272.2 Hz), 123.9, 26.3, 19.5; **IR** (cm⁻¹): 2916, 1603, 1409, 1324, 1264, 1166, 1122, 1078, 1027, 908, 821, 762, 723, 653; **HRMS**: *m/z* calculated for C₁₁H₁₀BrF₃⁺ [M]⁺: 277.9918; found: 277.9908.



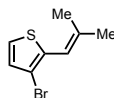
2-Bromo-4-chloro-1-(2-methylprop-1-en-1-yl)benzene (A1.5): Prepared according to GP-1.1 from 2-bromo-4-chlorobenzaldehyde (4.56 mmol). Purification by flash column chromatography (100% hexanes) afforded the title compound as a colorless oil (990 mg, 89%).

¹H NMR (500 MHz, CDCl₃): δ 7.57 (d, *J* = 2.0 Hz, 1H), 7.24 (dd, *J* = 8.3, 2.0 Hz, 1H), 7.15 (d, *J* = 8.3 Hz, 1H), 6.18 (s, 1H), 1.93 (s, 3H), 1.73 (s, 3H); **¹³C NMR** (126 MHz, CDCl₃): δ 137.7, 137.3, 132.5, 132.1, 131.7, 127.2, 124.6, 123.9, 26.3, 19.5; **IR** (cm⁻¹): 2973, 2908, 1654, 1581, 1548, 1465, 1374, 1180, 1097, 1034, 864, 841, 801, 746, 690; **HRMS**: *m/z* calculated for C₁₀H₁₀BrCl⁺ [M]⁺: 243.9654; found: 243.9660.



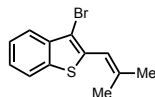
5-Bromo-6-(2-methylprop-1-en-1-yl)benzo[d][1,3]dioxole (A1.6): Prepared according to GP-1.1 from 6-bromobenzo[d][1,3]dioxole-5-carbaldehyde (4.37 mmol). Purification by flash column chromatography (100% hexanes) afforded the title compound as a colorless oil (1.04 g, 93%).

$^1\text{H NMR}$ (700 MHz, CDCl_3): δ 7.02 (s, 1H), 6.72 (s, 1H), 6.13 (s, 1H), 5.96 (s, 2H), 1.90 (s, 3H), 1.73 (s, 3H); $^{13}\text{C NMR}$ (176 MHz, CDCl_3): δ 146.9, 146.8, 136.3, 132.0, 124.8, 114.8, 112.5, 110.6, 101.7, 26.2, 19.5; **IR** (cm^{-1}): 2970, 2907, 1501, 1470, 1407, 1319, 1226, 1161, 1113, 1036, 972, 933, 871, 836, 682, 644; **HRMS**: m/z calculated for $\text{C}_{11}\text{H}_{11}\text{BrO}_2^+$ $[\text{M}]^+$: 253.9942; found: 253.9935.



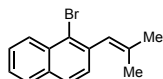
3-Bromo-2-(2-methylprop-1-en-1-yl)thiophene (A1.7): Prepared according to GP-1.1 from **A1.13** (5.23 mmol). Purification by flash column chromatography (100% hexanes) afforded the title compound as a pale-yellow oil (948 mg, 83%).

$^1\text{H NMR}$ (400 MHz, CDCl_3): δ 7.19 (d, $J = 5.3$ Hz, 1H), 6.97 (d, $J = 5.3$ Hz, 1H), 6.40 (s, 1H), 1.97 (d, $J = 3.7$ Hz, 6H); $^{13}\text{C NMR}$ (126 MHz, CDCl_3): δ 137.7, 135.4, 129.8, 123.8, 117.2, 109.8, 27.5, 20.3; **IR** (cm^{-1}): 2969, 2909, 1644, 1492, 1448, 1373, 1336, 1186, 1141, 1080, 1048, 974, 867, 794, 691, 607; **HRMS**: m/z calculated for $\text{C}_8\text{H}_9\text{BrS}^+$ $[\text{M}]^+$: 215.9608; found: 215.9609.



3-Bromo-2-(2-methylprop-1-en-1-yl)benzo[b]thiophene (A1.8): Prepared according to GP-1.1 from 3-bromobenzo[b]thiophene-2-carbaldehyde (3.11 mmol). Purification by flash column chromatography (100% hexanes) afforded the title compound as a colorless oil (682 mg, 82%).

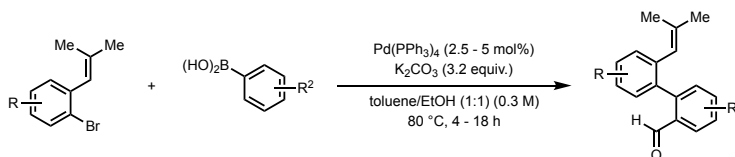
¹H NMR (500 MHz, CDCl₃): δ 7.80 (d, *J* = 8.0 Hz, 1H), 7.76 (d, *J* = 8.0 Hz, 1H), 7.43 (t, *J* = 7.6 Hz, 1H), 7.35 (t, *J* = 7.5 Hz, 1H), 6.60 (s, 1H), 2.08 (s, 3H), 2.03 (s, 3H); **¹³C NMR** (126 MHz, CDCl₃): δ 140.4, 137.9, 137.5, 135.7, 125.2, 125.1, 123.0, 122.1, 117.8, 107.0, 27.8, 20.6; **IR** (cm⁻¹): 3058, 2968, 2852, 1641, 1444, 1375, 1303, 1255, 1218, 1174, 1018, 924, 846, 750, 725; **HRMS**: *m/z* calculated for C₁₂H₁₁BrS⁺ [M]⁺: 265.9765; found: 265.9760.



1-Bromo-2-(2-methylprop-1-en-1-yl)naphthalene (A1.9): Prepared according to GP-1.1 from 1-bromo-2-naphthaldehyde (1.12 mmol). Purification by flash column chromatography (100% hexanes) afforded the title compound as a colorless oil (251 mg, 85%).

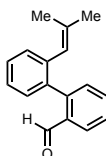
¹H NMR (500 MHz, CDCl₃): δ 8.34 (d, *J* = 8.5 Hz, 1H), 7.81 (d, *J* = 8.1 Hz, 1H), 7.75 (d, *J* = 8.4 Hz, 1H), 7.58 (t, *J* = 7.7 Hz, 1H), 7.49 (t, *J* = 7.4 Hz, 1H), 7.37 (d, *J* = 8.4 Hz, 1H), 6.48 (s, 1H), 2.00 (s, 3H), 1.79 (s, 3H); **¹³C NMR** (126 MHz, CDCl₃): δ 137.1, 137.0, 133.2, 132.6, 128.7, 128.1, 127.4, 127.3, 127.0, 126.2, 126.1, 123.8, 26.6, 19.7; **IR** (cm⁻¹): 3054, 2969, 2908, 1650, 1550, 1376, 1323, 1187, 1061, 975, 835, 806, 759, 663, 641; **HRMS**: *m/z* calculated for C₁₄H₁₃Br⁺ [M]⁺: 260.0201; found: 260.0194.

General Procedure for Suzuki-Miyaura Cross-Coupling (GP-1.2)



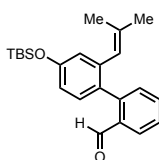
A flame-dried round-bottom flask was charged with aryl bromide (1.0 equiv.), aryl boronic acid (1.2 equiv.), K₂CO₃ (3.2 equiv.) and Pd(PPh₃)₄ (2.5–5 mol%). After addition of a solution of toluene/EtOH (1:1, 0.3 M), the flask was equipped with a reflux condenser and heated at 80 °C under a nitrogen atmosphere until judged completed by TLC (2–18 h). After cooling down to rt,

the mixture was diluted with EtOAc and washed with water (3x) and brine (1x). The organic phase was dried over Na₂SO₄, filtered and concentrated *in vacuo*. The crude product was purified by flash column chromatography to afford the pure cross-coupled product.



2'-(2-Methylprop-1-en-1-yl)-[1,1'-biphenyl]-2-carbaldehyde (1.31): Prepared according to GP-1.2 with **A1.1** (16.6 mmol). Purification by flash column chromatography (0–5% EtOAc/hexanes) afforded the title compound as a colorless oil (3.59 g, 92%).

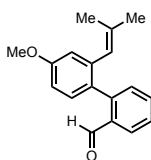
¹H NMR (700 MHz, CD₃OD): δ 9.52 (s, 1H), 7.91 (d, *J* = 7.8 Hz, 1H), 7.68 (t, *J* = 7.9 Hz, 1H), 7.51 (t, *J* = 7.6 Hz, 1H), 7.42 (t, *J* = 7.1 Hz, 1H), 7.36 (t, *J* = 7.4 Hz, 1H), 7.33 (d, *J* = 7.5 Hz, 2H), 7.31 (d, *J* = 7.6 Hz, 1H), 5.72 (s, 1H), 1.71 (s, 3H), 1.65 (s, 3H); **¹³C NMR** (176 MHz, CD₃OD): δ 193.2, 146.6, 139.4, 138.5, 138.0, 135.4, 134.9, 132.2, 131.2, 130.9, 129.1, 128.9, 127.8, 127.4, 125.7, 26.1, 19.3; **IR** (cm⁻¹): 3059, 2907, 2847, 2747, 1692, 1595, 1441, 1390, 1252, 1194, 1111, 1047, 825, 752, 646; **HRMS**: *m/z* calculated for C₁₇H₁₆NaO⁺ [M+H]⁺: 259.1093; found: 259.1100.



4'-((*Tert*-butyldimethylsilyloxy)-2'-(2-methylprop-1-en-1-yl)-[1,1'-biphenyl]-2-carbaldehyde (S1.35): Prepared according to GP-1.2 with **A1.2** (8.79 mmol). Purification by flash column chromatography (0–5% EtOAc/hexanes) afforded the title compound as a white solid (2.54 g, 79%).

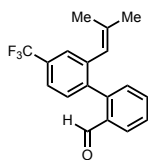
¹H NMR (500 MHz, CDCl₃): δ 9.60 (s, 1H), 7.95 (d, *J* = 7.8 Hz, 1H), 7.59 (t, *J* = 7.5 Hz, 1H), 7.43 (t, *J* = 7.5 Hz, 1H), 7.29 (d, *J* = 7.6 Hz, 1H), 7.16 (d, *J* = 8.2 Hz, 1H), 6.82 (dd, *J* = 8.2, 2.2 Hz,

1H), 6.78 (d, $J = 2.0$ Hz, 1H), 5.70 (s, 1H), 1.75 (s, 3H), 1.67 (s, 3H), 1.02 (s, 9H), 0.26 (s, 6H); ^{13}C NMR (126 MHz, CDCl_3): δ 192.4, 155.5, 145.1, 139.5, 137.3, 134.4, 133.5, 131.5, 131.4, 130.2, 127.5, 126.7, 124.5, 121.2, 118.4, 26.2, 25.8, 19.3, 18.3, -4.2; IR (cm^{-1}): 2928, 2857, 1688, 1594, 1471, 1403, 1279, 1254, 1229, 1182, 981, 863, 823, 775, 637; HRMS: m/z calculated for $\text{C}_{23}\text{H}_{30}\text{O}_2\text{SiNa}^+ [\text{M}+\text{H}]^+$: 389.1907; found: 389.1908.



4'-Methoxy-2'-(2-methylprop-1-en-1-yl)-[1,1'-biphenyl]-2-carbaldehyde (1.68): Prepared according to GP-1.2 with **A1.3** (0.82 mmol). Purification by flash column chromatography (5% EtOAc/hexanes) afforded the title compound as a white solid (151 mg, 69%).

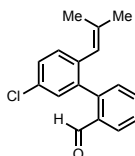
^1H NMR (500 MHz, CD_3OD): δ 9.52 (s, 1H), 7.88 (d, $J = 7.8$ Hz, 1H), 7.65 (t, $J = 7.5$ Hz, 1H), 7.47 (t, $J = 7.5$ Hz, 1H), 7.32 (d, $J = 7.6$ Hz, 1H), 7.25 (d, $J = 8.4$ Hz, 1H), 6.94 (dd, $J = 8.4, 2.1$ Hz, 1H), 6.84 (d, $J = 2.0$ Hz, 1H), 5.71 (s, 1H), 3.85 (s, 3H), 1.71 (s, 3H), 1.64 (s, 3H); ^{13}C NMR (126 MHz, CD_3OD): δ 193.5, 160.9, 146.4, 140.6, 138.3, 135.7, 134.8, 132.5, 132.4, 130.8, 128.6, 127.4, 125.8, 116.3, 113.2, 55.8, 26.1, 19.4; IR (cm^{-1}): 2909, 2836, 1690, 1596, 1467, 1441, 1389, 1295, 1230, 1194, 1166, 1048, 1002, 828, 763, 710, 639; HRMS: m/z calculated for $\text{C}_{18}\text{H}_{18}\text{O}_2\text{Na}^+ [\text{M}+\text{H}]^+$: 289.1199; found: 289.1200.



2'-(2-Methylprop-1-en-1-yl)-4'-(trifluoromethyl)-[1,1'-biphenyl]-2-carbaldehyde (1.69): Prepared according to GP-1.2 with **A1.4** (2.00 mmol). Purification by flash column

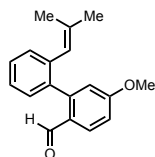
chromatography (5% EtOAc/hexanes) afforded the title compound as a colorless oil (560 mg, 92%).

¹H NMR (700 MHz, CDCl₃): δ 9.57 (s, 1H), 8.00 (dd, *J* = 7.8, 1.1 Hz, 1H), 7.65 (td, *J* = 7.5, 1.3 Hz, 1H), 7.59 (d, *J* = 8.0 Hz, 1H), 7.56 (s, 1H), 7.52 (t, *J* = 7.6 Hz, 1H), 7.43 (d, *J* = 7.9 Hz, 1H), 7.28 (d, *J* = 7.6 Hz, 1H), 5.74 (s, 1H), 1.75 (d, *J* = 1.0 Hz, 3H), 1.70 (d, *J* = 1.1 Hz, 3H); **¹³C NMR** (176 MHz, CDCl₃): δ 191.1, 143.4, 140.7, 138.9, 138.8, 133.9, 133.6, 130.7, 130.6, 130.2 (q, *J* = 32.3 Hz), 128.4, 127.1, 126.5 (q, *J* = 3.8 Hz), 124.1 (q, *J* = 272.4 Hz), 123.2 (q, *J* = 3.8 Hz), 123.1, 26.1, 19.1; **IR** (cm⁻¹): 2913, 1695, 1597, 1327, 1285, 1165, 1119, 1077, 909, 836, 765, 730, 657; **HRMS**: *m/z* calculated for C₁₈H₁₅F₃ONa⁺ [M+Na]⁺: 327.0967; found: 327.0971.



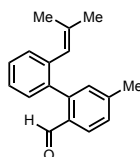
5'-Chloro-2'-(2-methylprop-1-en-1-yl)-[1,1'-biphenyl]-2-carbaldehyde (1.67): Prepared according to GP-1.2 with **A1.5** (2.04 mmol). Purification by flash column chromatography (2% EtOAc/hexanes) afforded the title compound as a colorless oil (425 mg, 77%).

¹H NMR (500 MHz, CDCl₃): δ 9.58 (s, 1H), 7.97 (d, *J* = 7.7 Hz, 1H), 7.63 (t, *J* = 7.5 Hz, 1H), 7.49 (t, *J* = 7.6 Hz, 1H), 7.37 (dd, *J* = 8.3, 2.0 Hz, 1H), 7.32 (d, *J* = 2.0 Hz, 1H), 7.29 (d, *J* = 7.6 Hz, 1H), 7.23 (d, *J* = 8.3 Hz, 1H), 5.66 (s, 1H), 1.72 (s, 3H), 1.67 (s, 3H); **¹³C NMR** (126 MHz, CDCl₃): δ 191.6, 143.7, 138.9, 138.2, 136.8, 134.1, 133.8, 132.3, 131.1, 130.8, 130.1, 128.3, 128.1, 127.1, 123.3, 26.2, 19.3; **IR** (cm⁻¹): 2974, 2850, 2747, 1694, 1597, 1466, 1442, 1385, 1253, 1194, 1101, 1019, 867, 766, 736, 681, 647; **HRMS**: *m/z* calculated for C₁₇H₁₅ClONa⁺ [M+Na]⁺: 293.0704; found: 293.0707.



5-Methoxy-2'-(2-methylprop-1-en-1-yl)-[1,1'-biphenyl]-2-carbaldehyde (1.72): Prepared according to GP-1.2 with **A1.1** (2.00 mmol). Purification by flash column chromatography (5–15% EtOAc/hexanes) afforded the title compound as a colorless oil (530 mg, 99%).

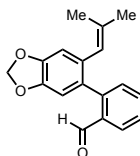
¹H NMR (500 MHz, CD₃OD): δ 9.35 (s, 1H), 7.90 (d, *J* = 8.7 Hz, 1H), 7.41 (t, *J* = 7.4 Hz, 1H), 7.35 (t, *J* = 7.3 Hz, 1H), 7.31 (t, *J* = 7.1 Hz, 2H), 7.05 (dd, *J* = 8.7, 2.0 Hz, 1H), 6.80 (d, *J* = 2.3 Hz, 1H), 5.76 (s, 1H), 3.89 (s, 3H), 1.73 (s, 3H), 1.67 (s, 3H); **¹³C NMR** (126 MHz, CD₃OD): δ 192.3, 165.5, 149.3, 139.2, 138.4, 137.7, 131.0, 130.8, 130.0, 129.1, 128.9, 127.7, 125.6, 116.7, 114.9, 56.2, 26.2, 19.3; **IR** (cm⁻¹): 2970, 2839, 1682, 1591, 1438, 1394, 1329, 1297, 1222, 1124, 1031, 1016, 825, 766, 741, 633, 616; **HRMS**: *m/z* calculated for C₁₈H₁₈O₂Na⁺ [M+H]⁺: 289.1199; found: 289.1202.



5-Methyl-2'-(2-methylprop-1-en-1-yl)-[1,1'-biphenyl]-2-carbaldehyde (1.71): Prepared according to GP-1.2 with **A1.1** (2.0 mmol). Purification by flash column chromatography (3% EtOAc/hexanes) afforded the title compound as a colorless oil (420 mg, 84%).

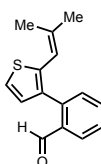
¹H NMR (700 MHz, CD₃OD): δ 9.42 (s, 1H), 7.79 (d, *J* = 8.0 Hz, 1H), 7.39 (t, *J* = 7.5 Hz, 1H), 7.33 (t, *J* = 7.5 Hz, 1H), 7.30 (d, *J* = 8.0 Hz, 1H), 7.29 – 7.27 (m, 2H), 7.12 (s, 1H), 5.70 (s, 1H), 2.43 (s, 3H), 1.71 (s, 3H), 1.63 (s, 3H); **¹³C NMR** (176 MHz, CD₃OD): δ 193.0, 146.7, 146.2, 139.3, 138.6, 137.8, 133.2, 132.5, 131.1, 130.8, 129.7, 129.0, 127.8, 127.6, 125.8, 26.2, 21.8, 19.3;

IR (cm⁻¹): 2972, 2910, 2845, 2745, 1690, 1602, 1441, 1391, 1256, 1207, 1177, 1122, 981, 822, 766, 741, 705, 637; **HRMS**: *m/z* calculated for C₁₈H₁₈ONa⁺ [M+Na]⁺: 273.1250; found: 273.1251.



2-(6-(2-Methylprop-1-en-1-yl)benzo[d][1,3]dioxol-5-yl)benzaldehyde (1.70): Prepared according to GP-1.2 with **A1.6** (2.40 mmol). Purification by flash column chromatography (5–15% EtOAc/hexanes) afforded the title compound as a pale-yellow oil (460 mg, 82%).

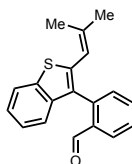
¹H NMR (400 MHz, CDCl₃): δ 9.60 (s, 1H), 7.94 (dd, *J* = 7.8, 1.1 Hz, 1H), 7.59 (td, *J* = 7.5, 1.4 Hz, 1H), 7.44 (t, *J* = 7.5 Hz, 1H), 7.27 (d, *J* = 6.9 Hz, 1H), 6.79 (d, *J* = 9.5 Hz, 2H), 6.03 (s, 2H), 5.61 (s, 1H), 1.72 (s, 3H), 1.63 (s, 3H); **¹³C NMR** (176 MHz, CD₃OD): δ 193.4, 148.9, 147.9, 146.3, 137.5, 135.8, 134.9, 133.4, 132.3, 131.8, 128.8, 127.4, 125.6, 111.0, 110.7, 102.8, 26.0, 19.3; **IR** (cm⁻¹): 2973, 2906, 1691, 1595, 1473, 1446, 1360, 1246, 1214, 1192, 1035, 933, 875, 824, 765, 737, 643; **HRMS**: *m/z* calculated for C₁₈H₁₆O₃Na⁺ [M+Na]⁺: 303.0992; found: 303.0995.



2-(2-(2-Methylprop-1-en-1-yl)thiophen-3-yl)benzaldehyde (S1.56): Prepared according to GP-1.2 with **A1.7** (3.60 mmol). Purification by flash column chromatography (0–5% EtOAc/hexanes) afforded the title compound as a pale-yellow oil (820 mg, 94%).

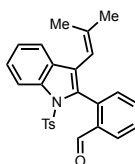
¹H NMR (400 MHz, CDCl₃): δ 9.81 (s, 1H), 8.01 (dd, *J* = 7.8, 1.1 Hz, 1H), 7.63 (td, *J* = 7.5, 1.4 Hz, 1H), 7.48 (t, *J* = 7.6 Hz, 1H), 7.37 (d, *J* = 7.7 Hz, 1H), 7.30 (d, *J* = 5.2 Hz, 1H), 7.03 (d, *J* = 5.2 Hz, 1H), 6.00 (s, 1H), 1.91 (s, 3H), 1.78 (s, 3H); **¹³C NMR** (176 MHz, CDCl₃): δ 192.6,

140.9, 138.9, 137.9, 134.8, 134.5, 133.7, 131.5, 129.7, 127.9, 127.4, 123.6, 116.8, 27.3, 20.3; **IR** (cm⁻¹): 2910, 2848, 1691, 1596, 1448, 1390, 1373, 1255, 1193, 1047, 887, 765, 738, 689, 660, 646; **HRMS**: *m/z* calculated for C₁₅H₁₄OSNa⁺ [M+Na]⁺: 265.0658; found: 265.0661.



2-(2-(2-Methylprop-1-en-1-yl)benzo[b]thiophen-3-yl)benzaldehyde (S1.57): Prepared according to GP-1.2 with **A1.8** (1.87 mmol). Purification by flash column chromatography (0–5% EtOAc/hexanes) afforded the title compound as a pale-yellow oil (468 mg, 86%).

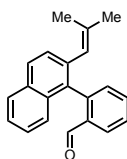
¹H NMR (700 MHz, CDCl₃): δ 9.69 (s, 1H), 8.11 (d, *J* = 7.8 Hz, 1H), 7.85 (d, *J* = 8.0 Hz, 1H), 7.72 (td, *J* = 7.5, 1.1 Hz, 1H), 7.57 (t, *J* = 7.6 Hz, 1H), 7.43 (d, *J* = 7.5 Hz, 1H), 7.35 – 7.32 (m, 1H), 7.32 – 7.29 (m, 2H), 6.08 (s, 1H), 2.03 (s, 3H), 1.82 (s, 3H); **¹³C NMR** (176 MHz, CDCl₃): δ 192.3, 140.2, 140.0, 139.6, 139.5, 138.7, 135.3, 134.2, 132.1, 129.6, 128.5, 127.6, 124.9, 124.7, 122.6, 122.1, 117.4, 27.7, 20.5; **IR** (cm⁻¹): 2969, 2845, 1692, 1596, 1444, 1393, 1264, 1193, 932, 847, 825, 761, 687, 651, 633; **HRMS**: *m/z* calculated for C₁₉H₁₆OSNa⁺ [M+Na]⁺: 315.0814; found: 315.0812.



2-(3-(2-Methylprop-1-en-1-yl)-1-tosyl-1H-indol-2-yl)benzaldehyde (S1.58): Prepared according to GP-1.2 with **A1.10** (4.55 mmol). Purification by flash column chromatography (10–20% EtOAc/hexanes) afforded the title compound as a pale-yellow foam (1.40 g, 72%).

¹H NMR (500 MHz, CDCl₃): δ 9.31 (s, 1H), 8.41 (d, *J* = 8.4 Hz, 1H), 7.98 (d, *J* = 7.8 Hz, 1H), 7.64 (td, *J* = 7.6, 1.2 Hz, 1H), 7.54 (t, *J* = 7.5 Hz, 1H), 7.48 (d, *J* = 7.7 Hz, 1H), 7.45 (m, 1H), 7.40

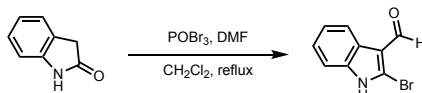
– 7.32 (m, 2H), 7.22 (d, $J = 8.3$ Hz, 2H), 7.05 (d, $J = 8.1$ Hz, 2H), 5.58 (s, 1H), 2.30 (s, 3H), 1.70 (s, 3H), 1.30 (s, 3H); ^{13}C NMR (176 MHz, CDCl_3): δ 191.0, 145.3, 141.4, 137.8, 135.3, 134.9, 134.6, 133.8, 132.6, 131.9, 130.4, 129.7, 129.1, 126.7, 126.6, 126.0, 125.8, 124.4, 120.7, 116.4, 113.9, 25.6, 21.7, 20.4; IR (cm^{-1}): 2912, 2851, 1735, 1693, 1597, 1444, 1372, 1244, 1174, 1089, 1065, 967, 850, 813, 749, 704, 663; HRMS: m/z calculated for $\text{C}_{26}\text{H}_{23}\text{NO}_3\text{SNa}^+$ $[\text{M}+\text{Na}]^+$: 452.1291; found: 452.1286.



2-(2-(2-Methylprop-1-en-1-yl)naphthalen-1-yl)benzaldehyde (1.73): Prepared according to GP-1.2 with **A1.9** (0.88 mmol). Purification by flash column chromatography (0–5% EtOAc/hexanes) afforded the title compound as a pale-green oil (199 mg, 79%).

^1H NMR (700 MHz, CDCl_3): δ 9.46 (s, 1H), 8.10 (d, $J = 7.8$ Hz, 1H), 7.89 (d, $J = 8.4$ Hz, 2H), 7.70 (td, $J = 7.5, 1.1$ Hz, 1H), 7.57 (t, $J = 7.6$ Hz, 1H), 7.49 (d, $J = 8.5$ Hz, 1H), 7.46 (t, $J = 7.3$ Hz, 1H), 7.36 (t, $J = 7.5$ Hz, 1H), 7.34 – 7.30 (m, 2H), 5.82 (s, 1H), 1.78 (s, 3H), 1.69 (s, 3H); ^{13}C NMR (176 MHz, CDCl_3): δ 192.3, 143.5, 136.9, 136.2, 135.1, 133.9, 133.3, 133.2, 132.3, 131.9, 128.2, 128.1, 128.0, 127.9, 127.1, 126.6, 126.1, 125.7, 124.8, 26.3, 19.6; IR (cm^{-1}): 3056, 2974, 2582, 1693, 1596, 1505, 1445, 1375, 1263, 1194, 1061, 867, 839, 762, 741, 645, 622; HRMS: m/z calculated for $\text{C}_{21}\text{H}_{18}\text{ONa}^+$ $[\text{M}+\text{Na}]^+$: 309.1250; found: 309.1248.

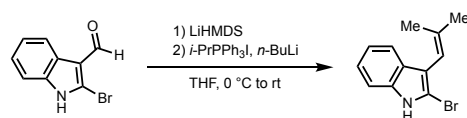
Miscellaneous Procedures



2-Bromo-1H-indole-3-carbaldehyde (A1.11): A 250-mL three-neck round-bottom flask equipped with a stir bar and reflux condenser was charged with DMF (3.5 mL, 45.1 mmol,

3.0 equiv.) and CH₂Cl₂ (12 mL) under a nitrogen atmosphere. A solution of phosphorus oxybromide (10.21 g, 35.6 mmol, 2.4 equiv.) in CH₂Cl₂ (18 mL) was added dropwise at 0 °C and the resulting mixture heated at reflux for 15 min. After cooling down to rt, 2-oxindole (2.00 g, 15.0 mmol, 1.0 equiv.) was added carefully and the reaction mixture heated at reflux for 1 h. The reaction was allowed to cool down to rt and quenched by the addition of ice. The aqueous layer was separated, neutralized with K₂CO₃ to pH 8–10 and stirred for 15 min. The resulting precipitate was collected via filtration and washed with water. The crude product was purified by flash column chromatography (30–50% EtOAc/hexanes) to afford the pure title compound as a orange solid (2.65 g, 79%). Spectroscopic data were consistent with those reported in the literature.

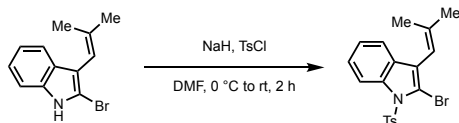
¹H NMR (400 MHz, CD₃OD): δ 9.91 (s, 1H), 8.13 (dd, *J* = 6.7, 1.7 Hz, 1H), 7.39 (dd, *J* = 6.9, 1.4 Hz, 1H), 7.25 (pd, *J* = 7.2, 1.5 Hz, 2H).



2-Bromo-3-(2-methylprop-1-en-1-yl)-1H-indole (A1.12): A 50-mL round-bottom flask equipped with a magnetic stir bar was charged with isopropyltriphenylphosphonium iodide (3.62 g, 8.40 mmol, 1.25 equiv.) and THF (15 mL), before cooling the resulting suspension to 0 °C. Next, *n*-BuLi (1.6 M in hexanes; 5.0 mL, 8.0 mmol, 1.2 equiv.) was added and the solution stirred at 0 °C for 30 min under a nitrogen atmosphere. A solution of **A1.11** (1.50 g, 6.70 mmol, 1.0 equiv.) in THF (7 mL) that was pretreated with LiHMDS (1 M in THF, 6.7 mL, 6.7 mmol, 1.0 equiv.) at 0 °C, was transferred to the reaction mixture at 0 °C via canula. The solution was gradually warmed up to rt and stirred for 1 h. Next, NH₄Cl solution (aq., sat.) was added and the mixture partitioned between water and EtOAc. The organic layer was separated and the aqueous layer extracted with EtOAc (3x). The combined organic extracts were dried over Na₂SO₄, filtered

and concentrated *in vacuo*. The crude product was purified by flash column chromatography (10% EtOAc/hexanes) to afford the pure title compound as a yellow oil (1.40 g, 84%).

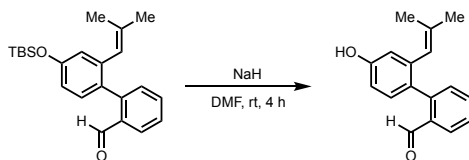
¹H NMR (500 MHz, CDCl₃): δ 8.04 (s, 1H), 7.43 (d, *J* = 7.8 Hz, 1H), 7.28 (d, *J* = 8.0 Hz, 1H), 7.17 (t, *J* = 7.5 Hz, 1H), 7.11 (t, *J* = 7.5 Hz, 1H), 6.08 (s, 1H), 1.98 (s, 3H), 1.74 (s, 3H); **¹³C NMR** (126 MHz, CDCl₃): δ 138.6, 136.1, 128.0, 122.4, 120.2, 119.7, 115.1, 115.0, 110.4, 108.5, 26.0, 20.9; **IR** (cm⁻¹): 3394, 2967, 2928, 1516, 1445, 1338, 1238, 1190, 1039, 742; **HRMS**: *m/z* calculated for C₁₂H₁₂BrN⁺ [M]⁺: 249.0153; found: 249.0165.



2-Bromo-3-(2-methylprop-1-en-1-yl)-1-tosyl-1H-indole (A1.10): A 100-mL round-bottom flask equipped with a magnetic stir bar was charged with **A1.12** (1.21 g, 4.84 mmol, 1.0 equiv.) and DMF (50 mL). NaH (60% dispersion in mineral oil; 271 mg, 6.77 mmol, 1.4 equiv.) was added at 0 °C and the solution stirred for 30 min at that temperature. Next, *p*-TsCl (1.44 g, 7.55 mmol, 1.6 equiv.) was added and the mixture gradually warmed up to rt and stirred for 1.5 h under a nitrogen atmosphere. Then, NH₄Cl solution (aq., sat.) was added and the mixture partitioned between water and EtOAc. The organic layer was separated and the aqueous layer extracted with EtOAc (3x). The combined organic extracts were washed with water (3x) and brine (1x), dried over Na₂SO₄, filtered and concentrated *in vacuo*. The crude product was purified by flash column chromatography (10% EtOAc/hexanes) to afford the pure title compound as a pale-yellow foam (1.92 g, 98%).

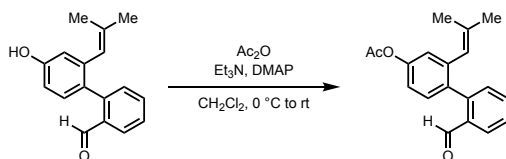
¹H NMR (500 MHz, CDCl₃): δ 8.28 (d, *J* = 8.4 Hz, 1H), 7.74 (d, *J* = 8.2 Hz, 2H), 7.31 (dd, *J* = 16.1, 8.0 Hz, 2H), 7.27 – 7.22 (m, 1H), 7.19 (d, *J* = 8.0 Hz, 2H), 5.88 (s, 1H), 2.34 (s, 3H), 1.94 (s, 3H), 1.53 (s, 3H); **¹³C NMR** (126 MHz, CDCl₃): δ 145.2, 141.3, 137.5, 135.3, 130.2, 129.8,

127.2, 125.0, 124.6, 124.0, 119.9, 115.7, 114.2, 109.5, 25.8, 21.7, 20.8; **IR** (cm⁻¹): 2912, 1596, 1440, 1375, 1217, 1178, 1088, 1049, 971, 909, 811, 736, 703, 676, 657; **HRMS**: *m/z* calculated for C₁₉H₁₈BrNO₂SH⁺ [M+H]⁺: 404.0314; found: 404.0316.



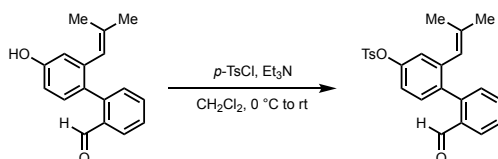
4'-Hydroxy-2'-(2-methylprop-1-en-1-yl)-[1,1'-biphenyl]-2-carbaldehyde (S1.52): Adapted from a literature procedure with minor modifications.⁷⁹ A 250-mL round-bottom flask equipped with a magnetic stir bar was charged with **S1.35** (1.50 g, 4.09 mmol, 1.0 equiv.) and DMF (50 mL). NaH (60% dispersion in mineral oil; 491 mg, 12.3 mmol, 3.0 equiv.) was added in portions and the reaction stirred at rt for 4 h under a nitrogen atmosphere. The reaction mixture was cooled down to 0 °C, and NH₄Cl solution (aq., sat.) was added. After diluting with EtOAc and separating the aqueous layer, the organic layer was washed with water (3x) and brine (1x), dried over Na₂SO₄, filtered and concentrated in vacuo. The crude product was purified by flash column chromatography (40% EtOAc/hexanes) to afford the pure title compound as a pale-yellow solid (1.03 g, quant.).

¹H NMR (500 MHz, CD₃OD): δ 9.53 (s, 1H), 7.87 (d, *J* = 7.7 Hz, 1H), 7.64 (t, *J* = 7.5 Hz, 1H), 7.45 (t, *J* = 7.5 Hz, 1H), 7.31 (d, *J* = 7.6 Hz, 1H), 7.16 (d, *J* = 8.2 Hz, 1H), 6.80 (dd, *J* = 8.2, 2.2 Hz, 1H), 6.75 (d, *J* = 1.9 Hz, 1H), 5.67 (s, 1H), 1.72 (s, 3H), 1.63 (s, 3H); **¹³C NMR** (126 MHz, CD₃OD): δ 193.7, 158.5, 146.8, 140.6, 137.9, 135.7, 134.8, 132.5, 132.4, 129.5, 128.4, 127.3, 125.9, 117.4, 114.8, 26.1, 19.3; **IR** (cm⁻¹): 3217, 1656, 1596, 1472, 1396, 1293, 1263, 1170, 970, 884, 836, 721, 629; **HRMS**: *m/z* calculated for C₁₇H₁₆O₂Na⁺ [M+Na]⁺: 275.1043; found: 275.1046.



2'-Formyl-2-(2-methylprop-1-en-1-yl)-[1,1'-biphenyl]-4-yl acetate (S1.51): A 25-mL round-bottom flask equipped with a magnetic stir bar was charged with **S1.52** (202 mg, 0.80 mmol, 1.0 equiv.) and CH_2Cl_2 (5 mL). After cooling to $0\text{ }^\circ\text{C}$, acetic anhydride (0.09 mL, 0.96 mmol, 1.2 equiv.), DMAP (4.9 mg, 0.04 mmol, 0.05 equiv.) and triethylamine (0.22 mL, 1.60 mmol, 2.0 equiv.) were added sequentially under a nitrogen atmosphere and the reaction mixture allowed to warm up to rt. After stirring for 1.5 h, NH_4Cl solution (aq., sat.) was added and the mixture extracted with EtOAc (3x). The combined organic extracts were dried over Na_2SO_4 , filtered and concentrated *in vacuo*. Purification by flash column chromatography (10% EtOAc/hexanes) afforded the pure title compound as a white solid (216 mg, 92%).

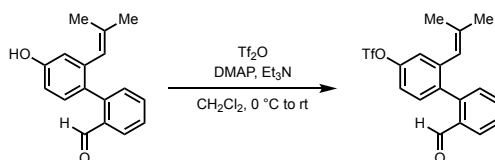
$^1\text{H NMR}$ (700 MHz, CD_3OD): δ 9.55 (s, 1H), 7.92 (d, $J = 7.7$ Hz, 1H), 7.70 (td, $J = 7.5, 1.1$ Hz, 1H), 7.53 (t, $J = 7.6$ Hz, 1H), 7.37 (d, $J = 8.2$ Hz, 1H), 7.35 (d, $J = 7.6$ Hz, 1H), 7.12 (dd, $J = 8.2, 2.3$ Hz, 1H), 7.06 (d, $J = 2.3$ Hz, 1H), 5.70 (s, 1H), 2.32 (s, 3H), 1.73 (s, 3H), 1.66 (s, 3H); **$^{13}\text{C NMR}$** (176 MHz, CD_3OD): δ 193.1, 171.2, 151.9, 145.6, 140.7, 139.2, 136.1, 135.6, 135.0, 132.3, 132.2, 129.1, 127.6, 124.9, 124.0, 121.0, 26.1, 21.0, 19.2; **IR** (cm^{-1}): 2971, 2928, 1764, 1683, 1596, 1443, 1373, 1258, 1203, 1155, 1005, 910, 836, 772, 728, 637; **HRMS**: m/z calculated for $\text{C}_{19}\text{H}_{18}\text{O}_3\text{Na}^+$ $[\text{M}+\text{Na}]^+$: 317.1148; found: 317.1152.



2'-Formyl-2-(2-methylprop-1-en-1-yl)-[1,1'-biphenyl]-4-yl 4-methylbenzenesulfonate (S1.48): A 25-mL round-bottom flask equipped with a magnetic stir bar was charged with **S1.52**

(221 mg, 0.88 mmol, 1.0 equiv.) and CH₂Cl₂ (5 mL). After cooling to 0 °C *p*-TsCl (201 mg, 1.05 mmol, 1.2 equiv.) and triethylamine (0.25 mL, 1.75 mmol, 2.0 equiv.) were added sequentially under a nitrogen atmosphere and the reaction mixture allowed to warm up to rt. After stirring for 1.5 h, NH₄Cl solution (aq., sat.) was added and the mixture extracted with EtOAc (3x). The combined organic extracts were dried over Na₂SO₄, filtered and concentrated *in vacuo*. Purification by flash column chromatography (10% EtOAc/hexanes) afforded the pure title compound as a colorless foam (343 mg, 96%).

¹H NMR (700 MHz, CD₃OD): δ 9.42 (s, 1H), 7.90 (d, *J* = 7.3 Hz, 1H), 7.76 (d, *J* = 8.3 Hz, 2H), 7.68 (td, *J* = 7.5, 1.0 Hz, 1H), 7.53 (t, *J* = 7.6 Hz, 1H), 7.44 (d, *J* = 8.3 Hz, 2H), 7.31 (d, *J* = 8.3 Hz, 1H), 7.29 (d, *J* = 7.6 Hz, 1H), 7.07 (dd, *J* = 8.3, 2.5 Hz, 1H), 6.86 (d, *J* = 2.4 Hz, 1H), 5.58 (s, 1H), 2.45 (s, 3H), 1.61 (s, 3H), 1.50 (s, 3H); **¹³C NMR** (176 MHz, CD₃OD): δ 192.7, 150.6, 147.8, 144.9, 141.0, 139.7, 137.7, 135.5, 135.0, 133.6, 132.4, 132.1, 131.2, 129.7, 129.4, 127.9, 124.5, 124.4, 121.7, 26.1, 21.6, 19.1; **IR** (cm⁻¹): 2928, 2852, 1736, 1694, 1597, 1445, 1372, 1241, 1191, 1144, 1092, 965, 840, 805, 765, 709, 661; **HRMS**: *m/z* calculated for C₂₄H₂₂O₄SNa⁺ [M+Na]⁺: 429.1131; found: 429.1131.

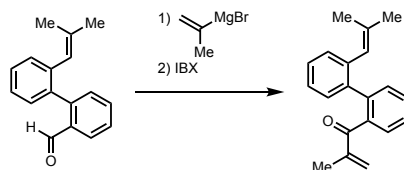


2'-Formyl-2-(2-methylprop-1-en-1-yl)-[1,1'-biphenyl]-4-yl trifluoromethanesulfonate

(S1.53): A 25-mL round-bottom flask equipped with a magnetic stir bar was charged with **S1.52** (204 mg, 0.81 mmol, 1.0 equiv.) and CH₂Cl₂ (5 mL). After cooling to 0 °C triflic anhydride (0.16 mL, 0.97 mmol, 1.2 equiv.), DMAP (4.9 mg, 0.04 mmol, 0.05 equiv.) and triethylamine (0.23 mL, 1.62 mmol, 2.0 equiv.) were added sequentially under a nitrogen atmosphere and the reaction mixture allowed to warm up to rt. After stirring for 1.5 h, NH₄Cl solution (aq., sat.) was

added and the mixture extracted with EtOAc (3x). The combined organic extracts were dried over Na₂SO₄, filtered and concentrated *in vacuo*. Purification by flash column chromatography (5% EtOAc/hexanes) afforded the pure title compound as a white solid (229 mg, 74%).

¹H NMR (700 MHz, CD₂Cl₂): δ 9.57 (s, 1H), 7.95 (d, *J* = 7.5 Hz, 1H), 7.66 (td, *J* = 7.5, 1.1 Hz, 1H), 7.53 (t, *J* = 7.6 Hz, 1H), 7.41 (d, *J* = 8.4 Hz, 1H), 7.30 (d, *J* = 7.6 Hz, 1H), 7.27 (dd, *J* = 8.4, 2.5 Hz, 1H), 7.25 (d, *J* = 2.5 Hz, 1H), 5.71 (s, 1H), 1.77 (s, 3H), 1.69 (s, 3H); **¹³C NMR** (176 MHz, CD₂Cl₂): δ 191.5, 149.6, 143.4, 141.1, 140.1, 138.3, 134.6, 134.2, 132.4, 131.5, 128.9, 127.6, 123.3, 122.8, 119.6, 119.4 (q, *J* = 320.7 Hz), 26.4, 19.4; **IR** (cm⁻¹): 2917, 2849, 1696, 1597, 1423, 1244, 1209, 1138, 961, 894, 858, 830, 766, 656, 608; **HRMS**: *m/z* calculated for C₁₈H₁₅F₃O₄SNa⁺ [M+Na]⁺: 407.0535; found: 407.0538.



2-Methyl-1-(2'-(2-methylprop-1-en-1-yl)-[1,1'-biphenyl]-2-yl)prop-2-en-1-one (S1.55): A 25-mL round-bottom flask equipped with a magnetic stir bar was charged with **1.31** (250 mg, 1.06 mmol, 1.0 equiv.) and THF (4 mL) under a nitrogen atmosphere. After cooling down to 0 °C, isopropenylmagnesium bromide (0.5 M in THF; 2.3 mL, 1.15 mmol, 1.1 equiv.) was added dropwise and the reaction mixture stirred for 30 min at 0 °C. Then, NH₄Cl solution (aq., sat.) was added and the mixture extracted with EtOAc (3x). The combined organic extracts were dried over Na₂SO₄, filtered and concentrated *in vacuo* to yield the crude alcohol, which was used for the next step without further purification.

A 10-mL round-bottom flask equipped with a magnetic stir bar was charged with crude alcohol from the previous step and DMSO (2 mL). 2-Iodoxybenzoic acid (355 mg, 1.27 mmol, 1.2 equiv.) was added at rt and the mixture stirred for 4 h. Water was added and the resulting

precipitate removed via filtration through celite. The filtrate was extracted with EtOAc (3x), and the combined organic extracts were dried over Na₂SO₄, filtered and concentrated *in vacuo*. The crude product was purified by flash column chromatography (0–5% EtOAc/hexanes) to afford the pure title compound as a colorless oil (201 mg, 69%).

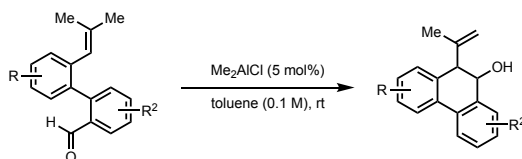
¹H NMR (700 MHz, CDCl₃): δ 7.46 – 7.43 (m, 2H), 7.37 (t, *J* = 7.5 Hz, 1H), 7.28 – 7.25 (m, 2H), 7.22 (d, *J* = 7.3 Hz, 1H), 7.18 (t, *J* = 7.4 Hz, 1H), 7.08 (d, *J* = 7.5 Hz, 1H), 5.84 (s, 1H), 5.63 (s, 1H), 5.40 (s, 1H), 1.73 (s, 3H), 1.72 (s, 3H), 1.70 (s, 3H); **¹³C NMR** (176 MHz, CDCl₃): δ 200.0, 145.0, 140.7, 139.84, 139.78, 136.7, 135.7, 131.3, 130.4, 130.0, 129.5, 128.6, 127.5, 127.2, 126.7, 126.1, 124.8, 26.5, 19.5, 17.4; **IR** (cm⁻¹): 3058, 2969, 2024, 1657, 1435, 1374, 1326, 1195, 1050, 1015, 977, 933, 748, 691; **HRMS**: *m/z* calculated for C₂₀H₂₀ONa⁺ [M+Na]⁺: 299.1406; found: 299.1410.



3-Bromothiophene-2-carbaldehyde (A1.13): To a round-bottom flask equipped with a magnetic stir bar containing a freshly prepared 0.5 M solution of LDA in THF (20 mL, 10 mmol, 1.1 equiv.), which was cooled at –78 °C, was added dropwise a solution of 3-bromothiophene (0.86 mL, 9.2 mmol, 1.0 equiv.) in THF (2.5 mL). The resulting solution was stirred for 0.5 h at that temperature, before being gradually warmed up to 0 °C. Next, DMF (0.85 mL, 11.0 mmol, 1.2 equiv.) was added dropwise and the reaction allowed to warm up to rt and stirred for 1 h. Then, NH₄Cl (aq., sat.) was added and the resulting mixture stirred for 0.5 h, before extracting with EtOAc (3x). The combined organic extracts were washed with water (3x) and brine, dried over Na₂SO₄, filtered and concentrated *in vacuo*. Purification by flash column chromatography (5% EtOAc/hexanes) afforded the pure title compound as a pale-yellow oil (1.35 g, 77%). Spectroscopic data was consistent with those reported in the literature.⁸⁰

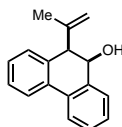
Synthesis of Carbonyl–Ene Products and Characterization

General Procedure for Carbonyl–Ene Reaction with Me₂AlCl (GP-1.3)



A 20-mL glass scintillation vial equipped with a magnetic stir bar was charged with aryl aldehyde (0.20 mmol, 1.0 equiv.). The vial was sealed with a rubber septum under a nitrogen atmosphere and toluene (2 mL) was added. To this solution was added Me₂AlCl (1 M in hexane; 10 μ L, 1.0×10^{-2} mmol, 5 mol%) and the resulting mixture stirred for the indicated time at rt. Upon completion as determined by TLC analysis, the reaction mixture was passed through a short silica plug eluting with CH₂Cl₂ (25–50 mL). The filtrate was concentrated *in vacuo* and the crude product purified by flash column chromatography to obtain the pure alcohol product.

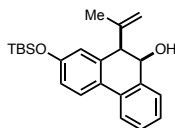
Note: Relative stereochemistry was found to be *syn* for all alcohol products, as assigned based on ¹H NMR NOE correlations and coupling constants of $J = 5.9$ – 6.4 Hz between both benzylic protons.⁸¹



10-(Prop-1-en-2-yl)-9,10-dihydrophenanthren-9-ol (1.33): Prepared according to GP-1.3 with aryl aldehyde **1.31** (0.20 mmol, 1.0 equiv.) with a total reaction time of 1 h. Purification by flash column chromatography (10% EtOAc/hexanes) afforded the pure title compound as a white solid (47 mg, 99%).

¹H NMR (700 MHz, CDCl₃): δ 7.82 (d, $J = 7.8$ Hz, 1H), 7.74 – 7.71 (m, 1H), 7.65 – 7.63 (m, 1H), 7.39 – 7.34 (m, 3H), 7.30 – 7.26 (m, 2H), 5.10 (d, $J = 6.3$ Hz, 1H), 5.00 (s, 1H), 4.93 (s, 1H), 3.82 (d, $J = 6.4$ Hz, 1H), 2.11 (b, 1H), 1.27 (s, 3H); ¹³C NMR (126 MHz, CDCl₃): δ 143.8, 138.5,

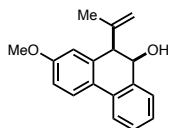
136.1, 133.8, 133.3, 129.5, 128.4, 128.1, 128.0, 127.9, 124.7, 123.8, 124.6, 116.0, 69.5, 53.3, 21.0;
IR (cm⁻¹): 3288, 3068, 2959, 1636, 1482, 1451, 1374, 1199, 1099, 1074, 1011, 946, 886, 737, 675;
HRMS: *m/z* calculated for C₁₇H₁₆ONa⁺ [M+Na]⁺: 259.1093; found: 259.1096.



2-((Tert-butyldimethylsilyloxy)-10-(prop-1-en-2-yl)-9,10-dihydrophenanthren-9-ol (1.35):

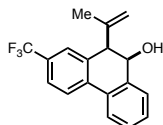
Prepared according to GP-1.3 with aryl aldehyde **S1.35** (73 mg, 0.20 mmol, 1.0 equiv.) with a total reaction time of 20 min. Purification by flash column chromatography (5–10% EtOAc/hexanes) afforded the pure title compound as a colorless oil (64 mg, 87%).

¹H NMR (700 MHz, CDCl₃): δ 7.68 (d, *J* = 8.5 Hz, 1H), 7.63 (d, *J* = 7.5 Hz, 1H), 7.59 (d, *J* = 7.4 Hz, 1H), 7.33 (t, *J* = 7.3 Hz, 1H), 7.29 (t, *J* = 7.0 Hz, 1H), 6.84 (dd, *J* = 8.4, 2.5 Hz, 1H), 6.74 (d, *J* = 2.4 Hz, 1H), 5.05 (t, *J* = 5.7 Hz, 1H), 4.98 (s, 1H), 4.94 (s, 1H), 3.72 (d, *J* = 6.2 Hz, 1H), 2.07 (b, 1H), 1.30 (s, 3H), 1.01 (s, 9H), 0.24 (s, 6H); **¹³C NMR** (176 MHz, CDCl₃): δ 155.7, 143.8, 137.7, 137.6, 133.3, 127.9, 127.5, 127.3, 125.1, 124.8, 123.0, 120.8, 119.6, 115.9, 69.6, 53.5, 25.8, 21.1, 18.4, -4.18, -4.21; **IR** (cm⁻¹): 2954, 2928, 2856, 1602, 1502, 1478, 1286, 1251, 1153, 1126, 1077, 987, 869, 837, 770, 732, 680; **HRMS**: *m/z* calculated for C₂₃H₃₀O₂SiNa⁺ [M+Na]⁺: 389.1907; found: 389.1900.



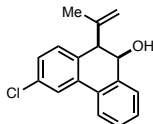
2-Methoxy-10-(prop-1-en-2-yl)-9,10-dihydrophenanthren-9-ol (1.36): Prepared according to GP-1.3 with aryl aldehyde **1.68** (53 mg, 0.20 mmol, 1.0 equiv.) with a total reaction time of 20 min. Purification by flash column chromatography (5–10% EtOAc/hexanes) afforded the pure title compound as a colorless oil (49 mg, 92%).

¹H NMR (700 MHz, CDCl₃): δ 7.74 (d, *J* = 8.6 Hz, 1H), 7.64 (d, *J* = 7.6 Hz, 1H), 7.59 (d, *J* = 7.4 Hz, 1H), 7.33 (t, *J* = 7.5 Hz, 1H), 7.29 (t, *J* = 7.4 Hz, 1H), 6.91 (dd, *J* = 8.6, 2.7 Hz, 1H), 6.80 (d, *J* = 2.6 Hz, 1H), 5.06 (s, 1H), 4.99 (s, 1H), 4.94 (s, 1H), 3.85 (s, 3H), 3.76 (d, *J* = 6.3 Hz, 1H), 2.08 (b, 1H), 1.30 (s, 3H); **¹³C NMR** (176 MHz, CDCl₃): δ 159.6, 143.8, 137.7, 137.6, 133.3, 127.9, 127.4, 126.7, 125.2, 124.7, 122.9, 116.1, 114.5, 113.6, 69.6, 55.5, 53.7, 21.0; **IR** (cm⁻¹): 2433, 2914, 2837, 1609, 1453, 1315, 1265, 1232, 1134, 1076, 1049, 899, 819, 770, 733; **HRMS**: *m/z* calculated for C₁₈H₁₈O₂Na⁺ [M+Na]⁺: 289.1199; found: 289.1203.



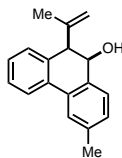
10-(Prop-1-en-2-yl)-2-(trifluoromethyl)-9,10-dihydrophenanthren-9-ol (1.40): Prepared according to GP-1.3 with aryl aldehyde **1.69** (61 mg, 0.20 mmol, 1.0 equiv.) with a total reaction time of 20 min. Purification by flash column chromatography (5–10% EtOAc/hexanes) afforded the pure title compound as a colorless oil (58 mg, 95%).

¹H NMR (700 MHz, CDCl₃): δ 7.90 (d, *J* = 8.2 Hz, 1H), 7.75 (d, *J* = 7.1 Hz, 1H), 7.66 (d, *J* = 7.1 Hz, 1H), 7.61 (d, *J* = 8.1 Hz, 1H), 7.53 (s, 1H), 7.41 (pd, *J* = 7.4, 1.6 Hz, 2H), 5.09 (d, *J* = 5.1 Hz, 1H), 5.02 (s, 1H), 4.99 (s, 1H), 3.85 (d, *J* = 6.2 Hz, 1H), 2.13 (b, 1H), 1.30 (s, 3H); **¹³C NMR** (176 MHz, CDCl₃): δ 142.9, 138.8, 137.3, 136.7, 132.0, 129.9 (q, *J* = 32.4 Hz), 129.5, 128.3, 126.3 (q, *J* = 3.8 Hz), 125.2, 124.9 (q, *J* = 3.8 Hz), 124.24 (q, *J* = 272.1 Hz), 124.19, 124.15, 116.9, 69.2, 53.1, 21.0; **IR** (cm⁻¹): 3427, 3071, 2920, 1619, 1418, 1329, 1295, 1162, 1117, 1072, 961, 903, 835, 738, 683, 647; **HRMS**: *m/z* calculated for C₁₈H₁₅F₃ONa⁺ [M+Na]⁺: 327.0967; found: 327.0973.



3-Chloro-10-(prop-1-en-2-yl)-9,10-dihydrophenanthren-9-ol (1.41): Prepared according to GP-1.3 with aryl aldehyde **1.67** (54 mg, 0.20 mmol, 1.0 equiv.) with a total reaction time of 15 min. Purification by flash column chromatography (5–10% EtOAc/hexanes) afforded the pure title compound as a colorless oil (53 mg, 98%).

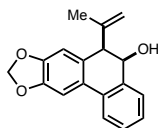
¹H NMR (500 MHz, CDCl₃): δ 7.77 (d, *J* = 1.7 Hz, 1H), 7.69 – 7.65 (m, 1H), 7.65 – 7.59 (m, 1H), 7.40 – 7.34 (m, 2H), 7.24 (dd, *J* = 8.1, 2.0 Hz, 1H), 7.19 (d, *J* = 8.1 Hz, 1H), 5.04 (d, *J* = 6.1 Hz, 1H), 4.97 (s, 1H), 4.93 (s, 1H), 3.77 (d, *J* = 6.3 Hz, 1H), 2.13 (b, 1H), 1.26 (s, 3H); **¹³C NMR** (126 MHz, CDCl₃): δ 143.3, 138.4, 135.5, 134.4, 133.8, 132.1, 130.8, 129.0, 128.1, 127.9, 125.0, 123.9, 123.7, 116.4, 69.3, 52.7, 20.9; **IR** (cm⁻¹): 3435, 3069, 2919, 1637, 1595, 1559, 1483, 1446, 1375, 1264, 1208, 1097, 1023, 946, 881, 818, 733, 690, 663; **HRMS**: *m/z* calculated for C₁₇H₁₅ClONa⁺ [M+Na]⁺: 293.0704; found: 293.0707.



6-Methyl-10-(prop-1-en-2-yl)-9,10-dihydrophenanthren-9-ol (1.46): Prepared according to GP-1.3 with aryl aldehyde **1.71** (50 mg, 0.20 mmol, 1.0 equiv.) with a total reaction time of 40 min. Purification by flash column chromatography (5–10% EtOAc/hexanes) afforded the pure title compound as a colorless oil (47 mg, 95%).

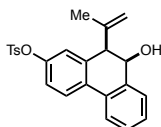
¹H NMR (700 MHz, CDCl₃): δ 7.80 (d, *J* = 7.8 Hz, 1H), 7.53 (s, 1H), 7.49 (d, *J* = 7.6 Hz, 1H), 7.35 (td, *J* = 8.1, 7.4, 2.3 Hz, 1H), 7.29 – 7.24 (m, 2H), 7.16 (d, *J* = 7.8 Hz, 1H), 5.05 (d, *J* = 6.2 Hz, 1H), 4.98 (s, 1H), 4.93 (s, 1H), 3.79 (d, *J* = 6.3 Hz, 1H), 2.41 (s, 3H), 1.29 (s, 3H); **¹³C NMR** (176 MHz, CDCl₃): δ 144.0, 137.5, 136.2, 135.7, 134.0, 133.2, 129.5, 129.1, 127.98, 127.95, 124.8,

124.4, 123.8, 115.9, 69.5, 53.5, 21.6, 21.1; **IR** (cm⁻¹): 3433, 3032, 2918, 1638, 1447, 1375, 1188, 1140, 1124, 942, 897, 816, 738, 720; **HRMS**: *m/z* calculated for C₁₈H₁₈ONa⁺ [M+Na]⁺: 273.1250; found: 273.1245.



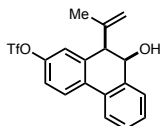
6-(Prop-1-en-2-yl)-5,6-dihydrophenanthro[2,3-d][1,3]dioxol-5-ol (1.47): Prepared according to GP-1.3 with aryl aldehyde **1.70** (56 mg, 0.20 mmol, 1.0 equiv.) with a total reaction time of 20 min. Purification by flash column chromatography (10% EtOAc/hexanes) afforded the pure title compound as a white solid (52 mg, 93%).

¹H NMR (700 MHz, CDCl₃): δ 7.59 (d, *J* = 7.3 Hz, 1H), 7.55 (d, *J* = 7.5 Hz, 1H), 7.33 (t, *J* = 7.1 Hz, 1H), 7.30 (t, *J* = 6.9 Hz, 1H), 7.28 (s, 1H), 6.73 (s, 1H), 5.98 (d, *J* = 10.2 Hz, 2H), 5.04 (t, *J* = 7.3 Hz, 1H), 4.96 (s, 1H), 4.92 (s, 1H), 3.68 (d, *J* = 6.4 Hz, 1H), 2.04 (d, *J* = 9.2 Hz, 1H), 1.25 (s, 3H); **¹³C NMR** (176 MHz, CDCl₃): δ 147.8, 147.5, 143.8, 137.8, 133.8, 130.3, 127.94, 127.86, 127.7, 124.6, 123.1, 116.1, 109.4, 104.2, 101.3, 69.6, 53.5, 20.8; **IR** (cm⁻¹): 3310, 3908, 1638, 1485, 1452, 1257, 1240, 1086, 1039, 938, 736, 619; **HRMS**: *m/z* calculated for C₁₈H₁₆O₃Na⁺ [M+Na]⁺: 303.0992; found: 303.0997.



9-Hydroxy-10-(prop-1-en-2-yl)-9,10-dihydrophenanthren-2-yl 4-methylbenzenesulfonate (1.48): Prepared according to GP-1.3 with aryl aldehyde **S1.48** (81 mg, 0.20 mmol, 1.0 equiv.) with a total reaction time of 20 min. Purification by flash column chromatography (20% EtOAc/hexanes) afforded the pure title compound as a white foam (74 mg, 91%).

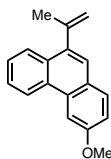
¹H NMR (700 MHz, CDCl₃): δ 7.74 – 7.70 (m, 3H), 7.65 – 7.62 (m, 1H), 7.60 – 7.57 (m, 1H), 7.37 – 7.33 (m, 2H), 7.30 (d, *J* = 8.1 Hz, 2H), 7.02 (dd, *J* = 8.5, 2.4 Hz, 1H), 6.80 (d, *J* = 2.4 Hz, 1H), 5.00 (d, *J* = 6.1 Hz, 1H), 4.90 (s, 1H), 4.86 (s, 1H), 3.65 (d, *J* = 6.1 Hz, 1H), 2.44 (s, 3H), 1.94 (b, 1H), 1.23 (s, 3H); **¹³C NMR** (176 MHz, CDCl₃): δ 149.1, 145.5, 142.9, 138.1, 137.7, 132.8, 132.4, 132.1, 129.9, 128.8, 128.7, 128.2, 125.2, 125.1, 123.8, 123.2, 122.0, 116.4, 69.2, 52.9, 21.9, 21.1; **IR** (cm⁻¹): 3532, 3067, 2919, 1733, 1597, 1479, 1451, 1370, 1187, 1175, 1141, 1091, 941, 835, 813, 696, 658; **HRMS**: *m/z* calculated for C₂₄H₂₂O₄SNa⁺ [M+Na]⁺: 429.1131; found: 429.1127.



9-Hydroxy-10-(prop-1-en-2-yl)-9,10-dihydrophenanthren-2-yl trifluoromethanesulfonate (1.53): Prepared according to GP-1.3 with aryl aldehyde **S1.53** (77 mg, 0.20 mmol, 1.0 equiv.) with a total reaction time of 20 min. Purification by flash column chromatography (5–10% EtOAc/hexanes) afforded the pure title compound as a white foam (72 mg, 94%).

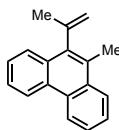
¹H NMR (500 MHz, CDCl₃): δ (d, *J* = 8.7 Hz, 1H), 7.71 – 7.67 (m, 1H), 7.64 – 7.60 (m, 1H), 7.43 – 7.37 (m, 2H), 7.27 (dd, *J* = 8.4, 2.7 Hz, 1H), 7.20 (d, *J* = 2.5 Hz, 1H), 5.08 – 5.03 (m, 1H), 5.01 (d, *J* = 3.3 Hz, 2H), 3.80 (d, *J* = 5.9 Hz, 1H), 2.06 (d, *J* = 8.6 Hz, 1H), 1.37 (s, 3H); **¹³C NMR** (126 MHz, CDCl₃): δ 148.94, 142.61, 138.66, 138.18, 134.28, 131.66, 129.28, 128.44, 125.68, 125.47, 124.00, 122.1, 120.7, 118.9 (q, *J* = 320.9 Hz), 117.0, 69.19, 53.01, 21.24; **IR** (cm⁻¹): 3430, 2920, 1480, 1423, 1209, 1139, 1078, 971, 940, 884, 865, 772, 734, 639, 607; **HRMS**: *m/z* calculated for C₁₈H₁₅F₃O₄SNa⁺ [M+Na]⁺: 407.0535; found: 407.0530.

Stoichiometric Carbonyl–Ene Reaction with Me₂AlCl



3-Methoxy-9-(prop-1-en-2-yl)phenanthrene (1.42): A 20-mL glass scintillation vial equipped with a magnetic stir bar was charged with **1.72** (53 mg, 0.20 mmol, 1.0 equiv.), the vial sealed with a rubber septum under a nitrogen atmosphere and toluene (2 mL) was added. After cooling the solution to $-20\text{ }^{\circ}\text{C}$, Me₂AlCl (1 M in hexane; 0.20 mL, 0.22 mmol, 1.0 equiv.) was added dropwise. The resulting mixture was allowed to warm up to rt and stirred for 0.5 h. Then, the reaction mixture was passed through a short silica plug eluting with CH₂Cl₂ (25–50 mL). The filtrate was concentrated and dried *in vacuo*. The yield was determined to be 66% by ¹H NMR analysis from the crude mixture using dimethyl terephthalate as the internal standard.

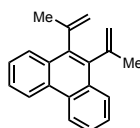
¹H NMR (500 MHz, CDCl₃): δ 8.65 (d, $J = 8.1$ Hz, 1H), 8.08 (d, $J = 8.0$ Hz, 1H), 8.05 (s, 1H), 7.78 (d, $J = 8.7$ Hz, 1H), 7.62 (td, $J = 14.8, 7.0$ Hz, 2H), 7.52 (s, 1H), 7.24 (d, $J = 8.7$ Hz, 1H), 5.43 (s, 1H), 5.14 (s, 1H), 4.03 (s, 3H), 2.25 (s, 3H); **¹³C NMR** (126 MHz, CDCl₃): δ 158.5, 145.3, 138.6, 131.2, 130.7, 130.1, 130.0, 126.7 (2C), 126.5, 126.0, 124.7, 123.1, 117.0, 116.2, 104.0, 55.7, 25.2; **IR** (cm⁻¹): 3059, 2917, 2850, 1642, 1492, 1447, 1423, 1370, 1188, 1144, 1042, 1010, 908, 856, 770, 750, 734, 627; **HRMS**: m/z calculated for C₁₈H₁₆O⁺ [M+H]⁺: 249.1274; found: 249.1270.



9-Methyl-10-(prop-1-en-2-yl)phenanthrene (1.54): A 20-mL glass scintillation vial equipped with a magnetic stir bar was charged with 1-(2'-(2-methylprop-1-en-1-yl)-[1,1'-biphenyl]-2-yl)ethan-1-one³⁰ (50 mg, 0.20 mmol, 1.0 equiv.), the vial sealed with a rubber septum under a

nitrogen atmosphere and toluene (2 mL) was added. After cooling the solution to 0 °C, Me₂AlCl (1 M in hexane; 0.22 mL, 0.22 mmol, 1.1 equiv.) was added, the resulting mixture allowed to warm up to rt and stirred for 0.5 h. Then, the reaction mixture was passed through a short silica plug eluting with CH₂Cl₂ (25–50 mL). The filtrate was concentrated and dried *in vacuo*. The yield was determined to be 81% by ¹H NMR analysis from the crude mixture using dimethyl terephthalate as the internal standard.

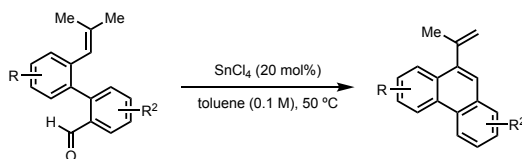
¹H NMR (500 MHz, CDCl₃): δ 8.75 – 8.72 (m, 1H), 8.71 (d, *J* = 8.5 Hz, 1H), 8.15 – 8.11 (m, 1H), 8.02 (d, *J* = 7.7 Hz, 1H), 7.67 – 7.63 (m, 2H), 7.59 (pd, *J* = 6.9, 1.5 Hz, 2H), 5.58 (s, 1H), 5.01 (s, 1H), 2.70 (s, 3H), 2.15 (s, 3H); **¹³C NMR** (126 MHz, CDCl₃): δ 144.6, 138.6, 132.1, 130.6, 129.8, 129.7, 127.7, 126.8, 126.67, 126.65, 126.1, 125.7, 125.0, 122.9, 122.7, 116.9, 25.0, 16.6; **IR** (cm⁻¹): 3073, 2962, 1949, 1804, 1642, 1490, 1423, 1369, 1239, 1048, 1027, 1004, 898, 751, 723, 619; **HRMS**: *m/z* calculated for C₁₈H₁₆⁺ [M]⁺: 232.1252; found: 232.1249.



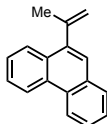
9,10-Di(prop-1-en-2-yl)phenanthrene (1.55): A 20-mL glass scintillation vial equipped with a magnetic stir bar was charged with aryl enone **S1.55** (55 mg, 0.20 mmol, 1.0 equiv.), the vial sealed with a rubber septum under a nitrogen atmosphere and toluene (2 mL) was added. After cooling the solution to 0 °C, Me₂AlCl (1 M in hexane; 0.22 mL, 0.22 mmol, 1.1 equiv.) was added, the resulting mixture allowed to warm up to rt and stirred for 0.5 h. Then, the reaction mixture was passed through a short silica plug eluting with CH₂Cl₂ (25–50 mL). The filtrate was concentrated and *in vacuo*. Purification by flash column chromatography (100% hexanes) afforded the pure title compound as a white solid as mixture of rotamers (A/B = 3.3:1) (26 mg, 51%).

¹H NMR (700 MHz, CDCl₃): δ 8.72 (d, *J* = 8.2 Hz, 8.6H, A+B), 8.08 (d, *J* = 8.1 Hz, 2H, B), 8.03 (d, *J* = 8.1 Hz, 6.6H, A), 7.64 (td, *J* = 8.1, 6.9, 1.2 Hz, 8.6H, A+B), 7.60 (td, *J* = 7.5, 6.9, 1.3 Hz, 8.6H, A+B), 5.57 (s, 2H, B), 5.47 (s, 6.6H, A), 5.02 (s, 2H, B), 5.00 (s, 6.6H, A), 2.20 (s, 19.8H, A), 2.15 (s, 6H, B); **¹³C NMR** (176 MHz, CDCl₃): δ 144.5 (A), 142.9 (B), 136.9 (A), 136.7 (B), 130.5 (A), 130.4 (B), 130.0 (B), 129.9 (A), 127.3 (B), 126.78 (A), 126.75 (A), 126.7 (B), 126.2 (2C, A+B), 122.7 (2C, A+B), 119.0 (B), 116.3 (A), 26.0 (A), 24.8 (B); **IR** (cm⁻¹): 3070, 2967, 2942, 1639, 1488, 1442, 1370, 1239, 1198, 1048, 1002, 915, 906, 863, 765, 629; **HRMS**: *m/z* calculated for C₂₀H₁₈H⁺ [M+H]⁺: 259.1481; found: 259.1478.

General Procedure for Carbonyl–Ene Reaction with SnCl₄ (GP-1.4)

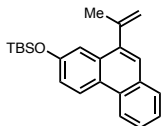


A 20-mL glass scintillation vial equipped with a magnetic stir bar was charged with aryl aldehyde (0.20 mmol, 1.0 equiv.). The vial was sealed with a rubber septum under a nitrogen atmosphere and toluene (2 mL) was added. After heating the solution to 50 °C, a freshly prepared SnCl₄ solution (1 M in toluene; 10 μL, 1.0×10⁻² mmol, 20–30 mol%) was added and the resulting mixture stirred for the indicated time at 50 °C. Upon completion (as determined by TLC analysis) the reaction mixture was allowed to cool down to rt and passed through a short silica plug eluting with CH₂Cl₂ (25–50 mL). The filtrate was concentrated and dried *in vacuo* and the yield determined by quantitative ¹H NMR analysis from the crude mixture or after purification by flash column chromatography.



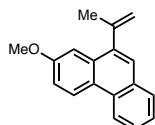
9-(Prop-1-en-2-yl)phenanthrene (1.34): Prepared according to GP-1.4 with aryl aldehyde **1.31** (47 mg, 0.20 mmol, 1.0 equiv.) with a total reaction time of 0.5 h. Purification by flash column chromatography (100% hexanes) afforded the pure title compound as a white solid (43 mg, 99%). Spectroscopic data are consistent with those reported in the literature.³⁰

¹H NMR (500 MHz, CDCl₃): δ 8.76 (d, *J* = 8.1 Hz, 1H), 8.70 (d, *J* = 8.0 Hz, 1H), 8.14 (d, *J* = 8.0 Hz, 1H), 7.89 (d, *J* = 7.6 Hz, 1H), 7.72 – 7.59 (m, 5H), 5.49 (s, 1H), 5.20 (s, 1H), 2.30 (s, 3H).



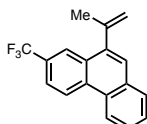
Tert-butyldimethyl((10-(prop-1-en-2-yl)phenanthren-2-yl)oxy)silane (1.37): Prepared according to GP-1.4 with aryl aldehyde **S1.35** (73 mg, 0.20 mmol, 1.0 equiv.) with a total reaction time of 0.5 h. The yield was determined to be 99% by quantitative ¹H NMR analysis using dimethyl terephthalate as the internal standard.

¹H NMR (700 MHz, CDCl₃): δ 8.59 (d, *J* = 8.9 Hz, 1H), 8.56 (d, *J* = 8.3 Hz, 1H), 7.81 (d, *J* = 7.8 Hz, 1H), 7.59 (td, *J* = 8.1, 7.0, 1.3 Hz, 1H), 7.53 (s, 1H), 7.51 (t, *J* = 7.4 Hz, 1H), 7.46 (d, *J* = 2.5 Hz, 1H), 7.21 (dd, *J* = 8.9, 2.5 Hz, 1H), 5.43 (s, 1H), 5.12 (s, 1H), 2.23 (s, 3H), 1.03 (s, 9H), 0.27 (s, 6H); **¹³C NMR** (176 MHz, CDCl₃): δ 154.5, 145.1, 140.3, 131.9, 130.9, 130.0, 128.6, 126.5, 125.9, 125.41, 125.39, 124.5, 122.2, 121.0, 116.1, 115.3, 25.9, 25.0, 18.5, -4.2; **IR** (cm⁻¹): 2955, 2928, 2856, 1611, 1528, 1483, 1462, 1390, 1265, 1218, 1167, 1104, 961, 862, 832, 777, 745, 678; **HRMS**: *m/z* calculated for C₂₃H₂₈OSiH⁺ [M+H]⁺: 349.1982; found: 349.1974.



2-Methoxy-10-(prop-1-en-2-yl)phenanthrene (1.38): Prepared according to GP-1.4 with aryl aldehyde **1.68** (52 mg, 0.20 mmol, 1.0 equiv.) with a total reaction time of 0.5 h. The yield was determined to be 86% by quantitative ^1H NMR analysis using dimethyl terephthalate as the internal standard.

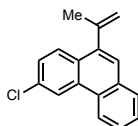
^1H NMR (700 MHz, CDCl_3): δ 8.63 (d, $J = 9.0$ Hz, 1H), 8.57 (d, $J = 8.3$ Hz, 1H), 7.83 (d, $J = 7.8$ Hz, 1H), 7.60 (td, $J = 8.1, 7.1, 1.3$ Hz, 1H), 7.56 (s, 1H), 7.52 (td, $J = 7.7, 6.9, 0.8$ Hz, 1H), 7.47 (d, $J = 2.6$ Hz, 1H), 7.29 (dd, $J = 9.0, 2.7$ Hz, 1H), 5.44 (s, 1H), 5.17 (s, 1H), 3.96 (s, 3H), 2.25 (s, 3H); ^{13}C NMR (176 MHz, CDCl_3): δ 158.3, 145.2, 140.4, 131.8, 130.8, 130.1, 128.6, 126.6, 125.9, 125.7, 125.0, 124.7, 122.1, 116.5, 116.2, 107.4, 55.5, 24.9; IR (cm^{-1}): 2930, 2837, 1614, 1531, 1451, 1434, 1361, 1276, 1221, 1106, 856, 898, 747, 710; HRMS: m/z calculated for $\text{C}_{18}\text{H}_{16}\text{O}^+$ $[\text{M}+\text{H}]^+$: 249.1274; found: 249.1268.



10-(Prop-1-en-2-yl)-2-(trifluoromethyl)phenanthrene (1.39): Prepared according to GP-1.4 with aryl aldehyde **1.69** (61 mg, 0.20 mmol, 1.0 equiv.) with a total reaction time of 0.5 h. The yield was determined to be 88% by quantitative ^1H NMR analysis using dimethyl terephthalate as the internal standard.

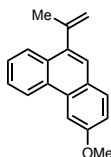
^1H NMR (700 MHz, CDCl_3): δ 8.82 (d, $J = 8.6$ Hz, 1H), 8.68 (d, $J = 7.9$ Hz, 1H), 8.37 (s, 1H), 7.90 (d, $J = 7.5$ Hz, 1H), 7.85 (d, $J = 8.6$ Hz, 1H), 7.70 – 7.64 (m, 3H), 5.51 (s, 1H), 5.17 (s, 1H), 2.26 (s, 3H); ^{13}C NMR (176 MHz, CDCl_3): δ 144.1, 140.8, 132.8, 132.5, 129.9, 129.2, 128.8, 128.4 (q, $J = 32.3$ Hz), 128.0, 127.0, 126.4, 124.7 (q, $J = 271.8$ Hz), 123.98, 123.95, 123.0, 122.4

(q, $J = 3.4$ Hz), 117.33, 25.21; **IR** (cm^{-1}): 3081, 2917, 1626, 1418, 1372, 1323, 1238, 1124, 1081, 1015, 912, 871, 786, 749, 693, 640; **HRMS**: m/z calculated for $\text{C}_{18}\text{H}_{13}\text{F}_3^+$ $[\text{M}]^+$: 286.0969; found: 289.0959.



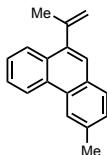
3-Chloro-10-(prop-1-en-2-yl)phenanthrene (1.43): Prepared according to GP-1.4 with aryl aldehyde **1.67** (54 mg, 0.20 mmol, 1.0 equiv.) with a total reaction time of 1 h. The yield was determined to be 85% by quantitative ^1H NMR analysis using dimethyl terephthalate as the internal standard.

^1H NMR (700 MHz, CDCl_3): δ 8.67 (s, 1H), 8.58 (d, $J = 8.0$ Hz, 1H), 8.02 (d, $J = 8.7$ Hz, 1H), 7.86 (d, $J = 7.6$ Hz, 1H), 7.63 (dt, $J = 19.7, 7.0$ Hz, 2H), 7.56 (s, 1H), 7.54 (d, $J = 8.7$ Hz, 1H), 5.45 (s, 1H), 5.13 (s, 1H), 2.23 (s, 3H); **^{13}C NMR** (176 MHz, CDCl_3): δ 144.6, 140.5, 132.7, 132.2, 132.0, 129.0, 128.8, 128.7, 128.2, 127.5, 127.1, 126.8, 125.3, 122.73, 122.69, 116.7, 25.2; **IR** (cm^{-1}): 3075, 2972, 1592, 1515, 1488, 1424, 1368, 1268, 1109, 1091, 1008, 887, 823, 818, 746, 642; **HRMS**: m/z calculated for $\text{C}_{17}\text{H}_{13}\text{ClH}^+$ $[\text{M}+\text{H}]^+$: 253.0779; found: 253.0776.



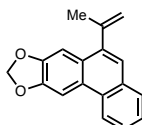
3-Methoxy-9-(prop-1-en-2-yl)phenanthrene (1.42): Prepared according to GP-1.4 with aryl aldehyde **1.72** (53 mg, 0.20 mmol, 1.0 equiv.) with a total reaction time of 0.5 h. The yield was determined to be 80% by quantitative ^1H NMR analysis using dimethyl terephthalate as the internal standard.

¹H NMR (500 MHz, CDCl₃): δ 8.65 (d, *J* = 8.1 Hz, 1H), 8.08 (d, *J* = 8.0 Hz, 1H), 8.05 (s, 1H), 7.78 (d, *J* = 8.7 Hz, 1H), 7.62 (td, *J* = 14.8, 7.0 Hz, 2H), 7.52 (s, 1H), 7.24 (d, *J* = 8.7 Hz, 1H), 5.43 (s, 1H), 5.14 (s, 1H), 4.03 (s, 3H), 2.25 (s, 3H); **¹³C NMR** (126 MHz, CDCl₃): δ 158.5, 145.3, 138.6, 131.2, 130.7, 130.1, 130.0, 126.7 (2C), 126.5, 126.0, 124.7, 123.1, 117.0, 116.2, 104.0, 55.7, 25.2; **IR** (cm⁻¹): 3059, 2917, 2850, 1642, 1492, 1447, 1423, 1370, 1188, 1144, 1042, 1010, 908, 856, 770, 750, 734, 627; **HRMS**: *m/z* calculated for C₁₈H₁₆OH⁺ [M+H]⁺: 249.1274; found: 249.1270.



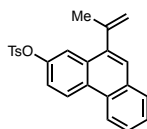
3-Methyl-9-(prop-1-en-2-yl)phenanthrene (1.44): Prepared according to GP-1.4 with aryl aldehyde **1.71** (50 mg, 0.20 mmol, 1.0 equiv.) with a total reaction time of 0.5 h. The yield was determined to be 96% by quantitative ¹H NMR analysis using dimethyl terephthalate as the internal standard.

¹H NMR (500 MHz, CDCl₃): δ 8.72 (d, *J* = 8.2 Hz, 1H), 8.46 (s, 1H), 8.07 (d, *J* = 8.0 Hz, 1H), 7.75 (d, *J* = 8.0 Hz, 1H), 7.64 (td, *J* = 8.0, 6.9, 1.0 Hz, 1H), 7.59 (td, *J* = 7.6, 6.9, 1.4 Hz, 1H), 7.54 (s, 1H), 7.42 (d, *J* = 8.1 Hz, 1H), 5.43 (s, 1H), 5.14 (s, 1H), 2.63 (s, 3H), 2.25 (s, 3H); **¹³C NMR** (126 MHz, CDCl₃): δ 145.31, 140.0, 136.1, 130.5, 130.4, 130.0, 129.7, 128.6, 128.4, 126.6, 126.4, 126.2, 124.9, 123.0, 122.4, 116.1, 25.2, 22.3; **IR** (cm⁻¹): 3076, 2917, 1914, 1602, 1502, 1444, 1370, 1257, 1184, 1162, 1045, 1014, 889, 804, 764, 724, 643; **HRMS**: *m/z* calculated for C₁₈H₁₆H⁺ [M+H]⁺: 233.1325; found: 233.1329.



6-(Prop-1-en-2-yl)phenanthro[2,3-*d*][1,3]dioxole (1.45): Prepared according to GP-1.4 with aryl aldehyde **1.70** (56 mg, 0.20 mmol, 1.0 equiv.) with a total reaction time of 0.5 h. The yield was determined to be 99% by quantitative ^1H NMR analysis using dimethyl terephthalate as the internal standard.

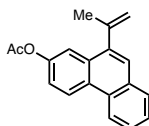
^1H NMR (500 MHz, CDCl_3): δ 8.45 (d, $J = 8.3$ Hz, 1H), 8.06 (s, 1H), 7.82 (d, $J = 7.8$ Hz, 1H), 7.57 (t, $J = 7.5$ Hz, 1H), 7.52 (t, $J = 7.4$ Hz, 1H), 7.48 (s, 1H), 7.45 (s, 1H), 6.11 (s, 2H), 5.42 (s, 1H), 5.12 (s, 1H), 2.22 (s, 3H); ^{13}C NMR (126 MHz, CDCl_3): δ 147.9, 147.7, 145.4, 140.6, 131.2, 129.7, 128.6, 127.0, 126.8, 126.2, 126.0, 123.6, 122.4, 116.3, 104.2, 101.5, 101.2, 25.1; IR (cm^{-1}): 2916, 1633, 1498, 1466, 1378, 1259, 1340, 1208, 1120, 1040, 936, 882, 853, 826, 741, 617; HRMS: m/z calculated for $\text{C}_{18}\text{H}_{14}\text{O}_2\text{H}^+$ $[\text{M}+\text{H}]^+$: 263.1067; found: 263.1061.



10-(Prop-1-en-2-yl)phenanthren-2-yl 4-methylbenzenesulfonate (1.49): Prepared according to GP-1.4 with aryl aldehyde **S1.48** (82 mg, 0.20 mmol, 1.0 equiv.) with a total reaction time of 0.5 h. The yield was determined to be 95% by quantitative ^1H NMR analysis using dimethyl terephthalate as the internal standard.

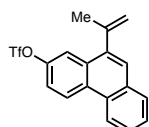
^1H NMR (700 MHz, CDCl_3): δ 8.65 (d, $J = 9.0$ Hz, 1H), 8.57 (d, $J = 8.2$ Hz, 1H), 7.84 (d, $J = 7.7$ Hz, 1H), 7.71 (d, $J = 8.2$ Hz, 2H), 7.63 (t, $J = 7.1$ Hz, 1H), 7.60 (t, $J = 7.2$ Hz, 1H), 7.56 (s, 1H), 7.50 (d, $J = 2.4$ Hz, 1H), 7.38 (dd, $J = 9.0, 2.5$ Hz, 1H), 7.28 (d, $J = 8.1$ Hz, 2H), 5.32 (s, 1H), 4.93 (s, 1H), 2.43 (s, 3H), 2.04 (s, 3H); ^{13}C NMR (176 MHz, CDCl_3): δ 148.1, 145.5, 144.0, 140.2, 132.3, 131.7, 131.1, 129.9, 129.4, 129.3, 128.8, 128.7, 127.3, 127.0, 126.2, 124.9, 122.7, 121.3,

119.3, 116.8, 24.8, 21.8; **IR** (cm^{-1}): 2920, 1597, 1527, 1486, 1449, 1371, 1251, 1176, 1092, 1019, 937, 897, 830, 776, 735, 703, 670, 652; **HRMS**: m/z calculated for $\text{C}_{24}\text{H}_{20}\text{O}_3\text{SH}^+$ $[\text{M}+\text{H}]^+$: 389.1206; found: 389.1201.



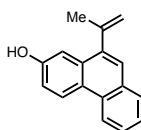
10-(Prop-1-en-2-yl)phenanthren-2-yl acetate (1.51): Prepared according to GP-1.4 with aryl aldehyde **S1.51** (59 mg, 0.20 mmol, 1.0 equiv.) with a total reaction time of 0.5 h. The yield was determined to be 96% by quantitative ^1H NMR analysis using dimethyl terephthalate as the internal standard.

^1H NMR (700 MHz, CDCl_3): δ 8.73 (d, $J = 8.9$ Hz, 1H), 8.62 (d, $J = 8.2$ Hz, 1H), 7.85 (d, $J = 7.7$ Hz, 1H), 7.78 (d, $J = 2.4$ Hz, 1H), 7.63 (t, $J = 7.5$ Hz, 1H), 7.60 (s, 1H), 7.59 (t, $J = 7.2$ Hz, 1H), 7.42 (dd, $J = 8.9, 2.4$ Hz, 1H), 5.45 (s, 1H), 5.15 (s, 1H), 2.38 (s, 3H), 2.23 (s, 3H); ^{13}C NMR (176 MHz, CDCl_3): δ 169.8, 149.2, 144.6, 140.4, 131.6, 131.4, 129.7, 128.7, 128.6, 126.9, 126.8, 125.9, 124.5, 122.6, 120.8, 118.1, 116.7, 25.1, 21.4; **IR** (cm^{-1}): 3075, 2962, 1742, 1617, 1488, 1452, 1371, 1223, 1193, 1153, 1020, 946, 888, 825, 749, 666; **HRMS**: m/z calculated for $\text{C}_{19}\text{H}_{16}\text{O}_2\text{H}^+$ $[\text{M}+\text{H}]^+$: 277.1223; found: 277.1223.



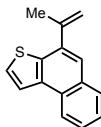
10-(Prop-1-en-2-yl)phenanthren-2-yl trifluoromethanesulfonate (1.50): Prepared according to GP-1.4 with aryl aldehyde **S1.53** (77 mg, 0.20 mmol, 1.0 equiv.) with a total reaction time of 1 h. The yield was determined to be 97% by quantitative ^1H NMR analysis using dimethyl terephthalate as the internal standard.

¹H NMR (500 MHz, CDCl₃): δ 8.78 (d, *J* = 9.1 Hz, 1H), 8.62 (d, *J* = 8.1 Hz, 1H), 7.99 (d, *J* = 2.5 Hz, 1H), 7.89 (d, *J* = 7.6 Hz, 1H), 7.72 – 7.62 (m, 3H), 7.55 (dd, *J* = 9.1, 2.6 Hz, 1H), 5.51 (s, 1H), 5.17 (s, 1H), 2.24 (s, 3H); **¹³C NMR** (126 MHz, CDCl₃): δ 148.1, 143.8, 140.2, 132.0, 131.5, 130.3, 129.2, 128.9, 127.7, 127.3, 127.0, 125.6, 122.8, 119.5, 119.0 (d, *J* = 320.9 Hz), 118.5, 117.5, 25.0; **IR** (cm⁻¹): 2921, 1488, 1416, 1374, 1250, 1236, 1196, 1140, 1126, 1017, 935, 901, 829, 743, 665; **HRMS**: *m/z* calculated for C₁₈H₁₃F₃O₃SH⁺ [M+H]⁺: 367.0610; found: 367.0605.



10-(Prop-1-en-2-yl)phenanthren-2-ol (1.52): Prepared according to GP-1.4 with aryl aldehyde **S1.52** (51 mg, 0.20 mmol, 1.0 equiv.) with a total reaction time of 1 h. The yield was determined to be 74% by quantitative ¹H NMR analysis using dimethyl terephthalate as the internal standard.

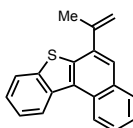
¹H NMR (700 MHz, CDCl₃): δ 8.62 (d, *J* = 8.9 Hz, 1H), 8.55 (d, *J* = 8.3 Hz, 1H), 7.82 (d, *J* = 7.8 Hz, 1H), 7.60 (t, *J* = 7.6 Hz, 1H), 7.55 (s, 1H), 7.52 (t, *J* = 7.4 Hz, 1H), 7.44 (d, *J* = 2.5 Hz, 1H), 7.22 (dd, *J* = 8.9, 2.6 Hz, 1H), 5.42 (s, 1H), 5.13 (s, 1H), 5.06 (s, 1H), 2.23 (s, 3H); **¹³C NMR** (176 MHz, CDCl₃): δ 154.2, 145.0, 140.0, 132.0, 130.7, 130.0, 128.6, 126.6, 126.0, 125.8, 125.1, 125.0, 122.1, 116.4, 116.3, 110.2, 25.0; **IR** (cm⁻¹): 3304, 3077, 2917, 1614, 1531, 1263, 1215, 1164, 1037, 1019, 939, 895, 822, 777, 735, 672; **HRMS**: *m/z* calculated for C₁₇H₁₄OH⁺ [M+H]⁺: 235.1117; found: 235.1113.



4-(Prop-1-en-2-yl)naphtho[2,1-*b*]thiophene (1.56): Prepared according to GP-1.4 with aryl aldehyde **S1.56** (49 mg, 0.20 mmol, 1.0 equiv.) with a total reaction time of 0.5 h. The yield was

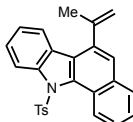
determined to be 59% by quantitative ^1H NMR analysis using dimethyl terephthalate as the internal standard.

^1H NMR (500 MHz, CDCl_3): δ 8.32 (d, $J = 8.1$ Hz, 1H), 8.03 (d, $J = 5.4$ Hz, 1H), 7.93 (d, $J = 8.0$ Hz, 1H), 7.66 (s, 1H), 7.62 (d, $J = 5.4$ Hz, 1H), 7.58 (t, $J = 7.6$ Hz, 1H), 7.52 (t, $J = 7.4$ Hz, 1H), 5.65 (s, 1H), 5.47 (s, 1H), 2.35 (s, 3H); ^{13}C NMR (126 MHz, CDCl_3): δ 143.9, 136.6 (2C), 136.0, 131.6, 128.74, 128.67, 126.4, 126.3, 125.7, 123.6, 122.7, 122.4, 116.0, 23.7; IR (cm^{-1}): 3058, 2970, 2919, 1626, 1498, 1447, 1374, 1284, 1208, 1181, 1162, 1140, 1092, 902, 883, 849, 749, 715; HRMS: m/z calculated for $\text{C}_{15}\text{H}_{12}\text{H}^+$ $[\text{M}+\text{H}]^+$: 225.0732; found: 225.0734.



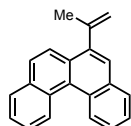
6-(Prop-1-en-2-yl)benzo[*b*]naphtho[1,2-*d*]thiophene (1.57): Prepared according to GP-1.4 with aryl aldehyde **S1.57** (59 mg, 0.20 mmol, 1.0 equiv.) and 30 mol% SnCl_4 solution (60 μL , 0.06 mmol, 0.3 equiv.) with a total reaction time of 0.5 h. The yield was determined to be 64% by quantitative ^1H NMR analysis using dimethyl terephthalate as the internal standard.

^1H NMR (700 MHz, CDCl_3): δ 9.03 (d, $J = 8.5$ Hz, 1H), 8.89 (d, $J = 8.2$ Hz, 1H), 8.02 (d, $J = 7.9$ Hz, 2H), 7.79 (s, 1H), 7.72 (t, $J = 7.1$ Hz, 1H), 7.60 (dt, $J = 14.4, 7.6$ Hz, 2H), 7.51 (t, $J = 7.4$ Hz, 1H), 5.61 (s, 1H), 5.53 (s, 1H), 2.38 (s, 3H); ^{13}C NMR (176 MHz, CDCl_3): δ 144.1, 140.0, 138.3, 137.1, 136.5, 132.3, 129.9, 129.7, 129.5, 127.0, 125.33, 125.32, 125.2, 124.82, 124.79, 123.2, 123.1, 116.5, 23.9; IR (cm^{-1}): 3055, 2970, 1630, 1497, 1462, 1443, 1344, 1213, 1167, 1072, 1025, 904, 885, 785, 746, 723, 626; HRMS: m/z calculated for $\text{C}_{19}\text{H}_{14}\text{SH}^+$ $[\text{M}+\text{H}]^+$: 275.0889; found: 275.0890.



6-(Prop-1-en-2-yl)-11-tosyl-11H-benzo[a]carbazole (1.58): Prepared according to GP-1.4 with aryl aldehyde **S1.58** (86 mg, 0.20 mmol, 1.0 equiv.) with a total reaction time of 20 min. Purification by flash column chromatography (5-10% EtOAc/hexanes) afforded the title compound as a white solid (74 mg, 90%).

¹H NMR (500 MHz, CDCl₃): δ 8.89 (d, *J* = 8.5 Hz, 1H), 8.31 (d, *J* = 8.2 Hz, 1H), 7.89 (d, *J* = 8.1 Hz, 1H), 7.76 (d, *J* = 7.8 Hz, 1H), 7.64 (t, *J* = 7.6 Hz, 1H), 7.59 – 7.53 (m, 2H), 7.42 (t, *J* = 7.7 Hz, 1H), 7.31 – 7.24 (m, 1H), 6.74 – 6.67 (m, 4H), 5.31 (s, 1H), 4.97 (s, 1H), 2.14 (s, 3H), 1.99 (s, 3H); **¹³C NMR** (126 MHz, CDCl₃): δ 144.3, 144.2, 142.4, 137.8, 136.6, 133.4, 130.6, 130.5, 128.2, 127.8, 127.20, 127.19, 126.41, 126.37, 126.0, 125.9, 125.8 (2C), 125.6, 121.8, 120.4, 116.0, 24.2, 21.5; **IR** (cm⁻¹): 2917, 1597, 1448, 1365, 1173, 1054, 1026, 936, 911, 886, 872, 791, 757, 661; **HRMS**: *m/z* calculated for C₂₆H₂₁NO₂SH⁺ [M+H]⁺: 412.1366; found: 412.1358.



6-(Prop-1-en-2-yl)benzo[c]phenanthrene (1.59): Prepared according to GP-1.4 with aryl aldehyde **1.73** (57 mg, 0.20 mmol, 1.0 equiv.) with a total reaction time of 0.5 h. The yield was determined to be 69% by quantitative ¹H NMR analysis using dimethyl terephthalate as the internal standard.

¹H NMR (500 MHz, CDCl₃): δ 9.10 (d, *J* = 8.3 Hz, 1H), 9.06 (d, *J* = 8.1 Hz, 1H), 8.05 – 8.00 (m, 2H), 7.99 (d, *J* = 7.6 Hz, 1H), 7.89 (d, *J* = 8.8 Hz, 1H), 7.73 (s, 1H), 7.69 – 7.58 (m, 4H), 5.48 (s, 1H), 5.17 (s, 1H), 2.27 (s, 3H); **¹³C NMR** (126 MHz, CDCl₃): δ 145.4, 140.8, 133.3, 133.1, 130.5, 129.7, 129.0, 128.5, 128.43, 128.37, 128.2, 128.1, 127.1, 126.2, 126.10, 126.07, 125.9, 125.8,

124.4, 116.7, 25.6; **IR** (cm^{-1}): 3048, 2964, 1639, 1518, 1427, 1371, 1230, 1133, 1060, 946, 895, 846, 748, 625; **HRMS**: m/z calculated for $\text{C}_{21}\text{H}_{16}\text{H}^+$ $[\text{M}+\text{H}]^+$: 269.1325; found: 269.1319.

1.7.4. Computational Details

Full list of authors in the Gaussian09 reference

M. J. Frisch, G. W. Trucks, H. B. Schlegel, G. E. Scuseria, M. A. Robb, J. R. Cheeseman, G. Scalmani, V. Barone, B. Mennucci, G. A. Petersson, H. Nakatsuji, M. Caricato, X. Li, H. P. Hratchian, A. F. Izmaylov, J. Bloino, G. Zheng, J. L. Sonnenberg, M. Hada, M. Ehara, K. Toyota, R. Fukuda, J. Hasegawa, M. Ishida, T. Nakajima, Y. Honda, O. Kitao, H. Nakai, T. Vreven, J. A. Montgomery, Jr., J. E. Peralta, F. Ogliaro, M. Bearpark, J. J. Heyd, E. Brothers, K. N. Kudin, V. N. Staroverov, T. Keith, R. Kobayashi, J. Normand, K. Raghavachari, A. Rendell, J. C. Burant, S. S. Iyengar, J. Tomasi, M. Cossi, N. Rega, J. M. Millam, M. Klene, J. E. Knox, J. B. Cross, V. Bakken, C. Adamo, J. Jaramillo, R. Gomperts, R. E. Stratmann, O. Yazyev, A. J. Austin, R. Cammi, C. Pomelli, J. W. Ochterski, R. L. Martin, K. Morokuma, V. G. Zakrzewski, G. A. Voth, P. Salvador, J. J. Dannenberg, S. Dapprich, A. D. Daniels, O. Farkas, J. B. Foresman, J. V. Ortiz, J. Cioslowski, and D. J. Fox, Gaussian, Inc., Wallingford CT, 2013.

Catalyst-substrate structures were optimized in the gas-phase with the M06 density functional,⁸² and the triple- ζ valence quality def2-TZVP basis set of Weigend and Ahlrichs,⁸³ as implemented in Gaussian 09 (revision D.01).⁸⁴ All of the optimized geometries were verified by frequency computations as minima (zero imaginary frequencies). Parameters were acquired from these ground state structures. NBO charges were calculated using NBO6,⁸⁵ at the same level. Sterimol values were calculated using a modified version of Paton's Python script.⁸⁶ Multidimensional regression analyses were performed using MATLAB[®].⁸⁷

Transition states were located with the B97-D density functional,⁸⁸ and the double- ζ , polarized basis set, 6-31G* as implemented in Gaussian 09 (revision D.01).⁸⁹ Free energies in solution were derived from structures optimized in the gas phase by means of a single point calculation at the B97-D/6-31G(d) level of theory and the CPCM implicit solvent model

(dichloroethane).⁹⁰ Cartesian coordinates of all stationary point structures utilized herein can be obtained free of charge from <https://pubs.acs.org/doi/10.1021/acscatal.0c00489>.

Parameters Collected

The parameters calculated and considered for the systems are reported in Tables 1.3–1.11. Sterimol parameters L, B1 and B5, respectively, represent the length, minimum and maximum widths of the considered substituent and are calculated using the Bondi radii.^{91,92} IR stretching frequencies, intensities, NBO charges have been found to be useful descriptors of electronic and steric properties, hence these have been calculated.⁶² The following substrates have been used for parameter collection: **1.31** (SubA); **1.67** (SubB); **1.68** (SubC); **1.69** (SubD); **1.71** (SubE); **1.70** (SubF); **1.72** (SubG).

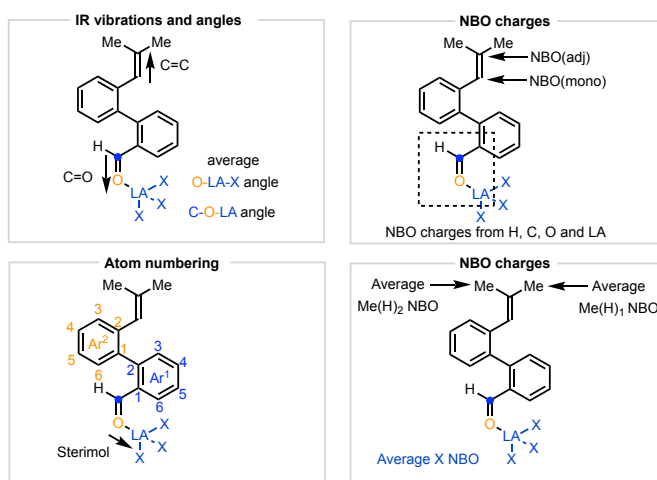


Figure 1.13: Overview of collected parameters for the statistical analysis.

Table 1.3: Collected carbonyl vibration parameters.

Reaction	$\nu\text{C=O}$	iC=O	$\nu\text{C=C}$	iC=C
AlCl ₃ /SubA	1681.96	457.0976	1715.84	104.9521
ScCl ₃ /SubA	1683.36	537.9386	1717.24	110.1830
FeCl ₃ /SubA	1687.77	508.8963	1719.22	103.1393
AlMe ₂ Cl/SubA	1701.83	398.3102	1722.62	88.1080
AlEtCl ₂ /SubA	1691.29	449.4920	1715.94	129.3676
AlEt ₂ Cl/SubA	1700.97	388.9121	1720.46	69.5907
AlCl ₃ /SubB	1684.67	579.3010	1725.88	48.3762
ScCl ₃ /SubB	1719.99	504.6393	1718.51	285.7938
FeCl ₃ /SubB	1717.13	666.4732	1721.80	38.1829
AlMe ₂ Cl/SubB	1698.39	482.8228	1731.53	47.8177
AlEtCl ₂ /SubB	1721.03	544.6320	1727.97	100.5127
AlCl ₃ /SubC	1703.31	627.2359	1721.69	58.7228
ScCl ₃ /SubC	1717.70	820.7021	1733.33	51.5321
FeCl ₃ /SubC	1682.20	555.5332	1726.00	32.3757
AlMe ₂ Cl/SubC	1736.18	563.9618	1723.23	20.1851
AlEtCl ₂ /SubC	1716.32	569.7800	1722.49	101.8149
AlCl ₃ /SubD	1686.54	549.3741	1722.52	56.5875
ScCl ₃ /SubD	1720.21	706.1832	1722.94	96.3907
FeCl ₃ /SubD	1717.75	661.8064	1724.86	54.6612
AlMe ₂ Cl/SubD	1701.00	462.2865	1733.98	48.3201
AlEtCl ₂ /SubD	1719.71	456.4744	1724.29	184.9137
AlCl ₃ /SubE	1706.77	623.5470	1726.37	57.3256
ScCl ₃ /SubE	1704.87	680.7312	1725.61	58.4823
FeCl ₃ /SubE	1710.34	643.7958	1727.90	57.5678
AlMe ₂ Cl/SubE	1729.41	459.2451	1731.66	171.8927
AlEtCl ₂ /SubE	1683.18	399.1027	1730.68	39.8689
AlCl ₃ /SubF	1707.46	629.0949	1724.89	31.6066
ScCl ₃ /SubF	1722.72	692.9357	1719.13	147.1537
FeCl ₃ /SubF	1714.40	657.7707	1728.31	45.1628
AlMe ₂ Cl/SubF	1723.58	417.5163	1726.93	115.8390
AlEtCl ₂ /SubF	1720.50	549.3308	1732.61	44.3065
AlCl ₃ /SubG	1700.85	344.2036	1724.11	60.6351
ScCl ₃ /SubG	1702.74	433.8963	1724.31	48.5639
FeCl ₃ /SubG	1701.63	372.3702	1725.76	39.0981
AlMe ₂ Cl/SubG	1719.09	373.1416	1723.53	137.7508
AlEtCl ₂ /SubG	1687.39	335.3090	1736.45	25.4866
AlCl ₃ /SubH	1685.31	638.3559	1733.03	38.2085
ScCl ₃ /SubH	1718.30	460.8191	1720.27	323.0098
FeCl ₃ /SubH	1717.05	491.7560	1720.28	208.7566
AlMe ₂ Cl/SubH	1731.25	329.8320	1728.21	129.7487
AlEtCl ₂ /SubH	1716.99	502.5801	1721.48	128.4073

Table 1.4: Collected carbonyl lengths and angles.

Reaction	LA-O	C=O	COLA
AlCl ₃ /SubA	1.87	1.24	129.9
ScCl ₃ /SubA	2.10	1.24	132.5
FeCl ₃ /SubA	2.02	1.23	128.3
AlMe ₂ Cl/SubA	1.93	1.23	130.5
AlEtCl ₂ /SubA	1.90	1.24	130.4
AlEt ₂ Cl/SubA	1.93	1.23	129.2
AlCl ₃ /SubB	1.87	1.24	128.2
ScCl ₃ /SubB	2.11	1.23	130.3
FeCl ₃ /SubB	2.03	1.23	123.3
AlMe ₂ Cl/SubB	1.94	1.23	129.2
AlEtCl ₂ /SubB	1.92	1.23	122.8
AlCl ₃ /SubC	1.87	1.23	126.8
ScCl ₃ /SubC	2.08	1.23	148.1
FeCl ₃ /SubC	2.02	1.23	126.3
AlMe ₂ Cl/SubC	1.94	1.22	128.0
AlEtCl ₂ /SubC	1.90	1.23	127.4
AlCl ₃ /SubD	1.88	1.24	128.6
ScCl ₃ /SubD	2.10	1.23	132.9
FeCl ₃ /SubD	2.04	1.23	123.2
AlMe ₂ Cl/SubD	1.94	1.23	129.5
AlEtCl ₂ /SubD	1.92	1.23	123.4
AlCl ₃ /SubE	1.87	1.23	126.8
ScCl ₃ /SubE	2.10	1.23	127.8
FeCl ₃ /SubE	2.02	1.23	123.4
AlMe ₂ Cl/SubE	1.95	1.23	124.4
AlEtCl ₂ /SubE	1.90	1.24	128.7
AlCl ₃ /SubF	1.87	1.23	127.1
ScCl ₃ /SubF	2.09	1.23	141.3
FeCl ₃ /SubF	2.03	1.23	124.4
AlMe ₂ Cl/SubF	1.95	1.23	125.4
AlEtCl ₂ /SubF	1.90	1.23	133.7
AlCl ₃ /SubG	1.86	1.24	126.0
ScCl ₃ /SubG	2.08	1.23	133.2
FeCl ₃ /SubG	2.01	1.23	123.2
AlMe ₂ Cl/SubG	1.93	1.23	126.8
AlEtCl ₂ /SubG	1.90	1.24	127.8
AlCl ₃ /SubH	1.87	1.24	128.3
ScCl ₃ /SubH	2.10	1.23	132.6
FeCl ₃ /SubH	2.02	1.23	124.9
AlMe ₂ Cl/SubH	1.93	1.22	132.0
AlEtCl ₂ /SubH	1.92	1.23	123.5

Table 1.5: Collected key NBO charges.

Reaction	LA	O	C	H	C(mono)	C(adj)
AlCl ₃ /SubA	1.533	-0.689	0.505	0.186	-0.266	0.087
ScCl ₃ /SubA	1.350	-0.652	0.500	0.177	-0.265	0.083
FeCl ₃ /SubA	1.376	-0.655	0.486	0.175	-0.264	0.083
AlMe ₂ Cl/SubA	1.689	-0.653	0.492	0.181	-0.260	0.080
AlEtCl ₂ /SubA	1.625	-0.677	0.499	0.184	-0.268	0.089
AlEt ₂ Cl/SubA	1.702	-0.657	0.488	0.183	-0.261	0.080
AlCl ₃ /SubB	1.530	-0.684	0.500	0.188	-0.269	0.086
ScCl ₃ /SubB	1.356	-0.623	0.501	0.149	-0.258	0.081
FeCl ₃ /SubB	1.370	-0.624	0.484	0.150	-0.256	0.081
AlMe ₂ Cl/SubB	1.691	-0.653	0.490	0.182	-0.262	0.075
AlEtCl ₂ /SubB	1.630	-0.649	0.504	0.162	-0.259	0.081
AlCl ₃ /SubC	1.536	-0.668	0.506	0.160	-0.256	0.075
ScCl ₃ /SubC	1.354	-0.637	0.509	0.144	-0.244	0.055
FeCl ₃ /SubC	1.378	-0.659	0.481	0.178	-0.269	0.083
AlMe ₂ Cl/SubC	1.700	-0.627	0.496	0.150	-0.243	0.068
AlEtCl ₂ /SubC	1.633	-0.656	0.507	0.159	-0.256	0.081
AlCl ₃ /SubD	1.529	-0.681	0.500	0.187	-0.273	0.090
ScCl ₃ /SubD	1.354	-0.622	0.504	0.149	-0.262	0.085
FeCl ₃ /SubD	1.368	-0.623	0.485	0.150	-0.261	0.085
AlMe ₂ Cl/SubD	1.690	-0.649	0.489	0.182	-0.265	0.079
AlEtCl ₂ /SubD	1.629	-0.649	0.506	0.162	-0.264	0.088
AlCl ₃ /SubE	1.536	-0.670	0.503	0.158	-0.256	0.078
ScCl ₃ /SubE	1.354	-0.630	0.495	0.146	-0.256	0.078
FeCl ₃ /SubE	1.374	-0.631	0.480	0.148	-0.254	0.077
AlMe ₂ Cl/SubE	1.698	-0.630	0.495	0.149	-0.245	0.063
AlEtCl ₂ /SubE	1.625	-0.685	0.495	0.185	-0.266	0.080
AlCl ₃ /SubF	1.534	-0.665	0.509	0.161	-0.252	0.067
ScCl ₃ /SubF	1.359	-0.630	0.510	0.147	-0.248	0.064
FeCl ₃ /SubF	1.372	-0.628	0.486	0.148	-0.249	-0.066
AlMe ₂ Cl/SubF	1.702	-0.631	0.498	0.159	-0.251	0.067
AlEtCl ₂ /SubF	1.626	-0.652	0.499	0.158	-0.240	0.053
AlCl ₃ /SubG	1.540	-0.684	0.490	0.158	-0.258	0.086
ScCl ₃ /SubG	1.359	-0.643	0.486	0.144	-0.254	0.077
FeCl ₃ /SubG	1.376	-0.643	0.470	0.148	-0.253	0.074
AlMe ₂ Cl/SubG	1.703	-0.645	0.487	0.153	-0.255	0.078
AlEtCl ₂ /SubG	1.623	-0.687	0.493	0.180	-0.258	0.066
AlCl ₃ /SubH	1.530	-0.685	0.502	0.189	-0.270	0.080
ScCl ₃ /SubH	1.356	-0.624	0.504	0.145	-0.256	0.075
FeCl ₃ /SubH	1.373	-0.626	0.488	0.148	-0.254	0.072
AlMe ₂ Cl/SubH	1.693	-0.627	0.485	0.162	-0.242	0.059
AlEtCl ₂ /SubH	1.624	-0.643	0.500	0.162	-0.257	0.082

Table 1.6: Collected average angles and NBO charges.

Reaction	Average O-LA-Halogen angle	Average Halogen NBO	Average Me(H) ₁ NBO	Average Me(H) ₂ NBO
AlCl ₃ /SubA	103.1	-0.557	0.219	0.227
ScCl ₃ /SubA	102.2	-0.501	0.219	0.226
FeCl ₃ /SubA	103.1	-0.497	0.218	0.225
AlMe ₂ Cl/SubA	101.4	-1.049	0.216	0.224
AlEtCl ₂ /SubA	102.1	-0.727	0.219	0.227
AlEt ₂ Cl/SubA	100.7	-0.877	0.213	0.223
AlCl ₃ /SubB	102.9	-0.556	0.221	0.219
ScCl ₃ /SubB	101.6	-0.501	0.213	0.226
FeCl ₃ /SubB	102.3	-0.495	0.212	0.224
AlMe ₂ Cl/SubB	101.2	-1.050	0.218	0.218
AlEtCl ₂ /SubB	101.4	-0.734	0.214	0.223
AlCl ₃ /SubC	102.7	-0.559	0.211	0.224
ScCl ₃ /SubC	103.2	-0.503	0.209	0.221
FeCl ₃ /SubC	103.2	-0.499	0.219	0.218
AlMe ₂ Cl/SubC	100.1	-1.056	0.210	0.222
AlEtCl ₂ /SubC	101.7	-0.734	0.213	0.223
AlCl ₃ /SubD	102.8	-0.555	0.222	0.219
ScCl ₃ /SubD	100.9	-0.500	0.213	0.228
FeCl ₃ /SubD	102.2	-0.493	0.212	0.225
AlMe ₂ Cl/SubD	101.1	-1.050	0.218	0.217
AlEtCl ₂ /SubD	101.4	-0.733	0.215	0.225
AlCl ₃ /SubE	102.6	-0.559	0.211	0.225
ScCl ₃ /SubE	102.2	-0.503	0.212	0.225
FeCl ₃ /SubE	102.5	-0.498	0.211	0.224
AlMe ₂ Cl/SubE	100.4	-1.057	0.210	0.221
AlEtCl ₂ /SubE	102.3	-0.727	0.220	0.217
AlCl ₃ /SubF	102.5	-0.559	0.210	0.224
ScCl ₃ /SubF	102.3	-0.504	0.210	0.224
FeCl ₃ /SubF	102.7	-0.497	0.210	0.223
AlMe ₂ Cl/SubF	100.7	-1.057	0.211	0.223
AlEtCl ₂ /SubF	101.3	-0.725	0.208	0.223
AlCl ₃ /SubG	102.9	-0.562	0.211	0.225
ScCl ₃ /SubG	102.0	-0.506	0.211	0.225
FeCl ₃ /SubG	102.8	-0.501	0.211	0.223
AlMe ₂ Cl/SubG	100.8	-1.058	0.211	0.224
AlEtCl ₂ /SubG	102.3	-0.729	0.216	0.215
AlCl ₃ /SubH	102.9	-0.556	0.220	0.218
ScCl ₃ /SubH	101.8	-0.502	0.211	0.225
FeCl ₃ /SubH	102.1	-0.496	0.210	0.223
AlMe ₂ Cl/SubH	100.2	-1.050	0.209	0.219
AlEtCl ₂ /SubH	101.1	-0.731	0.211	0.222

Table 1.7: Collected Lewis acid Sterimol descriptors.

Reaction	L	B1	B5
AlCl ₃ /SubA	4.54	2.76	3.82
ScCl ₃ /SubA	4.86	2.80	4.05
FeCl ₃ /SubA	4.72	2.77	3.89
AlMe ₂ Cl/SubA	4.91	2.88	3.90
AlEtCl ₂ /SubA	4.93	2.86	4.98
AlEt ₂ Cl/SubA	4.92	2.97	5.01
AlCl ₃ /SubB	4.51	2.75	3.83
ScCl ₃ /SubB	4.94	2.82	4.05
FeCl ₃ /SubB	4.72	2.77	3.89
AlMe ₂ Cl/SubB	4.93	2.92	3.90
AlEtCl ₂ /SubB	4.96	2.89	4.97
AlCl ₃ /SubC	4.53	2.75	3.84
ScCl ₃ /SubC	5.00	2.81	4.03
FeCl ₃ /SubC	4.72	2.76	3.89
AlMe ₂ Cl/SubC	4.71	2.77	3.89
AlEtCl ₂ /SubC	5.54	2.72	4.74
AlCl ₃ /SubD	4.52	2.75	3.83
ScCl ₃ /SubD	4.84	2.83	4.05
FeCl ₃ /SubD	4.75	2.76	3.89
AlMe ₂ Cl/SubD	4.93	2.92	3.91
AlEtCl ₂ /SubD	4.96	2.79	4.97
AlCl ₃ /SubE	4.52	2.74	3.83
ScCl ₃ /SubE	4.99	2.81	4.05
FeCl ₃ /SubE	4.73	2.76	3.90
AlMe ₂ Cl/SubE	4.71	2.79	3.89
AlEtCl ₂ /SubE	4.96	2.77	4.98
AlCl ₃ /SubF	4.52	2.75	3.83
ScCl ₃ /SubF	4.92	2.83	4.05
FeCl ₃ /SubF	4.75	2.77	3.89
AlMe ₂ Cl/SubF	4.86	2.83	3.91
AlEtCl ₂ /SubF	4.87	2.82	4.98
AlCl ₃ /SubG	4.53	2.74	3.84
ScCl ₃ /SubG	4.89	2.83	4.04
FeCl ₃ /SubG	4.74	2.77	3.89
AlMe ₂ Cl/SubG	4.89	2.84	3.91
AlEtCl ₂ /SubG	4.98	2.85	4.98
AlCl ₃ /SubH	4.52	2.75	3.83
ScCl ₃ /SubH	4.95	2.81	4.05
FeCl ₃ /SubH	4.69	2.76	3.90
AlMe ₂ Cl/SubH	4.94	2.90	3.90
AlEtCl ₂ /SubH	4.99	2.79	4.97

Table 1.8: Collected NBO charges on the first aromatic ring.

Reaction	C1	C2	C3	C4	C5	C6
AlCl ₃ /SubA	-0.202	0.061	-0.210	-0.132	-0.215	-0.117
ScCl ₃ /SubA	-0.201	0.058	-0.210	-0.133	-0.215	-0.120
FeCl ₃ /SubA	-0.197	0.053	-0.209	-0.138	-0.214	-0.122
AlMe ₂ Cl/SubA	-0.194	0.051	-0.208	-0.142	-0.214	-0.126
AlEtCl ₂ /SubA	-0.199	0.059	-0.210	-0.136	-0.215	-0.121
AlEt ₂ Cl/SubA	-0.199	0.060	-0.210	-0.138	-0.216	-0.122
AlCl ₃ /SubB	-0.200	0.054	-0.208	-0.140	-0.212	-0.127
ScCl ₃ /SubB	-0.201	0.071	-0.205	-0.123	-0.223	-0.113
FeCl ₃ /SubB	-0.198	0.067	-0.205	-0.127	-0.223	-0.116
AlMe ₂ Cl/SubB	-0.192	0.046	-0.207	-0.149	-0.212	-0.135
AlEtCl ₂ /SubB	-0.199	0.065	-0.205	-0.126	-0.222	-0.111
AlCl ₃ /SubC	-0.207	0.086	-0.210	-0.123	-0.288	-0.112
ScCl ₃ /SubC	-0.204	0.091	-0.211	-0.120	-0.227	-0.114
FeCl ₃ /SubC	-0.202	0.062	-0.213	-0.146	-0.218	-0.133
AlMe ₂ Cl/SubC	-0.201	0.077	-0.210	-0.132	-0.226	-0.119
AlEtCl ₂ /SubC	-0.204	0.077	-0.208	-0.129	-0.225	-0.115
AlCl ₃ /SubD	-0.200	0.052	-0.208	-0.141	-0.210	-0.127
ScCl ₃ /SubD	-0.199	0.066	-0.205	-0.126	-0.220	-0.115
FeCl ₃ /SubD	-0.199	0.065	-0.207	-0.128	-0.220	-0.116
AlMe ₂ Cl/SubD	-0.192	0.043	-0.207	-0.150	-0.210	-0.134
AlEtCl ₂ /SubD	-0.199	0.062	-0.205	-0.128	-0.220	-0.112
AlCl ₃ /SubE	-0.215	0.090	-0.215	0.078	-0.235	-0.097
ScCl ₃ /SubE	-0.212	0.085	-0.214	0.075	-0.234	-0.100
FeCl ₃ /SubE	-0.210	0.082	-0.214	0.070	-0.232	-0.104
AlMe ₂ Cl/SubE	-0.208	0.078	-0.214	0.066	-0.231	-0.105
AlEtCl ₂ /SubE	-0.212	0.070	-0.217	0.051	-0.221	-0.121
AlCl ₃ /SubF	-0.205	0.083	-0.209	-0.124	-0.226	-0.122
ScCl ₃ /SubF	-0.203	0.081	-0.208	-0.127	-0.225	-0.118
FeCl ₃ /SubF	-0.200	0.075	-0.208	-0.129	-0.226	-0.118
AlMe ₂ Cl/SubF	-0.194	0.064	-0.206	-0.138	-0.221	-0.124
AlEtCl ₂ /SubF	-0.199	0.085	-0.209	-0.128	-0.225	-0.118
AlCl ₃ /SubG	-0.237	-0.093	-0.273	0.386	-0.311	0.114
ScCl ₃ /SubG	-0.235	0.111	-0.311	0.385	-0.272	-0.096
FeCl ₃ /SubG	-0.233	0.108	-0.311	0.381	-0.272	-0.098
AlMe ₂ Cl/SubG	-0.225	0.082	-0.252	0.373	-0.327	-0.091
AlEtCl ₂ /SubG	-0.235	0.084	-0.262	0.366	-0.318	-0.094
AlCl ₃ /SubH	-0.204	0.067	-0.209	-0.147	-0.214	-0.131
ScCl ₃ /SubH	-0.209	0.093	-0.210	-0.122	-0.225	-0.114
FeCl ₃ /SubH	-0.205	0.086	-0.208	-0.127	-0.224	-0.117
AlMe ₂ Cl/SubH	-0.200	0.080	-0.211	-0.133	-0.222	-0.119
AlEtCl ₂ /SubH	-0.208	0.085	-0.209	-0.127	-0.224	-0.114

Table 1.9: Collected NBO charges on the second aromatic ring.

Reaction	C1	C2	C3	C4	C5	C6
AlCl ₃ /SubA	-0.074	-0.033	-0.185	-0.181	-0.202	-0.179
ScCl ₃ /SubA	-0.073	-0.033	-0.185	-0.181	-0.202	-0.179
FeCl ₃ /SubA	-0.071	-0.033	-0.185	-0.183	-0.202	-0.180
AlMe ₂ Cl/SubA	-0.068	-0.033	-0.185	-0.184	-0.202	-0.181
AlEtCl ₂ /SubA	-0.073	-0.032	-0.184	-0.182	-0.203	-0.180
AlEt ₂ Cl/SubA	-0.070	-0.035	-0.183	-0.186	-0.202	-0.183
AlCl ₃ /SubB	-0.058	-0.039	-0.164	-0.199	-0.031	-0.203
ScCl ₃ /SubB	-0.043	-0.035	-0.168	-0.204	-0.030	-0.209
FeCl ₃ /SubB	-0.041	-0.030	-0.169	-0.207	-0.031	-0.208
AlMe ₂ Cl/SubB	-0.054	-0.040	-0.163	-0.203	-0.032	-0.205
AlEtCl ₂ /SubB	-0.039	-0.029	-0.173	-0.212	-0.032	-0.208
AlCl ₃ /SubC	-0.102	0.003	-0.281	0.324	-0.247	-0.159
ScCl ₃ /SubC	-0.107	-0.010	-0.279	0.326	-0.244	-0.162
FeCl ₃ /SubC	-0.114	-0.002	-0.285	0.330	-0.247	-0.157
AlMe ₂ Cl/SubC	-0.091	-0.001	-0.287	0.319	-0.250	-0.165
AlEtCl ₂ /SubC	-0.095	0.002	-0.288	0.316	-0.249	-0.161
AlCl ₃ /SubD	-0.058	-0.028	-0.156	-0.125	-0.172	-0.177
ScCl ₃ /SubD	-0.039	-0.026	-0.154	-0.131	-0.174	-0.184
FeCl ₃ /SubD	-0.036	-0.022	-0.155	-0.136	-0.175	-0.184
AlMe ₂ Cl/SubD	-0.054	-0.028	-0.155	-0.128	-0.173	-0.179
AlEtCl ₂ /SubD	-0.037	-0.018	-0.161	-0.136	-0.178	-0.183
AlCl ₃ /SubE	-0.061	-0.025	-0.181	-0.185	-0.200	-0.186
ScCl ₃ /SubE	-0.060	-0.027	-0.183	-0.186	-0.200	-0.186
FeCl ₃ /SubE	-0.057	-0.025	-0.183	-0.188	-0.201	-0.186
AlMe ₂ Cl/SubE	-0.049	-0.029	-0.184	-0.194	-0.199	-0.188
AlEtCl ₂ /SubE	-0.076	-0.030	-0.179	-0.179	-0.202	-0.181
AlCl ₃ /SubF	-0.065	-0.025	-0.229	0.250	0.236	-0.235
ScCl ₃ /SubF	-0.063	-0.037	-0.228	0.253	0.240	-0.241
FeCl ₃ /SubF	-0.061	-0.026	-0.232	0.246	0.236	-0.237
AlMe ₂ Cl/SubF	-0.055	-0.027	-0.233	0.242	0.234	-0.236
AlEtCl ₂ /SubF	-0.065	-0.038	-0.225	0.252	0.241	-0.240
AlCl ₃ /SubG	-0.065	-0.021	-0.181	-0.185	-0.201	-0.187
ScCl ₃ /SubG	-0.061	-0.028	-0.181	-0.184	-0.199	-0.190
FeCl ₃ /SubG	-0.059	-0.025	-0.182	-0.189	-0.200	-0.189
AlMe ₂ Cl/SubG	-0.052	-0.026	-0.185	-0.193	-0.202	-0.186
AlEtCl ₂ /SubG	-0.077	-0.032	-0.179	-0.180	-0.201	-0.181
AlCl ₃ /SubH	-0.060	-0.019	-0.188	-0.147	-0.057	-0.035
ScCl ₃ /SubH	-0.046	-0.024	-0.185	-0.156	-0.054	-0.038
FeCl ₃ /SubH	-0.042	-0.021	-0.184	-0.159	-0.054	-0.037
AlMe ₂ Cl/SubH	-0.032	-0.031	-0.187	-0.166	-0.055	-0.035
AlEtCl ₂ /SubH	-0.039	-0.022	-0.187	-0.165	-0.056	-0.039

Table 1.10: Collected Sterimol parameters from the C4 position on the first aromatic ring.

Reaction	L C4	B1 C4	B5 C4
AlCl ₃ /SubA	2.57	1.09	1.09
ScCl ₃ /SubA	2.57	1.09	1.09
FeCl ₃ /SubA	2.57	1.09	1.09
AlMe ₂ Cl/SubA	2.57	1.09	1.09
AlEtCl ₂ /SubA	2.57	1.09	1.09
AlEt ₂ Cl/SubA	2.57	1.09	1.09
AlCl ₃ /SubB	2.57	1.09	1.09
ScCl ₃ /SubB	2.57	1.09	1.09
FeCl ₃ /SubB	2.57	1.09	1.09
AlMe ₂ Cl/SubB	2.57	1.09	1.09
AlEtCl ₂ /SubB	2.57	1.09	1.09
AlCl ₃ /SubC	2.57	1.09	1.09
ScCl ₃ /SubC	2.57	1.09	1.09
FeCl ₃ /SubC	2.57	1.09	1.09
AlMe ₂ Cl/SubC	2.57	1.09	1.09
AlEtCl ₂ /SubC	2.57	1.09	1.09
AlCl ₃ /SubD	2.57	1.09	1.09
ScCl ₃ /SubD	2.57	1.09	1.09
FeCl ₃ /SubD	2.57	1.09	1.09
AlMe ₂ Cl/SubD	2.57	1.09	1.09
AlEtCl ₂ /SubD	2.57	1.09	1.09
AlCl ₃ /SubE	3.59	1.70	2.11
ScCl ₃ /SubE	3.59	1.70	2.11
FeCl ₃ /SubE	3.59	1.70	2.12
AlMe ₂ Cl/SubE	3.59	1.70	2.11
AlEtCl ₂ /SubE	3.59	1.70	2.11
AlCl ₃ /SubF	2.57	1.09	1.09
ScCl ₃ /SubF	2.57	1.09	1.09
FeCl ₃ /SubF	2.57	1.09	1.09
AlMe ₂ Cl/SubF	2.57	1.09	1.09
AlEtCl ₂ /SubF	2.57	1.09	1.09
AlCl ₃ /SubG	4.57	1.39	3.12
ScCl ₃ /SubG	4.57	1.39	3.12
FeCl ₃ /SubG	4.57	1.39	3.12
AlMe ₂ Cl/SubG	4.57	1.39	3.12
AlEtCl ₂ /SubG	4.57	1.39	3.12
AlCl ₃ /SubH	2.57	1.09	1.09
ScCl ₃ /SubH	2.57	1.09	1.09
FeCl ₃ /SubH	2.57	1.09	1.09
AlMe ₂ Cl/SubH	2.57	1.09	1.09
AlEtCl ₂ /SubH	2.57	1.09	1.09

Table 1.11: Collected Sterimol parameters from the C4–C6 position on the second aromatic ring.

Reaction	L C4	B1 C4	B5 C4	L C5	B1 C5	B5 C5	L C6	B1 C6	B5 C6
AlCl ₃ /SubA	2.57	1.09	1.09	2.57	1.09	1.09	2.57	1.09	1.09
ScCl ₃ /SubA	2.57	1.09	1.09	2.57	1.09	1.09	2.57	1.09	1.09
FeCl ₃ /SubA	2.57	1.09	1.09	2.57	1.09	1.09	2.57	1.09	1.09
AlMe ₂ Cl/SubA	2.57	1.09	1.09	2.57	1.09	1.09	2.57	1.09	1.09
AlEtCl ₂ /SubA	2.57	1.09	1.09	2.57	1.09	1.09	2.57	1.09	1.09
AlEt ₂ Cl/SubA	2.57	1.09	1.09	2.57	1.09	1.09	2.57	1.09	1.09
AlCl ₃ /SubB	2.57	1.09	1.09	3.88	1.75	1.75	2.57	1.09	1.09
ScCl ₃ /SubB	2.57	1.09	1.09	3.88	1.75	1.75	2.57	1.09	1.09
FeCl ₃ /SubB	2.57	1.09	1.09	3.88	1.75	1.75	2.57	1.09	1.09
AlMe ₂ Cl/SubB	2.57	1.09	1.09	3.88	1.75	1.75	2.57	1.09	1.09
AlEtCl ₂ /SubB	2.57	1.09	1.09	3.88	1.75	1.75	2.57	1.09	1.09
AlCl ₃ /SubC	4.56	1.39	3.13	2.57	1.09	1.09	2.57	1.09	1.09
ScCl ₃ /SubC	4.56	1.52	3.13	2.57	1.09	1.09	2.57	1.09	1.09
FeCl ₃ /SubC	4.57	1.39	3.13	2.57	1.09	1.09	2.57	1.09	1.09
AlMe ₂ Cl/SubC	4.56	1.39	3.14	2.57	1.09	1.09	2.57	1.09	1.09
AlEtCl ₂ /SubC	4.56	1.52	3.13	2.57	1.09	1.09	2.57	1.09	1.09
AlCl ₃ /SubD	3.88	2.08	2.72	2.57	1.09	1.09	2.57	1.09	1.09
ScCl ₃ /SubD	3.88	2.08	2.72	2.57	1.09	1.09	2.57	1.09	1.09
FeCl ₃ /SubD	3.88	2.08	2.72	2.57	1.09	1.09	2.57	1.09	1.09
AlMe ₂ Cl/SubD	3.88	2.08	2.72	2.57	1.09	1.09	2.57	1.09	1.09
AlEtCl ₂ /SubD	3.88	2.08	2.71	2.57	1.09	1.09	2.57	1.09	1.09
AlCl ₃ /SubE	2.57	1.09	1.09	2.57	1.09	1.09	2.57	1.09	1.09
ScCl ₃ /SubE	2.57	1.09	1.09	2.57	1.09	1.09	2.57	1.09	1.09
FeCl ₃ /SubE	2.57	1.09	1.09	2.57	1.09	1.09	2.57	1.09	1.09
AlMe ₂ Cl/SubE	2.57	1.09	1.09	2.57	1.09	1.09	2.57	1.09	1.09
AlEtCl ₂ /SubE	2.57	1.09	1.09	2.57	1.09	1.09	2.57	1.09	1.09
AlCl ₃ /SubF	4.04	2.53	7.39	4.03	2.21	7.56	2.57	1.09	1.09
ScCl ₃ /SubF	4.06	2.53	7.71	4.05	2.23	7.74	2.57	1.09	1.09
FeCl ₃ /SubF	4.04	2.61	7.50	4.03	2.23	7.69	2.57	1.09	1.09
AlMe ₂ Cl/SubF	4.03	2.60	7.67	4.03	2.23	7.82	2.57	1.09	1.09
AlEtCl ₂ /SubF	4.07	2.47	7.35	4.07	2.21	7.26	2.57	1.09	1.09
AlCl ₃ /SubG	2.57	1.09	1.09	2.57	1.09	1.09	2.57	1.09	1.09
ScCl ₃ /SubG	2.57	1.09	1.09	2.57	1.09	1.09	2.57	1.09	1.09
FeCl ₃ /SubG	2.57	1.09	1.09	2.57	1.09	1.09	2.57	1.09	1.09
AlMe ₂ Cl/SubG	2.57	1.09	1.09	2.57	1.09	1.09	2.57	1.09	1.09
AlEtCl ₂ /SubG	2.57	1.09	1.09	2.57	1.09	1.09	2.57	1.09	1.09
AlCl ₃ /SubH	2.57	1.09	1.09	4.69	2.57	7.96	4.70	2.41	9.29
ScCl ₃ /SubH	2.57	1.09	1.09	4.69	2.12	8.06	4.69	2.42	7.88
FeCl ₃ /SubH	2.57	1.09	1.09	4.69	2.12	8.02	4.69	2.42	7.88
AlMe ₂ Cl/SubH	2.57	1.09	1.09	4.69	2.09	7.97	4.69	2.32	7.80
AlEtCl ₂ /SubH	2.57	1.09	1.09	4.69	2.16	8.17	4.69	2.48	8.02

Model Development

Calculated ΔG^\ddagger values were computed using TS analysis and are quoted relative to the Lewis Acid-carbonyl complex. Linear regression models were developed using an in-house script implemented in MATLAB[®] (version R2018b), to obtain the predicted ΔG^\ddagger .⁹³ A good linear correlation (R^2 close to 1.0 and intercept close to 0.0) between the predicted ΔG^\ddagger and the calculated ΔG^\ddagger indicates that the obtained model adequately approximates the system under study.

Carbonyl–Olefin Metathesis Model

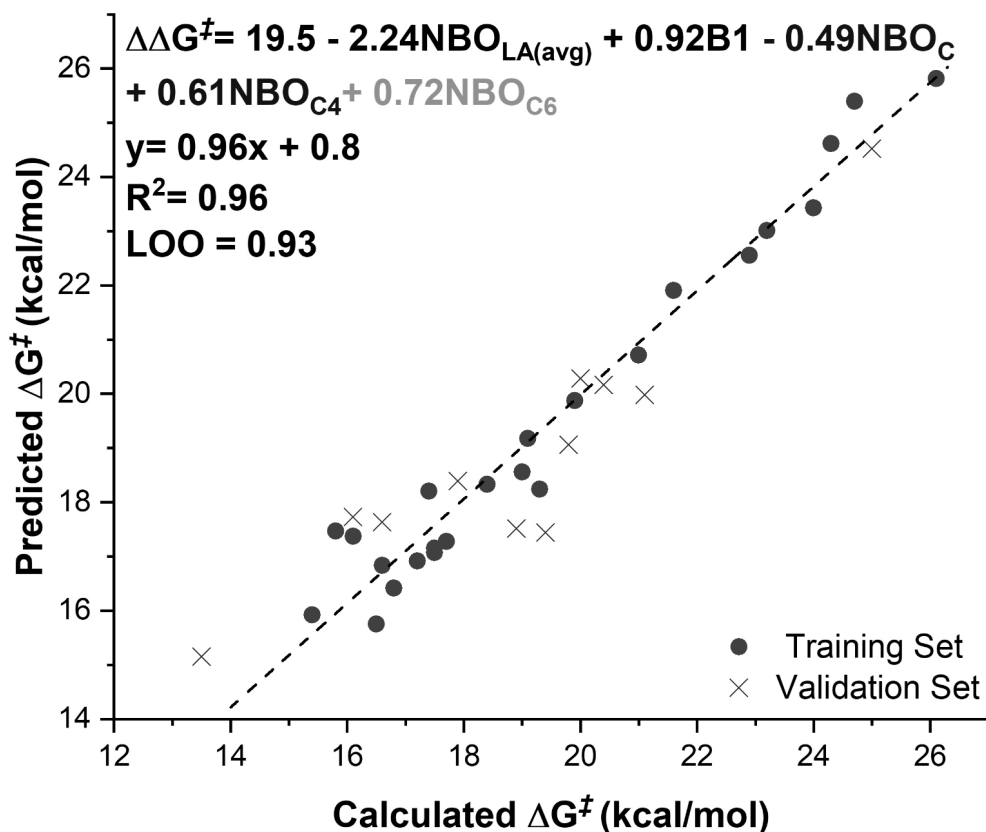


Figure 1.14: Developed statistical model for the carbonyl–olefin metathesis pathway.

Table 1.12: Training set used for the development of the carbonyl–olefin metathesis model.

Measured ΔG^\ddagger	Predicted ΔG^\ddagger	LOO
17.5	17.1	17.0
21.0	20.7	20.6
16.8	16.4	16.4
17.2	16.9	16.9
16.6	16.8	16.9
24.3	24.6	24.8
15.8	17.5	17.9
19.3	18.2	17.8
23.2	23.0	22.9
19.0	18.6	18.4
17.5	17.1	17.1
17.7	17.3	17.2
24.7	25.4	25.9
19.1	19.2	19.2
16.1	17.4	17.7
17.4	18.2	18.4
24.0	23.4	23.3
16.5	15.8	15.3
15.4	15.9	16.1
21.6	21.9	22.1
18.4	18.3	18.3
19.9	19.9	19.9
26.1	25.8	25.6
22.9	22.6	22.3

Table 1.13: Validation set used for the development of the carbonyl–olefin metathesis model.

Measured ΔG^\ddagger	Predicted ΔG^\ddagger
19.4	17.4
18.9	17.5
25	24.5
20	20.3
16.1	17.7
16.6	17.6
17.9	18.4
21.1	20.0
13.5	15.2
19.8	19.1
20.4	20.2

Carbonyl–Ene Reaction Model

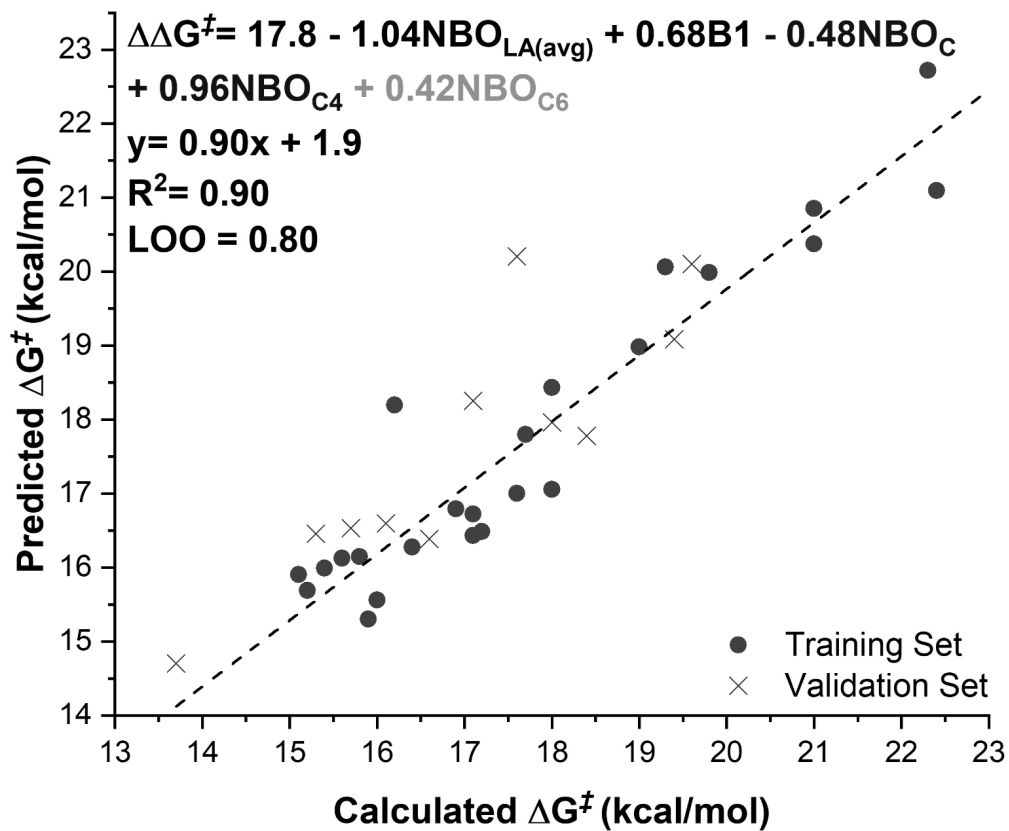


Figure 1.15: Developed statistical model for the carbonyl–ene reaction pathway.

Table 1.14: Training set used for the development of the carbonyl-ene reaction model.

Measured ΔG^\ddagger	Predicted ΔG^\ddagger	LOO
15.1	15.9	16.0
16.2	18.2	18.7
16	15.6	15.5
15.8	16.1	16.2
16.4	16.3	16.2
21	20.4	20.1
15.6	16.1	16.3
18	17.1	16.6
19	19.0	19.0
17.1	16.4	16.2
15.4	16.0	16.1
17.2	16.5	16.4
21	20.9	20.8
17.6	17.0	16.9
16.9	16.8	16.8
17.7	17.8	17.8
19.8	20.0	20.0
15.9	15.3	14.9
15.2	15.7	15.9
18	18.4	18.7
17.1	16.7	16.6
19.3	20.1	20.7
22.3	22.7	23.0
22.4	21.1	20.2

Table 1.15: Validation set used for the development of the carbonyl-ene reaction model.

Measured ΔG^\ddagger	Predicted ΔG^\ddagger
16.6	16.4
16.1	16.6
17.6	20.2
18.0	18.0
15.3	16.5
15.7	16.5
18.4	17.8
17.1	18.3
13.7	14.7
19.4	19.1
19.6	20.1

Development of Secondary Model for Carbonyl–Olefin Metathesis

In our analyses we collect a diverse array of molecular descriptor values from DFT optimized geometries to describe the structural features of the substrate and catalyst. Unfortunately, the lack of structural commonality for particular molecular subsets creates a challenge in identifying readily comprehensible and extensive parameter sets for each of these components. Despite this, we developed a model that contains features that would apply to a broader scope of substrates. We evaluated this secondary model for the carbonyl-olefin metathesis reaction of an aromatic ketone (**1.78**) using FeCl₃ as the Lewis acid catalyst. The model predicts this result with complete precision despite being trained on a different substrate class. However, it is clear from the validation data that prediction in the biaryl substrate space with this model is compromised (secondary model PredR2 = 0.64 compared to the focused COM model PredR2 = 0.86, values are derived from models in which all training data is used).

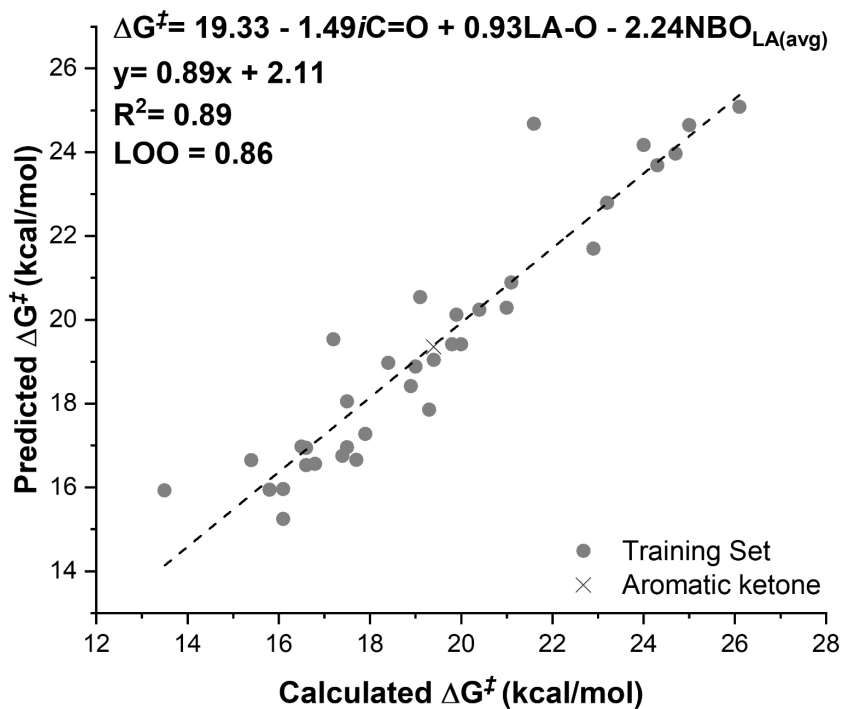


Figure 1.16: Developed secondary model for carbonyl–olefin metathesis relying on a more broadly applicable descriptor set.

Table 1.16: Training set used for the development of the secondary model for carbonyl–olefin metathesis.

Measured ΔG^\ddagger	Predicted ΔG^\ddagger	LOO
17.5	18.0	18.1
19.4	19.0	19.0
18.9	18.4	18.4
25.0	24.6	24.6
21.0	20.3	20.2
16.8	16.6	16.5
17.2	19.5	20.0
16.6	16.5	16.5
24.3	23.7	23.6
20.0	19.4	19.4
15.8	15.9	16.0
16.1	15.2	15.0
19.3	17.9	17.8
23.2	22.8	22.7
19.0	18.9	18.9
17.5	17.0	16.9
16.6	16.9	17.0
17.7	16.7	16.6
24.7	24.0	23.9
19.1	20.5	20.6
16.1	16.0	15.9
17.9	17.3	17.2
17.4	16.7	16.7
24.0	24.2	24.2
21.1	20.9	20.9
13.5	15.9	16.3
16.5	17.0	17.0
15.4	16.6	16.7
21.6	24.7	25.2
18.4	19.0	19.0
19.8	19.4	19.3
20.4	20.2	20.2
19.9	20.1	20.2
26.1	25.1	24.9
22.9	21.7	21.5

Table 1.17: Validation set used for the development of the secondary model for carbonyl–olefin metathesis.

Measured ΔG^\ddagger	Predicted ΔG^\ddagger
19.4	19.4

Chapter 2: Development of Intramolecular Visible Light-Mediated [2+2] Cycloaddition Reactions for the Synthesis of Functionalized Azetidines

Portions of this chapter have been published in Becker, M.R.; Richardson, A.D.; Schindler, C.S. Functionalized azetidines via visible light-enabled aza Paternò-Büchi reactions. *Nat. Commun.* **2019**, *10*, 5095. DOI: 10.1038/s41467-019-13072-x and Richardson, A.D.; Becker, M.R.; Schindler, C.S. Synthesis of Azetidines by Aza Paternò-Büchi Reactions. *Chem. Sci.* **2020**, *11*, 7553–7561.

2.1. Introduction

2.1.1. Azetidines in Pharmaceuticals

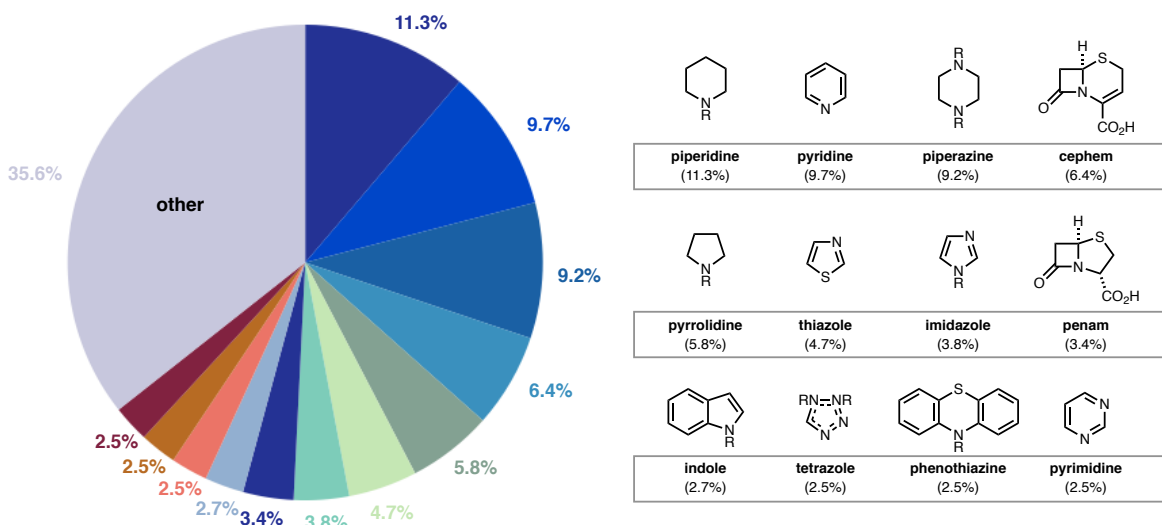


Figure 2.1: Overview of the most commonly used nitrogen heterocycles in FDA-approved small-molecule drugs (2014).

Nitrogen heterocycles are among the most significant components in current pharmaceuticals. This is highlighted by the fact that out of the 33 small-molecule drugs approved by the U.S. Food and Drug Administration (FDA) in 2019, a total of 27 (81%) contained at least one nitrogen heterocycle.⁹⁴ Similarly, a 2014 study by Njardarson and coworkers revealed that

59% of all small-molecule pharmaceuticals approved by the FDA contained at least one nitrogen heterocycle (Figure 2.1).⁹⁵

Six-membered heterocycles, such as piperidines, pyridines and piperazines, were the most frequently used motif, found in 59% of all small-molecule drugs. The next most common heterocycle class (39%) consists of five-membered rings, for example pyrrolidines, thiazoles, imidazoles and indoles. In contrast, four-membered nitrogen heterocycles are less commonly found in current pharmaceuticals. The majority of these compounds consists of β -lactam scaffolds, while other heterocycles, specifically azetidines are highly underrepresented among current pharmaceuticals. To date, a total of three pharmaceuticals that contain an azetidine ring have found approval (Figure 2.2). Cobimetinib (**2.1**) is a kinase inhibitor that has been approved in 2015 for the treatment of unresectable or metastatic melanoma.⁹⁶ Delafloxacin (**2.2**) is an antibiotic that is used against acute bacterial skin and skin structure infections as well as pneumonia and has acquired approval in 2017.⁹⁷ Additionally, baricitinib (**2.3**) has obtained its approval in 2018 as a kinase inhibitor for the treatment of severely active rheumatoid arthritis.⁹⁸

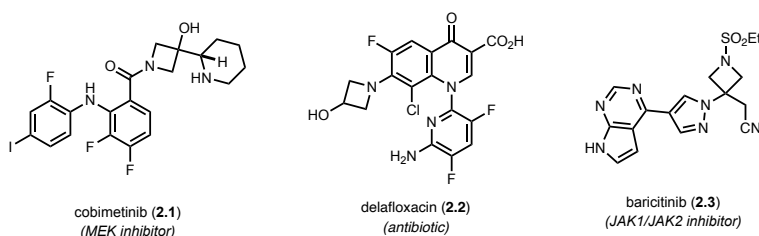


Figure 2.2: FDA-approved drugs containing an azetidine ring.

In light of the increasing demand of new, saturated building blocks for drug discovery, the lack of azetidines in current pharmaceutical scaffolds can be considered as surprising, since the well-defined, three-dimensional structure and high degree of saturated content provides access to unique chemical space.^{99–102} At the same time, azetidine-containing lead compounds can exhibit highly desirable properties, oftentimes superior to those of their corresponding five- or six-

membered analogs. Azetidines are generally considered to display an increased metabolic stability due to the decreased carbon–content that provides less sites for metabolic degradation as well as a low lipophilicity.¹⁰³ Similarly, azetidines exhibit an increased polarity in comparison to five- or six-membered rings, which was exploited by Brown and coworkers to improve the aqueous solubility of oxytocin antagonist **2.4**.¹⁰⁴ Structure-activity relationship (SAR) studies revealed aryloxyazetidines (**2.5**) as competent bioisosteres of the pyrazine ring in **2.4**, resulting in a 10-fold improvement in aqueous solubility, while maintaining a high selectivity for the respective receptor (Figure 2.3A).

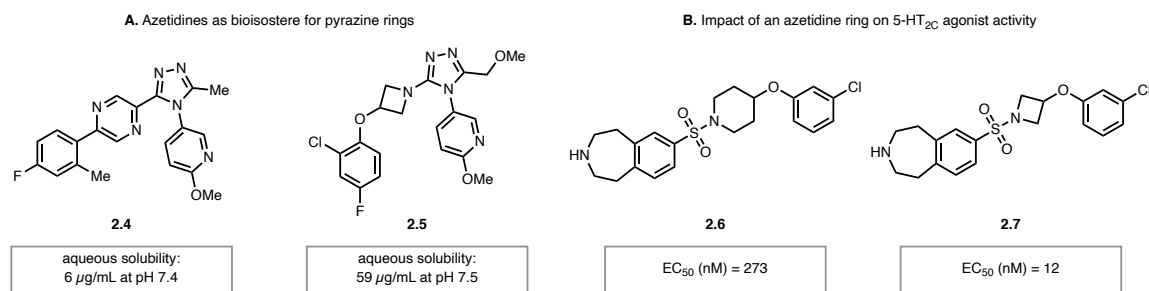


Figure 2.3: Examples of azetidines in lead compounds. (A) Azetidines as bioisostere for pyrazine rings (B) Impact of an azetidine ring on the 5-HT_{2C} agonist activity.

Brown and coworkers also investigated lead scaffolds with high activity for the serotonin 2C (5-HT_{2C}) receptor, a common target for the treatment of conditions such as obesity, schizophrenia, sexual dysfunction, and urinary incontinence.¹⁰⁵ SAR studies were carried out that specifically focused on varying the central nitrogen heterocycle, which showed that substitution of the larger piperidine ring in **2.6** with a smaller azetidine (**2.7**) led to a significant increase in 5-HT_{2C} activity (Figure 2.3B).

2.1.2. Traditional Methods for the Synthesis of Azetidines

The small number of azetidines in current pharmaceuticals in comparison to their five- or six-membered counterparts is often attributed to the lack of synthetic methods to construct and functionalize the small heterocycle.^{106–109} One of the most common ways to synthesize saturated

nitrogen heterocycles relies on intramolecular ring-closing reactions with substrates containing both a nitrogen nucleophile and a leaving group. However, the reactivity of these substrates is highly dependent on the chain length, and can alter drastically depending on the size of the ring being formed. While five- and six-membered undergo cyclization quite readily, the relative rate for ring-closing is diminished for aziridine and azetidines formation by several magnitudes (Figure 2.4A).¹¹⁰ The decreased reactivity for smaller rings can be attributed to the build-up of strain during the transition state for cyclization. However, ring strain alone does not explain the reactivity differences that can be observed between three- and four-membered rings. Specifically, the relative rate for aziridine formation is increased by a factor of 700 in comparison to azetidines. This can be rationalized by analyzing the reactive conformation undergoing cyclization for each substrate. For aziridines the reactive conformation also represents the most stable conformation, while in the case of azetidines, cyclization occurs from an unfavored eclipsed conformation.¹¹⁰ Consequently, elevated temperature or highly activated leaving groups are typically required to obtain sufficient reactivity in azetidines-forming cyclization reactions (Figure 2.4A).

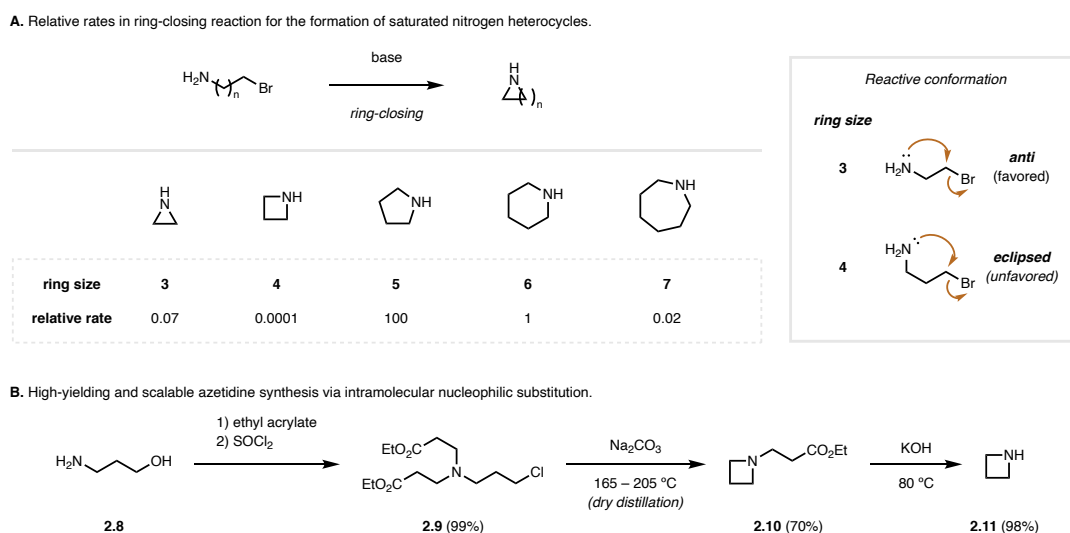


Figure 2.4: Synthesis of azetidines. (A) Relative rates for the intramolecular ring-closing reaction of aliphatic amines (B) High-yielding and scalable azetidines synthesis via intramolecular nucleophilic substitution.

For example, an efficient synthetic route for the synthesis of azetidine (**2.11**) was reported by Wadsworth, in which cyclization proceeded from tertiary amine **2.9** via an intermediate ammonium salt intermediate that subsequently undergoes dealkylation providing **2.10** (Figure 2.4B).¹¹¹ While this four-step sequence allowed access to azetidine (**2.11**) in high yields starting from 3-aminopropanol (**2.8**), high temperatures of 165–205 °C were necessary to obtain sufficient reactivity in the intramolecular cyclization step.

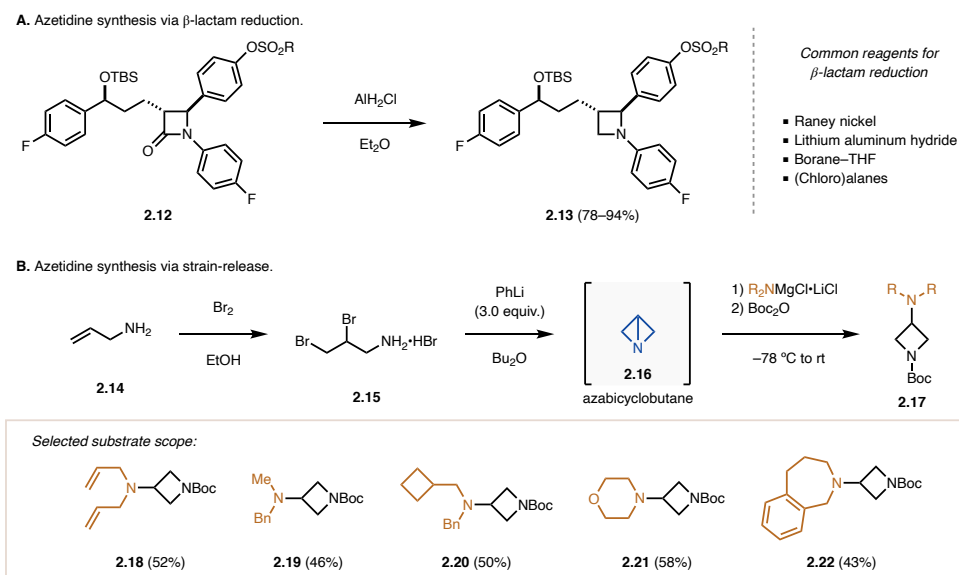


Figure 2.5: Alternative methods for azetidine synthesis. (A) Synthesis via β -lactam reduction (B) Azetidine synthesis via strain-release of azabicyclobutanes.

Consequently, alternative strategies for the synthesis of azetidines containing sensitive functional groups have been developed. One common approach to access azetidines under mild conditions is the reduction of β -lactams, as these scaffolds are readily synthesized,^{112,113} and the reduction process is facile. Common reagents to accomplish efficient lactam-reduction are diborane in tetrahydrofuran, LiAlH_4 or Raney nickel (Figure 2.5A).¹⁰⁶ Additionally, alanes such as DIBAL-H or chloroalanes (AlH_2Cl , AlHCl_2) have been demonstrated to be highly selective reagents for this process, as they often avoid undesired side reactions such as reductive cleavage of the four-membered ring. During their synthesis of glycosylated analogs of ezetimibe, a small-

molecule cholesterol absorption inhibitor, Carreira and coworkers identified AlH_2Cl as optimal reagent for the reduction of β -lactams (**2.12**) in the presence of various sensitive functional groups in high yields, while other reagents such as LiAlH_4 exclusively provided reductive cleavage of the lactam ring (Figure 2.5A).¹¹⁴

More recently, the rapid synthesis of azetidines with functionalization in the 3-position has been accomplished through the strain-release reaction of azabicyclobutanes (**2.16**) with nitrogen nucleophiles (Figure 2.5B). This reactivity, initially reported by Funke in 1969,^{115,116} has been exploited by Baran and coworkers for the synthesis of a variety of azetidinylated amines (**2.18**–**2.22**) in 42–60% yield.^{117–119} Azabicyclobutane (**2.16**) can be readily accessed in two steps via bromination of allylamine (**2.14**) and subsequent phenyllithium-mediated cyclization at cryogenic temperatures. The advantage of this method relies on the fact that **2.16** readily reacts with a series of amines, including drug scaffolds, to provide a series of azetidine products.

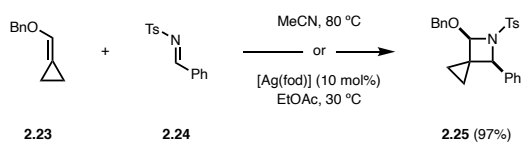


Figure 2.6: Azetidine synthesis via a thermal [2+2] cycloaddition reaction.

The [2+2] cycloaddition reaction between an alkene and an imine component represents a highly efficient way to synthesize azetidines. Overall, there exist only a limited number of examples in which azetidines are directly formed through a cycloaddition reaction, proceeding under either thermal or photochemical conditions.¹⁰⁶ The thermal reaction typically requires highly polarized reagents to achieve successful cycloaddition, specifically imines featuring electron-withdrawing substituents such as sulfonamides, while electron-rich alkenes such as enol ethers or allenes are commonly used as the alkene component (Figure 2.6). Additionally, these compounds require further activation to undergo cycloaddition, for example through high-pressure¹²⁰ or the addition of a Lewis acid catalyst.^{121–125}

2.1.3. Synthesis of Azetidines via Photochemical [2+2] Cycloaddition Reactions

The photochemical [2+2] cycloaddition between an imine and an alkene, often referred to as the aza Paternò-Büchi reaction, was first reported by Tsuge in 1968.¹²⁶ In contrast to photocycloadditions with carbonyls or alkenes, which have been used extensively for the synthesis of oxetanes^{127,128} or cyclobutanes,¹²⁹ the aza Paternò-Büchi reaction is significantly less advanced as a result of the decreased reactivity of imines in the excited state towards [2+2] cycloadditions. In addition to common relaxation pathways such as fragmentation, photoreduction or rearrangement reactions,^{130,131} the imine excited state (**2.27**) is susceptible to radiationless decay to the ground state through rotation around the carbon–nitrogen π -bond (**2.29**), rendering it difficult to engage imines in photocycloadditions (Figure 2.7A).¹³² Nevertheless, some examples have been reported in which imines participate in both intra- and intermolecular aza Paternò-Büchi reactions, oftentimes utilizing cyclic imines to avoid the limiting isomerization. Generally, these reactions can occur from either the singlet or the triplet excited state. Direct irradiation of an imine (**2.30**) leads to population of the corresponding singlet excited state (**2.31**), which is short-lived, but can participate in cycloaddition reactions with an alkene (Figure 2.7B). Ultraviolet (UV) light is typically required to achieve successful excitation of an imine scaffold. Singlet state reactions often proceed in a concerted fashion, therefore, high levels of stereoselectivity can be accomplished. Alternatively, the singlet excited state imine (**2.31**) can undergo intersystem crossing (ISC) to the triplet excited state (**2.33**), which has a significantly longer lifetime as relaxation back to the ground state is spin-forbidden (Figure 2.7C).¹³³ In contrast to the singlet state reaction, the cycloaddition process of a triplet state imine occurs stepwise via biradical intermediate **2.34**. Upon intersystem crossing, which produces a highly reactive singlet state intermediate, cyclization occurs rapidly to afford the respective azetidine product (**2.32**). An

alternative way to access the triplet excited state represents transferring the triplet excited state from a sensitizer, a process referred to as triplet energy transfer or triplet sensitization, which will be described in more detail in chapter 2.14 (Figure 2.7D).

A. Challenges in aza Paternò-Büchi reactions.

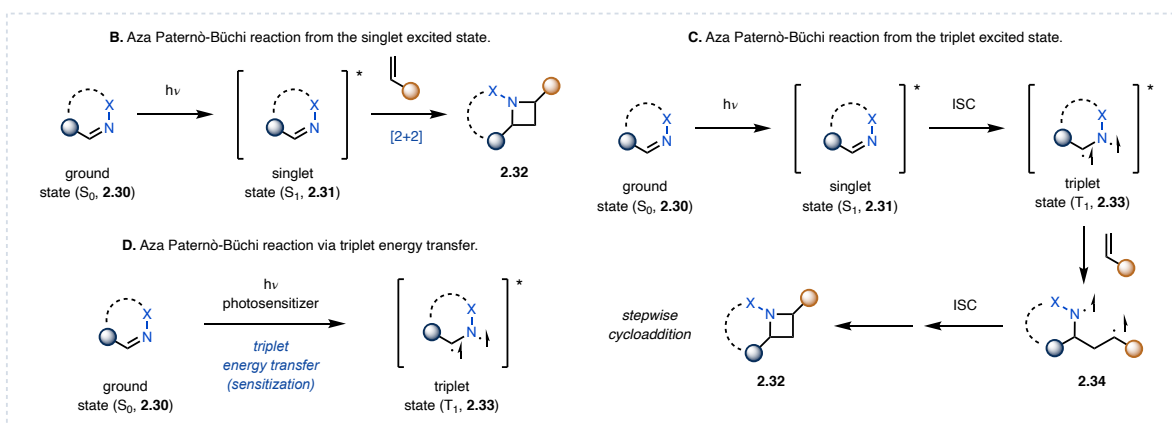
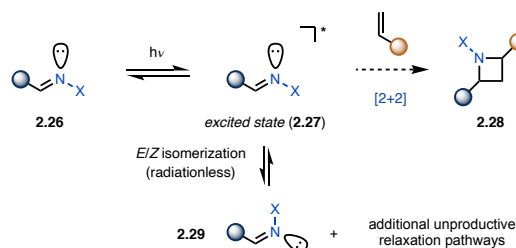


Figure 2.7: Overview of imine photochemistry. (A) Challenges in aza Paternò-Büchi reactions (B) Singlet state reaction (C) Triplet state reaction (D) Aza Paternò-Büchi reactions via triplet energy transfer.

The most common variant of the aza Paternò-Büchi reaction is the intermolecular process, which typically utilizes cyclic imines to increase the lifetime of the imine excited state by preventing rotation around the carbon–nitrogen bond. After the first report by Tsuge in 1968 relying on 1,3,4-oxadiazoles (**2.35**),¹²⁶ a series of other imine reagents have been reported, which show distinct differences in their structure, mechanism and scope of alkenes (Figure 2.8). Koch and coworkers reported the use of 3-ethoxyisoindolones (**2.36**) that react under UV light irradiation from the singlet state, although in low yields.^{134–137} In contrast, a quite efficient photocycloaddition in high yields can be achieved by using 6-azauracils (**2.37**) and a variety of aliphatic or electron-rich alkenes, originally reported by Swenton and coworkers.^{138–140} In this case, acetone is used as a solvent that also functions as a triplet sensitizer to access the excited state of **2.37**. Other imine

reagents that can be engaged in aza Paternò-Büchi reactions include 9-cyanophenanthridines (**2.38**)^{141,142} as well as quinoxaline-2(1*H*)-ones (**2.39**) and related compounds.^{143–146}

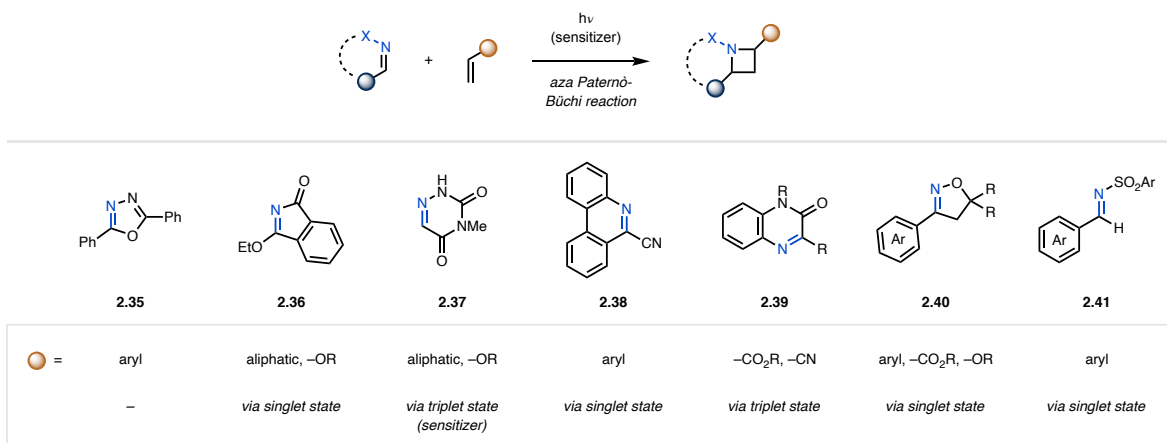


Figure 2.8: Overview of imines that participate in intermolecular aza Paternò-Büchi reactions.

Mukai and coworkers established that 3-aryl-2-isoxazolines (**2.40**) are competent substrates to react in an intermolecular photocycloaddition under UV light irradiation, representing the first example in which oximes are used in this transformation.^{147–149} Based on the observed regioselectivity, the reaction was proposed to occur via a singlet exciplex between **2.40** and the styrenyl alkene. The mechanism was later corroborated computationally by Sampedro and coworkers, who found that an electron-withdrawing substituent on the aromatic substituent of **2.40** was necessary to extend the lifetime of the imine excited state.^{150,151} To date, the only example in which an acyclic excited state imine was successfully used in an intermolecular aza Paternò-Büchi reaction has been reported by Maruoka and coworkers.¹⁵² In this reaction, aromatic *N*-(arylsulfonyl)imines (**2.41**) undergo cycloaddition with styrenyl alkenes via a singlet exciplex intermediate, and as a result, the reaction was found stereospecific.

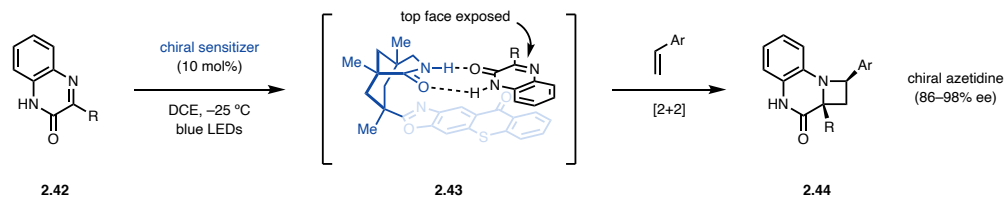


Figure 2.9: Enantioselective [2+2] cycloaddition between quinoxalinones and styrenes mediated by a chiral photosensitizer.

More recently, Bach and coworkers reported the first example of an enantioselective aza Paternò-Büchi reaction utilizing quinoxalinones (**2.42**) as the imine reagents, similar to those previously reported by Nishio, for the synthesis of chiral azetidines (Figure 2.9).¹⁵³ The reaction relied on a chiral catalyst that contains an amide functionality, which is capable of interacting with the imine substrate via hydrogen-bonding, as well as a thioxanthone moiety that can sensitize the hydrogen-bonded quinoxalinone via energy transfer. The hydrogen-bonded complex (**2.43**) subsequently undergoes the enantioselective [2+2] cycloaddition reaction with a styrenyl alkene, resulting in the formation of the desired chiral azetidine product (**2.44**). Utilizing 10 mol% of chiral catalyst, the cycloaddition proceeded in 50–99% yield and 86–98% ee. Although the transformation was limited to styrenyl alkenes, the authors demonstrated that this cycloaddition reaction can be carried out intramolecularly with a tethered aliphatic alkene.

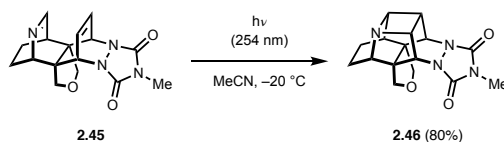


Figure 2.10: Intramolecular aza Paternò-Büchi reaction reported by Prinzbach and coworkers.

During their investigations of bichromophoric systems, Prinzbach and coworkers synthesized polycyclic compound **2.45**.¹⁵⁴ In this scaffold the proximal imine and alkene moieties were poised to undergo photocycloaddition upon UV light irradiation, which was achieved via direct or acetone-sensitized excitation in 80–85% yield, representing the first example of an intramolecular aza Paternò-Büchi reaction (Figure 2.10).

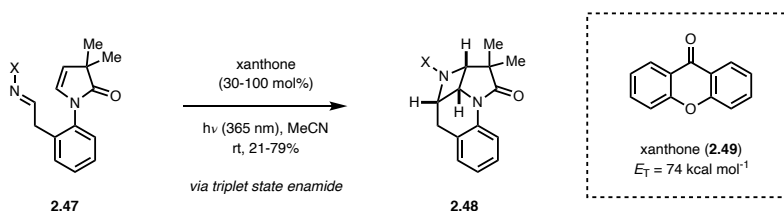


Figure 2.11: Transposed aza Paternò-Büchi reaction relying on a triplet state enamide. X = –OH, –OR, –NHTs, –NHbz, –NR₂

Recently, Sivaguru and coworkers reported an alternative approach to achieve an intramolecular aza Paternò-Büchi reaction.¹⁵⁵ To avoid the challenging photochemical behavior of excited state imines, the authors developed a “transposed” reaction protocol that instead relied on an excited state alkene initiating the cycloaddition process (Figure 2.11). Specifically, the authors demonstrated that enamides (**2.47**) can be used in this reaction to undergo cycloaddition with an adjacent oxime or hydrazone. The triplet excited state of the enamide was accessed through the use of 30–100 mol% xanthone as a photosensitizer under UV light irradiation. Under these conditions a series of polycyclic azetidines (**2.48**) were synthesized in 21–79% yield. Additionally, the authors carried out extensive mechanistic experiments that provided support for the proposed mechanism proceeding via a triplet state enamide intermediate. Based on the reaction efficiency observed with photosensitizers varying in triplet energy (E_T) such as xanthone ($E_T = 74 \text{ kcal mol}^{-1}$) the authors propose a triplet energy of 63–74 kcal mol^{-1} for the enamide scaffold.¹⁵⁶

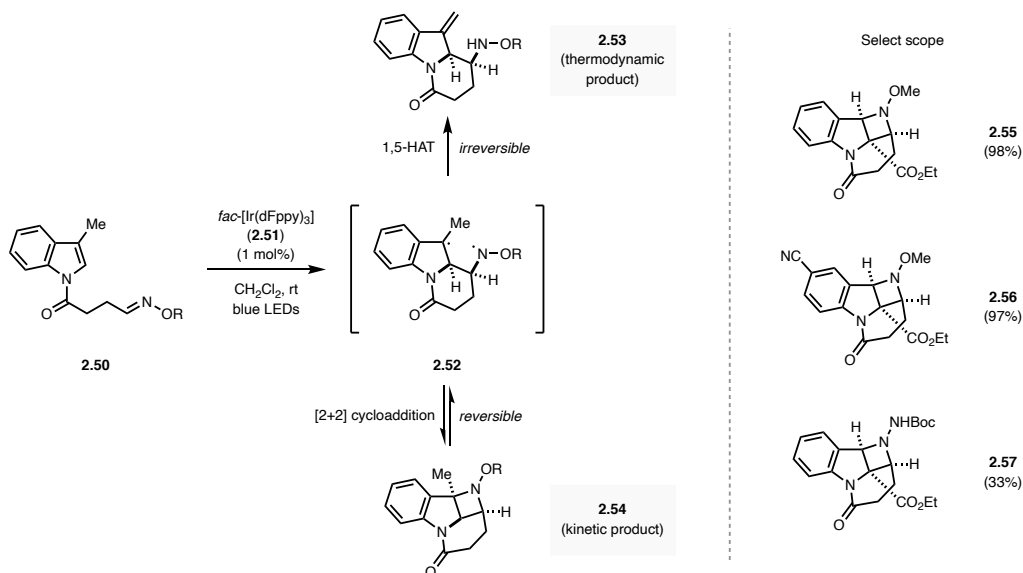


Figure 2.12: Dearomatization reaction of indoles via an energy transfer-mediated [2+2] cycloaddition reaction with oximes.

Using a similar approach, You and coworkers developed a [2+2] cycloaddition reaction for the dearomatization of indoles resulting in the construction of functionalized indoles.¹⁵⁷ Using an iridium photosensitizer (**2.51**), triplet sensitization of the indole (**2.50**) achieved an efficient

intramolecular cycloaddition reaction with a tethered oxime, obtaining the corresponding azetidine products (**2.54–2.57**) in 33–99% yield and typically excellent diastereoselectivity (Figure 2.12). Interestingly, the authors observed divergent reactivity for indoles containing a methyl group in the 3-position (**2.50**). Triplet sensitization resulted in the formation of biradical intermediate **2.52**, which rapidly undergoes the [2+2] cycloaddition reaction. Mechanistic studies including a series of control reactions and DFT studies indicated that the cycloaddition pathway is reversible. As a result, extended reaction times lead to the formation of **2.53** as the thermodynamically favored product, resulting from an irreversible 1,5-HAT from biradical intermediate **2.52**. The authors demonstrated the utility of the 1,5-HAT pathway by synthesizing a broad range of indoles containing an exocyclic alkene moiety in 40–96% yield.

2.1.4. Triplet Energy Transfer Catalysis

In the context of photocatalysis, energy transfer and the corresponding electron transfer need to be clearly distinguished (Figure 2.13). Electron transfer catalysis, often referred to as photoredox catalysis, utilizes a photocatalyst with high redox potentials to achieve a single electron transfer event with a substrate. While this process occurs from an excited state catalyst, the substrate, which is oxidized or reduced during this process, remains in its ground state.^{158,159}

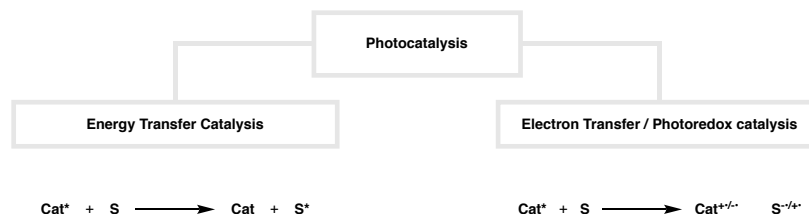


Figure 2.13. Distinguishing energy transfer and electron transfer (photoredox) catalysis. Cat* = catalyst (excited state); S = substrate (ground state); Cat = catalyst (ground state); S* = substrate (excited state).

In contrast, triplet energy transfer represents an alternative way to access the triplet excited state of an organic molecule, which typically involves a photosensitizer that can transfer its triplet excited state to a substrate in its ground state.^{160–163} This process can have distinct advantages over

direct irradiation, since the absorbance properties of most organic molecules require irradiation with UV light, which can negatively impact the selectivity, functional group tolerance and the operational simplicity of a reaction. These limitations are avoided by utilizing a visible light-absorbing photocatalyst that can achieve substrate sensitization without undesired background reactivity. Additionally, for substrates with inefficient intersystem crossing, where direct excitation is not an effective means to achieve high population of the triplet excited state, energy transfer provides a unique opportunity to access the reactivity of the triplet excited state.

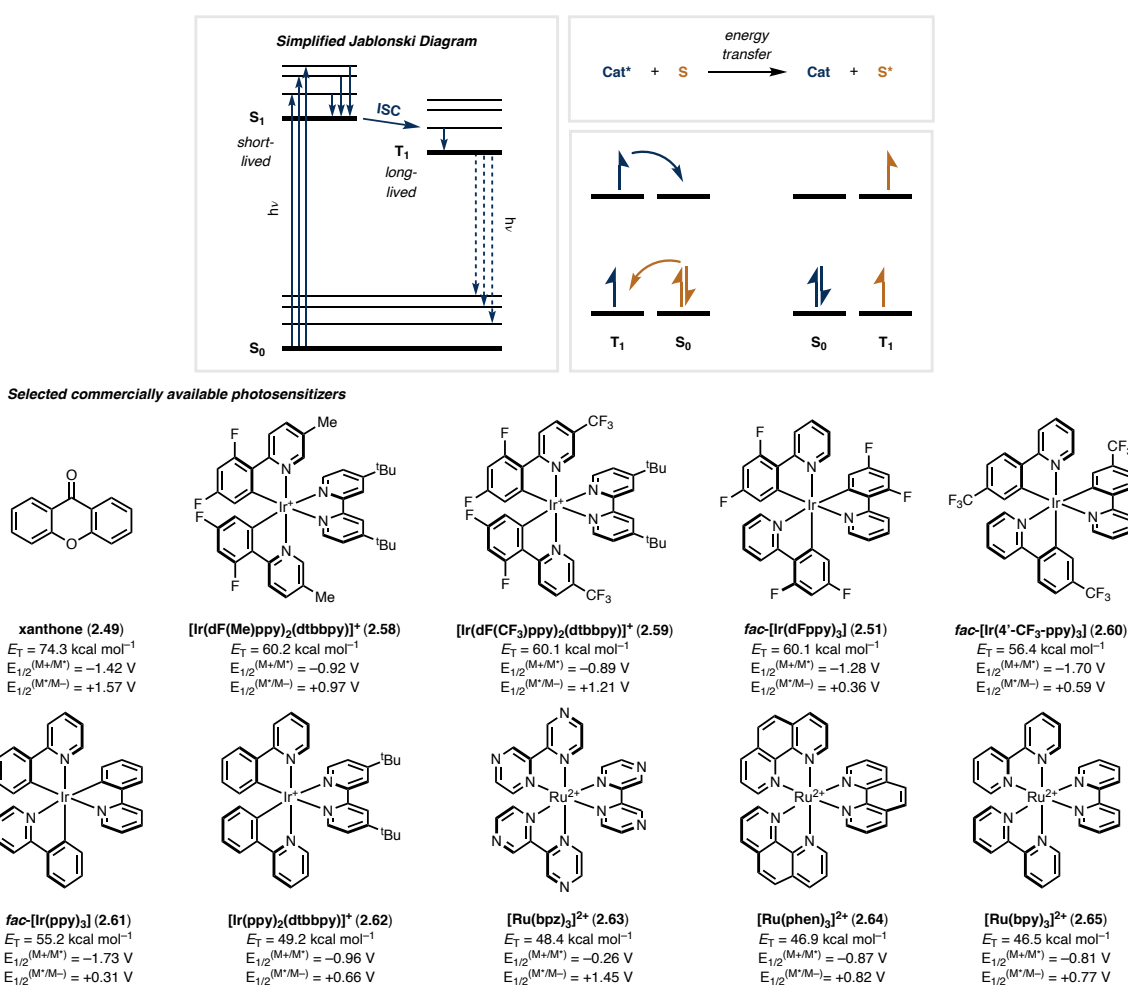


Figure 2.14: Photophysical principles for triplet energy transfer (top) and selected commercially available photosensitizers (bottom). Cat* = catalyst (excited state); S = substrate (ground state); Cat = catalyst (ground state); S* = substrate (excited state).

The energy transfer process relies on a photosensitizer, typically a transition metal complex or an organic dye, for which light irradiation results in excitation to an excited singlet state (S_1)

(Figure 2.14, top). The singlet state is often short-lived and rapidly relaxes back to the ground state (S_0) via fluorescence and radiationless internal conversion, or undergoes intersystem crossing (ISC) to an excited triplet state (S_1). Considering that relaxation back to the ground state for example via emission of a photon is spin-forbidden, the triplet state lifetime is sufficiently long to enable bimolecular interactions with a substrate. In addition to a long triplet state lifetime, a good photosensitizer should also possess a high intersystem crossing rate to achieve a high population of the triplet excited state. The energy transfer event typically proceeds via a simultaneous intermolecular exchange of an excited state electron from the photosensitizer and a corresponding ground state electron from the substrate (Figure 2.14, top). During this process, often referred to a Dexter energy transfer, both reaction components have to be in close proximity to afford sufficient electronic coupling. Similarly, energy transfer typically has to be energetically favored, which can be estimated based on the difference in triplet energy (E_T) of the photosensitizer and the triplet energy of the substrate (Equation 2.1).

$$\Delta E_T = E_T(\text{S}) - E_T(\text{Cat}) \quad \text{Equation 2.1}$$

An efficient energy transfer is likely when the difference between the two components is $\Delta E_T < 0$ (exergonic), in other words the triplet energy of the photosensitizer should be higher than that of the substrate. In contrast, an endergonic energy transfer ($\Delta E_T > 0$) is generally slow or does not occur at all.

Over the last years, several research groups have recognized that many visible light photocatalysts, which have previously only been used in the context of photoredox catalysis, also hold great potential as photosensitizers for energy transfer-mediated transformations such as isomerization, cycloaddition or bond homolysis reactions.¹⁶⁴ Figure 2.14 shows a selection of commercially available visible light photocatalysts (**2.51**, **2.58–2.65**), which have found use as

triplet sensitizers.¹⁶⁵ These catalysts possess triplet energy of up to 60 kcal mol⁻¹, while sensitizers with higher triplet energies such as xanthone (**2.49**, $E_T = 74.3$ kcal mol⁻¹) require irradiation with UV light. As a result, transformations that can be currently carried out with visible light photosensitizers are limited to substrates with triplet energies that are not substantially higher than 60 kcal mol⁻¹.

2.2. Reaction Design and Optimization

To realize an aza Paternò-Büchi reaction of general synthetic utility, we sought to develop a reaction protocol that would avoid excitation of the imine component and associated undesired relaxation pathways. Specifically, we envisioned an orthogonal approach that would rely on selective excitation of the alkene component of the substrate (Figure 2.15). Activated alkenes such as styrenes and dienes possess relatively low triplet energies of approximately 60 kcal mol⁻¹ that are amenable to triplet energy transfer from a visible light photocatalyst.¹⁶⁶

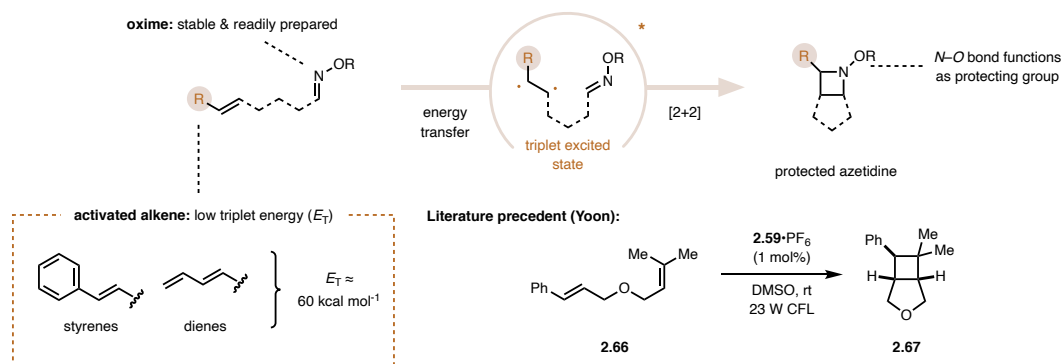


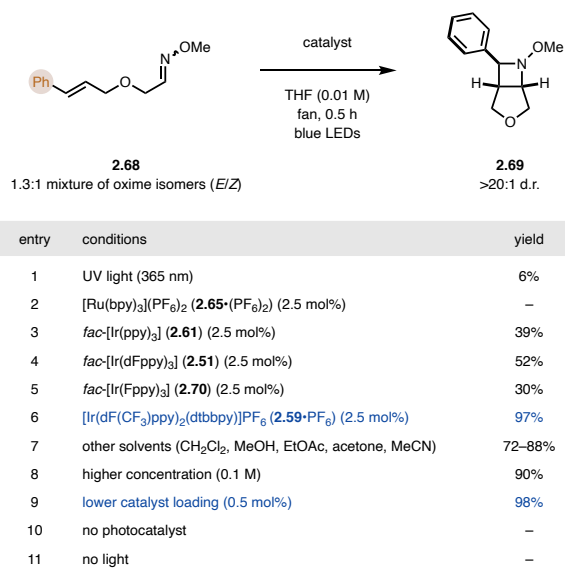
Figure 2.15: Reaction design for the intramolecular aza Paternò-Büchi reaction.

Yoon and coworkers previously recognized this reactivity for the synthesis of cyclobutanes (**2.67**) via an alkene [2+2] photocycloaddition reaction. Under irradiation with visible light, the photocatalyst [Ir(dF(CF₃)ppy)₂(dtbbpy)]PF₆ (**2.59**•PF₆) successfully engaged with the styrene moiety to access a triplet styrene, which underwent intramolecular cycloaddition with the adjacent alkene in 83% yield and excellent diastereoselectivity.¹⁶⁷ Later, the same group also reported a

similar protocol relying on dienes as alternative activated alkenes, although proceeding with lower stereoselectivities.¹⁶⁸

We hypothesized that a similar triplet excited state alkene might undergo cycloaddition with an adjacent imine to provide the desired azetidine product (Figure 2.15). Towards that goal, initial investigations were focused on oximes considering their straightforward preparation and increased stability towards hydrolysis in comparison to imines. At the same time, the azetidine product from the proposed cycloaddition reaction would contain a nitrogen–oxygen bond that could function as a nitrogen protecting group and could be cleaved in a subsequent, reductive step. To test this hypothesis, substrate **2.68** containing both a styrene and oxime moiety was submitted to a variety of reaction conditions. Direct irradiation with UV light (365 nm) provided only trace amounts of the desired product **2.69**, while significant amount of substrate decomposition and oxime isomerization was observed (Table 2.1, entry 1).

Table 2.1: Reaction optimization of the intramolecular aza Paternò-Büchi reaction.



Consequently, a series of commercially available visible light photosensitizers were evaluated under irradiation with blue LED lights (427 nm). While ruthenium catalyst **2.65**•(PF₆)₂

did not result in any reactivity (Table 2.1, entry 2), iridium-based photocatalysts **2.51**, **2.61** and **2.70** provided 30–52% yield of **2.69** (Table 2.1, entries 3–5). Further optimization identified iridium catalyst $[\text{Ir}(\text{dF}(\text{CF}_3)\text{ppy})_2(\text{dtbbpy})]\text{PF}_6$ (**2.59**• PF_6) as the optimal photosensitizer for the desired transformation to afford the desired product in 97% yield and >20:1 d.r. (Table 2.1, entry 6). The reaction was tolerant of solvents other than tetrahydrofuran and provided 72–88% yield with solvents such as dichloromethane, methanol, ethyl acetate or acetonitrile (Table 2.1, entry 7). Increasing the reaction concentration from 0.01 M to 0.1 M only led to a small reduction in yield (Table 2.1, entry 8). The reaction could be readily carried out with low catalyst loadings of 0.5 mol% providing **2.69** in 98% yield (Table 2.1, entry 9). Finally, control reactions revealed that both the photocatalyst and light irradiation are essential to obtain the desired reactivity, as removing one of the two components from the reaction did not provide any reactivity (Table 2.1, entries 10+11).

2.3. Substrate Scope

With optimal conditions identified, the scope of the imine moiety in the substrate was tested. Similar to the previously used *O*-methyl oxime **2.68**, *O*-benzyl oxime **2.71** provided **2.75** in excellent yield of 96%, which could be readily reproduced on gram-scale (Table 2.2, entry 2). Free oxime **2.72** provided the desired product in slightly diminished yields of 54% (Table 2.2, entry 3). Additionally, hydrazones were identified as a compatible class of substrates. *N*-Boc hydrazone **2.73** smoothly underwent the developed intramolecular cycloaddition reaction in 62% yield and 13:1 d.r. (Table 2.2, entry 4). Notably, the structural assignment of the azetidine products was further confirmed by X-ray crystallographic analysis of azetidine **2.77**. Interestingly, dimethyl hydrazone **2.74** was found unreactive under optimal conditions with photocatalyst **2.59**• PF_6 . Other substrates such *N*-tosyl imines could also be successfully engaged in the reaction, however, due to their poor stability towards hydrolysis these substrates could not be purified. While all evaluated

oxime and hydrazone substrates were typically isolated as an inconsequential mixture of *E/Z* isomers, the high diastereoselectivity observed in all reactions indicates that the isomer ratio is not important for the stereoselectivity of the cycloaddition process.

Table 2.2: Evaluation of oxime and hydrazone substrates. *Yields in parentheses were obtained from a reaction on gram-scale.

2.68, 2.71–2.74

2.69, 2.75–2.78

2.59·PF₆

entry	substrate	<i>E/Z</i> ratio	yield	d.r.	
1		2.68	1.3:1	96% (91%)*	>20:1
2		2.71	1.3:1	96% (90%)*	16:1
3		2.72	1.1:1	54%	>20:1
4		2.73	2.6:1	62%	13:1
5		2.74	>20:1	0%	–

2.77

X-ray

Based on the high yields obtained with *O*-alkyl substituted oximes, this class of oximes was used for the subsequent evaluation of the substrate scope of the intramolecular aza Paternò-Büchi reaction (Figure 2.16). A series of electronically differentiated styrenes smoothly underwent the cycloaddition reaction in very good to excellent yields and stereoselectivities (**2.79–2.83**). Modifications to the substrate backbone were well tolerated and allowed for the incorporation of functional groups such as sulfonamides, esters or silyl ethers into the azetidine product (**2.84–2.88**). The reaction protocol was also found tolerant of oxime substrates derived from a corresponding ketone precursor, as products **2.89–2.91** could be isolated 74–97% yield. Notably, **2.91** contains a pyridine ring, which is a common motif found in pharmaceutical compounds. Lactone-containing azetidine **2.92** could be accessed in 60% yield and 14:1 d.r., although the reaction had to be conducted in acetonitrile at 80 °C to obtain sufficient reactivity.

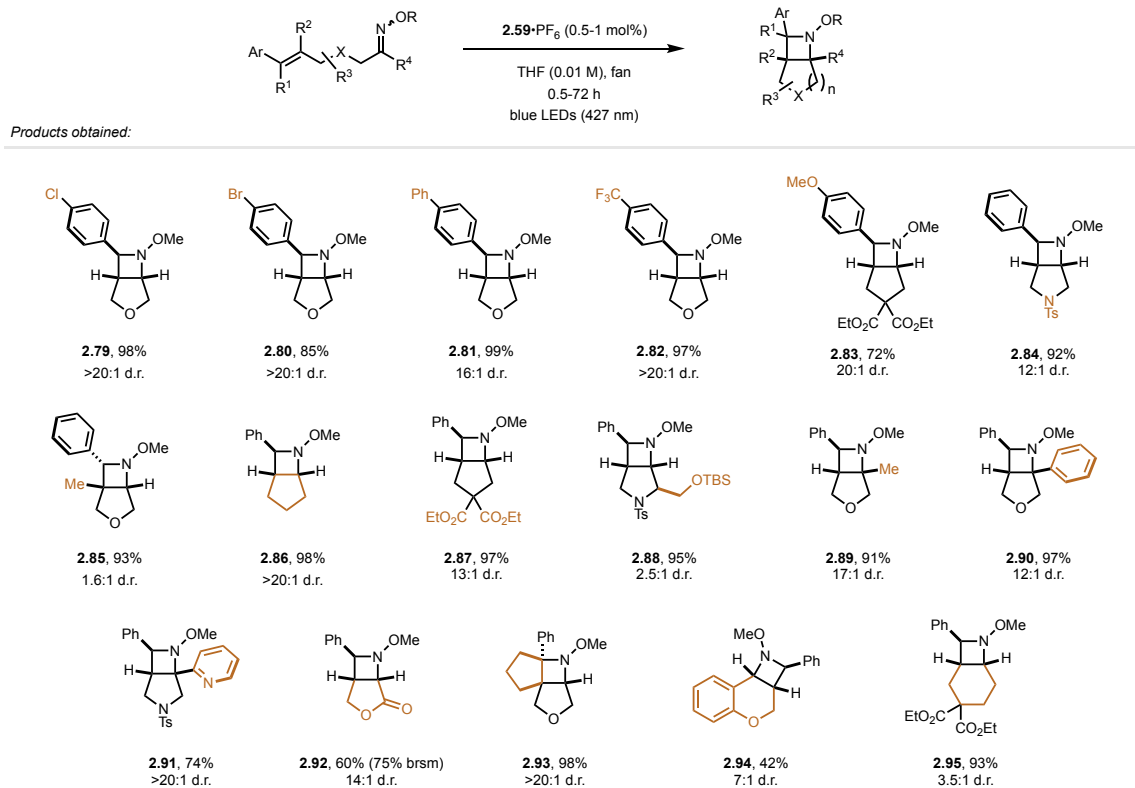


Figure 2.16: Scope of the developed intramolecular aza Paternò-Büchi reaction.

Furthermore, the reaction is amenable to tetrasubstituted styrenes (**2.93**) and also allows for the construction of six-membered rings, as azetidines **2.94** and **2.95** could be isolated in 42% and 93% yield, respectively. In light of the fact that many pharmaceutical or agrochemical products contain oxime or hydrazone motifs, we sought to demonstrate that the developed reaction protocol can be utilized for their late-stage modification. Therefore, oxime **2.97** was synthesized in two steps from herbicide safener isoxadifen ethyl (**2.96**) and submitted to the optimized conditions of the [2+2] photocycloaddition. The corresponding azetidine **2.98** could subsequently be isolated in 87% yield and 4:1 d.r. (Figure 2.17).

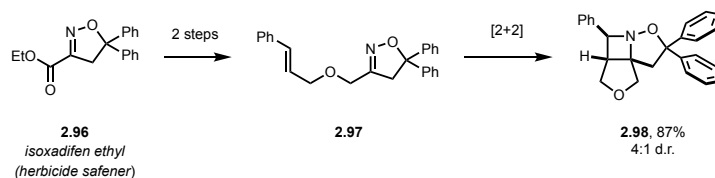


Figure 2.17: Modification of herbicide safener isoxadifen ethyl via an intramolecular aza Paternò-Büchi reaction.

Further investigations were focused on the compatibility of dienes as activated alkene components. These scaffolds possess similarly low triplet energies of approximately 60 kcal mol⁻¹ that are accessible for photocatalysts such as **2.59**•PF₆ via triplet energy transfer, as previously demonstrated by Yoon and coworkers.¹⁶⁸ Towards that goal, diene **2.99** was submitted to the optimized reaction conditions and smoothly underwent the desired cycloaddition reaction, providing azetidine **2.100** in 99% yield, although in diminished diastereoselectivity (Figure 2.18). Similarly, diene-containing cyclopentane **2.101** was identified as a viable substrate for this transformation and could be converted to strained bicycle **2.102** in 39% yield. Notably, both **2.100** and **2.102** contain an exocyclic alkene that could be potentially used for further synthetic modifications.

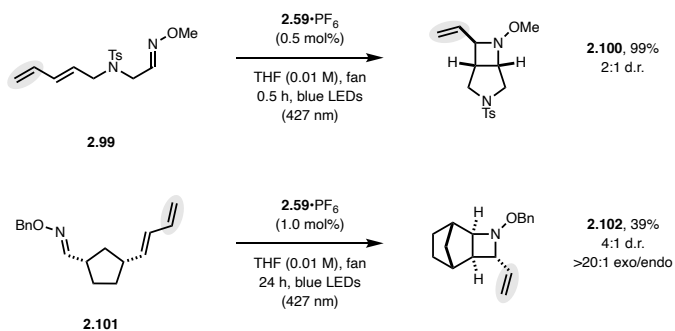


Figure 2.18: Intramolecular aza Paternò-Büchi reaction with dienes.

2.4. Mechanistic Studies

To corroborate the initially postulated mechanism proceeding via triplet energy transfer from the iridium catalyst to the styrene moiety of the substrate, a Stern-Volmer quenching study was carried out. Quenching of photocatalyst **2.59**•PF₆ was observed for substrate **2.68**, containing both a styrene and an oxime moiety (Figure 2.19). Similar quenching behavior was observed for **2.103** lacking the oxime moiety, indicating that this structural feature is not important for efficient quenching. In agreement with that observation, substrate **2.104** lacking a styrene moiety did not quench the photocatalyst.

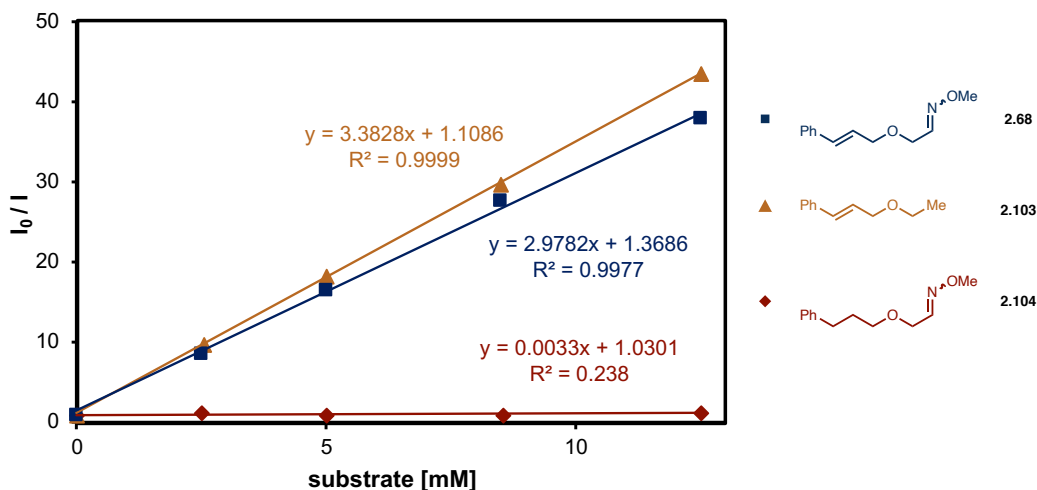
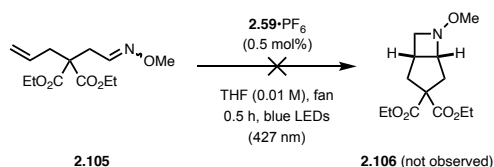


Figure 2.19: Stern-Volmer quenching study.

Furthermore, the quenching interaction is unlikely to result from a single electron transfer process considering that the redox properties of **2.59**•PF₆ ($E_{1/2}^{\text{III}^*/\text{III}} = +1.21$ V vs. SCE; $E_{1/2}^{\text{IV}/\text{III}^*} = -0.89$ V vs. SCE) are not sufficient to oxidize or reduce substrate **2.68** ($E_{\text{p}/2} = +1.82$ V vs SCE).¹⁶⁵ In contrast, triplet energy transfer from the iridium photocatalyst **2.59**•PF₆ ($E_{\text{T}} = 60.1$ kcal mol⁻¹) to the styrene moiety (E_{T} approx. 60 kcal mol⁻¹) is energetically favored, while the reaction efficiency decreases with photocatalysts with a triplet energy lower than 60 kcal mol⁻¹.

A. Control reaction with a terminal alkene.



B. Stereoconvergence of the intramolecular aza Paternò-Büchi reaction.

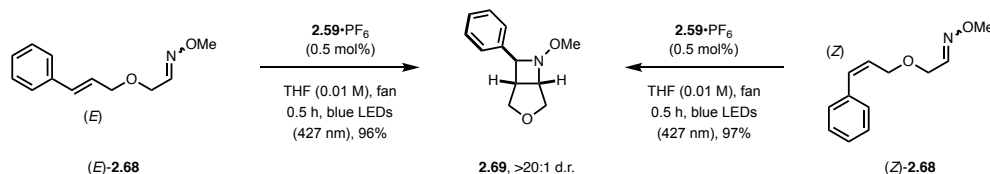


Figure 2.20: Control reactions demonstrating (A) the lack of reactivity of terminal alkenes, (B) the stereoconvergence of the developed [2+2] cycloaddition reaction.

Similarly, the reaction protocol is not compatible with alkenes possessing triplet energies higher than those of the photocatalyst. No reactivity was observed with terminal alkene **2.105**

under standard reaction conditions as a result of the high triplet energy ($E_T > 76 \text{ kcal mol}^{-1}$) that is inaccessible for photocatalyst **2.59**•PF₆ (Figure 2.20A).¹⁶⁶ Next, we tested whether the styrene geometry is influencing the diastereoselectivity of the intramolecular aza Paternò-Büchi reaction. Previous experiments had shown that (*E*)-**2.68** provided **2.69** in 96% yield and >20:1 d.r. (Table 2.2, entry 1). When the corresponding (*Z*)-**2.68** was subjected to identical reaction conditions, **2.69** was isolated in almost identical yield and diastereoselectivity, highlighting that the developed reaction is stereoconvergent (Figure 2.20B).

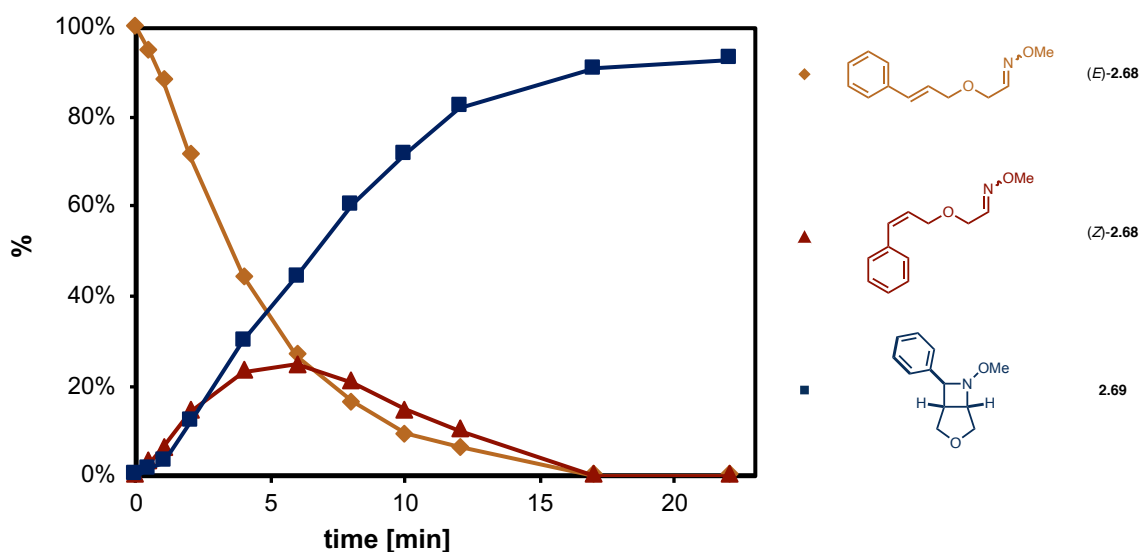


Figure 2.21: Monitoring *in situ* styrene *E/Z* isomerization by ¹H NMR.

Monitoring the reaction by ¹H NMR revealed rapid interconversion between both styrene isomers (Figure 2.21). Under standard reaction conditions, formation of (*Z*)-**2.68** occurs at a similar rate than product formation. However, both isomers are ultimately converted to product **2.69**. The same experiment also allowed to observe the change in oxime *E/Z* isomer ratio of substrate **2.68**, which was initially prepared as a 1.6:1 (*E/Z*) mixture of oxime isomers. Interestingly, scrambling of the oxime isomer ratio was observed when submitting **2.68** to standard reaction conditions. The ratio changed from 1.6:1 (*E/Z*) to 1:1 within a reaction time of two minutes (Figure 2.22). While the obtained data indicates that the *E*-isomer (*E*_O-**2.68**) reacts faster than *Z*_O-

2.68, it does not explain the overall increase in concentration of *Z*_O-**2.68**. Importantly, no oxime isomer scrambling was observed with oxime **2.104** lacking a styrene moiety.

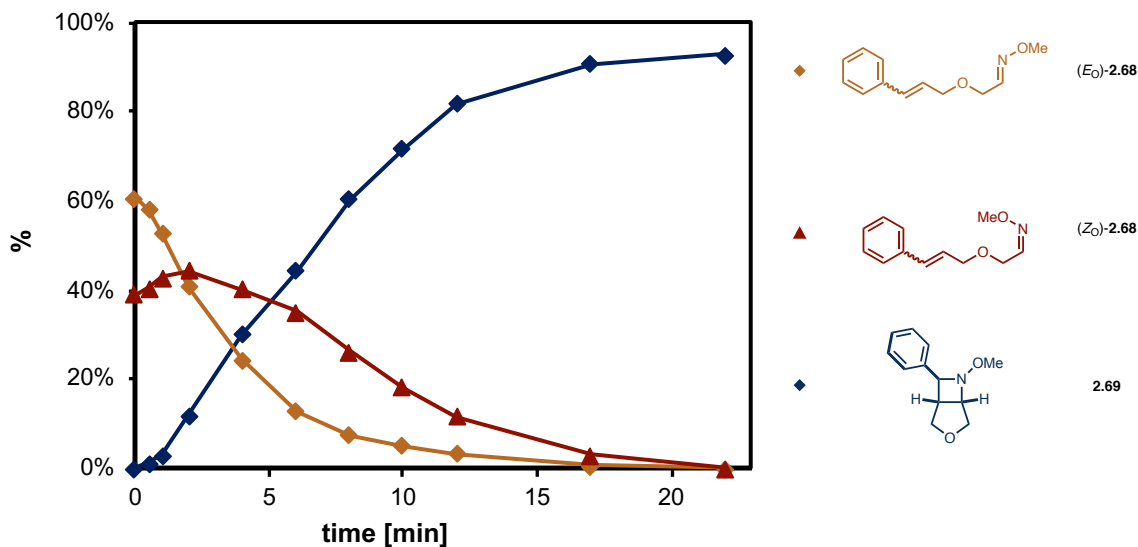


Figure 2.22: Monitoring *in situ* oxime *E/Z* isomerization by ¹H NMR.

Based on the conducted mechanistic experiments, a mechanistic proposal is outlined that starts out with efficient triplet energy transfer of the excited state iridium photocatalyst to the styrene moiety of **2.68** (Figure 2.23). The resulting triplet styrene (**2.107**) can subsequently undergo unproductive rotation around the carbon–carbon bond, which results in the observed *E/Z* styrene isomerization. Alternatively, the triplet styrene can undergo a stepwise [2+2] cycloaddition reaction with the oxime moiety. This step likely proceeds through an initial carbon–carbon bond formation to afford intermediate **2.108**, which can freely rotate around the carbon–nitrogen single bond. We propose that this step is reversible based on the observed oxime isomer scrambling, which can occur upon relaxation back to the ground state. Intermediate **2.108** can subsequently undergo intersystem crossing (ISC) to provide a highly reactive singlet state biradical (**2.109**) that will rapidly recombine to the final azetidine product (**2.69**). Due to the biradical nature of the involved triplet state intermediates, the stereoinformation of both the oxime and alkene component is lost during the course of the reaction. Consequently, the diastereoselectivity of the

intramolecular cycloaddition reaction is independent of both the starting oxime and styrene isomer ratio.

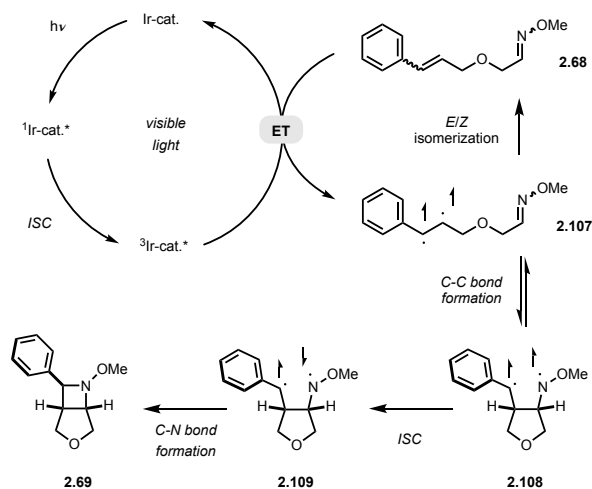


Figure 2.23: Proposed mechanism for the intramolecular aza Paternò-Büchi reaction. ET = energy transfer.

2.5. Synthetic Applications

We next sought to demonstrate the synthetic utility of the novel azetidine building blocks that are accessible via the developed intramolecular aza Paternò-Büchi reaction. Initial efforts focused on validating our initial hypothesis that the *N*-*O* bond can function as a readily removable protecting group. Common conditions for this type of reaction typically rely on zinc in acetic acid or palladium-mediated hydrogenolysis. While conditions relying on zinc in acetic acid did not provide any reactivity, we observed reduction of azetidine **2.75** with palladium on carbon under a hydrogen gas atmosphere. Interestingly, in addition to the desired nitrogen–oxygen bond cleavage, reduction of the benzylic carbon–nitrogen bond was also observed under these conditions, as tetrahydrofuran derivative **2.110** was isolated in 98% yield upon tosylation (Figure 2.24). In contrast, using zinc in hydrochloric acid resulted in selective cleavage of the nitrogen–oxygen bond to afford the deprotected azetidine **2.111** in 87% yield. Additionally, we could demonstrate that the 2-phenylazetidine motif of the cycloadducts can be converted to the corresponding azetidine-2-carboxylic acid. After changing the protecting group of azetidine **2.86** to the *N*-tosyl

derivative **2.112**, oxidation of the phenyl moiety was achieved using a RuO₄-oxidant system and azetidine carboxylic acid **2.113** isolated in 38% yield.¹⁶⁹ Finally, monocyclic azetidines can be accessed through reductive cleavage of azetidines containing a lactone functionality in the cyclic backbone. Utilizing LiAlH₄ resulted in efficient reduction of **2.92** to afford the corresponding diol **2.114** in 84% yield.

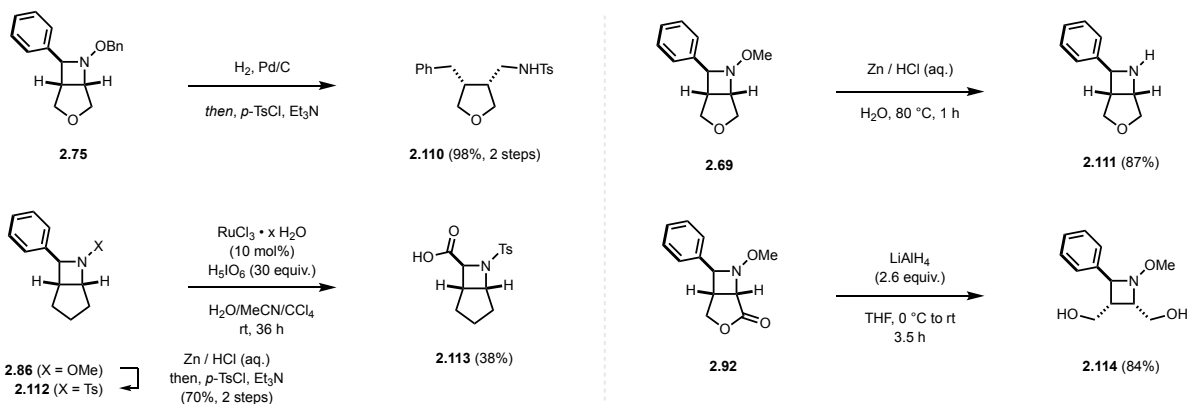


Figure 2.24: Synthetic modification of the accessible azetidine products.

2.6. Conclusion

In summary, an intramolecular aza Paternò-Büchi reaction was developed that proceeds under very mild conditions enabled by visible light triplet energy transfer catalysis. Previously reported procedures for aza Paternò-Büchi reactions rely on direct excitation with UV light, limiting the functional group tolerance in addition to the inherently challenging reactivity of excited state imines. This work circumvents these limitations through selective activation of the alkene component via triplet energy transfer from a commercially available iridium photocatalyst, which allowed for the synthesis of highly functionalized azetidine products in generally high yields (39–99%) and diastereoselectivities (2:1 to >20:1 d.r.). The developed reaction platform enables the synthesis of novel azetidine building blocks and is expected to advance the development of further photochemical [2+2] cycloaddition reactions with imines.

2.7. Experimental Section

2.7.1. General Information

General Laboratory Procedures. All air- or moisture-sensitive reaction were carried out in flame-dried glassware under an atmosphere of nitrogen. Thin-layer chromatography (TLC) was performed on Merck silica gel 60 F₂₅₄ plates using UV light (254 or 366 nm), KMnO₄ or CAM stain for visualization. Flash chromatography was performed using silica gel Silia Flash[®] 40-63 micron (230-400 mesh) from Silicycle unless noted.

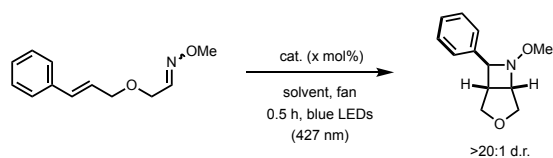
Materials and Instrumentation. All chemicals were purchased from Sigma-Aldrich, Alfa Aesar, Acros Organics, Oakwood, TCI America, Frontier Scientific, Matrix Scientific, Ark Pharm, Strem, and Chem Impex International, and were used as received unless otherwise stated. THF, CH₂Cl₂, Et₂O, MeOH, MeCN and DMF were dried by being passed through a column of activated alumina under argon using a JC-Meyer Solvent Systems. Triethylamine and diisopropylamine were freshly distilled prior to use over calcium hydride and potassium hydroxide, respectively. [Ir(dF(CF₃)ppy)₂(dtbbpy)]PF₆ (**2.59**•PF₆) was prepared according to the procedure described by Stephenson.¹⁷⁰ 2-Iodoxybenzoic acid (IBX) was prepared as described by Santagostino.¹⁷¹ Proton nuclear magnetic resonance (¹H NMR) spectra were recorded on Varian MR400, Varian vnmrs 500, Varian Inova 500, and Varian vnmrs 700 spectrometers and are referenced to residual protic NMR solvent (CDCl₃: δ 7.26 ppm, CD₂Cl₂: δ 5.32 ppm). Data for ¹H NMR are reported as follows: chemical shift (δ ppm), multiplicity (s = singlet, d = doublet, t = triplet, q = quartet, m = multiplet, br = broad), coupling constant (Hz), integration. Carbon nuclear magnetic resonance (¹³C NMR) spectra were recorded on Varian vnmrs 500 and Varian vnmrs 700 spectrometers and are referenced to the carbon resonances of the NMR solvent (CDCl₃: δ 77.16 ppm, CD₂Cl₂: δ 54.00 ppm). High-resolution mass spectroscopic (MS) data was recorded at the Mass

Spectrometry Facility at the Department of Chemistry of the University of Michigan in Ann Arbor, MI on an Agilent 6230 TOF HPLC-MS (ESI) or Micromass AutoSpec Ultima Magnetic Sector mass spectrometer (ESI, EI). Infrared (IR) spectra were obtained using a Thermo-Nicolet IS-50 spectrometer. IR data are represented as frequency of absorption (cm^{-1}). Stereochemistry indicators with asterisk (R^* , S^*) were used to indicate relative stereochemistry of diastereomers.

2.7.2. Reaction Optimization

A test tube was charged with **2.68** (21 mg, 0.1 mmol, 1.0 equiv.), photocatalyst and solvent, then sealed with a rubber septum and placed in front of a 40 W PR160-427 nm Kessil light at a distance of approximately 5 cm, which was set to 100% intensity (reactions involving UV light were carried out in a Luzchem LZG-ORG photoreactor). After stirring for 0.5 h, the reaction mixture was transferred to a 50-mL round-bottom flask and the solvent removed *in vacuo*. The crude reaction mixture was analyzed by ¹H NMR to determine the yield of **2.69** using mesitylene as the internal standard.

Table 2.3: Reaction optimization of the intramolecular aza Paternò-Büchi reaction.



entry	catalyst (mol%)	solvent	conc. (M)	yield
1 ^{a,b}	–	CH ₂ Cl ₂	0.01	6%
2 ^{b,c}	xanthone (30)	MeCN	0.01	43%
3	[Ru(bpy) ₃](PF ₆) ₂ (2.5)	THF	0.01	–
4	<i>fac</i> -[Ir(Fppy) ₃] (2.5)	THF	0.01	30%
5	<i>fac</i> -[Ir(ppy) ₃] (2.5)	THF	0.01	39%
6	<i>fac</i> -[Ir(dFppy) ₃] (2.5)	THF	0.01	52%
7	2.59 •PF ₆ (2.5)	THF	0.01	97%
8	2.59 •PF ₆ (2.5)	CH ₂ Cl ₂	0.025	72%
9	2.59 •PF ₆ (2.5)	MeOH	0.025	87%
10	2.59 •PF ₆ (2.5)	EtOAc	0.025	87%
11	2.59 •PF ₆ (2.5)	acetone	0.025	86%
12	2.59 •PF ₆ (2.5)	MeCN	0.025	88%
13	2.59 •PF ₆ (2.5)	THF	0.025	93%
14	2.59 •PF ₆ (2.5)	THF	0.05	88%
15	2.59 •PF ₆ (2.5)	THF	0.10	90%
16	2.59 •PF ₆ (1.0)	THF	0.01	96%
17	2.59 •PF ₆ (0.5)	THF	0.01	98%
18	–	THF	0.01	–
19 ^d	2.59 •PF ₆ (2.5)	THF	0.01	–

^afor 24 h; ^brun under UV light irradiation (365 nm); ^cfor 12 h; ^drun in the dark.

2.7.3. Mechanistic Experiments

Electrochemical Measurements

Cyclic voltammetry was performed on a CHI620E electrochemical analyzer (CH instruments) using a 3-mL five-necked electrochemical cell equipped with a carbon working electrode, a platinum counter or auxiliary electrode, an Ag/AgCl (3 M KCl) reference electrode and a scan rate of 100 mV/s. The experimental setup was calibrated using ferrocene (Fc^+/Fc) prior to each experiment. Samples were prepared with 0.03 mmol substrate in 3 mL $n\text{-Bu}_4\text{NPF}_6$ electrolyte (0.1 M in MeCN) and degassed by sparging with argon gas for 10 min prior to use. The potential ($E_{p/2}$) was determined and converted to SCE as described by Nicewicz.¹⁷²

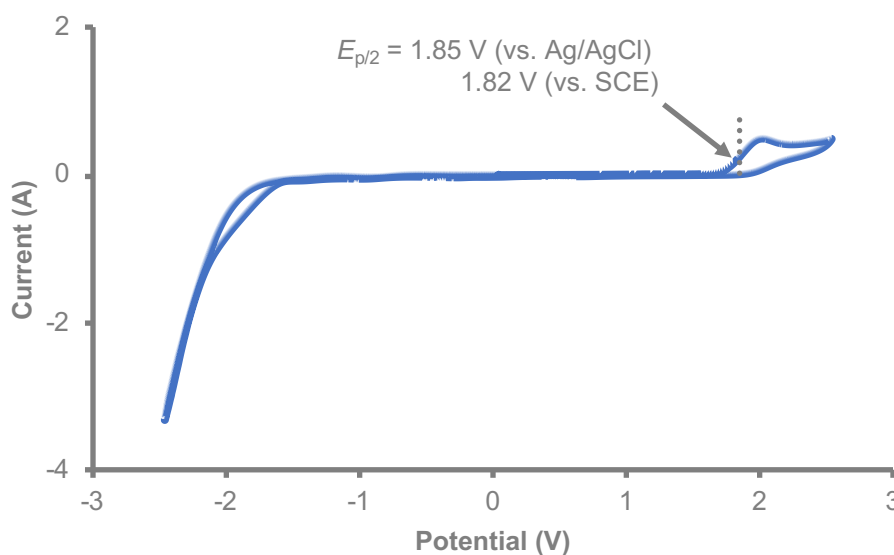


Figure 2.25: Cyclic voltammogram of compound (E)-2.68.

The cyclic voltammogram shows an irreversible oxidation process with $E_{p/2} = +1.82 \text{ V (vs. SCE)}$. $[\text{Ir}(\text{dF}(\text{CF}_3)\text{ppy})_2(\text{dtbbpy})]\text{PF}_6$ ($E_{1/2}^{\text{III}^*/\text{II}} = +1.21 \text{ V vs. SCE}$) does not possess an excited state oxidation potential sufficient to oxidize (E)-2.68, thus, a photoredox process is unlikely.¹⁵⁹

UV/Vis Absorption Spectra

UV/Vis absorption spectra were recorded on a Shimadzu UV-1601 UV/Vis spectrometer. Samples were prepared in THF with substrate (*E*)-**2.68** (10 mM) and photocatalyst **2.59**•PF₆ (0.05 mM).

The photocatalyst is the only species absorbing at 427 nm.

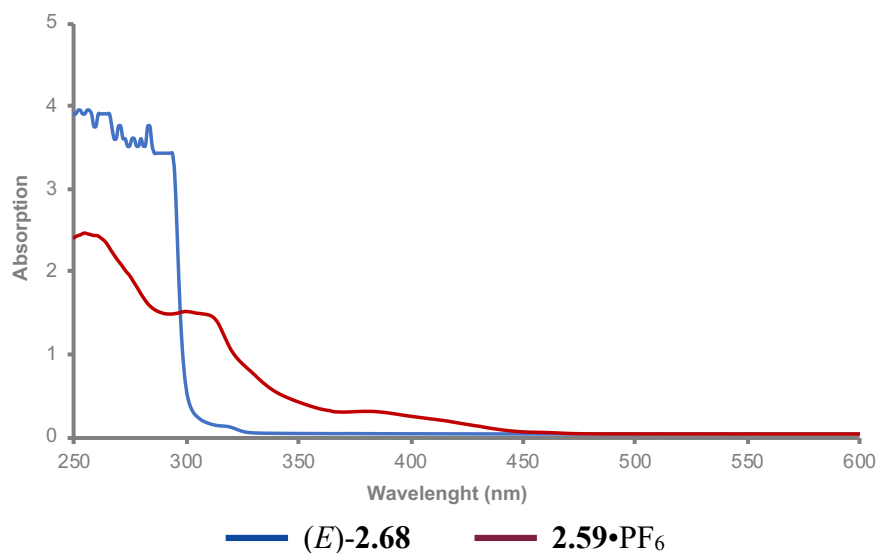


Figure 2.26: UV/Vis spectra of a representative reaction mixture.

Stern-Volmer Quenching Studies

All samples were prepared using stock solutions of **2.59**•PF₆ (0.11 mM), (*E*)-**2.68** (102.9 mM), (*E*)-**2.103** (144.8 mM) or **2.104** (102.4 mM) in dry MeCN. To a volumetric flask was added **2.59**•PF₆ (190 μL) with the respective amount of quencher and the volume adjusted to 4 mL with dry MeCN. The solution was transferred to a 1-cm quartz cuvette and degassed by sparging with nitrogen gas for 15 min. Emission spectra were recorded using a PTI QuantaMaster fluorimeter (Horiba) with an excitation wavelength of 420 nm. The emission intensities for the Stern-Volmer analysis were observed at 471 nm. The ratio of I₀/I was plotted as a function of the quencher concentration (I₀: emission intensity of **2.59**•PF₆ without quencher; I: emission intensity of **2.59**•PF₆ in the presence of quencher). The plotted data from the Stern-Volmer quenching studies is shown in Figure 2.19.

Table 2.4: Quenching data from the Stern-Volmer quenching study.

	0.0 mM	2.5 mM	5.0 mM	8.5 mM	12.5 mM
I ₀ / I (2.68)	1.0	8.7	16.4	27.7	37.8
I ₀ / I (2.103)	1.0	9.7	18.2	29.6	43.5
I ₀ / I (2.104)	1.0	1.1	1.0	1.0	1.1

NMR Time Study

A 1-dram vial was charged with (*E*)-**2.68** (6.2 mg, 0.03 mmol, 1.0 equiv.), **2.59**•PF₆ (0.2 mg, 0.5 mol%), dimethyl terephthalate (4.7 mg) and d₃-MeCN (3 mL). From the resulting solution 1 mL was transferred to a NMR tube, which was placed in front of a 40 W PR160-427 nm Kessil light (~5 cm distance) and the solution irradiated under ambient atmosphere at 50% light intensity. Conversion and yield were determined at several time points by quantitative ¹H NMR using dimethyl terephthalate as the internal standard. The plots displaying the concentrations of all reagents and reaction intermediates during the course of the reaction are shown in Figure 2.21 and Figure 2.22.

Table 2.5: Data from the NMR time study.

t (min)	% 2.68 (<i>E</i> -oxime)	% 2.68 (<i>Z</i> -oxime)	% 2.68 (<i>E</i> -styrene)	% 2.68 (<i>Z</i> -styrene)	% 2.69
0.0	61	39	100	0	0
0.5	58	41	95	3	1
1.0	53	43	88	6	3
2.0	41	44	71	14	12
4.0	24	40	44	23	30
6.0	13	35	27	25	44
8.0	8	26	17	21	60
10.0	5	18	9	15	72
12.0	3	12	6	10	82
17.0	1	3	0	0	91
22.0	0	0	0	0	93

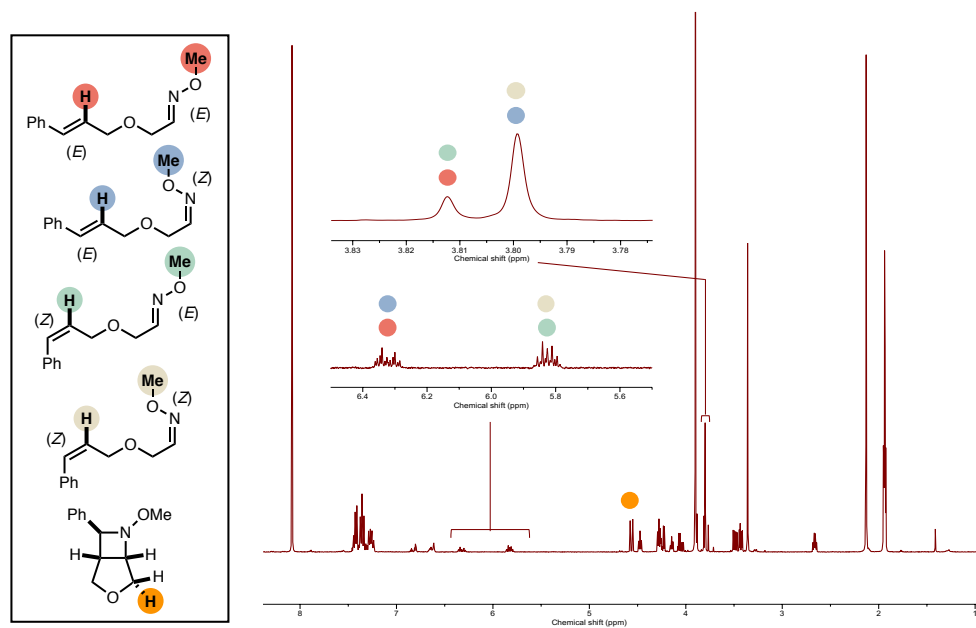
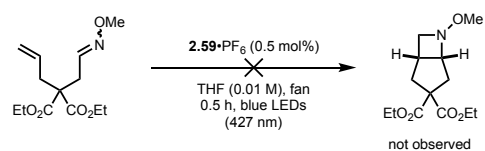


Figure 2.27: NMR signals utilized for the time study. The NMR spectra was obtained at $t = 8$ min.

Control Reactions

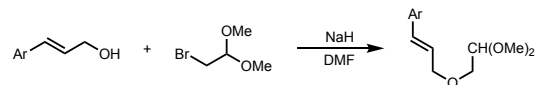


Reaction was carried out according to GP-2.6a on a 0.25 mmol scale. No formation of desired azetidine product was observed after 0.5 h, and only unreacted starting material was observed in the crude reaction mixture.

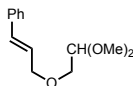
2.7.4. Experimental Procedures

Synthesis of Starting Materials and Characterization

General Procedure for Alkylation of Cinnamyl Alcohols (GP-2.1)

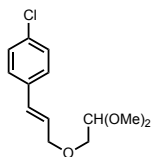


A round-bottom flask equipped with a magnetic stir bar was charged with NaH (60% dispersion in mineral oil; 1.5 equiv.) and dry DMF (0.5 M). The mixture was cooled to 0 °C and the corresponding cinnamyl alcohol was added slowly and the reaction mixture stirred for 1 h. Next, 2-bromo-1,1-dimethoxyethane (2.0 equiv.) was added and the reaction heated at 110 °C for 24 h. After cooling to rt, NH₄Cl solution (aq., sat.) and water were sequentially added, and the mixture extracted with EtOAc (3x). The combined organic extracts were washed with water (2x) and brine (2x), dried over Na₂SO₄, filtered and concentrated *in vacuo*. The crude product was purified by flash column chromatography (EtOAc/hexane) to afford the corresponding pure alkylated cinnamyl alcohol.



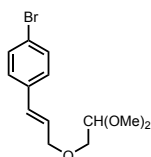
(E)-(3-(2,2-Dimethoxyethoxy)prop-1-en-1-yl)benzene (A2.1): Prepared according to GP-2.1 from (*E*)-cinnamyl alcohol (37.3 mmol). Purification by flash column chromatography (5–15% EtOAc/hexanes) afforded the pure title compound as a yellow oil (2.90 g, 35%).

¹H NMR (700 MHz, CDCl₃): δ 7.39 (d, *J* = 7.4 Hz, 2H), 7.32 (t, *J* = 7.6 Hz, 2H), 7.24 (t, *J* = 7.3 Hz, 1H), 6.61 (d, *J* = 15.9 Hz, 1H), 6.29 (dt, *J* = 15.9, 6.2 Hz, 1H), 4.56 (t, *J* = 5.2 Hz, 1H), 4.21 (dd, *J* = 6.2, 1.2 Hz, 2H), 3.54 (d, *J* = 5.2 Hz, 2H), 3.41 (s, 6H); **¹³C NMR** (176 MHz, CDCl₃): δ 136.7, 133.0, 128.7, 127.9, 126.7, 125.9, 102.9, 72.3, 69.8, 54.1; **IR** (cm⁻¹): 2936, 2834, 1724, 1450, 1366, 1312, 1194, 1111, 1067, 966, 841, 750, 697; **HRMS**: *m/z* calculated for C₁₃H₁₈O₃Na⁺ [M+Na]⁺: 245.1148; found: 245.1163.



(E)-1-Chloro-4-(3-(2,2-dimethoxyethoxy)prop-1-en-1-yl)benzene (A2.2): Prepared according to GP-2.1 from (*E*)-4-chlorocinnamyl alcohol¹⁷³ (5.7 mmol). Purification by flash column chromatography (5–20% EtOAc/hexanes) afforded the pure title compound as a yellow oil (482 mg, 33%).

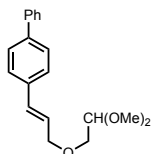
¹H NMR (500 MHz, CDCl₃): δ 7.31 (d, *J* = 8.7 Hz, 2H), 7.28 (d, *J* = 8.8 Hz, 2H), 6.56 (d, *J* = 15.9 Hz, 1H), 6.26 (dt, *J* = 15.9, 6.0 Hz, 1H), 4.55 (t, *J* = 5.2 Hz, 1H), 4.19 (dd, *J* = 6.0, 1.3 Hz, 2H), 3.54 (d, *J* = 5.2 Hz, 2H), 3.41 (s, 6H); **¹³C NMR** (126 MHz, CDCl₃): δ 135.3, 133.5, 131.6, 128.9, 127.8, 126.6, 102.9, 72.1, 70.0, 54.1; **IR** (cm⁻¹): 2909, 2831, 1491, 1447, 1193, 1112, 1090, 1012, 967, 849, 797; **HRMS**: *m/z* calculated for C₁₃H₁₇ClO₃Na⁺ [M+Na]⁺: 279.0758; found: 279.0760.



(E)-1-Bromo-4-(3-(2,2-dimethoxyethoxy)prop-1-en-1-yl)benzene (A2.3): Prepared according to GP-2.1 from (*E*)-4-bromocinnamyl alcohol¹⁷⁴ (4.7 mmol). Purification by flash column chromatography (5–20% EtOAc/hexanes) afforded the pure title compound as a yellow oil (433 mg, 31%).

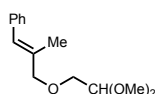
¹H NMR (400 MHz, CDCl₃): δ 7.43 (d, *J* = 8.4 Hz, 2H), 7.24 (d, *J* = 8.5 Hz, 2H), 6.55 (d, *J* = 15.9 Hz, 1H), 6.28 (dt, *J* = 15.9, 6.0 Hz, 1H), 4.55 (t, *J* = 5.2 Hz, 1H), 4.19 (dd, *J* = 6.0, 1.2 Hz, 2H), 3.54 (d, *J* = 5.2 Hz, 2H), 3.41 (s, 6H); **¹³C NMR** (176 MHz, CDCl₃): δ 135.7, 131.8, 131.7, 128.2, 126.8, 121.7, 102.9, 72.1, 70.0, 54.1; **IR** (cm⁻¹): 2928, 2831, 1488, 1401, 1323, 1201,

1114, 1072, 1009, 969, 848; **HRMS**: m/z calculated for $C_{13}H_{17}BrO_3Na^+$ $[M+Na]^+$: 323.0253; found: 323.0252.



(E)-4-(3-(2,2-Dimethoxyethoxy)prop-1-en-1-yl)-1,1'-biphenyl (A2.4): Prepared according to GP-2.1 from (*E*)-4-phenylcinnamyl alcohol¹⁷⁴ (5.6 mmol). Purification by flash column chromatography (5–20% EtOAc/hexanes) afforded the pure title compound as a pale-yellow foam (624 mg, 38%).

¹H NMR (700 MHz, $CDCl_3$): δ 7.60 (d, $J = 7.3$ Hz, 2H), 7.56 (d, $J = 8.2$ Hz, 2H), 7.48 – 7.42 (m, 4H), 7.34 (t, $J = 7.4$ Hz, 1H), 6.65 (d, $J = 15.9$ Hz, 1H), 6.34 (dt, $J = 15.9, 6.2$ Hz, 1H), 4.57 (t, $J = 5.2$ Hz, 1H), 4.23 (dd, $J = 6.1, 1.0$ Hz, 2H), 3.56 (d, $J = 5.2$ Hz, 2H), 3.42 (s, 6H); **¹³C NMR** (176 MHz, $CDCl_3$): δ 140.7, 140.6, 135.7, 132.5, 128.9, 127.4, 127.4, 127.1, 127.0, 125.9, 102.9, 72.3, 69.8, 54.1; **IR** (cm^{-1}): 2915, 2832, 1487, 1449, 1408, 1364, 1193, 1109, 1077, 971, 911, 853, 756, 731, 695; **HRMS**: m/z calculated for $C_{19}H_{22}O_3Na^+$ $[M+Na]^+$: 321.1461; found: 321.1466.



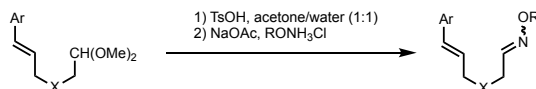
(E)-3-(2,2-dimethoxyethoxy)-2-methylprop-1-en-1-ylbenzene (A2.5): Prepared according to GP-2.1 from (*E*)-2-methyl-3-phenylprop-2-en-1-ol (6.8 mmol). Purification by flash column chromatography (5–20% EtOAc/hexanes) afforded the pure title compound as a yellow oil (530 mg, 33%).

¹H NMR (500 MHz, $CDCl_3$): δ 7.33 (t, $J = 7.6$ Hz, 2H), 7.28 (d, $J = 7.5$ Hz, 2H), 7.22 (t, $J = 7.2$ Hz, 1H), 6.50 (s, 1H), 4.56 (t, $J = 5.2$ Hz, 1H), 4.09 (s, 2H), 3.52 (d, $J = 5.2$ Hz, 2H), 3.42 (s, 6H), 1.90 (s, 3H); **¹³C NMR** (126 MHz, $CDCl_3$): δ 137.6, 135.0, 129.0, 128.2, 127.5, 126.6, 103.0,

77.8, 69.5, 54.0, 15.5; **IR** (cm⁻¹): 2911, 2831, 1445, 1358, 1110, 1072, 964, 918, 855, 746, 699;

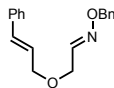
HRMS: *m/z* calculated for C₁₄H₂₀O₃Na⁺ [M+Na]⁺: 259.1305; found: 259.1308.

General Procedure for Oxime Synthesis from Acetals (GP-2.2)



A 100-mL round-bottom flask equipped with a magnetic stir bar was charged with the corresponding acetal (1.0 equiv.) and a 1:1 mixture (v/v) of water/acetone (0.1 M). *p*-TsOH (0.2 equiv.) was added and the reaction heated at 85 °C until complete as determined by TLC analysis (4–8 h). After cooling to rt, NaHCO₃ solution (aq., sat.) was added and the resulting mixture extracted with EtOAc (3x). The combined organic extracts were dried over Na₂SO₄, filtered, concentrated *in vacuo* and dried using high-vac.

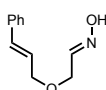
The crude aldehyde was dissolved in CH₂Cl₂ (0.1 M), before adding NaOAc (4.0 equiv.) and the corresponding hydroxylamine hydrochloride (2.0 equiv.). The mixture was stirred at rt until complete as judged by TLC analysis (4–18 h). NaHCO₃ solution (aq., sat.) was added, the organic layer separated, and the aqueous layer extracted with EtOAc (3x). The combined organic extracts were washed with brine, dried over Na₂SO₄, filtered and concentrated *in vacuo*. Purification by flash column chromatography (EtOAc/hexanes) afforded the corresponding pure oxime, typically as a mixture of *E/Z* oxime isomers.



2-(Cinnamyloxy)acetaldehyde *O*-benzyl oxime (2.71): Prepared according to GP-2.2 from **A2.1** (500 mg, 2.3 mmol, 1.0 equiv.) and *O*-benzylhydroxylamine hydrochloride (718 mg, 4.5 mmol, 2.0 equiv.). Purification by flash column chromatography (5–10% EtOAc/hexanes) afforded the pure title compound as a pale-yellow oil (444 mg, 70%; *E/Z* (oxime) = 1.3:1).

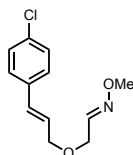
¹H NMR (700 MHz, CDCl₃): δ 7.56 (t, *J* = 5.7 Hz, 1.3H; major), 7.41 – 7.30 (m, 20.7H; major+minor), 7.28 – 7.24 (m, 2.3H; major+minor), 6.94 (t, *J* = 3.6 Hz, 1H; minor), 6.61 (dd, *J* = 18.9, 16.1 Hz, 2.3H; major+minor), 6.27 (dq, *J* = 15.9, 6.1 Hz, 2.3H; major+minor), 5.12 (d, *J* =

3.3 Hz, 4.6H; major+minor), 4.37 (d, $J = 3.6$ Hz, 2H; minor), 4.17 (ddd, $J = 12.0, 6.1, 1.3$ Hz, 4.6H; major+minor), 4.14 (d, $J = 5.7$ Hz, 2.6H; major); $^{13}\text{C NMR}$ (176 MHz, CDCl_3): δ 150.9, 147.7, 137.7, 137.5, 136.7, 136.6, 133.4, 133.3, 128.72, 128.70, 128.57, 128.56, 128.4, 128.2, 128.10, 128.08, 127.99, 127.95, 126.68, 126.67, 125.3, 125.2, 76.4, 76.2, 71.9, 71.2, 66.8, 64.6; **IR** (cm^{-1}): 3028, 2851, 1495, 1453, 1365, 1107, 1013, 966, 914, 842, 733, 691; **HRMS**: m/z calculated for $\text{C}_{18}\text{H}_{19}\text{NO}_2\text{Na}^+$ $[\text{M}+\text{Na}]^+$: 304.1308; found: 304.1312.



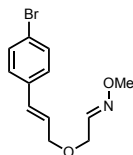
2-(Cinnamyloxy)acetalddehyde oxime (2.72): Prepared according to GP-2.2 from **A2.1** (500 mg, 2.3 mmol, 1.0 equiv.) and hydroxylamine hydrochloride (313 mg, 4.5 mmol, 2.0 equiv.). Purification by flash column chromatography (10–30% EtOAc/hexanes) afforded the pure title compound as a pale-yellow oil (287 mg, 67%; E/Z (oxime) = 1.1:1).

$^1\text{H NMR}$ (700 MHz, CDCl_3): δ 8.13 (b, 1H; minor), 7.85 (b, 1.1H; major), 7.54 (t, $J = 5.6$ Hz, 1.1H; major), 7.41 – 7.38 (m, 4.2H; major+minor), 7.34 – 7.30 (m, 4.2H; major+minor), 7.27 – 7.23 (m, 2.1H; major+minor), 6.96 (t, $J = 3.7$ Hz, 1H; minor), 6.63 (dd, $J = 15.9, 9.8$ Hz, 2.1H; major+minor), 6.28 (dq, $J = 15.9, 6.2$ Hz, 2.1H; major+minor), 4.40 (d, $J = 3.7$ Hz, 2H; minor), 4.19 (ddd, $J = 9.7, 6.1, 1.3$ Hz, 4.2H; major+minor), 4.15 (d, $J = 5.6$ Hz, 2.2H; major); $^{13}\text{C NMR}$ (176 MHz, CDCl_3): δ 151.5, 148.7, 136.61, 136.57, 133.5, 133.4, 128.73, 128.71, 128.02, 127.99, 126.69, 126.68, 125.24, 125.15, 72.0, 71.3, 66.7, 64.0; **IR** (cm^{-1}): 3203, 3027, 2868, 1448, 1395, 1348, 1284, 1116, 967, 920, 829, 731, 689; **HRMS**: m/z calculated for $\text{C}_{11}\text{H}_{13}\text{NO}_2\text{H}^+$ $[\text{M}+\text{H}]^+$: 192.1019; found: 192.1026.



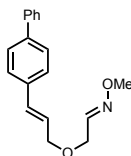
2-(((E)-3-(4-Chlorophenyl)allyl)oxy)acetaldehyde O-methyl oxime (S2.79): Prepared according to GP-2.2 from **A2.2** (438 mg, 1.7 mmol, 1.0 equiv.) and *O*-methylhydroxylamine hydrochloride (285 mg, 3.4 mmol, 2.0 equiv.). Purification by flash column chromatography (5–10% EtOAc/hexanes) afforded the pure title compound as a colorless oil (312 mg, 76%; *E/Z* (oxime) = 1.5:1).

¹H NMR (500 MHz, CDCl₃): δ 7.46 (t, *J* = 5.7 Hz, 1.5H; major), 7.33 – 7.27 (m, 10H; major+minor), 6.86 (t, *J* = 3.9 Hz, 1H; minor), 6.58 (d, *J* = 15.9 Hz, 2.5H; major+minor), 6.25 (dt, *J* = 15.9, 6.0 Hz, 2.5H; major+minor), 4.31 (d, *J* = 3.7 Hz, 2H; minor), 4.16 (d, *J* = 6.0 Hz, 5H; major+minor), 4.12 (d, *J* = 5.7 Hz, 3H; major), 3.89 – 3.86 (m, 7.5H; major+minor); **¹³C NMR** (126 MHz, CDCl₃): δ 150.0, 146.9, 135.13, 135.07, 133.6, 133.5, 131.82, 131.80, 128.9, 128.8, 127.82, 127.81, 126.1, 126.0, 71.6, 71.0, 66.9, 64.5, 62.2, 61.8; **IR** (cm⁻¹): 2938, 2899, 1491, 1464, 1359, 1089, 1040, 1012, 967, 846, 796; **HRMS**: *m/z* calculated for C₁₂H₁₄ClNO₂Na⁺ [M+Na]⁺: 262.0605; found: 262.0603.



2-(((E)-3-(4-Bromophenyl)allyl)oxy)acetaldehyde O-methyl oxime (S2.80): Prepared according to GP-2.2 from **A2.3** (434 mg, 1.4 mmol, 1.0 equiv.) and *O*-methylhydroxylamine hydrochloride (241 mg, 2.9 mmol, 2.0 equiv.). Purification by flash column chromatography (5–10% EtOAc/hexanes) afforded the pure title compound as a colorless foam (308 mg, 75%; *E/Z* (oxime) = 1.3:1).

¹H NMR (700 MHz, CDCl₃): δ 7.46 (t, *J* = 5.7 Hz, 1.3H; major), 7.45 – 7.42 (m, 4.6H; major+minor), 7.27 – 7.23 (m, 4.6H; major+minor), 6.86 (t, *J* = 3.7 Hz, 1H; minor), 6.56 (dd, *J* = 15.9, 3.8 Hz, 2.3H; major+minor), 6.26 (dt, *J* = 15.9, 6.0 Hz, 2.3H; major+minor), 4.31 (d, *J* = 3.7 Hz, 2H; minor), 4.17 – 4.15 (m, 4.6H; major+minor), 4.12 (d, *J* = 5.7 Hz, 2.6H; major), 3.87 (d, *J* = 0.7 Hz, 6.9H; major+minor); **¹³C NMR** (176 MHz, CDCl₃): δ 150.0, 146.9, 135.6, 135.5, 131.9, 131.83, 131.80, 131.79, 128.14, 128.13, 126.2, 126.1, 121.74, 121.70, 71.6, 71.0, 66.9, 64.5, 62.2, 61.8; **IR** (cm⁻¹): 2937, 2851, 1487, 1401, 1358, 1109, 1072, 1040, 1008, 966, 844, 793; **HRMS**: *m/z* calculated for C₁₂H₁₄BrNO₂Na⁺ [M+Na]⁺: 306.0100; found: 306.0107.

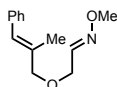


2-(((*E*)-3-((1,1'-Biphenyl)-4-yl)allyl)oxy)acetaldehyde *O*-methyl oxime (S2.81): Prepared according to GP-2.2 from **A2.4** (497 mg, 1.7 mmol, 1.0 equiv.) and *O*-methylhydroxylamine hydrochloride (278 mg, 3.3 mmol, 2.0 equiv.). Purification by flash column chromatography (5–10% EtOAc/hexanes) afforded the pure title compound as a colorless solid (364 mg, 78%; *E/Z* (oxime) = 1.1:1).

¹H NMR (700 MHz, CDCl₃): δ 7.60 (d, *J* = 7.4 Hz, 4.2H; major+minor), 7.57 (dd, *J* = 8.3, 2.8 Hz, 4.2H; major+minor), 7.50 – 7.42 (m, 9.5H; major+minor), 7.36 – 7.33 (m, 2.1H; major+minor), 6.88 (t, *J* = 3.7 Hz, 1H; minor), 6.69 – 6.64 (m, 2.1H; major+minor), 6.32 (dtd, *J* = 15.9, 6.1, 1.4 Hz, 2.1H; major+minor), 4.33 (d, *J* = 3.7 Hz, 2H; minor), 4.22 – 4.19 (m, 4.2H; major+minor), 4.14 (d, *J* = 5.7 Hz, 2.2H; major), 3.88 (d, *J* = 1.0 Hz, 6.3H; major+minor); **¹³C NMR** (176 MHz, CDCl₃): δ 150.2, 147.0, 140.74 (2C), 140.72, 140.69, 135.7, 135.6, 132.84, 132.82, 128.9 (2C), 127.48, 127.46, 127.39, 127.37, 127.09, 127.08, 127.05 (2C), 125.4, 125.3, 71.9, 71.3, 66.8, 64.4,

62.2, 61.9; **IR** (cm⁻¹): 2940, 2848, 1486, 1448, 1349, 1264, 1104, 1042, 967, 851, 754, 689;

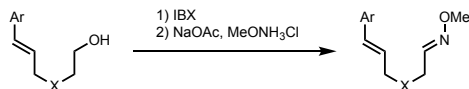
HRMS: *m/z* calculated for C₁₈H₁₉NO₂Na⁺ [M+Na]⁺: 304.1308; found: 304.1301.



2-(((E)-2-Methyl-3-phenylallyl)oxy)acetaldehyde O-methyl oxime (S2.85): Prepared according to GP-2.2 from **A2.5** (499 mg, 2.1 mmol, 1.0 equiv.) and *O*-methylhydroxylamine hydrochloride (353 mg, 4.2 mmol, 2.0 equiv.). Purification by flash column chromatography (5–10% EtOAc/hexanes) afforded the pure title compound as a pale-yellow oil (407 mg, 88%; *E/Z* (oxime) = 1.4:1).

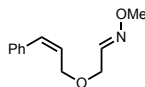
¹H NMR (500 MHz, CDCl₃): δ 7.48 (t, *J* = 5.7 Hz, 1.4H; major), 7.34 (td, *J* = 7.7, 2.0 Hz, 4.8H; major+minor), 7.28 (dd, *J* = 6.7, 3.8 Hz, 4.8H; major+minor), 7.23 (dt, *J* = 8.7, 3.8 Hz, 2.4H, major+minor), 6.88 (t, *J* = 3.6 Hz, 1H; minor), 6.52 (s, 2.4H; major+minor), 4.29 (d, *J* = 3.7 Hz, 2H; minor), 4.11 (d, *J* = 5.7 Hz, 2.8H; major), 4.06 (s, 4.8H; major+minor), 3.88 (d, *J* = 1.6 Hz, 7.2H; major+minor), 1.92 – 1.87 (m, 7.2H; major+minor); **¹³C NMR** (176 MHz, CDCl₃): δ 150.2, 147.1, 137.42, 137.36, 134.5, 134.4, 129.00, 128.99, 128.22, 128.20, 127.8, 127.7, 126.70, 126.65, 77.4, 76.9, 66.6, 64.1, 62.1, 61.8, 15.6, 15.5; **IR** (cm⁻¹): 2938, 2900, 144, 1351, 1091, 1039, 918, 848, 744, 697; **HRMS**: *m/z* calculated for C₁₃H₁₇NO₂H⁺ [M+H]⁺: 220.1332; found: 220.1333.

General Procedure for Oxime Synthesis from Alcohols (GP-2.3)



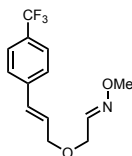
A 25-mL round-bottom flask equipped with a magnetic stir bar was charged with the corresponding alcohol (1.0 equiv.) and DMSO (0.3 M). IBX (1.5 equiv.) was added and the mixture stirred at rt until complete as judged by TLC analysis (4–18 h). Water was added to the reaction mixture and precipitated solids removed by filtration through a pad of celite. After washing the filter cake with Et₂O, the filtrate was collected, the organic layer separated and the aqueous layer extracted with Et₂O (3x). The combined organic extracts were washed with water (2x) and brine (2x), dried over MgSO₄, filtered, concentrated *in vacuo* and dried using high-vac.

The crude aldehyde was dissolved in CH₂Cl₂ (0.1 M), before adding NaOAc (4.0 equiv.) and the respective hydroxylamine hydrochloride (2.0 equiv.). The mixture was stirred at rt until complete as judged by TLC analysis (4–18 h). NaHCO₃ solution (aq., sat.) was added, the organic layer separated and the aqueous layer extracted with EtOAc (3x). The combined organic layers were washed with brine, dried over Na₂SO₄, filtered and concentrated *in vacuo*. Purification by flash column chromatography (EtOAc/hexanes) afforded the corresponding pure oxime, typically as a mixture of *E/Z* oxime isomers.



2-(((*Z*)-3-Phenylallyl)oxy)acetaldehyde *O*-methyl oxime ((*Z*)-2.68): Prepared according to GP-2.3 from **A2.6** (207 mg, 1.2 mmol, 1.0 equiv.) and *O*-methylhydroxylamine hydrochloride (194 mg, 2.3 mmol, 2.0 equiv.). Purification by flash column chromatography (20–30% EtOAc/hexanes) afforded the pure title compound as a colorless oil (84 mg, 35%; *E/Z* (oxime) = 1.3:1).

¹H NMR (700 MHz, CDCl₃): δ 7.43 (t, *J* = 5.7 Hz, 1.3H; major), 7.35 (t, *J* = 7.6 Hz, 4.6H; major+minor), 7.29 – 7.26 (m, 2.3H; major+minor), 7.20 (d, *J* = 7.4 Hz, 4.6H; major+minor), 6.84 (t, *J* = 3.7 Hz, 1H; minor), 6.64 (dd, *J* = 11.8, 4.9 Hz, 2.3H; major+minor), 5.86 – 5.81 (m, 2.3H; major+minor), 4.29 – 4.27 (m, 6.6H; major+minor), 4.09 (d, *J* = 5.7 Hz, 2.6H; major), 3.86 (s, 3H; minor), 3.84 (s, 3.9H; major); **¹³C NMR** (176 MHz, CDCl₃): δ 150.2, 147.0, 136.59, 136.55, 132.5, 132.4, 128.89, 128.87, 128.41, 128.40, 128.3, 128.2, 127.5, 127.4, 68.0, 67.4, 67.1, 64.7, 62.2, 61.8; **IR** (cm⁻¹): 2938, 1494, 1447, 1340, 1098, 1041, 866, 851, 772, 698; **HRMS**: *m/z* calculated for C₁₂H₁₅NO₂Na⁺ [*M*+Na]⁺: 228.0995; found: 228.0995.

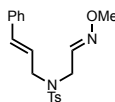


2-(((*E*)-3-(4-(Trifluoromethyl)phenyl)allyl)oxy)acetaldehyde *O*-methyl oxime (S2.82):

Prepared according to GP-2.3 from **A2.7** (437 mg, 1.8 mmol, 1.0 equiv.) and *O*-methylhydroxylamine hydrochloride (296 mg, 3.6 mmol, 2.0 equiv.). Purification by flash column chromatography (5–10% EtOAc/hexanes) afforded the pure title compound as a colorless solid (343 mg, 71%; *E/Z* (oxime) = 1.4:1).

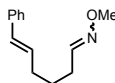
¹H NMR (700 MHz, CDCl₃): δ 7.57 (dd, *J* = 8.2, 2.8 Hz, 4.8H; major+minor), 7.49 – 7.45 (m, 6.2H; major+minor), 6.87 (t, *J* = 3.7 Hz, 1H; minor), 6.66 (dd, *J* = 16.0, 4.1 Hz, 2.4H; major+minor), 6.36 (dt, *J* = 16.0, 5.8 Hz, 2.4H; major+minor), 4.32 (d, *J* = 3.7 Hz, 2H; minor), 4.20 (d, *J* = 5.8 Hz, 4.8H; major+minor), 4.14 (d, *J* = 5.7 Hz, 2.8H; major), 3.88 (s, 7.2H; major+minor); **¹³C NMR** (176 MHz, CDCl₃): δ 149.9, 146.8, 140.2, 140.1, 131.3, 131.2, 129.7 (q, *J* = 32.4 Hz), 129.6 (q, *J* = 32.4 Hz), 128.3, 128.1, 126.73, 126.72, 125.7 – 125.5 (m, 2C), 124.3 (q, *J* = 271.9 Hz, 2C), 71.4, 70.8, 67.0, 64.6, 62.1, 61.8; **IR** (cm⁻¹): 2943, 1615, 1323, 1106, 1066,

1040, 1016, 967, 854, 821, 728, 651; **HRMS**: m/z calculated for $C_{13}H_{14}F_3NO_2H^+$ $[M+H]^+$: 274.1049; found: 274.1044.



***N*-Cinnamyl-*N*-(2-(methoxyimino)ethyl)-4-methylbenzenesulfonamide (S.84)**: Prepared according to GP-2.3 from *N*-cinnamyl-*N*-(2-hydroxyethyl)-4-methylbenzenesulfonamide¹⁷⁵ (700 mg, 2.1 mmol, 1.0 equiv.) and *O*-methylhydroxylamine hydrochloride (353 mg, 4.2 mmol, 2.0 equiv.). Purification by flash column chromatography (10–30% EtOAc/hexanes) afforded the pure title compound as a colorless oil (371 mg, 49%; *E/Z* (oxime) = 1.2:1).

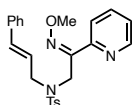
¹H NMR (700 MHz, $CDCl_3$): δ 7.73 (d, $J = 7.6$ Hz, 4.4H; major+minor), 7.34 – 7.28 (m, 8.8H; major+minor), 7.27 (d, $J = 7.4$ Hz, 4.4H; major+minor), 7.26 – 7.23 (m, 2.2H; major+minor), 7.21 (t, $J = 5.9$ Hz, 1.2H; major), 6.65 (t, $J = 4.3$ Hz, 1H; minor), 6.45 (d, $J = 15.7$ Hz, 2.2H; major+minor), 6.01 – 5.93 (m, 2.2H; major+minor), 4.04 (d, $J = 4.3$ Hz, 2H; minor), 3.96 (dd, $J = 9.6, 7.0$ Hz, 4.4H; major+minor), 3.93 (d, $J = 5.9$ Hz, 2.4H; major), 3.79 (s, 3H; minor), 3.77 (s, 3.6H; major), 2.44 (s, 3H; minor), 2.43 (s, 3.6H; major); **¹³C NMR** (176 MHz, $CDCl_3$): δ 147.9, 145.6, 143.9, 143.8, 137.0, 136.5, 136.3, 136.1, 135.0, 134.9, 130.1, 130.0, 128.74, 128.69, 128.2, 128.1, 127.43, 127.43, 126.7, 126.6, 123.3, 123.0, 62.2, 61.9, 51.5, 50.0, 45.9, 42.9, 21.7, 21.6; **IR** (cm^{-1}): 2937, 1597, 1495, 1448, 1337, 1156, 1089, 1030, 968, 897, 814, 731, 654; **HRMS**: m/z calculated for $C_{19}H_{22}N_2O_3SNa^+$ $[M+Na]^+$: 381.1243; found: 381.1245.



(5*E*)-6-Phenylhex-5-enal *O*-methyl oxime (S2.86): Prepared according to GP-2.3 from 6-phenylhex-5-en-1-ol¹⁷⁶ (763 mg, 4.3 mmol, 1.0 equiv.; *E/Z* = 2.6:1) and *O*-methylhydroxylamine hydrochloride (723 mg, 8.7 mmol, 2.0 equiv.) Purification by flash column chromatography (2–

10% EtOAc/hexanes) afforded the pure title compound as a colorless oil (797 mg, 91%; *E/Z* (styrene) = 2.6:1; *E/Z* (oxime) = 1.5:1). Characterization data is provided for the two major (*E*)-styrene isomers.

¹H NMR (700 MHz, CDCl₃): δ 7.39 (t, *J* = 6.2 Hz, 1.5H; major), 7.36 – 7.30 (m, 5H; major+minor), 7.31 – 7.27 (m, 5H; major+minor), 7.24 – 7.18 (m, 2.5H; major+minor), 6.66 (t, *J* = 5.5 Hz, 1H; minor), 6.40 (d, *J* = 15.8 Hz, 2.5H; major+minor), 6.19 (dtd, *J* = 15.6, 6.9, 1.5 Hz, 2.5H; major+minor), 3.87 (s, 3H; minor), 3.82 (s, 4.5H; major), 2.41 – 2.32 (m, 4H; minor), 2.29 – 2.19 (m, 6H; major), 1.71 – 1.60 (m, 5H; major+minor)¹⁷; **¹³C NMR** (176 MHz, CDCl₃): δ 151.5, 151.4, 150.6, 150.5, 137.74, 137.73, 137.6 (2C), 131.9 (2C), 130.80, 130.79, 129.84 (2C), 129.81, 129.76, 128.8 (2C), 128.62, 128.62, 128.3 (2C), 127.1 (2C), 126.74, 126.73, 126.1 (2C), 61.71, 61.69, 61.4, 61.3, 32.7, 32.5, 29.2, 29.1, 28.4, 28.1, 27.1, 26.64, 26.56, 26.1, 25.4, 25.2; **IR** (cm⁻¹): 3024, 2936, 1493, 1448, 1047, 964, 917, 883, 847, 803, 741, 692; **HRMS**: *m/z* calculated for C₁₃H₁₇NOH⁺ [M+H]⁺: 204.1383; found: 204.1376.

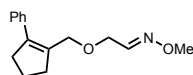


***N*-Cinnamyl-*N*-((*Z*)-2-(methoxyimino)-2-(pyridin-2-yl)ethyl)-4-methylbenzenesulfonamide**

(S2.91): Prepared according to GP-2.3 from **A2.8** (225 mg, 0.55 mmol, 1.0 equiv.) and *O*-methylhydroxylamine hydrochloride (92 mg, 1.1 mmol, 2.0 equiv.). The oxime formation was carried out in methanol (5 mL) at reflux for 16 h. Purification by flash column chromatography (10–60% EtOAc/hexanes) afforded the pure title compound as a colorless oil (602 mg, 64%; *E/Z* (oxime) = 1:1.3).

¹H NMR (500 MHz, CDCl₃): δ 8.58 (d, *J* = 4.8 Hz, 1H; minor), 8.54 (d, *J* = 4.3 Hz, 1.3H; major), 7.74 – 7.60 (m, 8.2H; major+minor), 7.57 (d, *J* = 7.9 Hz, 1H; minor), 7.32 – 7.14 (m, 18.4H;

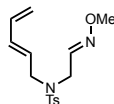
major+minor), 6.43 (d, $J = 15.8$ Hz, 1H; minor), 6.32 (d, $J = 15.9$ Hz, 1.3H; major), 5.94 (ddt, $J = 15.9, 11.2, 6.7$ Hz, 2.3H; major+minor), 4.62 (s, 2.6H; major), 4.47 (s, 2H; minor), 3.99 – 3.96 (m, 8.5H; major+minor), 3.83 (s, 3H; minor), 2.41 (s, 6.9H; major+minor); $^{13}\text{C NMR}$ (176 MHz, CDCl_3): δ 154.2, 152.9, 151.7, 149.7, 149.2, 148.8, 143.3, 143.1, 137.05, 137.03, 136.53, 136.46, 136.4, 135.7, 134.2, 133.7, 129.52, 129.51, 128.6, 128.5, 127.9, 127.8, 127.6, 127.5, 126.51, 126.45, 126.21, 124.2, 124.1, 123.9, 123.8, 122.0, 62.7, 62.5, 51.4, 50.4, 49.1, 40.4, 21.6, 21.5; **IR** (cm^{-1}): 2936, 2821, 1598, 1566, 1582, 1495, 1435, 1339, 1156, 1091, 1044, 994, 997, 906, 814, 729, 692, 667, 650; **HRMS**: m/z calculated for $\text{C}_{24}\text{H}_{25}\text{N}_3\text{O}_3\text{SH}^+$ $[\text{M}+\text{H}]^+$: 436.1689; found: 436.1687.



(2-((2-Phenylcyclopent-1-en-1-yl)methoxy)acetaldehyde O-methyl oxime (S2.93): Prepared according to GP-2.3 from **A2.9** (834 mg, 3.8 mmol, 1.0 equiv.) and *O*-methylhydroxylamine hydrochloride (638 mg, 7.6 mmol, 2.0 equiv.) Purification by flash column chromatography (0–10% EtOAc/hexanes) afforded the pure title compound as a colorless oil (602 mg, 64%; *E/Z* (oxime) = 1:1.6).

$^1\text{H NMR}$ (700 MHz, CDCl_3): δ 7.42 (t, $J = 5.8$ Hz, 1H; minor), 7.34 (t, $J = 7.6$ Hz, 5.2H; major+minor), 7.27 – 7.25 (m, 2.6H; major+minor), 7.24 – 7.21 (m, 5.2H; major+minor), 6.83 (t, $J = 3.6$ Hz, 1.6H; major), 4.22 (d, $J = 3.6$ Hz, 3.2H; major), 4.14 (d, $J = 5.2$ Hz, 5.2H; major+minor), 4.02 (d, $J = 5.8$ Hz, 2H; minor), 3.85 (s, 4.8H; major), 3.83 (s, 3H; minor), 2.81 – 2.77 (m, 5.2H; major+minor), 2.66 – 2.61 (m, 5.2H; major+minor), 2.00 – 1.94 (m, 5.2H; major+minor); $^{13}\text{C NMR}$ (176 MHz, CDCl_3): δ 150.5, 147.2, 141.51, 141.49, 137.64, 137.60, 135.03, 134.96, 128.31, 128.29, 127.88, 127.86, 127.14, 127.09, 68.2, 67.6, 67.0, 64.6, 62.2, 61.8, 37.9 (2C), 35.9 (2C), 22.12, 22.10; **IR** (cm^{-1}): 2937, 2843, 1493, 1442, 1341, 1250, 1100, 1042,

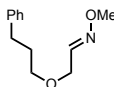
850, 761, 698, 655; **HRMS**: m/z calculated for $C_{15}H_{19}NO_2Na^+$ $[M+Na]^+$: 268.1308; found: 268.1307.



***N*-(2-(Methoxyimino)ethyl)-4-methyl-*N*-((*E*)-penta-2,4-dien-1-yl)benzenesulfonamide**

(S2.100): Prepared according to GP-2.3 from **A2.10** (500 mg, 1.8 mmol, 1.0 equiv.) and *O*-methylhydroxylamine hydrochloride (297 mg, 3.6 mmol, 2.0 equiv.). Purification by flash column chromatography (20% EtOAc/hexanes) afforded the pure title compound as a colorless oil (337 mg, 62%; *E/Z* (oxime) = 1.3:1; *E/Z* (diene) = 8:1).

¹H NMR (700 MHz, CDCl₃): δ 7.69 (dd, $J = 8.3, 2.2$ Hz, 4.6H; major+minor), 7.31 (t, $J = 8.4$ Hz, 4.6H; major+minor), 7.17 (t, $J = 5.9$ Hz, 1.3H; major), 6.61 (t, $J = 4.3$ Hz, 1H; minor), 6.29 – 6.22 (m, 2.3H; major+minor), 6.10 (dd, $J = 15.2, 10.7$ Hz, 2.3H; major+minor), 5.54 – 5.43 (m, 2.3H; major+minor), 5.18 (d, $J = 17.0$ Hz, 2.3H; major+minor), 5.11 (dd, $J = 10.0, 7.8$ Hz, 2.3H; major+minor), 3.98 (d, $J = 4.3$ Hz, 2H; minor), 3.88 (d, $J = 5.9$ Hz, 2.6H; major), 3.84 – 3.81 (m, 7.6H; major+minor), 3.79 (s, 3.9H; major+minor), 2.43 (d, $J = 2.2$ Hz, 6.9H; major+minor); **¹³C NMR** (176 MHz, CDCl₃): δ 147.9, 145.5, 143.9, 143.7, 136.8, 136.3, 135.8, 135.7, 135.64, 135.56, 130.0, 129.9, 127.38, 127.37, 127.2, 127.0, 118.6, 118.4, 62.2, 61.9, 51.0, 49.9, 45.9, 42.8, 21.64, 21.63; **IR** (cm⁻¹): 2938, 1598, 1441, 1337, 1156, 1090, 1030, 1005, 911, 854, 814, 743, 658; **HRMS**: m/z calculated for $C_{15}H_{20}N_2O_3SNa^+$ $[M+Na]^+$: 331.1087; found: 331.1088.

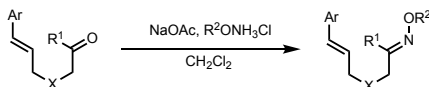


2-(3-Phenylpropoxy)acetaldehyde *O*-methyl oxime (2.104): Prepared according to GP-2.3 from **A2.11** (926 mg, 5.1 mmol, 1.0 equiv.) and *O*-methylhydroxylamine hydrochloride (858 mg,

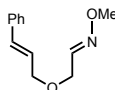
10.3 mmol, 2.0 equiv.). Purification by flash column chromatography (2–10% EtOAc/hexanes) afforded the pure title compound as a colorless oil (338 mg, 32%; *E/Z* (oxime) = 1:1.1).

¹H NMR (700 MHz, CDCl₃): δ 7.44 (t, *J* = 5.8 Hz, 1H; minor), 7.28 (td, *J* = 7.9, 2.2 Hz, 4.2H; major+minor), 7.21 – 7.17 (m, 6.3H; major+minor), 6.83 (t, *J* = 3.7 Hz, 1.1H; major), 4.24 (d, *J* = 3.7 Hz, 2.2H; major), 4.06 (d, *J* = 5.8 Hz, 2H; minor), 3.87 (s, 3.3H; major), 3.86 (s, 3H; minor), 3.46 (q, *J* = 6.2 Hz, 4.2H; major+minor), 2.70 (q, *J* = 7.7 Hz, 4.2H; major+minor), 1.95 – 1.88 (m, 4.2H; major+minor); **¹³C NMR** (176 MHz, CDCl₃): δ 150.6, 147.3, 141.9, 141.8, 128.6 (2C), 128.49, 128.47, 125.99, 125.96, 70.6, 70.0, 67.5, 65.1, 62.2, 61.8, 32.34, 32.33, 31.3, 31.2; **IR** (cm⁻¹): 2938, 2861, 1496, 1454, 1114, 1040, 911, 850, 744, 698; **HRMS**: *m/z* calculated for C₁₂H₁₇NO₂H⁺ [M+H]⁺: 208.1332; found: 208.1328.

General Procedure for Oxime Synthesis from Carbonyl Compounds (GP-2.4)



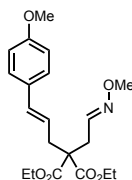
A 50-mL round-bottom flask equipped with a magnetic stir bar was charged with the corresponding aldehyde (1.0 equiv.) and CH_2Cl_2 (0.1 M). Next, NaOAc (4.0 equiv.) and the corresponding hydroxylamine hydrochloride (2.0 equiv.) were added sequentially and the mixture stirred at rt until complete as judged by TLC analysis (4–18 h). Then, NaHCO_3 solution (aq., sat.) was added and the organic layer separated. The aqueous layer was extracted with EtOAc (3x) and the combined organic extracts washed with brine, dried over Na_2SO_4 , filtered and concentrated in vacuo. Purification by flash column chromatography (EtOAc/hexanes) afforded the pure oxime, typically as a mixture of *E/Z* oxime isomers.



2-(Cinnamyloxy)acetaldehyde *O*-methyl oxime ((*E*)-2.68): Prepared according to GP-2.4 from 2-(cinnamyloxy)acetaldehyde¹⁷⁷ (1.33 g, 7.6 mmol, 1.0 equiv.) and *O*-methylhydroxylamine hydrochloride (1.26 g, 15.1 mmol, 2.0 equiv.). Purification by flash column chromatography (10–20% EtOAc/hexanes) afforded the pure title compound as a colorless oil (1.05 g, 68%; *E/Z* (oxime) = 1.4:1).

¹H NMR (700 MHz, CDCl_3): δ 7.47 (t, $J = 5.7$ Hz, 1.4H; major), 7.41 – 7.37 (m, 4.8H; major+minor), 7.34 – 7.30 (m, 4.8H; major+minor), 7.27 – 7.23 (m, 2.4H; major+minor), 6.87 (t, $J = 3.6$ Hz, 1H; minor), 6.62 (d, $J = 15.9$ Hz, 2.4H; major+minor), 6.27 (dtd, $J = 15.9, 6.1, 1.0$ Hz, 2.4H; major+minor), 4.31 (d, $J = 3.7$ Hz, 2H; minor), 4.20 – 4.16 (m, 4.8H; major+minor), 4.13 (d, $J = 5.7$ Hz, 2.8H; major), 3.87 (s, 7.2H; major+minor); **¹³C NMR** (176 MHz, CDCl_3): δ 150.2, 147.0, 136.7, 136.6, 133.37, 133.35, 128.73, 128.71, 128.01, 127.97, 126.69, 126.68, 125.4, 125.3,

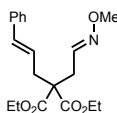
71.9, 71.3, 66.8, 64.4, 62.2, 61.9; **IR** (cm⁻¹): 2938, 2850, 1449, 1358, 1108, 1040, 965, 851, 735, 691; **HRMS**: *m/z* calculated for C₁₂H₁₅NO₂Na⁺ [M+Na]⁺: 228.0995; found: 228.0999.



Diethyl 2-(2-(methoxyimino)ethyl)-2-((E)-3-(4-methoxyphenyl)allyl)malonate (S.83):

Prepared according to GP-2.4 from **A2.12** (190 mg, 0.6 mmol, 1.0 equiv.) and *O*-methylhydroxylamine hydrochloride (91 mg, 1.1 mmol, 2.0 equiv.). Purification by flash column chromatography (2–20% EtOAc/hexanes) afforded the pure title compound as a yellow oil (150 mg, 73%; *E/Z* (oxime) = 2:1).

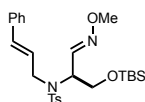
¹H NMR (500 MHz, CD₂Cl₂): δ 7.38 – 7.31 (m, 2H; major), 7.26 (dd, *J* = 8.8, 3.0 Hz, 6H), 6.85 – 6.81 (m, 6H), 6.70 (t, *J* = 5.4 Hz, 1H), 6.40 (dd, *J* = 15.7, 7.3 Hz, 3H), 5.91 (dt, *J* = 15.5, 7.6 Hz, 3H), 4.19 (q, *J* = 7.1 Hz, 12H), 3.83 (s, 3H), 3.78 (s, 15H), 2.87 (d, *J* = 5.4 Hz, 2H), 2.77 (dd, *J* = 7.5, 3.8 Hz, 6H), 2.73 (d, *J* = 6.4 Hz, 4H), 1.24 (t, *J* = 7.1 Hz, 18H); **¹³C NMR** (126 MHz, CD₂Cl₂): δ 170.9, 170.7, 159.8 (2C), 147.1, 147.0, 134.44 (2C), 134.3 (2C), 130.3, 127.9 (2C), 121.62, 121.60, 114.4, 62.22, 62.15, 62.1, 61.9, 57.4, 56.5, 55.8 (2C), 38.0, 37.5, 33.4, 29.6, 14.5, 14.4; **IR** (cm⁻¹): 2980, 2936, 1729, 1608, 1512, 1301, 1250, 1205, 1032, 971, 841; **HRMS**: *m/z* calculated for C₂₀H₂₇NO₆H⁺ [M+H]⁺: 378.1911; found: 378.1910.



Diethyl 2-cinnamyl-2-(2-(methoxyimino)ethyl)malonate (S2.87): Prepared according to GP-2.4 from **A2.13** (350 mg, 1.1 mmol, 1.0 equiv.) and *O*-methylhydroxylamine hydrochloride (184 mg,

2.2 mmol, 2.0 equiv.). Purification by flash column chromatography (20% EtOAc/hexanes) afforded the pure title compound as a pale-yellow oil (366 mg, 96%; *E/Z* (oxime) = 1.3:1).

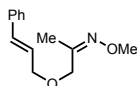
¹H NMR (500 MHz, CDCl₃): δ 7.37 (t, *J* = 6.4 Hz, 1.3H; major), 7.33 – 7.27 (m, 9.2H; major+minor), 7.22 (t, *J* = 6.5 Hz, 2.3H; major+minor), 6.73 (t, *J* = 5.4 Hz, 1H; minor), 6.46 (dd, *J* = 15.7, 5.2 Hz, 2.3H; major+minor), 6.10 – 6.02 (m, 2.3H; major+minor), 4.22 (q, *J* = 7.1 Hz, 9.2H; major+minor), 3.86 (s, 3H; minor), 3.81 (s, 3.9H; major), 2.93 (d, *J* = 5.4 Hz, 2H; minor), 2.86 – 2.80 (m, 4.6H; major+minor), 2.78 (d, *J* = 6.4 Hz, 2.6H; major), 1.26 (t, *J* = 7.1 Hz, 13.8H; major+minor); **¹³C NMR** (176 MHz, CDCl₃): δ 170.5, 170.3, 146.62, 146.57, 137.1 (2C), 134.74, 134.73, 128.6 (2C), 127.6 (2C), 126.4 (2C), 123.5, 123.4, 61.84, 61.83, 61.76, 61.6, 56.9, 56.1, 37.7, 37.3, 33.2, 29.4, 14.22, 14.21; **IR** (cm⁻¹): 2981, 2938, 1727, 1445, 1367, 1185, 1095, 1041, 968, 851, 741, 693; **HRMS**: *m/z* calculated for C₁₉H₂₅NO₅Na⁺ [M+Na]⁺: 370.1625; found: 370.1630.



***N*-Cinnamyl-4-methyl-*N*-((*S,E*)-8,8,9,9-tetramethyl-2,7-dioxa-3-aza-8-siladec-3-en-5-yl)benzenesulfonamide (S2.88)**: Prepared according to GP-2.4 from crude **A2.14** (343 mg, 0.72 mmol, 1.0 equiv.) and *O*-methylhydroxylamine hydrochloride (121 mg, 1.45 mmol, 2.0 equiv.). Purification by flash column chromatography (2–18% EtOAc/hexanes) afforded the pure title compound as a colorless oil (326 mg, 90%; *E/Z* (oxime) = 1.1:1).

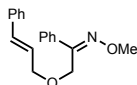
¹H NMR (500 MHz, CDCl₃): δ 7.73 (dd, *J* = 10.2, 8.3 Hz, 4.2H; major+minor), 7.36 – 7.18 (m, 15.8H; major+minor), 6.75 (d, *J* = 5.6 Hz, 1H; minor), 6.46 (dd, *J* = 20.2, 15.9 Hz, 2.1H; major+minor), 6.09 (ddt, *J* = 32.6, 15.9, 6.7 Hz, 2.1H; major+minor), 4.83 (q, *J* = 6.1 Hz, 1H; minor), 4.61 (q, *J* = 6.3 Hz, 1.1H; major), 4.17 – 3.91 (m, 6.3H; major+minor), 3.88 (ddd, *J* = 10.6,

6.7, 1.7 Hz, 2.1H; major+minor), 3.74 (s, 3.3H; major), 3.67 (s, 3H; minor), 2.40 (s, 3H; minor), 2.39 (s, 3.3H; major), 0.87 – 0.78 (m, 18.9H; major+minor), 0.00 (d, $J = 3.2$ Hz, 12.6H; major+minor); $^{13}\text{C NMR}$ (176 MHz, CDCl_3): δ 147.5, 147.0, 143.32, 143.26, 138.1, 137.7, 136.5, 136.4, 133.5, 133.0, 129.6, 129.5, 128.7, 128.6, 128.0, 127.9, 127.68, 127.65, 126.59, 126.57, 126.3, 126.0, 63.4, 62.7, 62.0, 61.9, 58.6, 54.8, 49.3, 48.1, 25.9 (2C), 21.6 (2C), 18.34, 18.30, -5.35 (3C), -5.41; **IR** (cm^{-1}): 2928.4, 2855.9, 1462.9, 13339.7, 1253.1, 1156.5, 1090.2, 1043.9, 967.1, 900.1, 834.0, 813.1, 776.5, 727.4, 691.6, 657.8.; **HRMS**: m/z calculated $\text{C}_{26}\text{H}_{38}\text{N}_2\text{O}_4\text{SSiH}^+$ for $[\text{M}+\text{H}]^+$: 503.2394; found: 503.2393.

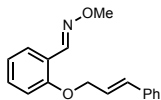


1-(Cinnamyloxy)propan-2-one *O*-methyl oxime (S2.89): Prepared according to GP-2.4 from **A2.15** (295 mg, 1.6 mmol, 1.0 equiv.) and *O*-methylhydroxylamine hydrochloride (259 mg, 3.1 mmol, 2.0 equiv.). Purification by flash column chromatography (5–15% EtOAc/hexanes) afforded the pure title compound as a colorless oil (316 mg, 93%; *E/Z* (oxime) = 1:3.3).

$^1\text{H NMR}$ (700 MHz, CDCl_3): δ 7.41 – 7.37 (m, 8.6H; major+minor), 7.34 – 7.29 (m, 8.6H; major+minor), 7.24 (t, $J = 7.3$ Hz, 4.3H; major+minor), 6.62 (dd, $J = 15.7, 3.7$ Hz, 4.3H; major+minor), 6.31 – 6.25 (m, 4.3H; major+minor), 4.32 (s, 2H; minor), 4.14 (td, $J = 6.5, 1.4$ Hz, 8.6H; major+minor), 4.04 (s, 6.6H; major), 3.88 (s, 9.9H; major), 3.81 (s, 3H; minor), 1.97 (s, 3H; minor), 1.91 (s, 9.9H; major); $^{13}\text{C NMR}$ (176 MHz, CDCl_3): δ 157.2, 154.9, 136.72, 136.67, 133.0, 132.9, 128.69, 128.67, 127.90, 127.86, 126.6 (2C), 125.59, 125.55, 71.9, 71.5, 70.9, 65.6, 61.7, 61.6, 16.7, 12.2; **IR** (cm^{-1}): 2937, 2852, 1495, 1448, 1366, 1115, 1045, 965, 888, 831, 735, 691; **HRMS**: m/z calculated for $\text{C}_{13}\text{H}_{17}\text{NO}_2\text{Na}^+$ $[\text{M}+\text{Na}]^+$: 242.1151; found: 242.1155.



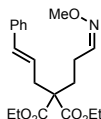
(Z)-2-(Cinnamyloxy)-1-phenylethan-1-one O-methyl oxime (S2.90): Prepared according to GP-2.4 from crude **A2.16** (stoichiometry based on 2.9 mmol **A2.17**) and *O*-methylhydroxylamine hydrochloride (482 mg, 5.8 mmol, 2.0 equiv.). Purification by flash column chromatography (5–15% EtOAc/hexanes) afforded the pure title compound as a colorless oil (255 mg, 31%; *Z* only). **¹H NMR** (700 MHz, CDCl₃): δ 7.71 (dd, *J* = 6.5, 2.9 Hz, 2H), 7.39 – 7.34 (m, 5H), 7.31 (t, *J* = 7.6 Hz, 2H), 7.24 (t, *J* = 7.3 Hz, 1H), 6.55 (d, *J* = 15.9 Hz, 1H), 6.22 (dt, *J* = 15.9, 6.1 Hz, 1H), 4.69 (s, 2H), 4.13 (d, *J* = 6.1 Hz, 2H), 4.00 (s, 3H); **¹³C NMR** (176 MHz, CDCl₃): δ 155.5, 136.7, 134.4, 133.1, 129.3, 128.7, 128.4, 127.9, 127.2, 126.6, 125.6, 71.5, 62.4, 62.0; **IR** (cm⁻¹): 2936, 1724, 1494, 1445, 1327, 1184, 1115, 1041, 965, 885, 763, 743, 690; **HRMS**: *m/z* calculated for C₁₈H₁₉NO₂H⁺ [M+H]⁺: 282.1489; found: 282.1494.



(E)-2-(Cinnamyloxy)benzaldehyde O-methyl oxime (S2.94): Prepared according to GP-2.4 from 2-(cinnamyloxy)benzaldehyde¹⁷⁸ (508 mg, 2.1 mmol, 1.0 equiv.) and *O*-methylhydroxylamine hydrochloride (356 mg, 4.3 mmol, 2.0 equiv.). Purification by flash column chromatography (10% EtOAc/hexanes) afforded the pure title compound as a colorless oil (459 mg, 81%; *E* only).

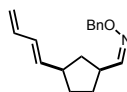
¹H NMR (700 MHz, CDCl₃): δ 8.53 (s, 1H), 7.81 (dd, *J* = 7.7, 1.6 Hz, 1H), 7.41 (d, *J* = 7.6 Hz, 2H), 7.34 (t, *J* = 7.6 Hz, 3H), 7.29 – 7.26 (m, 1H), 6.96 (t, *J* = 7.5 Hz, 1H), 6.94 (d, *J* = 8.3 Hz, 1H), 6.72 (d, *J* = 16.0 Hz, 1H), 6.40 (dt, *J* = 16.0, 5.7 Hz, 1H), 4.73 (dd, *J* = 5.7, 1.4 Hz, 2H), 3.98 (s, 3H); **¹³C NMR** (176 MHz, CDCl₃): δ 156.8, 145.0, 136.5, 133.2, 131.2, 128.8, 128.1, 126.7, 126.6, 124.2, 121.3, 121.2, 112.7, 69.3, 62.0; **IR** (cm⁻¹): 2934, 1598, 1486, 1449, 1340, 1241, 1108,

1051, 1005, 963, 917, 743, 690; **HRMS**: m/z calculated for $C_{17}H_{17}NO_2Na^+$ $[M+Na]^+$: 290.1151; found: 290.1147.



Diethyl 2-cinnamyl-2-(3-(methoxyimino)propyl)malonate (S2.95): Prepared according to GP-2.4 from **A.18** (500 mg, 1.5 mmol, 1.0 equiv.) and *O*-methylhydroxylamine hydrochloride (251 mg, 3.0, 2.0 equiv.). Purification by flash column chromatography (20% EtOAc/hexanes) afforded the pure title compound as a pale-yellow oil (476 mg, 88%; *E/Z* (oxime) = 1.2:1).

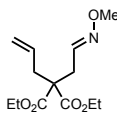
¹H NMR (500 MHz, $CDCl_3$): δ 7.35 – 7.27 (m, 10H; major+minor), 7.21 (t, J = 6.8 Hz, 2.2H; major+minor), 6.62 (t, J = 5.3 Hz, 1H; minor), 6.45 (d, J = 15.7 Hz, 2.2H; major+minor), 6.03 (dtd, J = 15.4, 7.5, 2.6 Hz, 2.2H; major+minor), 4.25 – 4.17 (m, 8.8H; major+minor), 3.84 (s, 3H; minor), 3.80 (s, 3.6H; major), 2.82 (d, J = 7.5 Hz, 4.4H; major+minor), 2.34 – 2.27 (m, 2H; minor), 2.24 – 2.17 (m, 2.4H; major), 2.14 – 2.06 (m, 4.4H; major+minor), 1.25 (t, J = 7.1 Hz, 13.2H; major+minor); **¹³C NMR** (176 MHz, $CDCl_3$): δ 170.9 (2C), 150.2, 149.5, 137.12, 137.10, 134.2 (2C), 128.6 (2C), 127.6 (2C), 126.34, 126.33, 123.81, 123.79, 61.8, 61.6 (2C), 61.4, 57.5, 57.4, 36.8, 36.4, 29.7, 29.1, 24.8, 20.8, 14.2 (2C); **IR** (cm^{-1}): 2980, 1725, 1446, 1367, 1263, 1180, 1094, 1049, 1028, 967, 858, 741, 693; **HRMS**: m/z calculated for $C_{20}H_{27}NO_5Na^+$ $[M+Na]^+$: 384.1781; found: 384.1783.



3-(Buta-1,3-dien-1-yl)cyclopentane-1-carbaldehyde O-benzyl oxime (2.101): Prepared according to GP-2.4 from (1*S**,3*R**)-3-(buta-1,3-dien-1-yl)cyclopentane-1-carbaldehyde¹⁷⁹ (172 mg, 1.2 mmol, 1.0 equiv.; *E/Z* (diene) = 4:1) and *O*-benzylhydroxylamine hydrochloride

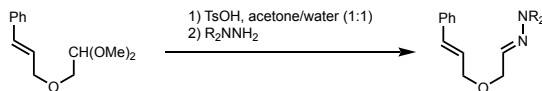
(366 mg, 2.3 mmol, 2.0 equiv.). Purification by flash column chromatography (0–10% EtOAc/hexanes) afforded the pure title compound as a colorless oil (205 mg, 70%; *E/Z* (oxime) = 2:1; *E/Z* (diene) = 10:1). Characterization data is provided for the two major (*E*)-diene isomers.

¹H NMR (700 MHz, CDCl₃): δ 7.38 (d, *J* = 7.4 Hz, 2H; major), 7.37 – 7.33 (m, 12H; major+minor), 7.31 – 7.28 (m, 3H; major+minor), 6.65 (d, *J* = 6.9 Hz, 1H, minor), 6.29 (dt, *J* = 17.2, 10.3 Hz, 3H; major+minor), 6.05 (dd, *J* = 15.2, 10.6 Hz, 3H; major+minor), 5.69 – 5.63 (m, 3H; major+minor), 5.10 (d, *J* = 18.0 Hz, 5H; major+minor), 5.04 (s, 4H; major), 4.98 (d, *J* = 10.1 Hz, 3H; major+minor), 3.38 – 3.31 (m, 1H; minor), 2.80 – 2.71 (m, 2H; major), 2.66 – 2.52 (m, 3H; major+minor), 2.17 – 2.10 (m, 1H; minor), 2.06 – 2.00 (m, 2H; major), 1.99 – 1.83 (m, 6H; major+minor), 1.69 – 1.60 (m, 3H; major+minor), 1.49 – 1.41 (m, 3H; major+minor), 1.33 (dt, *J* = 12.6, 10.3 Hz, 2H; major), 1.21 (dt, *J* = 12.5, 10.3 Hz, 1H; minor); **¹³C NMR** (176 MHz, CDCl₃): δ 156.9, 156.5, 154.9, 154.8, 138.7, 138.6, 137.24, 137.22, 129.89, 129.86, 128.53, 128.50, 128.44, 128.43, 127.98, 127.98, 115.41, 115.39, 75.8, 75.7, 43.34, 43.33, 39.90, 39.90, 38.28, 38.26, 32.3, 32.1, 30.0, 29.8; **IR** (cm⁻¹): 2950, 2866, 1496, 1453, 1366, 1040, 1003, 899, 732, 696; **HRMS**: *m/z* calculated for C₁₇H₂₁NOH⁺ [M+H]⁺: 256.1696; found: 256.1701.



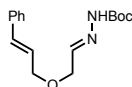
Diethyl 2-allyl-2-(2-(methoxyimino)ethyl)malonate (2.105): Prepared according to GP-2.4 from diethyl 2-allyl-2-(2-oxoethyl)malonate¹⁸⁰ (271 mg, 1.0 mmol, 1.0 equiv.) and *O*-methylhydroxylamine hydrochloride (167 mg, 2.0 mmol, 2.0 equiv.). Purification by flash column chromatography (10% EtOAc/hexanes) afforded the pure title compound as a colorless oil (233 mg, 86%; *E/Z* (oxime) = 1.3:1). Spectroscopic data were consistent with those reported in the literature.¹⁸¹

General Procedure for Hydrazone Synthesis (GP-2.5)



A 100-mL round-bottom flask equipped with a magnetic stir bar was charged with acetal (1.0 equiv.) and a 1:1 mixture (*v/v*) of water/acetone (0.1 M). *p*-TsOH (0.2 equiv.) was added and the solution heated at 85 °C until complete as determined by TLC analysis (4–8 h). After cooling to rt, NaHCO₃ solution (aq., sat.) was added and the mixture extracted with EtOAc (3x). The combined organic extracts were dried over Na₂SO₄, filtered, concentrated *in vacuo* and dried using high-vac.

The crude aldehyde was dissolved in MeOH (0.1 M), the corresponding hydrazide/hydrazine (1.5 equiv.) added and the reaction stirred overnight at rt. Then, the solvent was removed *in vacuo* and the crude product purified by flash column chromatography (EtOAc/hexanes) to afford the corresponding pure hydrazone.

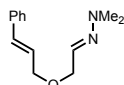


***Tert*-butyl 2-(2-(cinnamyloxy)ethylidene)hydrazine-1-carboxylate (2.73):** Prepared according to GP-2.5 from **A2.1** (500 mg, 2.3 mmol, 1.0 equiv.) and *tert*-butyl carbazate (446 mg, 3.4 mmol, 1.5 equiv.). Purification by flash column chromatography (20–40% EtOAc/hexanes) afforded the pure title compound as a pale-yellow solid (402 mg, 62%; *E/Z* (hydrazone) = 3.9:1).

¹H NMR (700 MHz, CDCl₃): δ 7.86 (s, 3.9H; major), 7.41 – 7.36 (m, 9.8H; major+minor), 7.35 – 7.29 (m, 9.8H; major+minor), 7.24 (t, *J* = 7.3 Hz, 5.9H; major+minor), 6.65 (d, *J* = 7.8 Hz, 1H; minor), 6.61 (d, *J* = 15.8 Hz, 3.9H; major), 6.26 (dt, *J* = 15.9, 6.1 Hz, 4.9H; major+minor), 4.24 – 4.19 (m, 9.8H; major+minor), 4.19 – 4.15 (m, 9.8H; major+minor), 1.50 (s, 44.1H; major+minor);

¹³C NMR (176 MHz, CDCl₃): δ 152.8, 152.5, 143.1, 139.4, 136.6, 136.2, 134.2, 133.1, 128.7,

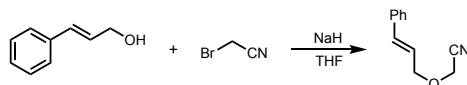
128.6, 128.2, 127.8, 126.7, 126.6, 125.4, 124.2, 81.4, 81.2, 71.8, 71.3, 69.3, 66.7, 28.3 (2C); **IR** (cm^{-1}): 3232, 2978, 2931, 1706, 1533, 1449, 1366, 1269, 1247, 1164, 1133, 1042, 1015, 966, 859, 723, 691; **HRMS**: m/z calculated for $\text{C}_{16}\text{H}_{22}\text{N}_2\text{O}_3\text{Na}^+$ $[\text{M}+\text{Na}]^+$: 313.1523; found: 313.1530.



(E)-2-(2-(Cinnamyloxy)ethylidene)-1,1-dimethylhydrazine (2.74): Prepared according to GP-2.5 from **A2.1** (300 mg, 1.4 mmol, 1.0 equiv.) and *N,N*-dimethylhydrazine (0.15 mL, 2.0 mmol, 1.5 equiv.). Purification by flash column chromatography (5–10% EtOAc/hexanes) afforded the pure title compound as a pale-yellow oil (116 mg, 39%; *E* only).

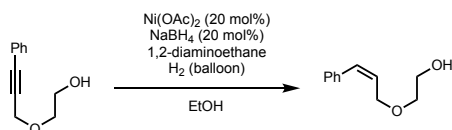
$^1\text{H NMR}$ (700 MHz, CDCl_3): δ 7.38 (d, $J = 8.0$ Hz, 2H), 7.31 (t, $J = 7.2$ Hz, 2H), 7.23 (t, $J = 7.3$ Hz, 1H), 6.65 – 6.59 (m, 2H), 6.31 (dt, $J = 15.9, 6.1$ Hz, 1H), 4.18 (d, $J = 6.1$ Hz, 2H), 4.15 (d, $J = 5.3$ Hz, 2H), 2.83 (s, 6H); **$^{13}\text{C NMR}$** (176 MHz, CDCl_3): δ 136.9, 132.9, 131.8, 128.7, 127.8, 126.6, 126.1, 71.0, 70.7, 42.8; **IR** (cm^{-1}): 2854, 1598, 1496, 1447, 1262, 1116, 1036, 968, 817, 745, 693; **HRMS**: m/z calculated for $\text{C}_{13}\text{H}_{18}\text{N}_2\text{OH}^+$ $[\text{M}+\text{H}]^+$: 219.1492; found: 219.1498.

Miscellaneous Procedures



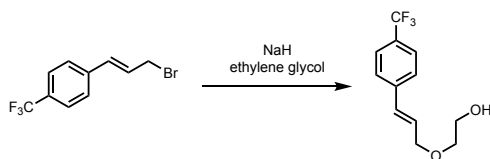
2-((Cinnamyloxy)acetonitrile (A2.17): A 100-mL round-bottom flask equipped with a stir bar was charged with NaH (60% dispersion in mineral oil; 1.79 g, 44.7 mmol, 1.2 equiv.) and THF (35 mL). The mixture was cooled to 0 °C and a solution of cinnamyl alcohol (5.00 g, 37.3 mmol, 1.0 equiv.) in THF (5 mL) was added dropwise. After stirring for 30 min at 0 °C, bromoacetonitrile (3.1 mL, 44.7 mmol, 1.2 equiv.) was added and the reaction mixture allowed to warm up to rt and stirred overnight. Then, NH₄Cl solution (aq., sat.) was added and the biphasic mixture diluted with water and EtOAc. The organic layer was separated and the aqueous layer extracted with EtOAc (3x). The combined organic extracts were washed with brine, dried over Na₂SO₄, filtered and concentrated *in vacuo*. Purification by flash column chromatography (5–10% EtOAc/hexanes) afforded the pure title compound as a pale-yellow oil (3.23 g, 50%).

¹H NMR (700 MHz, CDCl₃): δ 7.41 (d, *J* = 7.4 Hz, 2H), 7.34 (t, *J* = 7.6 Hz, 2H), 7.28 (t, *J* = 7.3 Hz, 1H), 6.70 (d, *J* = 15.9 Hz, 1H), 6.23 (dt, *J* = 15.9, 6.4 Hz, 1H), 4.31 (dd, *J* = 6.5, 1.2 Hz, 2H), 4.29 (s, 2H); **¹³C NMR** (176 MHz, CDCl₃): δ 136.0, 135.4, 128.8, 128.4, 126.8, 123.2, 116.1, 71.8, 54.8; **IR** (cm⁻¹): 3027, 2861, 1494, 1450, 1352, 1091, 967, 883, 744, 692; **HRMS**: *m/z* calculated for C₁₁H₁₁NONa⁺ [M+Na]⁺: 196.0733; found: 196.0730.



(Z)-2-((3-Phenylallyl)oxy)ethan-1-ol (A2.6): A 25-mL round-bottom flask equipped with a stir bar was charged with nickel(II) acetate tetrahydrate (71 mg, 0.28 mmol, 0.2 equiv.), sodium borohydride (11 mg, 0.28 mmol, 0.2 equiv.) and EtOH (4 mL). The mixture was sparged with hydrogen gas from a balloon and stirred for 1 h at rt. A solution containing 2-((3-phenylprop-2-

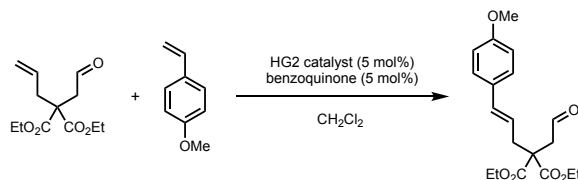
yn-1-yl)oxy)ethan-1-ol¹⁸² (250 mg, 1.4 mmol, 1.0 equiv.) and 1,2-diaminoethane (38 μ L, 0.57 mmol, 0.4 equiv.) in EtOH (1 mL) was added and the reaction stirred for 5.5 h at rt under an atmosphere of hydrogen. The mixture was filtered through celite and the filtrate concentrated *in vacuo*. Purification by flash column chromatography (30% EtOAc/hexanes) afforded the pure title compound as a colorless oil (207 mg, 82%). Spectroscopic data were consistent with those reported in the literature.¹⁷⁶



(E)-2-((3-(4-(Trifluoromethyl)phenyl)allyl)oxy)ethan-1-ol (A2.7): In a 25-mL round-bottom flask equipped with a magnetic stir bar, NaH (60% dispersion in mineral oil; 148 mg, 3.7 mmol, 1.2 equiv.) was added to a solution of ethylene glycol (0.31 mL, 5.6 mmol, 1.9 equiv.) in THF (8 mL) at 0 °C and the resulting mixture stirred for 0.5 h at that temperature, before adding 4-(trifluoromethyl)cinnamyl bromide¹⁸³ (800 mg, 3.0 mmol, 1.0 equiv.) as solution in THF (2 mL) dropwise. Then, the reaction mixture was allowed to warm up to rt and heated at reflux overnight. After cooling down to rt, NH₄Cl solution (aq., sat.) was added and the biphasic mixture diluted with water and EtOAc. The organic layer was separated and the aqueous layer extracted with EtOAc (3x). The combined organic extracts were washed with brine, dried over Na₂SO₄, filtered and concentrated *in vacuo*. Purification by flash column chromatography (5–50% EtOAc/hexanes) afforded the pure title compound as colorless oil (470 mg, 64%).

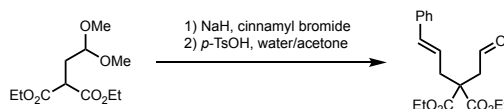
¹H NMR (700 MHz, CDCl₃): δ 7.57 (d, J = 8.2 Hz, 2H), 7.48 (d, J = 8.2 Hz, 2H), 6.66 (d, J = 16.0 Hz, 1H), 6.39 (dt, J = 16.0, 5.8 Hz, 1H), 4.23 (dd, J = 5.8, 1.4 Hz, 2H), 3.80 (t, J = 4.6 Hz, 2H), 3.64 (t, J = 4.6 Hz, 2H); ¹³C NMR (176 MHz, CDCl₃): δ 140.2, 131.0, 129.7 (q, J = 32.4 Hz), 128.7, 126.8, 125.7 (q, J = 3.8 Hz), 124.3 (q, J = 271.4 Hz), 71.7, 71.6, 62.0; IR (cm⁻¹): 3396, 2860,

1615, 1322, 1162, 1106, 1065, 1016, 968, 852, 730; **HRMS**: m/z calculated for $C_{12}H_{13}F_3O_2Na^+$ $[M+Na]^+$: 269.0760; found: 269.0762.



Diethyl (*E*)-2-(3-(4-methoxyphenyl)allyl)-2-(2-oxoethyl)malonate (A2.12): A 25-mL round-bottom flask equipped with a magnetic stir bar was charged with diethyl 2-allyl-2-(2-oxoethyl)malonate¹⁸⁰ (300 mg, 1.2 mmol, 1.0 equiv.) and CH_2Cl_2 (2.5 mL). Hoveyda-Grubbs catalyst (2nd generation) (39 mg, 0.06 mmol, 5 mol%), 4-methoxystyrene (332 mg, 2.5 mmol, 2.0 eq.), and benzoquinone (7 mg, 0.06 mmol, 5 mol%) were added sequentially and the reaction was heated at reflux for 16 h. After cooling to room temperature, the solvent was removed *in vacuo* and the crude product purified by flash column chromatography (2–30% EtOAc/hexanes) to afford the pure title compound as a yellow oil (220 mg, 55%).

¹H NMR (500 MHz, CD_2Cl_2): δ 9.70 (s, 1H), 7.26 (d, $J = 8.6$ Hz, 2H), 6.83 (d, $J = 8.7$ Hz, 2H), 6.37 (d, $J = 15.7$ Hz, 1H), 5.90 (dt, $J = 15.5, 7.6$ Hz, 1H), 4.27 – 4.12 (m, 4H), 3.78 (s, 3H), 2.96 (s, 2H), 2.86 (d, $J = 7.6$ Hz, 2H), 1.25 (t, $J = 7.1$ Hz, 6H); **¹³C NMR** (126 MHz, CD_2Cl_2): δ 199.6, 170.8, 159.9, 134.6, 130.2, 127.9, 121.8, 114.4, 62.5, 55.8, 55.7, 46.8, 38.2, 14.4; **IR** (cm^{-1}): 2981, 2839, 1723, 1607, 1511, 1247, 1190, 1176, 1094, 1031, 972, 843; **HRMS**: m/z calculated for $C_{19}H_{24}O_6Na^+$ $[M+Na]^+$: 371.1465; found: 371.1465.

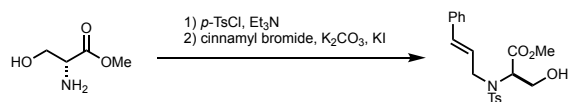


Diethyl 2-cinnamyl-2-(2-oxoethyl)malonate (A2.13): A 25-mL round-bottom flask equipped with a magnetic stir bar was charged with NaH (60% dispersion in mineral oil; 193 mg, 4.8 mmol,

1.2 equiv.) and THF (13 mL). After cooling the mixture to 0 °C, diethyl 2-(2,2-dimethoxyethyl)malonate¹⁸⁴ (1.00 g, 4.0 mmol, 1.0 equiv.) was added dropwise and the solution allowed to warm up to rt and stirred for 1 h. The solution was cooled to 0 °C, then, cinnamyl bromide (1.19 g, 6.0 mmol, 1.5 equiv.) was added subsequently and the solution allowed to warm up to rt and stirred overnight. Next, NH₄Cl solution (aq., sat.) was added and the biphasic mixture diluted with water and Et₂O. The organic layer was separated and the aqueous layer extracted with Et₂O (3x). The combined organic extracts were dried over MgSO₄, filtered, concentrated *in vacuo* and dried using high-vac.

The crude acetal was dissolved in a 1:1 mixture (v/v) of water/acetone (40 mL). *p*-TsOH (153 mg, 0.8 mmol, 0.2 equiv.) was added and the reaction heated at 85 °C for 2 h. After cooling down to rt, NaHCO₃ solution (aq., sat.) was added and the mixture extracted with EtOAc (3x). The combined organic extracts were dried over Na₂SO₄, filtered and concentrated *in vacuo*. Purification by flash column chromatography (20% EtOAc/hexanes) afforded the pure title compound as colorless oil (950 mg, 74%).

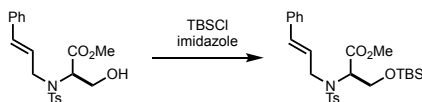
¹H NMR (500 MHz, CDCl₃): δ 9.73 (s, 1H), 7.34 – 7.27 (m, 4H), 7.25 – 7.21 (m, 1H), 6.43 (d, *J* = 15.7 Hz, 1H), 6.05 (dt, *J* = 15.5, 7.6 Hz, 1H), 4.24 (q, *J* = 7.1 Hz, 4H), 3.01 (s, 2H), 2.92 (d, *J* = 7.6 Hz, 2H), 1.27 (t, *J* = 7.1 Hz, 6H); **¹³C NMR** (176 MHz, CDCl₃): δ 199.0, 170.1, 136.8, 134.9, 128.7, 127.8, 126.4, 123.6, 62.1, 55.2, 46.4, 37.7, 14.1; **IR** (cm⁻¹): 2982, 1721, 1446, 1367, 1188, 1093, 1020, 969, 860, 741, 693; **HRMS**: *m/z* calculated for C₁₈H₂₂O₅Na⁺ [M+Na]⁺: 341.1359; found: 341.1362.



Methyl *N*-cinnamyl-*N*-tosyl-*D*-serinate (A2.19): A 100-mL round-bottom flask equipped with a magnetic stir bar was charged with *D*-serine methyl ester hydrochloride (1.00 g, 6.43 mmol, 1.0 equiv.) and CH₂Cl₂ (30 mL), before adding tosyl chloride (1.76 g, 9.23 mmol, 1.4 equiv.) and triethylamine (2.93 mL, 21.0 mmol, 3.3 equiv.). After stirring at rt for 16 h, NaHCO₃ solution (aq., sat.) was added, the organic layer separated, and the aqueous layer extracted with CH₂Cl₂ (3x). The combined organic extracts were washed with brine, dried over Na₂SO₄, filtered and concentrated *in vacuo*, then dried using high-vac.

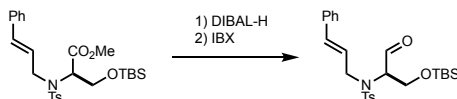
The crude *N*-tosyl amine was dissolved in acetone (30 mL), before adding K₂CO₃ (1.74 g, 12.6 mmol, 2.0 equiv.), cinnamyl bromide (2.49 g, 12.6 mmol, 2.0 equiv.), and KI (140 mg, 0.84 mmol, 0.1 equiv.). The resulting mixture was stirred at 60 °C for 3 h. Next, NaHCO₃ solution (aq., sat.) was added, the organic layer separated, and the aqueous layer extracted with Et₂O (3x). The combined organic extracts were washed with brine, dried over MgSO₄, filtered and concentrated *in vacuo*. Purification by flash column chromatography (5–65% EtOAc/hexanes) afforded the pure title compound as a pale-yellow oil (1.17 g, 47%).

¹H NMR (700 MHz, CDCl₃): δ 7.73 (d, *J* = 8.2 Hz, 2H), 7.26 (m, 6H), 7.21 (m, 1H), 6.48 – 6.43 (m, 1H), 6.10 (dt, *J* = 15.9, 6.7 Hz, 1H), 4.62 (t, *J* = 6.4 Hz, 1H), 4.10 (dd, *J* = 16.1, 6.2 Hz, 1H), 4.06 (dd, *J* = 11.8, 6.1 Hz, 1H), 3.94 (dd, *J* = 16.0, 7.2 Hz, 1H), 3.86 (dd, *J* = 11.8, 6.8 Hz, 1H), 3.55 (s, 3H), 2.39 (s, 3H); **¹³C NMR** (176 MHz, CDCl₃): δ 170.4, 143.8, 137.1, 136.1, 133.8, 129.7, 128.7, 128.2, 127.7, 126.6, 125.2, 61.5, 60.9, 52.5, 49.1, 21.7; **IR** (cm⁻¹): 3522, 2953, 1739, 1336, 1290, 1246, 1155, 1089, 1038, 970, 731, 660; **HRMS**: *m/z* calculated for C₂₀H₂₃NO₅SNH₄⁺ [M+NH₄]⁺: 407.1635; found: 407.1635.



Methyl *O*-(*tert*-butyldimethylsilyl)-*N*-cinnamyl-*N*-tosyl-*D*-serinate (A2.20): A 100-mL round-bottom flask equipped with a magnetic stir bar was charged with **A2.19** (1.17 g, 3.00 mmol, 1.0 equiv.), imidazole (205 mg, 3.00 mmol, 1.0 equiv.), TBSCl (543 mg, 3.60 mmol, 1.2 equiv.) and CH₂Cl₂ (30.0 mL). After stirring for 16 h at rt, the NaHCO₃ solution (aq., sat.) was added and the organic layer separated. Then, the aqueous layer was extracted with CH₂Cl₂ (3x) and the combined organic extracts washed with brine, dried over Na₂SO₄, filtered and concentrated *in vacuo*. Purification by flash chromatography (2–20% EtOAc/hexanes) afforded the pure title compound as a colorless oil (1.30 g, 86%).

¹H NMR (400 MHz, CDCl₃): δ 7.72 (d, *J* = 8.2 Hz, 2H), 7.31 – 7.18 (m, 7H), 6.46 (d, *J* = 15.9 Hz, 1H), 6.22 – 6.07 (m, 1H), 4.71 (t, *J* = 5.5 Hz, 1H), 4.23 – 4.08 (m, 2H), 4.04 (d, *J* = 5.5 Hz, 2H), 3.57 (s, 3H), 2.37 (s, 3H), 0.82 (s, 9H), 0.00 (d, *J* = 3.9 Hz, 6H); **¹³C NMR** (100 MHz, CD₂Cl₂): δ 170.3, 144.1, 138.2, 137.3, 132.6, 130.0, 129.0, 128.1, 128.0, 127.5, 126.9, 63.2, 61.9, 52.5, 49.1, 26.0, 21.8, 18.6, –5.3, –5.5; **IR** (cm⁻¹): 2952, 2929, 2884, 2856, 1743, 1342, 1254, 1157, 1093, 837, 813, 779, 753, 693, 657; **HRMS**: *m/z* calculated for C₂₆H₃₇NO₅SSiNH₄⁺ [M+NH₄]⁺: 521.2500; found: 521.2501.



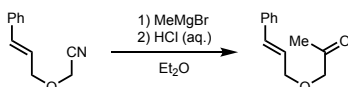
(*R*)-*N*-(1-((*tert*-butyldimethylsilyl)oxy)-3-oxopropan-2-yl)-*N*-cinnamyl-4-

methylbenzenesulfonamide (A2.14): A 100-mL round-bottom flask equipped with a magnetic stir bar was charged with **A2.20** (1.17 g, 2.32 mmol, 1.0 equiv.) and CH₂Cl₂ (25 mL). After cooling the solution to –78 °C, a freshly prepared 1 M solution of DIBAL-H (0.91 mL, 5.11 mmol, 2.2 equiv.) in CH₂Cl₂ was added slowly over 12 min. After stirring for 0.5 h at –78 °C, the flask

was transferred to an ice bath and allowed to warm to 0 °C. The mixture was diluted with diethyl ether (25 mL), then, water (0.2 mL) was added dropwise, followed by the addition of 15% NaOH (aq., 0.2 mL) and water (0.5 mL). The mixture was allowed to warm to rt and stirred for 15 min. Next, MgSO₄ was added and the mixture stirred for an additional 15 min. Solids were removed by filtration and the filtrate concentrated *in vacuo* to afford the corresponding crude alcohol.

The crude alcohol was dissolved in DMSO (20 mL) and IBX (971 mg, 3.47 mmol, 1.5 equiv.) was added sequentially. The mixture was stirred at rt for 12 h, after which Et₂O (20 mL) and water (20 mL) were added. The mixture was filtered through celite, and the organic layer was separated from the biphasic filtrate. The aqueous layer was extracted with Et₂O (3x), and the combined organic extracts were washed with brine, dried over MgSO₄, filtered and concentrated *in vacuo*. Purification by flash chromatography (2–20% EtOAc/hexanes) afforded the pure title compound as a colorless oil (343 mg, 31%).

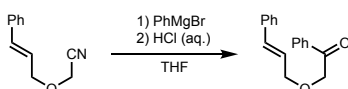
¹H NMR (500 MHz, CDCl₃): δ 9.68 (s, 1H), 7.77 (d, *J* = 8.3 Hz, 2H), 7.34 – 7.21 (m, 7H), 6.47 (d, *J* = 15.9 Hz, 1H), 6.12 (dt, *J* = 15.8, 6.8 Hz, 1H), 4.34 (dd, *J* = 7.3, 5.0 Hz, 1H), 4.20 – 4.05 (m, 3H), 4.02 (dd, *J* = 11.0, 7.4 Hz, 1H), 2.41 (s, 3H), 0.82 (s, 9H), 0.00 (d, *J* = 10.6 Hz, 6H); **¹³C NMR** (100 MHz, CDCl₃): δ 198.8, 143.7, 137.5, 136.1, 134.4, 129.8, 128.7, 128.2, 127.6, 126.6, 125.0, 67.5, 61.0, 49.7, 25.8, 21.6, 18.2, –5.5, –5.6; **IR** (cm⁻¹): 2954, 2928, 2856, 1734, 1471, 1338, 1256, 1157, 1092, 837, 781, 751; **HRMS**: *m/z* calculated for C₂₅H₃₅NO₄SSiNH₄⁺ [M+NH₄]⁺: 491.2394; found: 491.2400.



1-(Cinnamyloxy)propan-2-one (A2.15): A 25-mL round-bottom flask equipped with a magnetic stir bar was charged with **A2.17** (500 mg, 2.9 mmol, 1.0 equiv.) and THF (10 mL). After cooling to 0 °C, methylmagnesium bromide (3 M solution in Et₂O, 1.2 mL, 3.6 mmol, 1.2 equiv.) was

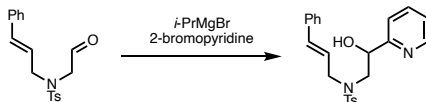
added dropwise and the reaction mixture allowed to warm up to rt and stirred for 2 h. Then, a 2 M aqueous solution of HCl (5 mL) was added at 0 °C, the mixture allowed to warm up to rt and stirred vigorously for 0.5 h. The biphasic mixture was diluted with water and EtOAc, the organic layer separated and the aqueous layer extracted with EtOAc (3x). The combined organic extracts were washed with NaHCO₃ solution (aq., sat.), brine, dried over MgSO₄, filtered and concentrated *in vacuo*. Purification by flash column chromatography (5–15% EtOAc/hexanes) afforded the pure title compound as a colorless oil (328 mg, 60%).

¹H NMR (700 MHz, CDCl₃): δ 7.39 (d, *J* = 7.5 Hz, 2H), 7.33 (t, *J* = 7.6 Hz, 2H), 7.26 (t, *J* = 7.8 Hz, 1H), 6.63 (d, *J* = 15.9 Hz, 1H), 6.29 (dt, *J* = 15.9, 6.2 Hz, 1H), 4.23 (dd, *J* = 6.2, 1.1 Hz, 2H), 4.11 (s, 2H), 2.18 (s, 3H); ¹³C NMR (176 MHz, CDCl₃): δ 206.8, 136.5, 133.7, 128.8, 128.1, 126.7, 125.1, 75.4, 72.1, 26.6; IR (cm⁻¹): 3027, 2852, 1729, 1716, 1495, 1449, 1354, 1119, 966, 733, 692; HRMS: *m/z* calculated for C₁₂H₁₄O₂Na⁺ [M+Na]⁺: 213.0886; found: 213.0893.



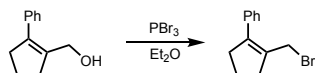
2-(Cinnamyloxy)-1-phenylethan-1-one (A2.16): A 50-mL round-bottom flask equipped with a magnetic stir bar was charged with freshly grinded magnesium turnings (105 mg, 4.3 mmol, 1.5 equiv.). THF (4 mL) and bromobenzene (0.48 mL, 4.6 mmol, 1.6 equiv.) were added sequentially and the mixture brought to reflux with a heat gun, then allowed to stir at rt for 2 h. After diluting the solution with THF (4 mL), CuBr (8 mg, 0.06 mmol, 0.02 equiv.) and **A2.17** (500 mg, 2.9 mmol, 1.0 equiv.) were added and the reaction heated at reflux for 0.5 h. Then, the mixture was cooled to 0 °C and 2 M aqueous HCl solution (5 mL) was added followed by vigorous stirring for 0.5 h. The biphasic mixture was partitioned between water and Et₂O, the organic layer separated and the aqueous layer extracted with Et₂O (3x). The combined organic extracts were washed with NaHCO₃ solution (aq., sat.) and brine, dried over MgSO₄, filtered and concentrated

in vacuo, then dried using high-vac. The crude phenyl ketone was used for the synthesis of **S2.90** without further purification.

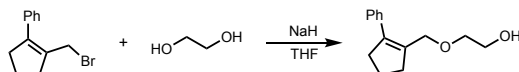


***N*-Cinnamyl-*N*-(2-hydroxy-2-(pyridin-2-yl)ethyl)-4-methylbenzenesulfonamide (A2.8):** A 25-mL round-bottom flask with a magnetic stir bar was charged with 2-bromopyridine (0.16 mL, 1.61 mmol, 1.0 equiv.) and THF (1 mL), and a 1 M solution of isopropylmagnesium bromide in THF (1.6 mL, 1.0 equiv.) was added over 5 minutes. After stirring for 2 h at rt, a solution of *N*-cinnamyl-*N*-(2-hydroxyethyl)-4-methylbenzenesulfonamide¹⁷⁵ (530 mg, 1.61 mmol, 1.0 equiv.) in THF (1 mL) was added dropwise. The mixture was stirred for 12 h at rt followed by addition of NH₄Cl solution (aq., sat.). The organic layer was separated, and the aqueous layer extracted with diethyl ether (3x). The combined organic extracts were washed with brine, dried over MgSO₄, filtered and concentrated *in vacuo*. Purification by flash column chromatography (10–70% EtOAc/hexanes) afforded the pure title compound as a yellow oil (225 mg, 34%).

¹H NMR (500 MHz, CDCl₃): δ 8.47 (d, *J* = 4.7 Hz, 1H), 7.74 (d, *J* = 8.3 Hz, 2H), 7.70 (td, *J* = 7.7, 1.7 Hz, 1H), 7.48 (d, *J* = 7.8 Hz, 1H), 7.32 – 7.27 (m, 4H), 7.25 – 7.13 (m, 4H), 6.37 (d, *J* = 15.9 Hz, 1H), 5.80 (dt, *J* = 15.8, 6.8 Hz, 1H), 5.02 (q, *J* = 5.0 Hz, 1H), 4.27 (d, *J* = 5.4 Hz, 1H), 4.03 (dd, *J* = 15.5, 5.8 Hz, 1H), 3.92 (dd, *J* = 15.5, 7.3 Hz, 1H), 3.51 (dd, *J* = 14.7, 4.5 Hz, 1H), 3.44 (dd, *J* = 14.8, 7.4 Hz, 1H), 2.41 (s, 3H); **¹³C NMR** (126 MHz, CDCl₃): δ 159.5, 148.6, 143.7, 136.9, 136.8, 136.3, 134.4, 129.9, 128.6, 128.0, 127.6, 126.6, 123.7, 123.0, 121.7, 72.4, 54.2, 52.0, 21.6; **IR** (cm⁻¹): 3026, 2924, 1596, 1438, 1335, 1305, 1155, 1089, 969, 925, 815, 732, 693, 662; **HRMS**: *m/z* calculated for C₂₃H₂₄N₂O₄SH⁺ [M+H]⁺: 409.1580; found: 409.1578.



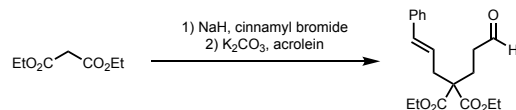
(2-(Bromomethyl)cyclopent-1-en-1-yl)benzene (A2.21): A 25-mL round-bottom flask equipped with a magnetic stir bar was charged with (2-phenylcyclopent-1-en-1-yl)methanol¹⁸⁵ (940 mg, 5.4 mmol, 1.0 equiv.) and Et₂O (6 mL). PBr₃ (0.21 mL, 2.2 mmol, 0.4 equiv.) was added dropwise at 0 °C and the reaction stirred for 1 h at that temperature. Then, brine (1 mL) was added and the aqueous layer separated. The organic layer was washed sequentially with NaHCO₃ solution (aq., sat., 3x) and brine, dried over MgSO₄, filtered and concentrated *in vacuo* and dried using high-vac to afford the crude title compound as a colorless oil (1.18 g, 92%), which was directly used for the next step without further purification.



2-((2-Phenylcyclopent-1-en-1-yl)methoxy)ethan-1-ol (A2.9): NaH (60% dispersion in mineral oil; 498 mg, 12.4 mmol, 2.5 equiv.) was carefully added to a solution of ethylene glycol (2.8 mL, 49.8 mmol, 10.0 equiv.) in THF (10 mL) at 0 °C. After stirring for 15 min, the mixture was transferred to a 50-mL round-bottom flask equipped with a magnetic stir bar containing a solution of **A2.21** (1.18 g, 5.0 mmol, 1.0 equiv.) in THF (10 mL) and the resulting mixture refluxed for 4 h. After cooling down to rt, NH₄Cl solution (aq., sat.) was added and the mixture extracted with EtOAc (3x). The combined organic extracts were washed with brine, dried over Na₂SO₄, filtered and concentrated *in vacuo*. Purification by flash column chromatography (5–50% EtOAc/hexanes) afforded the pure title compound as a colorless oil (869 mg, 80%).

¹H NMR (700 MHz, CDCl₃): δ 7.34 (t, *J* = 7.6 Hz, 2H), 7.27 – 7.25 (m, 1H), 7.25 – 7.22 (m, 2H), 4.17 (s, 2H), 3.74 – 3.70 (m, 2H), 3.52 – 3.48 (m, 2H), 2.79 (t, *J* = 7.5 Hz, 2H), 2.65 (t, *J* = 7.5 Hz, 2H), 1.97 (p, *J* = 7.5 Hz, 2H), 1.91 (t, *J* = 6.2 Hz, 1H); ¹³C NMR (176 MHz, CDCl₃): δ 140.9, 137.8, 135.51, 128.3, 127.9, 127.1, 71.4, 68.1, 62.1, 37.9, 36.0, 22.1; IR (cm⁻¹): 3386, 2843, 1493,

1442, 1355, 1253, 1207, 1105, 1054, 1035, 1005, 889, 760, 732, 698, 655; **HRMS**: m/z calculated for $C_{14}H_{18}O_2^+$ $[M]^+$: 218.1307; found: 218.1312.

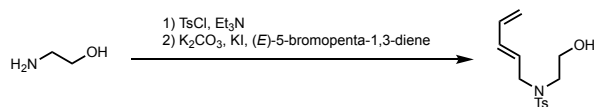


Diethyl 2-cinnamyl-2-(3-oxopropyl)malonate (A2.18): A round-bottom flask equipped with a magnetic stir bar was charged with NaH (60% dispersion in mineral oil; 457 mg, 11.4 mmol, 1.5 equiv.) and THF (15 mL). After cooling to 0 °C, diethyl malonate (1.7 mL, 11.4 mmol, 1.5 equiv.) was added dropwise and the reaction mixture stirred for 1 h at that temperature. Next, a solution of cinnamyl bromide (1.50 g, 7.6 mmol, 1.0 equiv.) in THF (2 mL) was added and the reaction mixture allowed to warm up to rt and stirred overnight. NH_4Cl solution (aq., sat.) and water were sequentially added, the organic layer separated and the aqueous layer extracted with EtOAc (3x). The combined organic extracts were dried over Na_2SO_4 , filtered and concentrated *in vacuo*. Excess diethyl malonate was removed under high-vac at 70 °C, and the crude product was taken to the next step without further purification.

A 100-mL round-bottom flask equipped with a magnetic stir bar was charged with crude diethyl 2-cinnamylmalonate, K_2CO_3 (1.16 g, 8.4 mmol, 1.1 equiv.), acrolein (0.85 mL, 11.4 mmol, 1.5 equiv.) and CH_2Cl_2 (20 mL) and the mixture stirred at rt overnight. Water and EtOAc were added, the organic layer separated and the aqueous layer extracted with EtOAc (3x). The combined organic extracts were washed with brine, dried over Na_2SO_4 , filtered and concentrated *in vacuo*. Purification by flash column chromatography (20% EtOAc/hexanes) afforded the pure title compound as a pale-yellow oil (914 mg, 36%).

1H NMR (500 MHz, $CDCl_3$): δ 9.74 (s, 1H), 7.33 – 7.27 (m, 4H), 7.24 – 7.20 (m, 1H), 6.45 (d, J = 15.7 Hz, 1H), 6.04 (dt, J = 15.5, 7.5 Hz, 1H), 4.26 – 4.15 (m, 4H), 2.80 (d, J = 7.5 Hz, 2H),

2.53 (t, $J = 7.8$ Hz, 2H), 2.24 (t, $J = 8.1$ Hz, 2H), 1.26 (t, $J = 7.1$ Hz, 6H); ^{13}C NMR (176 MHz, CDCl_3): δ 200.9, 170.9, 137.0, 134.3, 128.6, 127.6, 126.3, 123.6, 61.6, 57.0, 39.3, 37.5, 25.4, 14.2; IR (cm^{-1}): 2981, 1721, 1446, 1367, 1233, 1184, 1095, 1025, 968, 858, 739, 693; HRMS: m/z calculated for $\text{C}_{19}\text{H}_{24}\text{O}_5\text{Na}^+$ $[\text{M}+\text{Na}]^+$: 355.1516; found: 355.1518.



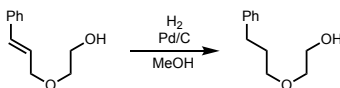
(E)-N-(2-Hydroxyethyl)-4-methyl-N-(penta-2,4-dien-1-yl)benzenesulfonamide (A2.10):

Ethanolamine (0.25 mL, 4.1 mmol, 1.0 equiv.) was converted to *N*-(2-hydroxyethyl)-4-toluenesulfonamide following a literature procedure¹⁷⁵ and the crude product used for the next step without further purification.

A 25-mL round-bottom flask equipped with a magnetic stir bar was charged with crude *N*-(2-hydroxyethyl)-4-toluenesulfonamide from the previous step and acetone (10 mL), followed by the sequential addition of K_2CO_3 (859 mg, 6.2 mmol, 1.5 equiv.), potassium iodide (69 mg, 0.41 mmol, 0.1 equiv.) and freshly prepared (*E*)-5-bromopenta-1,3-diene¹⁸⁶ (913 mg, 6.2 mmol, 1.5 equiv.). Then, the reaction was heated to reflux overnight. After cooling to rt, the reaction mixture was diluted with water and EtOAc, the organic layer separated and the aqueous layer extracted with EtOAc (3x). The combined organic extracts were washed with brine, dried over Na_2SO_4 , filtered and concentrated *in vacuo*. Purification by flash column chromatography (30–50% EtOAc/hexanes) afforded the pure title compound as a pale-yellow oil (994 mg, 85%; *E/Z* (diene) = 15:1).

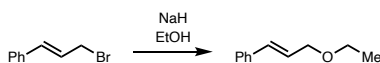
^1H NMR (700 MHz, CDCl_3): δ 7.71 (d, $J = 8.3$ Hz, 2H), 7.32 (d, $J = 7.9$ Hz, 2H), 6.25 (dt, $J = 17.0, 10.3$ Hz, 1H), 6.11 (dd, $J = 15.2, 10.5$ Hz, 1H), 5.51 (dt, $J = 15.0, 6.8$ Hz, 1H), 5.18 (d, $J = 17.0$ Hz, 1H), 5.11 (d, $J = 10.1$ Hz, 1H), 3.89 (d, $J = 6.8$ Hz, 2H), 3.73 (t, $J = 5.3$ Hz, 2H), 3.24 (t,

$J = 5.3$ Hz, 2H), 2.44 (s, 3H); ^{13}C NMR (176 MHz, CDCl_3): δ 143.7, 136.4, 135.7, 135.1, 129.9, 127.9, 127.4, 118.6, 61.2, 51.3, 49.8, 21.6; IR (cm^{-1}): 3510, 2925, 1598, 1447, 1329, 1152, 1047, 1003, 950, 909, 814, 752, 726, 657; HRMS: m/z calculated for $\text{C}_{14}\text{H}_{19}\text{NO}_3\text{SNa}^+$ $[\text{M}+\text{Na}]^+$: 304.0978; found: 304.0982.



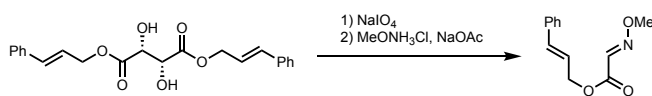
2-(3-Phenylpropoxy)ethan-1-ol (A2.11): A 100-mL round-bottom flask equipped with a magnetic stir bar was charged with 2-(cinnamyloxy)ethan-1-ol¹⁸⁷ (1.00 g, 5.6 mmol, 1.0 equiv.), palladium on activated carbon (10 wt%; 299 mg, 5 mol%) and MeOH (30 mL). The mixture was sparged for 20 min with hydrogen gas from a balloon and stirred at rt for 2 h under a hydrogen atmosphere. Then, the reaction mixture was passed through a pad of celite. After washing the pad with EtOAc, the filtrate was concentrated *in vacuo* and dried using high-vac to obtain the pure title compound as a colorless oil (1.00 g, 99%).

^1H NMR (700 MHz, CDCl_3): δ 7.29 (t, $J = 7.6$ Hz, 2H), 7.21 – 7.18 (m, 3H), 3.73 (q, $J = 5.4$ Hz, 2H), 3.53 (t, $J = 4.5$ Hz, 2H), 3.49 (t, $J = 6.4$ Hz, 2H), 2.70 (t, $J = 7.8$ Hz, 2H), 1.96 – 1.90 (m, 3H); ^{13}C NMR (176 MHz, CDCl_3): δ 141.9, 128.54, 128.46, 125.9, 71.9, 70.5, 62.0, 32.4, 31.3; IR (cm^{-1}): 3418, 2927, 2862, 1496, 1453, 1361, 1118, 1044, 891, 745, 698; HRMS: m/z calculated for $\text{C}_{11}\text{H}_{16}\text{O}_2\text{Na}^+$ $[\text{M}+\text{Na}]^+$: 203.1043; found: 203.1037.



(E)-(3-ethoxyprop-1-en-1-yl)benzene (2.103): A 50-mL round-bottom flask equipped with a magnetic stir bar was charged with NaH (60% dispersion in mineral oil; 507 mg, 12.7 mmol, 2.5 equiv.) and THF (15 mL). After cooling to 0 °C, EtOH (0.74 mL, 12.7 mmol, 2.5 equiv.) was added dropwise and the mixture stirred for 0.5 h. Next, a solution of cinnamyl bromide (1.00 g,

5.1 mmol, 1.0 equiv.) in THF (2.5 mL) was added at 0 °C, and the mixture heated at reflux for 2 h. After cooling down to rt, NH₄Cl solution (aq., sat.) was added and the resulting mixture partitioned between water and EtOAc. The organic layer was separated and the aqueous layer extracted with EtOAc (3x). The combined organic extracts were washed with brine, dried over MgSO₄, filtered and concentrated *in vacuo*. Purification by flash column chromatography (2.5% Et₂O/pentane) provided the pure title compound as a colorless oil (452 mg, 52%). Spectroscopic data were consistent with those reported in the literature.¹⁸⁸

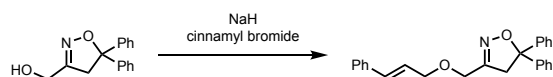


Cinnamyl 2-(methoxyimino)acetate (S2.92): A 25-mL round-bottom flask equipped with a magnetic stir bar was charged with dicinnamyl (2*R*,3*R*)-2,3-dihydroxysuccinate¹⁸⁹ (1.00 g, 2.6 mmol, 1.0 equiv.) and a 2:1 THF/water mixture. NaIO₄ (1.12 g, 5.2 mmol, 2.0 equiv.) was added and the reaction stirred overnight at rt. Then, solids were removed by filtration through a pad of celite and NaHSO₃ solution (aq., sat.) was added to the filtrate. The resulting mixture was extracted with Et₂O (3x) and the combined organic extracts washed with brine, dried over MgSO₄, filtered and concentrated *in vacuo*, then dried using high-vac. The crude oxoacetate was used for the next step without further purification.

To a 50-mL round-bottom flask equipped with magnetic stir bar containing crude oxoacetate and CH₂Cl₂ (25 mL) was sequentially added NaOAc (1.72 g, 20.9 mmol, 8.0 equiv.) and *O*-methylhydroxylamine hydrochloride (874 mg, 10.5 mmol, 4.0 equiv.). After stirring the resulting mixture overnight at rt, NaHCO₃ solution (aq., sat.) was added, the organic layer separated and the aqueous layer extracted with EtOAc (3x). The combined organic extracts were washed with brine, dried over Na₂SO₄, filtered and concentrated *in vacuo*. Purification by flash

column chromatography (5–10% EtOAc/hexanes) afforded the pure title compound as a colorless oil (453 mg, 40%; *E/Z* (oxime) = 6.7:1).

¹H NMR (500 MHz, CDCl₃): δ 7.52 (s, 6.7H; major), 7.40 (d, *J* = 7.3 Hz, 15.4H; major+minor), 7.33 (t, *J* = 7.4 Hz, 15.4H; major+minor), 7.29 – 7.25 (m, 7.7H; major+minor), 6.99 (s, 1H; minor), 6.71 (d, *J* = 15.9 Hz, 7.7H; major+minor), 6.39 – 6.26 (m, 7.7H; major+minor), 4.92 (dd, *J* = 6.6, 1.3 Hz, 13.4H; major), 4.86 (dd, *J* = 6.6, 1.3 Hz, 2H; minor), 4.07 (s, 20.1H; major), 4.05 (s, 3H; minor); **¹³C NMR** (176 MHz, CDCl₃): δ 161.9, 158.8, 140.7, 136.9, 136.1 (2C), 135.5, 135.3, 128.77, 128.75, 128.40, 128.39, 126.84, 126.82, 122.3, 122.2, 66.3, 65.9, 64.0, 63.7; **IR** (cm⁻¹): 2941, 1719, 1598, 1494, 1449, 1382, 1318, 1265, 1198, 1171, 1047, 962, 917, 735, 691; **HRMS**: *m/z* calculated for C₁₂H₁₃NO₃Na⁺ [M+Na]⁺: 242.0788; found: 242.0794.



3-((Cinnamyloxy)methyl)-5,5-diphenyl-4,5-dihydroisoxazole (2.97): A 25-mL round-bottom flask equipped with a magnetic stir bar was charged with NaH (60% dispersion in mineral oil; 71 mg, 1.8 mmol, 1.5 equiv.) and THF (10 mL). Next, a solution of (5,5-diphenyl-4,5-dihydroisoxazol-3-yl)methanol¹⁹⁰ (300 mg, 1.2 mmol, 1.0 equiv.) in THF (2 mL) was added dropwise at 0 °C and then, after stirring for 15 min, a solution of cinnamyl bromide (257 mg, 1.3 mmol, 1.1 equiv.) in THF (2 mL) and the reaction allowed to warm up to rt and stirred overnight. NH₄Cl solution (aq., sat.) was added and the mixture extracted with EtOAc (3x). The combined organic extracts were washed with brine, dried over Na₂SO₄, filtered and concentrated *in vacuo*. Purification by flash column chromatography (2–10% EtOAc/hexanes) afforded the pure title compound as a pale-yellow oil (384 mg, 88%).

¹H NMR (700 MHz, CDCl₃): δ 7.44 – 7.41 (m, 4H), 7.36 – 7.30 (m, 8H), 7.29 – 7.26 (m, 2H), 7.27 – 7.23 (m, 1H), 6.50 (d, *J* = 15.9 Hz, 1H), 6.18 (dt, *J* = 15.9, 6.2 Hz, 1H), 4.32 (s, 2H), 4.03

(dd, $J = 6.2, 1.4$ Hz, 2H), 3.70 (s, 2H); ^{13}C NMR (176 MHz, CDCl_3): δ 156.7, 144.0, 136.5, 133.6, 128.7, 128.5, 128.00, 127.8, 126.7, 126.2, 124.9, 91.8, 71.0, 64.7, 48.4; IR (cm^{-1}): 3025, 2852, 1598, 1492, 1447, 1363, 1328, 1221, 1109, 1058, 966, 894, 865, 747, 692; HRMS: m/z calculated for $\text{C}_{25}\text{H}_{23}\text{NO}_2\text{Na}^+$ $[\text{M}+\text{Na}]^+$: 392.1621; found: 392.1619.

Synthesis of Azetidine Products and Characterization

General Procedure for [2+2] Cycloaddition

General Procedure for small-scale reactions (GP-2.6). An oven-dried test tube (25x150 mm) equipped with a magnetic stir bar was charged with substrate (0.25 mmol, 1.0 equiv.), [Ir(dF(CF₃)ppy)₂(dtbbpy)](PF₆) (1.4 mg or 2.8 mg, 0.5 or 1 mol%) and THF (25 mL). When a substrate required extended reaction times (>2 h), the reaction mixture was degassed by sparging with nitrogen gas for 30 min prior to irradiation and the reaction conducted under a nitrogen atmosphere. The test tube was sealed with a rubber septum and placed in front of a 40 W PR160-427 nm Kessil light at a distance of approximately 5 cm. The light was set to 100% intensity and the reaction stirred until complete as judged by TLC analysis (0.5–72 h). The internal temperature of the photoreactor was maintained below 45 °C by a fan. Upon completion, the reaction mixture was transferred to a 100-mL round-bottom flask and the solvent removed *in vacuo*. The diastereomeric ratio was determined by ¹H NMR analysis from the crude mixture, before purifying the crude product by flash column chromatography (EtOAc/hexanes) to afford the corresponding pure azetidine.

General Procedure for gram-scale reactions (GP-2.7). A 500-mL round-bottom flask equipped with a magnetic stir bar was charged with substrate (1.0 equiv.), [Ir(dF(CF₃)ppy)₂(dtbbpy)](PF₆) (0.5 mol%) and THF (0.025 M). The flask was placed in between a 40 W PR160-427 nm Kessil light (100% intensity) and a 34 W H150-BLUE Kessil light at a distance of approximately 5 cm and the reaction stirred under ambient atmosphere until complete as judged by TLC analysis. Solvent was removed *in vacuo* and the diastereomeric ratio determined by ¹H NMR analysis from the crude mixture. Purification of the crude product by flash column chromatography (EtOAc/hexanes) afforded the corresponding pure azetidine.

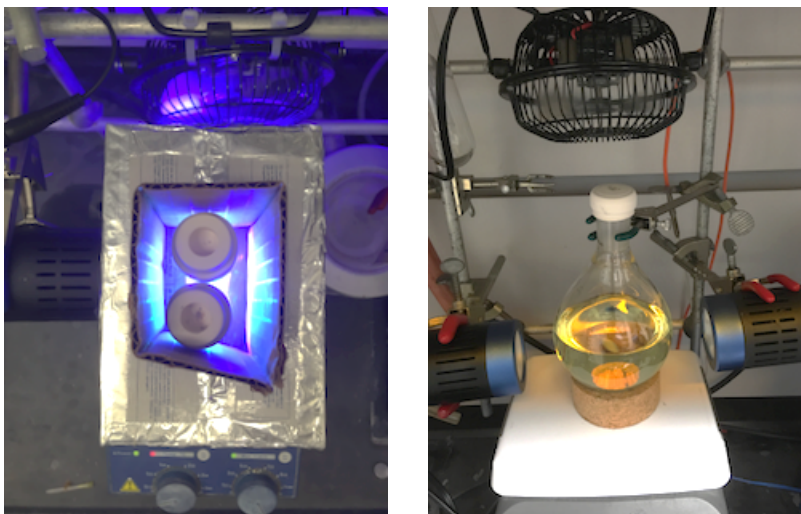
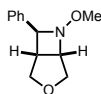


Figure 2.28: Reaction setup used for the [2+2] cycloaddition reactions. left: setup for small scale reactions (0.25 mmol). right: setup for gram-scale reactions.



(1*R,5*S**,7*S**)-6-Methoxy-7-phenyl-3-oxa-6-azabicyclo[3.2.0]heptane (2.69):** Prepared according to GP-2.6 using (*E*)-**2.68** (51 mg, 0.25 mmol, 1.0 equiv.), **2.59**•PF₆ (1.4 mg, 0.5 mol%) and THF (25 mL) with a reaction time of 0.5 h. The diastereomeric ratio was determined to be >20:1 by ¹H NMR analysis of the crude mixture. Purification by flash column chromatography (10–20% EtOAc/hexanes) afforded the pure title compound as a colorless oil (49 mg, 96%; combined yield).

¹H NMR (500 MHz, CDCl₃): δ 7.43 (d, *J* = 7.5 Hz, 2H), 7.37 (t, *J* = 7.6 Hz, 2H), 7.29 (t, *J* = 7.2 Hz, 1H), 4.76 (d, *J* = 10.6 Hz, 1H), 4.54 (t, *J* = 5.5 Hz, 1H), 4.42 (d, *J* = 5.8 Hz, 1H), 3.98 (d, *J* = 9.4 Hz, 1H), 3.58 (dd, *J* = 10.6, 5.3 Hz, 1H), 3.52 (dd, *J* = 9.4, 3.6 Hz, 1H), 3.45 (s, 3H), 2.72 (td, *J* = 5.8, 3.9 Hz, 1H); **¹³C NMR** (126 MHz, CDCl₃): δ 141.9, 128.6, 127.6, 126.4, 73.9, 70.8, 67.5, 67.2, 60.6, 42.1; **IR** (cm⁻¹): 2949, 2852, 1466, 1162, 1084, 1059, 1019, 909, 730, 697; **HRMS**: *m/z* calculated for C₁₂H₁₅NO₂H⁺ [M+H]⁺: 206.1176; found: 206.1175.



(1*R,5*S**,7*S**)-6-Methoxy-7-phenyl-3-oxa-6-azabicyclo[3.2.0]heptane (2.69):** Prepared according to GP-2.6 using (*Z*)-**2.68** (51 mg, 0.25 mmol, 1.0 equiv.), **2.59**•PF₆ (1.4 mg, 0.5 mol%) and THF (25 mL) with a reaction time of 0.5 h. The diastereomeric ratio was determined to be >20:1 by ¹H NMR analysis of the crude mixture. Purification by flash column chromatography (10–20% EtOAc/hexanes) afforded the pure title compound as a colorless oil (50 mg, 97%; combined yield). Spectroscopic data was found consistent with those obtained when (*E*)-**2.68** was used.



(1*R,5*S**,7*S**)-6-Methoxy-7-phenyl-3-oxa-6-azabicyclo[3.2.0]heptane (2.69):** Prepared according to GP-2.7 using (*E*)-**2.68** (1.40 g, 6.8 mmol, 1.0 equiv.), **2.59**•PF₆ (38 mg, 0.5 mol%) and THF (300 mL) with a reaction time of 1 h. The diastereomeric ratio was determined to be >20:1 by ¹H NMR analysis of the crude mixture. Purification by flash column chromatography (5–20% EtOAc/hexanes) afforded the pure title compound as a colorless oil (1.27 g, 91%; combined yield). Spectroscopic data was found consistent with those obtained when the reaction was conducted on 0.25 mmol scale.



(1*R,5*S**,7*S**)-6-(Benzyloxy)-7-phenyl-3-oxa-6-azabicyclo[3.2.0]heptane (2.75):** Prepared according to GP-2.6 using **2.71** (70 mg, 0.25 mmol, 1.0 equiv.), **2.59**•PF₆ (1.4 mg, 0.5 mol%) and THF (25 mL) with a reaction time of 0.5 h. The diastereomeric ratio was determined to be 16:1 by

¹H NMR analysis of the crude mixture. Purification by flash column chromatography (5–10% EtOAc/hexanes) afforded the pure title compound as a colorless oil (67 mg, 96%; combined yield). **¹H NMR** (700 MHz, CDCl₃): δ 7.37 – 7.35 (m, 2H), 7.33 (t, *J* = 7.6 Hz, 2H), 7.29 – 7.23 (m, 6H), 4.76 (d, *J* = 10.5 Hz, 1H), 4.62 (s, 2H), 4.48 (d, *J* = 5.8 Hz, 1H), 4.30 (t, *J* = 5.6 Hz, 1H), 3.95 (d, *J* = 9.4 Hz, 1H), 3.50 – 3.45 (m, 2H), 2.65 (td, *J* = 5.9, 3.6 Hz, 1H) **¹³C NMR** (176 MHz, CDCl₃): δ 141.9, 138.4, 128.6, 128.5, 128.3, 127.7, 127.5, 126.5, 75.6, 74.1, 70.8, 68.5, 67.6, 42.6; **IR** (cm⁻¹): 2850, 1495, 1453, 1366, 1204, 1084, 1061, 977, 909, 742, 695; **HRMS**: *m/z* calculated for C₁₈H₁₉NO₂H⁺ [M+H]⁺: 282.1489; found: 282.1491.



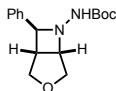
(1R*,5S*,7S*)-6-(Benzyloxy)-7-phenyl-3-oxa-6-azabicyclo[3.2.0]heptane (2.75): Prepared according to GP-2.7 using **2.71** (1.20 g, 4.3 mmol, 1.0 equiv.), **2.59**•PF₆ (24 mg, 0.5 mol%) and THF (300 mL) with a reaction time of 1 h. The diastereomeric ratio was determined to be 20:1 by ¹H NMR analysis of the crude mixture. Purification by flash column chromatography (5–20% EtOAc/hexanes) afforded the pure title compound as a colorless oil (1.08 g, 90%; combined yield). Spectroscopic data was found consistent with those obtained when the reaction was conducted on 0.25 mmol scale.



(1R*,5S*,7S*)-7-Phenyl-3-oxa-6-azabicyclo[3.2.0]heptan-6-ol (2.76): Prepared according to GP-2.6 using **2.72** (48 mg, 0.25 mmol, 1.0 equiv.), **2.59**•PF₆ (1.4 mg, 0.5 mol%) and THF (25 mL) with a reaction time of 0.5 h. The diastereomeric ratio was determined to be >20:1 by ¹H NMR analysis of the crude mixture. Purification by flash column chromatography (20–40%

EtOAc/hexanes) afforded the pure title compound as an off-white solid (48 mg, 54%; combined yield).

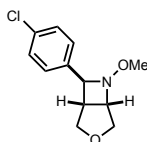
¹H NMR (700 MHz, CDCl₃): δ 7.35 – 7.30 (m, 4H), 7.29 – 7.26 (m, 1H), 4.79 (d, *J* = 10.7 Hz, 1H), 4.36 (d, *J* = 5.9 Hz, 1H), 4.32 (t, *J* = 5.6 Hz, 1H), 3.92 (d, *J* = 9.4 Hz, 1H), 3.51 – 3.45 (m, 2H), 2.74 (td, *J* = 5.9, 3.6 Hz, 1H); **¹³C NMR** (176 MHz, CDCl₃): δ 140.8, 128.6, 127.9, 126.9, 75.5, 70.7, 69.1, 66.8, 41.8; **IR** (cm⁻¹): 3243, 2853, 1454, 1353, 1266, 1162, 1084, 1055, 954, 815, 741, 697; **HRMS**: *m/z* calculated for C₁₁H₁₃NO₂Na⁺ [M+Na]⁺: 214.0838; found: 214.0838.



***Tert*-butyl ((1*R**,5*S**,7*S**)-7-phenyl-3-oxa-6-azabicyclo[3.2.0]heptan-6-yl)carbamate (2.77):**

Prepared according to GP-2.6 using **2.73** (73 mg, 0.25 mmol, 1.0 equiv.), **2.59**•PF₆ (1.4 mg, 0.5 mol%) and THF (25 mL) with a reaction time of 0.5 h. The diastereomeric ratio was determined to be 13:1 by ¹H NMR analysis of the crude mixture. Purification by flash column chromatography (30–40% EtOAc/hexanes) afforded the pure title compound as a pale-yellow solid (45 mg, 62%; combined yield).

¹H NMR (700 MHz, CDCl₃): δ 7.50 (d, *J* = 7.4 Hz, 2H), 7.36 (t, *J* = 7.7 Hz, 2H), 7.26 (t, *J* = 7.4 Hz, 1H), 5.91 (b, 1H), 4.60 (t, *J* = 4.8 Hz, 1H), 4.49 (d, *J* = 11.5 Hz, 1H), 4.22 (d, *J* = 4.8 Hz, 1H), 4.03 (d, *J* = 9.5 Hz, 1H), 3.50 (dd, *J* = 9.5, 3.9 Hz, 1H), 3.47 (dd, *J* = 11.5, 4.1 Hz, 1H), 2.75 (q, *J* = 4.9 Hz, 1H), 1.41 (s, 9H); **¹³C NMR** (176 MHz, CDCl₃): δ 154.9, 141.6, 128.6, 127.5, 126.0, 80.3, 77.2, 71.9, 68.7, 67.5, 43.2, 28.4; **IR** (cm⁻¹): 3262, 2975, 2857, 1734, 1695, 1522, 1455, 1366, 1247, 1161, 1049, 993, 906, 743, 670; **HRMS**: *m/z* calculated for C₁₆H₂₂N₂O₃Na⁺ [M+Na]⁺: 313.1523; found: 313.1528.



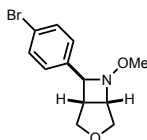
(1*R,5*S**,7*S**)-7-(4-Chlorophenyl)-6-methoxy-3-oxa-6-azabicyclo[3.2.0]heptane (2.79):**

Prepared according to GP-2.6 using **S2.79** (62 mg, 0.26 mmol, 1.0 equiv.), **2.59**•PF₆ (1.4 mg, 0.5 mol%) and THF (25 mL) with a reaction time of 0.5 h. The diastereomeric ratio was determined to be >20:1 by ¹H NMR analysis of the crude mixture. Purification by flash column chromatography (2–20% EtOAc/hexanes) afforded the pure title compound as a colorless oil (61 mg, 98%; combined yield).

¹H NMR (500 MHz, CDCl₃): δ 7.35 (d, *J* = 8.6 Hz, 2H), 7.32 (d, *J* = 8.6 Hz, 2H), 4.73 (d, *J* = 10.7 Hz, 1H), 4.52 (t, *J* = 5.6 Hz, 1H), 4.36 (d, *J* = 5.8 Hz, 1H), 3.94 (d, *J* = 9.5 Hz, 1H), 3.55 (dd, *J* = 10.7, 5.3 Hz, 1H), 3.49 (dd, *J* = 9.5, 3.6 Hz, 1H), 3.42 (s, 3H), 2.66 (td, *J* = 5.9, 3.5 Hz, 1H);

¹³C NMR (100 MHz, CDCl₃): δ 140.4, 133.3, 128.7, 127.8, 73.1, 70.7, 67.5, 67.1, 60.6, 42.2; IR (cm⁻¹): 2951, 2895, 2852, 1491, 1466, 1081, 1064, 1050, 1023, 1014, 979, 913, 820, 803, 725;

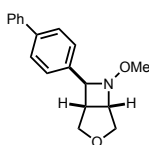
HRMS: *m/z* calculated for C₁₂H₁₄ClNO₂H⁺ [M+H]⁺: 240.0786; found: 240.0786.



(1*R,5*S**,7*S**)-7-(4-Bromophenyl)-6-methoxy-3-oxa-6-azabicyclo[3.2.0]heptane (2.80):**

Prepared according to GP-2.6 using **S2.80** (71 mg, 0.25 mmol, 1.0 equiv.), **2.59**•PF₆ (1.4 mg, 0.5 mol%) and THF (25 mL) with a reaction time of 0.5 h. The diastereomeric ratio was determined to be >20:1 by ¹H NMR analysis of the crude mixture. Purification by flash column chromatography (10–20% EtOAc/hexanes) afforded the pure title compound as a white solid (60 mg, 85%; combined yield).

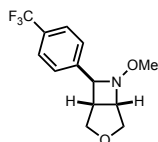
¹H NMR (500 MHz, CDCl₃): δ 7.48 (d, *J* = 8.3 Hz, 2H), 7.29 (d, *J* = 8.3 Hz, 2H), 4.73 (d, *J* = 10.7 Hz, 1H), 4.51 (t, *J* = 5.5 Hz, 1H), 4.34 (d, *J* = 5.8 Hz, 1H), 3.94 (d, *J* = 9.5 Hz, 1H), 3.55 (dd, *J* = 10.7, 5.3 Hz, 1H), 3.49 (dd, *J* = 9.5, 3.6 Hz, 1H), 3.41 (s, 3H), 2.65 (td, *J* = 5.8, 3.7 Hz, 1H); **¹³C NMR** (126 MHz, CDCl₃): δ 141.0, 131.7, 128.2, 121.4, 73.2, 70.7, 67.5, 67.1, 60.7, 42.2; **IR** (cm⁻¹): 2929, 2843, 1485, 1161, 1059, 1007, 937, 903, 858, 814, 792, 718; **HRMS**: *m/z* calculated for C₁₂H₁₄BrNO₂H⁺ [M+H]⁺: 284.0281; found: 284.0279.



(1*R,5*S**,7*S**)-7-([1,1'-Biphenyl]-4-yl)-6-methoxy-3-oxa-6-azabicyclo[3.2.0]heptane (2.81):**

Prepared according to GP-2.6 using **S2.81** (70 mg, 0.25 mmol, 1.0 equiv.), **2.59**•PF₆ (1.4 mg, 0.5 mol%) and THF (25 mL) with a reaction time of 0.5 h. The diastereomeric ratio was determined to be 16:1 by ¹H NMR analysis of the crude mixture. Purification by flash column chromatography (10–20% EtOAc/hexanes) afforded the pure title compound as a colorless oil (70 mg, 99%; combined yield).

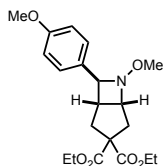
¹H NMR (500 MHz, CDCl₃): δ 7.60 (d, *J* = 8.1 Hz, 4H), 7.49 (d, *J* = 8.1 Hz, 2H), 7.44 (t, *J* = 7.6 Hz, 2H), 7.35 (t, *J* = 7.4 Hz, 1H), 4.77 (d, *J* = 10.6 Hz, 1H), 4.56 (t, *J* = 5.5 Hz, 1H), 4.45 (d, *J* = 5.8 Hz, 1H), 3.99 (d, *J* = 9.4 Hz, 1H), 3.58 (dd, *J* = 10.6, 5.3 Hz, 1H), 3.53 (dd, *J* = 9.3, 3.6 Hz, 1H), 3.46 (s, 3H), 2.75 (td, *J* = 5.8, 3.8 Hz, 1H); **¹³C NMR** (126 MHz, CDCl₃): δ 141.1, 141.0, 140.6, 128.9, 127.4 (2C), 127.2, 126.9, 73.7, 70.8, 67.5, 67.2, 60.7, 42.2; **IR** (cm⁻¹): 2930, 2849, 1486, 1098, 1079, 1008, 978, 911, 832, 760, 734, 695; **HRMS**: *m/z* calculated for C₁₈H₁₉NO₂Na⁺ [M+Na]⁺: 304.1308; found: 304.1311.



(1*R,5*S**,7*S**)-6-Methoxy-7-(4-(trifluoromethyl)phenyl)-3-oxa-6-azabicyclo[3.2.0]heptane**

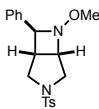
(2.82): Prepared according to GP-2.6 using **S2.82** (68 mg, 0.25 mmol, 1.0 equiv.), **2.59**•PF₆ (1.4 mg, 0.5 mol%) and THF (25 mL) with a reaction time of 0.5 h. The diastereomeric ratio was determined to be >20:1 by ¹H NMR analysis of the crude mixture. Purification by flash column chromatography (5–20% EtOAc/hexanes) afforded the pure title compound as a colorless oil (66 mg, 97%; combined yield).

¹H NMR (700 MHz, CDCl₃): δ 7.61 (d, *J* = 8.1 Hz, 2H), 7.53 (d, *J* = 8.1 Hz, 2H), 4.75 (d, *J* = 10.6 Hz, 1H), 4.54 (t, *J* = 5.5 Hz, 1H), 4.45 (d, *J* = 5.7 Hz, 1H), 3.97 (d, *J* = 9.5 Hz, 1H), 3.57 (dd, *J* = 10.6, 5.2 Hz, 1H), 3.52 (dd, *J* = 9.5, 3.5 Hz, 1H), 3.44 (s, 3H), 2.68 (td, *J* = 5.8, 3.6 Hz, 1H); ¹³C NMR (176 MHz, CDCl₃): δ 145.9, 129.8 (q, *J* = 32.3 Hz), 126.6, 125.5 (q, *J* = 3.8 Hz), 124.3 (q, *J* = 272 Hz), 73.1, 70.7, 67.6, 67.1, 60.6, 42.2; IR (cm⁻¹): 2940, 2854, 1620, 1417, 1322, 1161, 1118, 1064, 1017, 913, 832, 807, 712, 639; HRMS: *m/z* calculated for C₁₃H₁₄F₃NO₂H⁺ [M+H]⁺: 274.1049; found: 274.1044.



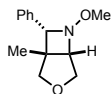
Diethyl (1*S,5*R**,7*S**)-6-methoxy-7-(4-methoxyphenyl)-6-azabicyclo[3.2.0]heptane-3,3-dicarboxylate (2.83):** Prepared according to GP-2.6 using **S2.83** (94 mg, 0.25 mmol, 1.0 equiv.), **2.59**•PF₆ (1.4 mg, 0.5 mol%) and THF (25 mL) with a reaction time of 1.5 h. The diastereomeric ratio was determined to be 20:1 by ¹H NMR analysis of the crude mixture. Purification by flash column chromatography (2–30% EtOAc/hexanes) afforded the pure title compound as a colorless oil (68 mg, 72%; combined yield).

¹H NMR (400 MHz, C₆D₆): δ 7.37 (d, *J* = 8.6 Hz, 2H), 6.83 (d, *J* = 8.6 Hz, 2H), 4.57 (d, *J* = 6.0 Hz, 1H), 4.52 (q, *J* = 6.9 Hz, 1H), 4.13 – 4.02 (m, 2H), 3.98 – 3.87 (m, 2H), 3.41 (dd, *J* = 14.7, 4.6 Hz, 1H), 3.32 (s, 3H), 3.31 (s, 3H), 2.89 – 2.79 (m, 2H), 2.39 (qd, *J* = 7.1, 6.2, 1.8 Hz, 1H), 2.29 (dd, *J* = 14.0, 7.9 Hz, 1H), 0.99 (t, *J* = 7.1 Hz, 3H), 0.89 (t, *J* = 7.1 Hz, 3H); **¹³C NMR** (126 MHz, C₆D₆): δ 172.3, 171.7, 159.8, 134.2, 128.5, 114.2, 76.6, 69.9, 63.9, 61.52, 61.49, 60.5, 54.8, 42.6, 38.5, 34.7, 14.1, 14.0; **IR** (cm⁻¹): 2937, 1725, 1611, 1513, 1464, 1443, 1300, 1244, 1206, 1178, 1094, 1062, 1034, 859, 809; **HRMS**: *m/z* calculated for C₂₀H₂₇NO₆H⁺ [M+H]⁺: 378.1911; found: 378.1917.



(1R*,5S*,7S*)-6-Methoxy-7-phenyl-3-tosyl-3,6-diazabicyclo[3.2.0]heptane (2.84): Prepared according to GP-2.6 using **S2.84** (90 mg, 0.25 mmol, 1.0 equiv.), **2.59**•PF₆ (1.4 mg, 0.5 mol%) and THF (25 mL) with a reaction time of 0.5 h. The diastereomeric ratio was determined to be 12:1 by ¹H NMR analysis of the crude mixture. Purification by flash column chromatography (10–30% EtOAc/hexanes) afforded the pure title compound as a white solid (83 mg, 92%; combined yield).

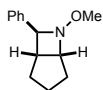
¹H NMR (700 MHz, CDCl₃): δ 7.77 (d, *J* = 8.2 Hz, 2H), 7.39 – 7.32 (m, 6H), 7.30 – 7.26 (m, 1H), 4.51 (d, *J* = 6.0 Hz, 1H), 4.40 – 4.33 (m, 2H), 3.61 (d, *J* = 10.0 Hz, 1H), 3.40 (s, 3H), 2.82 – 2.75 (m, 2H), 2.57 (q, *J* = 5.8 Hz, 1H), 2.45 (s, 3H); **¹³C NMR** (176 MHz, CDCl₃): δ 143.9, 141.3, 132.5, 129.8, 128.6, 128.1, 127.8, 126.5, 73.8, 66.2, 60.8, 51.5, 46.4, 40.5, 21.7; **IR** (cm⁻¹): 2936, 1597, 1466, 1343, 1158, 1093, 1055, 1023, 813, 735, 699, 665; **HRMS**: *m/z* calculated for C₁₉H₂₂N₂O₃SNa⁺ [M+Na]⁺: 381.1243; found: 381.1245.



(1R*,5S*,7S*)-6-Methoxy-1-methyl-7-phenyl-3-oxa-6-azabicyclo[3.2.0]heptane (2.85):

Prepared according to GP-2.6 using **S2.85** (55 mg, 0.25 mmol, 1.0 equiv.), **2.59**•PF₆ (1.4 mg, 0.5 mol%) and THF (25 mL) with a reaction time of 1.5 h. The diastereomeric ratio was determined to be 1.6:1 by ¹H NMR analysis of the crude mixture. Purification by flash column chromatography (1–5% EtOAc/hexanes) afforded the pure title compound as a colorless oil (51 mg, 93%; combined yield).

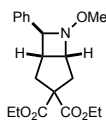
(1R*,5S*,7S*) Diastereomer (major): ¹H NMR (700 MHz, CDCl₃): δ 7.41 (d, *J* = 7.5 Hz, 2H), 7.36 (t, *J* = 7.6 Hz, 2H), 7.27 (t, *J* = 7.4 Hz, 1H), 4.48 (s, 1H), 4.12 (d, *J* = 9.8 Hz, 1H), 3.83 (d, *J* = 2.8 Hz, 1H), 3.54 – 3.50 (m, 5H), 2.98 (d, *J* = 9.8 Hz, 1H), 1.44 (s, 3H); ¹³C NMR (176 MHz, CDCl₃): δ 138.7, 128.5, 127.5, 126.8, 77.6, 77.2, 73.0, 72.5, 61.8, 45.0, 22.7; **IR** (cm⁻¹): 2952, 2894, 2844, 1495, 1466, 1452, 1062, 1032, 1023, 911, 744, 721; **HRMS:** *m/z* calculated for C₁₃H₁₇NO₂H⁺ [M+H]⁺: 220.1332; found: 220.1333; **(1R*,5S*,7R*) Diastereomer (minor):** ¹H NMR (500 MHz, CDCl₃): δ 7.39 (d, *J* = 7.1 Hz, 2H), 7.35 (t, *J* = 7.6 Hz, 2H), 7.27 (t, *J* = 7.1 Hz, 1H), 4.72 (d, *J* = 10.7 Hz, 1H), 4.58 (s, 1H), 4.05 (d, *J* = 5.1 Hz, 1H), 3.83 (d, *J* = 9.1 Hz, 1H), 3.68 (dd, *J* = 10.7, 5.1 Hz, 1H), 3.48 (s, 3H), 3.29 (d, *J* = 9.1 Hz, 1H), 0.86 (s, 3H); ¹³C NMR (176 MHz, CDCl₃): δ 139.5, 128.3, 127.3, 126.8, 76.8, 75.3, 72.3, 67.8, 60.8, 46.2, 14.3; **IR** (cm⁻¹): 2935, 2849, 1495, 1467, 1451, 1056, 1032, 1008, 943, 911, 734, 701; **HRMS:** *m/z* calculated for C₁₃H₁₇NO₂H⁺ [M+H]⁺: 220.1332; found: 220.1331.



(1S*,5R*,7S*)-6-Methoxy-7-phenyl-6-azabicyclo[3.2.0]heptane (2.86): Prepared according to GP-2.7 using **S2.86** (0.50 g, 2.50 mmol, 1.0 equiv.), **2.59**•PF₆ (14 mg, 0.5 mol%) and THF

(250 mL) with a reaction time of 4 h. The diastereomeric ratio was determined to be >20:1 by ^1H NMR analysis of the crude mixture. Purification by flash column chromatography (1–5% EtOAc/hexanes) afforded the pure title compound as a pale-yellow oil (0.49 g, 98%; combined yield).

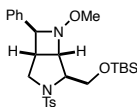
^1H NMR (700 MHz, CDCl_3): δ 7.39 (d, $J = 7.3$ Hz, 2H), 7.34 (t, $J = 7.7$ Hz, 2H), 7.25 (t, $J = 7.3$ Hz, 1H), 4.40 (t, $J = 6.5$ Hz, 1H), 4.15 (d, $J = 5.8$ Hz, 1H), 3.44 (s, 3H), 2.54 (q, $J = 5.8$ Hz, 1H), 2.48 – 2.43 (m, 1H), 2.00 – 1.93 (m, 2H), 1.82 – 1.77 (m, 1H), 1.62 – 1.50 (m, 2H); ^{13}C NMR (176 MHz, CDCl_3): δ 143.1, 128.4, 127.1, 126.2, 74.0, 68.4, 60.5, 42.5, 30.8, 25.99, 25.95; IR (cm^{-1}): 2934, 1853, 1494, 1465, 1451, 1325, 1267, 1179, 1058, 1022, 970, 944, 907, 833, 751, 734, 697; HRMS: m/z calculated for $\text{C}_{13}\text{H}_{17}\text{NOH}^+$ $[\text{M}+\text{H}]^+$: 204.1383; found: 204.1376.



Diethyl (1*S,5*R**,7*S**)-6-Methoxy-7-phenyl-6-azabicyclo[3.2.0]heptane-3,3-dicarboxylate (2.87)**: Prepared according to GP-2.6 using **S2.87** (87 mg, 0.25 mmol, 1.0 equiv.), **2.59**• PF_6 (1.4 mg, 0.5 mol%) and THF (25 mL) with a reaction time of 0.5 h. The diastereomeric ratio was determined to be 13:1 by ^1H NMR analysis of the crude mixture. Purification by flash column chromatography (5–10% EtOAc/hexanes) afforded the pure title compound as a colorless oil (84 mg, 97%; combined yield).

^1H NMR (500 MHz, CDCl_3): δ 7.39 (d, $J = 7.5$ Hz, 2H), 7.34 (t, $J = 7.5$ Hz, 2H), 7.29 – 7.24 (m, 1H), 4.50 (q, $J = 6.6$ Hz, 1H), 4.34 (d, $J = 6.0$ Hz, 1H), 4.30 – 4.23 (m, 2H), 4.23 – 4.14 (m, 2H), 3.38 (s, 3H), 3.04 (dd, $J = 14.7, 4.8$ Hz, 1H), 2.62 (d, $J = 14.4$ Hz, 1H), 2.55 (q, $J = 7.4$ Hz, 2H), 2.33 (dd, $J = 14.2, 7.9$ Hz, 1H), 1.30 (t, $J = 7.1$ Hz, 3H), 1.25 (t, $J = 7.1$ Hz, 3H); ^{13}C NMR (126 MHz, CDCl_3): δ 172.5, 171.7, 141.3, 128.5, 127.6, 126.7, 76.6, 69.5, 63.6, 61.9, 61.8, 60.5,

41.5, 38.8, 34.2, 14.3, 14.2; **IR** (cm⁻¹): 2980, 2938, 1726, 1445, 1366, 1252, 1180, 1094, 1061, 1039, 934, 746, 698; **HRMS**: *m/z* calculated for C₁₉H₂₅NO₅Na⁺ [M+Na]⁺: 370.1625; found: 370.1629.



(1R*,4S*,5S*,7S*)-4-(((Tert-butyldimethylsilyloxy)methyl)-6-methoxy-7-phenyl-3-tosyl-3,6-diazabicyclo[3.2.0]heptane (2.88): Prepared according to GP-2.6 using **S2.88** (126 mg, 0.25 mmol, 1.0 equiv.), **2.59**•PF₆ (1.4 mg, 0.5 mol%) and THF (25 mL) with a reaction time of 0.5 h. The diastereomeric ratio was determined to be 2.5:1 by ¹H NMR analysis of the crude mixture. Purification by flash column chromatography (2–20% diethyl ether/pentane) afforded the pure title compound as a colorless oil (120 mg, 95%; combined yield).

¹H NMR (500 MHz, CDCl₃): δ 7.87 (d, *J* = 8.2 Hz, 2H), 7.35 (d, *J* = 8.2 Hz, 2H), 7.28 (m, 2H), 7.24 (m, 1H), 7.06 (d, *J* = 7.0 Hz, 2H), 4.79 (t, *J* = 4.0 Hz, 1H), 4.46 (d, *J* = 6.1 Hz, 1H), 3.85 (d, *J* = 4.0 Hz, 2H), 3.53 – 3.44 (m, 3H), 3.33 (s, 3H), 2.50 (tt, *J* = 6.0, 2.4 Hz, 1H), 2.43 (s, 3H), 0.86 (s, 9H), 0.06 (d, *J* = 15.9 Hz, 6H); **¹³C NMR** (176 MHz, CDCl₃): δ 143.5, 140.8, 137.5, 129.9, 128.5, 127.8, 127.6, 126.5, 73.1, 71.2, 66.2, 60.4, 58.8, 51.8, 41.2, 25.9, 21.7, 18.2, -5.36, -5.43; **IR** (cm⁻¹): 2929, 2883, 2856, 1463, 1345, 1251, 1187, 1156, 1091, 1033, 1005, 956, 869, 831, 813, 776, 751, 699, 666; **HRMS**: *m/z* calculated for C₂₆H₃₈N₂O₄SSiH⁺ [M+H]⁺: 503.2394; found: 503.2394.



(1R*,5S*,7S*)-6-Methoxy-5-methyl-7-phenyl-3-oxa-6-azabicyclo[3.2.0]heptane (2.89): Prepared according to GP-2.6 using **S2.89** (55 mg, 0.25 mmol, 1.0 equiv.), **2.59**•PF₆ (2.8 mg, 1 mol%) and degassed THF (25 mL) with a reaction time of 18 h. The diastereomeric ratio was

determined to be 17:1 by ^1H NMR analysis of the crude mixture. Purification by flash column chromatography (5–15% EtOAc/hexanes) afforded the pure title compound as a colorless oil (50 mg, 91%; combined yield).

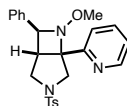
^1H NMR (700 MHz, CDCl_3): δ 7.43 (d, $J = 7.3$ Hz, 2H), 7.36 (t, $J = 7.6$ Hz, 2H), 7.28 (t, $J = 7.3$ Hz, 1H), 4.73 (d, $J = 10.1$ Hz, 1H), 4.28 (d, $J = 5.8$ Hz, 1H), 3.93 (d, $J = 9.4$ Hz, 1H), 3.63 (dd, $J = 9.4, 3.5$ Hz, 1H), 3.49 (s, 3H), 3.37 (d, $J = 10.1$ Hz, 1H), 2.23 (dd, $J = 5.7, 3.5$ Hz, 1H), 1.51 (s, 3H); ^{13}C NMR (126 MHz, CDCl_3): δ 142.4, 128.5, 127.4, 126.6, 74.3, 71.8, 70.9, 70.7, 62.2, 48.4, 23.5; IR (cm^{-1}): 2935, 2851, 1452, 1375, 1192, 1130, 1061, 1045, 939, 913, 792, 746, 697; HRMS: m/z calculated for $\text{C}_{13}\text{H}_{17}\text{NO}_2\text{H}^+$ $[\text{M}+\text{H}]^+$: 220.1332; found: 220.1329.



(1R*,5R*,7S*)-6-Methoxy-5,7-diphenyl-3-oxa-6-azabicyclo[3.2.0]heptane (2.90): Prepared according to GP-2.6 using **S2.90** (70 mg, 0.25 mmol, 1.0 equiv.), **2.59**• PF_6 (2.8 mg, 1 mol%) and degassed THF (25 mL) with a reaction time of 18 h. The diastereomeric ratio was determined to be 12:1 by ^1H NMR analysis of the crude mixture. Purification by flash column chromatography (1–10% EtOAc/hexanes) afforded the pure title compound as a colorless oil (68 mg, 97%; combined yield).

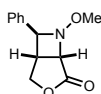
^1H NMR (700 MHz, CDCl_3): δ 7.51 (d, $J = 7.1$ Hz, 2H), 7.42 – 7.38 (m, 4H), 7.33 (t, $J = 7.6$ Hz, 2H), 7.29 (t, $J = 7.4$ Hz, 1H), 7.28 – 7.24 (m, 1H), 5.03 (d, $J = 10.5$ Hz, 1H), 4.47 (d, $J = 5.7$ Hz, 1H), 4.12 (d, $J = 9.6$ Hz, 1H), 3.91 (dd, $J = 9.6, 3.5$ Hz, 1H), 3.79 (d, $J = 10.5$ Hz, 1H), 3.59 (s, 3H), 2.60 (dd, $J = 5.6, 3.5$ Hz, 1H); ^{13}C NMR (176 MHz, CDCl_3): δ 143.0, 142.2, 128.56, 128.55, 127.6, 127.1, 126.9, 125.5, 79.3, 73.6, 71.9, 71.6, 61.6, 51.0; IR (cm^{-1}): 2933, 2851, 1602, 1492,

1446, 1262, 1059, 1043, 1022, 964, 914, 840, 748, 696; **HRMS**: m/z calculated for $C_{18}H_{19}NO_2H^+$ $[M+H]^+$: 282.1489; found: 282.1491.



(1R*,5S*,7S*)-6-Methoxy-7-phenyl-5-(pyridin-2-yl)-3-tosyl-3,6-diazabicyclo[3.2.0]heptane (2.91): Prepared according to GP-2.6 using **S2.91** (109 mg, 0.25 mmol, 1.0 equiv.), **2.59**•PF₆ (1.4 mg, 0.5 mol%) and degassed THF (25 mL) with a reaction time of 17 h. The diastereomeric ratio was determined to be >20:1 by ¹H NMR analysis of the crude mixture. Purification by flash column chromatography (10–60% EtOAc/hexanes) afforded the pure title compound as a colorless oil (80 mg, 74%; combined yield).

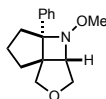
¹H NMR (500 MHz, CDCl₃): δ 8.39 (d, $J = 4.7$ Hz, 1H), 7.81 (d, $J = 7.9$ Hz, 3H), 7.70 (t, $J = 7.7$ Hz, 1H), 7.35 (dt, $J = 15.5, 7.5$ Hz, 6H), 7.31 – 7.23 (m, 1H), 7.17 – 7.10 (m, 1H), 4.61 (d, $J = 10.8$ Hz, 1H), 4.56 (d, $J = 6.0$ Hz, 1H), 3.73 (d, $J = 10.0$ Hz, 1H), 3.58 (d, $J = 10.8$ Hz, 1H), 3.54 (s, 3H), 3.20 (dd, $J = 10.0, 4.5$ Hz, 1H), 2.55 – 2.49 (m, 1H), 2.46 (s, 3H); **¹³C NMR** (176 MHz, CDCl₃): δ 161.6, 149.2, 143.7, 141.5, 136.7, 133.4, 129.8, 128.6, 128.1, 127.8, 126.9, 122.2, 120.8, 79.3, 71.2, 61.8, 52.0, 50.9, 48.4, 21.7; **IR** (cm⁻¹): 2934, 1590, 1465, 1161, 1091, 1027, 1012, 911, 815, 784, 749, 731, 698, 666; **HRMS**: m/z calculated for $C_{24}H_{25}N_3O_3SNa^+$ $[M+Na]^+$: 458.1509; found: 458.1507.



(1R*,5S*,7S*)-6-methoxy-7-phenyl-3-oxa-6-azabicyclo[3.2.0]heptan-4-one (2.92): Prepared according to GP-2.6, the reaction was conducted in a sealed 30-mL microwave vial using **S2.92** (55 mg, 0.25 mmol, 1.0 equiv.), **2.59**•PF₆ (2.8 mg, 1 mol%) and degassed MeCN (25 mL) at 82 °C with a reaction time of 70 h. The diastereomeric ratio was determined to be 14:1 by ¹H NMR

analysis of the crude mixture. Purification by flash column chromatography (5–40% EtOAc/hexanes) afforded the pure title compound as a yellow oil (33 mg, 60%; combined yield; 75% brsm).

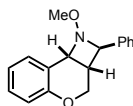
¹H NMR (500 MHz, CDCl₃): δ 7.43 – 7.37 (m, 4H), 7.36 – 7.32 (m, 1H), 4.57 (ddd, *J* = 12.8, 6.1, 1.2 Hz, 2H), 4.40 (d, *J* = 9.7 Hz, 1H), 4.34 (dd, *J* = 9.8, 5.0 Hz, 1H), 3.54 (s, 3H), 2.87 (q, *J* = 5.7 Hz, 1H); **¹³C NMR** (126 MHz, CDCl₃): δ 171.9, 139.3, 128.9, 128.6, 126.7, 75.6, 70.5, 63.2, 61.2, 37.1; **IR** (cm⁻¹): 2934, 1774, 1456, 1371, 1266, 1160, 1046, 993, 974, 943, 731, 698; **HRMS**: *m/z* calculated for C₁₂H₁₃NO₃Na⁺ [M+Na]⁺: 242.0788; found: 242.0787.



(3a*S,4a*S**,7a*S**)-4-methoxy-4a-phenylhexahydro-1*H*,3*H*-cyclopenta[*b*]furo[3,4-*c*]azete**

(2.93): Prepared according to GP-2.6 using **S2.93** (61 mg, 0.25 mmol, 1.0 equiv.), **2.59**•PF₆ (2.8 mg, 1 mol%) and degassed THF (25 mL) with a reaction time of 15 h. The diastereomeric ratio was determined to be >20:1 by ¹H NMR analysis of the crude mixture. Purification by flash column chromatography (2–10% EtOAc/hexanes) afforded the pure title compound as a white solid (60 mg, 98%; combined yield).

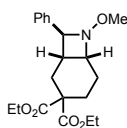
¹H NMR (700 MHz, CDCl₃): δ 7.43 (dd, *J* = 8.2, 1.1 Hz, 2H), 7.35 (t, *J* = 7.8 Hz, 2H), 7.20 (tt, *J* = 7.2, 1.3 Hz, 1H), 4.02 (d, *J* = 10.0 Hz, 1H), 3.76 (d, *J* = 3.7 Hz, 1H), 3.61 (s, 3H), 3.48 (d, *J* = 10.0 Hz, 1H), 3.36 (dd, *J* = 10.0, 3.7 Hz, 1H), 3.18 (d, *J* = 10.0 Hz, 1H), 2.82 (dd, *J* = 14.8, 6.8 Hz, 1H), 2.11 – 2.02 (m, 2H), 1.94 – 1.87 (m, 1H), 1.87 – 1.81 (m, 2H); **¹³C NMR** (176 MHz, CDCl₃): δ 144.2, 128.2, 126.3, 126.2, 80.9, 73.5, 72.8, 69.3, 61.4, 59.0, 35.6, 32.6, 25.7; **IR** (cm⁻¹): 2959, 2941, 2841, 1492, 1461, 1446, 1061, 1043, 992, 902, 786, 757, 736, 717, 704, 653; **HRMS**: *m/z* calculated for C₁₅H₁₉NO₂Na⁺ [M+Na]⁺: 268.1308; found: 268.1314.



(2*R,2*aS**,8*bR**)-1-Methoxy-2-phenyl-1,2*a*,3,8*b*-tetrahydro-2*H*-chromeno[4,3-*b*]azete**

(2.94): Prepared according to GP-2.6 using **S2.94** (67 mg, 0.25 mmol, 1.0 equiv.), **2.59**•PF₆ (2.8 mg, 1 mol%) and degassed THF (25 mL) with a reaction time of 72 h. The diastereomeric ratio was determined to be 7:1 by ¹H NMR analysis of the crude mixture. Purification by flash column chromatography (1–10% EtOAc/hexanes) afforded the pure title compound as a colorless oil (28 mg, 42%).

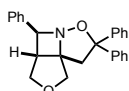
¹H NMR (700 MHz, CDCl₃): δ 7.51 (d, *J* = 7.3 Hz, 2H), 7.39 (t, *J* = 7.6 Hz, 2H), 7.34 – 7.27 (m, 2H), 7.24 (dd, *J* = 7.8, 1.4 Hz, 1H), 7.06 – 7.02 (m, 2H), 4.97 (d, *J* = 7.6 Hz, 1H), 4.61 (d, *J* = 8.4 Hz, 1H), 4.17 (dd, *J* = 11.9, 1.5 Hz, 1H), 3.90 (dd, *J* = 11.9, 1.9 Hz, 1H), 3.48 (s, 3H), 2.68 – 2.63 (m, 1H); ¹³C NMR (176 MHz, CDCl₃): δ 155.4, 141.0, 133.4, 129.4, 128.6, 127.8, 126.9, 121.2, 118.9, 117.8, 70.5, 63.4, 61.2, 59.9, 36.8; IR (cm⁻¹): 2823, 1581, 1486, 1447, 1220, 1209, 1079, 1051, 1030, 1001, 940, 929, 747, 699; HRMS: *m/z* calculated for C₁₇H₁₇NO₂Na⁺ [M+Na]⁺: 290.1151; found: 290.1150.



Diethyl (1*S,6*R**,8*S**)-7-Methoxy-8-phenyl-7-azabicyclo[4.2.0]octane-3,3-dicarboxylate**

(2.95): Prepared according to GP-2.6 using **S2.95** (90 mg, 0.25 mmol, 1.0 equiv.), **2.59**•PF₆ (2.8 mg, 1 mol%) and degassed THF (25 mL) with a reaction time of 72 h. The diastereomeric ratio was determined to be 3.5:1 by ¹H NMR analysis of the crude mixture. Purification by flash column chromatography (5–10% EtOAc/hexanes) afforded the pure title compound as a colorless oil (84 mg, 93%; combined yield). Characterization data was obtained for a 5:1 mixture of (1*S**,6*R**,8*S**) diastereomer (major) and (1*S**,6*R**,8*R**) diastereomer (minor).

¹H NMR (700 MHz, CDCl₃): δ 7.48 (d, *J* = 6.1 Hz, 9H; major+minor), 7.39 – 7.31 (m, 15H; major+minor), 7.29 – 7.24 (m, 6H; major+minor), 4.47 (d, *J* = 8.0 Hz, 5H; major), 4.29 (q, *J* = 7.2 Hz, 10H; major), 4.21 – 4.11 (m, 15H; major), 4.04 (d, *J* = 9.4 Hz, 1H; minor), 3.98 (q, *J* = 7.6 Hz, 5H; minor), 3.49 (s, 3H; minor), 3.44 (s, 15H; major), 2.80 (td, *J* = 11.2, 3.2 Hz, 1H; minor), 2.64 (dd, *J* = 12.5, 3.1 Hz, 1H; minor), 2.59 – 2.54 (m, 1H; minor), 2.52 – 2.34 (m, 10H; major+minor), 2.21 – 2.01 (m, 13H; major+minor), 1.97 – 1.73 (m, 15H; major+minor), 1.44 – 1.36 (m, 1H minor), 1.30 (t, *J* = 7.1 Hz, 16H; major+minor), 1.23 (td, *J* = 7.1, 1.6 Hz, 20H; major+minor); **¹³C NMR** (176 MHz, CDCl₃): δ 172.5, 172.0, 171.7, 170.9, 141.6, 140.1, 128.5, 128.4, 127.7, 127.4, 126.9, 126.5, 78.8, 74.0, 72.8, 61.73, 61.66, 61.59, 61.56, 60.9, 60.8 (2C), 56.0, 53.4, 36.5, 34.9, 32.9, 30.7, 28.6, 27.6, 26.2, 17.8, 14.21, 14.15, 14.13, 14.11; **IR** (cm⁻¹): 2938, 1726, 1449, 1367, 1228, 1175, 1111, 1024, 952, 860, 733, 699; **HRMS**: *m/z* calculated for C₂₀H₂₇NO₅Na⁺ [M+Na]⁺: 384.1781; found: 384.1784.

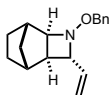


(3aR*,4S*,8aS*)-4,7,7-Triphenyltetrahydro-1H,3H-furo[3',4':2,3]azeto[1,2-b]isoxazole

(2.98): Prepared according to GP-2.6 using **2.97** (94 mg, 0.25 mmol, 1.0 equiv.), **2.59**•PF₆ (2.8 mg, 1 mol%) and degassed THF (25 mL) with a reaction time of 14.5 h. The diastereomeric ratio was determined to be 4:1 by ¹H NMR analysis of the crude mixture. Purification by flash column chromatography (10–60% EtOAc/hexanes) afforded the pure title compound as an off-white solid (82 mg, 87%; combined yield).

¹H NMR (700 MHz, CDCl₃): δ 7.45 – 7.42 (m, 4H), 7.39 – 7.33 (m, 3H), 7.30 (t, *J* = 7.8 Hz, 2H), 7.21 (t, *J* = 7.3 Hz, 1H), 7.14 – 7.10 (m, 3H), 7.02 – 6.99 (m, 2H), 4.84 (d, *J* = 6.4 Hz, 1H), 4.04 (d, *J* = 9.8 Hz, 1H), 3.71 (dd, *J* = 9.9, 5.1 Hz, 1H), 3.69 (d, *J* = 10.2 Hz, 1H), 3.54 (t, *J* = 5.6 Hz,

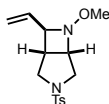
1H), 3.37 (d, $J = 10.2$ Hz, 1H), 3.18 (s, 2H); ^{13}C NMR (176 MHz, CDCl_3): δ 144.3, 143.2, 135.7, 129.6, 128.5, 128.14, 128.10, 127.9, 127.3, 127.2, 126.06, 126.06, 89.4, 78.3, 74.7, 71.5, 68.2, 48.0, 47.8; IR (cm^{-1}): 3058, 2968, 2850, 1598, 1492, 1448, 1265, 1189, 1125, 1043, 1032, 985, 912, 866, 731, 694; HRMS: m/z calculated for $\text{C}_{25}\text{H}_{23}\text{NO}_2\text{H}^+$ $[\text{M}+\text{H}]^+$: 370.1802; found: 370.1799.



(1S*,2R*,4R*,5R*,6R*)-3-(Benzyloxy)-4-vinyl-3-azatricyclo[4.2.1.0^{2,5}]nonane (2.102):

Prepared according to GP-2.6 using **2.101** (64 mg, 0.25 mmol, 1.0 equiv.), **2.59**• PF_6 (2.8 mg, 1 mol%) and degassed THF (25 mL) with a reaction time of 24 h. The diastereomeric ratio was determined to be 4:1 (exo/endo >20:1) by ^1H NMR analysis of the crude mixture. Purification by flash column chromatography (0–10% EtOAc/hexanes) afforded the pure title compound as a colorless oil (25 mg, 39%; combined yield). Characterization data was obtained for the (1S*,2R*,4R*,5R*,6R*) diastereomer (major).

^1H NMR (700 MHz, CDCl_3): δ 7.34 – 7.30 (m, 4H), 7.28 – 7.24 (m, 1H), 5.96 (ddd, $J = 17.1$, 10.2, 6.8 Hz, 1H), 5.11 (d, $J = 17.1$ Hz, 1H), 5.01 (d, $J = 10.3$ Hz, 1H), 4.60 (d, $J = 11.7$ Hz, 1H), 4.56 (d, $J = 11.7$ Hz, 1H), 3.90 (t, $J = 5.4$ Hz, 1H), 3.70 (d, $J = 5.6$ Hz, 1H), 2.46 (s, 1H), 2.17 (d, $J = 10.6$ Hz, 2H), 1.98 (t, $J = 4.9$ Hz, 1H), 1.49 – 1.42 (m, 2H), 1.30 (d, $J = 10.5$ Hz, 1H), 1.02 – 0.91 (m, 2H); ^{13}C NMR (176 MHz, CDCl_3): δ 139.1, 138.8, 128.4, 128.3, 127.6, 114.6, 75.8, 73.4, 71.5, 43.2, 37.9, 37.8, 34.1, 27.6, 25.2; IR (cm^{-1}): 2952, 1871, 1453, 1364, 1023, 987, 916, 846, 733, 695; HRMS: m/z calculated for $\text{C}_{17}\text{H}_{21}\text{NOH}^+$ $[\text{M}+\text{H}]^+$: 256.1696; found: 256.1700.

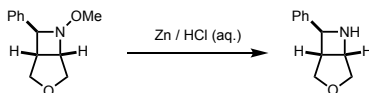


(1R*,5S*,7R*)-6-Methoxy-3-tosyl-7-vinyl-3,6-diazabicyclo[3.2.0]heptane (2.100): Prepared according to GP-2.6 using **2.99** (77 mg, 0.25 mmol, 1.0 equiv.), **2.59**•PF₆ (1.4 mg, 0.5 mol%) and THF (25 mL) with a reaction time of 0.5 h. The diastereomeric ratio was determined to be 2:1 by ¹H NMR analysis of the crude mixture. Purification by flash column chromatography (25% EtOAc/hexanes) afforded the pure title compound as a pale-yellow solid (76 mg, 99%; combined yield).

(1R*,5S*,7R*) Diastereomer (major): ¹H NMR (500 MHz, CDCl₃): δ 7.73 (d, *J* = 8.2 Hz, 2H), 7.34 (d, *J* = 8.0 Hz, 2H), 5.94 (ddd, *J* = 17.3, 10.3, 7.0 Hz, 1H), 5.23 (d, *J* = 17.2 Hz, 1H), 5.12 (d, *J* = 10.3 Hz, 1H), 4.29 – 4.21 (m, 2H), 3.97 (t, *J* = 6.4 Hz, 1H), 3.49 (d, *J* = 10.0 Hz, 1H), 3.42 (s, 3H), 2.72 (td, *J* = 11.6, 10.6, 5.8 Hz, 2H), 2.48 (q, *J* = 5.7 Hz, 1H), 2.44 (s, 3H); ¹³C NMR (126 MHz, CDCl₃): δ 143.9, 137.8, 132.6, 129.8, 128.1, 116.8, 73.2, 66.7, 60.8, 51.2, 46.6, 38.2, 21.7; IR (cm⁻¹): 2936, 2890, 1598, 1472, 1338, 1156, 1125, 1053, 1013, 928, 809, 708, 667; HRMS: *m/z* calculated for C₁₅H₂₀N₂O₃SNa⁺ [M+Na]⁺: 331.1087; found: 331.1089;

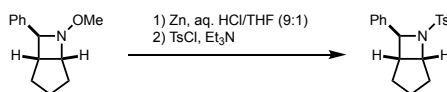
(1R*,5S*,7S*) Diastereomer (minor): ¹H NMR (500 MHz, CDCl₃): δ 7.73 (d, *J* = 8.2 Hz, 2H), 7.32 (d, *J* = 8.0 Hz, 2H), 5.76 (ddd, *J* = 16.9, 10.5, 6.1 Hz, 1H), 5.31 (d, *J* = 17.2 Hz, 1H), 5.23 (d, *J* = 10.5 Hz, 1H), 4.02 – 3.93 (m, 2H), 3.66 (d, *J* = 10.6 Hz, 1H), 3.51 (dd, *J* = 10.6, 2.5 Hz, 1H), 3.43 (s, 3H), 2.99 (qd, *J* = 8.7, 2.3 Hz, 1H), 2.89 – 2.82 (m, 2H), 2.43 (s, 3H); ¹³C NMR (126 MHz, CDCl₃): δ 143.6, 133.9, 133.6, 129.6, 128.0, 118.8, 70.1, 69.0, 61.9, 53.8, 46.9, 35.6, 21.8; IR (cm⁻¹): 2939, 2889, 1464, 1334, 1176, 1155, 1093, 1045, 1030, 988, 923, 812, 737, 665; HRMS: *m/z* calculated for C₁₅H₂₀N₂O₃SNa⁺ [M+Na]⁺: 331.1087; found: 331.1090.

Synthetic Modifications of Azetidine Products



(1R*,5S*,7S*)-7-Phenyl-3-oxa-6-azabicyclo[3.2.0]heptane (2.111): A 25-mL round-bottom flask equipped with a magnetic stir bar was charged with azetidine **2.69** (51 mg, 0.25 mmol, 1.0 equiv.). Then, 2 M aqueous HCl solution (5 mL) and zinc powder (82 mg, 1.25 mmol, 5 equiv.) were added sequentially and the resulting mixture stirred at 80 °C for 1 h. The reaction was cooled to 0 °C and 2 M aqueous NaOH solution was added dropwise until pH 10-12 was reached. The mixture was subsequently extracted with CH₂Cl₂ (3x) and the combined organic layers dried over Na₂SO₄, filtered and concentrated *in vacuo*. Purification by flash column chromatography (1–10% MeOH/CH₂Cl₂) afforded the pure title compound as a yellow oil (38 mg, 87%).

¹H NMR (500 MHz, CDCl₃): δ 7.43 (d, *J* = 7.3 Hz, 2H), 7.37 (t, *J* = 7.6 Hz, 2H), 7.28 – 7.24 (m, 1H), 4.60 (d, *J* = 4.5 Hz, 1H), 4.38 (dd, *J* = 6.3, 3.6 Hz, 1H), 4.16 (d, *J* = 9.7 Hz, 1H), 4.08 (d, *J* = 10.4 Hz, 1H), 3.57 (dd, *J* = 10.4, 3.6 Hz, 1H), 3.54 (dd, *J* = 9.7, 4.6 Hz, 1H), 3.07 (dt, *J* = 6.3, 4.6 Hz, 1H); **¹³C NMR** (126 MHz, CDCl₃): δ 145.1, 128.7, 127.2, 125.9, 76.0, 72.9, 64.0, 60.4, 48.1; **IR** (cm⁻¹): 3314, 3025, 2929, 2844, 1603, 1491, 1452, 1338, 1165, 1094, 1070, 977, 909, 881, 735, 697; **HRMS**: *m/z* calculated for C₁₁H₁₃NOH⁺ [M+H]⁺: 176.1070; found: 176.1067.

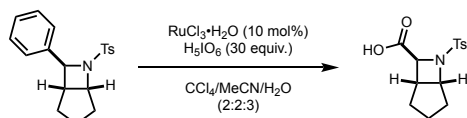


(1S*,5R*,7S*)-7-Phenyl-6-tosyl-6-azabicyclo[3.2.0]heptane (2.112): A 100-mL round-bottom flask equipped with a magnetic stir bar was charged with **2.86** (178 mg, 0.88 mmol, 1.0 equiv.) and a 9:1 mixture (*v/v*) of 2 M HCl solution (aq.) and THF (20 mL). The mixture was heated at reflux until the substrate completely dissolved, then, Zn (286 mg, 4.38 mmol, 5.0 equiv.) was

added and the mixture continued to reflux for 1.5 h. After cooling to 0 °C, 2 M NaOH solution (aq.) was added until pH 12 and the mixture sequentially extracted with CH₂Cl₂ (3x) and EtOAc (3x). The combined organic layers were dried over Na₂SO₄, filtered and concentrated *in vacuo*, then dried using high-vac to afford the crude azetidine (quant. yield), which was used in the next step without further purification.

The crude azetidine was dissolved in CH₂Cl₂ (10 mL) and the solution cooled to 0 °C. Et₃N (0.13 mL, 0.96 mmol, 1.1 equiv.) and *p*-TsCl (184 mg, 0.96 mmol, 1.1 equiv.) were added sequentially and the solution allowed to warm up to rt and stirred for 1.5 h. Then, water was added, the organic layer separated and the aqueous layer extracted with CH₂Cl₂ (3x). The combined organic layers were dried over Na₂SO₄, filtered and concentrated *in vacuo*. Purification by flash column chromatography (5–15% EtOAc/hexanes) afforded the pure title compound as a white solid (200 mg, 70%).

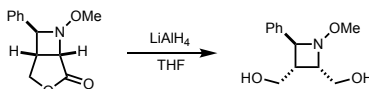
¹H NMR (700 MHz, CDCl₃): δ 7.43 (d, *J* = 8.2 Hz, 2H), 7.22 (s, 5H), 7.10 (d, *J* = 8.0 Hz, 2H), 4.85 (t, *J* = 5.5 Hz, 1H), 4.65 (d, *J* = 4.1 Hz, 1H), 2.76 (q, *J* = 6.3 Hz, 1H), 2.57 (dd, *J* = 14.1, 5.6 Hz, 1H), 2.36 (s, 3H), 1.89 – 1.79 (m, 2H), 1.80 – 1.71 (m, 1H), 1.52 – 1.39 (m, 2H); **¹³C NMR** (176 MHz, CDCl₃): δ 142.8, 140.2, 137.9, 129.3, 128.5, 127.9, 127.2, 126.9, 70.9, 68.9, 44.6, 32.2, 30.7, 24.1, 21.6; **IR** (cm⁻¹): 3030, 2952, 1598, 1495, 1455, 1338, 1186, 1152, 1121, 1090, 1059, 1028, 997, 951, 815, 754, 698, 665; **HRMS**: *m/z* calculated for C₁₉H₂₁NO₂SNa⁺ [M+Na]⁺: 350.1185; found: 350.1185.



(1S*,5R*,7S*)-6-Tosyl-6-azabicyclo[3.2.0]heptane-7-carboxylic acid (2.113): Adapted from a literature procedure with minor modifications.¹⁶⁹ A 10-mL microwave vial equipped with a

magnetic stir bar was charged with **2.112** (100 mg, 0.31 mmol, 1.0 equiv.). CCl₄ (0.7 mL), MeCN (0.7 mL) and water (1.0 mL) were added and the mixture stirred until all solids were dissolved. Then, periodic acid (879 mg, 4.6 mmol, 15.0 equiv.) and RuCl₃ hydrate (3.4 mg, 0.015 mmol, 0.05 equiv.) were added sequentially and the vial sealed with a rubber septa pierced with a needle to maintain an open atmosphere. The biphasic mixture was vigorously stirred for 24 h, before adding additional periodic acid (879 mg, 4.6 mmol, 15.0 equiv.) and RuCl₃ hydrate (3.4 mg, 0.015 mmol, 0.05 equiv.), and the reaction was continued to stir for 12 h. Et₂O was added and the mixture stirred for 0.5 h, before the addition of water. The organic layer was separated and the aqueous layer sequentially extracted with Et₂O (3x) and EtOAc (3x). The combined organic layers were dried over MgSO₄, filtered and concentrated *in vacuo*. Purification by flash column chromatography (94:5:1 CH₂Cl₂/MeOH/AcOH) afforded the pure title compound as a pale-yellow oil (34 mg, 38%).

¹H NMR (700 MHz, CDCl₃): δ 7.75 (d, *J* = 8.0 Hz, 2H), 7.35 (d, *J* = 7.9 Hz, 2H), 4.74 (t, *J* = 5.4 Hz, 1H), 4.19 (d, *J* = 4.1 Hz, 1H), 3.06 (q, *J* = 5.6 Hz, 1H), 2.46 (s, 3H), 2.31 (dd, *J* = 14.7, 5.9 Hz, 1H), 1.81 (dd, *J* = 13.7, 6.3 Hz, 1H), 1.71 (dt, *J* = 13.1, 6.6 Hz, 1H), 1.50 (h, *J* = 13.5, 6.8 Hz, 1H), 1.33 (h, *J* = 19.6, 12.5, 5.7 Hz, 1H), 1.20 – 1.11 (m, 1H); **¹³C NMR** (176 MHz, CDCl₃): δ 174.2, 144.2, 136.5, 129.9, 127.5, 69.5, 65.7, 39.9, 31.2, 30.6, 23.6, 21.8; **IR** (cm⁻¹): 2960, 1716, 1598, 1434, 1335, 1289, 1241, 1150, 1090, 1060, 1001, 907, 815, 727, 708, 674, 648; **HRMS**: *m/z* calculated for C₁₄H₁₇NO₄SNa⁺ [M+Na]⁺: 318.0770; found: 318.0769.



((2*S,3*R**,4*S**)-1-Methoxy-4-phenylazetidine-2,3-diyl)dimethanol (**2.114**):** A 10-mL round-bottom flask equipped with a magnetic stir bar was charged with LiAlH₄ (12 mg, 0.32 mmol, 2.6 equiv.) and THF (1.5 mL). After cooling to 0 °C, a solution of **2.92** (27 mg, 0.12 mmol,

1.0 equiv.) in THF (0.5 mL) was added dropwise. Then, the reaction mixture was allowed to warm up to rt and stirred for 3.5 h. Water was carefully added at 0 °C, followed by Rochelle salt solution (aq., sat.), and the resulting mixture was allowed to gradually warm up to rt and stirred for 3 h. The resulting clear biphasic mixture was extracted with Et₂O (3x) and the combined organic layers dried over MgSO₄, filtered and concentrated *in vacuo*. Purification by flash column chromatography (30–95% EtOAc/hexanes) afforded the pure title compound as a white solid (23 mg, 84%).

¹H NMR (700 MHz, CDCl₃): δ 7.43 (d, *J* = 7.3 Hz, 2H), 7.36 (t, *J* = 7.6 Hz, 2H), 7.28 (t, *J* = 7.3 Hz, 1H), 4.76 (d, *J* = 9.0 Hz, 1H), 4.31 – 4.24 (m, 1H), 4.17 – 4.10 (m, 2H), 3.91 – 3.83 (m, 2H), 3.52 (s, 3H), 3.03 (t, *J* = 5.2 Hz, 1H), 2.90 (dd, *J* = 7.6, 4.4 Hz, 1H), 2.50 (bs, 1H); **¹³C NMR** (176 MHz, CDCl₃): δ 141.2, 128.6, 127.7, 126.6, 73.4, 66.6, 62.1, 59.8, 59.6, 40.7; **IR** (cm⁻¹): 3319, 2935, 1596, 1495, 1453, 1370, 1266, 1155, 1091, 1020, 736, 698; **HRMS**: *m/z* calculated for C₁₂H₁₇NO₃Na⁺ [M+Na]⁺: 246.1101; found: 246.1105.

Representative NOE Data

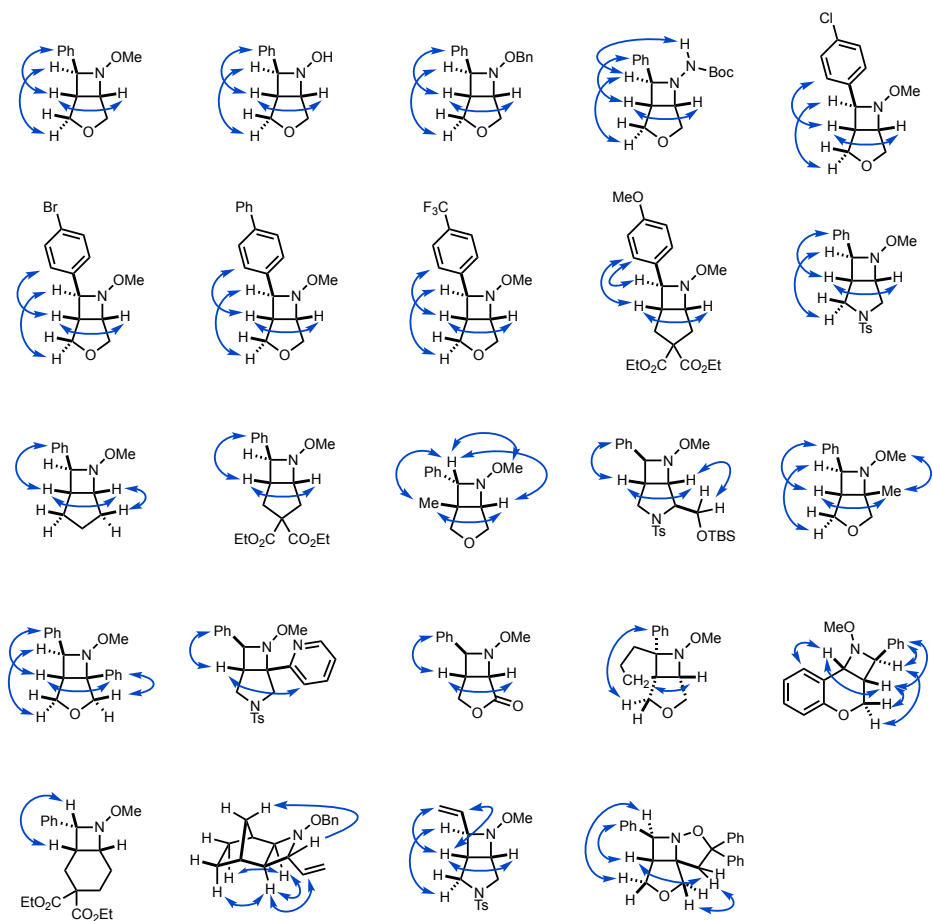
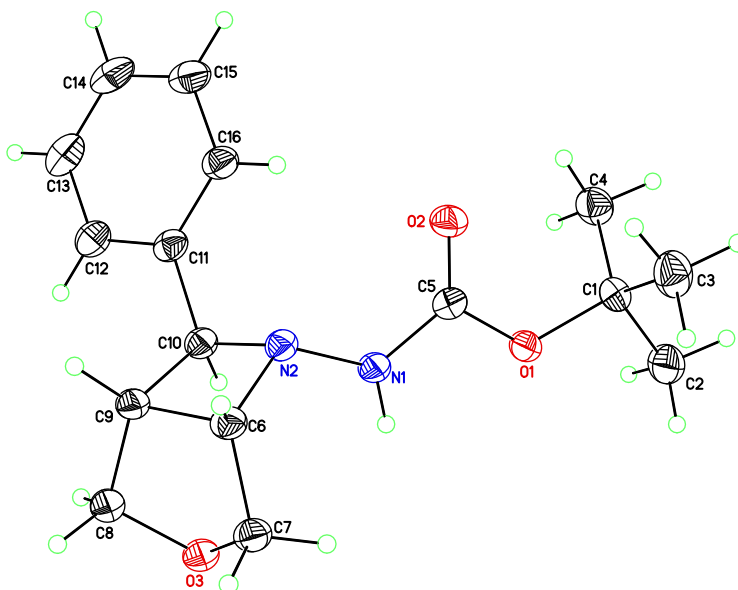


Figure 2.29: Selected NOE data for the synthesized azetidine products.

X-Ray Crystallographic Data



CCDC 1873931

Colorless blocks of *tert*-butyl ((1*R**,5*S**,7*S**)-7-phenyl-3-oxa-6-azabicyclo[3.2.0]heptan-6-yl)carbamate (**2.77**) were grown via vapor diffusion (pentane/ethyl acetate) of the compound at ambient temperature. A crystal of dimensions 0.18 x 0.14 x 0.10 mm was mounted on a Rigaku AFC10K Saturn 944+ CCD-based X-ray diffractometer equipped with a low temperature device and Micromax-007HF Cu-target micro-focus rotating anode ($\lambda = 1.54187$ Å) operated at 1.2 kW power (40 kV, 30 mA). The X-ray intensities were measured at 85(1) K with the detector placed at a distance 42.00 mm from the crystal. A total of 2028 images were collected with an oscillation width of 1.0° in ω . The exposure times were 1 sec. for the low angle images, 2 sec. for high angle. Rigaku d*trek images were exported to CrysAlisPro for processing and corrected for absorption. The integration of the data yielded a total of 23789 reflections to a maximum 2θ value of 138.67° of which 2901 were independent and 2802 were greater than $2\sigma(I)$. The final cell constants (Table 2) were based on the xyz centroids of 17770 reflections above $10\sigma(I)$. Analysis of the data showed

negligible decay during data collection. The structure was solved and refined with the Bruker SHELXTL (version 2016/6) software package, using the space group P2(1)/c with $Z = 4$ for the formula $C_{16}H_{22}N_2O_3$. All non-hydrogen atoms were refined anisotropically with the hydrogen atoms placed in a combination of idealized and refined positions. Full matrix least-squares refinement based on F^2 converged at $R1 = 0.0505$ and $wR2 = 0.1183$ [based on $I > 2\sigma(I)$], $R1 = 0.0512$ and $wR2 = 0.1191$ for all data. Acknowledgement is made for funding from NSF grant CHE-0840456 for X-ray instrumentation.

G.M. Sheldrick (2015) "Crystal structure refinement with SHELXL", *Acta Cryst.*, C71, 3-8 (Open Access).

CrystalClear Expert 2.0 r16, Rigaku Americas and Rigaku Corporation (2014), Rigaku Americas, 9009, TX, USA 77381-5209, Rigaku Tokyo, 196-8666, Japan.

CrysAlisPro 1.171.38.41 (Rigaku Oxford Diffraction, 2015).

Table 2.6: Crystallographic parameters and structure refinement for compound 2.77.

Identification code	<i>tert</i> -butyl ((1 <i>R</i> *,5 <i>S</i> *,7 <i>S</i> *)-7-phenyl-3-oxa-6-azabicyclo[3.2.0]heptan-6-yl)carbamate
Empirical formula	C16 H22 N2 O3
Formula weight	290.35
Temperature	85(2) K
Wavelength	1.54184 Å
Crystal system, space group	Monoclinic, P2(1)/c
Unit cell dimensions	a = 9.81308(10) Å alpha = 90 deg. b = 16.02162(18) Å beta = 96.5969(9) deg. c = 10.02249(9) Å gamma = 90 deg.
Volume	1565.32(3) Å ³
Z, Calculated density	4, 1.232 Mg/m ³
Absorption coefficient	0.693 mm ⁻¹
F(000)	624
Crystal size	0.180 x 0.140 x 0.100 mm
Theta range for data collection	4.536 to 69.335 deg.
Limiting indices	-11 ≤ h ≤ 11, -19 ≤ k ≤ 18, -11 ≤ l ≤ 12
Reflections collected / unique	23789 / 2901 [R(int) = 0.0747]
Completeness to theta = 67.684	99.70%
Absorption correction	Semi-empirical from equivalents
Max. and min. transmission	1.00000 and 0.76509
Refinement method	Full-matrix least-squares on F ²
Data / restraints / parameters	2901 / 0 / 198
Goodness-of-fit on F ²	1.105
Final R indices [I > 2σ(I)]	R1 = 0.0505, wR2 = 0.1183
R indices (all data)	R1 = 0.0512, wR2 = 0.1191
Extinction coefficient	0.041(2)
Largest diff. peak and hole	0.283 and -0.352 e.Å ⁻³

Chapter 3: Synthesis of Azetidines via Intermolecular Visible Light-Mediated [2+2] Cycloaddition Reactions

Portions of this chapter have been published in Becker, M.R.; Wearing, E.R.; Schindler, C.S. Synthesis of azetidines via visible light-mediated intermolecular [2+2] photocycloadditions. *Nat. Chem.* **2020**, 12, 898–905.

3.1. Introduction

3.1.1. Photochemistry of Oximes

Oximes can undergo a wide variety of different transformation from their excited state, which has been extensively summarized by Roth and Sivaguru.^{191,192} Similar to the reactivity of excited state imines, acyclic excited oximes readily undergo *E/Z* isomerization upon irradiation with UV light (typically 254 nm)^{193,194} or in the presence of a triplet sensitizer.^{195,196} Padwa and Albrecht studied the photoisomerization of *O*-methyl acetophenone oxime (**3.1**) by measuring the photostationary state in the presence of a range of triplet sensitizers (Figure 3.1).

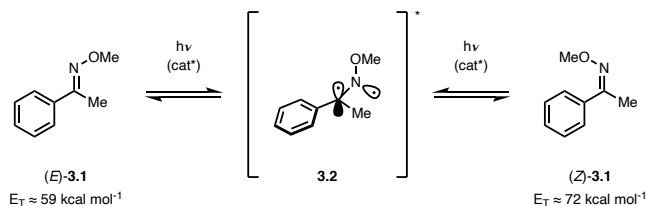


Figure 3.1: Photosensitized isomerization of oxime *O*-methyl acetophenone oxime.

Evaluation of photosensitizers ranging in triplet energies between 53.7–74.6 kcal mol⁻¹ revealed drastic differences in the photostationary state of **3.1**. The highest *E/Z* ratios were observed with triplet sensitizers with $E_T \approx 59 \text{ kcal mol}^{-1}$ (*E/Z* = 1:13), while a stark decrease in *E/Z* ratio was observed with sensitizers of both higher and lower triplet energies. This observation was

rationalized based on photosensitization of the oxime, generating a twisted excited state (**3.2**) (Figure 3.1). Based on the observed isomerization efficiencies, the triplet energies of (*E*)-**3.1** and (*Z*)-**3.1** were estimated to be approximately 59 and 72 kcal mol⁻¹.

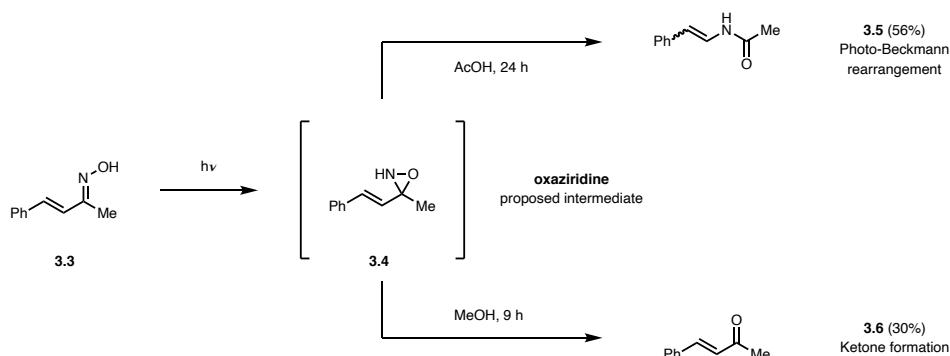


Figure 3.2: Photo-Beckmann rearrangement and ketone formation as photoproducts via irradiation of an oxime.

While the photochemical *E/Z* isomerization represents one of the most common relaxation pathways of excited oximes, these compounds can exhibit additional reactivity from their excited state. The Beckmann rearrangement is the acid-catalyzed conversion of an oxime to a corresponding amide. Albeit less general, the same transformation can be achieved through irradiation of an oxime with UV light, known as the photo-Beckmann rearrangement. This reaction was first discovered by Amin and de Mayo in 1963, who reported the conversion of benzaldoxime to benzamide under UV light irradiation in up to 41% yield.¹⁹⁷ The authors proposed an oxaziridine as key intermediate of the rearrangement, a hypothesis that was later supported via spectroscopic studies by Mukai.¹⁹⁸ Specifically, Mukai and coworkers were able to form **3.4** in approximately 50% yield through irradiation of oxime **3.3** (Figure 3.2). Interestingly, this intermediate either decomposed to the corresponding photo-Beckmann rearrangement product **3.5** or ketone **3.6** depending on the solvent used in the reaction. With acetic acid as the solvent amide **3.5** was isolated in 56% yield, while performing the reaction in MeOH provided ketone **3.6** in 30% yield, the latter arising via loss of nitrogen from **3.4**. Although an interesting alternative to the traditional

Beckmann-rearrangement, the synthetic utility of the photo-Beckmann rearrangement is limited due to its narrow scope and generally poor yields.¹⁹¹

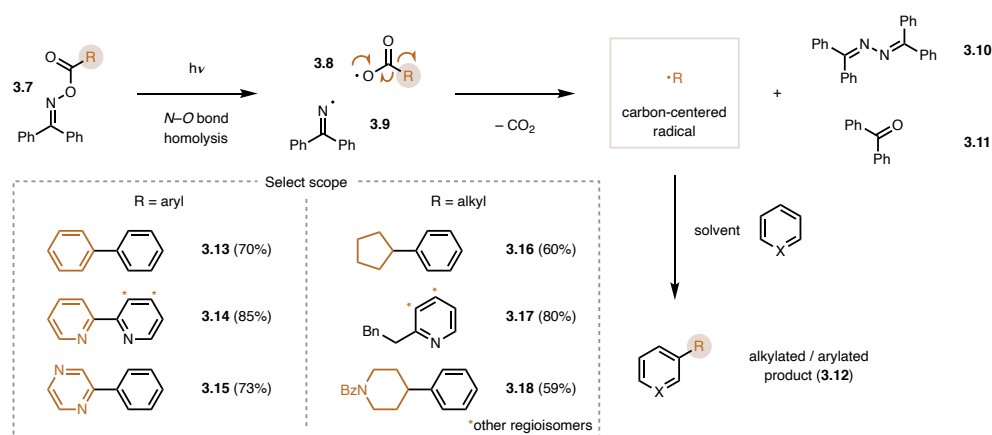


Figure 3.3: Nitrogen-oxygen bond cleavage as relaxation pathway for the alkylation and arylation of (hetero)aromatics.

Similar to *E/Z* isomerization, homolytic nitrogen–oxygen bond scission represents a common photoreaction of excited state oximes for the generation of iminyl radicals. This reactivity has been reported for both aliphatic and aromatic oximes under UV light irradiation, while both the unsubstituted as well as *O*-alkylated oximes are tolerated.¹⁹¹ While in most examples reported in the literature, an iminyl radical was generated to undergo intramolecular radical addition to an adjacent aromatic ring, Hasebe and Tsuchiya developed a decarboxylative variant, in which alkyl and aryl radicals are generated and added to aromatic substrates. (Figure 3.3).^{199,200} Irradiation of benzophenone oxime ester **3.7** resulted in $N-O$ bond homolysis affording iminyl radical **3.9** and acyloxy radical **3.8**. Upon decarboxylation of **3.8**, the resulting carbon-centered radical can subsequently react with the benzene or pyridine solvent. Importantly, the homolysis step is proposed to occur from the triplet excited state. Besides the desired product **3.12**, dimer **3.10** and benzophenone (**3.11**) were observed in 70–85% and 8–18% yield, respectively. Using solvent-quantities of either benzene or pyridine, arylation and alkylation was achieved with a series of different oxime ester precursor in generally good yields (**3.13–3.18**). The reaction with pyridine typically provided a mixture of regioisomers with preference for the ortho-position. In addition to

reaction of 3-aryl-2-isoxazolines both experimentally as well as computationally.^{150,151} The computations did not provide any evidence for the involvement of triplet excited state intermediates, thus supporting the mechanism proposed by Mukai. Interestingly, the electron-withdrawing substituent of the 3-aryl-2-isoxazolines (**3.19**) was found crucial for reactivity as it prevents rapid deactivation back to the ground state. Furthermore, the authors observed a strong dependence of the regioselectivity of the cycloaddition process on the electronic properties of the alkene substrate, particularly when comparing furans (**3.24**) and acrylates (**3.26**). This was attributed to a match of partial charges between the alkene and oxime reaction partners (Figure 3.4).

3.1.2. Triplet State Oximes via Visible Light Energy Transfer Catalysis

Although the photochemistry of oximes has been studied for over a century, examples in which photoexcited oximes are successfully utilized in synthetic organic transformations remain limited.²⁰¹ In general, most examples have a narrow scope and only provide low yields of the desired product. Additionally, UV light is required to achieve efficient excitation of the oxime chromophore, thus providing limited selectivity issues as other organic functional group can also adsorb UV light. In recent years, visible light triplet energy transfer catalysis has emerged as an attractive tool to access the triplet excited state of organic molecules under mild conditions. Glorius and coworkers recognized that benzophenone oximes, similar to those originally used by Hasebe and Tsuchiya, can be sensitized with a commercially available iridium photosensitizer for the decarboxylative functionalization of carboxylic acids.^{199,200,202} Aryl (**3.27**) or aliphatic carboxylic acids (**3.28**) were functionalized with benzophenone derived oxime **3.29** to obtain the corresponding oxime ester **3.30** or **3.31**, respectively (Figure 3.5). Under blue LED irradiation and in the presence of photocatalyst **2.59**•PF₆ these compounds underwent decarboxylation to generate a carbon-centered aryl or alkyl radical intermediate that could subsequently be functionalized with

various electrophiles. The authors successfully demonstrated the utility of this reaction protocol for deuteration (**3.34**), trifluoromethylthiolation (**3.35**), iodination (**3.36**), chlorination (**3.37**), borylation (**3.38**) and arylation (**3.39**) in 47–83% yield (Figure 3.5).

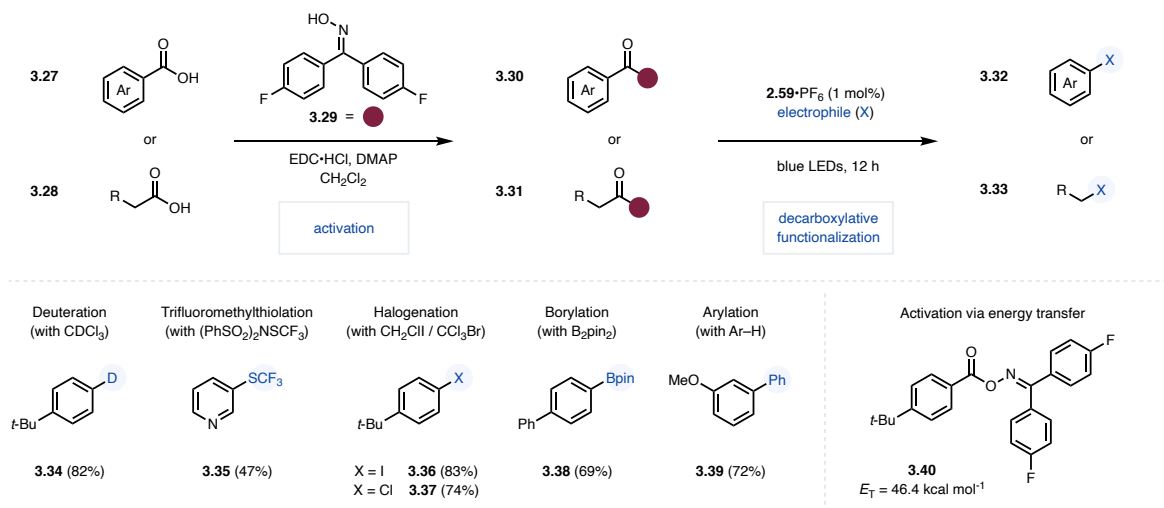


Figure 3.5: Visible light-sensitized decarboxylative functionalization reactions.

A series of mechanistic experiments were carried out that provided strong support for a mechanism proceeding via triplet energy transfer. Computational analysis revealed that oxime **3.40** possesses a triplet energy of $E_T = 46.4 \text{ kcal mol}^{-1}$, supporting an exergonic energy transfer process from photocatalyst **2.59**·PF₆ ($E_T = 60.1 \text{ kcal mol}^{-1}$). Interestingly, analysis of the mechanistic profile of the reaction via DFT calculations suggested a concerted *N*–*O* bond cleavage/decarboxylation, rather than a stepwise process proceeding via a carboxyl radical as proposed by Hasebe and Tsuchiya.

Glorius and coworkers further expanded the utility of activating oxime esters via triplet energy transfer for the carboimination of alkenes.²⁰³ Under very similar conditions to their previous work, energy transfer to the oxime ester results in decarboxylative *N*–*O* bond cleavage, providing a carbon-centered radical and an iminyl radical. The transient carbon-centered radical can then add to the terminal position of an alkene, typically an acrylate or styrene. The resulting

stabilized radical subsequently undergoes radical–radical combination with the iminyl radical to the desired product (Figure 3.6).

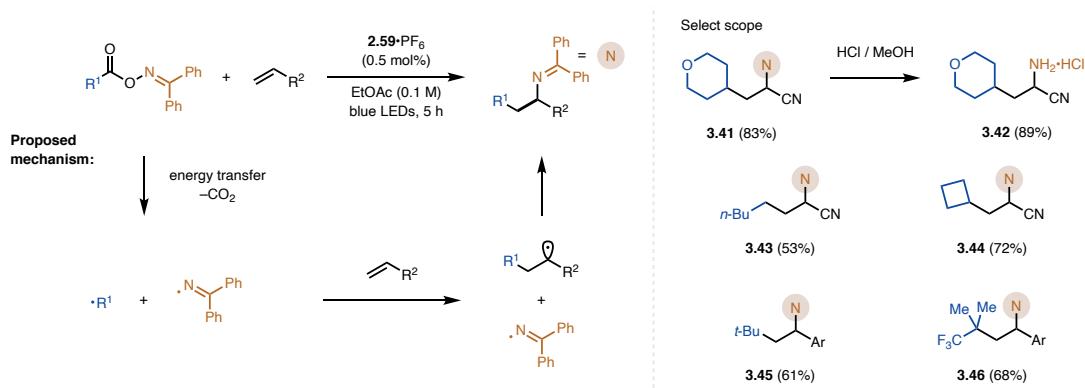


Figure 3.6: Photosensitized intermolecular carboimination of alkenes.

In contrast to the decarboxylative functionalization discussed above, the carboimination reaction protocol was unsuccessful with aromatic carboxylic acids. Nevertheless, the authors demonstrated the utility of the reaction protocol on a variety of primary, secondary and tertiary aliphatic carboxylic acids in 36–85% yield (**3.41**, **3.43–3.46**) (Figure 3.6). Notably, the benzophenone imine motif can be readily hydrolyzed to reveal the corresponding free amine **3.42** in 89% yield. This protocol was recently expanded to achieve the oxyimination of unactivated alkenes by utilizing oxime carbonates as bifunctional reagents.²⁰⁴

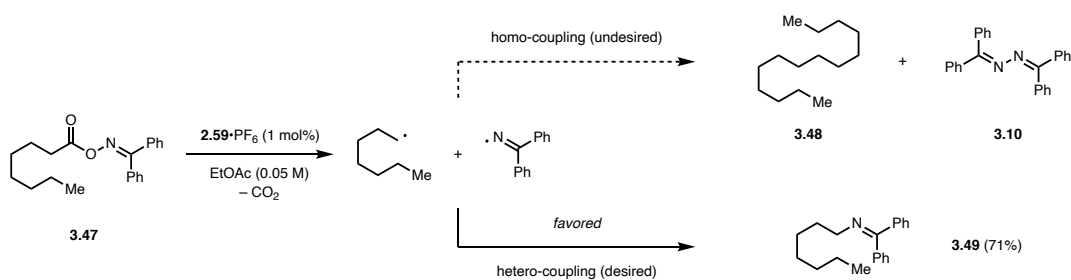


Figure 3.7: Radical-radical cross coupling via photocatalytic energy transfer.

You and Cho utilized a similar reaction design for the synthesis of functionalized imine building blocks via radical–radical cross-coupling in which triplet energy transfer to oxime esters such as **3.47** provided decarboxylative *N–O* bond cleavage (Figure 3.7).²⁰⁵ The authors developed

conditions that resulted in selective hetero-coupling between the carbon-centered and the iminyl radical to provide imine **3.49**. The use of ethyl acetate as solvent at a low reaction concentration was found crucial for achieving high selectivity. The reaction scope was demonstrated on a series of primary, secondary and tertiary alkyl carboxylic acids in 30–75% yield.

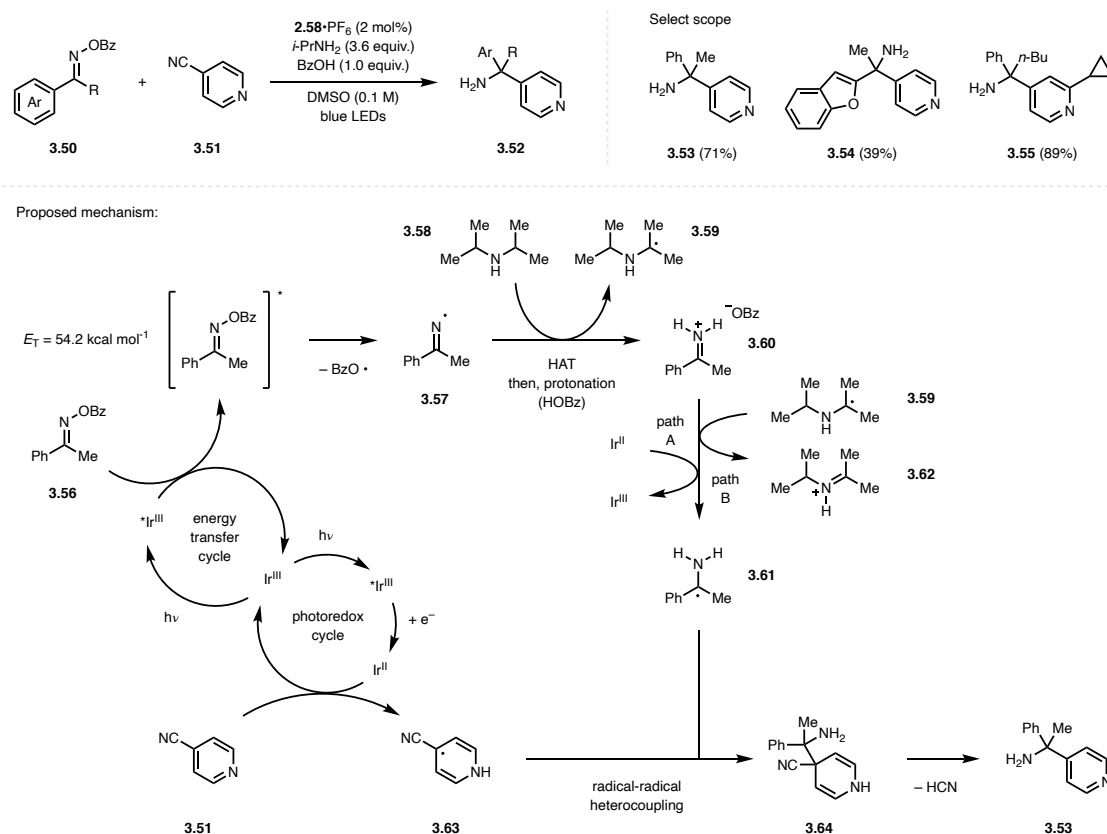


Figure 3.8: Synthesis of sterically hindered primary amines via tandem energy transfer and photoredox catalysis.

Rovis and Lehnher reported a tandem energy transfer/photoredox-based method for the synthesis of sterically hindered primary amines, which represent important motifs in active pharmaceutical ingredients.²⁰⁶ The reaction protocol reductively couples aromatic *O*-benzoyl oximes and cyanoarenes relying on **2.58**·PF₆ as the photocatalyst (Figure 3.8). High-throughput experimentation identified diisopropylamine as the optimal stoichiometric reductant and DMSO as the optimal solvent for the developed transformation. These conditions were amenable to a broad scope of aromatic oximes and cyanoarenes to provide the corresponding primary amines

products (**3.53–3.55**) in 10–95% yield. Although the authors initially hypothesized a cleavage of the oxime *N–O* bond via a single-electron reduction, collected reaction data was not in support of such a mechanism. Instead, mechanistic experiments were in favor of an initial triplet energy transfer process of the iridium photocatalyst to the aromatic oxime resulting in *N–O* bond cleavage. Based on DFT calculation, the triplet energy of **3.56** was determined as $E_T = 54.2 \text{ kcal mol}^{-1}$. Next, hydrogen atom abstraction of the iminyl radical (**3.57**) from diisopropylamine was proposed to occur, providing iminium salt **3.60** after protonation with benzoic acid. This intermediate can be reduced via single electron transfer from a strongly reducing iridium(II) intermediate regenerating catalyst **2.58**, or alternatively from the α -amino radical of *i*-Pr₂NH (**3.59**). Intermediate **3.61** can subsequently undergo heterocoupling with persistent radical **3.63**, which is generated through proton-coupled electron transfer by an iridium(II) intermediate and the cyanoarene (**3.51**). Net loss of a proton and cyanide leads to the formation of the final product **3.53**.

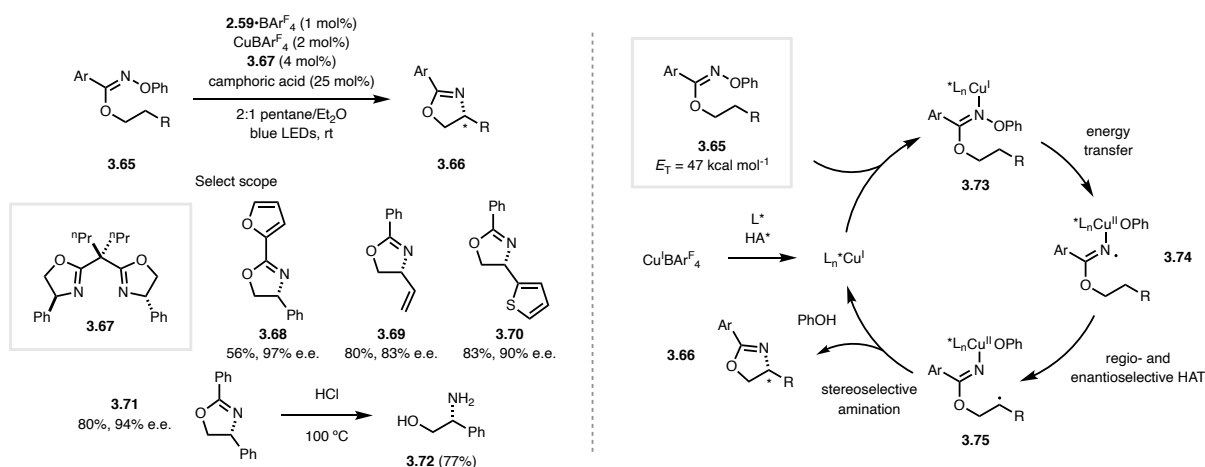


Figure 3.9: Enantioselective radical C–H amination via triplet energy transfer for the synthesis of chiral β -amino alcohols.

Over the last years, Nagib and coworkers have pioneered the synthesis of medicinally valuable β -amino alcohols via β -functionalization of alcohols utilizing *C–H* abstraction of *in situ* generated nitrogen centered radicals, typically derived from imidates.^{207–210,210,211} While these transformations traditionally produce achiral products, the authors recently developed a

enantioselective variant of this reaction through the merger of triplet energy transfer and chiral copper catalysis.²¹² This report relies on the use of aryl oxime imidates (**3.65**) that are converted to chiral oxazolines with catalytic amounts of **2.59**•BAr^F₄, CuBAr^F₄, camphoric acid, and chiral bisoxazoline ligand **3.67** in typically high yields and 79–99% e.e. (Figure 3.9). The majority of substrates contained an activating group in the β-position, thus *C–H* functionalization occurred at benzylic, allylic or propargylic *C–H* bonds (**3.68–3.71**). Nevertheless, the authors demonstrated that the *C–H* functionalization could also be successfully carried out on unactivated *C–H* bonds, although adjacent sterically demanding substituents were required to achieve high enantioselectivities. The desired chiral β-amino alcohols could be obtained through hydrolysis of the oxazoline to provide products such as **3.72** in 77% yield and 98% enantiospecificity. Based on Stern-Volmer quenching studies the authors proposed that the triplet energy transfer occurs from the iridium photocatalyst to a copper-bound imidate (**3.73**) resulting in subsequent *N–O* bond fission. The resulting nitrogen-centered radical can undergo enantio- and regioselective hydrogen atom transfer (HAT) to generate a carbon-centered radical (**3.75**), which is rapidly trapped by the copper catalyst. Based on radical trap experiments, the rate of alkyl radical trapping was estimated to be between 10⁸–10¹¹ s⁻¹. Finally, stereoselective amination provides the desired chiral oxazoline product (Figure 3.9).

3.2. Reaction Design and Optimization

Towards the development of an intermolecular aza Paternò-Büchi reaction, we envisioned a reaction design relying on activation via triplet energy transfer from a visible light photocatalyst. Based on our previous work on intramolecular aza Paternò-Büchi reactions that showed that styrenes are readily activated via triplet sensitization, initial efforts were focused on styrene substrates such as β-methylstyrene (**3.76**).²¹³ Towards that goal, **3.76** was reacted with hexanal *O*-

methyl oxime (**3.77**) in the presence of **2.59**•PF₆ under blue LEDs irradiation (Figure 3.10). No azetidine product arising from a cycloaddition reaction was observed, although isomerization of **3.76** from >20:1 to 1:4 *E/Z* indicated that triplet sensitization of the styrene likely occurred. Similarly, no reaction was observed with benzaldehyde *O*-methyl oxime (**3.78**) under otherwise identical conditions, indicating that styrene isomerization is outcompeting the desired cycloaddition process. Interestingly, we also observed isomerization of oxime **3.78** under these reaction conditions (20:1 to 1:4 *E/Z*), which suggested that photocatalyst **2.59**•PF₆ is capable of sensitizing the aromatic oxime moiety of **3.78**.

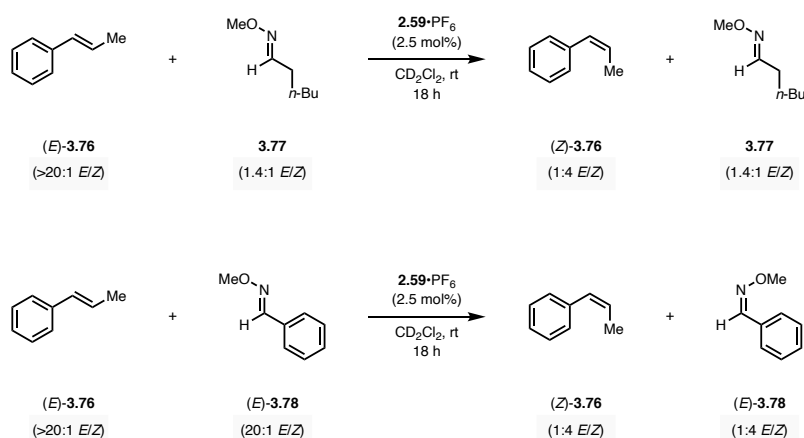


Figure 3.10: Probing the feasibility of an intermolecular aza Paternò-Büchi reaction relying on styrene sensitization.

This observation is in agreement with reports that determined the triplet energies of similar aromatic oximes to be approximately 54–59 kcal mol⁻¹.^{196,206} Therefore, we next evaluated the feasibility of an intermolecular aza Paternò-Büchi reaction via activation of the oxime component by triplet energy transfer. For the development of this reaction, we envisioned a reaction design relying on a cyclic oxime to prevent competitive oxime isomerization (Figure 3.11). Changes to the functional group adjacent to the oxime was expected to allow for control of the triplet energy of the oxime moiety. Photocycloaddition with an unactivated alkene would provide the desired bicyclic azetidine product containing an isoxazoline ring, which could be converted to the corresponding free azetidine via *N*–*O* bond cleavage. At the outset of our investigations, we chose

1-hexene as an unactivated reaction partner that is unable to interact with the iridium photocatalyst **2.59**•PF₆. Considering that triplet energies are only known for a limited number of oximes, we measured the quenching fraction for each substrate to inform about their quenching ability.²¹⁴

$$F = 100 \cdot \frac{I}{I_0} \quad \text{Equation 3.1}$$

The quenching fraction (F) was calculated based on the ratio of luminescence intensity in the presence of a substrate (I_0) and without (I) (Equation 3.1). Two distinct scenarios can be distinguished through this hypothesis-driven approach. Specifically, substrates that lack quenching ($F < 25\%$) are likely unable to interact with the photocatalyst, for example due to a mismatch in triplet energies. Thus, no reactivity would be expected, which was confirmed with aliphatic oxime **2.104** ($F = 24\%$) (Figure 3.11).

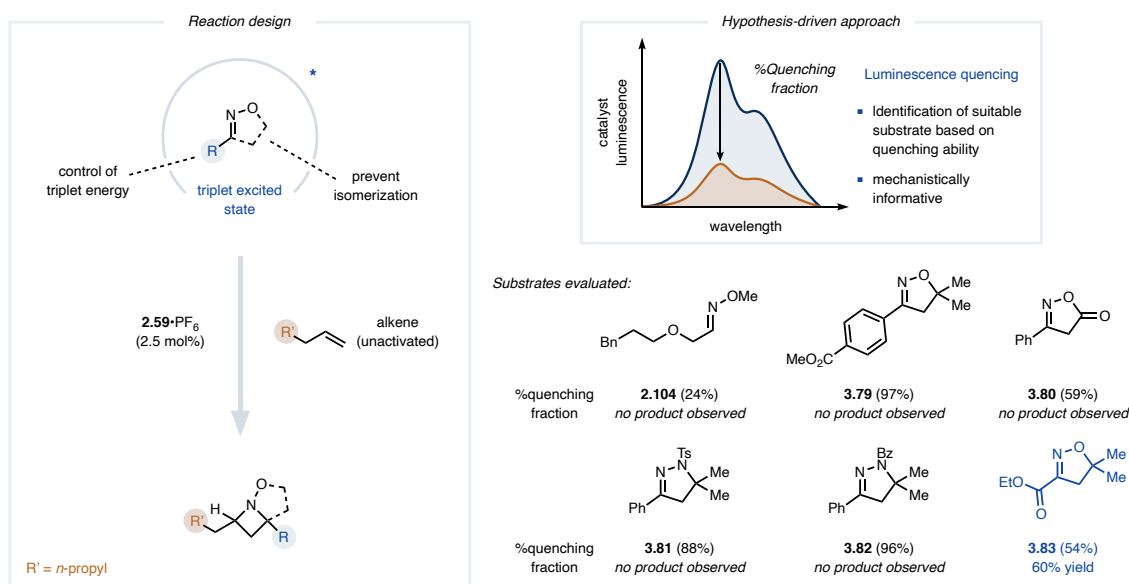
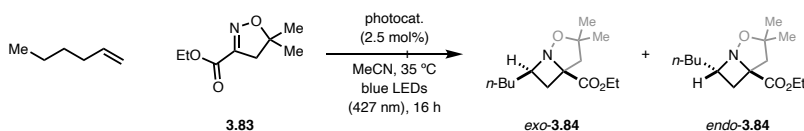


Figure 3.11: Development of an intermolecular aza Paternò-Büchi reaction.

In contrast, some substrates might possess a matching triplet energy, thus quenching would be expected ($F > 25\%$), but are not reactive towards [2+2] photocycloaddition reactions. Aromatic oxime **3.79** was identified as a strong quencher of **2.59**•PF₆ ($F = 97\%$), however, no azetidine formation was observed. Similar substrates have been successfully engaged in intermolecular

cycloaddition reactions by Sampedro and Mukai. However, it is important to note that those reactions were performed with activated alkenes and occurred from the singlet state. Interestingly, isoxazolone **3.80** showed high reactivity (>95% conversion) under the reaction conditions, but only provided a complex mixture of products, which could be a result of cleavage of the relatively weak *N*–*O* bond. Similarly, *N*-tosyl hydrazone **3.81** showed high conversion to a complex mixture of products while *N*-benzoyl hydrazone **3.82** did not provide any reactivity. Although all of these aromatic oximes and hydrazones were quenchers of **2.59**•PF₆ (*F* > 0.25), the lack of reactivity indicates that their triplet state is not reactive in intermolecular [2+2] cycloaddition reactions. Thus, substrates with alternative conjugating groups adjacent to the oxime were evaluated. When isoxazoline carboxylate **3.83** (*F* = 54%) was reacted under the reaction conditions, the desired azetidine (**3.84**) was isolated in 60% yield as the sole product of the reaction.

Table 3.1: Photocatalyst evaluation of the developed intermolecular aza Paternò-Büchi reaction. Yields were determined by ¹H NMR from the crude reaction mixture using an internal standard.



entry	photocatalyst	E_T (kcal mol ⁻¹)	$E_{1/2}^{III/IV}$ (V)	$E_{1/2}^{III/II^*}$ (V)	d.r.	yield
1	[Ir(dF(Me)ppy) ₂ (dtbbpy)]PF ₆ (2.58 •PF ₆)	60.2	-0.92	+0.97	>20:1	54%
2	[Ir(dF(CF ₃)ppy) ₂ (dtbbpy)]PF ₆ (2.59 •PF ₆)	60.1	-0.89	+1.21	9:1	69%
3	fac-[Ir(dFppy) ₃] (2.51)	60.1	-1.28	+0.36	3:1	94%
4	fac-[Ir(4'-CF ₃ -ppy) ₃] (2.60)	56.4	-1.70	+0.59	3:1	8%
5	fac-[Ir(ppy) ₃] (2.61)	55.2	-1.73	+0.31	–	0%
6	[Ir(ppy) ₂ (dtbbpy)]PF ₆ (2.62 •PF ₆)	49.2	-0.96	+0.66	–	0%
7	[Ru(bpz) ₃](PF ₆) ₂ (2.63 •(PF ₆) ₂)	48.4	-0.26	+1.45	–	0%
8	[Ru(phen) ₃](PF ₆) ₂ (2.64 •(PF ₆) ₂)	46.9	-0.87	+0.82	–	0%
9	[Ru(bpy) ₃](PF ₆) ₂ (2.65 •(PF ₆) ₂)	46.5	-0.81	+0.77	–	0%

Having identified a suitable substrate for an intermolecular aza Paternò-Büchi reaction, we next focused on optimizing relevant reaction parameters. Although photocatalyst [Ir(dF(Me)ppy)₂(dtbbpy)]PF₆ (**2.58**•PF₆) provided **3.84** in similar yield (54%), a drastic difference in diastereoselectivity was observed (Table 3.1, entries 1+2). Further analysis revealed that the

difference in stereoselectivity originated from different amounts of minor diastereomer (*endo*-**3.84**) present in the crude reaction mixture, while similar quantities of the major diastereomer (*exo*-**3.84**) were detected. This observation led us to perform a control reaction, in which both diastereomers were independently irradiated with blue LEDs in the presence of photocatalyst **2.59**•PF₆. While *exo*-**3.84** could be fully recovered after 16 h, we observed an intriguing 41% conversion of *endo*-**3.84** to unidentifiable degradation products, indicating that the decomposition of the minor diastereomer caused the observed difference in yield and stereoselectivity (Figure 3.12).

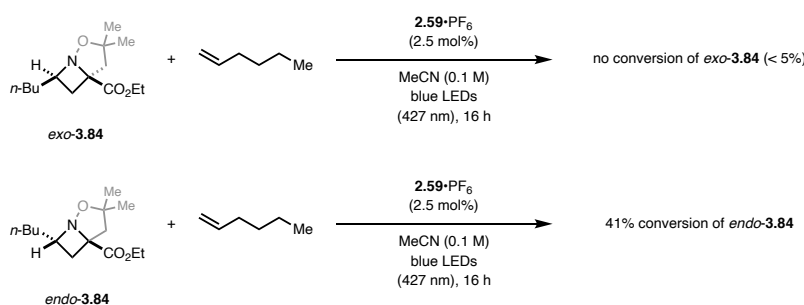


Figure 3.12: Control reactions probing the stability of both azetidine diastereomers.

Considering that **2.58**•PF₆ and **2.59**•PF₆ are both relatively strong oxidants, we carried out cyclic voltammetry experiments of azetidine products. These experiments revealed that the *endo*-diastereomer is amenable to single-electron oxidation with an oxidation process at $E_{p/2} = +1.33$ V (vs. SCE), while the *exo*-diastereomer is oxidized at a more positive potential of $E_{p/2} = +1.51$ V (vs. SCE) (Figure 3.26). In addition, the concave structure of the *endo*-diastereomer is more accessible for the photocatalyst to engage with the substrate through undesired single-electron transfer. Thus, less oxidizing photocatalysts were evaluated, which identified *fac*-[Ir(dFppy)₃] (**2.51**) as optimal, providing the desired product in 94% yield (Table 3.1, entry 3). Other photocatalysts with lower triplet energies but similar redox properties did not facilitate the reaction, indicating that the reaction indeed occurs via energy transfer as opposed to a photoredox-based transformation (Table 3.1, entries 4–9).

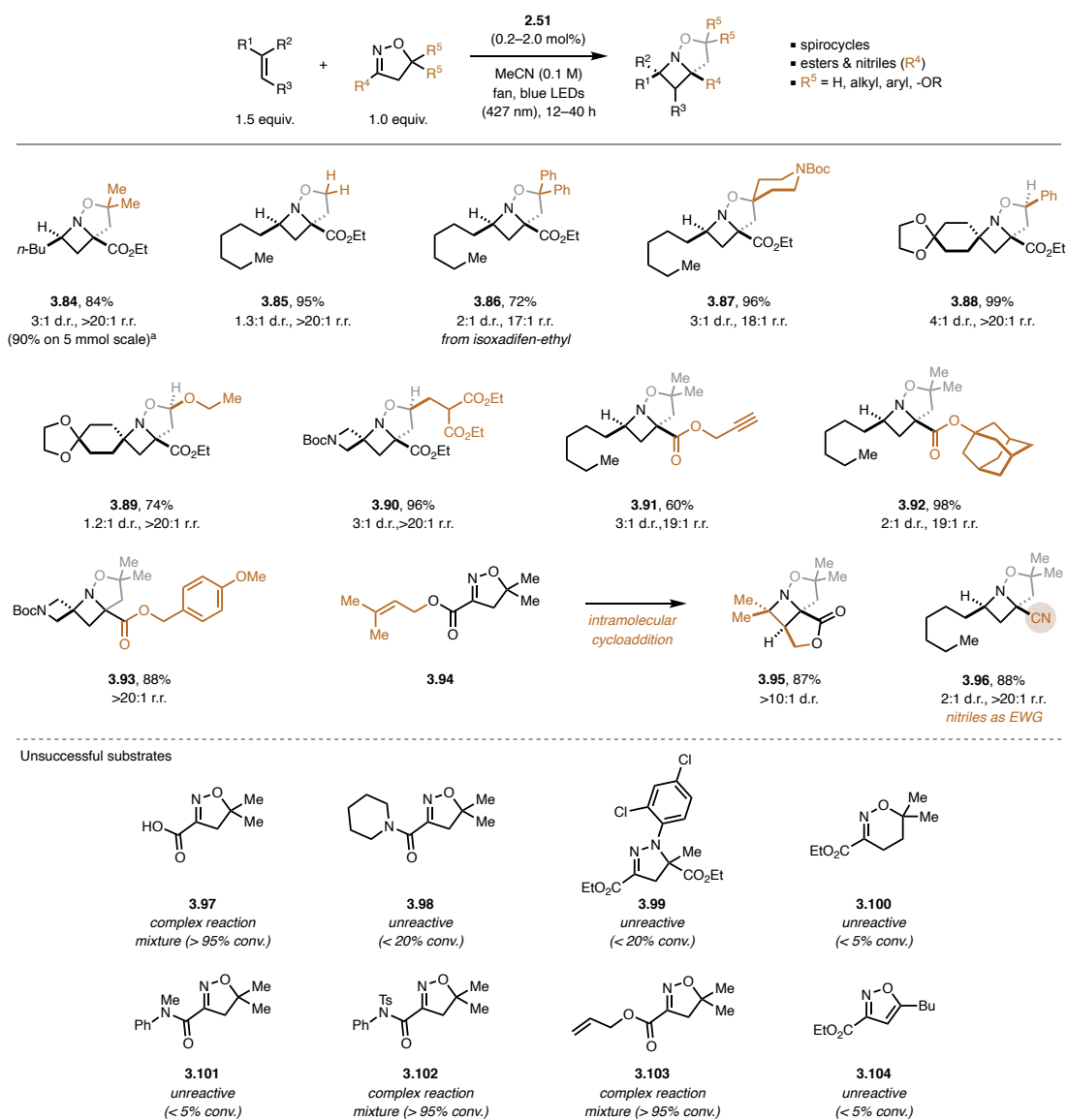


Figure 3.13: Scope of the oxime component in the developed intermolecular aza Paternò-Büchi reaction (major diastereomer is shown). EWG = electron-withdrawing group.

3.3. Substrate Scope

With optimized conditions identified, we next evaluated the scope of the oxime component in the developed reaction. Thus, a series of 2-isoxazolines bearing various substitution patterns were tested (Figure 3.13, top). Importantly, azetidine **3.84** could be readily synthesized on larger scale in 90% yield providing gram-quantities of **3.84**. Substitution in the 5-position of the isoxazoline was not required as the unsubstituted substrate smoothly underwent cycloaddition in

95% yield (**3.85**), albeit in diminished stereoselectivity of 1.3:3. The reaction allowed incorporation of various synthetic motifs into the 2-isoxazoline ring, including aromatic substituents (**3.86** and **3.88**), nitrogen spirocycles (**3.87**), ethers (**3.89**) and esters (**3.90**) in 72–99% yield. Notably, in the case of mono-substituted substrates such as **3.88** and **3.90**, the cycloaddition preferentially occurs at the less substituted face, which highlights how 2-isoxazoline substitution can control the cycloaddition process. Variations of the ester moiety allowed the integration of synthetic handles such as alkynes (**3.91**) in 60% yield, while sterically bulky and electron-rich substituents were similarly tolerated, affording azetidines **3.92** and **3.93** in 98% and 88% yield, respectively. In contrast, alkene-containing esters (**3.94**) preferentially undergo intramolecular cycloaddition resulting in intriguing scaffolds such as tricyclic azetidine **3.95** in 87% yield. Finally, we were able to convert 2-isoxazolines containing other electron-withdrawing substituents than ester in the title reaction. While functional groups such as carboxylic acids (**3.97**) or amides did not provide any desired reactivity (Figure 3.13, bottom), we identified nitriles as a compatible group, affording azetidine **3.96** in 88% yield.

Subsequent efforts were directed at evaluating the alkene scope of the developed reaction (Figure 3.14). Notably, feedstock reagents such as ethylene gas can be directly used in the cycloaddition reaction, allowing access to azetidines such as **3.105** in 70% yield. Furthermore, primary alkenes were found to be competent substrates in the cycloaddition and allowed incorporation of various functional groups including nitriles, amides, alcohols, sulfonamides as well as aromatic functional groups in 67–98% yield (**3.106–3.113**). Notably, the successful formation of azetidines **3.111** and **3.112** highlights that pharmaceutical scaffolds can be readily integrated into the azetidine scaffolds, as both alkene precursors were derived from probenecid or aspirin, respectively.

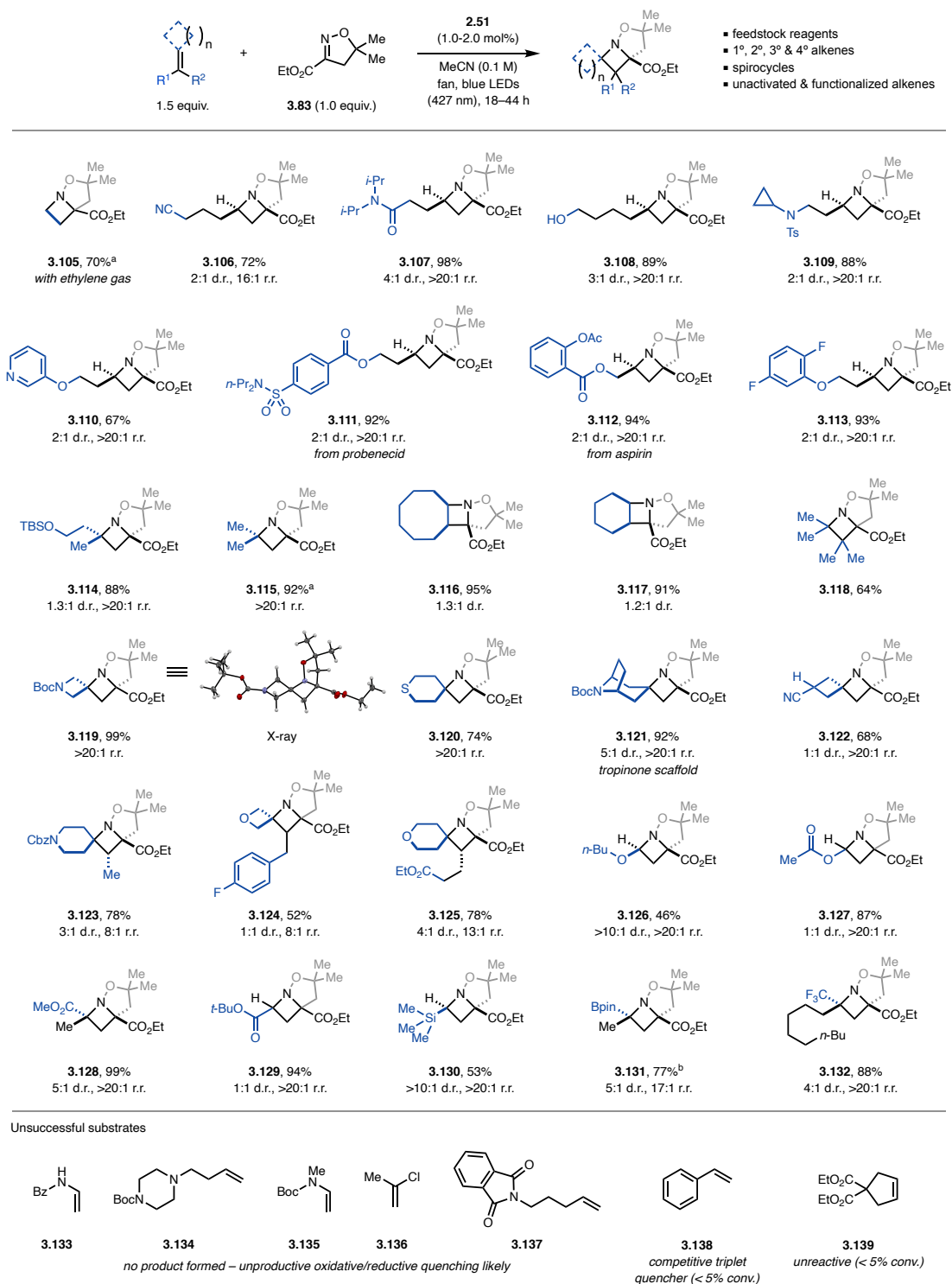


Figure 3.14: Alkene scope of the developed intermolecular aza Paternò-Büchi reaction.

1,1-Disubstituted alkenes as well as internal alkenes readily underwent the cycloaddition reaction, providing azetidines **3.114–3.117** in very good to excellent yields. Interestingly, while 6-

and 8-membered alkenes were well tolerated, smaller 5-membered alkenes (**3.139**) were found unreactive under the reaction conditions (Figure 3.14, bottom). Quaternary alkenes can be used in the developed reaction, which subsequently afford fully substituted azetidine products such as **3.118**. Given the interest in azetidine spirocycles for medicinal chemistry application, we hypothesized utilizing exocyclic alkenes as the substrates that would afford the corresponding spirocyclic azetidines products in a single synthetic transformation from readily available starting materials.²¹⁵ Indeed, we were able to isolate bis-azetidine spirocycle **3.119** in 99% yield using the developed reaction protocol, and the structure of this compound was further confirmed by X-ray crystallographic analysis. Similarly, this method allows for the incorporation of sulfur or nitrogen heterocycles, as well as cyclobutanes, yielding the corresponding spirocycles **3.120–3.125** in generally good yields. Even though **3.123–3.125** were derived from trisubstituted alkenes, the azetidine product were obtained in only slightly diminished regioselectivity of 8:1 to 13:1. Finally, we investigated functionalized alkenes as substrates with which functional groups could be incorporated directly at the azetidine ring. Vinyl ethers, vinyl acetates as well as acrylates readily participated in the cycloaddition reaction and provided the desired products **3.126–3.129** in 46–99% yield. The enhanced diastereoselectivity of **3.126** is likely a result of decomposition of the minor diastereomer via undesired single-electron oxidation under the reaction conditions, which could be attributed to the additional electron-rich vinyl ether substituent. Similarly, silane **3.130** was afforded as a single diastereomer, but in a diminished yield of 53%. Finally, the reaction protocol enables incorporation of valuable synthetic handles such as boronic esters (**3.131**) or trifluoromethyl substituents (**3.132**) in very good yields. Our extensive investigations into the scope of the cycloaddition reaction also revealed functional groups that were not tolerated, including enamines (**3.133**, **3.135**), tertiary amines (**3.134**), vinyl chlorides (**3.136**) and

phthalimides (**3.137**). These scaffolds represent challenging substrates in energy transfer-mediated transformations, as they likely interact with the photocatalyst via oxidative or reductive quenching. Additionally, we found that styrene (**3.138**) did not participate in the cycloaddition reaction, likely due to competitive quenching of the iridium photocatalyst via energy transfer.

3.4. Synthetic Applications

To further demonstrate the synthetic utility of the developed intermolecular cycloaddition reaction, we next focused on converting the obtained cycloadducts to the corresponding free azetidines via cleavage of the nitrogen–oxygen (*N–O*) bond. Towards that goal, we evaluated a series of heterogeneous catalyst to achieve *N–O* bond cleavage via hydrogenolysis. Utilizing **3.84** as a model substrate for the transformation, we observed only poor conversion of < 25% with a series of catalysts, including palladium on carbon, platinum(IV) oxide, ruthenium on carbon or palladium(II) hydroxide (Table 3.2, entries 1, 3–5).

Table 3.2: Catalyst evaluation for the *N–O* bond cleavage reaction.

Reaction scheme: **3.84** (a bicyclic spirocyclic intermediate with an *N–O* bond) reacts with H_2 (1 atm) and a catalyst (20 mol%) in EtOH at 45 °C for 24 h to form **3.140** (a spirocyclic product where the *N–O* bond has been cleaved).

entry	catalyst	deviation from conditions	yield	conversion
1	Pd/C	–	12%	12%
2	Raney nickel	–	58%	67%
3	PtO ₂	–	–	< 5%
4	Ru/C	–	12%	17%
5	Pd(OH) ₂	–	23%	25%
6	Pd(OH) ₂	50 mol% [Pd]	27%	39%
7	Pd(OH) ₂	high temperature (78 °C)	23%	85%
8	Pd(OH) ₂	high pressure (4.1 atm)	16%	46%

In contrast, Raney nickel provided higher conversion, however, this result was unfortunately challenging to reproduce, likely due to difficulties to accurately measure consistent amounts of the slurry (Table 3.2, entry 2). Interestingly, the product formed in these reaction was spirocycle **3.140**, highlighting that the amino alcohol formed upon *N–O* bond cleavage undergoes

lactonization. The poor conversion can likely be attributed to catalyst inhibition by the basic amine moiety in the product **3.140**. Therefore, other reaction parameters were evaluated with palladium(II) hydroxide as the catalyst. Increasing the catalyst loading to 50 mol% only led to a subtle increase in conversion, while increasing the reaction temperature substantially improved conversion, however, it did not provide increased yields (Table 3.2, entries 6+7). Similarly, performing the hydrogenolysis at elevated pressure was not successful, and only resulted in increased decomposition (Table 3.2, entry 8).

Table 3.3: Reaction optimization of the palladium-mediated *N*-*O* bond cleavage reaction.

entry	solvent	deviation from conditions	yield	conversion
1	EtOH/H ₂ O (1:1)	–	< 5%	28%
2	EtOH/AcOH (3:1)	–	–	58%
3	EtOH/AcOH/H ₂ O (1:1:1)	–	76%	>95%
4	EtOH/AcOH/H ₂ O (2:1:1)	–	–	>95%
5	EtOH/AcOH/H ₂ O (1:2:2)	–	10%	>95%
6	EtOH/H ₂ O (1:1)	NaOAc (5.0 equiv.)	8%	8%
7	EtOH/H ₂ O (1:1)	NH ₄ OAc (5.0 equiv.)	14%	17%
8	EtOH	<i>p</i> -TsOH (2.0 equiv.)	85%	87%
9	EtOH	oxalic acid (2.0 equiv.)	14%	40%
10	EtOH	HCl (aq.) (2.6 equiv.)	79%	80%
11	EtOH	TFA (3.4 equiv.)	33%	61%

Next, different solvents were evaluated in the *N*-*O* bond cleavage reaction. While addition of water or acetic acid resulted in trace amounts of the desired product (Table 3.3, entries 1+2), a 1:1:1 mixture of ethanol, water and acetic acid provided >95% conversion and 76% yield of **3.140**, indicating that acidic conditions can prevent catalyst inhibition through protonation of the free amine moiety in the product (Table 3.3, entry 3). However, subtle changes to the composition of the solvent system resulted in substantial decomposition of the product, which made it challenging to reproduce as well as to scale up these conditions (Table 3.3, entries 4+5). As a result, other acidic additives were tested on their ability to prevent catalyst inhibition through amine

protonation. While oxalic acid or trifluoroacetic acid resulted in slightly increased conversions (Table 3.3, entries 9+11), utilizing hydrochloric acid and *p*-toluenesulfonic acid provided the desired product in 79% and 85% yield, respectively (Table 3.3, entries 8+10).

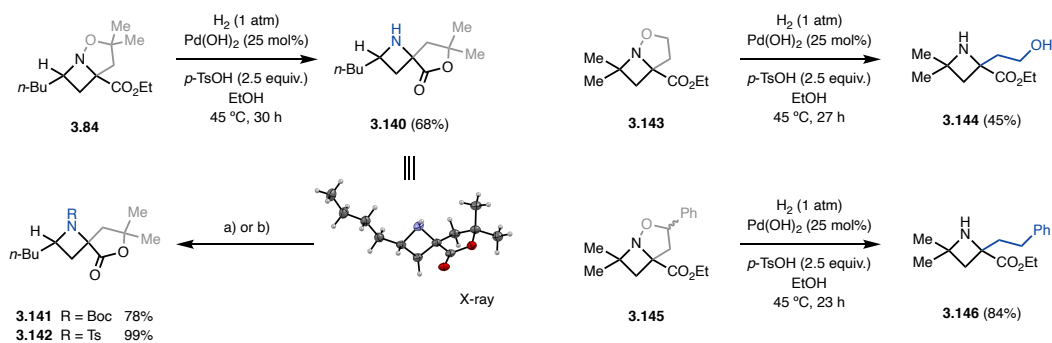


Figure 3.15: Synthesis of free azetidines via *N*–*O* bond cleavage through palladium-mediated hydrogenolysis reactions. (a) Boc₂O, DMAP, CH₂Cl₂, rt (for **3.141**) (b) *p*-TsCl, K₂CO₃, MeCN, 80 °C (for **3.142**).

Importantly, 2.5 equivalents of *p*-toluenesulfonic acid were found optimal and afforded the desired product in 68% yield on a 50-mg scale (Figure 3.15). The structure of **3.140** was further confirmed via X-ray crystallographic analysis. In contrast, reacting azetidine **3.143** containing an unsubstituted isoxazolidine ring afforded the uncyclized amino alcohol **3.144** in 45% yield. Interestingly, stopping the reaction at shorter reaction times allowed to isolate mixtures containing both the cyclized lactone and the amino alcohol, which indicates that lactonization initially occurs, however, the lactone is ultimately opened under the reaction conditions. When the isoxazolidine ring contains a phenyl substituent, such as in **3.145**, hydrogenolysis of the *N*–*O* bond as well as the benzylic *C*–*O* bond takes place, giving rise to free azetidine **3.146** in 84% yield.

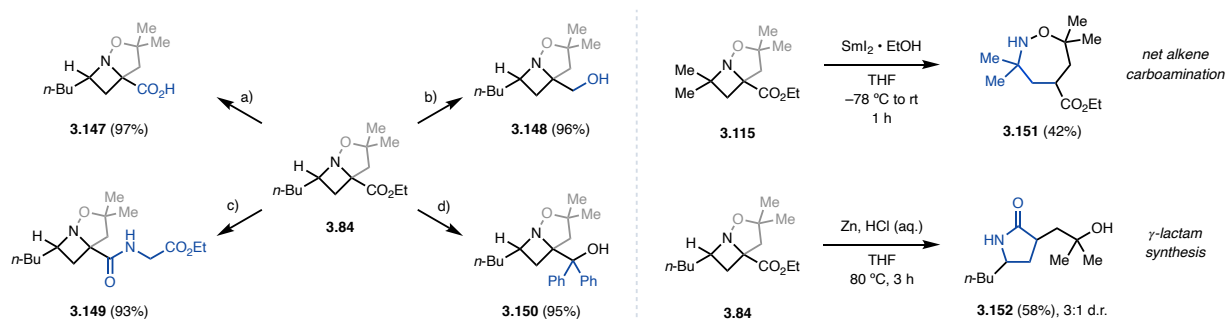


Figure 3.16: Synthesis modification of the obtained azetidine products. (a) LiOH, H₂O, MeOH, rt (b) LiAlH₄, Et₂O, 0 °C (c) LiOH, H₂O, MeOH, rt; then, glycine ethyl ester•HCl, DMAP, EDC•HCl, CH₂Cl₂, rt (d) PhMgBr, THF, 0 °C.

These building blocks are amenable to further functionalization of the free amino moiety, for example **3.141** and **3.142** were readily obtained via Boc-protection or tosylation in 78% and 99% yield, respectively.

While the *N*-*O* bond in the azetidine products can be readily cleaved through hydrogenolysis, it also functions as a nitrogen protecting group that enables various synthetic manipulations of these compounds in high yields. For example, **3.84** readily underwent hydrolysis (**3.147**), reduction (**3.148**), amide formation (**3.149**) and Grignard addition reactions (**3.150**) in 93–97% yield (Figure 3.16). At the outset of our investigations, we also investigated single-electron reductants for the cleavage of the *N*-*O* bond. Interestingly, utilizing samarium(II) iodide, a common reagent used for *N*-*O* bond reduction, resulted in the formation of oxazepane **3.151** in 42% yield.²¹⁶ This product likely originates from single-electron reduction of the ester moiety to the corresponding α -alkoxy radical rather than the *N*-*O* bond, which subsequently induces fragmentation of the internal *C*-*N* bond.^{217,218} In contrast, utilizing zinc as the stoichiometric reductant under acidic conditions afforded γ -lactam **3.152** in 58% yield as a 3:1 mixture of diastereomers. Under these conditions, the internal *C*-*N* bond as well as the *N*-*O* bond is cleaved, resulting in an amino alcohol intermediate that subsequently undergoes lactam formation. These results highlight that the developed intermolecular cycloaddition reaction not only allows for access to novel azetidine products, but that these building blocks can also function as precursor for the synthesis of other heterocycles.

3.5. Mechanistic Studies

The next step of this study aimed at corroborating the postulated triplet energy transfer mechanism and to gain further insights into the previously unexplored triplet reactivity of glyoxylate-derived oximes such as **3.83**. In agreement with the initially outlined mechanism, Stern-

Volmer studies confirmed oxime **3.83** as the only species in solution that is quenching the iridium photocatalyst *fac*-[Ir(dF(ppy)₃)], while the alkene component does not interact with the catalyst (Figure 3.17). The quenching process is unlikely to result from an electron transfer interaction as the redox potentials for **3.83** ($E_{\text{red}} = +2.01$ V versus SCE) are out of range for *fac*-[Ir(dF(ppy)₃)] ($\text{Ir}^{\text{III}*/\text{II}} = +0.36$ V versus SCE; $\text{Ir}^{\text{IV}/\text{III}*} = -1.28$ V versus SCE) (Figure 3.25).¹⁶⁵

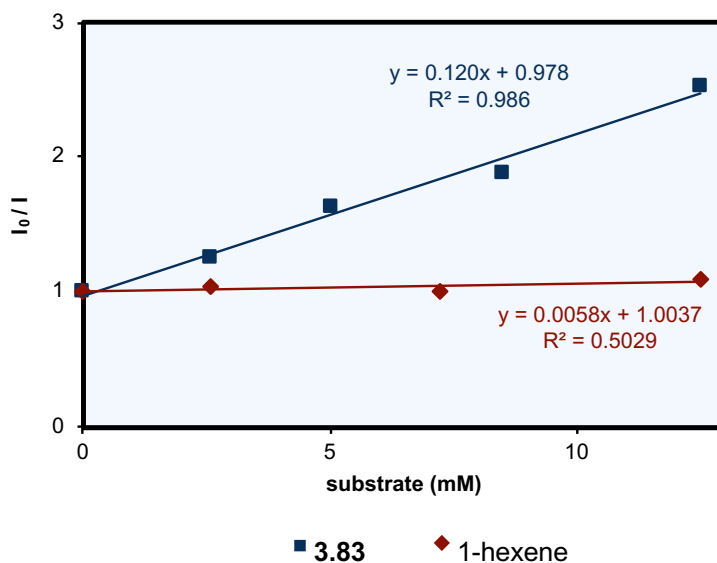


Figure 3.17: Stern-Volmer quenching studies with iridium catalyst *fac*-[Ir(dF(ppy)₃)].

In contrast, the reaction can be carried out with xanthone, an established organic photosensitizer. Utilizing 20 mol% of the catalyst, the desired product **3.84** was obtained in 54% yield relying on irradiation with UV light (Figure 3.18). Further control reactions revealed that a photocatalyst is essential to harvest the triplet reactivity of glyoxylate-derived oximes as direct irradiation **3.83** with various light sources in the absence of a catalyst did not lead to any product formation. Thus, it can be concluded that the singlet state of **3.83** is not reactive towards [2+2] cycloaddition reactions. This reactivity is in stark contrast to the 3-aryl-2-isoxazolines utilized by Mukai and Sampedro, which participated in cycloaddition reactions, although exclusively from the singlet excited state.^{147–150} Furthermore, the lack of reactivity of **3.83** further highlights that

direct irradiation does not result in sufficient population of the excited triplet state, indicating that intersystem crossing of **3.83** is likely inefficient.

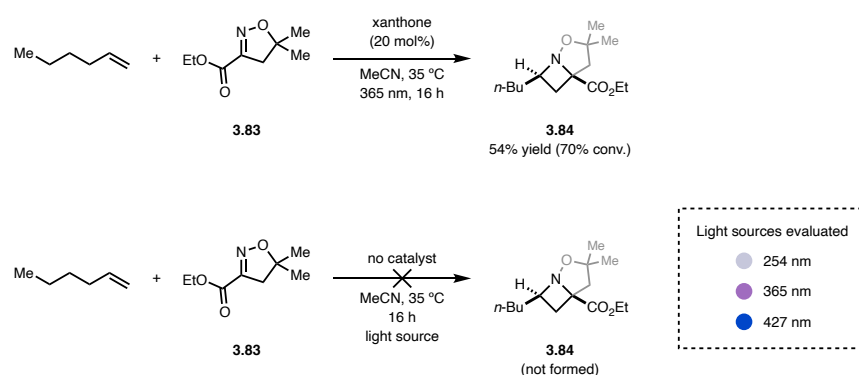


Figure 3.18: Control reactions using an organic photosensitizer (top) and different light sources without a catalyst (bottom).

We next investigated the structural features that are necessary for desired reactivity. Reacting alcohol **3.153** lacking the ester moiety under standard conditions did not result in product formation (Figure 3.19). This result is in agreement with previously made observations that aliphatic oximes have relatively high triplet energy that are not accessible for visible light photocatalysts. Next, we tested acyclic oxime **3.154** as substrate under our reaction conditions. Interestingly, no reaction with the alkene was observed, however, we detected a drastic change in the oxime isomer ratio from 20:1 to 1:1.2 *E/Z*. Based on this observation we postulate that triplet energy transfer to the acyclic oxime occurs. However, as a result of the lacking cyclic backbone, *E/Z* isomerization outcompetes the desired cycloaddition process.

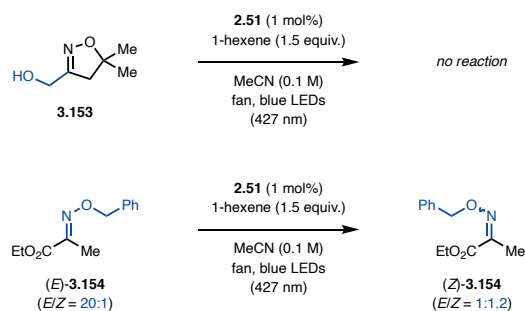


Figure 3.19: Investigations into the structure-activity relationships of oximes in the intermolecular cycloaddition reaction.

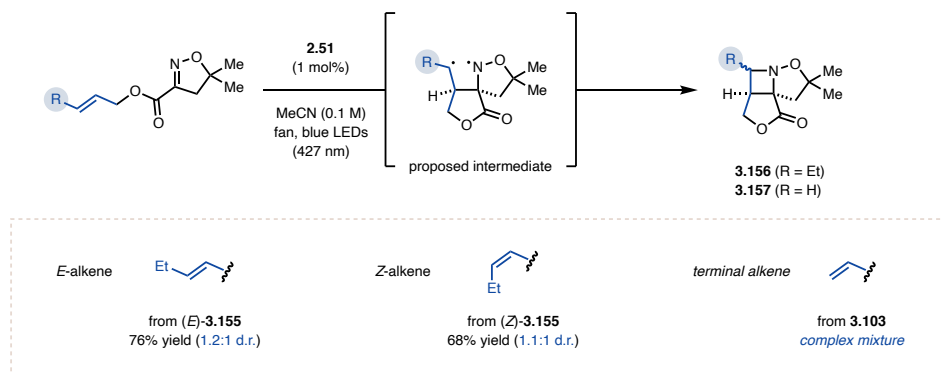


Figure 3.20: Probing the impact of alkene properties in the intermolecular cycloaddition reaction.

Considering that biradicals would be likely intermediates in a mechanism proceeding via the triplet state, we designed an intramolecular probe (**3.155**) containing either an (*E*)- or (*Z*)-alkene (Figure 3.20). Next, (*E*)- and (*Z*)-**3.155** were independently irradiated with visible light in the presence of catalytic amounts of **2.51**. Both reactions produced an almost identical mixture of diastereomers (**3.156**) in similar yields, indicative of a biradical intermediate that allows for free rotation of the alkene substituent. In contrast, irradiation of **3.103** containing a terminal alkene under our standard reaction conditions resulted in a complex mixture of inter- and intramolecular cycloaddition products.

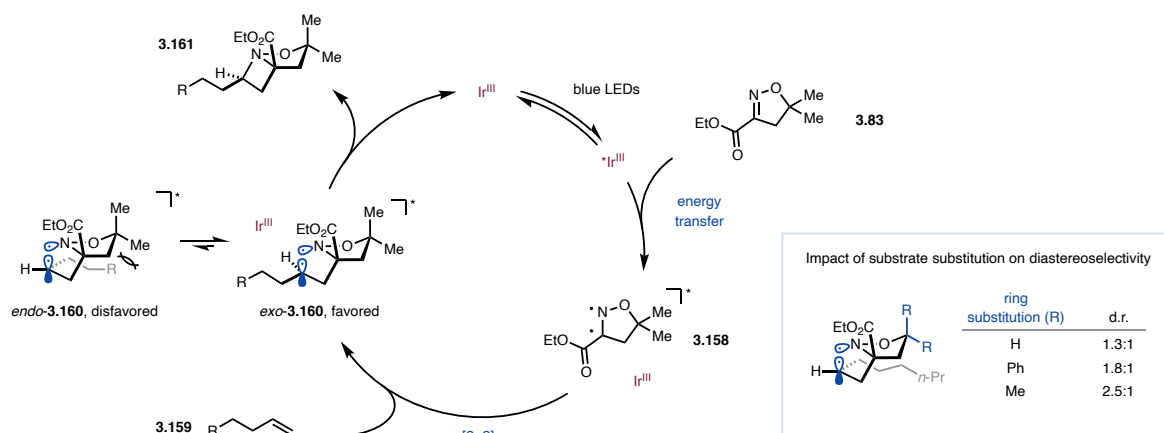


Figure 3.21: Proposed mechanism for the developed intermolecular aza Paternò-Büchi reaction.

This stark difference in reactivity can be attributed to the lack of stabilization of the biradical intermediate, and further shows that the first step of the cycloaddition process is likely carbon–carbon bond formation as opposed to an initial formation of the carbon–nitrogen bond.

selectivity likely arises from the fact that this stereocenter is set during the first step of the cycloaddition process, and that this position does not contain any biradical character.

3.6. Conclusion and Outlook

In summary, we have developed an intermolecular aza Paternò-Büchi reaction that relies on activation of cyclic glyoxylate-derived oximes via triplet energy transfer from a visible light photocatalyst. This method provides a highly versatile approach for the synthesis of azetidines that avoids limitations of previously reported procedures such as the need of direct irradiation via UV light, or the use of activated alkenes. The glyoxylate-derived oximes used in the developed transformation display distinct differences to the reactivity of the previously reported 3-aryl-2-isoxazolines, as they react from the triplet excited state that is exclusively accessible via triplet energy transfer. In addition, the investigated triplet state oximes tolerate a broad scope of unactivated alkene substrates. Finally, the obtained azetidine products are readily converted to a range of valuable building blocks, including free azetidine accessed via *N–O* bond cleavage.

Although the aza Paternò-Büchi reactions discussed herein represent highly efficient protocols to access complex azetidine scaffolds, some challenges remain that will require further investigations in the future. For example, these reactions, specifically those proceeding via triplet sensitization of oximes, are currently limited to cyclic imines due to the competing photoisomerization of acyclic substrates. Consequently, the successful design of novel, acyclic imine reagents that could engage in intermolecular [2+2] cycloaddition reactions would substantially expand the scope and the utility of current aza Paternò-Büchi reaction protocols, and enable access to additional types of novel azetidines products. Furthermore, the aza Paternò-Büchi reactions developed herein typically rely on the use of iridium photocatalysts. However, the prohibitively high cost of these catalysts provides challenges for conducting these reactions on large scale. Therefore, the development of cycloaddition reactions that proceed without any

catalyst or, alternatively, can be mediated by cheaper organic photocatalysts would represent a valuable improvement in this regard. Finally, advancing our understanding of the unprecedented excited state reactivity of the isoxazoline carboxylates discussed in this dissertation will likely accelerate the process of addressing current limitations, as well as hold the potential to utilize this reactivity for the development of other novel, photochemical transformations.

3.7. Experimental Section

3.7.1. General Information

General Laboratory Procedures. All air- or moisture-sensitive reaction were carried out in flame-dried glassware under an atmosphere of nitrogen. Thin-layer chromatography (TLC) was performed on *Merck* silica gel 60 F₂₅₄ plates using UV light (254 or 366 nm), KMnO₄ or CAM stain for visualization. Flash chromatography was performed using silica gel Silia Flash[®] 40-63 micron (230-400 mesh) from Silicycle unless noted.

Materials and Instrumentation. All chemicals were purchased from Sigma-Aldrich, Alfa Aesar, Acros Organics, Oakwood, TCI America, Frontier Scientific, Matrix Scientific, Ark Pharm, and Chem Impex International, and were used as received unless otherwise stated. THF, CH₂Cl₂, Et₂O, MeOH, MeCN and DMF were dried by being passed through a column of activated alumina under argon using a JC-Meyer Solvent Systems. [Ir(dF(CF₃)ppy)₂(dtbbpy)]PF₆ was prepared according to a literature procedure.¹⁷⁰ All other photocatalysts including *fac*-[Ir(dFppy)₃] were purchased from Sigma-Aldrich and used as received. 2-(3-phenylpropoxy)acetaldehyde *O*-methyl oxime (**2.104**),²¹³ 3-phenylisoxazol-5(4*H*)-one (**3.80**),²¹⁹ 5,5-dimethyl-3-phenyl-1-tosyl-4,5-dihydro-1*H*-pyrazole (**3.81**)²²⁰ and (5,5-dimethyl-4,5-dihydroisoxazol-3-yl)methanol (**3.153**)¹⁹⁰ were prepared according to literature procedures. Proton nuclear magnetic resonance (¹H NMR) spectra were recorded on Varian MR400, Varian vnmrs 500, Varian Inova 500, and Varian vnmrs 700 spectrometers and are referenced to residual protic NMR solvent (CDCl₃: δ 7.26 ppm). Data for ¹H NMR are reported as follows: chemical shift (δ ppm), multiplicity (s = singlet, d = doublet, t = triplet, q = quartet, m = multiplet, b = broad), coupling constant (Hz), integration. Carbon nuclear magnetic resonance (¹³C NMR) spectra were recorded on Varian vnmrs 500 and Varian vnmrs 700 spectrometers and are referenced to the carbon resonances of the NMR solvent (CDCl₃:

δ 77.16 ppm). High-resolution mass spectrometry (MS) data was recorded at the Mass Spectrometry Facility at the Department of Chemistry of the University of Michigan in Ann Arbor, MI on an Agilent 6230 TOF HPLC-MS (ESI) or Micromass AutoSpec Ultima Magnetic Sector mass spectrometer (ESI, EI). Infrared (IR) spectra were obtained using a Thermo-Nicolet IS-50 spectrometer. IR data are represented as frequency of absorption (cm^{-1}). Stereochemistry indicators with asterisk (R^* , S^*) were used to indicate relative stereochemistry of diastereomers.

Photochemical Setup.

Visible light-mediated reactions were carried out using two 40 W PR160-427 Kessil lights (100% intensity) that were placed at both sides of the reaction vessel at a distance of approximately 10 cm. The reactor temperature was monitored throughout the reaction with a temperature probe placed adjacent to the reaction vessel and maintained at 35 °C by cooling with a fan positioned above the reaction (Figure 3.23).

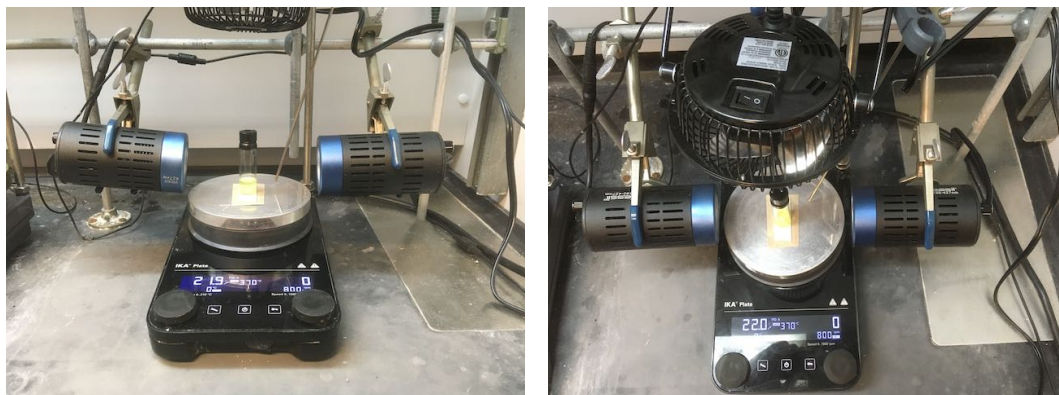


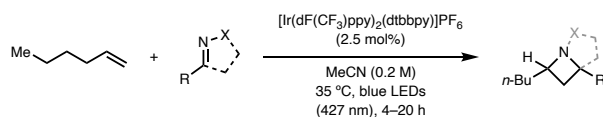
Figure 3.23: Photochemical setup used for intermolecular [2+2] photocycloaddition.

3.7.2. Reaction Optimization

Evaluations of Substrates

A 1-dram vial was charged with the corresponding substrate (0.1 mmol, 1.0 equiv.), [Ir(dF(CF₃)ppy)₂(dtbbpy)]PF₆ (3 mg, 2.5 mol%) and MeCN (0.5 mL). The vial was subsequently sealed with a septum-equipped cap and the reaction mixture degassed by sparging with nitrogen gas for 5 min. Then, 1-hexene (67 μL, 0.54 mmol, 5.0 equiv.) was added via syringe, the vial sealed with electrical tape and the reaction stirred under irradiation with blue LED lights (427 nm) at ambient temperature (fan cooling) for 4–20 h. The solvent was removed *in vacuo* and crude reaction mixture purified by flash column chromatography.

Table 3.4: Evaluation of substrates for photochemical [2+2] photocycloaddition.



entry	substrate	reaction time (h)	quenching percentage (%)	yield (%)
1		18	24	0 ^a
2		18	97	0 ^a
3		4	59	0 ^b
4		4	88	0 ^b
5		18	96	0 ^a
6		18	54	60

^ano reaction was observed; ^brapid decomposition of the substrate was observed.

The quenching percentage was calculated using the following equation: $100(1-I/I_0)$ (I: luminescence of $[\text{Ir}(\text{dF}(\text{CF}_3)\text{ppy})_2(\text{dtbbpy})]\text{PF}_6$ in the absence of quencher; I_0 : luminescence of $[\text{Ir}(\text{dF}(\text{CF}_3)\text{ppy})_2(\text{dtbbpy})]\text{PF}_6$ in the presence of 2500 equiv. of substrate).²¹⁴ 190 μL of a 0.11 mM stock solution of catalyst in MeCN and the respective amount of a 50–60 mM stock solution of substrate (2500 equiv.) were added to a 4-mL volumetric flask and the volume adjusted with MeCN. The solution was transferred to a 1-cm cuvette, which was sealed with a septum-equipped cap and the solution degassed by sparging for 15 min with argon gas, before measuring the luminescence using a PTI quantaMaster fluorimeter (Horiba) (excitation at 420 nm; luminescence was observed at 427 nm).

Reaction Optimization of Photochemical [2+2] Cycloaddition

A 1-dram vial was charged with **3.83** (17 mg, 0.1 mmol, 1.0 equiv.), photocatalyst and solvent. The vial was subsequently sealed with a septum-equipped cap and the reaction mixture degassed by sparging with nitrogen gas for 5 min. Then, 1-hexene was added via syringe, the vial sealed with electrical tape and the reaction stirred under irradiation with blue LED lights (427 nm) at ambient temperature (fan cooling) for 16 h. The solvent was removed *in vacuo* and the crude reaction mixture analyzed by ¹H NMR using mesitylene as the internal standard.

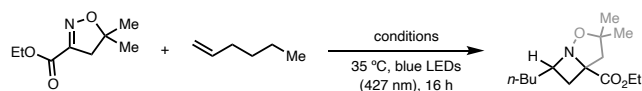


Table 3.5: Photocatalyst evaluation.

entry	photocatalyst	yield (%)	d.r.	r.r.	conversion (%)
1	xanthone ^a	54	4:1	16:1	70
2	[Ir(dF(Me)ppy) ₂ (dtbbpy)]PF ₆	54	>20:1	9:1	>95
3	[Ir(dF(CF ₃)ppy) ₂ (dtbbpy)]PF ₆	69	9:1	13:1	>95
4	<i>fac</i> -[Ir(dFppy) ₃]	94	3:1	>20:1	>95
5	<i>fac</i> -[Ir(4'-CF ₃ -ppy) ₃]	8	3:1	>20:1	9
6	<i>fac</i> -[Ir(ppy) ₃]	0	–	–	<5
7	[Ir(ppy) ₂ (dtbbpy)]PF ₆	0	–	–	<5
8	[Ru(bpz) ₃](PF ₆) ₂	0	–	–	<5
9	[Ru(phen) ₃](PF ₆) ₂	0	–	–	<5
10	[Ru(bpy) ₃](PF ₆) ₂	0	–	–	<5

Conditions: Reactions performed with 0.5 mmol 1-hexene (5.0 equiv.) and 2.5 mol% photocatalyst in MeCN (1 mL) for 16 h. d.r. = diastereomer ratio; r.r. = regioisomer ratio; ^arun with 20 mol% catalyst under UV light irradiation (365 nm).

Table 3.6: Solvent evaluation.

entry	solvent	yield (%)	d.r.	r.r.	conversion (%)
1	acetonitrile	94	3:1	>20:1	>95
2	CH ₂ Cl ₂	>95	3:1	>20:1	>95
3	1,2-dichloroethane	>95	3:1	19:1	>95
4	THF	50	3:1	11:1	>95
5	ethyl acetate	89	3:1	16:1	>95
6	methanol	89	2:1	17:1	94
7	toluene	91	4:1	16:1	>95
8	acetone	92	3:1	18:1	>95
9	1,4-dioxane	94	3:1	>20:1	>95
10	DMF	94	3:1	>20:1	>95
11	DMSO	84	2:1	19:1	>95

Conditions: Reactions performed with 0.5 mmol 1-hexene (5.0 equiv.) and 2.5 mol% *fac*-[Ir(dFppy)₃] in the corresponding solvents (1 mL) for 16 h. d.r. = diastereomer ratio; r.r. = regioisomer ratio.

Table 3.7: Reaction concentration evaluation.

entry	concentration (M)	yield (%)	d.r.	r.r.	conversion (%)
1	0.05	94	3:1	>20:1	>95
2	0.10	94	3:1	>20:1	>95
3	0.25	93	3:1	>20:1	>95
4	0.50	90	3:1	19:1	>95
5	no solvent (neat)	10	–	–	12

Conditions: Reactions performed with 0.5 mmol 1-hexene (5.0 equiv.) and 2.5 mol% *fac*-[Ir(dFppy)₃] in MeCN (x mL) for 16 h. d.r. = diastereomer ratio; r.r. = regioisomer ratio.

Table 3.8: Alkene equivalents evaluation.

entry	equivalents (alkene)	yield (%)	d.r.	r.r.	conversion (%)
1	1.1	75	3:1	18:1	79
2	1.5	93	3:1	>20:1	>95
3	2.0	92	3:1	19:1	>95
4	5.0	94	3:1	>20:1	>95

Conditions: Reactions performed with x mmol 1-hexene (x equiv.) and 2.5 mol% *fac*-[Ir(dFppy)₃] in MeCN (1 mL) for 16 h. d.r. = diastereomer ratio; r.r. = regioisomer ratio.

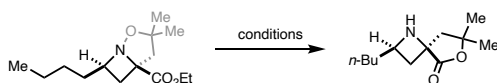
Table 3.9: Catalyst loading evaluation.

entry	catalyst loading (mol%)	yield (%)	d.r.	r.r.	conversion (%)
1	0.1	88	3:1	19:1	>95
2	0.5	86	3:1	17:1	>95
3	1.0	91	3:1	19:1	>95
4	2.5	93	3:1	>20:1	>95

Conditions: Reactions performed with 0.15 mmol 1-hexene (1.5 equiv.) and x mol% *fac*-[Ir(dFppy)₃] in MeCN (1 mL) for 16 h. d.r. = diastereomer ratio; r.r. = regioisomer ratio.

Reaction Optimization of *N*-*O* Bond Cleavage of Azetidine Products

A 1-dram vial was charged with *exo*-**3.84** (10 mg, 0.04 mmol, 1.0 equiv.), reagents and solvent (1 mL). The vial was subsequently sealed with a septum-equipped cap and reaction mixture sparged with hydrogen gas for 5–10 min, before being stirred at the corresponding temperature for 24 h under a hydrogen atmosphere (ballon, 1 atm). The reaction mixture was filtered through celite, the filter cake washed with CH₂Cl₂ and the filtrate concentrated *in vacuo*. The residue was taken up in CH₂Cl₂ and water and the aqueous layer brought to pH 10–11 with 2 M NaOH solution (aq.). Next, the organic layer was separated and the aqueous layer extracted with CH₂Cl₂ (2x). The combined organic extracts were dried over Na₂SO₄, filtered and concentrated *in vacuo*. The crude reaction mixture was analyzed by ¹H NMR to determine yield and conversion using mesitylene as the internal standard.

Table 3.10: Reaction optimization of *N*-*O* bond cleavage reaction.

entry	reagents (mol%)	solvent	temperature (°C)	yield (%)	conversion (%)
1	Zn (xs)	HCl (aq.)/THF	80	0	>95
2	Zn (xs)	AcOH	60	38	53
3	Pd/C (20)	EtOH	40	12	11
4	Pd(OH) ₂ (20), H ₂ (1 atm)	EtOH	40	23	16
5	Raney-Ni, H ₂ (1 atm)	EtOH	40	58	67
6	PtO ₂ (20), H ₂ (1 atm)	EtOH	40	0	<5
7	Ru/C (20), H ₂ (1 atm)	EtOH	40	12	17
8	Pd(OH) ₂ (50), H ₂ (1 atm)	EtOH	40	27	39
9	Pd(OH) ₂ (20), H ₂ (4 atm)	EtOH	60	16	46
10	Pd(OH) ₂ (20), H ₂ (1 atm)	EtOH	78	14	>95
11	Pd(OH) ₂ (20), H ₂ (1 atm)	EtOH/H ₂ O (1:1)	40	4	28
12	Pd(OH) ₂ (20), H ₂ (1 atm)	DMF	40	0	<5
13	Pd(OH) ₂ (20), H ₂ (1 atm)	acetone	40	0	51
14	Pd(OH) ₂ (20), H ₂ (1 atm)	H ₂ O/AcOH (1:1)	40	0	>95
15	Pd(OH) ₂ (20), H ₂ (1 atm)	EtOH/H ₂ O/AcOH	40	61	>95
16	Pd(OH)₂ (20), H₂ (1 atm) <i>p</i>-TsOH (2.0 equiv.)	EtOH	40	85	87
17	Pd(OH) ₂ (20), H ₂ (1 atm) oxalic acid (2.0 equiv.)	EtOH	40	14	40
18	Pd(OH) ₂ (20), H ₂ (1 atm) TFA (3.4 equiv.)	EtOH	40	33	61
19	Pd(OH) ₂ (20), H ₂ (1 atm) HCl (aq., 2.6 equiv.)	EtOH	40	79	80

3.7.3. Mechanistic Investigations

UV/Vis Absorption Spectra

UV/Vis absorption spectra were recorded on a Varian Cary 50 UV/Vis spectrophotometer. Samples were prepared in MeCN with **3.83** (2.5 mM) and *fac*-[Ir(dFppy)₃] (0.025 mM). The photocatalyst is the only species absorbing at 427 nm.

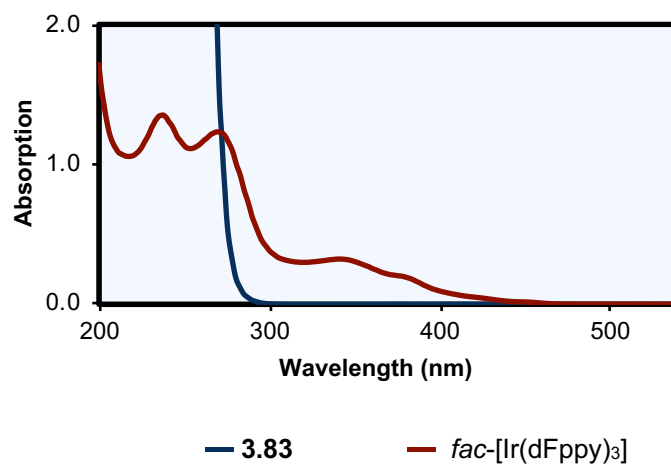


Figure 3.24: UV/Vis absorption spectra of *fac*-[Ir(dFppy)₃] and compound **3.83**.

Electrochemical Measurements

Cyclic voltammetry was performed on a CHI620E electrochemical analyzer (CH instruments) using a 3-mL five-neck electrochemical cell equipped with a glassy carbon working electrode, a platinum counter or auxiliary electrode and an Ag/AgCl (3 M KCl) reference electrode. The experimental setup was calibrated using ferrocene (Fc^+/Fc) prior to each experiment. Samples were prepared with 0.03 mmol substrate in 3 mL $n\text{-Bu}_4\text{NPF}_6$ electrolyte (0.1 M in MeCN) and degassed prior to use by sparging with argon gas for 10 min. Data acquisition was performed at a scan rate of 100 mV/s and the potential ($E_{p/2}$) determined according to literature procedures.¹⁷² All potentials are reported versus the saturated calomel electrode (SCE). The cyclic voltamogram for 2-isoxazoline **3.83** shows an irreversible reduction process at $E_{p/2} = -2.01$ V (vs. SCE) (Figure 3.25).

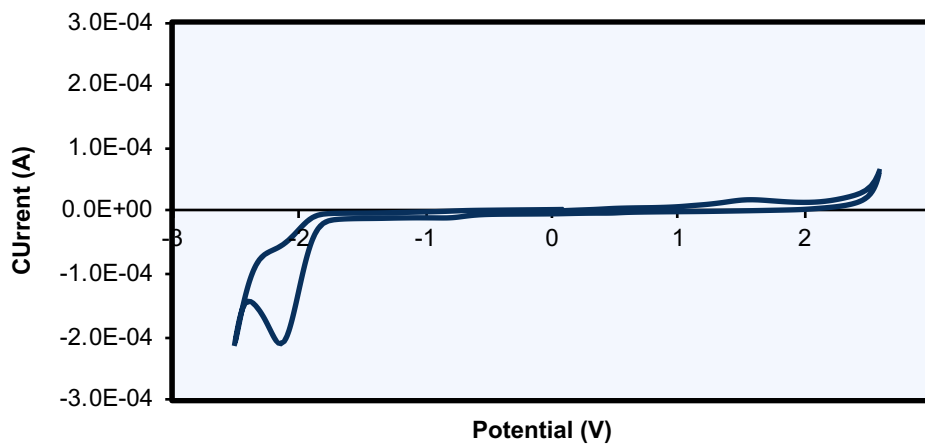


Figure 3.25: Cyclic voltammogram of compound **3.83**.

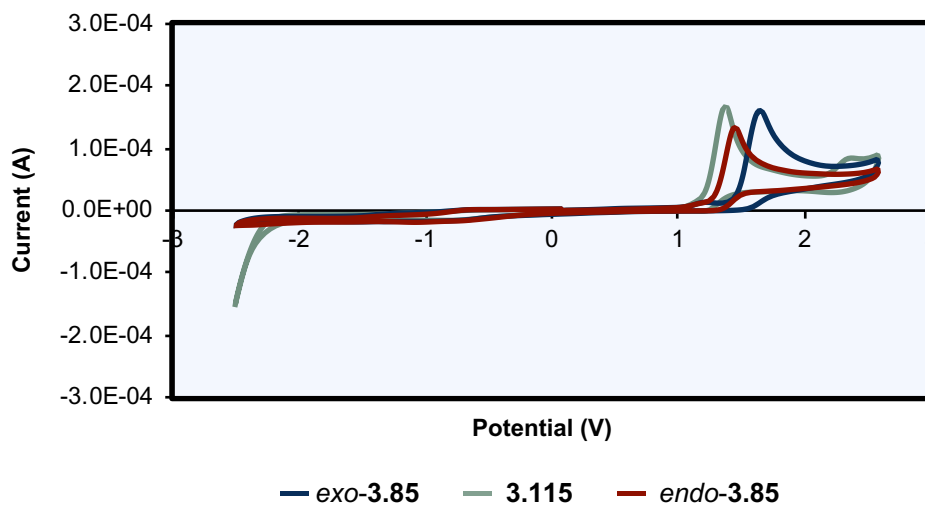


Figure 3.26: Cyclic voltammograms of azetidines *exo*-**3.85**, **3.115** and *endo*-**3.85**. The compounds show an irreversible oxidation process at $E_{p/2}$ (*exo*-**3.85**) = +1.51 V, $E_{p/2}$ (**3.115**) = +1.25 V and $E_{p/2}$ (*endo*-**3.85**) = +1.33 V, respectively (vs. SCE).

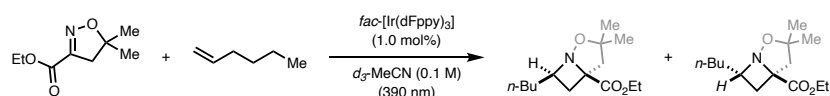
Stern-Volmer Quenching Study

Samples for the quenching study were prepared using stock solutions of **3.83** (103 mM), 1-hexene (103 mM) and *fac*-[Ir(dFppy)₃] (0.05 mM) in dry MeCN. To a 4-mL volumetric flask was added *fac*-[Ir(dFppy)₃] (572 μL) and the respective amount of quencher (for **3.83**: 0 μL, 100 μL, 195 μL, 332 μL, 488 μL; for 1-hexene: 0 μL; 100 μL, 280 μL, 485 μL) and the volume adjusted to 4 mL with dry MeCN. The solution was transferred to a 1-cm quartz cuvette, which was sealed with a septum-equipped cap and degassed by sparging with nitrogen gas for 15 min. Emission spectra were recorded using a PTI quantaMaster fluorimeter (Horiba) with an excitation wavelength of 420 nm. Emissions were observed at 480 nm and the ratio of I₀/I plotted as a function of the quencher concentration (I₀: emission intensity without quencher; I: emission intensity with quencher). The Stern-Volmer analysis shows that 2-isoxazoline **3.83** is a quencher of the photocatalyst *fac*-[Ir(dFppy)₃], while 1-hexene does not interact with the photocatalyst. The plotted data from the Stern-Volmer quenching study can be found in Figure 3.17.

Table 3.11: Stern-Volmer quenching data.

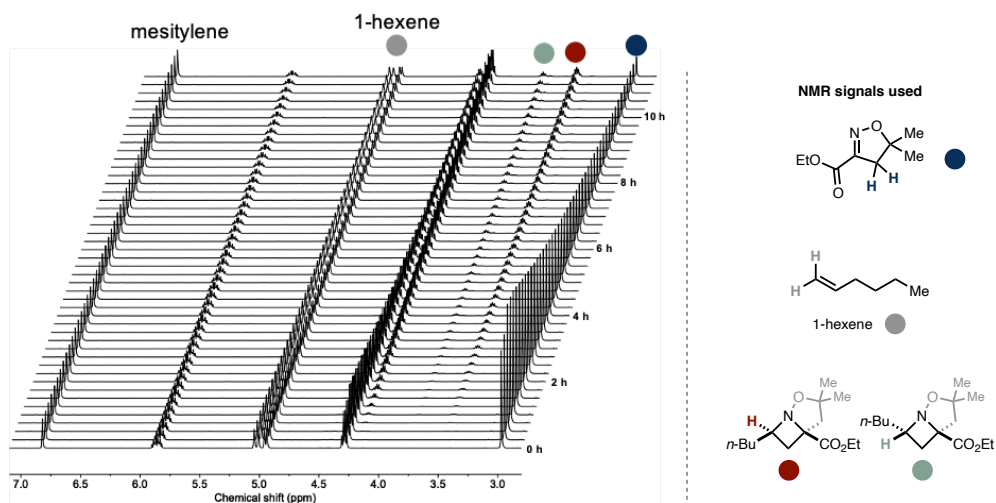
concentration (mM)	I ₀ / I (3.83)
0.0	1.0
2.6	1.3
5.0	1.6
8.5	1.9
12.5	2.5
concentration (mM)	I ₀ / I (1-hexene)
0.0	1.0
2.6	1.0
7.2	1.0
12.5	1.1

In Situ ^1H NMR Experiment



A 1-dram vial was charged with **3.83** (34 mg, 0.2 mmol, 1.0 equiv.), $fac\text{-}[\text{Ir}(\text{dFppy})_3]$ (2 mg, 1 mol%) and $d_3\text{-MeCN}$ (2 mL). The mixture was homogenized by sonicating for 1 min. Then, mesitylene ($\sim 5 \mu\text{L}$) and 1-hexene (37 μL , 0.3 mmol, 1.5 equiv.) were added. The reaction was carried out with a LED NMR setup by Goldstone Scientific (Mic-LED-NMR). A volume of 600 μL of the prepared solution was transferred to a 5 mm thin-wall NMR tube, which was fitted with a coaxial glass insert containing a fiber-optic cable and the tube sealed with a cap and parafilm. The sample was inserted into a Varian vnmrs 500 and the reaction mixture irradiated through the fiber-optic cable with a LED light (390 nm) at ambient temperature. Concentrations of all reactants and products were monitored by ^1H NMR in 15 min increments in reference to mesitylene as the internal standard. After a reaction time of 11.5 h the reaction reached 84% conversion with 81% yield of product. The product diastereomer ratio was found to be constant (d.r. = 2.9) during the course of the reaction.

A. Stacked NMR data of the kinetic experiment



B. ¹H NMR time study of title reaction

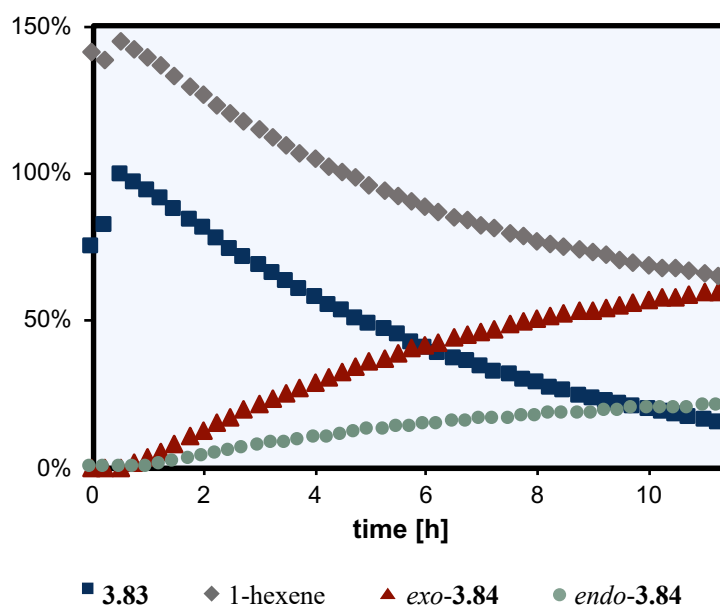


Figure 3.27: NMR time study. (A) Stacked NMR data of the NMR experiment (B) Plot of the NMR time study.

Table 3.12: Data from the NMR time study.

time [h]	3.83 (%)	1-hexene (%)	<i>exo</i> - 3.84 (%)	<i>endo</i> - 3.84 (%)
0.00	76	142	0	0
0.25	83	139	0	0
0.50	100	145	0	0
0.75	98	143	2	0
1.00	95	140	4	1
1.25	92	137	6	2
1.50	88	133	8	3
1.75	85	130	11	3
2.00	82	127	13	4
2.25	78	124	16	5
2.50	75	121	18	6
2.75	72	118	20	7
3.00	69	115	22	7
3.25	66	113	24	8
3.50	64	110	26	9
3.75	61	107	28	10
4.00	58	105	30	10
4.25	56	103	32	11
4.50	54	101	33	12
4.75	51	99	35	12
5.00	49	96	37	13
5.25	47	94	38	13
5.50	45	93	39	14
5.75	43	91	41	14
6.00	41	89	42	15
6.25	40	88	43	15
6.50	38	86	45	16
6.75	36	85	46	16
7.00	35	83	47	16
7.25	33	82	48	17
7.50	32	80	49	17
7.75	30	79	50	17
8.00	29	78	51	18
8.25	28	77	52	18
8.50	26	76	53	18
8.75	25	74	54	19
9.00	24	73	54	19
9.25	23	72	55	19
9.50	22	71	56	20
9.75	21	70	57	20
10.00	20	70	58	20
10.25	19	69	58	20
10.50	18	68	59	21
10.75	17	67	59	21
11.00	17	67	60	21
11.25	16	66	60	21

Control Reactions

A 1-dram vial was charged with substrate (0.1 mmol, 1.0 equiv.), photocatalyst (1.0–2.5 mol%) and MeCN (1 mL). The vial was subsequently sealed with a septum-equipped cap and the reaction mixture degassed by sparging with nitrogen gas for 5 min. Then, 1-hexene was added via syringe, the vial sealed with electrical tape and the reaction stirred under irradiation with blue LED lights (427 nm) at ambient temperature (fan cooling) for 16–18 h. The solvent was removed *in vacuo* and the crude reaction mixture analyzed by ^1H NMR using mesitylene as the internal standard.

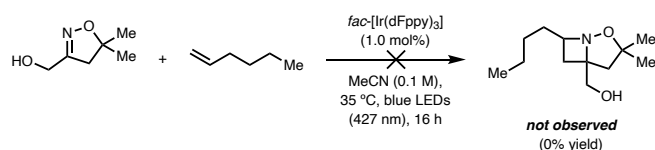


Figure 3.28: Control reactions testing the requirements of light and a catalyst for the cycloaddition reaction.

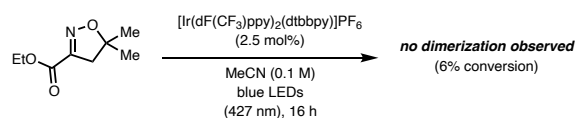


Figure 3.29: Control reaction to demonstrate the stability of the 2-isoxazoline substrates under the reaction conditions.

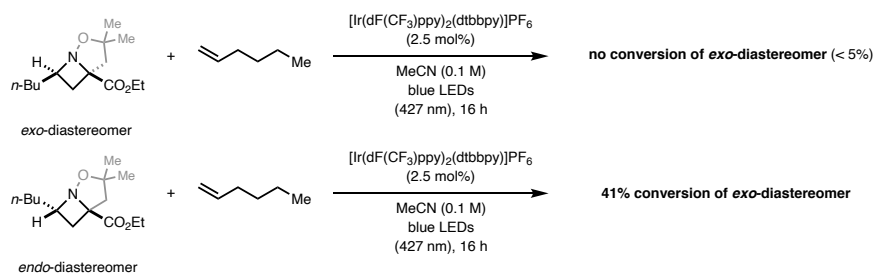


Figure 3.30: Control reactions to test the stability of both azetidine diastereomers under the reaction conditions.

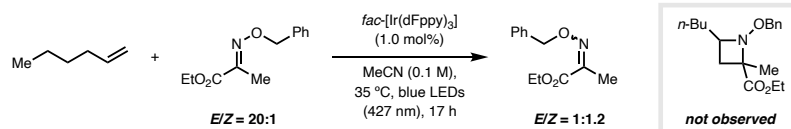


Figure 3.31: Control reaction demonstrating the requirement of a cyclic backbone.

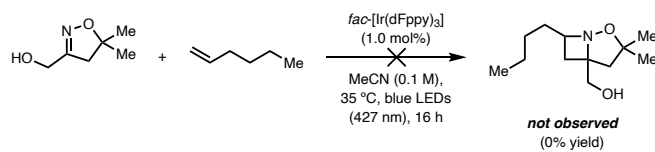


Figure 3.32: Control reaction demonstrating the requirement of an electron-withdrawing group.

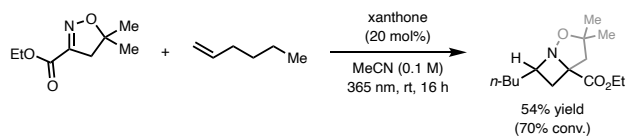


Figure 3.33: Control reaction with xanthone as an organic triplet sensitizer.

Other Evaluated Substrates in the Photochemical [2+2] Cycloaddition

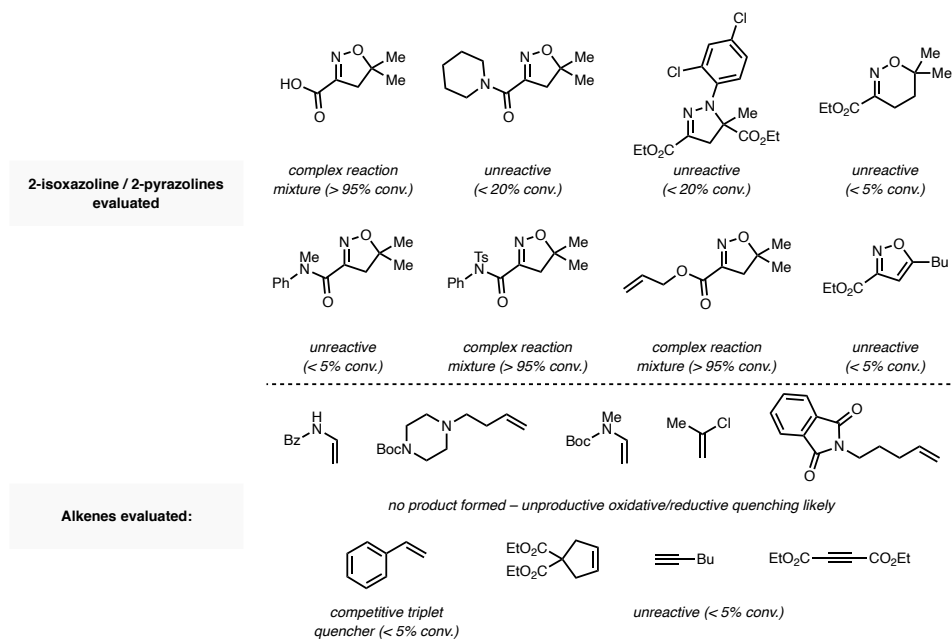
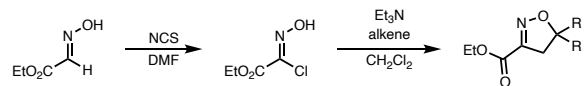


Figure 3.34: Overview of unsuccessful substrates in the intermolecular [2+2] cycloaddition reaction.

3.7.4. Experimental Procedures

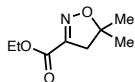
General Procedure for Synthesis of 2-Isoxazolines via (3+2) Cycloaddition (GP-3.1)



A round-bottom flask equipped with a magnetic stir bar was charged with ethyl 2-(hydroxyimino)acetate²²¹ (1.0 equiv.) and DMF (0.5 M). *N*-chlorosuccinimide (1.0 equiv.) was added and the resulting mixture stirred at 60 °C for 2 h. After cooling to rt, the reaction mixture was partitioned between water and EtOAc. The organic layer was separated, and the aqueous layer extracted with EtOAc (2x). The combined organic extracts were washed with water (2x) and brine, then dried over Na₂SO₄, filtered and concentrated *in vacuo* to afford ethyl 2-chloro-2-(hydroxyimino)acetate as a colorless solid, which was used for the next step without further purification.

A round-bottom flask containing ethyl 2-chloro-2-(hydroxyimino)acetate was equipped with a magnetic stir bar, charged with the corresponding alkene (1.5–33.4 equiv.) and CH₂Cl₂ (0.3 M), and subsequently sealed with a rubber septum. Next, Et₃N (1.0 equiv.) was added dropwise over 2–4 h using a syringe pump, and, after completion of addition, the reaction stirred for additional 0.5–12 h. The resulting reaction mixture was washed with 0.5 M HCl solution (aq.) and the aqueous layer extracted with CH₂Cl₂ (2x). The combined organic extracts were washed with brine, dried over Na₂SO₄, filtered and concentrated *in vacuo*. The crude mixture was purified by flash column chromatography to afford the pure title compound.

Note: For cyclic 2-isoxazolines **3.83** and **S3.85**, the alkene was added by sparging the solution with the corresponding gaseous alkene after sealing the flask with a rubber septum, and the reaction carried out under an atmosphere of the alkene. The amount of added alkene was determined by weighing the gas container before and after addition of alkene.



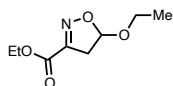
Ethyl 5,5-dimethyl-4,5-dihydroisoxazole-3-carboxylate (3.83): Prepared according to GP-3.1 using ethyl 2-(hydroxyimino)acetate²²¹ (5.00 g, 42.7 mmol, 1.0 equiv.), *N*-chlorosuccinimide (5.70 g, 42.7 mmol, 1.0 equiv.), Et₃N (6.0 mL, 42.7 mmol, 1.0 equiv.) and 2-methylpropene (24.0 g, 427 mmol, 10.0 equiv.). Purification by flash column chromatography (5–20% EtOAc/hexanes) afforded the pure title compound as a colorless low-melting solid (4.62 g, 63%). Spectroscopic data were consistent with those reported in the literature.¹⁹⁰

¹H NMR (400 MHz, CDCl₃): δ 4.34 (q, *J* = 7.1 Hz, 2H), 2.96 (s, 2H), 1.46 (s, 6H), 1.37 (t, *J* = 7.1 Hz, 3H).



Ethyl 4,5-dihydroisoxazole-3-carboxylate (S3.85): Prepared according to GP-3.1 using ethyl 2-(hydroxyimino)acetate²²¹ (750 mg, 6.4 mmol, 1.0 equiv.), *N*-chlorosuccinimide (855 mg, 6.4 mmol, 1.0 equiv.), Et₃N (0.89 mL, 6.4 mmol, 1.0 equiv.) and ethylene (6.00 g, 214 mmol, 33.4 equiv.). Purification by flash column chromatography (5–35% EtOAc/hexanes) afforded the pure title compound as a colorless oil (600 mg, 65%).

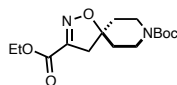
¹H NMR (700 MHz, CDCl₃): δ 4.54 (t, *J* = 10.7 Hz, 2H), 4.36 (q, *J* = 7.1 Hz, 2H), 3.21 (t, *J* = 10.7 Hz, 2H), 1.37 (t, *J* = 7.1 Hz, 3H).; **¹³C NMR** (176 MHz, CDCl₃): δ 160.8, 151.9, 71.4, 62.2, 33.9, 14.2; **IR** (cm⁻¹): 2984, 2361, 2338, 1715, 1685, 1587, 1404, 1333, 1254, 1118, 1017, 916, 858, 818, 748; **HRMS**: *m/z* calculated for C₆H₁₀NO₃⁺ [M+H]⁺: 144.0655; found: 144.0656.



Ethyl 5-ethoxy-4,5-dihydroisoxazole-3-carboxylate (S3.89): Prepared according to GP-3.1 using ethyl 2-(hydroxyimino)acetate²²¹ (293 mg, 2.5 mmol, 1.0 equiv.), *N*-chlorosuccinimide

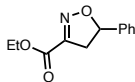
(334 mg, 2.5 mmol, 1.0 equiv.), Et₃N (0.35 mL, 2.5 mmol, 1.0 equiv.) and ethyl vinyl ether (1.2 mL, 12.5 mmol, 5.0 equiv.). Purification by flash column chromatography (2–15% EtOAc/hexanes) afforded the pure title compound as a colorless oil (328 mg, 70%).

¹H NMR (500 MHz, CDCl₃): δ 5.70 (d, *J* = 6.9 Hz, 1H), 4.36 (q, *J* = 6.7 Hz, 2H), 3.90 (p, *J* = 7.4 Hz, 1H), 3.61 (p, *J* = 7.5 Hz, 1H), 3.23 (dd, *J* = 18.4, 6.9 Hz, 1H), 3.08 (d, *J* = 18.4 Hz, 1H), 1.37 (t, *J* = 7.1 Hz, 3H), 1.22 (t, *J* = 7.0 Hz, 3H); **¹³C NMR** (126 MHz, CDCl₃): δ 160.4, 152.0, 105.0, 64.5, 62.2, 40.3, 15.1, 14.2; **IR** (cm⁻¹): 2981, 2361, 2338, 1718, 1589, 1374, 1339, 1260, 1190, 1130, 1090, 1017, 904, 850, 761, 741; **HRMS**: *m/z* calculated for C₈H₁₄NO₄⁺ [M+H]⁺: 188.0917; found: 188.0916.



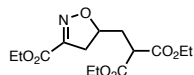
8-(*Tert*-butyl) 3-ethyl 1-oxa-2,8-diazaspiro[4.5]dec-2-ene-3,8-dicarboxylate (S3.87): Prepared according to GP-3.1 using ethyl 2-(hydroxyimino)acetate²²¹ (293 mg, 2.5 mmol, 1.0 equiv.), *N*-chlorosuccinimide (334 mg, 2.5 mmol, 1.0 equiv.), Et₃N (0.35 mL, 2.5 mmol, 1.0 equiv.) and *tert*-butyl 4-methylenepiperidine-1-carboxylate²²² (740 mg, 3.8 mmol, 1.5 equiv.). Purification by flash column chromatography (7–40% EtOAc/hexanes) afforded the pure title compound as a colorless solid (463 mg, 59%).

¹H NMR (700 MHz, CDCl₃): δ 4.35 (q, *J* = 7.1 Hz, 2H), 3.65 (b, 2H), 3.49 – 3.39 (m, 2H), 2.96 (s, 2H), 1.88 (d, *J* = 13.3 Hz, 2H), 1.70 (t, *J* = 9.0 Hz, 2H), 1.46 (s, 9H), 1.37 (t, *J* = 7.1 Hz, 3H); **¹³C NMR** (176 MHz, CDCl₃): δ 160.9, 154.7, 151.2, 88.0, 79.9, 62.2, 43.8, 40.7, 35.8, 28.5, 14.2; **IR** (cm⁻¹): 2979, 2927, 2361, 2338, 1734, 1695, 1429, 1366, 1152, 1110, 1077, 949, 855, 749; **HRMS**: *m/z* calculated for C₁₅H₂₄N₂NaO₅⁺ [M+Na]⁺: 335.1577; found: 335.1581.



Ethyl 5-phenyl-4,5-dihydroisoxazole-3-carboxylate (S3.88): Prepared according to GP-3.1 using ethyl 2-(hydroxyimino)acetate²²¹ (293 mg, 2.5 mmol, 1.0 equiv.), *N*-chlorosuccinimide (334 mg, 2.5 mmol, 1.0 equiv.), Et₃N (0.35 mL, 2.5 mmol, 1.0 equiv.) and styrene (0.57 mL, 5.0 mmol, 2.0 equiv.). Purification by flash column chromatography (7–40% EtOAc/hexanes) afforded the pure title compound as a colorless oil (413 mg, 75%).

¹H NMR (700 MHz, CDCl₃): δ 7.42 – 7.37 (m, 2H), 7.37 – 7.31 (m, 3H), 5.79 (dd, *J* = 11.6, 8.9 Hz, 1H), 4.37 (q, *J* = 7.1 Hz, 2H), 3.64 (dd, *J* = 17.8, 11.6 Hz, 1H), 3.22 (dd, *J* = 17.8, 8.9 Hz, 1H), 1.38 (t, *J* = 7.1 Hz, 3H); **¹³C NMR** (176 MHz, CDCl₃): δ 160.7, 151.3, 139.6, 129.0, 128.8, 126.0, 85.1, 62.3, 41.6, 14.2; **IR** (cm⁻¹): 2983, 2361, 2338, 1717, 1588, 1379, 1333, 1243, 1119, 1016, 921, 860, 745, 698; **HRMS**: *m/z* calculated for C₁₂H₁₄NO₃⁺ [M+H]⁺: 220.0968; found: 220.0970.

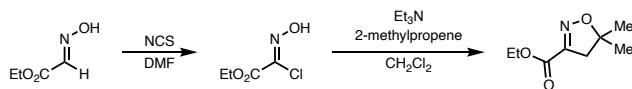


Diethyl 2-((3-(ethoxycarbonyl)-4,5-dihydroisoxazol-5-yl)methyl)malonate (S3.90): Prepared according to GP-3.1 using ethyl 2-(hydroxyimino)acetate²²¹ (293 mg, 2.5 mmol, 1.0 equiv.), *N*-chlorosuccinimide (334 mg, 2.5 mmol, 1.0 equiv.), Et₃N (0.35 mL, 2.5 mmol, 1.0 equiv.) and diethyl allylmalonate (0.99 mL, 5.0 mmol, 2.0 equiv.). Purification by flash column chromatography (5–40% EtOAc/hexanes) afforded the pure title compound as a colorless oil (571 mg, 72%).

¹H NMR (700 MHz, CDCl₃): δ 4.90 – 4.83 (m, 1H), 4.35 (qd, *J* = 7.1, 1.4 Hz, 2H), 4.28 – 4.17 (m, 4H), 3.63 (dd, *J* = 8.8, 5.8 Hz, 1H), 3.33 (dd, *J* = 17.6, 10.9 Hz, 1H), 2.89 (dd, *J* = 17.6, 7.4 Hz, 1H), 2.28 – 2.18 (m, 2H), 1.36 (t, *J* = 7.1 Hz, 3H), 1.28 (dt, *J* = 10.3, 7.1 Hz, 6H); **¹³C NMR**

(176 MHz, CDCl₃): δ 168.9, 168.8, 160.6, 151.6, 81.1, 62.3, 61.9 (2C), 48.4, 39.2, 34.3, 14.23, 14.15, 14.1; **IR** (cm⁻¹): 2983, 1721, 1590, 1446, 1370, 1239, 1175, 1149, 1018, 924, 859, 793, 748; **HRMS**: *m/z* calculated for C₁₄H₂₁NNaO₇⁺ [M+Na]⁺: 338.1210; found: 338.1214.

Procedure for Gram-Scale Synthesis of 3.83

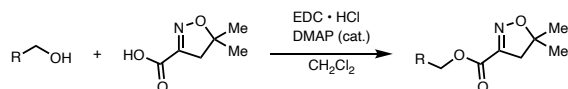


To a 250-mL round-bottom flask equipped with a magnetic stir bar containing ethyl 2-(hydroxyimino)acetate²²¹ (10.00 g, 85.4 mmol, 1.0 equiv.) and DMF (100 mL) was added *N*-chlorosuccinimide, and the resulting mixture heated at 60 °C for 3.5 h. After cooling to rt, the reaction mixture was diluted with water (300 mL) and extracted with Et₂O (3x 200 mL). The combined organic extracts were washed with water (200 mL) and brine (200 mL), then dried over MgSO₄, filtered and concentrated *in vacuo* to afford ethyl 2-chloro-2-(hydroxyimino)acetate as a white solid, which was used for the next step without further purification.

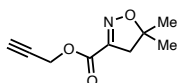
Next, a 1-L three-neck round-bottom flask was equipped with a magnetic stir bar, nitrogen gas inlet and a condenser, which was cooled to -78 °C and connected to a lecture bottle containing 2-methylpropene. The three-neck flask was cooled to approximately -20 °C and 2-methylpropene gas (56 g, 998 mmol, 11.7 equiv.) was condensed into the flask. Ethyl 2-chloro-2-(hydroxyimino)acetate was added as a solution in CH₂Cl₂ (300 mL) and the resulting mixture warmed up to 0 °C with an ice bath. The ice bath was removed and Et₃N (12.0 mL, 85.4 mmol, 1.0 equiv.) was subsequently added dropwise using a syringe pump over 6 h. After stirring for 10 h at rt, water (100 mL) was added, the organic layer separated and the aqueous layer extracted with CH₂Cl₂ (2x 50 mL). The combined organic layers were washed with brine (100 mL), dried over Na₂SO₄, filtered and concentrated *in vacuo*. Purification by flash column chromatography (0–10% EtOAc/hexanes) afforded the pure title compound as a colorless, low-melting solid (9.89 g, 68%). Spectroscopic data were consistent with those reported in the literature.¹⁹⁰

¹H NMR (400 MHz, CDCl₃): δ 4.34 (q, *J* = 7.1 Hz, 2H), 2.96 (s, 2H), 1.46 (s, 6H), 1.37 (t, *J* = 7.1 Hz, 3H).

General Procedure for Synthesis of 2-Isoxazolines via Steglich Esterification (GP-3.2)

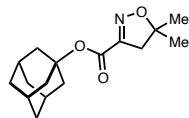


To a round-bottom flask equipped with a magnetic stir bar containing **3.97** (1.0 equiv.) and CH₂Cl₂ (0.1 M) were added the corresponding alcohol (1.0–2.0 equiv.) EDC·HCl (1.2 equiv.) and DMAP (0.2 equiv.). The resulting reaction mixture was stirred at rt until complete as judged by TLC analysis (6–24 h). Then, 1 M HCl solution (aq.) was added, the organic layer separated, and the aqueous layer extracted with CH₂Cl₂ (3x). The combined organic layers were washed with brine, dried over Na₂SO₄, filtered and concentrated *in vacuo*. The crude product was purified by flash column chromatography to afford the pure title compound.



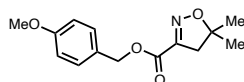
Prop-2-yn-1-yl 5,5-dimethyl-4,5-dihydroisoxazole-3-carboxylate (S3.91): Prepared according to GP-3.2 using **3.97** (150 mg, 1.1 mmol, 1.0 equiv.), propargyl alcohol (0.12 mL, 2.1 mmol, 2.0 equiv.), EDC·HCl (241 mg, 1.3 mmol, 1.2 equiv.) and DMAP (26 mg, 0.2 mmol, 0.2 equiv.) with a reaction time of 6 h. Purification by flash column chromatography (5–30% EtOAc/hexanes) afforded the pure title compound as a colorless oil (167 mg, 88%)

¹H NMR (700 MHz, CDCl₃): δ 4.87 (d, *J* = 2.5 Hz, 2H), 2.98 (s, 2H), 2.52 (t, *J* = 2.5 Hz, 1H), 1.47 (s, 6H); **¹³C NMR** (176 MHz, CDCl₃): δ 160.4, 150.4, 89.1, 76.9, 75.9, 53.1, 45.1, 27.3; **IR** (cm⁻¹): 3279, 2977, 2362, 2337, 1723, 1581, 1437, 1380, 1338, 1285, 1230, 1118, 942, 742, 668; **HRMS**: *m/z* calculated for C₉H₁₂NO₃⁺ [M+H]⁺: 182.0812; found: 182.0809.



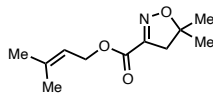
Adamantan-1-yl 5,5-dimethyl-4,5-dihydroisoxazole-3-carboxylate (S3.92): Prepared according to GP-3.2 using **3.97** (150 mg, 1.1 mmol, 1.0 equiv.), 1-adamantanol (191 mg, 1.3 mmol, 1.2 equiv.), EDC • HCl (241 mg, 1.3 mmol, 1.2 equiv.) and DMAP (26 mg, 0.2 mmol, 0.2 equiv.) with a reaction time of 24 h. Purification by flash column chromatography (1–10% EtOAc/hexanes) afforded the pure title compound as a white solid (143 mg, 49%).

¹H NMR (700 MHz, CDCl₃): δ 2.92 (s, 2H), 2.20 (s, 9H), 1.73 – 1.64 (m, 6H), 1.44 (s, 6H); **¹³C NMR** (176 MHz, CDCl₃): δ 160.0, 152.4, 88.2, 83.4, 45.6, 41.4, 36.2, 31.1, 27.4; **IR** (cm⁻¹): 2912, 2856, 2362, 2337, 1724, 1577, 1457, 1344, 1279, 1235, 1054, 954, 741; **HRMS**: *m/z* calculated for C₁₆H₂₃NNaO₃⁺ [M+Na]⁺: 300.1570; found: 300.1571.



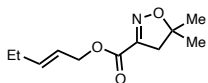
4-Methoxybenzyl 5,5-dimethyl-4,5-dihydroisoxazole-3-carboxylate (S3.93): Prepared according to GP-3.2 using **3.97** (100 mg, 0.7 mmol, 1.0 equiv.), 4-methoxybenzyl alcohol (97 mg, 0.7 mmol, 1.0 equiv.), EDC • HCl (148 mg, 0.8 mmol, 1.1 equiv.) and DMAP (17 mg, 0.1 mmol, 0.2 equiv.) with a reaction time of 24 h. Purification by flash column chromatography (5–30% EtOAc/hexanes) afforded the pure title compound as a colorless oil (135 mg, 73%).

¹H NMR (700 MHz, CDCl₃): δ 7.36 (d, *J* = 8.6 Hz, 2H), 6.89 (d, *J* = 8.7 Hz, 2H), 5.24 (s, 2H), 3.81 (s, 3H), 2.95 (s, 2H), 1.44 (s, 6H); **¹³C NMR** (176 MHz, CDCl₃): δ 161.0, 159.9, 151.0, 130.6, 127.2, 114.0, 88.6, 67.3, 55.3, 45.2, 27.3; **IR** (cm⁻¹): 2959, 2836, 2361, 2338, 1712, 1513, 1298, 1234, 1179, 1121, 1092, 1033, 925, 851, 832, 768, 759; **HRMS**: *m/z* calculated for C₁₄H₁₇NO₄⁺ [M]⁺: 263.1152; found: 263.1158.



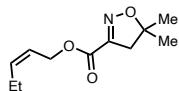
3-Methylbut-2-en-1-yl 5,5-dimethyl-4,5-dihydroisoxazole-3-carboxylate (3.94): Prepared according to GP-3.2 using **3.97** (143 mg, 1.0 mmol, 1.0 equiv.), 3-methyl-2-buten-1-ol (0.20 mL, 2.0 mmol, 2.0 equiv.), EDC • HCl (230 mg, 1.2 mmol, 1.2 equiv.) and DMAP (24 mg, 0.2 mmol, 0.2 equiv.) with a reaction time of 6 h. Purification by flash column chromatography (2–15% EtOAc/hexanes) afforded the pure title compound as a colorless oil (198 mg, 94%).

¹H NMR (700 MHz, CDCl₃): δ 5.39 (t, *J* = 7.3 Hz, 1H), 4.75 (d, *J* = 7.4 Hz, 2H), 2.94 (d, *J* = 1.0 Hz, 2H), 1.74 (d, *J* = 16.9 Hz, 6H), 1.44 (s, 6H); **¹³C NMR** (176 MHz, CDCl₃): δ 161.2, 151.2, 140.3, 117.9, 88.5, 62.8, 45.3, 27.3, 25.9, 18.2; **IR** (cm⁻¹): 2975, 2934, 1713, 1583, 1440, 1400, 1286, 1231, 1123, 940, 731; **HRMS**: *m/z* calculated for C₁₁H₁₇NNaO₃⁺ [M+Na]⁺: 234.1101; found: 234.1101.



(E)-Pent-2-en-1-yl 5,5-dimethyl-4,5-dihydroisoxazole-3-carboxylate ((E)-3.155): Prepared according to GP-3.2 using **3.97** (143 mg, 1.0 mmol, 1.0 equiv.), *trans*-2-penten-1-ol (0.20 mL, 2.0 mmol, 2.0 equiv.), EDC • HCl (230 mg, 1.2 mmol, 1.2 equiv.) and DMAP (24 mg, 0.2 mmol, 0.2 equiv.) with a reaction time of 18 h. Purification by flash column chromatography (2–15% EtOAc/hexanes) afforded the pure title compound as a colorless oil (184 mg, 87%).

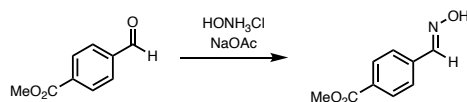
¹H NMR (400 MHz, CDCl₃): δ 5.94 – 5.85 (m, 1H), 5.67 – 5.56 (m, 1H), 4.71 (d, *J* = 6.6 Hz, 2H), 2.96 (s, 2H), 2.08 (p, *J* = 7.1 Hz, 2H), 1.46 (s, 6H), 1.00 (t, *J* = 7.5 Hz, 3H); **¹³C NMR** (176 MHz, CDCl₃): δ 161.0, 151.1, 139.5, 122.0, 88.6, 66.7, 45.3, 27.3, 25.4, 13.1; **IR** (cm⁻¹): 2969, 2935, 1714, 1583, 1440, 1372, 1285, 1231, 1121, 938, 765, 745; **HRMS**: *m/z* calculated for C₁₁H₁₇NNaO₃⁺ [M+Na]⁺: 234.1101; found: 234.1100.



(Z)-Pent-2-en-1-yl 5,5-dimethyl-4,5-dihydroisoxazole-3-carboxylate ((Z)-3.155): Prepared according to GP-3.2 using **3.97** (143 mg, 1.0 mmol, 1.0 equiv.), *cis*-2-penten-1-ol (0.20 mL, 2.0 mmol, 2.0 equiv.), EDC • HCl (230 mg, 1.2 mmol, 1.2 equiv.) and DMAP (24 mg, 0.2 mmol, 0.2 equiv.) with a reaction time of 18 h. Purification by flash column chromatography (2–15% EtOAc/hexanes) afforded the pure title compound as a colorless oil (195 mg, 92%).

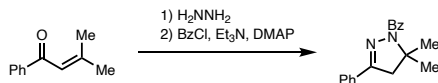
¹H NMR (400 MHz, CDCl₃): δ 5.74 – 5.65 (m, 1H), 5.61 – 5.52 (m, 1H), 4.82 (d, *J* = 6.9 Hz, 2H), 2.96 (s, 2H), 2.15 (p, *J* = 7.3 Hz, 2H), 1.46 (s, 6H), 1.00 (t, *J* = 7.5 Hz, 3H); **¹³C NMR** (176 MHz, CDCl₃): δ 161.1, 151.0, 138.0, 121.9, 88.6, 61.6, 45.3, 27.3, 21.0, 14.1; **IR** (cm⁻¹): 2971, 2876, 1715, 1583, 1390, 1371, 1336, 1286, 1230, 1120, 939, 765, 745; **HRMS**: *m/z* calculated for C₁₁H₁₇NNaO₃⁺ [M+Na]⁺: 234.1101; found: 234.1103.

Miscellaneous Procedures



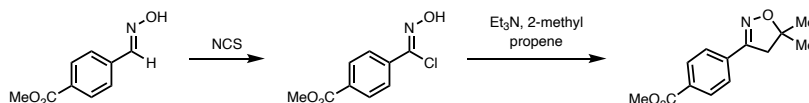
Methyl (*E*)-4-((hydroxyimino)methyl)benzoate (A3.1): A 50-mL round-bottom flask equipped with a magnetic stir bar was charged with methyl 4-formylbenzoate (1.00 g, 6.1 mmol, 1.0 equiv.) and MeOH (20 mL). Sodium acetate (1.50 g, 18.3 mmol, 3.0 equiv.) and hydroxylamine hydrochloride (466 mg, 6.7 mmol, 1.1 equiv.) were added sequentially and the resulting mixture stirred at rt for 18 h. NaHCO₃ solution (aq., sat.) was added and the organic solvent removed *in vacuo*. The residue was diluted with water and extracted with EtOAc (3x). The combined organic extracts were dried over Na₂SO₄, filtered and concentrated *in vacuo*, then dried using high-vac to afford the pure title compound as a white solid. Spectroscopic data were consistent with those reported in the literature.²²³

¹H NMR (400 MHz, CDCl₃): δ 8.17 (s, 1H), 8.05 (d, *J* = 8.0 Hz, 2H), 7.65 (d, *J* = 8.1 Hz, 2H), 7.51 (s, 1H), 3.93 (d, *J* = 2.1 Hz, 3H).



(5,5-Dimethyl-3-phenyl-4,5-dihydro-1*H*-pyrazol-1-yl)(phenyl)methanone (3.82): A 25-mL round-bottom flask was charged with 3-methyl-1-phenylbut-2-en-1-one²²⁴ (500 mg, 3.1 mmol, 1.0 equiv.) and EtOH (12 mL). Hydrazine hydrate (1.4 mL, 15.6 mmol, 5.0 equiv.) was added and the resulting reaction mixture heated at 70 °C for 6 h. After cooling to rt, the solvent was removed *in vacuo* and the resulting residue taken up in EtOAc. The organic layer was washed with NH₄Cl solution (aq., sat.) and brine, dried over Na₂SO₄, filtered and concentrated *in vacuo* to afford 5,5-dimethyl-3-phenyl-4,5-dihydro-1*H*-pyrazole.

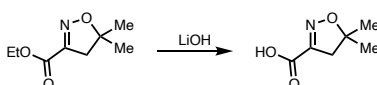
The crude compound was dissolved in CH₂Cl₂ (15 mL), and benzoyl chloride (0.54 mL, 4.7 mmol, 1.5 equiv.), Et₃N (0.65 mL, 4.7 mmol, 1.5 equiv.) and DMAP (76 mg, 0.6 mmol, 0.2 equiv.) were sequentially added. After stirring the reaction mixture for 18 h at rt, the mixture was diluted with CH₂Cl₂ and washed with 1 M HCl solution (aq.) and brine, dried over Na₂SO₄, filtered and concentrated *in vacuo*. Purification by flash column chromatography (2–20% EtOAc/hexanes) afforded the pure title compound as an off-white solid (235 mg, 27%). Spectroscopic data were found consistent with those reported in the literature.²²⁵



Methyl 4-(5,5-dimethyl-4,5-dihydroisoxazol-3-yl)benzoate (3.79): To a 25-mL round-bottom flask equipped with a magnetic stir bar containing **A3.1** (544 mg, 3.0 mmol, 1.0 equiv.) and DMF (10 mL) was added *N*-chlorosuccinimide (405 mg, 3.0 mmol, 1.0 equiv.). After heating for 2 h at 60 °C, the reaction mixture was poured onto ice water. The white precipitate was collected by

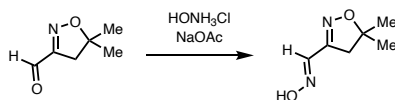
filtration to afford methyl (*Z*)-4-(chloro(hydroxyimino)methyl)benzoate, which was subsequently transferred to a 100-mL round-bottom flask and dissolved in CH₂Cl₂ (30 mL). The flask was sealed with a rubber septum and the solution sparged with 2-methylpropene for 20 min. Next, Et₃N (0.47 mL, 3.3 mmol, 1.1 equiv.) was added dropwise over 2 h using a syringe pump and the reaction stirred for additional 0.5 h at rt under an atmosphere of 2-methylpropene. The reaction mixture was diluted with CH₂Cl₂ and washed with 0.2 M HCl solution (aq.) and brine, dried over Na₂SO₄, filtered and concentrated *in vacuo*. Purification by flash column chromatography (5–30% EtOAc/hexanes) afforded the pure title compound as a white solid (448 mg, 63%).

¹H NMR (400 MHz, CDCl₃): δ 8.06 (d, *J* = 8.5 Hz, 2H), 7.71 (d, *J* = 8.5 Hz, 2H), 3.93 (s, 3H), 3.12 (s, 2H), 1.51 (s, 6H); **¹³C NMR** (126 MHz, CDCl₃): δ 166.7, 155.7, 134.7, 131.1, 130.0, 126.4, 85.9, 52.4, 46.6, 27.5; **IR** (cm⁻¹): 2972, 1709, 1609, 1588, 1436, 1370, 1274, 1101, 960, 904, 860, 770, 693; **HRMS**: *m/z* calculated for C₁₃H₁₆NO₃⁺ [M+H]⁺: 234.1125; found: 234.1125.



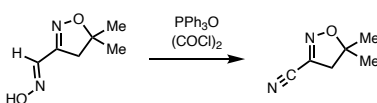
5,5-Dimethyl-4,5-dihydroisoxazole-3-carboxylic acid (3.97): To a 50-mL round-bottom flask equipped with a magnetic stir bar was added **3.83** (1.00 g, 5.8 mmol, 1.0 equiv.) and a 3:1 mixture of methanol/H₂O (20 mL). Lithium hydroxide monohydrate (270 mg, 6.4 mmol, 1.1 equiv.) was added and the reaction mixture stirred for 12 h at rt. Next, the solution was acidified with 1 M HCl solution (aq.) and subsequently extracted with CH₂Cl₂ (10x). The combined organic extracts were dried over Na₂SO₄, filtered and concentrated *in vacuo*, then dried using high-vac to afford the pure title compound as a white solid (773 mg, 92%).

¹H NMR (700 MHz, CDCl₃): δ 2.98 (s, 2H), 1.49 (s, 6H); **¹³C NMR** (176 MHz, CDCl₃): δ 164.2, 150.7, 90.2, 44.5, 27.4; **IR** (cm⁻¹): 3381, 2978, 1704, 1587, 1439, 1289, 1240, 1139, 1020, 949, 724; **HRMS**: *m/z* calculated for C₆H₁₀NO₃⁺ [M+H]⁺: 144.0655; found: 144.0655.



5,5-Dimethyl-4,5-dihydroisoxazole-3-carbaldehyde oxime (A3.2): A 25-mL round-bottom flask equipped with a magnetic stir bar was charged with 5,5-dimethyl-4,5-dihydroisoxazole-3-carbaldehyde²²⁵ (160 mg, 1.3 mmol, 1.0 equiv.). MeOH (10 mL) was added, followed by sequential addition of hydroxylamine hydrochloride (175 mg, 2.5 mmol, 2.0 equiv.) and sodium acetate (413 mg, 5.0 mmol, 4.0 equiv.). After stirring for 16 h at rt, the reaction mixture was concentrated *in vacuo*. The residue was diluted with NaHCO₃ solution (aq., sat.) and extracted with EtOAc (3x). The combined organic extracts were washed with brine, dried over Na₂SO₄, filtered and concentrated *in vacuo*, then dried using high-vac to afford the pure title compound as a white solid (123 mg, 69%; 4:1 mixture of oxime isomers).

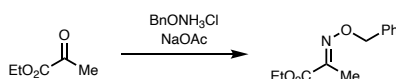
¹H NMR (500 MHz, CDCl₃): δ 8.48 (s, 1H; minor), 8.07 (s, 4H; major), 8.04 (s, 4H; major), 7.40 (s, 1H; minor), 3.25 (s, 2H; minor), 2.91 (s, 8H; major), 1.44 (d, *J* = 1.7 Hz, 30H; major+minor); **¹³C NMR** (126 MHz, CDCl₃): δ 154.0, 143.8 (2C), 139.6, 87.1, 86.5, 48.5, 44.5, 27.2, 27.1; **IR** (cm⁻¹): 3245, 3179, 3089, 2999, 2982, 2937, 2859, 1467, 1432, 1369, 1292, 1154, 907, 855, 760, 730; **HRMS**: *m/z* calculated for C₆H₁₁N₂O₂⁺ [M+H]⁺: 143.0815; found: 143.0815.



5,5-Dimethyl-4,5-dihydroisoxazole-3-carbonitrile (S3.96): Adapted from a literature procedure with minor modifications.²²⁶ To a 10-mL round-bottom flask equipped with a magnetic stir bar containing a solution of triphenylphosphine (22 mg, 0.08 mmol, 0.1 equiv.) in EtOAc (2 mL) was added oxalyl chloride (0.1 mL, 1.2 mmol, 1.5 equiv.) dropwise. After stirring for 5 min at rt, a solution of **A3.2** (110 mg, 0.8 mmol, 1.0 equiv.) in EtOAc (1 mL) was added dropwise over 0.5 h. The reaction mixture was stirred for 1 h at rt, after which it was concentrated *in vacuo*. The crude

mixture was purified by flash column chromatography (10–20% Et₂O/pentane) to afford the pure title compound as a colorless oil (77 mg, 80%).

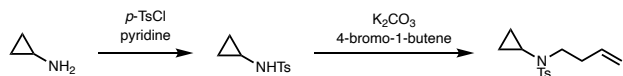
¹H NMR (500 MHz, CDCl₃): δ 2.93 (s, 2H), 1.49 (s, 6H); **¹³C NMR** (126 MHz, CDCl₃): δ 133.9, 111.6, 89.6, 46.9, 27.1; **IR** (cm⁻¹): 2982, 2236, 1555, 1462, 1374, 1324, 1263, 1150, 964, 827, 782, 663; **HRMS**: *m/z* calculated for C₆H₈N₂O⁺ [M]⁺: 124.0637; found: 124.0642.



Ethyl 2-((benzyloxy)imino)propanoate ((E)-3.154): To a 25-mL round-bottom flask equipped with a magnetic stir bar was added ethyl pyruvate (0.20 mL, 1.8 mmol, 1.0 equiv.) and EtOH (10 mL). After sequential addition of sodium acetate (591 mg, 7.2 mmol, 4.0 equiv.) and *O*-benzylhydroxylamine hydrochloride (575 mg, 3.6 mmol, 2.0 equiv.), the reaction was stirred for 14 h at rt. Next, NaHCO₃ solution (aq., sat.) was added and the organic solvent removed *in vacuo*. Water was added to the remaining residue and the mixture extracted with EtOAc (3x). The combined organic extracts were washed with brine, dried over Na₂SO₄, filtered and concentrated *in vacuo*. Purification by flash column chromatography (2–10% EtOAc/hexanes) afforded the pure title compound as a colorless oil (338 mg, 85%; 20:1 mixture of oxime isomers).

¹H NMR (500 MHz, CDCl₃): δ 7.40 – 7.31 (m, 5H), 5.31 (s, 2H), 4.32 (q, *J* = 7.1 Hz, 2H), 2.09 (s, 3H), 1.35 (t, *J* = 7.1 Hz, 3H); **¹³C NMR** (126 MHz, CDCl₃): δ 163.9, 149.6, 136.8, 128.6, 128.4, 128.3, 77.7, 61.9, 14.3, 11.8; **IR** (cm⁻¹): 2982, 1715, 1613, 1497, 1454, 1366, 1317, 1148, 1009, 955, 923, 855, 754, 715, 696; **HRMS**: *m/z* calculated for C₁₂H₁₅NNaO₃⁺ [M+Na]⁺: 244.0944; found: 244.0946.

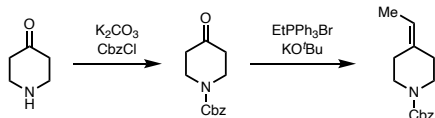
Synthesis of Alkene Starting Materials



***N*-(But-3-en-1-yl)-*N*-cyclopropyl-4-methylbenzenesulfonamide (S3.109):** A 10-mL round-bottom flask equipped with a magnetic stir bar was charged with cyclopropylamine (0.21 mL, 3.0 mmol, 1.0 equiv.) and water (3 mL). Pyridine (0.29 mL, 3.6 mmol, 1.2 equiv.) and 4-toluenesulfonyl chloride (636 mg, 3.3 mmol, 1.1 equiv.) were added sequentially and the reaction stirred for 1 h at rt. The resulting precipitate was collected by filtration and washed with water to afford *N*-cyclopropyl-4-methylbenzenesulfonamide as an orange solid.

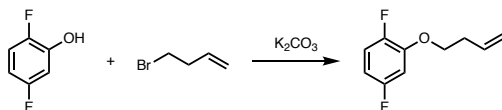
The compound was dissolved in DMF (10 mL) followed by the addition of K_2CO_3 (1.26 g, 9.1 mmol, 3.0 equiv.) and 4-bromo-1-butene (0.46 mL, 4.6 mmol, 1.5 equiv.). After stirring the reaction for 6 h at 80 °C, the mixture was allowed to cool down to rt and diluted with water. After extracting with EtOAc (3x) the combined organic extracts were washed with water (2x) and brine, dried over Na_2SO_4 , filtered and concentrated *in vacuo*. Purification by flash column chromatography (2–20% EtOAc/hexanes) afforded the product as a colorless oil (150 mg, 19%).

1H NMR (700 MHz, $CDCl_3$): δ 7.74 (d, $J = 8.2$ Hz, 2H), 7.31 (d, $J = 8.0$ Hz, 2H), 5.74 (ddt, $J = 17.1, 10.2, 6.8$ Hz, 1H), 5.07 – 5.01 (m, 2H), 3.26 – 3.22 (m, 2H), 2.43 (s, 3H), 2.35 (q, $J = 7.0$ Hz, 2H), 2.04 (h, $J = 6.9, 3.7$ Hz, 1H), 0.87 – 0.83 (m, 2H), 0.71 – 0.67 (m, 2H); **^{13}C NMR** (176 MHz, $CDCl_3$): δ 143.4, 135.8, 135.2, 129.6, 127.7, 116.9, 50.7, 33.1, 30.5, 21.6, 7.5; **IR** (cm^{-1}): 2924, 2361, 2338, 1457, 1341, 1160, 1090, 1028, 992, 916, 862, 814, 711, 691, 654; **HRMS**: m/z calculated for $C_{14}H_{19}NNaO_2S^+$ [$M+Na$] $^+$: 288.1029; found: 288.1024.



Benzyl 4-ethylidenepiperidine-1-carboxylate (S3.123): Benzyl 4-oxopiperidine-1-carboxylate was synthesized from piperidine-4-one hydrochloride (400 mg, 2.6 mmol, 1.0 equiv.) according to a literature procedure²²⁷ and used for the next step without further purification. To a 25-mL round-bottom flask equipped with a magnetic stir bar containing a suspension of ethyltriphenylphosphonium bromide (1.45 g, 3.9 mmol, 1.5 equiv.) in Et₂O (10 mL) was added KO^t-Bu (438 mg, 3.9 mmol, 1.5 equiv.) at 0 °C. After stirring the mixture for 0.5 h, a solution of crude benzyl 4-oxopiperidine-1-carboxylate in Et₂O (2 mL) was slowly added and the reaction allowed to warm up to rt. After stirring for 2.5 h at rt, NH₄Cl solution (aq., sat.) and water were added, the organic layer separated, and the aqueous layer extracted with Et₂O (3x). The combined organic extracts were washed with brine, dried over MgSO₄, filtered and concentrated *in vacuo*. Purification by flash column chromatography (1–10% EtOAc/hexanes) afforded the pure title compound as a colorless oil (455 mg, 71%).

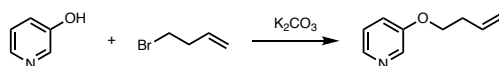
¹H NMR (700 MHz, CDCl₃): δ 7.39 – 7.29 (m, 5H), 5.29 (q, *J* = 6.5 Hz, 1H), 5.14 (s, 2H), 3.49 – 3.45 (m, 4H), 2.19 (d, *J* = 56.5 Hz, 4H), 1.60 (d, *J* = 6.7 Hz, 3H); ¹³C NMR (176 MHz, CDCl₃): δ 155.4, 137.1, 135.1, 128.6, 128.1, 128.0, 118.4, 67.2, 45.9, 44.9, 35.8, 27.9, 12.8; IR (cm⁻¹): 2861, 2362, 2337, 1695, 1425, 1363, 1014, 963, 824, 734, 696 ; HRMS: *m/z* calculated for C₁₅H₁₉NNaO₂⁺ [M+Na]⁺: 268.1308; found: 268;1308.



2-(But-3-en-1-yloxy)-1,4-difluorobenzene (S3.113): A 25-mL round-bottom flask equipped with a magnetic stir bar was charged with 2,5-difluorophenol (325 mg, 2.5 mmol, 1.0 equiv.) and DMF (5 mL). K₂CO₃ (1.04 g, 7.5 mmol, 3.0 equiv.) and 4-bromo-1-butene (0.38 mL, 3.8 mmol,

1.5 equiv.) were added and the resulting heterogeneous mixture stirred for 20 h at 80 °C. After cooling to rt, the mixture was diluted with water and extracted with EtOAc (3x). The combined organic extracts were washed with water (2x) and brine, dried over Na₂SO₄, filtered and concentrated *in vacuo*. Purification by flash column chromatography (1–5% EtOAc/hexanes) afforded the pure title compound as a colorless, volatile oil (173 mg, 38%).

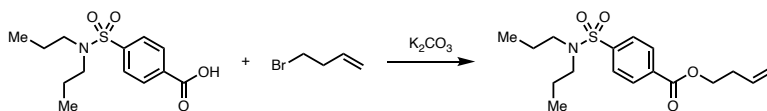
¹H NMR (500 MHz, CDCl₃): δ 7.05 – 6.96 (m, 1H), 6.73 – 6.65 (m, 1H), 6.61 – 6.53 (m, 1H), 5.90 (ddt, *J* = 17.1, 10.3, 6.7 Hz, 1H), 5.22 – 5.10 (m, 2H), 4.05 (t, *J* = 6.8 Hz, 2H), 2.58 (q, *J* = 6.7 Hz, 2H); **¹³C NMR** (176 MHz, CDCl₃): δ 158.9 (dd, *J* = 241.8, 2.5 Hz), 149.1 (dd, *J* = 241.1, 3.3 Hz), 147.7 (dd, *J* = 12.5, 10.5 Hz), 133.9, 117.7, 116.3 (dd, *J* = 20.7, 10.2 Hz), 106.7 (dd, *J* = 23.8, 6.9 Hz), 102.9 (dd, *J* = 27.4, 2.0 Hz), 68.9, 33.5; **IR** (cm⁻¹): 2934, 1626, 1510, 1472, 1432, 1387, 1323, 1286, 1248, 1204, 1157, 1099, 1025, 990, 918, 834, 791, 726; **HRMS**: *m/z* calculated for C₁₀H₁₀F₂O⁺ [M]⁺: 184.0694; found: 184.0697.



3-(But-3-en-1-yloxy)pyridine (S3.110): A 25-mL round-bottom flask equipped with a magnetic stir bar was charged with 3-hydroxypyridine (238 mg, 2.5 mmol, 1.0 equiv.) and DMF (5 mL). K₂CO₃ (1.04 g, 7.5 mmol, 3.0 equiv.) and 4-bromo-1-butene (0.38 mL, 3.8 mmol, 1.5 equiv.) were added and the resulting heterogeneous mixture stirred for 20 h at 80 °C. After cooling to rt, the mixture was diluted with water and extracted with EtOAc (3x). The combined organic extracts were washed with water (2x) and brine, dried over Na₂SO₄, filtered and concentrated *in vacuo*. Purification by flash column chromatography (10–40% EtOAc/hexanes) afforded the pure title compound as an orange, volatile oil (70 mg, 19%).

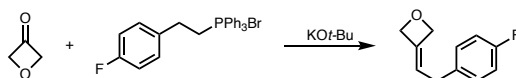
¹H NMR (500 MHz, CDCl₃): δ 8.32 (dd, *J* = 2.7, 1.1 Hz, 1H), 8.21 (dd, *J* = 4.3, 1.8 Hz, 1H), 7.24 – 7.15 (m, 2H), 5.96 – 5.84 (m, 1H), 5.18 (dt, *J* = 17.1, 1.7 Hz, 1H), 5.13 (dt, *J* = 10.3, 1.5 Hz,

1H), 4.06 (t, $J = 6.7$ Hz, 2H), 2.59 – 2.53 (m, 2H); ^{13}C NMR (176 MHz, CDCl_3): δ 155.2, 142.2, 138.2, 134.1, 123.9, 121.3, 117.5, 67.6, 33.6; IR (cm^{-1}): 2925, 1643, 1586, 1426, 1387, 1231, 1050, 1023, 991, 920, 798, 707; HRMS: m/z calculated for $\text{C}_9\text{H}_{12}\text{NO}^+$ $[\text{M}+\text{H}]^+$: 150.0913; found: 150.0908.



But-3-en-1-yl 4-(*N,N*-dipropylsulfamoyl)benzoate (S3.111): A 25-mL round-bottom flask equipped with a magnetic stir bar was charged with probenecid (713 mg, 2.5 mmol, 1.0 equiv.) and DMF (5 mL). K_2CO_3 (1.04 g, 7.5 mmol, 3.0 equiv.) and 4-bromo-1-butene (0.38 mL, 3.8 mmol, 1.5 equiv.) were added and the resulting heterogeneous mixture stirred for 2 h at 80 °C. After cooling to rt, the mixture was diluted with water and extracted with EtOAc (3x). The combined organic extracts were washed with water (2x) and brine, dried over Na_2SO_4 , filtered and concentrated *in vacuo*. Purification by flash column chromatography (2–10% EtOAc/hexanes) afforded the pure title compound as colorless oil (0.85 g, quant.).

^1H NMR (400 MHz, CDCl_3): δ 8.14 (d, $J = 8.3$ Hz, 2H), 7.87 (d, $J = 8.3$ Hz, 2H), 5.86 (ddt, $J = 17.0, 10.3, 6.8$ Hz, 1H), 5.15 (dd, $J = 22.6, 13.7$ Hz, 2H), 4.41 (t, $J = 6.6$ Hz, 2H), 3.12 – 3.06 (m, 4H), 2.54 (q, $J = 6.6$ Hz, 2H), 1.54 (dq, $J = 14.9, 7.3$ Hz, 4H), 0.86 (t, $J = 7.4$ Hz, 6H); ^{13}C NMR (176 MHz, CDCl_3): δ 165.3, 144.3, 133.9, 133.7, 130.3, 127.1, 117.7, 64.8, 50.0, 33.2, 22.1, 11.3; IR (cm^{-1}): 2966, 2876, 1721, 1478, 1342, 1269, 1157, 1105, 1087, 990, 916, 862, 778, 738, 693; HRMS: m/z calculated for $\text{C}_{17}\text{H}_{26}\text{NO}_4\text{S}^+$ $[\text{M}+\text{H}]^+$: 340.1577; found: 340.1581.

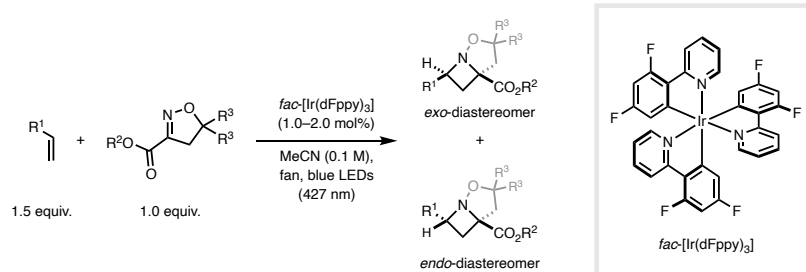


3-(2-(4-Fluorophenyl)ethylidene)oxetane (S3.124): To a 100-mL round bottom flask equipped with a magnetic stir bar containing a suspension of bromo(4-fluorophenethyl)triphenyl- l^5 -

phosphane²²² (5.88 g, 12.6 mmol, 1.5 equiv.) in Et₂O (40 mL) was added KO^t-Bu (1.42 g, 12.6 mmol, 1.5 equiv.) at 0 °C and the reaction mixture stirred for 0.5 h at that temperature. Oxetan-3-one (0.54 mL, 8.4 mmol, 1.0 equiv.) was added dropwise and the resulting mixture allowed to warm up to rt and stirred for 16 h. NH₄Cl solution (aq., sat.) and water were added, the organic layer separated and the aqueous layer extracted with Et₂O (3x). The combined organic extracts were washed with brine, dried over MgSO₄, filtered and concentrated *in vacuo*. Purification by flash column chromatography (5–20% Et₂O/pentane) afforded the pure title compound as a pale-yellow oil (688 mg, 46%).

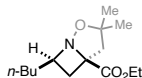
¹H NMR (400 MHz, CDCl₃): δ 7.16 – 7.10 (m, 2H), 7.01 – 6.94 (m, 2H), 5.35 – 5.25 (m, 1H), 5.25 – 5.17 (m, 2H), 5.18 – 5.12 (m, 2H), 3.18 (d, *J* = 7.1 Hz, 2H); **¹³C NMR** (126 MHz, CDCl₃): δ 161.6 (d, *J* = 243.9 Hz), 135.7, 135.4 (d, *J* = 3.4 Hz), 129.9 (d, *J* = 7.7 Hz), 118.1, 115.4 (d, *J* = 21.1 Hz), 79.5, 78.8, 33.8; **IR** (cm⁻¹): 2862, 1689, 1600, 1508, 1219, 1157, 1094, 1015, 946, 852, 822, 742; **HRMS**: *m/z* calculated for C₁₁H₁₁FO⁺ [M]⁺: 178.0794; found: 178.0799.

General Procedure for Photochemical [2+2] Cycloaddition (GP-3.3)



A 3-dram vial equipped with a magnetic stir bar was charged with 2-isoxazoline (0.25 mmol, 1.0 equiv.), alkene (if solid, 1.5 equiv.), $fac-[Ir(dFppy)_3]$ (0.2–2 mol%) and MeCN (2.5 mL). The vial was sealed with a septum-equipped cap and the reaction mixture degassed by sparging with nitrogen gas for 10 min. Then, alkene (if liquid, 1.5 equiv.) was added, the vial sealed with electrical tape and the reaction mixture homogenized by sonicating for approximately 30 seconds. Then, the reaction mixture was stirred at ambient temperature (fan cooling) under irradiation with blue LED lights (427 nm). After the indicated time (12–42 h), the reaction mixture was concentrated *in vacuo* and the crude reaction mixture analyzed by 1H NMR to determine the diastereomer (d.r.) and regioisomer (r.r.) ratio, before purification by flash column chromatography to afford the corresponding pure azetidine product (major diastereomer is drawn).

Note: For **3.105**, **3.115**, **3.143** and **3.145** the alkene was added by sparging the solution with the corresponding gaseous alkene after sealing the vial, and the reaction carried out under an atmosphere of the alkene.

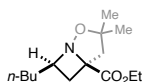


Ethyl 7-butyl-3,3-dimethyl-2-oxa-1-azabicyclo[3.2.0]heptane-5-carboxylate (3.84): Prepared according to GP-3.3 using **3.83** (43 mg, 0.25 mmol, 1.0 equiv.), 1-hexene (47 μ L, 0.38 mmol, 1.5 equiv.), *fac*-[Ir(dFppy)₃] (1.9 mg, 1 mol%) and MeCN (2.5 mL) with a reaction time of 19 h. ¹H NMR analysis of the crude reaction mixture revealed a diastereomer ratio of 3:1 and a regioisomer ratio of >20:1. Purification by flash column chromatography (5–40% EtOAc/hexanes) afforded the pure title compound as a pale-yellow oil (54 mg, 84% combined yield; d.r. = 3:1). Characterization data for both diastereomers was obtained after separation by flash column chromatography (5–40% EtOAc/hexanes).

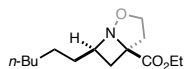
exo-Diastereomer (major): ¹H NMR (700 MHz, CDCl₃): δ 4.24 (q, J = 7.1 Hz, 2H), 3.46 (p, J = 8.4 Hz, 1H), 2.85 (d, J = 12.9 Hz, 1H), 2.47 (d, J = 12.9 Hz, 1H), 2.35 (dd, J = 11.1, 8.7 Hz, 1H), 1.98 (dd, J = 11.1, 8.5 Hz, 1H), 1.75 – 1.67 (m, 1H), 1.55 – 1.50 (m, 1H), 1.51 (s, 3H), 1.39 – 1.21 (m, 4H), 1.30 (t, J = 7.1 Hz, 3H), 1.20 (s, 3H), 0.88 (t, J = 7.2 Hz, 3H); ¹³C NMR (176 MHz, CDCl₃): δ 173.0, 87.2, 73.1, 67.4, 61.6, 51.1, 35.2, 30.4, 29.7, 28.5, 27.6, 22.8, 14.3, 14.2; IR (cm⁻¹): 2958, 2930, 2872, 1727, 1456, 1367, 1308, 1256, 1215, 1179, 1148, 1045, 864, 779, 733; HRMS: m/z calculated for C₁₄H₂₆NO₃⁺ [M+H]⁺: 256.1907; found: 256.1901.

endo-Diastereomer (minor): ¹H NMR (700 MHz, CDCl₃): δ 4.27 (qd, J = 7.1, 1.4 Hz, 2H), 3.88 (p, J = 7.8 Hz, 1H), 2.80 (dd, J = 11.6, 7.9 Hz, 1H), 2.72 (d, J = 12.4 Hz, 1H), 2.23 – 2.19 (m, 2H), 1.97 – 1.90 (m, 1H), 1.55 – 1.47 (m, 1H), 1.45 (s, 3H), 1.34 – 1.27 (m, 6H), 1.24 – 1.18 (m, 1H), 1.20 (s, 3H), 0.89 (t, J = 7.1 Hz, 3H); ¹³C NMR (176 MHz, CDCl₃): δ 173.1, 83.6, 72.7, 61.7, 60.6, 52.9, 36.8, 31.3, 28.1, 27.1, 26.0, 22.8, 14.3, 14.1; IR (cm⁻¹): 2955, 2930, 2872, 1729, 1457, 1367, 1301, 1254, 1184, 1152, 1020, 924, 863, 785, 730; HRMS: m/z calculated for C₁₄H₂₆NO₃⁺ [M+H]⁺: 256.1907; found: 256.1907.

Minor Regioisomer (2:1 mixture of diastereomers A/B): $^1\text{H NMR}$ (700 MHz, CDCl_3): δ 4.34 – 4.22 (m, 6H; A+B), 3.86 (dd, $J = 9.0, 7.7$ Hz, 2H; A), 3.54 – 3.47 (m, 2H; B), 3.01 (t, $J = 9.2$ Hz, 2H; A), 2.84 (d, $J = 12.8$ Hz, 1H; B), 2.63 (d, $J = 12.9$ Hz, 2H; A), 2.59 – 2.50 (m, 6H; A+B), 1.59 – 1.45 (m, 15H; A+B), 1.36 – 1.08 (m, 21H; A+B), 1.17 (s, 6H; A), 1.12 (s, 3H; B), 0.90 – 0.85 (m, 9H; A+B); $^{13}\text{C NMR}$ (176 MHz, CDCl_3): δ 173.3, 172.0, 86.2, 86.0, 80.0, 79.1, 62.7, 61.6, 61.4, 60.0, 52.5, 43.9, 39.2, 33.8, 30.6, 30.1, 29.4, 29.1, 29.0, 28.8, 28.4, 28.1, 22.7, 22.6, 14.5, 14.3, 14.10, 14.06; **IR** (cm^{-1}): 2959, 2928, 2859, 1724, 1466, 1368, 1302, 1254, 1183, 1143, 1046, 866, 779, 708; **HRMS**: m/z calculated for $\text{C}_{14}\text{H}_{26}\text{NO}_3^+$ $[\text{M}+\text{H}]^+$: 256.1907; found: 256.1901.



Ethyl 7-butyl-3,3-dimethyl-2-oxa-1-azabicyclo[3.2.0]heptane-5-carboxylate (3.84): Prepared according to GP-3.3 in a test tube (25x150 mm) using **3.83** (856 mg, 5.0 mmol, 1.0 equiv.), 1-hexene (0.93 mL, 7.5 mmol, 1.5 equiv.), *fac*- $[\text{Ir}(\text{dFppy})_3]$ (7.6 mg, 0.2 mol%) and MeCN (15 mL) with a reaction time of 24 h. $^1\text{H NMR}$ analysis of the crude reaction mixture revealed a diastereomer ratio of 3:1 and a regioisomer ratio of >20:1. Purification by flash column chromatography (1–10% EtOAc/ CH_2Cl_2) afforded the pure title compound as a pale-yellow oil (1.14 g, 90% combined yield; d.r. = 3:1). Spectroscopic data was found consistent with that obtained, when conducting the reaction on 0.25 mmol scale.

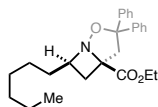


Ethyl 7-hexyl-2-oxa-1-azabicyclo[3.2.0]heptane-5-carboxylate (3.85): Prepared according to GP-3.3 using **S3.85** (36 mg, 0.25 mmol, 1.0 equiv.), 1-octene (59 μL , 0.38 mmol, 1.5 equiv.), *fac*- $[\text{Ir}(\text{dFppy})_3]$ (1.9 mg, 1 mol%) and MeCN (2.5 mL) with a reaction time of 18 h. $^1\text{H NMR}$ analysis of the crude reaction mixture revealed a diastereomer ratio of 1.3:1 and a regioisomer ratio of

>20:1. Purification by flash column chromatography (5–30% EtOAc/hexanes) afforded the pure *exo*-diastereomer as a pale-yellow oil (34 mg, 53%) and the *endo*-diastereomer as pale-yellow oil (27 mg, 42%).

***exo*-Diastereomer (major):** $^1\text{H NMR}$ (700 MHz, CDCl_3): δ 4.34 – 4.17 (m, 4H), 3.37 (p, $J = 8.4$ Hz, 1H), 2.59 (dt, $J = 12.6, 8.8$ Hz, 1H), 2.37 (ddd, $J = 12.7, 6.8, 3.0$ Hz, 1H), 2.27 (d, $J = 9.1$ Hz, 2H), 1.75 – 1.68 (m, 1H), 1.58 – 1.51 (m, 1H), 1.40 – 1.33 (m, 1H), 1.32 – 1.22 (m, 10H), 0.87 (t, $J = 7.0$ Hz, 3H); $^{13}\text{C NMR}$ (176 MHz, CDCl_3): δ 173.2, 71.6, 67.8, 61.7, 61.6, 39.1, 35.6, 31.9, 29.6, 29.2, 25.3, 22.7, 14.23, 14.16; **IR** (cm^{-1}): 2956, 2927, 2856, 1729, 1454, 1368, 1317, 1268, 1175, 1144, 1029, 907, 862, 725, 671; **HRMS**: m/z calculated for $\text{C}_{14}\text{H}_{26}\text{NO}_3^+$ $[\text{M}+\text{H}]^+$: 256.1907; found: 256.1904.

***endo*-Diastereomer (minor):** $^1\text{H NMR}$ (700 MHz, CDCl_3): δ 4.32 – 4.17 (m, 4H), 4.00 (p, $J = 8.4$ Hz, 1H), 2.94 (dd, $J = 12.1, 8.4$ Hz, 1H), 2.54 (ddd, $J = 12.3, 9.5, 7.5$ Hz, 1H), 2.26 (ddd, $J = 12.3, 5.9, 2.8$ Hz, 1H), 2.00 (dd, $J = 12.1, 8.9$ Hz, 1H), 1.88 – 1.82 (m, 1H), 1.45 – 1.39 (m, 12H), 0.87 (t, $J = 7.0$ Hz, 3H); $^{13}\text{C NMR}$ (176 MHz, CDCl_3): δ 172.8, 73.0, 71.1, 62.7, 61.8, 39.8, 34.3, 31.8, 30.0, 29.3, 26.0, 22.7, 14.24, 14.18; **IR** (cm^{-1}): 2926, 2857, 1729, 1445, 1369, 1320, 1271, 1176, 1140, 1096, 1025, 997, 917, 862, 720; **HRMS**: m/z calculated for $\text{C}_{14}\text{H}_{26}\text{NO}_3^+$ $[\text{M}+\text{H}]^+$: 256.1907; found: 256.1905.

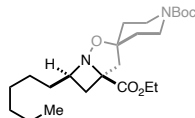


Ethyl 7-hexyl-3,3-diphenyl-2-oxa-1-azabicyclo[3.2.0]heptane-5-carboxylate (3.86): Prepared according to GP-3.3 using isoxadifen-ethyl (74 mg, 0.25 mmol, 1.0 equiv.), 1-octene (59 μL , 0.38 mmol, 1.5 equiv.), *fac*- $[\text{Ir}(\text{dFppy})_3]$ (3.8 mg, 2 mol%) and MeCN (2.5 mL) with a reaction time of 40 h. $^1\text{H NMR}$ analysis of the crude reaction mixture revealed a diastereomer ratio of 2:1

and a regioisomer ratio of 17:1. Purification by flash column chromatography (50–100% CH₂Cl₂/hexanes) afforded the pure title compound as a yellow oil (73 mg, 72% combined yield; d.r. = 2:1). Characterization data for both diastereomers was obtained after separation by flash column chromatography (5–40% EtOAc/hexanes).

exo-Diastereomer (major): ¹H NMR (700 MHz, CDCl₃): δ 7.44 (ddd, *J* = 15.3, 8.4, 1.3 Hz, 4H), 7.32 (t, *J* = 7.7 Hz, 2H), 7.27 – 7.22 (m, 3H), 7.18 – 7.13 (m, 1H), 3.88 (qd, *J* = 7.1, 2.1 Hz, 2H), 3.75 (d, *J* = 12.9 Hz, 1H), 3.58 (p, *J* = 8.0, 7.5 Hz, 1H), 3.24 (d, *J* = 12.9 Hz, 1H), 2.41 (dd, *J* = 11.1, 8.7 Hz, 1H), 1.93 (dd, *J* = 11.1, 8.5 Hz, 1H), 1.86 – 1.78 (m, 1H), 1.58 – 1.51 (m, 1H), 1.45 – 1.37 (m, 1H), 1.31 – 1.23 (m, 7H), 0.99 (t, *J* = 7.1 Hz, 3H), 0.87 (t, *J* = 7.0 Hz, 3H); ¹³C NMR (176 MHz, CDCl₃): δ 172.0, 144.7, 144.6, 128.4, 128.1, 127.5, 127.1, 126.4, 126.2, 93.4, 72.8, 66.8, 61.4, 50.7, 35.5, 31.9, 30.1, 29.2, 25.4, 22.7, 14.2, 14.0; **IR** (cm⁻¹): 2954, 2926, 2855, 1725, 1492, 1447, 1368, 1312, 1222, 1180, 1081, 1031, 911, 862, 778, 749, 697; **HRMS**: *m/z* calculated for C₂₆H₃₄NO₃⁺ [M+H]⁺: 408.2533; found: 408.2528.

endo-Diastereomer (minor): ¹H NMR (700 MHz, CDCl₃): δ 7.49 (d, *J* = 7.3 Hz, 2H), 7.43 (d, *J* = 8.0 Hz, 2H), 7.30 (t, *J* = 7.7 Hz, 2H), 7.27 – 7.20 (m, 3H), 7.14 (t, *J* = 7.3 Hz, 1H), 4.02 (p, *J* = 7.4 Hz, 1H), 3.92 – 3.81 (m, 3H), 2.98 (d, *J* = 12.5 Hz, 1H), 2.66 (dd, *J* = 11.8, 8.3 Hz, 1H), 2.22 (dd, *J* = 11.8, 6.6 Hz, 1H), 2.07 – 1.99 (m, 1H), 1.52 – 1.40 (m, 2H), 1.31 – 1.17 (m, 7H), 0.95 (t, *J* = 7.1 Hz, 3H), 0.86 (t, *J* = 7.1 Hz, 3H); ¹³C NMR (176 MHz, CDCl₃): δ 172.3, 144.2, 143.3, 128.4, 128.2, 127.4, 127.1, 126.0, 126.0, 90.4, 72.6, 61.7, 61.5, 52.2, 34.7, 32.4, 31.8, 29.3, 26.4, 22.7, 14.2, 14.0; **IR** (cm⁻¹): 2926, 2855, 1724, 1492, 1448, 1368, 1314, 1225, 1180, 1085, 1030, 965, 911, 860, 778, 749, 697; **HRMS**: *m/z* calculated for C₂₆H₃₄NO₃⁺ [M+H]⁺: 408.2533; found: 408.2528.

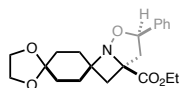


1'-(*Tert*-butyl) 5-ethyl 7-hexyl-2-oxa-1-azaspiro[bicyclo[3.2.0]heptane-3,4'-piperidine]-1',5-dicarboxylate (3.87): Prepared according to GP-3.3 using **S3.87** (78 mg, 0.25 mmol, 1.0 equiv.), 1-octene (59 mg, 0.38 mmol, 1.5 equiv.), *fac*-[Ir(dFppy)₃] (1.9 mg, 1 mol%) and MeCN (2.5 mL) with a reaction time of 19.5 h. ¹H NMR analysis of the crude reaction mixture revealed a diastereomer ratio of 3:1 and a regioisomer ratio of 18:1. Purification by flash column chromatography (5–40% EtOAc/hexanes) afforded the pure *exo*-diastereomer as a colorless oil (74 mg, 70%) and the *endo*-diastereomer as a colorless oil (28 mg, 26%).

***exo*-Diastereomer (major):** ¹H NMR (700 MHz, CDCl₃): δ 4.28 – 4.19 (m, 2H), 3.68 (b, 1H), 3.56 (b, 1H), 3.45 (p, *J* = 8.0 Hz, 1H), 3.31 (m, 2H), 2.89 (d, *J* = 13.1 Hz, 1H), 2.43 (d, *J* = 13.1 Hz, 1H), 2.34 (dd, *J* = 11.1, 8.6 Hz, 1H), 2.02 (dd, *J* = 11.2, 8.5 Hz, 1H), 1.93 – 1.86 (b, 1H), 1.86 – 1.79 (b, 1H), 1.76 – 1.65 (m, 2H), 1.55 – 1.50 (m, 1H), 1.48 – 1.44 (m, 1H), 1.44 (s, 9H), 1.40 – 1.33 (m, 1H), 1.32 – 1.24 (m, 10H), 0.87 (t, *J* = 7.0 Hz, 3H); ¹³C NMR (176 MHz, CDCl₃): δ 172.7, 154.8, 87.1, 79.6, 72.5, 67.6, 61.7, 49.6, 41.5 (2C), 38.9, 36.7, 35.4, 31.9, 30.1, 29.3, 28.6, 25.3, 22.7, 14.3, 14.2; IR (cm⁻¹): 2927, 2856, 1729, 1690, 1451, 1419, 1365, 1306, 1277, 1239, 1177, 1146, 1095, 967, 862, 825, 767; HRMS: *m/z* calculated for C₂₃H₄₁N₂O₅⁺ [M+H]⁺: 425.3010; found: 425.3004.

***endo*-Diastereomer (minor):** ¹H NMR (700 MHz, CDCl₃): δ 4.26 (q, *J* = 7.1 Hz, 2H), 3.90 (p, *J* = 7.7 Hz, 1H), 3.66 (b, 2H), 3.33 – 3.22 (m, 2H), 2.84 (dd, *J* = 11.7, 7.9 Hz, 1H), 2.74 (d, *J* = 12.6 Hz, 1H), 2.22 (dd, *J* = 11.7, 8.0 Hz, 1H), 2.15 (d, *J* = 12.7 Hz, 1H), 1.97 – 1.91 (m, 1H), 1.86 – 1.72 (m, 3H), 1.51 – 1.42 (m, 10H), 1.42 – 1.21 (m, 12H), 0.88 (t, *J* = 7.1 Hz, 3H); ¹³C NMR (176 MHz, CDCl₃): δ 172.8, 154.9, 83.2, 79.6, 71.9, 61.9, 60.8, 51.4, 41.2 (2C), 36.7, 35.0, 34.7,

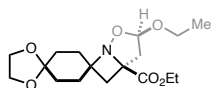
31.82, 31.77, 29.3, 28.6, 25.9, 22.7, 14.3, 14.2; **IR** (cm⁻¹): 2927, 2858, 1730, 1691, 1452, 1419, 1365, 1276, 1240, 1177, 1145, 1050, 967, 864, 828, 767; **HRMS**: *m/z* calculated for C₂₃H₄₁N₂O₅⁺ [M+H]⁺: 425.3010; found: 425.3001.



Ethyl 3-phenyl-4-oxa-5-azadispiro[bicyclo[3.2.0]heptane-6,1'-cyclohexane-4',2''-[1,3]dioxolane]-1-carboxylate (3.88): Prepared according to GP-3.3 using **S3.88** (55 mg, 0.25 mmol, 1.0 equiv.), 8-methylene-1,4-dioxaspiro[4.5]decane²²⁸ (58 mg, 0.38 mmol, 1.5 equiv.), *fac*-[Ir(dFppy)₃] (1.9 mg, 1 mol%) and MeCN (2.5 mL) with a reaction time of 19.5 h. ¹H NMR analysis of the crude reaction mixture revealed a diastereomer ratio of 4:1 and a regioisomer ratio of 18:1. Purification by flash column chromatography (5–30% EtOAc/hexanes) afforded the pure title compound as a yellow oil (94 mg, 99% combined yield; d.r. = 4:1). Characterization data was obtained for a 3.8:1 mixture of *exo/endo* diastereomers.

¹H NMR (700 MHz, CDCl₃): δ 7.45 (d, *J* = 7.2 Hz, 7.6H; major), 7.40 (d, *J* = 7.7 Hz, 2H; minor), 7.36 (t, *J* = 7.5 Hz, 9.6H; major+minor), 7.31 (t, *J* = 7.3 Hz, 4.8H; major+minor), 5.50 (dd, *J* = 10.2, 5.5 Hz, 3.8H; major), 5.19 (dd, *J* = 11.3, 4.9 Hz, 1H; minor), 4.35 – 4.19 (m, 9.6H; major+minor), 3.98 – 3.87 (m, 19.2H; major+minor), 3.08 (dd, *J* = 12.4, 4.9 Hz, 1H; minor), 2.70 (d, *J* = 12.3 Hz, 3.8H; major), 2.65 (dd, *J* = 12.7, 5.5 Hz, 3.8H; major), 2.58 (d, *J* = 12.0 Hz, 1H; minor), 2.50 (dd, *J* = 12.7, 10.2 Hz, 3.8H; major), 2.40 (dd, *J* = 12.4, 11.3 Hz, 1H; minor), 2.31 (d, *J* = 12.3 Hz, 3.8H; major), 2.30 – 2.26 (m, 1H; minor), 2.20 (d, *J* = 12.0 Hz, 1H; minor), 2.15 – 2.08 (m, 3.8H; major+minor), 2.02 – 1.74 (m, 24H; major+minor) 1.62 – 1.53 (m, 9.6H; major+minor), 1.35 (t, *J* = 7.1 Hz, 3H; minor), 1.30 (t, *J* = 7.1 Hz, 11.4H; major); **¹³C NMR** (176 MHz, CDCl₃): δ 173.2, 173.0, 138.4, 137.9, 128.7, 128.6, 128.4, 128.1, 126.8, 126.3, 108.2, 108.1, 84.9, 83.0, 71.7, 69.2, 65.3, 64.47, 64.46, 64.39, 64.35, 63.7, 62.0, 61.9, 49.0, 48.2, 38.7,

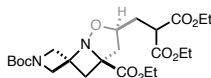
36.9, 36.3, 35.8, 31.39, 31.35, 31.3, 30.8, 30.6, 29.6, 14.3, 14.2; **IR** (cm⁻¹): 2951, 1723, 1445, 1375, 1300, 1241, 1180, 1156, 1102, 1032, 946, 926, 885, 751, 730, 699; **HRMS**: *m/z* calculated for C₂₁H₂₇NNaO₅⁺ [M+Na]⁺: 396.1781; found: 396.1771.



Ethyl 3-ethoxy-4-oxa-5-azadispiro[bicyclo[3.2.0]heptane-6,1'-cyclohexane-4',2''-[1,3]dioxolane]-1-carboxylate (3.89): Prepared according to GP-3.3 using **S3.89** (47 mg, 0.25 mmol, 1.0 equiv.), 8-methylene-1,4-dioxaspiro[4.5]decane²²⁸ (58 mg, 0.38 mmol, 1.5 equiv.), *fac*-[Ir(dFppy)₃] (3.8 mg, 2 mol%) and MeCN (2.5 mL) with a reaction time of 36 h. ¹H NMR analysis of the crude reaction mixture revealed a diastereomer ratio of 1.2:1 and a regioisomer ratio of >20:1. Purification by flash column chromatography (10–40% EtOAc/CH₂Cl₂) afforded the pure title compound as a pale-yellow oil (63 mg, 74% combined yield; d.r. = 1.2:1). Characterization data for both diastereomers was obtained after separation by flash column chromatography (20–30% EtOAc/CH₂Cl₂). Characterization data was obtained for a 1.1:1 mixture of *exo/endo* diastereomers.

¹H NMR (700 MHz, CDCl₃): δ 5.44 (dd, *J* = 5.8, 2.0 Hz, 2.1H; major+minor), 4.31 – 4.18 (m, 4.2H; major+minor), 3.96 – 3.88 (m, 8.4H; major+minor), 3.84 – 3.73 (m, 2.1H; major+minor), 3.51 (dq, *J* = 9.6, 7.1 Hz, 1.1H; major), 3.37 (dq, *J* = 9.5, 7.0 Hz, 1H; minor), 3.02 (d, *J* = 13.1 Hz, 1H; minor), 2.84 (dd, *J* = 13.6, 6.2 Hz, 1.1H; major), 2.55 – 2.50 (m, 2.2H; major), 2.48 (dd, *J* = 13.2, 4.9 Hz, 1H; minor), 2.45 (dd, *J* = 13.6, 1.9 Hz, 1.1H; major), 2.27 – 2.19 (m, 2.1H; major+minor), 2.14 (d, *J* = 11.6 Hz, 1H; minor), 2.05 – 1.99 (m, 2H; minor), 1.96 – 1.72 (m, 8.5H; major+minor), 1.67 – 1.60 (m, 1H; minor), 1.59 – 1.45 (m, 4.2H; major+minor), 1.30 (td, *J* = 7.1, 2.4 Hz, 6.3H; major+minor), 1.22 (t, *J* = 7.1 Hz, 3.3H; major), 1.11 (t, *J* = 7.0 Hz, 3H; minor); **¹³C NMR** (176 MHz, CDCl₃): δ 173.1, 172.5, 108.5, 108.3, 108.0, 104.7, 69.6, 67.6, 64.7, 64.6,

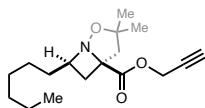
64.40, 64.37, 64.35, 64.3, 64.0, 62.6, 61.8, 61.6, 46.8, 46.5, 38.1, 37.4, 36.4, 35.8, 31.4, 30.9 (2C), 30.69, 30.68, 30.1, 15.0, 14.9, 14.24, 14.18; **IR** (cm⁻¹): 2944, 1726, 1444, 1374, 1267, 1225, 1143, 1101, 1033, 993, 945, 925, 882, 771, 713, 662; **HRMS**: *m/z* calculated for C₁₇H₂₇NNaO₆⁺ [M+Na]⁺: 364.1731; found: 364.1725.



1-(*Tert*-butyl) 1'-ethyl 3'-(3-ethoxy-2-(ethoxycarbonyl)-3-oxopropyl)-4'-oxa-5'-azaspiro[azetidine-3,6'-bicyclo[3.2.0]heptane]-1,1'-dicarboxylate (3.90): Prepared according to GP-3.3 using **S3.90** (79 mg, 0.25 mmol, 1.0 equiv.), *tert*-butyl 3-methyleneazetidine-1-carboxylate²²⁹ (64 mg, 0.38 mmol, 1.5 equiv.), *fac*-[Ir(dFppy)₃] (1.9 mg, 1 mol%) and MeCN (2.5 mL) with a reaction time of 24 h. ¹H NMR analysis of the crude reaction mixture revealed a diastereomer ratio of 3:1 and a regioisomer ratio of >20:1. Purification by flash column chromatography (3–50% EtOAc/CH₂Cl₂) afforded the pure title compound as a colorless oil (117 mg, 96% combined yield; d.r. = 3:1). Characterization data for both diastereomers was obtained after separation by flash column chromatography (30–50% EtOAc/hexanes).

exo-Diastereomer (major): ¹H NMR (700 MHz, CDCl₃): δ 4.31 (d, *J* = 9.5 Hz, 1H), 4.28 – 4.15 (m, 6H), 4.11 (d, *J* = 9.6 Hz, 1H), 4.00 – 3.94 (m, 1H), 3.88 (d, *J* = 9.6 Hz, 1H), 3.69 (d, *J* = 9.2 Hz, 1H), 3.63 (dd, *J* = 10.1, 4.9 Hz, 1H), 2.94 (d, *J* = 13.2 Hz, 1H), 2.40 (d, *J* = 13.2 Hz, 1H), 2.39 – 2.34 (m, 1H), 2.30 (dd, *J* = 12.7, 5.3 Hz, 1H), 2.21 – 2.11 (m, 2H), 1.40 (s, 9H), 1.28 (q, *J* = 7.2 Hz, 6H), 1.24 (t, *J* = 7.1 Hz, 3H); ¹³C NMR (176 MHz, CDCl₃): δ 171.8, 169.2, 169.0, 156.1, 79.9, 79.3, 72.1, 62.5, 62.0, 61.93, 61.86, 61.8, 55.7, 49.1, 43.6, 37.3, 31.7, 28.4, 14.2, 14.14, 14.10; **IR** (cm⁻¹): 2979, 1729, 1700, 1447, 1392, 1367, 1304, 1247, 1203, 1159, 1091, 1025, 961, 930, 860, 771, 732; **HRMS**: *m/z* calculated for C₂₃H₃₆N₂NaO₉⁺ [M+Na]⁺: 507.2313; found: 507.2314.

endo-Diastereomer (minor): $^1\text{H NMR}$ (700 MHz, CDCl_3): δ 4.63 (d, $J = 9.3$ Hz, 1H), 4.31 – 4.13 (m, 7H), 4.05 (d, $J = 9.9$ Hz, 1H), 3.90 (d, $J = 9.9$ Hz, 1H), 3.72 (d, $J = 9.4$ Hz, 1H), 3.56 (dd, $J = 9.0, 5.8$ Hz, 1H), 2.78 (dd, $J = 12.6, 4.7$ Hz, 1H), 2.73 (d, $J = 12.2$ Hz, 1H), 2.45 (d, $J = 12.2$ Hz, 1H), 2.37 (ddd, $J = 14.1, 9.0, 4.2$ Hz, 1H), 2.25 – 2.17 (m, 1H), 1.77 (dd, $J = 12.7, 11.2$ Hz, 1H), 1.43 (s, 9H), 1.30 – 1.25 (m, 9H); $^{13}\text{C NMR}$ (176 MHz, CDCl_3): δ 171.4, 169.0, 168.9, 156.2, 81.3, 78.0, 71.1, 63.1, 62.0, 61.89, 61.85, 61.0, 56.0, 49.7, 45.3, 34.11, 31.9, 28.5, 14.20, 14.17, 14.15; **IR** (cm^{-1}): 2979, 1730, 1699, 1447, 1392, 1367, 1329, 1302, 1159, 1093, 1055, 1022, 962, 931, 861, 771, 718; **HRMS**: m/z calculated for $\text{C}_{23}\text{H}_{36}\text{N}_2\text{NaO}_9^+$ $[\text{M}+\text{Na}]^+$: 507.2313; found: 507.2309.



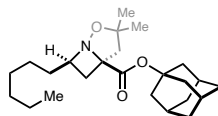
Prop-2-yn-1-yl-7-hexyl-3,3-dimethyl-2-oxa-1-azabicyclo[3.2.0]heptane-5-carboxylate (3.91):

Prepared according to GP-3.3 using **S3.91** (45 mg, 0.25 mmol, 1.0 equiv.), 1-octene (59 μL , 0.38 mmol, 1.5 equiv.), *fac*- $[\text{Ir}(\text{dFppy})_3]$ (1.9 mg, 1 mol%) and MeCN (2.5 mL) with a reaction time of 20 h. $^1\text{H NMR}$ analysis of the crude reaction mixture revealed a diastereomer ratio of 3:1 and a regioisomer ratio of 19:1. Purification by flash column chromatography (5–30% EtOAc/hexanes) afforded the pure *exo*-diastereomer as pale-yellow oil (31 mg, 43%) and the pure *endo*-diastereomer as a colorless oil (13 mg, 18%).

exo-Diastereomer (major): $^1\text{H NMR}$ (700 MHz, CDCl_3): δ 4.76 (m, 2H), 3.47 (p, $J = 8.4$ Hz, 1H), 2.87 (d, $J = 13.0$ Hz, 1H), 2.49 (d, $J = 13.0$ Hz, 1H), 2.45 (t, $J = 2.5$ Hz, 1H), 2.37 (dd, $J = 11.1, 8.6$ Hz, 1H), 2.00 (dd, $J = 11.1, 8.4$ Hz, 1H), 1.76 – 1.67 (m, 1H), 1.55 – 1.48 (m, 4H), 1.40 – 1.32 (m, 1H), 1.30 – 1.21 (m, 7H), 1.20 (s, 3H), 0.85 (t, $J = 7.0$ Hz, 3H); $^{13}\text{C NMR}$ (176 MHz, CDCl_3): δ 172.1, 87.4, 77.4, 75.2, 72.9, 67.5, 52.8, 51.0, 35.5, 31.9, 30.3, 29.7, 29.3, 28.5, 25.4,

22.7, 14.2; **IR** (cm⁻¹): ;**HRMS**: *m/z* calculated for C₁₇H₂₈NO₃⁺ [M+H]⁺: 294.2064; found: 294.2063.

endo-Diastereomer (minor): ¹H NMR (700 MHz, CDCl₃): δ 4.85 – 4.72 (m, 2H), 3.91 (p, *J* = 7.8 Hz, 1H), 2.83 (dd, *J* = 11.7, 8.0 Hz, 1H), 2.75 (d, *J* = 12.5 Hz, 1H), 2.47 (t, *J* = 2.5 Hz, 1H), 2.28 – 2.18 (m, 2H), 1.98 – 1.90 (m, 1H), 1.53 – 1.47 (m, 1H), 1.45 (s, 3H), 1.32 – 1.22 (m, 8H), 1.20 (s, 3H), 0.87 (t, *J* = 7.0 Hz, 3H); ¹³C NMR (176 MHz, CDCl₃): δ 172.3, 83.7, 77.4, 75.3, 72.5, 60.8, 53.0, 52.7, 36.6, 31.8, 31.6, 29.4, 27.1, 25.92, 25.86, 22.7, 14.2; **IR** (cm⁻¹): 2926, 2857, 1738, 1634, 1457, 1368, 1302, 1253, 1173, 1147, 1044, 993, 932, 786, 723, 666; **HRMS**: *m/z* calculated for C₁₇H₂₈NO₃⁺ [M+H]⁺: 294.2064; found: 294.2062.



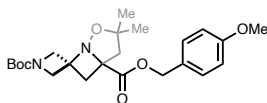
Adamantan-1-yl-7-hexyl-3,3-dimethyl-2-oxa-1-azabicyclo[3.2.0]heptane-5-carboxylate

(3.92): Prepared according to GP-3.3 using **S3.92** (69 mg, 0.25 mmol, 1.0 equiv.), 1-octene (59 μL, 0.38 mmol, 1.5 equiv.), *fac*-[Ir(dFppy)₃] (1.9 mg, 1 mol%) and MeCN (2.5 mL) with a reaction time of 18 h. ¹H NMR analysis of the crude reaction mixture revealed a diastereomer ratio of 2:1 and a regioisomer ratio of 19:1. Purification by flash column chromatography (5–15% EtOAc/hexanes) afforded the pure title compound as a colorless oil (95 mg, 98% combined yield; d.r. = 2:1). Characterization data for both diastereomers was obtained after separation by flash column chromatography (1–20% EtOAc/hexanes).

exo-Diastereomer (major): ¹H NMR (500 MHz, CDCl₃): δ 3.42 (p, *J* = 7.6 Hz, 1H), 2.82 (d, *J* = 12.7 Hz, 1H), 2.40 (d, *J* = 12.8 Hz, 1H), 2.29 (t, *J* = 9.8 Hz, 1H), 2.16 (d, *J* = 7.9 Hz, 9H), 1.97 (t, *J* = 9.6 Hz, 1H), 1.75 – 1.61 (m, 7H), 1.54 – 1.46 (m, 4H), 1.39 – 1.19 (m, 11H), 0.87 (t, *J* = 6.2 Hz, 3H); ¹³C NMR (126 MHz, CDCl₃): δ 171.8, 86.9, 81.6, 73.6, 67.1, 51.0, 41.2, 36.2, 35.4, 31.9,

31.0, 30.4, 29.6, 29.3, 28.4, 25.3, 22.7, 14.2; **IR** (cm⁻¹): 2911, 2853, 1720, 1456, 1366, 1326, 1298, 1255, 1186, 1151, 1103, 1055, 967, 872, 778; **HRMS**: *m/z* calculated for C₂₄H₃₉NNaO₃⁺ [M+Na]⁺: 412.2822; found: 412.2824.

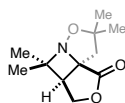
endo-Diastereomer (minor): **¹H NMR** (500 MHz, CDCl₃): δ 3.84 (p, *J* = 7.9 Hz, 1H), 2.79 (dd, *J* = 11.5, 7.8 Hz, 1H), 2.67 (d, *J* = 12.3 Hz, 1H), 2.21 – 2.08 (m, 11H), 1.95 – 1.85 (m, 1H), 1.72 – 1.63 (m, 6H), 1.55 – 1.46 (m, 1H), 1.43 (s, 3H), 1.31 – 1.24 (m, 8H), 1.22 (s, 3H), 0.87 (t, *J* = 6.3 Hz, 3H); **¹³C NMR** (126 MHz, CDCl₃): δ 171.9, 83.4, 81.8, 73.3, 60.5, 53.0, 41.2, 37.0, 36.3, 31.9, 31.5, 31.0, 29.4, 27.0, 26.1, 25.8, 22.7, 14.2; **IR** (cm⁻¹): 2911, 2852, 1723, 1456, 1366, 1328, 1299, 1253, 1184, 1103, 1055, 967, 875, 729; **HRMS**: *m/z* calculated for C₂₄H₄₀NO₃⁺ [M+H]⁺: 390.3003; found: 390.3003.



1-(Tert-butyl) 1'-(4-methoxybenzyl) 3',3'-dimethyl-4'-oxa-5'-azaspiro[azetidine-3,6'-bicyclo[3.2.0]heptane]-1,1'-dicarboxylate (3.93): Prepared according to GP-3.3 using **S3.93** (66 mg, 0.25 mmol, 1.0 equiv.), *tert*-butyl 3-methyleneazetidine-1-carboxylate²²⁹ (64 mg, 0.38 mmol, 1.5 equiv.), *fac*-[Ir(dFppy)₃] (1.9 mg, 1 mol%) and MeCN (2.5 mL) with a reaction time of 20 h. ¹H NMR analysis of the crude reaction mixture revealed a regioisomer ratio of >20:1. Purification by flash column chromatography (5–20% EtOAc/CH₂Cl₂) afforded the pure title compound as a colorless oil (95 mg, 88%).

¹H NMR (700 MHz, CDCl₃): δ 7.31 (d, *J* = 8.6 Hz, 2H), 6.87 (d, *J* = 8.6 Hz, 2H), 5.20 (d, *J* = 11.8 Hz, 1H), 5.13 (d, *J* = 11.9 Hz, 1H), 4.65 (d, *J* = 9.4 Hz, 1H), 4.12 (d, *J* = 9.9 Hz, 1H), 3.87 (d, *J* = 9.9 Hz, 1H), 3.81 (s, 3H), 3.71 (d, *J* = 9.4 Hz, 1H), 2.81 (d, *J* = 12.8 Hz, 1H), 2.60 (d, *J* = 12.0 Hz, 1H), 2.53 (d, *J* = 12.0 Hz, 1H), 1.98 (d, *J* = 12.9 Hz, 1H), 1.42 (d, *J* = 11.5 Hz, 12H), 1.12

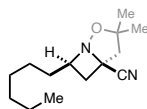
(s, 3H); ^{13}C NMR (176 MHz, CDCl_3): δ 171.7, 159.9, 156.2, 130.4, 127.5, 114.0, 86.8, 79.7, 71.9, 67.2, 63.0, 61.3, 56.0, 55.3, 50.2, 37.0, 28.4, 27.7, 26.4; IR (cm^{-1}): 2976, 2937, 2875, 1740, 1689, 1615, 1586, 1514, 1456, 1410, 1367, 1244, 1214, 1166, 1139, 1096, 1030, 963, 817, 798, 709; HRMS: m/z calculated for $\text{C}_{23}\text{H}_{33}\text{N}_2\text{O}_6^+$ $[\text{M}+\text{H}]^+$: 433.2333; found: 433.2325.



4,4,7,7-Tetramethyltetrahydro-1H,3H-furo[3',4':2,3]azeto[1,2-b]isoxazol-1-one (3.95):

Prepared according to GP-3.3 using **3.94** (53 mg, 0.25 mmol, 1.0 equiv.), *fac*-[Ir(dFppy) $_3$] (1.9 mg, 1 mol%) and MeCN (2.5 mL) with a reaction time of 12 h. ^1H NMR analysis of the crude reaction mixture revealed a diastereomer ratio of >10:1. Purification by flash column chromatography (2–30% EtOAc/ CH_2Cl_2) afforded the pure title compound as a white solid (46 mg, 87%).

^1H NMR (700 MHz, CDCl_3): δ 4.48 (d, J = 10.5 Hz, 1H), 4.34 (dd, J = 10.4, 8.0 Hz, 1H), 2.91 (d, J = 7.8 Hz, 1H), 2.54 (d, J = 12.5 Hz, 1H), 2.34 (d, J = 12.5 Hz, 1H), 1.50 (s, 3H), 1.42 (s, 3H), 1.38 (s, 3H), 1.35 (s, 3H); ^{13}C NMR (176 MHz, CDCl_3): δ 176.7, 86.3, 69.1, 66.8, 63.8, 48.0, 45.3, 27.0, 26.0, 24.58, 24.55; IR (cm^{-1}): 2974, 2930, 1771, 1457, 1367, 1288, 1207, 1157, 1131, 1095, 1060, 992, 948, 927, 866, 832, 785, 730, 710, 679; HRMS: m/z calculated for $\text{C}_{11}\text{H}_{18}\text{NO}_3^+$ $[\text{M}+\text{H}]^+$: 212.1281; found: 212.1277.



7-Hexyl-3,3-dimethyl-2-oxa-1-azabicyclo[3.2.0]heptane-5-carbonitrile (3.96): Prepared according to GP-3.3 using **S3.96** (31 mg, 0.25 mmol, 1.0 equiv.), 1-octene (59 μL , 0.38 mmol, 1.5 equiv.), *fac*-[Ir(dFppy) $_3$] (1.9 mg, 1 mol%) and MeCN (2.5 mL) with a reaction time of 20 h. ^1H NMR analysis of the crude reaction mixture revealed a diastereomer ratio of 2:1 and a

regioisomer ratio of >20:1. Purification by flash column chromatography (2–15% EtOAc/hexanes) afforded the pure title compound as a colorless oil (52 mg, 88% combined yield; d.r. = 2:1). Characterization data was obtained for a 2.2:1 mixture of diastereomers.

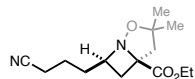
¹H NMR (500 MHz, CDCl₃): δ 3.99 (p, *J* = 7.7 Hz, 1H; minor), 3.46 (p, *J* = 8.4 Hz, 2.2H; major), 2.93 (dd, *J* = 11.9, 8.1 Hz, 1H; minor), 2.74 (d, *J* = 12.9 Hz, 2.2H; major), 2.65 (d, *J* = 12.6 Hz, 1H; minor), 2.56 (d, *J* = 13.0 Hz, 2.2H; major), 2.50 (dd, *J* = 11.3, 8.7 Hz, 2.2H; major), 2.34 (d, *J* = 12.7 Hz, 1H; minor), 2.29 (dd, *J* = 12.1, 7.3 Hz, 1H; minor), 2.20 (dd, *J* = 11.3, 8.6 Hz, 2.2H; major), 1.95 – 1.87 (m, 1H; minor), 1.76 – 1.65 (m, 2.2H; major), 1.59 – 1.17 (m, 48H; major+minor), 0.86 (t, *J* = 6.7 Hz, 9.6H; major+minor); **¹³C NMR** (126 MHz, CDCl₃): δ 121.0, 120.7, 88.1, 84.8, 69.3, 61.9, 61.3, 61.2, 54.3, 52.4, 36.7, 35.4, 31.8, 31.7, 31.7, 31.3, 29.23, 29.15, 28.4 (2C), 27.1, 25.7, 25.2, 25.1, 22.7 (2C), 14.1 (2C); **IR** (cm⁻¹): 2955, 2925, 2853, 2235, 1468, 1459, 1382, 1368, 1307, 1275, 1226, 1153, 1102, 1006, 970, 858, 824, 804, 722, 685, 646; **HRMS**: *m/z* calculated for C₁₄H₂₅N₂O⁺ [M+H]⁺: 237.1961; found: 237.1960.



Ethyl 3,3-dimethyl-2-oxa-1-azabicyclo[3.2.0]heptane-5-carboxylate (3.105): Prepared according to GP-3.3 using **3.83** (43 mg, 0.25 mmol, 1.0 equiv.), *fac*-[Ir(dFppy)₃] (3.8 mg, 2 mol%) and 1,2-dichloroethane (2.5 mL) with a reaction time of 44 h under an atmosphere of ethylene gas. Purification by flash column chromatography (2–35% EtOAc/CH₂Cl₂) afforded the pure title compound as a yellow oil (35 mg, 70%).

¹H NMR (400 MHz, CDCl₃): δ 4.26 (qd, *J* = 7.1, 2.5 Hz, 2H), 3.78 (ddd, *J* = 9.7, 8.4, 4.1 Hz, 1H), 3.46 (q, *J* = 9.5 Hz, 1H), 2.85 (d, *J* = 12.9 Hz, 1H), 2.55 (d, *J* = 12.9 Hz, 1H), 2.47 (dt, *J* = 11.3, 8.7 Hz, 1H), 2.29 (ddd, *J* = 11.3, 9.7, 4.1 Hz, 1H), 1.55 (s, 3H), 1.32 (t, *J* = 7.1 Hz, 3H), 1.20 (s, 3H); **¹³C NMR** (176 MHz, CDCl₃): δ 172.7, 87.0, 76.7, 61.6, 55.2, 51.0, 29.5, 28.3, 24.9, 14.2; **IR**

(cm^{-1}): 2973, 1725, 1448, 1383, 1313, 1256, 1221, 1179, 1144, 1024, 921, 864, 821, 782, 705, 672; **HRMS**: m/z calculated for $\text{C}_{10}\text{H}_{17}\text{NNaO}_3^+$ $[\text{M}+\text{Na}]^+$: 222.1101; found: 222.1099.



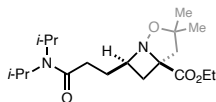
Ethyl 7-(3-cyanopropyl)-3,3-dimethyl-2-oxa-1-azabicyclo[3.2.0]heptane-5-carboxylate

(3.106): Prepared according to GP-3.3 using **3.83** (43 mg, 0.25 mmol, 1.0 equiv.), 5-hexenenitrile (43 μL , 0.38 mmol, 1.5 equiv.), *fac*- $[\text{Ir}(\text{dFppy})_3]$ (3.8 mg, 2 mol%) and MeCN (2.5 mL) with a reaction time of 36 h. ^1H NMR analysis of the crude reaction mixture revealed a diastereomer ratio of 2:1 and a regioisomer ratio of 16:1. Purification by flash column chromatography (20–80% EtOAc/hexanes) afforded the pure *exo*-diastereomer as a pale-yellow oil (33 mg, 49%) and the pure *endo*-diastereomer as a colorless oil (15 mg, 22%).

exo-Diastereomer (major): ^1H NMR (700 MHz, CDCl_3): δ 4.26 (q, $J = 7.0$ Hz, 2H), 3.54 – 3.47 (m, 1H), 2.88 (d, $J = 13.0$ Hz, 1H), 2.49 (d, $J = 13.0$ Hz, 1H), 2.47 – 2.35 (m, 3H), 2.04 (dd, $J = 11.2, 8.5$ Hz, 1H), 1.90 – 1.82 (m, 1H), 1.81 – 1.71 (m, 3H), 1.52 (s, 3H), 1.31 (t, $J = 7.1$ Hz, 3H), 1.21 (s, 3H); ^{13}C NMR (176 MHz, CDCl_3): δ 172.6, 119.7, 87.7, 73.2, 66.2, 61.7, 51.0, 33.9, 30.0, 29.8, 28.5, 21.6, 17.1, 14.3; **IR** (cm^{-1}): 2973, 2936, 2245, 1725, 1456, 1384, 1368, 1309, 1256, 1220, 1185, 1148, 1108, 1054, 1022, 861, 779, 729, 676; **HRMS**: m/z calculated for $\text{C}_{14}\text{H}_{23}\text{N}_2\text{O}_3^+$ $[\text{M}+\text{H}]^+$: 267.1703; found: 267.1703.

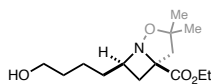
endo-Diastereomer (minor): ^1H NMR (700 MHz, CDCl_3): δ 4.28 (q, $J = 7.0$ Hz, 2H), 3.92 (qd, $J = 8.0, 5.3$ Hz, 1H), 2.87 (dd, $J = 11.8, 7.9$ Hz, 1H), 2.74 (d, $J = 12.4$ Hz, 1H), 2.38 (q, $J = 6.8$ Hz, 2H), 2.27 (dd, $J = 11.8, 8.1$ Hz, 1H), 2.21 (d, $J = 12.5$ Hz, 1H), 2.16 – 2.10 (m, 1H), 1.85 – 1.78 (m, 1H), 1.68 – 1.60 (m, 2H), 1.47 (s, 3H), 1.33 (t, $J = 7.1$ Hz, 3H), 1.21 (s, 3H); ^{13}C NMR (176 MHz, CDCl_3): δ 172.7, 119.7, 83.8, 72.5, 61.9, 59.5, 52.9, 36.8, 30.8, 26.9, 26.0, 22.6, 17.3,

14.3; **IR** (cm⁻¹): 2975, 2245, 1726, 1457, 1367, 1303, 1254, 1185, 1152, 1023, 894, 862, 786, 726, 665; **HRMS**: *m/z* calculated for C₁₄H₂₃N₂O₃⁺ [M+H]⁺: 267.1703; found: 267.1710.



Ethyl 7-(3-(diisopropylamino)-3-oxopropyl)-3,3-dimethyl-2-oxa-1-azabicyclo[3.2.0]heptane-5-carboxylate (3.107): Prepared according to GP-3.3 using **3.83** (43 mg, 0.25 mmol, 1.0 equiv.), *N,N*-diisopropylpent-4-enamide²²⁹ (69 mg, 0.38 mmol, 1.5 equiv.), *fac*-[Ir(dFppy)₃] (1.9 mg, 1 mol%) and MeCN (2.5 mL) with a reaction time of 24 h. ¹H NMR analysis of the crude reaction mixture revealed a diastereomer ratio of 4:1 and a regioisomer ratio of >20:1. Purification by flash column chromatography (30–95% EtOAc/hexanes) afforded the pure *exo*-diastereomer as a pale-yellow oil (65 mg, 73%) and the pure *endo*-diastereomer as a pale-yellow oil (22 mg, 25%). Characterization data is provided for the *exo*-diastereomer.

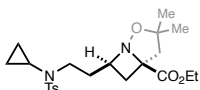
***exo*-Diastereomer (major)**: ¹H NMR (700 MHz, CDCl₃): δ 4.24 (qd, *J* = 7.1, 2.5 Hz, 2H), 4.05 (p, *J* = 6.8 Hz, 1H), 3.58 (qd, *J* = 8.8, 4.1 Hz, 1H), 3.42 (b, 1H), 2.83 (d, *J* = 12.9 Hz, 1H), 2.52 – 2.46 (m, 2H), 2.44 – 2.35 (m, 2H), 2.05 – 1.98 (m, 2H), 1.83 – 1.77 (m, 1H), 1.49 (s, 3H), 1.38 (d, *J* = 6.8 Hz, 6H), 1.30 (t, *J* = 7.1 Hz, 3H), 1.20 (s, 3H), 1.18 (d, *J* = 6.7 Hz, 6H); ¹³C NMR (176 MHz, CDCl₃): δ 172.9, 171.1, 87.5, 73.3, 66.6, 61.5, 51.1, 48.4, 45.7, 30.4, 30.1, 29.9, 28.7, 21.0, 20.9, 20.8, 14.3; **IR** (cm⁻¹): 2967, 2932, 1727, 1635, 1442, 1368, 1300, 1256, 1214, 1184, 1149, 1107, 1044, 888, 862, 779, 728, 677; **HRMS**: *m/z* calculated for C₁₉H₃₅N₂O₄⁺ [M+H]⁺: 355.2591; found: 355.2584.



Ethyl 7-(4-hydroxybutyl)-3,3-dimethyl-2-oxa-1-azabicyclo[3.2.0]heptane-5-carboxylate (3.108): Prepared according to GP-3.3 using **3.83** (43 mg, 0.25 mmol, 1.0 equiv.), 5-hexen-1-ol

(45 μ L, 0.38 mmol, 1.5 equiv.), *fac*-[Ir(dFppy)₃] (1.9 mg, 1 mol%) and MeCN (2.5 mL) with a reaction time of 20 h. ¹H NMR analysis of the crude reaction mixture revealed a diastereomer ratio of 3:1 and a regioisomer ratio of >20:1. Purification by flash column chromatography (30–99% EtOAc/CH₂Cl₂) afforded the pure *exo*-diastereomer as a pale-yellow oil (40 mg, 62%) and the pure *endo*-diastereomer as a pale-yellow oil (17 mg, 26%).

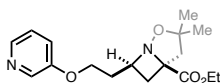
***exo*-Diastereomer (major):** ¹H NMR (700 MHz, CDCl₃): δ 4.25 (q, *J* = 7.1 Hz, 2H), 3.65 (td, *J* = 6.5, 2.0 Hz, 2H), 3.49 (qd, *J* = 8.4, 6.1 Hz, 1H), 2.86 (d, *J* = 12.9 Hz, 1H), 2.48 (d, *J* = 12.9 Hz, 1H), 2.37 (dd, *J* = 11.1, 8.7 Hz, 1H), 2.00 (dd, *J* = 11.1, 8.5 Hz, 1H), 1.78 – 1.70 (m, 1H), 1.63 – 1.54 (m, 3H), 1.52 (s, 3H), 1.51 – 1.45 (m, 1H), 1.44 – 1.37 (m, 1H), 1.31 (t, *J* = 7.1 Hz, 3H), 1.20 (s, 3H); ¹³C NMR (176 MHz, CDCl₃): δ 172.8, 87.3, 73.0, 67.3, 62.4, 61.6, 51.0, 34.7, 32.5, 30.3, 29.5, 28.4, 21.5, 14.2; IR (cm⁻¹): 3388, 2973, 2933, 2862, 1727, 1456, 1383, 1368, 1310, 1257, 1218, 1186, 1149, 1111, 1057, 1035, 863, 839, 779, 737, 674; HRMS: *m/z* calculated for C₁₄H₂₆NO₄⁺ [M+H]⁺: 272.1856; found: 272.1854.



Ethyl 7-(2-((*N*-cyclopropyl-4-methylphenyl)sulfonamido)ethyl)-3,3-dimethyl-2-oxa-1-azabicyclo[3.2.0]heptane-5-carboxylate (3.109): Prepared according to GP-3.3 using **3.83** (43 mg, 0.25 mmol, 1.0 equiv.), **S3.109** (100 mg, 0.38 mmol, 1.5 equiv.), *fac*-[Ir(dFppy)₃] (1.9 mg, 1 mol%) and MeCN (2.5 mL) with a reaction time of 20 h. ¹H NMR analysis of the crude reaction mixture revealed a diastereomer ratio of 2:1 and a regioisomer ratio of >20:1. Purification by flash column chromatography (1–35% EtOAc/CH₂Cl₂) afforded the pure *exo*-diastereomer as a pale-yellow oil (64 mg, 58%) and the pure *endo*-diastereomer as a pale-yellow oil (32 mg, 29%).

exo-Diastereomer (major): $^1\text{H NMR}$ (700 MHz, CDCl_3): δ 7.71 (d, $J = 8.2$ Hz, 2H), 7.30 (d, $J = 8.0$ Hz, 2H), 4.25 (q, $J = 7.1$ Hz, 2H), 3.60 – 3.53 (m, 1H), 3.23 (ddd, $J = 8.0, 6.5, 2.6$ Hz, 2H), 2.85 (d, $J = 12.9$ Hz, 1H), 2.50 (d, $J = 13.0$ Hz, 1H), 2.47 – 2.39 (m, 4H), 2.10 – 2.01 (m, 2H), 1.99 – 1.95 (m, 1H), 1.94 – 1.88 (m, 1H), 1.53 (s, 3H), 1.31 (t, $J = 7.1$ Hz, 3H), 1.21 (s, 3H), 0.94 – 0.89 (m, 1H), 0.89 – 0.85 (m, 1H), 0.72 – 0.64 (m, 2H); $^{13}\text{C NMR}$ (176 MHz, CDCl_3): δ 172.6, 143.5, 135.2, 129.6, 127.7, 87.6, 73.5, 64.9, 61.5, 50.9, 47.8, 34.4, 31.0, 30.1, 29.7, 28.5, 21.6, 14.2, 7.6, 7.2; **IR** (cm^{-1}): 2973, 1726, 1598, 1455, 1367, 1341, 1306, 1256, 1160, 1091, 1053, 1027, 860, 815, 775, 712, 690, 648; **HRMS**: m/z calculated for $\text{C}_{22}\text{H}_{33}\text{N}_2\text{O}_5\text{S}^+$ $[\text{M}+\text{H}]^+$: 437.2105; found: 437.2102.

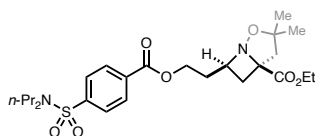
endo-Diastereomer (minor): $^1\text{H NMR}$ (500 MHz, CDCl_3): δ 7.71 (d, $J = 7.7$ Hz, 2H), 7.29 (d, $J = 7.8$ Hz, 2H), 4.27 (q, $J = 7.1$ Hz, 2H), 3.89 (p, $J = 7.7$ Hz, 1H), 3.25 – 3.10 (m, 2H), 2.83 (dd, $J = 11.5, 8.3$ Hz, 1H), 2.75 (d, $J = 12.5$ Hz, 1H), 2.42 (s, 3H), 2.39 – 2.28 (m, 1H), 2.25 (dd, $J = 11.6, 7.9$ Hz, 1H), 2.20 (d, $J = 12.5$ Hz, 1H), 2.07 – 1.98 (m, 1H), 1.87 – 1.76 (m, 1H), 1.44 (s, 3H), 1.32 (t, $J = 6.9$ Hz, 3H), 1.17 (s, 3H), 0.84 (q, $J = 9.8, 9.3$ Hz, 2H), 0.67 (d, $J = 6.8$ Hz, 2H); $^{13}\text{C NMR}$ (176 MHz, CDCl_3): δ 172.8, 143.47, 135.5, 129.7, 127.8, 83.8, 72.8, 61.8, 58.4, 52.8, 48.6, 36.3, 31.7, 31.0, 27.0, 25.9, 21.6, 14.3, 7.6, 7.3; **IR** (cm^{-1}): 2977, 1727, 1456, 1368, 1342, 1266, 1184, 1161, 1092, 1027, 979, 932, 860, 815, 732, 714, 700, 642; **HRMS**: m/z calculated for $\text{C}_{22}\text{H}_{33}\text{N}_2\text{O}_5\text{S}^+$ $[\text{M}+\text{H}]^+$: 437.2105; found: 437.2101.



Ethyl 3,3-dimethyl-7-(2-(pyridin-3-yloxy)ethyl)-2-oxa-1-azabicyclo[3.2.0]heptane-5-carboxylate (3.110): Prepared according to GP-3.3 using **3.83** (43 mg, 0.25 mmol, 1.0 equiv.), **S3.110** (56 mg, 0.38 mmol, 1.5 equiv.), *fac*- $[\text{Ir}(\text{dFppy})_3]$ (1.9 mg, 1 mol%) and MeCN (2.5 mL) with a reaction time of 21 h. $^1\text{H NMR}$ analysis of the crude reaction mixture revealed a

diastereomer ratio of 2:1 and a regioisomer ratio of >20:1. Purification by flash column chromatography (20–100% EtOAc/hexanes) afforded the pure title compound as a yellow oil (54 mg, 67% combined yield; d.r. = 2:1). Characterization data was obtained for the *exo*-diastereomer after purification by flash column chromatography (50–100% EtOAc/hexanes).

¹H NMR (400 MHz, CDCl₃): δ 8.29 (s, 1H), 8.19 (t, *J* = 3.1 Hz, 1H), 7.19 (dd, *J* = 3.3, 1.6 Hz, 2H), 4.24 (q, *J* = 7.1 Hz, 2H), 4.18 – 4.07 (m, 2H), 3.82 – 3.70 (m, 1H), 2.87 (d, *J* = 13.0 Hz, 1H), 2.51 (d, *J* = 13.0 Hz, 1H), 2.44 (dd, *J* = 11.2, 8.7 Hz, 1H), 2.21 – 2.03 (m, 3H), 1.50 (s, 3H), 1.29 (t, *J* = 7.1 Hz, 3H), 1.20 (s, 3H); **¹³C NMR** (176 MHz, CDCl₃): δ 172.7, 155.2, 142.1, 138.4, 123.9, 121.1, 87.7, 73.5, 64.8, 64.0, 61.7, 50.9, 34.6, 30.1, 29.7, 28.5, 14.2; **IR** (cm⁻¹): 2973, 1725, 1574, 1471, 1426, 1384, 1310, 1260, 1231, 1186, 1148, 1111, 1053, 1014, 925, 861, 800, 707, 678; **HRMS**: *m/z* calculated for C₁₇H₂₅N₂O₄⁺ [M+H]⁺: 321.1809; found: 321.1812.

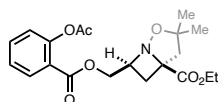


Ethyl 7-(2-((4-(*N,N*-dipropylsulfamoyl)benzoyl)oxy)ethyl)-3,3-dimethyl-2-oxa-1-azabicyclo[3.2.0]heptane-5-carboxylate (3.111): Prepared according to GP-3.3 using **3.83** (43 mg, 0.25 mmol, 1.0 equiv.), **S3.111** (128 mg, 0.38 mmol, 1.5 equiv.), *fac*-[Ir(dFppy)₃] (1.9 mg, 1 mol%) and MeCN (2.5 mL) with a reaction time of 23 h. ¹H NMR analysis of the crude reaction mixture revealed a diastereomer ratio of 2:1 and a regioisomer ratio of >20:1. Purification by flash column chromatography (2–40% EtOAc/CH₂Cl₂) afforded the pure title compound as a yellow oil (118 mg, 92% combined yield; d.r. = 2:1). Characterization data for both diastereomers was obtained after separation by flash column chromatography (5–40% EtOAc/CH₂Cl₂).

***exo*-Diastereomer (major)**: **¹H NMR** (500 MHz, CDCl₃): δ 8.12 (d, *J* = 8.4 Hz, 2H), 7.84 (d, *J* = 8.4 Hz, 2H), 4.49 – 4.40 (m, 2H), 4.24 (q, *J* = 7.1 Hz, 2H), 3.66 (p, *J* = 8.3 Hz, 1H), 3.11 – 3.04

(m, 4H), 2.86 (d, $J = 13.0$ Hz, 1H), 2.49 (d, $J = 13.0$ Hz, 1H), 2.43 (dd, $J = 11.2, 8.7$ Hz, 1H), 2.21 – 2.01 (m, 3H), 1.56 – 1.49 (m, 4H), 1.49 (s, 3H), 1.29 (t, $J = 7.1$ Hz, 3H), 1.20 (s, 3H), 0.84 (t, $J = 7.4$ Hz, 6H); $^{13}\text{C NMR}$ (176 MHz, CDCl_3): δ 172.6, 165.2, 144.3, 133.6, 130.3, 127.1, 87.7, 73.5, 64.2, 62.4, 61.7, 50.9, 50.0, 34.2, 30.2, 29.7, 28.4, 22.0, 14.2, 11.2; **IR** (cm^{-1}): 2968, 2876, 1721, 1458, 1342, 1271, 1217, 1177, 1157, 1105, 1087, 1052, 991, 863, 778, 740, 693; **HRMS**: m/z calculated for $\text{C}_{25}\text{H}_{39}\text{N}_2\text{O}_7\text{S}^+$ $[\text{M}+\text{H}]^+$: 511.2472; found: 511.2471.

endo-Diastereomer (minor): $^1\text{H NMR}$ (500 MHz, CDCl_3): δ 8.14 (d, $J = 8.3$ Hz, 2H), 7.86 (d, $J = 8.3$ Hz, 2H), 4.48 – 4.20 (m, 4H), 4.15 (p, $J = 7.9$ Hz, 1H), 3.14 – 3.08 (m, 4H), 2.94 (dd, $J = 11.8, 7.9$ Hz, 1H), 2.75 (d, $J = 12.4$ Hz, 1H), 2.47 (td, $J = 14.1, 6.0$ Hz, 1H), 2.37 (dd, $J = 11.8, 8.1$ Hz, 1H), 2.23 (d, $J = 12.5$ Hz, 1H), 2.05 – 1.96 (m, 1H), 1.57 – 1.50 (m, 4H), 1.47 (s, 3H), 1.32 (t, $J = 7.1$ Hz, 3H), 1.22 (s, 3H), 0.87 (t, $J = 7.4$ Hz, 6H); $^{13}\text{C NMR}$ (176 MHz, CDCl_3): δ 172.7, 165.3, 144.3, 133.7, 130.4, 127.1, 83.9, 72.7, 63.2, 61.9, 57.4, 52.9, 50.0, 36.9, 31.0, 26.9, 26.1, 22.0, 14.3, 11.3; **IR** (cm^{-1}): 2970, 2876, 1722, 1458, 1368, 1271, 1157, 1106, 1087, 992, 862, 734, 695; **HRMS**: m/z calculated for $\text{C}_{25}\text{H}_{39}\text{N}_2\text{O}_7\text{S}^+$ $[\text{M}+\text{H}]^+$: 511.2472; found: 511.2468.

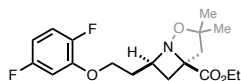


Ethyl 7-(((2-acetoxybenzoyl)oxy)methyl)-3,3-dimethyl-2-oxa-1-azabicyclo[3.2.0]heptane-5-carboxylate (3.112): Prepared according to GP-3.3 using **3.83** (43 mg, 0.25 mmol, 1.0 equiv.), allyl 2-acetoxybenzoate²³⁰ (83 mg, 0.38 mmol, 1.5 equiv.), *fac*-[Ir(dFppy)₃] (1.9 mg, 1 mol%) and MeCN (2.5 mL) with a reaction time of 23 h. $^1\text{H NMR}$ analysis of the crude reaction mixture revealed a diastereomer ratio of 2:1 and a regioisomer ratio of >20:1. Purification by flash column chromatography (1–40% EtOAc/ CH_2Cl_2) afforded the pure title compound as a pale-yellow oil

(92 mg, 94% combined yield; d.r. = 2:1). Characterization data for both diastereomers was obtained after separation by flash column chromatography (5–40% EtOAc/CH₂Cl₂).

exo-Diastereomer (major): ¹H NMR (500 MHz, CDCl₃): δ 8.07 (dd, *J* = 7.9, 1.7 Hz, 1H), 7.54 (td, *J* = 7.7, 1.7 Hz, 1H), 7.28 (td, *J* = 7.6, 1.2 Hz, 1H), 7.08 (dd, *J* = 8.1, 1.2 Hz, 1H), 4.45 – 4.35 (m, 2H), 4.25 (q, *J* = 7.1 Hz, 2H), 3.84 (tt, *J* = 8.7, 5.2 Hz, 1H), 2.90 (d, *J* = 13.0 Hz, 1H), 2.48 (d, *J* = 13.0 Hz, 1H), 2.42 (dd, *J* = 11.5, 9.0 Hz, 1H), 2.34 (s, 3H), 2.31 (dd, *J* = 11.5, 8.4 Hz, 1H), 1.53 (s, 3H), 1.28 (t, *J* = 7.1 Hz, 3H), 1.22 (s, 3H); ¹³C NMR (176 MHz, CDCl₃): δ 172.4, 169.9, 164.2, 151.0, 134.1, 132.1, 126.0, 123.8, 123.0, 87.8, 73.3, 66.1, 64.7, 61.8, 50.8, 29.5, 28.4, 27.5, 21.2, 14.2; IR (cm⁻¹): 2974, 2934, 1769, 1720, 1607, 1578, 1452, 1366, 1256, 1186, 1136, 1087, 1012, 917, 866, 817, 784, 755, 701, 671; HRMS: *m/z* calculated for C₂₀H₂₅NNaO₇⁺ [M+Na]⁺: 414.1523; found: 414.1527.

endo-Diastereomer (minor): ¹H NMR (500 MHz, CDCl₃): δ 8.03 (dd, *J* = 7.8, 1.5 Hz, 1H), 7.55 (td, *J* = 8.0, 1.6 Hz, 1H), 7.29 (td, *J* = 7.7, 1.0 Hz, 1H), 7.09 (dd, *J* = 8.1, 1.2 Hz, 1H), 4.70 (dd, *J* = 11.7, 8.1 Hz, 1H), 4.44 (dd, *J* = 11.8, 5.1 Hz, 1H), 4.34 – 4.24 (m, 3H), 2.89 (dd, *J* = 12.1, 8.3 Hz, 1H), 2.79 (d, *J* = 12.6 Hz, 1H), 2.41 (dd, *J* = 12.2, 8.0 Hz, 1H), 2.36 (s, 3H), 2.24 (d, *J* = 12.6 Hz, 1H), 1.45 (s, 3H), 1.33 (t, *J* = 7.1 Hz, 3H), 1.20 (s, 3H); ¹³C NMR (176 MHz, CDCl₃): δ 172.4, 169.9, 164.4, 150.9, 134.1, 132.1, 126.1, 123.9, 123.1, 84.3, 72.7, 63.9, 62.0, 57.7, 52.5, 33.5, 26.8, 25.9, 21.2, 14.3; IR (cm⁻¹): 2971, 1766, 1722, 1608, 1490, 1448, 1367, 1307, 1263, 1195, 1134, 1083, 1018, 969, 918, 840, 761, 711, 647; HRMS: *m/z* calculated for C₂₀H₂₆NO₇⁺ [M+H]⁺: 392.1704; found: 392.1707.



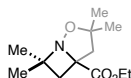
Ethyl 7-(2-(2,5-difluorophenoxy)ethyl)-3,3-dimethyl-2-oxa-1-azabicyclo[3.2.0]heptane-5-carboxylate (3.113): Prepared according to GP-3.3 using **3.83** (43 mg, 0.25 mmol, 1.0 equiv.),

S3.113 (69 mg, 0.38 mmol, 1.5 equiv.), *fac*-[Ir(dFppy)₃] (1.9 mg, 1 mol%) and MeCN (2.5 mL) with a reaction time of 20 h. ¹H NMR analysis of the crude reaction mixture revealed a diastereomer ratio of 2:1 and a regioisomer ratio of >20:1. Purification by flash column chromatography (1–20% EtOAc/CH₂Cl₂) afforded the pure title compound as a pale-yellow oil (83 mg, 93% combined yield; d.r. = 2:1). Characterization data for both diastereomers was obtained after separation by flash column chromatography (2–25% EtOAc/CH₂Cl₂).

exo-Diastereomer (major): ¹H NMR (500 MHz, CDCl₃): δ 7.01 – 6.93 (m, 1H), 6.74 – 6.67 (m, 1H), 6.57 – 6.50 (m, 1H), 4.23 (q, *J* = 7.1 Hz, 2H), 4.18 – 4.07 (m, 2H), 3.77 (p, *J* = 8.4 Hz, 1H), 2.86 (d, *J* = 12.9 Hz, 1H), 2.51 (d, *J* = 13.0 Hz, 1H), 2.44 (dd, *J* = 11.2, 8.8 Hz, 1H), 2.21 – 2.05 (m, 3H), 1.49 (s, 3H), 1.28 (t, *J* = 7.2 Hz, 3H), 1.20 (s, 3H); ¹³C NMR (126 MHz, CDCl₃): δ 172.7, 158.9 (dd, *J* = 241.9, 2.6 Hz), 149.0 (dd, *J* = 240.9, 3.2 Hz), 147.7 (dd, *J* = 12.4, 10.5 Hz), 116.1 (dd, *J* = 20.8, 10.2 Hz), 106.6 (dd, *J* = 23.9, 7.0 Hz), 103.0 (dd, *J* = 27.6, 1.9 Hz), 87.7, 73.6, 66.1, 64.0, 61.6, 51.0, 34.5, 30.1, 29.7, 28.6, 14.2; IR (cm⁻¹): 2974, 1726, 1625, 1512, 1469, 1432, 1368, 1309, 1249, 1186, 1156, 1099, 1053, 1019, 987, 836, 790, 721; HRMS: *m/z* calculated for C₁₈H₂₄F₂NO₄⁺ [M+H]⁺: 356.1668; found: 356.1665.

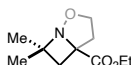
endo-Diastereomer (minor): ¹H NMR (500 MHz, CDCl₃): δ 6.98 (ddd, *J* = 10.8, 8.9, 5.3 Hz, 1H), 6.71 (ddd, *J* = 9.9, 6.8, 3.0 Hz, 1H), 6.59 – 6.50 (m, 1H), 4.28 (q, *J* = 7.1 Hz, 2H), 4.22 – 4.11 (m, 2H), 4.05 – 3.97 (m, 1H), 2.93 (dd, *J* = 11.9, 8.0 Hz, 1H), 2.75 (d, *J* = 12.4 Hz, 1H), 2.56 – 2.45 (m, 1H), 2.40 (dd, *J* = 11.9, 8.2 Hz, 1H), 2.23 (d, *J* = 12.4 Hz, 1H), 2.08 – 1.97 (m, 1H), 1.48 (s, 3H), 1.33 (t, *J* = 7.1 Hz, 3H), 1.22 (s, 3H); ¹³C NMR (126 MHz, CDCl₃): δ 172.7, 158.9 (dd, *J* = 241.9, 2.5 Hz), 149.0 (dd, *J* = 240.9, 3.2 Hz), 147.6 (dd, *J* = 12.7, 10.5 Hz), 116.1 (dd, *J* = 20.6, 10.1 Hz), 106.4 (dd, *J* = 23.9, 6.9 Hz), 102.6 (dd, *J* = 27.7, 2.0 Hz), 83.9, 72.7, 66.8, 61.9, 57.3, 53.0, 37.1, 31.3, 26.9, 26.0, 14.3; IR (cm⁻¹): 2975, 1727, 1625, 1512, 1473, 1433, 1368, 1314,

7.6, 6.6 Hz, 1H), 1.81 (dt, $J = 13.9, 5.7$ Hz, 1H), 1.45 (s, 3H), 1.35 – 1.28 (m, 6H), 1.15 (s, 3H), 0.86 (s, 9H), 0.02 (d, $J = 1.7$ Hz, 6H); $^{13}\text{C NMR}$ (126 MHz, CDCl_3): δ 173.6, 84.5, 70.8, 64.1, 61.6, 59.5, 52.0, 45.1, 40.1, 28.0, 26.0, 25.6, 22.1, 18.3, 14.3, -5.2, -5.3; **IR** (cm^{-1}): 2954, 2929, 2857, 1726, 1463, 1368, 1301, 1253, 1182, 1140, 1089, 1039, 1006, 938, 833, 774, 729, 663; **HRMS**: m/z calculated for $\text{C}_{19}\text{H}_{38}\text{NO}_4\text{Si}^+$ $[\text{M}+\text{H}]^+$: 372.2565; found: 272.2562.



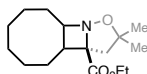
Ethyl 3,3,7,7-tetramethyl-2-oxa-1-azabicyclo[3.2.0]heptane-5-carboxylate (3.115): Prepared according to GP-3.3 using **3.83** (200 mg, 1.2 mmol, 1.0 equiv.), *fac*- $[\text{Ir}(\text{dFppy})_3]$ (1.8 mg, 0.2 mol%) and 1,2-dichloroethane (5 mL) with a reaction time of 24 h under an atmosphere of 2-methylpropene. Purification by flash column chromatography (1–10% EtOAc/ CH_2Cl_2) afforded the pure title compound as a yellow oil (244 mg, 92%).

$^1\text{H NMR}$ (500 MHz, CDCl_3): δ 4.37 – 4.16 (m, 2H), 2.84 (d, $J = 12.6$ Hz, 1H), 2.40 – 2.16 (m, 3H), 1.45 (s, 3H), 1.36 (s, 3H), 1.34 – 1.28 (m, 6H), 1.17 (s, 3H); $^{13}\text{C NMR}$ (126 MHz, CDCl_3): δ 173.5, 84.3, 69.4, 61.9, 61.6, 52.0, 41.6, 30.1, 27.6, 25.7, 24.4, 14.2; **IR** (cm^{-1}): ; **HRMS**: m/z calculated for $\text{C}_{12}\text{H}_{22}\text{NO}_3^+$ $[\text{M}+\text{H}]^+$: 228.1594; found: 228.1595.



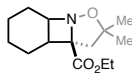
Ethyl 7,7-dimethyl-2-oxa-1-azabicyclo[3.2.0]heptane-5-carboxylate (3.143): Prepared according to GP-3.3 using **S3.85** (250 mg, 1.8 mmol, 1.0 equiv.), *fac*- $[\text{Ir}(\text{dFppy})_3]$ (2.7 mg, 0.2 mol%) and 1,2-dichloroethane (5 mL) with a reaction time of 24 h under an atmosphere of 2-methylpropene. Purification by flash column chromatography (1–10% EtOAc/ CH_2Cl_2) afforded the pure title compound as a yellow oil (301 mg, 87%).

¹H NMR (500 MHz, CDCl₃): δ 4.30 – 4.06 (m, 4H), 2.63 – 2.49 (m, 2H), 2.33 – 2.26 (m, 1H), 2.11 (d, *J* = 12.0 Hz, 1H), 1.31 (s, 3H), 1.28 (t, *J* = 7.1 Hz, 3H), 1.22 (s, 3H); **¹³C NMR** (126 MHz, CDCl₃): δ 173.4, 70.8, 69.4, 62.9, 61.7, 40.1, 39.8, 30.5, 22.7, 14.2; **IR** (cm⁻¹): 2967, 2872, 1727, 1446, 1367, 1318, 1281, 1215, 1175, 1135, 1096, 1027, 938, 877, 860, 782, 748, 703, 658; **HRMS**: *m/z* calculated for C₁₀H₁₈NO₃⁺ [M+H]⁺: 200.1281; found: 200.1277.



Ethyl 2,2-dimethyldecahydro-3aH-cycloocta[3,4]azeto[1,2-b]isoxazole-3a-carboxylate (3.116): Prepared according to GP-3.3 using **3.83** (43 mg, 0.25 mmol, 1.0 equiv.), cyclooctene (49 μL, 0.38 mmol, 1.5 equiv.), *fac*-[Ir(dFppy)₃] (1.9 mg, 1 mol%) and MeCN (2.5 mL) with a reaction time of 20 h. ¹H NMR analysis of the crude reaction mixture revealed a diastereomer ratio of 1.3:1. Purification by flash column chromatography (5–30% EtOAc/hexanes) afforded the pure title compound as a pale-yellow oil (67 mg, 95% combined yield; d.r. = 1.3:1). Characterization data for the *endo*-diastereomer was obtained after separation by flash column chromatography (5–30% EtOAc/hexanes).

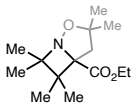
***endo*-Diastereomer (minor)**: **¹H NMR** (400 MHz, CDCl₃): δ 4.26 (qd, *J* = 7.1, 3.1 Hz, 2H), 3.19 (ddd, *J* = 11.1, 8.7, 3.8 Hz, 1H), 2.61 – 2.46 (m, 2H), 2.21 – 2.05 (m, 2H), 1.92 – 1.68 (m, 5H), 1.68 – 1.44 (m, 5H), 1.37 – 1.21 (m, 5H), 1.21 – 0.96 (m, 5H); **¹³C NMR** (176 MHz, CDCl₃): δ 173.4, 86.1, 77.5, 75.2, 61.4, 44.6, 40.1, 35.8, 30.3, 29.2, 28.6, 28.5, 28.2, 27.7, 26.6, 14.3; **IR** (cm⁻¹): 2972, 2923, 2853, 1745, 1721, 1454, 1366, 1300, 1250, 1210, 1180, 1148, 1123, 1041, 896, 856, 780, 732; **HRMS**: *m/z* calculated for C₁₆H₂₈NO₃⁺ [M+H]⁺: 282.2064; found: 282.2059.



Ethyl 2,2-dimethyloctahydro-3aH-benzo[3,4]azeto[1,2-b]isoxazole-3a-carboxylate (3.117):

Prepared according to GP-3.3 using **3.83** (43 mg, 0.25 mmol, 1.0 equiv.), cyclohexene (38 μ L, 0.38 mmol, 1.5 equiv.), *fac*-[Ir(dFppy)₃] (1.9 mg, 1 mol%) and MeCN (2.5 mL) with a reaction time of 20 h. ¹H NMR analysis of the crude reaction mixture revealed a diastereomer ratio of 1.2:1. Purification by flash column chromatography (5–30% EtOAc/CH₂Cl₂) afforded the pure title compound as a yellow oil (58 mg, 91% combined yield; d.r. = 1.2:1). Characterization data for the *exo*-diastereomer was obtained after separation by flash column chromatography (5–30% EtOAc/CH₂Cl₂).

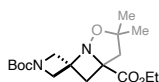
***exo*-Diastereomer (major):** ¹H NMR (700 MHz, CDCl₃): δ 4.36 – 4.23 (m, 2H), 3.57 (ddd, *J* = 8.4, 5.5, 1.7 Hz, 1H), 2.71 (d, *J* = 13.1 Hz, 1H), 2.63 (d, *J* = 13.1 Hz, 1H), 2.53 (q, *J* = 9.0 Hz, 1H), 2.03 – 1.96 (m, 1H), 1.91 – 1.83 (m, 1H), 1.65 – 1.59 (m, 1H), 1.55 – 1.51 (m, 2H), 1.51 (s, 3H), 1.47 – 1.39 (m, 1H), 1.34 – 1.27 (m, 4H), 1.18 (s, 3H), 1.03 – 0.92 (m, 1H); ¹³C NMR (176 MHz, CDCl₃): δ 172.6, 87.5, 78.2, 63.4, 61.2, 51.7, 33.8, 30.2, 29.0, 27.0, 25.3, 22.4, 20.9, 14.6; **IR** (cm⁻¹): 2966, 2935, 2861, 1737, 1464, 1366, 1289, 1252, 1178, 1139, 1045, 1015, 947, 861, 777, 728, 716; **HRMS**: *m/z* calculated for C₁₄H₂₄NO₃⁺ [M+H]⁺: 254.1751; found: 254.1750.



Ethyl 3,3,6,6,7,7-hexamethyl-2-oxa-1-azabicyclo[3.2.0]heptane-5-carboxylate (3.118):

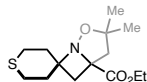
Prepared according to GP-3.3 using **3.83** (43 mg, 0.25 mmol, 1.0 equiv.), 2,3-dimethyl-2-butene (45 μ L, 0.38 mmol, 1.5 equiv.), *fac*-[Ir(dFppy)₃] (1.9 mg, 1 mol%) and MeCN (2.5 mL) with a reaction time of 22 h. Purification by flash column chromatography (3–30% EtOAc/CH₂Cl₂) afforded the pure title compound as a pale-yellow oil (41 mg, 64%).

¹H NMR (500 MHz, CDCl₃): δ 4.35 – 4.21 (m, 2H), 2.53 (d, *J* = 13.1 Hz, 1H), 2.45 (d, *J* = 13.1 Hz, 1H), 1.43 (s, 3H), 1.31 (t, *J* = 7.1 Hz, 3H), 1.20 (s, 3H), 1.18 (s, 3H), 1.16 (s, 3H), 1.12 (s, 3H), 1.08 (s, 3H); **¹³C NMR** (126 MHz, CDCl₃): δ 173.3, 84.0, 79.7, 68.0, 61.1, 47.6, 39.2, 28.4, 26.0, 25.7, 22.8, 21.7, 20.4, 14.5; **IR** (cm⁻¹): 2974, 2932, 1743, 1717, 1464, 1370, 1294, 1233, 1172, 1124, 1047, 1014, 937, 862, 837, 766, 726, 641; **HRMS**: *m/z* calculated for C₁₄H₂₆NO₃⁺ [M+H]⁺: 256.1907; found: 256.1908.



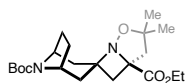
1-(*Tert*-butyl) 1'-ethyl 3',3'-dimethyl-4'-oxa-5'-azaspiro[azetidine-3,6'-bicyclo[3.2.0]heptane]-1,1'-dicarboxylate (3.119): Prepared according to GP-3.3 using **3.83** (43 mg, 0.25 mmol, 1.0 equiv.), *tert*-butyl 3-methyleneazetidine-1-carboxylate²²⁹ (64 mg, 0.38 mmol, 1.5 equiv.), *fac*-[Ir(dFppy)₃] (1.9 mg, 1 mol%) and MeCN (2.5 mL) with a reaction time of 24 h. ¹H NMR analysis of the crude reaction mixture revealed a regioisomer ratio of >20:1. Purification by flash column chromatography (5–30% EtOAc/CH₂Cl₂) afforded the pure title compound as a pale-yellow oil (85 mg, 99%).

¹H NMR (700 MHz, CDCl₃): δ 4.68 (d, *J* = 9.4 Hz, 1H), 4.26 (qd, *J* = 7.1, 1.4 Hz, 2H), 4.14 (d, *J* = 9.9 Hz, 1H), 3.91 (d, *J* = 9.9 Hz, 1H), 3.74 (d, *J* = 9.4 Hz, 1H), 2.85 (d, *J* = 12.8 Hz, 1H), 2.63 (d, *J* = 12.1 Hz, 1H), 2.57 (d, *J* = 12.0 Hz, 1H), 2.00 (d, *J* = 12.9 Hz, 1H), 1.46 (s, 3H), 1.42 (s, 9H), 1.31 (t, *J* = 7.1 Hz, 3H), 1.20 (s, 3H); **¹³C NMR** (176 MHz, CDCl₃): δ 171.9, 156.2, 86.8, 79.8, 71.9, 63.0, 61.8, 61.3, 56.2, 50.3, 37.1, 28.4, 27.9, 26.4, 14.2; **IR** (cm⁻¹): 2977, 2873, 2248, 1733, 1697, 1452, 1394, 1367, 1304, 1252, 1220, 1165, 1142, 1091, 1045, 916, 859, 772, 729, 646; **HRMS**: *m/z* calculated for C₁₇H₂₈N₂NaO₅⁺ [M+Na]⁺: 363.1890; found: 363.1898.



Ethyl 3,3-dimethyl-4-oxa-5-azaspiro[bicyclo[3.2.0]heptane-6,4'-thiopyran]-1-carboxylate (3.120): Prepared according to GP-3.3 using **3.83** (43 mg, 0.25 mmol, 1.0 equiv.), 4-methylenetetrahydro-2*H*-thiopyran²²² (43 mg, 0.38 mmol, 1.5 equiv.), *fac*-[Ir(dFppy)₃] (1.9 mg, 1 mol%) and MeCN (2.5 mL) with a reaction time of 20 h. ¹H NMR analysis of the crude reaction mixture revealed a regioisomer ratio of >20:1. Purification by flash column chromatography (3–50% EtOAc/CH₂Cl₂) afforded the pure title compound as a pale-yellow oil (53 mg, 74%).

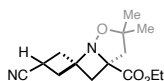
¹H NMR (700 MHz, CDCl₃): δ 4.33 – 4.20 (m, 2H), 2.89 (d, *J* = 12.6 Hz, 1H), 2.85 – 2.75 (m, 2H), 2.54 – 2.45 (m, 2H), 2.27 – 2.16 (m, 4H), 2.10 (ddd, *J* = 12.4, 8.9, 3.0 Hz, 1H), 2.02 (ddd, *J* = 13.1, 7.4, 2.7 Hz, 1H), 1.98 (ddd, *J* = 13.8, 7.8, 2.9 Hz, 1H), 1.43 (s, 3H), 1.32 (t, *J* = 7.1 Hz, 3H), 1.17 (s, 3H); ¹³C NMR (176 MHz, CDCl₃): δ 173.2, 84.4, 69.9, 63.1, 61.7, 52.3, 39.9, 39.7, 35.0, 27.4, 25.5, 25.11, 25.06, 14.2; IR (cm⁻¹): 2976, 2933, 2212, 1726, 1456, 1429, 1368, 1304, 1232, 1187, 1148, 1098, 1031, 912, 863, 827, 785, 725, 643; HRMS: *m/z* calculated for C₁₄H₂₄NO₃S⁺ [M+H]⁺: 286.1471; found: 286.1470.



8'-(*Tert*-butyl) 1-ethyl 3,3-dimethyl-4-oxa-5,8'-diazaspiro[bicyclo[3.2.0]heptane-6,3'-bicyclo[3.2.1]octane]-1,8'-dicarboxylate (3.121): Prepared according to GP-3.3 using **3.83** (43 mg, 0.25 mmol, 1.0 equiv.), *tert*-butyl 3-methylene-8-azabicyclo[3.2.1]octane-8-carboxylate²³¹ (84 mg, 0.38 mmol, 1.5 equiv.), *fac*-[Ir(dFppy)₃] (1.9 mg, 1 mol%) and MeCN (2.5 mL) with a reaction time of 24 h. ¹H NMR analysis of the crude reaction mixture revealed a diastereomer ratio of 5:1 and a regioisomer ratio of >20:1. Purification by flash column chromatography (2–35% EtOAc/CH₂Cl₂) afforded the pure major diastereomer as a colorless oil

(77 mg, 78%) and the pure minor diastereomer as a pale-yellow oil (14 mg, 14%). Characterization is provided for the major (1*S**,1'*R**,5'*S**,6'*r*'*)-diastereomer.

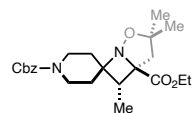
(1*S,1'*R**,5'*S**,6'*r*'*)-Diastereomer (major):** ¹H NMR (700 MHz, CDCl₃): δ 4.34 – 4.25 (m, 1H), 4.24 – 4.18 (m, 1H), 4.10 (b, 2H), 2.79 (d, *J* = 12.5 Hz, 1H), 2.53 (b, 1H), 2.27 (m, 2H), 2.20 (b, 2H), 2.12 (d, *J* = 12.3 Hz, 2H), 1.93 – 1.54 (m, 4H), 1.48 (s, 3H) 1.45 (s, 9H), 1.31 (t, *J* = 7.1 Hz, 3H), 1.18 (s, 3H); ¹³C NMR (176 MHz, CDCl₃): δ 173.4, 153.4, 84.6, 79.1, 70.0, 62.0, 61.6, 52.7 (dd, *J* = 144.5, 18.4 Hz, 3C), 43.4 (d, *J* = 148.1 Hz), 43.0, 37.1 (d, *J* = 157.1 Hz), 28.6, 27.6, 27.1 (d, *J* = 103.1 Hz), 26.0, 25.9 (d, *J* = 121.2 Hz), 14.2; **IR** (cm⁻¹): 2974, 1726, 1686, 1452, 1413, 1363, 1329, 1307, 1257, 1169, 1095, 1075, 1010, 971, 879, 846, 735; **HRMS**: *m/z* calculated for C₂₁H₃₅N₂O₅⁺ [M+H]⁺: 395.2540; found: 395.2535.



Ethyl 3'-cyano-3,3-dimethyl-4-oxa-5-azaspiro[bicyclo[3.2.0]heptane-6,1'-cyclobutane]-1-carboxylate (3.122): Prepared according to GP-3.3 using **3.83** (43 mg, 0.25 mmol, 1.0 equiv.), 3-methylenecyclobutane-1-carbonitrile (35 mg, 0.38 mmol, 1.5 equiv.), *fac*-[Ir(dFppy)₃] (1.9 mg, 1 mol%) and MeCN (2.5 mL) with a reaction time of 20 h. ¹H NMR analysis of the crude reaction mixture revealed a diastereomer ratio of 1:1 and a regioisomer ratio of >20:1. Purification by flash column chromatography (3–50% EtOAc/CH₂Cl₂) afforded the pure title compound as a pale-yellow oil (45 mg, 68% combined yield; d.r. = 1:1). Characterization data was obtained for a 1:1 mixture of diastereomers.

¹H NMR (700 MHz, CDCl₃): δ 4.26 (q, *J* = 7.1 Hz, 4H), 3.30 – 3.24 (m, 2H), 3.01 (tt, *J* = 9.3, 5.5 Hz, 1H), 2.87 – 2.81 (m, 2H), 2.83 – 2.79 (m, 1H), 2.75 (ddd, *J* = 11.9, 9.4, 1.8 Hz, 1H), 2.68 (dd, *J* = 12.2, 10.1 Hz, 1H), 2.61 – 2.53 (m, 2H), 2.53 – 2.42 (m, 4H), 2.31 – 2.25 (m, 2H), 2.08 (d, *J* = 12.9 Hz, 2H), 1.44 (d, *J* = 4.6 Hz, 6H), 1.31 (td, *J* = 7.1, 2.5 Hz, 6H), 1.19 (d, *J* = 2.2 Hz,

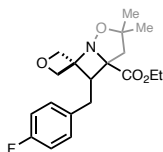
6H); ^{13}C NMR (176 MHz, CDCl_3): δ 172.1, 172.0, 122.5, 121.2, 86.7, 86.6, 71.89, 71.87, 66.7, 65.3, 61.8 (2C), 50.61, 50.55, 39.6, 39.4, 38.4, 37.4, 35.6, 34.7, 28.0, 27.9, 26.4, 26.2, 16.2, 14.4, 14.2 (2C); IR (cm^{-1}): 2977, 2237, 1724, 1456, 1369, 1281, 1221, 1185, 1127, 1050, 1022, 957, 856, 779, 718; HRMS: m/z calculated for $\text{C}_{14}\text{H}_{21}\text{N}_2\text{O}_3^+$ $[\text{M}+\text{H}]^+$: 265.1547; found: 265.1551.



1'-Benzyl 1-ethyl 3,3,7-trimethyl-4-oxa-5-azaspiro[bicyclo[3.2.0]heptane-6,4'-piperidine]-1,1'-dicarboxylate (3.123): Prepared according to GP-3.3 using **3.83** (43 mg, 0.25 mmol, 1.0 equiv.), **S3.123** (92 mg, 0.38 mmol, 1.5 equiv.), *fac*-[Ir(dFppy)₃] (1.9 mg, 1 mol%) and MeCN (2.5 mL) with a reaction time of 24 h. ^1H NMR analysis of the crude reaction mixture revealed a diastereomer ratio of 3:1 and a regioisomer ratio of 8:1. Purification by flash column chromatography (5–50% EtOAc/ CH_2Cl_2) afforded the pure title compound as a pale-yellow oil (82 mg, 78% combined yield; d.r. = 2.4:1). Characterization data was obtained for a 2.4:1 mixture of *exo/endo* diastereomers.

^1H NMR (700 MHz, CDCl_3): δ 7.37 – 7.29 (m, 17H; major+minor), 5.17 – 5.03 (m, 6.8H), 4.37 – 4.15 (m, 6.8H; major+minor), 3.82 (b, 6.8H; major+minor), 3.35 (b, 6.8H), 2.87 (d, $J = 12.7$ Hz, 1H; minor), 2.54 (d, $J = 12.8$ Hz, 2.4H; major), 2.45 (q, $J = 7.5$ Hz, 1H; minor), 2.30 (b, 5.8H; major+minor), 2.13 (b, 1H; minor), 1.90 (b, 5.8H; major+minor), 1.67 – 1.37 (m, 17H; major+minor), 1.34 – 1.28 (m, 10.2H; major+minor), 1.17 (s, 7.2H; major), 1.13 (s, 3H; minor), 1.03 (d, $J = 7.3$ Hz, 7.2H; major), 1.00 (d, $J = 7.5$ Hz, 3H; minor); ^{13}C NMR (176 MHz, CDCl_3): δ 173.6, 172.0, 155.3 (2C), 136.93, 136.91, 128.5 (2C), 128.0, 127.9, 127.9, 127.8, 84.1, 83.9, 74.8, 74.6, 67.00, 66.98, 66.0, 63.3, 61.5, 61.4, 54.0, 45.3, 44.4, 41.5 (2C), 40.4, 40.04, 40.02, 38.6 (d, $J = 50.2$ Hz), 34.9 (d, $J = 50.9$ Hz), 32.4 (d, $J = 58.5$ Hz), 28.8 (d, $J = 56.1$ Hz), 27.8, 27.5, 25.6,

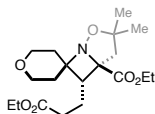
25.3, 14.5, 14.2, 10.8, 10.7; **IR** (cm⁻¹): 2976, 2248, 1690, 1432, 1368, 1282, 1235, 1212, 1144, 1090, 1029, 908, 867, 724, 697, 645; **HRMS**: *m/z* calculated for C₂₃H₃₃N₂O₅⁺ [M+H]⁺: 417.2384; found: 417.2379.



Ethyl 7-(4-fluorobenzyl)-3,3-dimethyl-4-oxa-5-azaspiro[bicyclo[3.2.0]heptane-6,3'-oxetane]-1-carboxylate (3.124): Prepared according to GP-3.3 using **3.83** (43 mg, 0.25 mmol, 1.0 equiv.), **S3.124** (67 mg, 0.38 mmol, 1.5 equiv.), *fac*-[Ir(dFppy)₃] (1.9 mg, 1 mol%) and MeCN (2.5 mL) with a reaction time of 22 h. ¹H NMR analysis of the crude reaction mixture revealed a diastereomer ratio of 1:1 and a regioisomer ratio of 8:1. Purification by flash column chromatography (2–40% EtOAc/CH₂Cl₂) afforded the pure title compound as a pale-yellow oil (46 mg, 52% combined yield; d.r. = 1:1). Characterization data was obtained for a 1:1 mixture of diastereomers (A/B).

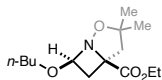
¹H NMR (500 MHz, CDCl₃): δ 7.19 – 7.09 (m, 4H), 6.97 (t, *J* = 8.2 Hz, 4H), 5.32 (d, *J* = 7.1 Hz, 1H), 5.26 (d, *J* = 7.3 Hz, 1H), 4.84 (d, *J* = 7.7 Hz, 1H), 4.78 (d, *J* = 7.8 Hz, 1H), 4.67 (d, *J* = 7.5 Hz, 2H), 4.44 (d, *J* = 7.1 Hz, 1H), 4.41 (d, *J* = 7.7 Hz, 1H), 4.21 – 4.08 (m, 2H), 4.06 – 3.92 (m, 2H), 3.17 (t, *J* = 8.1 Hz, 1H), 3.09 – 2.93 (m, 2H), 2.89 – 2.78 (m, 4H), 2.68 (d, *J* = 12.9 Hz, 1H), 1.90 (d, *J* = 12.9 Hz, 1H), 1.84 (d, *J* = 12.9 Hz, 1H), 1.41 (d, *J* = 10.8 Hz, 6H), 1.19 (t, *J* = 7.1 Hz, 3H), 1.16 – 1.09 (m, 9H); **¹³C NMR** (126 MHz, CDCl₃): δ 171.7, 170.4, 161.8 (d, *J* = 245.0 Hz), 161.7 (d, *J* = 245.2 Hz), 133.7 (d, *J* = 3.4 Hz), 133.3 (d, *J* = 3.5 Hz), 130.2 (d, *J* = 7.7 Hz), 129.7 (d, *J* = 8.0 Hz), 115.7 (d, *J* = 10.8 Hz), 115.5 (d, *J* = 10.9 Hz), 86.6, 85.9, 81.8, 78.3, 77.7, 75.9, 75.6, 72.9, 71.8, 70.2, 61.7, 61.7, 51.7, 48.0, 43.8, 42.7, 33.1, 31.7, 28.1, 27.8, 26.3, 26.1, 14.1, 14.0; **IR** (cm⁻¹): 2975, 2940, 2870, 1727, 1602, 1510, 1456, 1370, 1305, 1221, 1178, 1145, 1117, 1035,

975, 826, 777, 726, 709; **HRMS**: m/z calculated for $C_{19}H_{25}FNO_4^+$ $[M+H]^+$: 350.1762; found: 350.1760.



Ethyl 7-(3-ethoxy-3-oxopropyl)-3,3-dimethyltetrahydro-4-oxa-5-azaspiro[bicyclo[3.2.0]heptane-6,4'-pyran]-1-carboxylate (3.125): Prepared according to GP-3.3 using **3.83** (43 mg, 0.25 mmol, 1.0 equiv.), ethyl 4-(tetrahydro-4*H*-pyran-4-ylidene)butanoate²³² (75 mg, 0.38 mmol, 1.5 equiv.), *fac*-[Ir(dFppy)₃] (1.9 mg, 1 mol%) and MeCN (2.5 mL) with a reaction time of 24 h. ¹H NMR analysis of the crude reaction mixture revealed a diastereomer ratio of 4:1 and a regioisomer ratio of 13:1. Purification by flash column chromatography (5–85% EtOAc/CH₂Cl₂) afforded the pure title compound as a pale-yellow oil (72 mg, 78% combined yield; d.r. = 4:1). Characterization data was obtained for the *exo*-diastereomer after purification by flash column chromatography (40–60% EtOAc/hexanes).

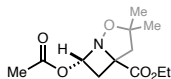
***exo*-Diastereomer (major)**: ¹H NMR (700 MHz, CDCl₃): δ 4.30 (dq, $J = 10.8, 7.1$ Hz, 1H), 4.20 (dq, $J = 10.8, 7.1$ Hz, 1H), 4.12 (q, $J = 7.1$ Hz, 2H), 3.81 (td, $J = 11.4, 2.4$ Hz, 1H), 3.78 – 3.70 (m, 3H), 2.63 (d, $J = 12.7$ Hz, 1H), 2.32 – 2.22 (m, 2H), 2.21 – 2.13 (m, 2H), 1.91 (dq, $J = 13.7, 2.7$ Hz, 1H), 1.86 – 1.78 (m, 3H), 1.78 – 1.72 (m, 1H), 1.69 – 1.62 (m, 1H), 1.40 (s, 3H), 1.29 (t, $J = 7.1$ Hz, 3H), 1.25 (t, $J = 7.1$ Hz, 3H), 1.16 (s, 3H); ¹³C NMR (176 MHz, CDCl₃): δ 173.7, 172.8, 84.1, 74.3, 65.4 (2C), 64.2, 61.8, 60.7, 45.1, 44.5, 39.8, 31.5, 29.7, 27.9, 25.7, 20.8, 14.3, 14.2; **IR** (cm⁻¹): 2972, 2874, 1729, 1463, 1368, 1301, 1231, 1179, 1117, 1101, 1040, 1024, 954, 848, 783, 731; **HRMS**: m/z calculated for $C_{19}H_{32}NO_6^+$ $[M+H]^+$: 370.2224; found: 370.2223.



Ethyl 7-butoxy-3,3-dimethyl-2-oxa-1-azabicyclo[3.2.0]heptane-5-carboxylate (3.126):

Prepared according to GP-3.3 using **3.83** (43 mg, 0.25 mmol, 1.0 equiv.), *n*-butyl vinyl ether (49 μ L, 0.38 mmol, 1.5 equiv.), *fac*-[Ir(dFppy)₃] (1.9 mg, 1 mol%) and MeCN (2.5 mL) with a reaction time of 22 h. ¹H NMR analysis of the crude reaction mixture revealed a diastereomer ratio of >10:1 and a regioisomer ratio of >20:1. Purification by flash column chromatography (2–30% EtOAc/hexanes) afforded the pure title compound as a colorless oil (31 mg, 46%).

¹H NMR (700 MHz, CDCl₃): δ 4.57 (t, *J* = 7.1 Hz, 1H), 4.24 (q, *J* = 7.1 Hz, 2H), 3.79 (dt, *J* = 9.3, 6.8 Hz, 1H), 3.41 (dt, *J* = 9.3, 6.9 Hz, 1H), 2.85 (d, *J* = 13.0 Hz, 1H), 2.52 (dd, *J* = 11.8, 7.4 Hz, 1H), 2.32 (dd, *J* = 11.8, 6.8 Hz, 1H), 2.25 (d, *J* = 13.0 Hz, 1H), 1.57 (p, *J* = 7.0 Hz, 2H), 1.49 (s, 3H), 1.35 (hd, *J* = 7.3, 2.2 Hz, 2H), 1.29 (t, *J* = 7.1 Hz, 3H), 1.22 (s, 3H), 0.89 (t, *J* = 7.4 Hz, 3H); ¹³C NMR (176 MHz, CDCl₃): δ 172.4, 94.8, 88.9, 68.0, 67.6, 61.8, 50.9, 31.6, 31.3, 29.6, 28.4, 19.3, 14.2, 14.0; IR (cm⁻¹): 2962, 2934, 2873, 1727, 1456, 1368, 1298, 1256, 1191, 1157, 1110, 1025, 984, 913, 866, 788, 746, 679; HRMS: *m/z* calculated for C₁₄H₂₆NO₄⁺ [M+H]⁺: 272.1856; found: 272.1851.

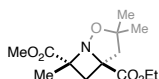


Ethyl 7-acetoxy-3,3-dimethyl-2-oxa-1-azabicyclo[3.2.0]heptane-5-carboxylate (3.127):

Prepared according to GP-3.3 using **3.83** (43 mg, 0.25 mmol, 1.0 equiv.), vinyl acetate (35 μ L, 0.38 mmol, 1.5 equiv.), *fac*-[Ir(dFppy)₃] (1.9 mg, 1 mol%) and MeCN (2.5 mL) with a reaction time of 22 h. ¹H NMR analysis of the crude reaction mixture revealed a diastereomer ratio of 1.4:1 and a regioisomer ratio of >20:1. Purification by flash column chromatography (1–30% EtOAc/CH₂Cl₂) afforded the pure title compound as a pale-yellow oil (56 mg, 87% combined

yield; d.r. = 1.4:1). Characterization data was obtained for a 1.4:1 mixture of *endo/exo* diastereomers.

¹H NMR (500 MHz, CDCl₃): δ 5.85 (dd, *J* = 5.8, 2.3 Hz, 1.4H; major), 5.71 (t, *J* = 7.1 Hz, 1H; minor), 4.28 – 4.20 (m, 4.8H; major+minor), 2.88 – 2.75 (m, 3.8H; major+minor), 2.67 (dd, *J* = 12.0, 7.5 Hz, 1H; minor), 2.45 (d, *J* = 12.7 Hz, 1.4H; major), 2.35 (dd, *J* = 12.1, 6.7 Hz, 1H; minor), 2.33 – 2.26 (m, 2.4H; major+minor), 2.14 (s, 4.2H; major), 2.05 (s, 3H; minor), 1.51 (s, 3H; minor), 1.44 (s, 4.2H; major), 1.28 (t, *J* = 7.1 Hz, 7.2H; major+minor), 1.20 (s, 3H; minor), 1.16 (s, 4.2H; major); **¹³C NMR** (126 MHz, CDCl₃): δ 172.3, 171.6, 169.6, 169.1, 89.5, 88.1, 87.7, 84.0, 74.9, 68.9, 62.0, 61.8, 50.4, 50.3, 33.0, 31.4, 29.3, 28.2 (2C), 26.4, 21.01, 20.97, 14.2, 14.1; **IR** (cm⁻¹): 2976, 2931, 1748, 1727, 1455, 1368, 1315, 1217, 1179, 1148, 1118, 1087, 1039, 1016, 913, 865, 828, 777, 692; **HRMS**: *m/z* calculated for C₁₂H₁₉NNaO₅⁺ [M+Na]⁺: 280.1155; found: 280.1153.

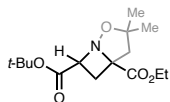


5-Ethyl 7-methyl 3,3,7-trimethyl-2-oxa-1-azabicyclo[3.2.0]heptane-5,7-dicarboxylate (3.128): Prepared according to GP-3.3 using **3.83** (43 mg, 0.25 mmol, 1.0 equiv.), methyl methacrylate (40 μL, 0.38 mmol, 1.5 equiv.), *fac*-[Ir(dFppy)₃] (1.9 mg, 1 mol%) and MeCN (2.5 mL) with a reaction time of 24 h. ¹H NMR analysis of the crude reaction mixture revealed a diastereomer ratio of 5:1 and a regioisomer ratio of >20:1. Purification by flash column chromatography (5–50% EtOAc/hexanes) afforded the pure major diastereomer as a pale-yellow oil (56 mg, 82%) and the pure minor diastereomer as a pale-yellow oil (13 mg, 19%).

***exo*(C₇-Me)-Diastereomer (major)**: **¹H NMR** (700 MHz, CDCl₃): δ 4.31 – 4.18 (m, 2H), 3.72 (s, 3H), 3.19 (d, *J* = 12.0 Hz, 1H), 2.72 (d, *J* = 12.4 Hz, 1H), 2.54 (d, *J* = 12.4 Hz, 1H), 2.27 (d, *J* = 12.0 Hz, 1H), 1.59 (s, 3H), 1.32 – 1.26 (m, 6H), 1.09 (s, 3H); **¹³C NMR** (176 MHz, CDCl₃):

δ 172.8, 171.8, 85.5, 70.2, 68.0, 61.8, 52.4, 50.0, 36.5, 27.0, 26.0, 24.2, 14.2; **IR** (cm^{-1}): 2976, 2361, 2338, 1729, 1451, 1368, 1297, 1255, 1188, 1141, 1094, 1027, 959, 863, 784, 685; **HRMS**: m/z calculated for $\text{C}_{13}\text{H}_{22}\text{NO}_5^+$ $[\text{M}+\text{H}]^+$: 272.1492; found: 272.1493.

endo(C₇-Me)-Diastereomer (minor): **¹H NMR** (700 MHz, CDCl_3): δ 4.31 – 4.19 (m, 2H), 3.77 (s, 3H), 3.04 (d, $J = 12.1$ Hz, 1H), 2.88 (d, $J = 12.8$ Hz, 1H), 2.31 (d, $J = 12.9$ Hz, 1H), 2.27 (d, $J = 12.1$ Hz, 1H), 1.54 (s, 3H), 1.48 (s, 3H), 1.29 (t, $J = 7.1$ Hz, 3H), 1.20 (s, 3H); **¹³C NMR** (176 MHz, CDCl_3): δ 174.3, 172.5, 86.0, 70.9, 66.4, 61.9, 52.8, 51.2, 37.0, 28.1, 25.6, 20.6, 14.2; **IR** (cm^{-1}): 2977, 2361, 2338, 1733, 1457, 1369, 1295, 1252, 1185, 1138, 1105, 1024, 994, 857, 771, 728, 682; **HRMS**: m/z calculated for $\text{C}_{13}\text{H}_{22}\text{NO}_5^+$ $[\text{M}+\text{H}]^+$: 272.1492; found: 272.1493.

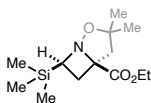


7-(Tert-butyl) 5-ethyl 3,3-dimethyl-2-oxa-1-azabicyclo[3.2.0]heptane-5,7-dicarboxylate (3.129): Prepared according to GP-3.3 using **3.83** (43 mg, 0.25 mmol, 1.0 equiv.), *tert*-butyl acrylate (55 μL , 0.38 mmol, 1.5 equiv.), *fac*-[Ir(dFppy)₃] (1.9 mg, 1 mol%) and MeCN (2.5 mL) with a reaction time of 42 h. ¹H NMR analysis of the crude reaction mixture revealed a diastereomer ratio of 1:1 and a regioisomer ratio of >20:1. Purification by flash column chromatography (5–35% EtOAc/hexanes) afforded the pure *endo*-diastereomer as a colorless oil (34 mg, 45%) and the pure *exo*-diastereomer as a white solid (37 mg, 49%).

exo-Diastereomer: **¹H NMR** (700 MHz, CDCl_3): δ 4.26 (qd, $J = 7.1, 1.1$ Hz, 2H), 3.97 (dd, $J = 9.6, 8.6$ Hz, 1H), 2.88 (d, $J = 13.0$ Hz, 1H), 2.60 (dd, $J = 11.5, 8.6$ Hz, 1H), 2.51 – 2.42 (m, 2H), 1.56 (s, 3H), 1.48 (s, 9H), 1.31 (t, $J = 7.1$ Hz, 3H), 1.26 (s, 3H); **¹³C NMR** (176 MHz, CDCl_3): δ 172.1, 169.6, 88.5, 81.9, 73.3, 66.4, 61.8, 50.8, 29.9, 28.6, 28.1, 27.9, 14.2; **IR** (cm^{-1}): 2977,

1727, 1455, 1365, 1314, 1225, 1144, 1021, 944, 911, 844, 754, 671; **HRMS**: m/z calculated for $C_{15}H_{25}NNaO_5^+$ $[M+H]^+$: 322.1625; found: 322.1624.

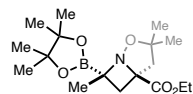
endo-Diastereomer: 1H NMR (700 MHz, $CDCl_3$): δ 4.42 (dd, $J = 8.2, 6.5$ Hz, 1H), 4.31 – 4.23 (m, 2H), 2.88 (dd, $J = 12.2, 6.5$ Hz, 1H), 2.73 (d, $J = 12.3$ Hz, 1H), 2.64 – 2.56 (m, 2H), 1.48 (s, 9H), 1.38 (s, 3H), 1.32 (t, $J = 7.1$ Hz, 3H), 1.13 (s, 3H); ^{13}C NMR (176 MHz, $CDCl_3$): δ 172.7, 168.4, 85.0, 82.0, 73.7, 62.6, 61.8, 50.8, 29.7, 28.2, 26.9, 25.7, 14.2; **IR** (cm^{-1}): 2974, 2933, 1718, 1452, 1367, 1308, 1247, 1186, 1147, 1116, 1055, 1015, 950, 908, 847, 776, 725, 680; **HRMS**: m/z calculated for $C_{15}H_{25}NNaO_5^+$ $[M+H]^+$: 322.1625; found: 322.1625.



Ethyl 3,3-dimethyl-7-(trimethylsilyl)-2-oxa-1-azabicyclo[3.2.0]heptane-5-carboxylate

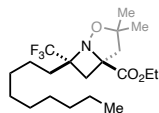
(3.130): Prepared according to GP-3.3 using **3.83** (43 mg, 0.25 mmol, 1.0 equiv.), vinyltrimethylsilane (55 μ L, 0.38 mmol, 1.5 equiv.), *fac*-[Ir(dFppy)₃] (1.9 mg, 1 mol%) and MeCN (2.5 mL) with a reaction time of 23 h. 1H NMR analysis of the crude reaction mixture revealed a diastereomer ratio of >10:1 and a regioisomer ratio of >20:1. Purification by flash column chromatography (2–20% EtOAc/hexanes) afforded the pure title compound as a pale-yellow oil (36 mg, 53%).

1H NMR (700 MHz, $CDCl_3$): δ 4.27 – 4.15 (m, 2H), 3.27 (t, $J = 10.2$ Hz, 1H), 2.85 (d, $J = 12.8$ Hz, 1H), 2.62 (d, $J = 12.8$ Hz, 1H), 2.26 (dd, $J = 10.3, 2.0$ Hz, 2H), 1.55 (s, 3H), 1.29 (t, $J = 7.1$ Hz, 3H), 1.20 (s, 3H), 0.06 (s, 9H); ^{13}C NMR (176 MHz, $CDCl_3$): δ 173.0, 86.6, 77.9, 61.4, 59.4, 51.5, 30.2, 28.8, 26.2, 14.2, -4.1; **IR** (cm^{-1}): 2973, 1727, 1454, 1367, 1313, 1247, 1215, 1181, 1144, 1040, 988, 915, 835, 728, 693; **HRMS**: m/z calculated for $C_{13}H_{26}NO_3Si^+$ $[M+H]^+$: 272.1676; found: 272.1673.



Ethyl 3,3,7-trimethyl-7-(4,4,5,5-tetramethyl-1,3,2-dioxaborolan-2-yl)-2-oxa-1-azabicyclo[3.2.0]heptane-5-carboxylate (3.131): Prepared according to GP-3.3 using **3.83** (43 mg, 0.25 mmol, 1.0 equiv.), isopropenylboronic acid pinacol ester (71 μ L, 0.38 mmol, 1.5 equiv.), *fac*-[Ir(dFppy)₃] (1.9 mg, 1 mol%) and MeCN (2.5 mL) with a reaction time of 18 h. ¹H NMR analysis of the crude reaction mixture revealed a diastereomer ratio of 5:1 and a regioisomer ratio of 17:1. The yield was determined to be 77% by ¹H NMR analysis of the crude reaction mixture using mesitylene as the internal standard. Characterization data for the *exo*(C₇-Me)-diastereomer was obtained after purification by flash column chromatography (florisil; 0–30% EtOAc/hexanes).

***exo*(C₇-Me)-Diastereomer (major):** ¹H NMR (700 MHz, CDCl₃): δ 4.33 – 4.17 (m, 2H), 2.81 (d, *J* = 11.3 Hz, 1H), 2.75 (d, *J* = 12.1 Hz, 1H), 2.54 (d, *J* = 12.1 Hz, 1H), 2.08 (d, *J* = 11.3 Hz, 1H), 1.42 (s, 6H), 1.32 (t, *J* = 7.1 Hz, 3H), 1.28 (s, 6H), 1.24 (s, 6H), 1.08 (s, 3H); ¹³C NMR (176 MHz, CDCl₃): δ 173.7, 84.3, 84.1, 70.4, 61.6, 51.3, 37.2, 26.4, 25.7, 25.5, 24.5, 14.3; **IR** (cm⁻¹): 2978, 1724, 1474, 1453, 1367, 1321, 1270, 1141, 983, 968, 926, 852, 733, 700, 674; **HRMS**: *m/z* calculated for C₁₇H₃₁BNO₅⁺ [M+H]⁺: 340.2290; found: 340.2295. The boron bearing quaternary carbon was not observed by ¹³C NMR.

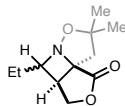


Ethyl 3,3-dimethyl-7-octyl-7-(trifluoromethyl)-2-oxa-1-azabicyclo[3.2.0]heptane-5-carboxylate (3.132): Prepared according to GP-3.3 using **3.83** (43 mg, 0.25 mmol, 1.0 equiv.), 2-(trifluoromethyl)undec-1-ene²³³ (84 mg, 0.38 mmol, 1.5 equiv.), *fac*-[Ir(dFppy)₃] (1.9 mg, 1 mol%) and MeCN (2.5 mL) with a reaction time of 19 h. ¹H NMR analysis of the crude reaction

mixture revealed a diastereomer ratio of 4:1 and a regioisomer ratio of >20:1. Purification by flash column chromatography (2–15% EtOAc/hexanes) afforded the pure *endo*(C₇-CF₃)-diastereomer as a colorless oil (68 mg, 69%) and the pure *exo*(C₇-CF₃)-diastereomer as a colorless oil (19 mg, 19%).

***endo*(CF₃)-Diastereomer (major):** ¹H NMR (700 MHz, CDCl₃): δ 4.33 – 4.21 (m, 2H), 2.77 (d, *J* = 12.5 Hz, 1H), 2.73 (d, *J* = 12.8 Hz, 1H), 2.49 (dd, *J* = 12.8, 2.9 Hz, 2H), 1.94 – 1.81 (m, 2H), 1.55 – 1.47 (b, 2H), 1.44 (s, 3H), 1.33 (t, *J* = 7.1 Hz, 3H), 1.32 – 1.21 (m, 12H), 1.18 (s, 3H), 0.87 (t, *J* = 7.0 Hz, 3H); ¹³C NMR (176 MHz, CDCl₃): δ 172.6, 125.5 (q, *J* = 283.4 Hz), 85.7, 69.7, 66.4 (q, *J* = 25.6 Hz), 62.0, 50.6, 35.9, 34.3 (d, *J* = 2.5 Hz), 32.0, 30.3, 29.7, 29.6, 29.4, 27.2, 25.5, 23.1, 22.8, 14.2 (2C); IR (cm⁻¹): 2925, 2855, 1731, 1459, 1369, 1306, 1252, 1190, 1173, 1141, 1114, 1096, 1055, 943, 882, 784, 722, 678; HRMS: *m/z* calculated for C₂₀H₃₅F₃NO₃⁺ [M+H]⁺: 394.2564; found: 394.2561.

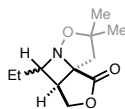
***exo*(CF₃)-Diastereomer (minor):** ¹H NMR (700 MHz, CDCl₃): δ 4.34 – 4.21 (m, 2H), 2.83 (d, *J* = 12.9 Hz, 1H), 2.75 (d, *J* = 12.6 Hz, 1H), 2.32 (d, *J* = 12.9 Hz, 1H), 2.28 (d, *J* = 12.6 Hz, 1H), 1.96 (t, *J* = 11.0 Hz, 1H), 1.79 (t, *J* = 13.9 Hz, 1H), 1.54 – 1.50 (m, 1H), 1.48 (s, 3H), 1.35 – 1.20 (m, 19H), 0.87 (t, *J* = 7.0 Hz, 3H); ¹³C NMR (176 MHz, CDCl₃): δ 172.4, 126.1 (q, *J* = 281 Hz), 85.7, 70.8, 66.6 (q, *J* = 27.9 Hz), 62.0, 52.5, 33.87 (d, *J* = 2.1 Hz), 32.0, 31.5, 30.6, 29.6, 29.4, 29.4, 27.9, 25.9, 23.4, 22.8, 14.3, 14.2; IR (cm⁻¹): 2925, 2855, 1729, 1461, 1370, 1305, 1253, 1148, 1122, 1094, 1020, 956, 933, 861, 783, 737; HRMS: *m/z* calculated for C₂₀H₃₅F₃NO₃⁺ [M+H]⁺: 394.2564; found: 394.2560.



4,7,7-Trimethyltetrahydro-1H,3H-furo[3',4':2,3]azeto[1,2-b]isoxazol-1-one (3.156): Prepared according to GP-3.3 using (*E*)-**3.155** (53 mg, 0.25 mmol, 1.0 equiv.), *fac*-[Ir(dFppy)₃] (1.9 mg, 1 mol%) and MeCN (2.5 mL) with a reaction time of 19 h. ¹H NMR analysis of the crude reaction mixture revealed a diastereomer ratio of 1.2:1. Purification by flash column chromatography (2–30% EtOAc/CH₂Cl₂) afforded the pure (3*aS**,4*R**,8*aR**)-diastereomer as a white solid (22 mg, 42%) and the pure (3*aS**,4*S**,8*aR**)-diastereomer as a pale-yellow oil (18 mg, 34%).

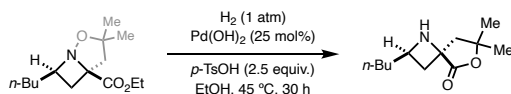
(3*aS,4*R**,8*aR**)-Diastereomer (major):** ¹H NMR (700 MHz, CDCl₃): δ 4.51 (d, *J* = 10.3 Hz, 1H), 4.39 (t, *J* = 9.4 Hz, 1H), 3.68 (q, *J* = 7.9 Hz, 1H), 3.30 (t, *J* = 8.6 Hz, 1H), 2.60 (d, *J* = 12.8 Hz, 1H), 2.45 (d, *J* = 12.8 Hz, 1H), 1.78 (dp, *J* = 14.9, 7.4 Hz, 1H), 1.62 – 1.51 (m, 4H), 1.40 (s, 3H), 0.91 (t, *J* = 7.2 Hz, 3H); ¹³C NMR (176 MHz, CDCl₃): δ 175.9, 88.5, 72.4, 70.8, 66.0, 46.6, 35.8, 28.3, 27.7, 23.5, 9.7; **IR** (cm⁻¹): 2960, 2939, 2361, 2337, 1770, 1457, 1368, 1264, 1233, 1211, 1155, 1100, 1048, 970, 949, 858, 824, 733, 706; **HRMS:** *m/z* calculated for C₁₁H₁₈NO₃⁺ [M+H]⁺: 212.1281; found: 212.1286.

(3*aS,4*S**,8*aR**)-Diastereomer (minor):** ¹H NMR (700 MHz, CDCl₃): δ 4.41 (t, *J* = 8.4 Hz, 1H), 4.35 (d, *J* = 9.8 Hz, 1H), 3.66 (q, *J* = 6.5 Hz, 1H), 3.00 (t, *J* = 6.4 Hz, 1H), 2.49 (d, *J* = 12.4 Hz, 1H), 2.27 (d, *J* = 12.4 Hz, 1H), 2.02 (dp, *J* = 14.2, 7.1 Hz, 1H), 1.66 (dp, *J* = 14.8, 7.4 Hz, 1H), 1.48 (s, 3H), 1.38 (s, 3H), 0.91 (t, *J* = 7.3 Hz, 3H); ¹³C NMR (176 MHz, CDCl₃): δ 176.1, 85.3, 71.6, 70.6, 68.9, 48.5, 43.8, 26.8, 26.0, 23.3, 10.1; **IR** (cm⁻¹): 2963, 2932, 2873, 2361, 2338, 1759, 1457, 1366, 1218, 1170, 1133, 1050, 969, 885, 869, 827, 806, 723, 662; **HRMS:** *m/z* calculated for C₁₁H₁₈NO₃⁺ [M+H]⁺: 212.1281; found: 212.1283.



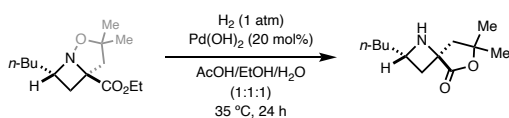
4,7,7-Trimethyltetrahydro-1*H*,3*H*-furo[3',4':2,3]azeto[1,2-*b*]isoxazol-1-one (3.156): Prepared according to GP-3.3 using (*Z*)-**3.155** (53 mg, 0.25 mmol, 1.0 equiv.), *fac*-[Ir(dFppy)₃] (1.9 mg, 1 mol%) and MeCN (2.5 mL) with a reaction time of 19 h. ¹H NMR analysis of the crude reaction mixture revealed a diastereomer ratio of 1.1:1. Purification by flash column chromatography (2–30% EtOAc/CH₂Cl₂) afforded the pure title compound as a pale-yellow oil (36 mg, 68% combined yield; 1.1:1 d.r.). Spectroscopic data was found consistent with that obtained, when conducting the reaction with (*E*)-**3.155**.

N-O Bond Cleavage of Azetidine Products



2-Butyl-7,7-dimethyl-6-oxa-1-azaspiro[3.4]octan-5-one (*cis*-3.140): A 3-dram vial equipped with a magnetic stir bar was charged with *exo*-**3.84** (50 mg, 0.2 mmol, 1.0 equiv.), Pd(OH)₂ (20wt%; 34 mg, 0.05 mmol, 0.25 equiv.) and *p*-TsOH (93 mg, 0.5 mmol, 2.5 equiv.). EtOH (5 mL) was added, the vial subsequently sealed with a septum-equipped cap and the reaction mixture sparged with hydrogen gas for 10 min. Then, the heterogenous reaction mixture was stirred vigorously at 45 °C for 30 h under a hydrogen atmosphere (balloon). After cooling to rt, the reaction mixture was passed through celite, the filter cake washed with CH₂Cl₂ and the filtrate concentrated *in vacuo*. The residue was taken up in CH₂Cl₂ and water and the aqueous layer brought to pH 10-11 with 2 M NaOH solution (aq.). The organic layer was separated and the aqueous layer extracted with CH₂Cl₂ (2x). The combined organic extracts were dried over MgSO₄, filtered and concentrated *in vacuo*. Purification by flash column chromatography (70–100% EtOAc/hexanes) afforded the pure title compound as a colorless solid (28 mg, 68%).

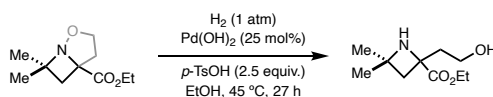
¹H NMR (400 MHz, CDCl₃): δ 3.70 (p, *J* = 7.2 Hz, 1H), 2.55 – 2.32 (m, 4H), 2.22 (d, *J* = 13.2 Hz, 1H), 1.89 – 1.66 (m, 2H), 1.42 (s, 3H), 1.37 – 1.14 (m, 7H), 0.89 (t, *J* = 7.2 Hz, 3H); **¹³C NMR** (176 MHz, CDCl₃): δ 179.4, 81.6, 62.9, 54.5, 50.1, 38.4, 37.3, 29.1, 28.0, 27.7, 22.6, 14.2; **IR** (cm⁻¹): 3318, 1957, 2928, 2857, 1761, 1456, 1387, 1374, 1273, 1243, 1204, 1154, 1075, 1027, 946, 923, 876, 810, 730, 677; **HRMS**: *m/z* calculated for C₁₂H₂₂NO₂⁺ [M+H]⁺: 212.1645; found: 212.1645.



2-Butyl-7,7-dimethyl-6-oxa-1-azaspiro[3.4]octan-5-one (*trans*-3.140): A 3-dram vial equipped with a magnetic stir bar was charged with *endo*-3.84 (100 mg, 0.4 mmol, 1.0 equiv.) and Pd(OH)₂ (20wt%; 55 mg, 0.08 mmol, 0.20 equiv.). A 1:1:1 mixture of EtOH, water and acetic acid (10 mL) was added, the vial subsequently sealed with a septum-equipped cap and the reaction mixture sparged with hydrogen gas for 12 min. Then, the heterogenous reaction mixture was stirred vigorously at 35 °C for 24 h under a hydrogen atmosphere (balloon). After cooling to rt, the reaction mixture was passed through celite, the filter cake washed with MeOH and the filtrate concentrated *in vacuo*. The residue was taken up in CH₂Cl₂ and water and the aqueous layer brought to pH 10-11 with 2 M NaOH solution (aq.). The organic layer was separated and the aqueous layer extracted with CH₂Cl₂ (2x). The combined organic extracts were dried over Na₂SO₄, filtered and concentrated *in vacuo*. Purification by flash column chromatography (20–100% EtOAc/hexanes) afforded the pure title compound as a white solid (53 mg, 64%)

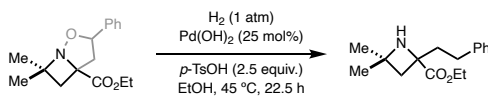
¹H NMR (700 MHz, CDCl₃): δ 4.09 (p, *J* = 6.8 Hz, 1H), 2.92 (b, 1H), 2.71 (t, *J* = 9.3 Hz, 1H), 2.27 (d, *J* = 13.4 Hz, 1H), 2.12 (d, *J* = 13.4 Hz, 1H), 2.07 (t, *J* = 9.4 Hz, 1H), 1.58 – 1.44 (m, 2H), 1.40 (s, 3H), 1.36 – 1.08 (m, 7H), 0.88 (t, *J* = 6.9 Hz, 3H); **¹³C NMR** (176 MHz, CDCl₃): δ 180.8,

81.8, 62.8, 54.0, 50.6, 39.1, 38.79, 3.12, 28.1, 27.4, 22.7, 14.2; **IR** (cm⁻¹): 3299, 2920, 2855, 1753, 1466, 1451, 1370, 1289, 1250, 1168, 1148, 1028, 933, 860, 799, 719, 695, 676; **HRMS**: *m/z* calculated for C₁₂H₂₂NO₂⁺ [M+H]⁺: 212.1645; found: 212.1650.



Ethyl 2-(2-hydroxyethyl)-4,4-dimethylazetidine-2-carboxylate (3.144): A 3-dram vial equipped with a magnetic stir bar was charged with **3.143** (40 mg, 0.2 mmol, 1.0 equiv.), Pd(OH)₂ (20wt%; 35 mg, 0.05 mmol, 0.25 equiv.) and *p*-TsOH (96 mg, 0.5 mmol, 2.5 equiv.). EtOH (5 mL) was added, the vial subsequently sealed with a septum-equipped cap and the reaction mixture sparged with hydrogen gas for 10 min. Then, the heterogenous reaction mixture was stirred vigorously at 45 °C for 27 h under a hydrogen atmosphere (balloon). After cooling to rt, the reaction mixture was passed through celite, the filter cake washed with CH₂Cl₂ and the filtrate concentrated *in vacuo*. The residue was taken up in CH₂Cl₂ and water and the aqueous layer brought to pH 10-11 with 2 M NaOH solution (aq.). The organic layer was separated and the aqueous layer extracted with CH₂Cl₂ (2x). The combined organic extracts were dried over MgSO₄, filtered and concentrated *in vacuo*. Purification by flash column chromatography (1–10% MeOH/CH₂Cl₂) afforded the pure title compound as a pale-yellow oil (18 mg, 45%).

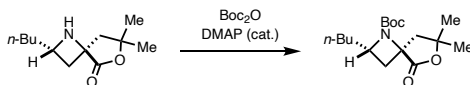
¹H NMR (700 MHz, CDCl₃): δ 4.24 (q, *J* = 7.1 Hz, 2H), 4.08 (t, *J* = 10.7 Hz, 1H), 3.82 – 3.73 (m, 1H), 2.40 (d, *J* = 12.0 Hz, 1H), 2.25 (d, *J* = 12.1 Hz, 1H), 1.91 (t, *J* = 12.2 Hz, 1H), 1.79 (dd, *J* = 14.6, 4.8 Hz, 1H), 1.30 (t, *J* = 7.9 Hz, 9H); **¹³C NMR** (176 MHz, CDCl₃): δ 180.8, 81.8, 62.8, 54.0, 50.6, 39.1, 38.8, 29.1, 28.1, 27.4, 22.7, 14.2; **IR** (cm⁻¹): 3301, 2958, 2868, 1724, 1447, 1376, 1279, 1263, 1208, 1149, 1086, 1054, 1023, 855, 808, 746; **HRMS**: *m/z* calculated for C₁₀H₂₀NO₃⁺ [M+H]⁺: 202.1438; found: 202.1437.



Ethyl 4,4-dimethyl-2-phenethylazetidine-2-carboxylate (3.146): A 3-dram vial equipped with a magnetic stir bar was charged with **3.145** (30 mg, 0.1 mmol, 1.0 equiv.), Pd(OH)₂ (20wt%; 19 mg, 0.25 mmol, 0.25 equiv.) and *p*-TsOH (52 mg, 0.25 mmol, 2.5 equiv.). EtOH (3 mL) was added, the vial subsequently sealed with a septum-equipped cap and the reaction mixture sparged with hydrogen gas for 15 min. Then, the heterogenous reaction mixture was stirred vigorously at 45 °C for 22.5 h under a hydrogen atmosphere (balloon). After cooling to rt, the reaction mixture was passed through celite, the filter cake washed with CH₂Cl₂ and the filtrate concentrated *in vacuo*. The residue was taken up in CH₂Cl₂ and water and the aqueous layer brought to pH 10-11 with 2 M NaOH solution (aq.). The organic layer was separated and the aqueous layer extracted with CH₂Cl₂ (2x). The combined organic extracts were dried over Na₂SO₄, filtered and concentrated *in vacuo*. Purification by flash column chromatography (20–60% EtOAc/hexanes) afforded the pure title compound as a pale-yellow oil (24 mg, 84%).

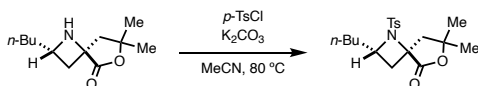
¹H NMR (700 MHz, CDCl₃): δ 7.26 (t, *J* = 7.5 Hz, 2H), 7.17 (d, *J* = 7.7 Hz, 2H), 4.19 (q, *J* = 7.1 Hz, 2H), 2.77 (s, 1H), 2.69 (td, *J* = 12.9, 4.7 Hz, 1H), 2.38 – 2.31 (m, 2H), 2.17 (td, *J* = 12.9, 5.4 Hz, 1H), 2.13 (d, *J* = 11.8 Hz, 1H), 2.06 (td, *J* = 12.7, 4.9 Hz, 1H), 1.31 – 1.27 (m, 9H); **¹³C NMR** (176 MHz, CDCl₃): δ 177.5, 141.8, 128.5, 128.4, 125.9, 61.3, 59.7, 54.1, 43.3, 43.1, 32.3, 30.2, 30.1, 14.4; **IR** (cm⁻¹): 3316, 2957, 2925, 1725, 1604, 1497, 1448, 1376, 1299, 1251, 1213, 1175, 1097, 1063, 1025, 857, 776, 745, 698; **HRMS**: *m/z* calculated for C₁₆H₂₄NO₂⁺ [M+H]⁺: 262.1802; found: 262.1802.

Synthetic Modifications of Azetidine Products



***Tert*-butyl 2-butyl-7,7-dimethyl-5-oxo-6-oxa-1-azaspiro[3.4]octane-1-carboxylate (3.141):** A 10-mL round-bottom flask equipped with a magnetic stir bar was charged with *trans*-**3.140** (21 mg, 0.1 mmol, 1.0 equiv.) and MeCN (2 mL). Boc₂O (50 μ L, 0.2 mmol, 2.0 equiv.) and DMAP (2.4 mg, 0.02 mmol, 0.2 equiv.) were added and the solution stirred at rt for 16 h. The reaction mixture was concentrated *in vacuo* and purified by flash column chromatography (5–40% EtOAc/hexanes) to afford the pure title compound as a white solid (24 mg, 78%). Characterization data is provided for a 1.7:1 mixture of rotamers (A/B).

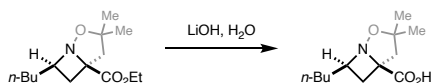
¹H NMR (700 MHz, CDCl₃): δ 4.55 – 4.49 (m, 2.7H; A+B), 2.79 (d, J = 13.5 Hz, 1.7H; A), 2.75 – 2.67 (m, 2.7H; A+B), 2.60 (d, J = 13.5 Hz, 1H; B), 2.37 (d, J = 13.4 Hz, 1H; B), 2.29 (d, J = 13.5 Hz, 1.7H; A), 2.05 – 1.95 (m, 3.7H; A+B), 1.95 – 1.84 (m, 1.7H; A), 1.66 – 1.21 (m, 54H; A+B) 0.94 – 0.85 (m, 8.1H; A+B); **¹³C NMR** (176 MHz, CDCl₃): δ 174.8, 174.7, 148.1 (d, J = 356.0 Hz), 147.5 (d, J = 371.7 Hz), 85.2, 85.0, 82.1, 81.8, 68.0, 67.1, 60.9, 59.7, 47.0, 45.7, 36.2, 35.8, 35.1, 35.0, 29.2, 29.1, 29.0, 28.9, 27.60, 27.58, 26.6, 26.1, 22.61, 22.57, 14.1 (2C); **IR** (cm⁻¹): 2977, 2934, 2872, 1797, 1762, 1722, 1468, 1398, 1372, 1237, 1134, 1095, 1057, 1026, 944, 923, 890, 826, 762, 694, 666; **HRMS**: m/z calculated for C₁₇H₃₀NO₄⁺ [M+H]⁺: 312.2169; found: 312.2170.



2-Butyl-7,7-dimethyl-1-tosyl-6-oxa-1-azaspiro[3.4]octan-5-one (3.142): A 10-mL round-bottom flask equipped with a magnetic stir bar was charged with *trans*-**3.140** (21 mg, 0.1 mmol, 1.0 equiv.) and MeCN (2 mL). *p*-TsCl (57 mg, 0.3 mmol, 3.0 equiv.) and K₂CO₃ (41 mg,

0.3 mmol, 3.0 equiv.) were added and the reaction mixture heated at 80 °C for 2.5 h. Then, the reaction was concentrated *in vacuo* and purified by flash column chromatography (5–40% EtOAc/hexanes) to afford the pure title compound as a viscous, colorless oil (36 mg, 99%).

¹H NMR (400 MHz, CDCl₃): δ 7.68 (d, *J* = 8.2 Hz, 2H), 7.30 (d, *J* = 8.0 Hz, 2H), 4.41 (qd, *J* = 7.9, 3.9 Hz, 1H), 2.84 (d, *J* = 13.7 Hz, 1H), 2.55 (dd, *J* = 10.5, 8.0 Hz, 1H), 2.43 (s, 3H), 2.36 (d, *J* = 13.7 Hz, 1H), 2.02 (dd, *J* = 10.5, 7.4 Hz, 1H), 1.92 – 1.78 (m, 1H), 1.64 – 1.50 (m, 4H), 1.33 (s, 3H), 1.30 – 1.11 (m, 4H), 0.85 (t, *J* = 7.1 Hz, 3H); **¹³C NMR** (176 MHz, CDCl₃): δ 174.7, 143.7, 136.7, 129.4, 127.7, 81.9, 70.5, 61.7, 48.2, 36.3, 35.2, 29.4, 29.0, 26.0, 22.5, 21.7, 14.0; **IR** (cm⁻¹): 2931, 2861, 1769, 1598, 1453, 1333, 1294, 1152, 1090, 923, 813, 753, 730, 669, 640; **HRMS**: *m/z* calculated for C₁₉H₂₇NNaO₄S⁺ [M+Na]⁺: 388.1553 found: 388.1548.

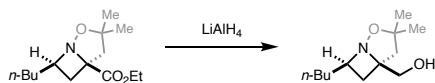


7-Butyl-3,3-dimethyl-2-oxa-1-azabicyclo[3.2.0]heptane-5-carboxylic acid (3.147): A 10-mL round-bottom flask equipped with a magnetic stir bar was charged with *exo*-**3.84** (51 mg, 0.2 mmol, 1.0 equiv.) and a 3:1 mixture of MeOH/water (2 mL). Lithium hydroxide monohydrate (13 mg, 0.3 mmol, 1.5 equiv.) was added and the resulting solution stirred at rt for 16 h. The reaction mixture acidified with 1 M HCl solution (aq.) to pH 1–2 and subsequently extracted with CH₂Cl₂ (5x). The combined organic extracts were dried over Na₂SO₄, filtered, concentrated *in vacuo*, then dried using high-vac to afford the pure title compound as a colorless oil (44 mg, 97%).

¹H NMR (500 MHz, CDCl₃): δ 7.12 (b, 1H), 3.72 (p, *J* = 7.9 Hz, 1H), 2.98 (d, *J* = 12.9 Hz, 1H), 2.55 (dd, *J* = 11.7, 8.9 Hz, 1H), 2.49 (d, *J* = 12.9 Hz, 1H), 2.14 (dd, *J* = 11.7, 8.1 Hz), 1.95 – 1.83 (m, 1H), 1.73 – 1.62 (m, 1H), 1.53 (s, 3H), 1.42 – 1.26 (m, 4H), 1.24 (s, 3H), 0.90 (t, *J* = 7.0 Hz, 3H); **¹³C NMR** (126 MHz, CDCl₃): δ 172.2, 89.9, 74.5, 68.4, 50.2, 33.8, 31.1, 28.3, 27.8, 27.3,

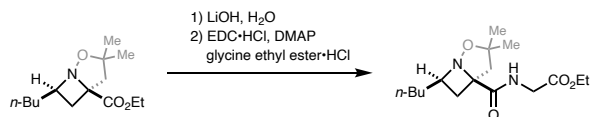
22.5, 14.1; **IR** (cm⁻¹): 2959, 2932, 2873, 1718, 1617, 1457, 1378, 1265, 1194, 1152, 854, 731, 700;

HRMS: *m/z* calculated for C₁₂H₂₂NO₃⁺ [M+H]⁺: 228.1594; found: 228.1594.



7-Butyl-3,3-dimethyl-2-oxa-1-azabicyclo[3.2.0]heptan-5-ylmethanol (3.148): To a 10-mL round-bottom flask equipped with a magnetic stir bar containing a suspension of LiAlH₄ (10 mg, 0.26 mmol, 1.35 equiv.) in Et₂O (1.25 mL) was added *exo*-**3.84** (50 mg, 0.2 mmol, 1.0 equiv.) as a solution in Et₂O (0.75 mL) dropwise at 0 °C. After stirring for 0.5 h at 0 °C, water was added carefully, the reaction mixture diluted with Et₂O and Rochelle salt solution (aq., sat.) and subsequently stirred for 12 h at rt. The organic layer was separated and the aqueous layer extracted with Et₂O (3x). The combined organic extracts were dried over MgSO₄, filtered and concentrated *in vacuo*, then dried using high-vac to obtain the pure title compound as a clear oil (40 mg, 96%).

¹H NMR (400 MHz, CDCl₃): δ 3.62 – 3.48 (m, 2H), 3.43 – 3.33 (m, 1H), 2.86 (d, *J* = 8.6 Hz, 1H), 2.45 (d, *J* = 13.0 Hz, 1H), 2.17 (d, *J* = 13.0 Hz, 1H), 2.08 (dd, *J* = 11.0, 8.9 Hz, 1H), 1.92 (dd, *J* = 11.0, 8.2 Hz, 1H), 1.69 – 1.53 (m, 4H), 1.53 – 1.40 (m, 1H), 1.40 – 1.18 (m, 7H), 0.88 (t, *J* = 6.9 Hz, 3H); **¹³C NMR** (126 MHz, CDCl₃): δ 87.7, 74.8, 66.2, 66.0, 51.4, 35.1, 31.7, 30.2, 27.8, 27.6, 22.8, 14.2; **IR** (cm⁻¹): 3386, 2955, 2928, 2858, 2361, 2337, 1457, 1380, 1303, 1249, 1226, 1150, 1078, 1043, 971, 864, 773, 686, 668, 640; **HRMS**: *m/z* calculated for C₁₂H₂₄NO₂⁺ [M+H]⁺: 214.1802; found: 214.1805.



Ethyl 7-butyl-3,3-dimethyl-2-oxa-1-azabicyclo[3.2.0]heptane-5-carbonyl)glycinate (3.149):

A 10-mL round-bottom flask equipped with a magnetic stir bar was charged with *exo*-**3.84** (51 mg, 0.2 mmol, 1.0 equiv.) and a 3:1 mixture of MeOH/water (2 mL). Lithium hydroxide monohydrate

(13 mg, 0.3 mmol, 1.5 equiv.) was added and the resulting solution stirred at rt for 2 h. The reaction mixture acidified with 1 M HCl (aq.) to pH 1–2 and subsequently extracted with CH₂Cl₂ (5x). The combined organic extracts were dried over Na₂SO₄, filtered, concentrated *in vacuo*, then dried using high-vac to afford pure **3.147**.

Next, the carboxylic acid (**3.147**) was dissolved in CH₂Cl₂ (5 mL) and DMAP (5 mg, 0.04 mmol, 0.2 equiv.), glycine ethyl ester hydrochloride (56 mg, 0.4 mmol, 2.0 equiv.) and EDC•HCl (57 mg, 0.3 mmol, 1.5 equiv.) were added sequentially. After stirring the resulting mixture for 16 h at rt, it was diluted with CH₂Cl₂ and washed with 1 M HCl solution (aq., 2x) and brine, dried over Na₂SO₄, filtered and concentrated *in vacuo*. Purification by flash column chromatography (20–40% EtOAc/hexanes) afforded the product as a colorless oil (58 mg, 93%).

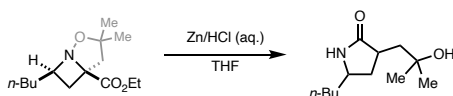
¹H NMR (500 MHz, CDCl₃): δ 7.82 (t, *J* = 6.1 Hz, 1H), 4.20 (q, *J* = 7.2 Hz, 2H), 4.14 – 3.95 (m, 2H), 3.50 (p, *J* = 8.0 Hz, 1H), 2.94 (d, *J* = 12.8 Hz, 1H), 2.52 – 2.38 (m, 2H), 1.79 (dd, *J* = 11.1, 8.5 Hz, 1H), 1.74 – 1.65 (m, 1H), 1.58 – 1.46 (m, 4H), 1.42 – 1.21 (m, 7H), 1.17 (s, 3H), 0.90 (t, *J* = 6.9 Hz, 3H); **¹³C NMR** (126 MHz, CDCl₃): δ 173.6, 169.5, 87.5, 73.2, 67.3, 61.4, 50.0, 41.0, 35.3, 31.5, 29.2, 28.6, 27.5, 22.7, 14.2, 14.1; **IR** (cm⁻¹): 3366, 2957, 2931, 2873, 2361, 2337, 1750, 1671, 1516, 1457, 1369, 1255, 1188, 1098, 1028, 919, 862, 729, 668, 646; **HRMS**: *m/z* calculated for C₁₆H₂₉N₂O₄⁺ [M+H]⁺: 313.2122; found: 313.2120.



7-Butyl-3,3-dimethyl-2-oxa-1-azabicyclo[3.2.0]heptan-5-yl)diphenylmethanol (3.150): To a 10-mL round-bottom flask equipped with a magnetic stir bar containing a solution of *exo*-**3.84** (51 mg, 0.2 mmol, 1.0 equiv.) in THF (2 mL) was added freshly prepared PhMgBr (0.5 M in THF, 4.0 mL, 2.0 mmol, 10.0 equiv.) dropwise at 0 °C. After stirring for 15 min at 0 °C, NH₄Cl solution

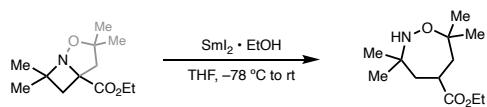
(aq., sat.) was added and the resulting mixture extracted with Et₂O (3x), the combined organic extracts dried over MgSO₄, filtered and concentrated *in vacuo*. Purification by flash column chromatography (5–10% EtOAc/hexanes) afforded the pure title compound as a colorless oil (69 mg, 95%).

¹H NMR (500 MHz, CDCl₃): δ 7.43 – 7.15 (m, 10H), 4.78 (s, 1H), 3.77 (p, *J* = 7.8 Hz, 1H), 2.59 (q, *J* = 13.1 Hz, 2H), 2.34 (dd, *J* = 11.5, 9.4 Hz, 1H), 1.92 (dd, *J* = 11.5, 7.8 Hz, 1H), 1.59 (s, 3H), 1.56 – 1.44 (m, 1H), 1.39 – 1.14 (m, 5H), 0.87 (t, *J* = 7.1 Hz, 3H), 0.52 (s, 3H); **¹³C NMR** (126 MHz, CDCl₃): δ 144.9, 143.1, 128.1, 128.0, 127.8, 127.7, 127.3, 127.2, 89.8, 81.4, 80.6, 65.1, 52.9, 34.7, 33.4, 32.1, 28.2, 27.6, 22.6, 14.2; **IR** (cm⁻¹): 2957, 2858, 2246, 1493, 1447, 1366, 1298, 1229, 1170, 1146, 1024, 907, 759, 728, 698, 668; **HRMS**: *m/z* calculated for C₂₄H₃₂NO₂⁺ [M+H]⁺: 266.2428; found: 266.2435.



5-Butyl-3-(2-hydroxy-2-methylpropyl)pyrrolidin-2-one (3.152): A 25-mL round-bottom flask equipped with a magnetic stir bar was charged with *exo*-**3.84** (50 mg, 0.2 mmol, 1.0 equiv.) and a 9:1 mixture of 1 M HCl (aq.)/THF (5 mL). Zinc powder (128 mg, 2.0 mmol, 10.0 equiv.) was added and the resulting mixture heated at 80 °C for 3 h. After cooling to rt, the reaction mixture was filtered and the filtrate brought to pH 10–11 with 2 M NaOH solution (aq.). The resulting cloudy mixture was extracted with CH₂Cl₂ (5x) and the combined organic extracts dried over Na₂SO₄, filtered and concentrated *in vacuo*. Purification by flash column chromatography (50–100% EtOAc/hexanes) afforded the pure title compound as a colorless oil as a 2.6:1 mixture of diastereomers (24 mg, 58%). Characterization data was obtained for a 2.6:1 mixture of diastereomers.

¹H NMR (700 MHz, CDCl₃): δ 6.42 (s, 1H; minor), 6.35 (s, 2.6H; major), 4.92 (s, 2.6H; major), 4.74 (s, 1H; minor), 3.64 – 3.51 (m, 3.6H; major+minor), 2.82 – 2.71 (m, 3.6H; major+minor), 2.46 – 2.39 (m, 2.6H; major), 2.04 (t, *J* = 11.1 Hz, 1H; minor), 1.99 – 1.86 (m, 4.6H; major+minor), 1.60 – 1.20 (m, 49.4H; major+minor), 0.93 – 0.86 (m, 10.8H; major+minor); **¹³C NMR** (176 MHz, CDCl₃): δ 181.2, 180.9, 69.4, 69.2, 53.7, 53.1, 45.2, 45.1, 39.1, 37.0, 36.7, 36.3, 36.1, 35.3, 31.5 (2C), 28.7 (2C), 28.3, 28.1, 22.7, 22.6, 14.11, 14.08; **IR** (cm⁻¹): 3205, 2960, 2927, 2858, 1681, 1662, 1456, 1378, 1362, 1317, 1274, 1186, 1151, 1084, 959, 907, 783, 731, 658; **HRMS**: *m/z* calculated for C₁₂H₂₃NNaO₂⁺ [M+Na]⁺: 236.1621; found: 236.1621.



Ethyl 3,3,7,7-tetramethyl-1,2-oxazepane-5-carboxylate (3.151): A Schlenk flask equipped with a magnetic stir bar was charged with **3.115** (45 mg, 0.2 mmol 1.0 equiv.) and the flask evacuated and refilled with nitrogen gas. This process was repeated twice, before adding a 2:1 mixture (*v/v*) of degassed THF/EtOH (2 mL). Next, the resulting solution was cooled to –78 °C and a freshly prepared samarium(II) iodide solution (0.1 M in THF; 12 mL, 1.2 mmol, 6.0 equiv.) was added dropwise. The resulting dark-blue solution was allowed to gradually warm up to rt over 1 h. Then, the reaction vessel was opened up to air, the reaction mixture diluted with water and sodium thiosulfate solution (aq., sat.) and extracted with EtOAc (3x). The combined organic extracts were washed with water and brine, dried over MgSO₄, filtered and concentrated *in vacuo*. Purification by flash column chromatography (2–10% EtOAc/hexanes) afforded the pure title compound as a pale-yellow oil (19 mg, 42%).

¹H NMR (400 MHz, CDCl₃): δ 4.43 (s, 1H), 4.11 (q, *J* = 7.1 Hz, 2H), 2.69 (t, *J* = 11.0 Hz, 1H), 1.97 (dd, *J* = 14.0, 10.1 Hz, 1H), 1.84 – 1.67 (m, 2H), 1.53 (t, *J* = 12.6 Hz, 1H), 1.29 – 1.19 (m,

9H), 1.10 (s, 3H), 0.98 (s, 3H); ^{13}C NMR (126 MHz, CDCl_3): δ 176.9, 77.6, 60.5, 56.1, 45.8, 43.4, 37.9, 27.6, 26.8, 25.9, 24.6, 14.4; IR (cm^{-1}): 2971, 1728, 1453, 1362, 1283, 1228, 1155, 1114, 1037, 1020, 911, 840, 787, 733; HRMS: m/z calculated for $\text{C}_{12}\text{H}_{24}\text{NO}_3^+$ $[\text{M}+\text{H}]^+$: 230.1751; found: 230.1750.

Stereo- and Regiochemistry of Azetidine Products

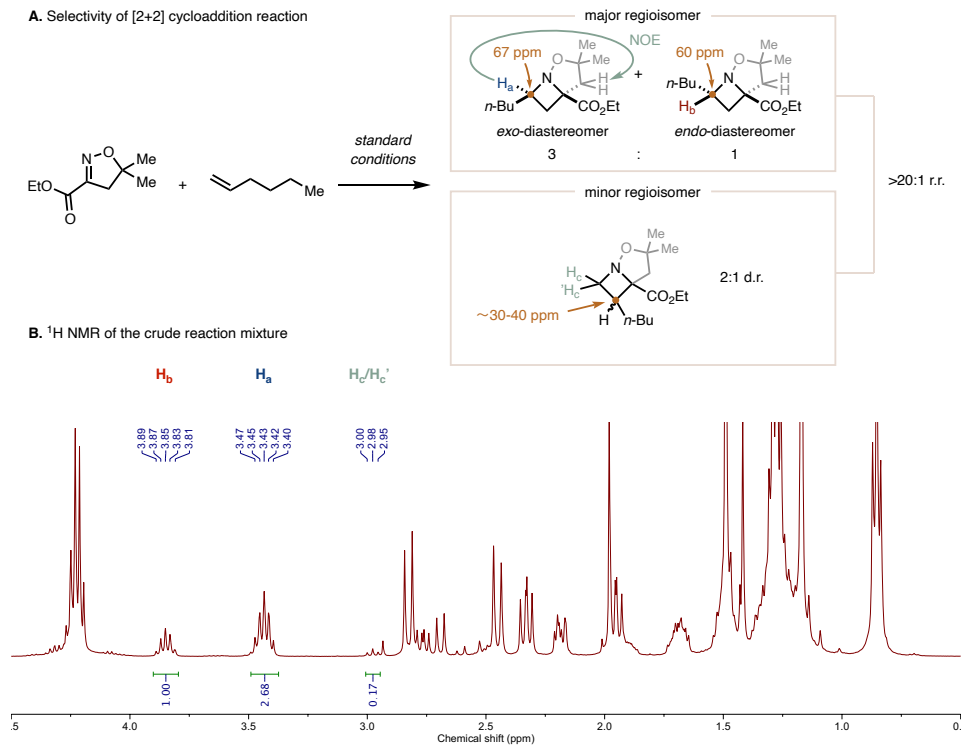
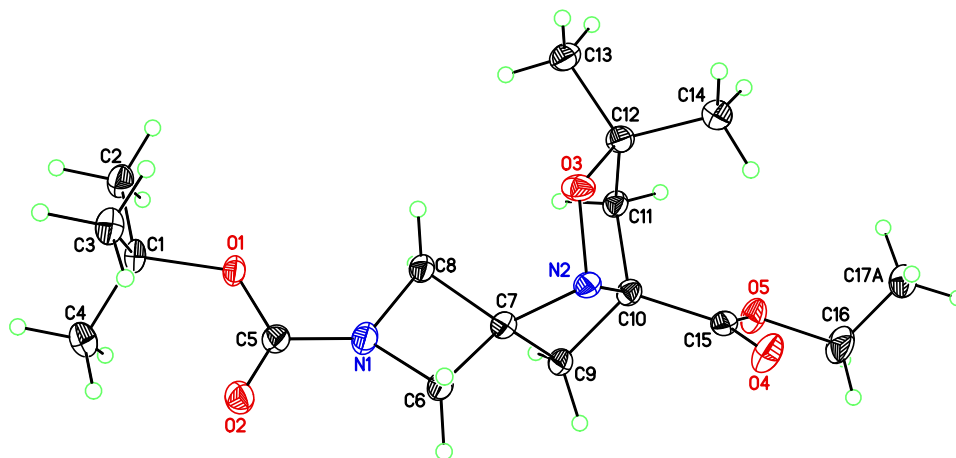


Figure 3.35: Stereo- and regiochemistry of the azetidine products. (A) Selectivity of the [2+2] cycloaddition reaction (B) ^1H NMR of the crude reaction mixture.

Diastereomer and regioisomer ratios of the intermolecular aza Paternò-Büchi reaction were determined by ^1H NMR analysis of the crude reaction mixture. The reaction exhibits high regioselectivity (8:1 to >20:1 r.r.) for the azetidine product, in which the side of an alkene with a higher degree of substitution ($2^\circ > 1^\circ$) adds to the 2-isoxazoline nitrogen. For mono- and 1,1-disubstituted alkenes the major diastereomer is typically the *exo*-isomer in which the larger substituent (R_L) ends up opposite to the isoxazolidine ring with diastereoselectivities between 1:1 to >10:1. For tertiary alkenes, the additional substituent was found to preferentially add in the *endo* position during the cycloaddition. Furthermore, in the case of monosubstituted 2-isoxazoline substrates, the cycloaddition occurs at the least hindered face. The regio- and stereochemical assignments for azetidine products were based on 1D NMR (^1H , ^{13}C), 2D NMR (gCOSY, gHMBCAD, gHSQCAD) and ^1H NMR NOE analysis. Specifically, the regiochemistry was typically assigned according to the ^{13}C NMR shift of the carbon signals adjacent to the azetidine nitrogen. The stereochemistry of the azetidine products was assigned based on NOE correlations of characteristic ^1H NMR signals. For example, in the case of products arising from the reaction with a primary alkene, a strong NOE correlation was observed for proton H_a with the methylene group in the backbone of the substrate, which was not observed for the corresponding other diastereomer. The regio- and stereochemical assignments were further confirmed by the X-ray crystallographic analyses of compounds **3.119**, **3.121** and *trans*-**3.140**.

X-Ray Crystallographic Data

Compound 3.119



CCDC 1980947

Colorless plates of **3.119** were grown from a hexane solution of the compound at 22 °C. A crystal of dimensions 0.12 x 0.10 x 0.03 mm was mounted on a Rigaku AFC10K Saturn 944+ CCD-based X-ray diffractometer equipped with a low temperature device and Micromax-007HF Cu-target micro-focus rotating anode ($\lambda = 1.54187 \text{ \AA}$) operated at 1.2 kW power (40 kV, 30 mA). The X-ray intensities were measured at 85(1) K with the detector placed at a distance 42.34 mm from the crystal. A total of 2028 images were collected with an oscillation width of 1.0° in ω . The exposure times were 1 sec. for the low angle images, 3 sec. for high angle. Rigaku d*trek images were exported to CrysAlisPro for processing and corrected for absorption. The integration of the data yielded a total of 13716 reflections to a maximum 2θ value of 138.76° of which 3286 were independent and 3158 were greater than $2\sigma(I)$. The final cell constants (Supplementary Table 9) were based on the xyz centroids of 9574 reflections above $10\sigma(I)$. Analysis of the data showed negligible decay during data collection. The structure was solved and refined with the Bruker SHELXTL (version 2018/3) software package, using the space group $P1\bar{1}$ with $Z = 2$ for the formula $C_{17}H_{28}N_2O_5$. All non-hydrogen atoms were refined anisotropically with the hydrogen

atoms placed in idealized positions. The terminal methyl group (C17) is disordered over two sites. Full matrix least-squares refinement based on F^2 converged at $R1 = 0.0403$ and $wR2 = 0.1030$ [based on $I > 2\sigma(I)$], $R1 = 0.0411$ and $wR2 = 0.1039$ for all data. Acknowledgement is made for funding from NSF grant CHE-0840456 for X-ray instrumentation.

G.M. Sheldrick (2015) "Crystal structure refinement with SHELXL", *Acta Cryst.*, C71, 3-8 (Open Access).

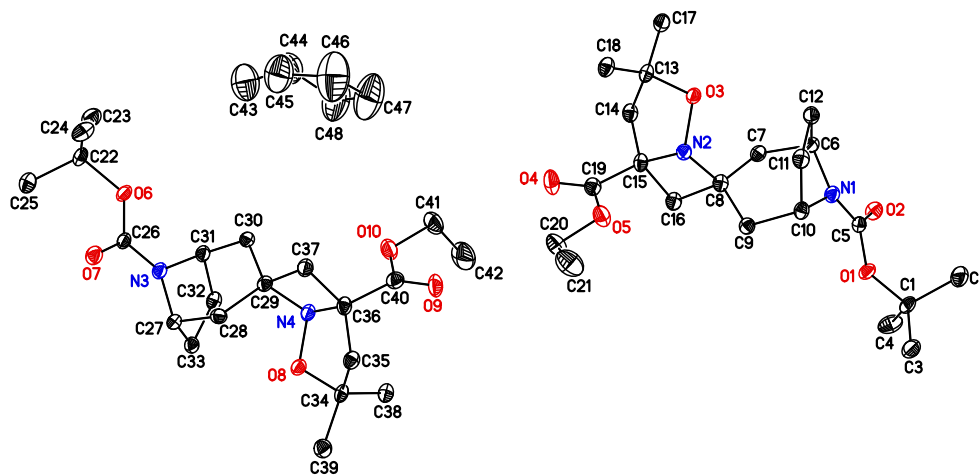
CrystalClear Expert 2.0 r16, Rigaku Americas and Rigaku Corporation (2014), Rigaku Americas, 9009, TX, USA 77381-5209, Rigaku Tokyo, 196-8666, Japan.

CrysAlisPro 1.171.38.41 (Rigaku Oxford Diffraction, 2015).

Table 3.13: Crystallographic parameters and structure refinement for compound **3.119**.

Identification code	1-(<i>Tert</i> -butyl) 1'-ethyl 3',3'-dimethyl-4'-oxa-5'-azaspiro[azetidine-3,6'-bicyclo[3.2.0]heptane]-1,1'-dicarboxylate
Empirical formula	C17 H28 N2 O5
Formula weight	340.41
Temperature	85(2) K
Wavelength	1.54184 Å
Crystal system, space group	Triclinic, P-1
Unit cell dimensions	a = 5.7853(2) Å alpha = 105.136(3) deg. b = 11.3896(3) Å beta = 97.310(3) deg. c = 14.8541(4) Å gamma = 100.774(3) deg.
Volume	912.02(5) Å ³
Z, Calculated density	2, 1.240 Mg/m ³
Absorption coefficient	0.748 mm ⁻¹
F(000)	368
Crystal size	0.120 x 0.100 x 0.030 mm
Theta range for data collection	3.137 to 69.386 deg.
Limiting indices	-7<=h<=6, -13<=k<=13, -16<=l<=17
Reflections collected / unique	13716 / 3286 [R(int) = 0.0427]
Completeness to theta = 67.684	97.90%
Absorption correction	Semi-empirical from equivalents
Max. and min. transmission	1.00000 and 0.84904
Refinement method	Full-matrix least-squares on F ²
Data / restraints / parameters	3286 / 1 / 234
Goodness-of-fit on F ²	1.066
Final R indices [I>2sigma(I)]	R1 = 0.0403, wR2 = 0.1030
R indices (all data)	R1 = 0.0411, wR2 = 0.1039
Extinction coefficient	0.0137(12)
Largest diff. peak and hole	0.356 and -0.279 e.Å ⁻³

Compound 3.121



CCDC 1980951

Colorless needles of **3.121** were grown from a hexane solution of the compound at 0 °C. A crystal of dimensions 0.13 x 0.03 x 0.03 mm was mounted on a Rigaku AFC10K Saturn 944+ CCD-based X-ray diffractometer equipped with a low temperature device and Micromax-007HF Cu-target micro-focus rotating anode ($\lambda = 1.54187$ Å) operated at 1.2 kW power (40 kV, 30 mA). The X-ray intensities were measured at 85(1) K with the detector placed at a distance 42.00 mm from the crystal. A total of 2028 images were collected with an oscillation width of 1.0° in ω . The exposure times were 1 sec. for the low angle images, 4 sec. for high angle. Rigaku d*trek images were exported to CrysAlisPro for processing and corrected for absorption. The integration of the data yielded a total of 35611 reflections to a maximum 2θ value of 138.69° of which 8411 were independent and 8004 were greater than $2\sigma(I)$. The final cell constants (Supplementary Table 10) were based on the xyz centroids of 15622 reflections above $10\sigma(I)$. Analysis of the data showed negligible decay during data collection. The structure was solved and refined with the Bruker SHELXTL (version 2018/3) software package, using the space group Pn with $Z = 2$ for the formula $C_{48}H_{80}N_4O_{10}$. All non-hydrogen atoms were refined anisotropically with the hydrogen atoms placed in idealized positions. Full matrix least-squares refinement based on F^2 converged at $R1 =$

0.0414 and $wR2 = 0.1080$ [based on $I > 2\sigma(I)$], $R1 = 0.0435$ and $wR2 = 0.1115$ for all data.

Acknowledgement is made for funding from NSF grant CHE-0840456 for X-ray instrumentation.

G.M. Sheldrick (2015) "Crystal structure refinement with SHELXL", *Acta Cryst.*, C71, 3-8 (Open Access).

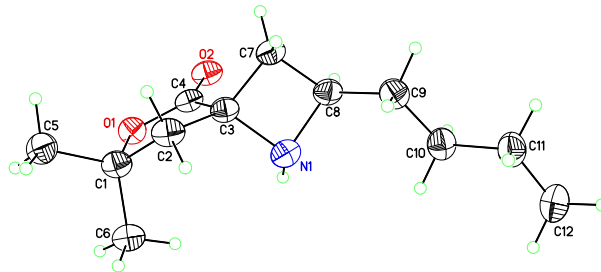
CrystalClear Expert 2.0 r16, Rigaku Americas and Rigaku Corporation (2014), Rigaku Americas, 9009, TX, USA 77381-5209, Rigaku Tokyo, 196-8666, Japan.

CrysAlisPro 1.171.38.41 (Rigaku Oxford Diffraction, 2015).

Table 3.14: Crystallographic parameters and structure refinement for compound **3.121**.

Identification code	8'-(<i>Tert</i> -butyl) 1-ethyl-3,3-dimethyl-4-oxa-5,8'-diazaspiro[bicyclo[3.2.0]heptane-6,3'-bicyclo[3.2.1]octane]-1,8'-dicarboxylate
Empirical formula	C ₄₈ H ₈₀ N ₄ O ₁₀
Formula weight	873.16
Temperature	85(2) K
Wavelength	1.54184 Å
Crystal system, space group	Monoclinic, Pn
Unit cell dimensions	a = 17.6585(2) Å alpha = 90 deg. b = 6.09660(10) Å beta = 98.4520(10) deg. c = 22.7527(3) Å gamma = 90 deg.
Volume	2422.88(6) Å ³
Z, Calculated density	2, 1.197 Mg/m ³
Absorption coefficient	0.669 mm ⁻¹
F(000)	952
Crystal size	0.130 x 0.030 x 0.030 mm
Theta range for data collection	2.966 to 69.343 deg.
Limiting indices	-21 ≤ h ≤ 20, -7 ≤ k ≤ 7, -25 ≤ l ≤ 27
Reflections collected / unique	35611 / 8411 [R(int) = 0.0621]
Completeness to theta = 67.684	100.00%
Absorption correction	Semi-empirical from equivalents
Max. and min. transmission	1.00000 and 0.78867
Refinement method	Full-matrix least-squares on F ²
Data / restraints / parameters	8411 / 2 / 573
Goodness-of-fit on F ²	1.043
Final R indices [I > 2σ(I)]	R ₁ = 0.0414, wR ₂ = 0.1080
R indices (all data)	R ₁ = 0.0435, wR ₂ = 0.1115
Absolute structure parameter	0.4(2)
Extinction coefficient	n/a
Largest diff. peak and hole	0.259 and -0.229 e.Å ⁻³

Compound *trans*-3.140



CCDC 1980952

Colorless needles of *trans*-3.140 were grown from a hexane solution of the compound at 0 °C. A crystal of dimensions 0.18 x 0.09 x 0.03 mm was mounted on a Rigaku AFC10K Saturn 944+ CCD-based X-ray diffractometer equipped with a low temperature device and Micromax-007HF Cu-target micro-focus rotating anode ($\lambda = 1.54187 \text{ \AA}$) operated at 1.2 kW power (40 kV, 30 mA). The X-ray intensities were measured at 85(1) K with the detector placed at a distance 42.00 mm from the crystal. A total of 2028 images were collected with an oscillation width of 1.0° in ω . The exposure times were 1 sec. for the low angle images, 5 sec. for high angle. Rigaku d*trek images were exported to CrysAlisPro for processing and corrected for absorption. The integration of the data yielded a total of 18752 reflections to a maximum 2θ value of 138.92° of which 2257 were independent and 2082 were greater than $2\sigma(I)$. The final cell constants (Supplementary Table 11) were based on the xyz centroids of 5417 reflections above $10\sigma(I)$. Analysis of the data showed negligible decay during data collection. The structure was solved and refined with the Bruker SHELXTL (version 2018/3) software package, using the space group $P2(1)2(1)2(1)$ with $Z = 4$ for the formula $C_{12}H_{21}NO_2$. All non-hydrogen atoms were refined anisotropically with the hydrogen atoms placed in a combination of refined and idealized positions. Full matrix least-squares refinement based on F^2 converged at $R1 = 0.0467$ and $wR2 = 0.1131$ [based on $I > 2\sigma(I)$], $R1$

= 0.0512 and $wR2 = 0.1195$ for all data. Acknowledgement is made for funding from NSF grant CHE-0840456 for X-ray instrumentation.

G.M. Sheldrick (2015) "Crystal structure refinement with SHELXL", *Acta Cryst.*, C71, 3-8 (Open Access).

CrystalClear Expert 2.0 r16, Rigaku Americas and Rigaku Corporation (2014), Rigaku Americas, 9009, TX, USA 77381-5209, Rigaku Tokyo, 196-8666, Japan.

CrysAlisPro 1.171.38.41 (Rigaku Oxford Diffraction, 2015).

Table 3.15: Crystallographic parameters and structure refinement for compound **3.140**.

Identification code	2-Butyl-7,7-dimethyl-6-oxa-1-azaspiro[3.4]octan-5-one
Empirical formula	C ₁₂ H ₂₁ N O ₂
Formula weight	211.3
Temperature	85(2) K
Wavelength	1.54184 Å
Crystal system, space group	Orthorhombic, P2(1)2(1)2(1)
Unit cell dimensions	a = 6.15494(18) Å alpha = 90 deg.
	b = 8.5930(4) Å beta = 90 deg.
	c = 23.1982(8) Å gamma = 90 deg.
Volume	1226.94(8) Å ³
Z, Calculated density	4, 1.144 Mg/m ³
Absorption coefficient	0.611 mm ⁻¹
F(000)	464
Crystal size	0.180 x 0.090 x 0.030 mm
Theta range for data collection	3.811 to 69.462 deg.
Limiting indices	-7<=h<=7, -9<=k<=8, -27<=l<=28
Reflections collected / unique	18752 / 2257 [R(int) = 0.0771]
Completeness to theta = 67.684	98.60%
Absorption correction	Semi-empirical from equivalents
Max. and min. transmission	1.00000 and 0.76113
Refinement method	Full-matrix least-squares on F ²
Data / restraints / parameters	2257 / 0 / 144
Goodness-of-fit on F ²	1.063
Final R indices [I>2sigma(I)]	R1 = 0.0467, wR2 = 0.1131
R indices (all data)	R1 = 0.0512, wR2 = 0.1195
Absolute structure parameter	0.2(4)
Extinction coefficient	n/a
Largest diff. peak and hole	0.233 and -0.235 e.Å ⁻³

Bibliography

- (1) *Lewis Acids in Organic Synthesis*; Yamamoto, H., Ed.; Wiley-VCH: Weinheim, 2008.
- (2) Santelli, M.; Pons, J.-M. *Lewis Acids and Selectivity in Organic Synthesis*, 1st ed.; CRC Press: Boca Raton, FL, 1996.
- (3) Alder, K.; Pascher, F.; Schmitz, A. Über Die Anlagerung von Maleinsäure-Anhydrid Und Azodicarbonsäure-Ester an Einfach Ungesättigte Kohlenwasserstoffe. Zur Kenntnis von Substitutionsvorgängen in Der Allyl-Stellung. *Ber. Dtsch. Chem. Ges.* **1943**, *76*, 27–53.
- (4) Snider, B. B. Lewis-Acid Catalyzed Ene Reactions. *Acc. Chem. Res.* **1980**, *13*, 426–432.
- (5) Mikami, K.; Shimizu, M. Asymmetric Ene Reactions in Organic Synthesis. *Chem. Rev.* **1992**, *92*, 1021–1050.
- (6) Oppolzer, W.; Snieckus, V. Intramolecular Ene Reactions in Organic Synthesis. *Angew. Chem. Int. Ed.* **1978**, *17*, 476–486.
- (7) Clarke, M. L.; France, M. B. The Carbonyl Ene Reaction. *Tetrahedron* **2008**, *64*, 9003–9031.
- (8) Adams, D. R.; Bhatnagar, S. P. The Prins Reaction. *Synthesis* **1977**, 661–672.
- (9) Olier, C.; Kaafarani, M.; Gastaldi, S.; Bertrand, M. P. Synthesis of Tetrahydropyrans and Related Heterocycles via Prins Cyclization; Extension to Aza-Prins Cyclization. *Tetrahedron* **2010**, *66*, 413–445.
- (10) Arundale, E.; Mikeska, L. A. The Olefin-Aldehyde Condensation: The Prins Reaction. *Chem. Rev.* **1952**, *51*, 505–555.

- (11) Kriewitz, O. Ueber Addition von Formaldehyd an Einige Terpene. *Ber. Dtsch. Chem. Ges.* **1899**, *32*, 57–60.
- (12) Ravindar, L.; Lekkala, R.; Rakesh, K. P.; Asiri, A. M.; Marwani, H. M.; Qin, H. L. Carbonyl-Olefin Metathesis: A Key Review. *Org. Chem. Front.* **2018**, *5*, 1381–1391.
- (13) Ludwig, J. R.; Zimmerman, P. M.; Gianino, J. B.; Schindler, C. S. Iron(III)-Catalysed Carbonyl-Olefin Metathesis. *Nature* **2016**, *533*, 374–379.
- (14) Ludwig, J. R.; Schindler, C. S. Lewis Acid Catalyzed Carbonyl-Olefin Metathesis. *Synlett* **2017**, *28*, 1501–1509.
- (15) Riehl, P. S.; Schindler, C. S. Lewis Acid-Catalyzed Carbonyl–Olefin Metathesis. *Trends Chem.* **2019**, *1*, 272–273.
- (16) Ludwig, J. R.; Watson, R. B.; Nasrallah, D. J.; Gianino, J. B.; Zimmerman, P. M.; Wiscons, R. A.; Schindler, C. S. Interrupted Carbonyl-Olefin Metathesis via Oxygen Atom Transfer. *Science* **2018**, *361*, 1363–1369.
- (17) Ludwig, J. R.; Phan, S.; McAtee, C. C.; Zimmerman, P. M.; Devery, J. J.; Schindler, C. S. Mechanistic Investigations of the Iron(III)-Catalyzed Carbonyl-Olefin Metathesis Reaction. *J. Am. Chem. Soc.* **2017**, *139*, 10832–10842.
- (18) Djurovic, A.; Vayer, M.; Li, Z.; Guillot, R.; Baltaze, J. P.; Gandon, V.; Bour, C. Synthesis of Medium-Sized Carbocycles by Gallium-Catalyzed Tandem Carbonyl-Olefin Metathesis/Transfer Hydrogenation. *Org. Lett.* **2019**, *21*, 8132–8137.
- (19) Ni, S.; Franzén, J. Carbocation Catalysed Ring Closing Aldehyde-Olefin Metathesis. *Chem. Commun.* **2018**, *54*, 12982–12985.
- (20) Zhu, Y.; Rebek, J.; Yu, Y. Cyclizations Catalyzed inside a Hexameric Resorcinarene Capsule. *Chem. Commun.* **2019**, *55*, 3573–3577.

- (21) Hanson, C. S.; Psaltakis, M. C.; Cortes, J. J.; Devery, J. J. Catalyst Behavior in Metal-Catalyzed Carbonyl-Olefin Metathesis. *J. Am. Chem. Soc.* **2019**, *141*, 11870–11880.
- (22) Tran, U. P. N.; Oss, G.; Pace, D. P.; Ho, J.; Nguyen, T. V. Tropylium-Promoted Carbonyl-Olefin Metathesis Reactions. *Chem. Sci.* **2018**, *9*, 5145–5151.
- (23) Catti, L.; Tiefenbacher, K. Brønsted Acid-Catalyzed Carbonyl-Olefin Metathesis inside a Self-Assembled Supramolecular Host. *Angew. Chem. Int. Ed.* **2018**, *57*, 14589–14592.
- (24) Ma, L.; Li, W.; Xi, H.; Bai, X.; Ma, E.; Yan, X.; Li, Z. FeCl₃-Catalyzed Ring-Closing Carbonyl–Olefin Metathesis. *Angew. Chem. Int. Ed.* **2016**, *55*, 10410–10413.
- (25) Davis, A. J.; Watson, R. B.; Nasrallah, D. J.; Gomez-Lopez, J. L.; Schindler, C. S. Superelectrophilic Aluminium(III)–Ion Pairs Promote a Distinct Reaction Path for Carbonyl–Olefin Ring-Closing Metathesis. *Nat. Catal.* **2020**, *3*, 787–796.
- (26) Rykaczewski, K. A.; Groso, E. J.; Vonesh, H. L.; Gaviria, M. A.; Richardson, A. D.; Zehnder, T. E.; Schindler, C. S. Tetrahydropyridines via FeCl₃-Catalyzed Carbonyl-Olefin Metathesis. *Org. Lett.* **2020**, *22*, 2844–2848.
- (27) Albright, H.; Riehl, P. S.; McAtee, C. C.; Reid, J. P.; Ludwig, J. R.; Karp, L. A.; Zimmerman, P. M.; Sigman, M. S.; Schindler, C. S. Catalytic Carbonyl-Olefin Metathesis of Aliphatic Ketones: Iron(III) Homo-Dimers as Lewis Acidic Superelectrophiles. *J. Am. Chem. Soc.* **2019**, *141*, 1690–1700.
- (28) Becker, M. R.; Rykaczewski, K. A.; Ludwig, J. R.; Schindler, C. S. Carbonyl-Olefin Metathesis for the Synthesis of Cyclic Olefins. *Org. Synth.* **2018**, *95*, 472–485.
- (29) Groso, E. J.; Golonka, A. N.; Harding, R. A.; Alexander, B. W.; Sodano, T. M.; Schindler, C. S. 3-Aryl-2,5-Dihydropyrroles via Catalytic Carbonyl-Olefin Metathesis. *ACS Catal.* **2018**, *8*, 2006–2011.

- (30) McAtee, C. C.; Riehl, P. S.; Schindler, C. S. Polycyclic Aromatic Hydrocarbons via Iron(III)-Catalyzed Carbonyl-Olefin Metathesis. *J. Am. Chem. Soc.* **2017**, *139*, 2960–2963.
- (31) Albright, H.; Vonesh, H. L.; Becker, M. R.; Alexander, B. W.; Ludwig, J. R.; Wiscons, R. A.; Schindler, C. S. GaCl₃-Catalyzed Ring-Opening Carbonyl-Olefin Metathesis. *Org. Lett.* **2018**, *20*, 4954–4958.
- (32) Naidu, V. R.; Bah, J.; Franzén, J. Direct Organocatalytic Oxo-Metathesis, a Trans-Selective Carbocation-Catalyzed Olefination of Aldehydes. *Eur. J. Org. Chem.* **2015**, 1834–1839.
- (33) Albright, H.; Vonesh, H. L.; Schindler, C. S. Superelectrophilic Fe(III)-Ion Pairs as Stronger Lewis Acid Catalysts for (E)-Selective Intermolecular Carbonyl-Olefin Metathesis. *Org. Lett.* **2020**, *22*, 3155–3160.
- (34) Riehl, P. S.; Nasrallah, D. J.; Schindler, C. S. Catalytic, Transannular Carbonyl-Olefin Metathesis Reactions. *Chem. Sci.* **2019**, *10*, 10267–10274.
- (35) Santelli, M.; Pons, J.-M. *Lewis Acids and Selectivity in Organic Synthesis*, 1st ed.; CRC Press: Boca Raton, FL, 1996; Vol. 34.
- (36) Jensen, W. B. The Lewis Acid-Base Definitions: A Status Report. *Chem. Rev.* **1978**, *78*, 1–22.
- (37) Lewis, G. N. The Atom and the Molecule. *J. Am. Chem. Soc.* **1916**, *38*, 762–785.
- (38) Himmel, D.; Radtke, V.; Butschke, B.; Krossing, I. Basic Remarks on Acidity. *Angew. Chem. Int. Ed.* **2018**, *57*, 4386–4411.
- (39) Gutmann, V. Solvent Effects on the Reactivities of Organometallic Compounds. *Coord. Chem. Rev.* **1976**, *18*, 225–255.
- (40) Sivaev, I. B.; Bregadze, V. I. Lewis Acidity of Boron Compounds. *Coord. Chem. Rev.* **2014**, *270–271*, 75–88.

- (41) Beckett, M. A.; Strickland, G. C.; Holland, J. R.; Varma, K. S. A Convenient n.m.r. Method for the Measurement of Lewis Acidity at Boron Centres: Correlation of Reaction Rates of Lewis Acid Initiated Epoxide Polymerizations with Lewis Acidity. *Polymer* **1996**, *37*, 4629–4631.
- (42) Childs, R. F.; Mulholland, D. L.; Nixon, A. The Lewis Acid Complexes of α,β -Unsaturated Carbonyl and Nitrile Compounds. A Nuclear Magnetic Resonance Study. *Can. J. Chem.* **1982**, *60*, 801–808.
- (43) Laszlo, P.; Teston, M. Determination of the Acidity of Lewis Acids. *J. Am. Chem. Soc.* **1990**, *112*, 8750–8754.
- (44) Cook, D. INFRARED SPECTRA OF 2,6-DIMETHYL-4-PYRONE COMPLEXES. *Can. J. Chem.* **1961**, *39*, 1184–1189.
- (45) Cook, D. INFRARED SPECTRA OF XANTHONE: LEWIS ACID COMPLEXES. *Can. J. Chem.* **1963**, *41*, 522–526.
- (46) Lappert, M. F. Co-Ordination Compounds Having Carboxylic Esters as Ligands. Part I. Stoichiometry, Structure, and Stereochemistry. *J. Chem. Soc.* **1961**, 817–822.
- (47) Mohammad, A.; Satchell, D. P. N.; Satchell, R. S. Quantitative Aspects of Lewis Acidity. Part VIII. The Validity of Infrared Carbonyl Shifts as Measures of Lewis Acid Strength. The Interaction of Lewis Acids and Phenalen-1-One(Perinaphthenone). *J. Chem. Soc. B* **1967**, 723–725.
- (48) Hanson, C. S.; Psaltakis, M. C.; Cortes, J. J.; Siddiqi, S. S.; Devery, J. J. Investigation of Lewis Acid-Carbonyl Solution Interactions via Infrared-Monitored Titration. *J. Org. Chem.* **2020**, *85*, 820–832.
- (49) Albright, H.; Riehl, P. S.; McAtee, C. C.; Reid, J. P.; Ludwig, J. R.; Karp, L. A.;

- Zimmerman, P. M.; Sigman, M. S.; Schindler, C. S. Catalytic Carbonyl-Olefin Metathesis of Aliphatic Ketones: Iron(III) Homo-Dimers as Lewis Acidic Superelectrophiles. *J. Am. Chem. Soc.* **2019**, *141*, 1690–1700.
- (50) Fukuzumi, S.; Ohkubo, K. Fluorescence Maxima of 10-Methylacridone-Metal Ion Salt Complexes: A Convenient and Quantitative Measure of Lewis Acidity of Metal Ion Salts. *J. Am. Chem. Soc.* **2002**, *124*, 10270–10271.
- (51) Gaffen, J. R.; Bentley, J. N.; Torres, L. C.; Chu, C.; Baumgartner, T.; Caputo, C. B. A Simple and Effective Method of Determining Lewis Acidity by Using Fluorescence. *Chem* **2019**, *5*, 1567–1583.
- (52) Bentley, J. N.; Elgadi, S. A.; Gaffen, J. R.; Demay-Drouhard, P.; Baumgartner, T.; Caputo, C. B. Fluorescent Lewis Adducts: A Practical Guide to Relative Lewis Acidity. *Organometallics* **2020**, *39*, 3645–3655.
- (53) Jupp, A. R.; Johnstone, T. C.; Stephan, D. W. The Global Electrophilicity Index as a Metric for Lewis Acidity. *Dalton Trans.* **2018**, *47*, 7029–7035.
- (54) Jupp, A. R.; Johnstone, T. C.; Stephan, D. W. Improving the Global Electrophilicity Index (GEI) as a Measure of Lewis Acidity. *Inorg. Chem.* **2018**, *57*, 14764–14771.
- (55) Christe, K. O.; Dixon, D. A.; McLemore, D.; Wilson, W. W.; Sheehy, J. A.; Boatz, J. A. On a Quantitative Scale for Lewis Acidity and Recent Progress in Polynitrogen Chemistry. *J. Fluor. Chem.* **2000**, *101*, 151–153.
- (56) Großekappenberg, H.; Reißmann, M.; Schmidtman, M.; Müller, T. Quantitative Assessment of the Lewis Acidity of Silylium Ions. *Organometallics* **2015**, *34*, 4952–4958.
- (57) Mallouk, T. E.; Rosenthal, G. L.; MÜLLER, G.; Brusasco, R.; Bartlett, N. Fluoride Ion Affinities of GeF₄ and BF₃ from Thermodynamic and Structural Data for (SF₃)₂GeF₆,

- $C_1O_2GeF_5$, and $C_1O_2BF_4$. *Inorg. Chem.* **1984**, *23*, 3167–3173.
- (58) Böhrer, H.; Trapp, N.; Himmel, D.; Schleep, M.; Krossing, I. From Unsuccessful H_2 -Activation with FLPs Containing $B(OHfip)_3$ to a Systematic Evaluation of the Lewis Acidity of 33 Lewis Acids Based on Fluoride, Chloride, Hydride and Methyl Ion Affinities. *Dalton Trans.* **2015**, *44*, 7489–7499.
- (59) Carlson, R.; Lundstedt, T.; Nordahl, Å.; Prochazka, M.; Tang, P.-F. L.; Ljungqvist, A. Lewis Acids in Organic Synthesis. Approach to a Selection Strategy for Screening Experiments. *Acta Chem. Scand.* **1986**, *40b*, 522–533.
- (60) Fortuna, C. G.; Musumarra, G.; Nardi, M.; Procopio, A.; Sindona, G.; Scirè, S. Principal Properties (PPs) for Lanthanide Triflates as Lewis-Acid Catalysts. *J. Chemom.* **2006**, *20*, 418–424.
- (61) Reid, J. P.; Sigman, M. S. Comparing Quantitative Prediction Methods for the Discovery of Small-Molecule Chiral Catalysts. *Nat. Rev. Chem.* **2018**, *2*, 290–305.
- (62) Santiago, C. B.; Guo, J. Y.; Sigman, M. S. Predictive and Mechanistic Multivariate Linear Regression Models for Reaction Development. *Chem. Sci.* **2018**, *9*, 2398–2412.
- (63) Sigman, M. S.; Harper, K. C.; Bess, E. N.; Milo, A. The Development of Multidimensional Analysis Tools for Asymmetric Catalysis and Beyond. *Acc. Chem. Res.* **2016**, *49*, 1292–1301.
- (64) Rosales, A. R.; Ross, S. P.; Helquist, P.; Norrby, P. O.; Sigman, M. S.; Wiest, O.; Wiest, O. Transition State Force Field for the Asymmetric Redox-Relay Heck Reaction. *J. Am. Chem. Soc.* **2020**, *142*, 9700–9707.
- (65) Miró, J.; Gensch, T.; Ellwart, M.; Han, S. J.; Lin, H. H.; Sigman, M. S.; Toste, F. D. Enantioselective Allenolate-Claisen Rearrangement Using Chiral Phosphate Catalysts. *J.*

- Am. Chem. Soc.* **2020**, *142*, 6390–6399.
- (66) Robinson, S. G.; Sigman, M. S. Integrating Electrochemical and Statistical Analysis Tools for Molecular Design and Mechanistic Understanding. *Acc. Chem. Res.* **2020**, *53*, 289–299.
- (67) Wu, K.; Doyle, A. G. Parameterization of Phosphine Ligands Demonstrates Enhancement of Nickel Catalysis via Remote Steric Effects. *Nat. Chem.* **2017**, *9*, 779–784.
- (68) Sevov, C. S.; Hickey, D. P.; Cook, M. E.; Robinson, S. G.; Barnett, S.; Minter, S. D.; Sigman, M. S.; Sanford, M. S. Physical Organic Approach to Persistent, Cyclable, Low-Potential Electrolytes for Flow Battery Applications. *J. Am. Chem. Soc.* **2017**, *139*, 2924–2927.
- (69) Brown, I. D. What Factors Determine Cation Coordination Numbers? *Acta Crystallogr. B* **1988**, *44*, 545–553.
- (70) Kepp, K. P. A Quantitative Scale of Oxophilicity and Thiophilicity. *Inorg. Chem.* **2016**, *55*, 9461–9470.
- (71) Zhang, Y. Electronegativities of Elements in Valence States and Their Applications. 1. Electronegativities of Elements in Valence States. *Inorg. Chem.* **1982**, *21*, 3886–3889.
- (72) Shannon, R. D. Revised Effective Ionic Radii and Systematic Studies of Interatomic Distances in Halides and Chalcogenides. *Acta Crystallogr. A* **1976**, *32*, 751–767.
- (73) Milo, A.; Bess, E. N.; Sigman, M. S. Interrogating Selectivity in Catalysis Using Molecular Vibrations. *Nature* **2014**, *507*, 210–214.
- (74) Brethomé, A. V.; Fletcher, S. P.; Paton, R. S. Conformational Effects on Physical-Organic Descriptors: The Case of Sterimol Steric Parameters. *ACS Catal.* **2019**, *9*, 2313–2323.
- (75) Harper, K. C.; Bess, E. N.; Sigman, M. S. Multidimensional Steric Parameters in the Analysis of Asymmetric Catalytic Reactions. *Nat. Chem.* **2012**, *4*, 366–374.

- (76) Reed, A. E.; Weinstock, R. B.; Weinhold, F. Natural Population Analysis. *J. Chem. Phys.* **1985**, *83*, 735–746.
- (77) Reed, A. E.; Weinhold, F. Natural Bond Orbital Analysis of Near-Hartree-Fock Water Dimer. *J. Chem. Phys.* **1983**, *78*, 4066–4073.
- (78) Yavari, K.; Moussa, S.; Ben Hassine, B.; Retailleau, P.; Voituriez, A.; Marinetti, A. 1H-Phosphindoles as Structural Units in the Synthesis of Chiral Helicenes. *Angew. Chem. Int. Ed.* **2012**, *51*, 6748–6752.
- (79) Fernandes, R. A.; Gholap, S. P.; Mulay, S. V. A Facile Chemoselective Deprotection of Aryl Silyl Ethers Using Sodium Hydride/DMF and in Situ Protection of Phenol with Various Groups. *RSC Adv.* **2014**, *4*, 16438–16443.
- (80) Manuela, M.; Raposo, M.; Herbivo, C.; Hugues, V.; Clermont, G.; Castro, M. C. R.; Comel, A.; Blanchard-Desce, M. Synthesis, Fluorescence, and Two-Photon Absorption Properties of Push–Pull 5-Arylthieno[3,2-b]Thiophene Derivatives. *Eur. J. Org. Chem.* **2016**, *2016*, 5263–5273.
- (81) Tamiya, M.; Jager, C.; Ohmori, K.; Suzuki, K. Stereoselective Access to Functionalized Dihydrophenanthrenes via Reductive Cyclization of Biaryl Ene-Aldehydes. *Synlett* **2007**, 780–784.
- (82) Zhao, Y.; Truhlar, D. G. The M06 Suite of Density Functionals for Main Group Thermochemistry, Thermochemical Kinetics, Noncovalent Interactions, Excited States, and Transition Elements: Two New Functionals and Systematic Testing of Four M06-Class Functionals and 12 Other Function. *Theor. Chem. Acc.* **2008**, *120*, 215–241.
- (83) Weigend, F.; Ahlrichs, R. Balanced Basis Sets of Split Valence, Triple Zeta Valence and Quadruple Zeta Valence Quality for H to Rn: Design and Assessment of Accuracy. *Phys.*

- Chem. Chem. Phys.* **2005**, *7*, 3297–3305.
- (84) Frisch, M. J.; Trucks, G. W.; Schlegel, H. B.; Scuseria, G. E.; Robb, M. A.; Cheeseman, J. R.; Scalmani, G.; Barone, V.; Mennucci, B.; Petersson, G. A.; et al. Gaussian Inc.: Wallingford CT. 2016.
- (85) Glendening, E. D.; Badenhoop, J. K.; Reed, A. E.; Carpenter, J. E.; Bohmann, J. A.; Morales, C. M.; Landis, C. R.; Weinhold, F. Theoretical Chemistry Institute, University of Wisconsin: Madison, WI.
- (86) Piou, T.; Romanov-Michailidis, F.; Romanova-Michaelides, M.; Jackson, K. E.; Semakul, N.; Taggart, T. D.; Newell, B. S.; Rithner, C. D.; Paton, R. S.; Rovis, T. Correlating Reactivity and Selectivity to Cyclopentadienyl Ligand Properties in Rh(III)-Catalyzed C-H Activation Reactions: An Experimental and Computational Study. *J. Am. Chem. Soc.* **2017**, *139*, 1296–1310.
- (87) The MathWorks, Inc.: Natick, Massachusetts, United States.
- (88) Grimme, S. Semiempirical GGA-Type Density Functional Constructed with a Long-Range Dispersion Correction. *J. Comput. Chem.* **2006**, *27*, 1787–1799.
- (89) Hehre, W. J.; Ditchfield, K.; Pople, J. A. Self-Consistent Molecular Orbital Methods. XII. Further Extensions of Gaussian-Type Basis Sets for Use in Molecular Orbital Studies of Organic Molecules. *J. Chem. Phys.* **1972**, *56*, 2257–2261.
- (90) Cossi, M.; Rega, N.; Scalmani, G.; Barone, V. Energies, Structures, and Electronic Properties of Molecules in Solution with the C-PCM Solvation Model. *J. Comput. Chem.* **2003**, *24*, 669–681.
- (91) Verloop, A.; Tipker, J. A Comparative Study of New Steric Parameters in Drug Design. *Pharmacochem. Libr.* **1977**, *2*, 63–81.

- (92) Verloop, A.; Tipker, J. Physical Basis of STERIMOL and Related Steric Constants. *Pharmacochem. Libr.* **1987**, *10*, 97–102.
- (93) Guo, J. Y.; Minko, Y.; Santiago, C. B.; Sigman, M. S. Developing Comprehensive Computational Parameter Sets to Describe the Performance of Pyridine-Oxazoline and Related Ligands. *ACS Catal.* **2017**, *7*, 4144–4151.
- (94) Novel Drug Approvals for 2019 <https://www.fda.gov/drugs/new-drugs-fda-cders-new-molecular-entities-and-new-therapeutic-biological-products/novel-drug-approvals-2019> (accessed Feb 16, 2021).
- (95) Vitaku, E.; Smith, D. T.; Njardarson, J. T. Analysis of the Structural Diversity, Substitution Patterns, and Frequency of Nitrogen Heterocycles among U.S. FDA Approved Pharmaceuticals. *J. Med. Chem.* **2014**, *57*, 10257–10274.
- (96) Cotellic (cobimetinib)
https://www.accessdata.fda.gov/drugsatfda_docs/nda/2015/206192Orig1s000TOC.cfm
(accessed Feb 16, 2021).
- (97) BAXDELA (delafloxacin)
https://www.accessdata.fda.gov/drugsatfda_docs/nda/2017/208610Orig1s000,208611Orig1s000TOC.cfm (accessed Feb 16, 2021).
- (98) Drug Approval Package: Olumiant (baricitinib)
https://www.accessdata.fda.gov/drugsatfda_docs/nda/2018/207924Orig1s000TOC.cfm
(accessed Feb 16, 2021).
- (99) Lovering, F.; Bikker, J.; Humblet, C. Escape from Flatland: Increasing Saturation as an Approach to Improving Clinical Success. *J. Med. Chem.* **2009**, *52*, 6752–6756.
- (100) Lovering, F. Escape from Flatland 2: Complexity and Promiscuity. *MedChemComm* **2013**,

- 4, 515–519.
- (101) Kerns, E. H.; Di, L. *Drug-Like Properties: Concepts, Structure Design and Methods*; Academic Press, 2008.
- (102) Shu, Y. Z.; Johnson, B. M.; Yang, T. J. Role of Biotransformation Studies in Minimizing Metabolism-Related Liabilities in Drug Discovery. *AAPS J.* **2008**, *10*, 178–192.
- (103) St. Jean, D. J.; Fotsch, C. Mitigating Heterocycle Metabolism in Drug Discovery. *J. Med. Chem.* **2012**, *55*, 6002–6020.
- (104) Brown, A.; Brown, T. B.; Calabrese, A.; Ellis, D.; Puhalo, N.; Ralph, M.; Watson, L. Triazole Oxytocin Antagonists: Identification of an Aryloxyazetidone Replacement for a Biaryl Substituent. *Bioorg. Med. Chem. Lett.* **2010**, *20*, 516–520.
- (105) Fish, P. V.; Brown, A. D.; Evrard, E.; Roberts, L. R. 7-Sulfonamido-3-Benzazepines as Potent and Selective 5-HT_{2C} Receptor Agonists: Hit-to-Lead Optimization. *Bioorg. Med. Chem. Lett.* **2009**, *19*, 1871–1875.
- (106) Brandi, A.; Cicchi, S.; Cordero, F. M. Novel Syntheses of Azetidines and Azetidinones. *Chem. Rev.* **2008**, *108*, 3988–4035.
- (107) Cromwell, N. H.; Phillips, B. The Azetidines. Recent Synthetic Developments. *Chem. Rev.* **1979**, *79*, 331–358.
- (108) Antermite, D.; Degennaro, L.; Luisi, R. Recent Advances in the Chemistry of Metallated Azetidines. *Org. Biomol. Chem.* **2017**, *15*, 34–50.
- (109) Yoda, H.; Takahashi, M.; Sengoku, T. Heterocycles in Natural Product Synthesis; Majumdar, K. C., Chattopadhyay, S. K., Eds.; Wiley-VCH, 2011.
- (110) Clayden, J.; Greeves, N.; Warren, S. *Organic Chemistry*; Oxford University Press, 2012; pp 805–807.

- (111) Wadsworth, D. H. A Facile Synthesis of Azetidines. *J. Org. Chem.* **1967**, *32*, 1184–1187.
- (112) Pitts, C. R.; Lectka, T. Chemical Synthesis of β -Lactams: Asymmetric Catalysis and Other Recent Advances. *Chem. Rev.* **2014**, *114*, 7930–7953.
- (113) Alcaide, B.; Almendros, P.; Aragoncillo, C. β -Lactams: Versatile Building Blocks for the Stereoselective Synthesis of Non- β -Lactam Products. *Chem. Rev.* **2007**, *107*, 4437–4492.
- (114) Kværnø, L.; Werder, M.; Hauser, H.; Carreira, E. M. Synthesis and in Vitro Evaluation of Inhibitors of Intestinal Cholesterol Absorption. *J. Med. Chem.* **2005**, *48*, 6035–6053.
- (115) Funke, W. Synthesis and Properties of 1-Azabicyclo[1.1.0]Butanes. *Angew. Chem.Int. Ed.* **1969**, *8*, 70–71.
- (116) Funke, W. Über Synthesen Und Reaktionen von 1-Aza-bicyclo[1.1.0]Butanen. *Chem. Ber.* **1969**, *102*, 3148–3158.
- (117) Gianatassio, R.; Lopchuk, J. M.; Wang, J.; Pan, C. M.; Malins, L. R.; Prieto, L.; Brandt, T. A.; Collins, M. R.; Gallego, G. M.; Sach, N. W.; et al. Strain-Release Amination. *Science* **2016**, *351*, 241–246.
- (118) Lopchuk, J. M.; Fjelbye, K.; Kawamata, Y.; Malins, L. R.; Pan, C. M.; Gianatassio, R.; Wang, J.; Prieto, L.; Bradow, J.; Brandt, T. A.; et al. Strain-Release Heteroatom Functionalization: Development, Scope, and Stereospecificity. *J. Am. Chem. Soc.* **2017**, *139*, 3209–3226.
- (119) Gianatassio, R.; Kadish, D. Direct Alkylation of 1-Azabicyclo[1.1.0]Butanes. *Org. Lett.* **2019**, *21*, 2060–2063.
- (120) Aben, R. W. M.; Smit, R.; Scheeren, J. W. High-Pressure-Promoted (2+2) Cycloadditions of Imines With Electron-Rich Alkenes. A Simple Route To Azetidines and β -Amino Carbonyl Compounds. *J. Org. Chem.* **1987**, *52*, 365–370.

- (121) Rainoldi, G.; Faltracco, M.; Lo Presti, L.; Silvani, A.; Lesma, G. Highly Diastereoselective Entry into Chiral Spirooxindole-Based 4-Methyleneazetidines: Via Formal [2+2] Annulation Reaction. *Chem. Commun.* **2016**, *52*, 11575–11578.
- (122) Nakamura, I.; Nemoto, T.; Yamamoto, Y.; De Armin, M. Thermally Induced and Silver-Salt-Catalyzed [2+2] Cycloadditions of Imines to (Alkoxymethylene)Cyclopropanes. *Angew. Chem. Int. Ed.* **2006**, *45*, 5176–5179.
- (123) Akiyama, T.; Daidouji, K.; Fuchibe, K. Cu(I)-Catalyzed Enantioselective [2+2] Cycloaddition of 1-Methoxyallenylsilane with α -Imino Ester: Chiral Synthesis of α,β -Unsaturated Acylsilanes. *Org. Lett.* **2003**, *5*, 3691–3693.
- (124) Uyehara, T.; Yuuki, M.; Masaki, H.; Matsumoto, M.; Ueno, M.; Sato, T. Lewis Acid-Promoted [2+2] Azetidine Annulation of N-Acylaldimines with Allyltriisopropylsilane. *Chem. Lett.* **1995**, *24*, 789–790.
- (125) Cabral, J.; Laszlo, P.; Montaufer, M. T. Schizoid Reactivity of N-Benzylidene Aniline toward Clay-Catalyzed cycloadditions. *Tetrahedron Lett.* **1988**, *29*, 547–550.
- (126) Tsuge, O.; Tashiro, M.; Oe, K. Photochemical Reaction of 2,5-Diphenyl-1,3,4-Oxadiazole with Indene. *Tetrahedron Lett.* **1968**, *9*, 3971–3974.
- (127) D'Auria, M.; Racioppi, R. Oxetane Synthesis through the Paternò-Büchi Reaction. *Molecules* **2013**, *18*, 11384–11428.
- (128) D'Auria, M. The Paternò-Büchi Reaction – a Comprehensive Review. *Photochem. Photobiol. Sci.* **2019**, *18*, 2297–2362.
- (129) Poplata, S.; Tröster, A.; Zou, Y. Q.; Bach, T. Recent Advances in the Synthesis of Cyclobutanes by Olefin [2 + 2] Photocycloaddition Reactions. *Chem. Rev.* **2016**, *116*, 9748–9815.

- (130) Pratt, A. C. The Photochemistry of Imines. *Chem. Soc. Rev.* **1977**, *6*, 63–81.
- (131) Padwa, A. Photochemistry of the Carbon–Nitrogen Double Bond. *Chem. Rev.* **1977**, *77*, 37–68.
- (132) Padwa, A.; Albrecht, F. Photoisomerization about the Carbon-Nitrogen Double Bond of an Oxime Ether. *J. Am. Chem. Soc.* **1972**, *94*, 1000–1002.
- (133) Anderson, D. R.; Keute, J. S.; Koch, T. H.; Moseley, R. H. Di-Tert-Butyl Nitroxide Quenching of the Photoaddition of Olefins to the Carbon-Nitrogen Double Bond of 3-Ethoxyisoindolenone. *J. Am. Chem. Soc.* **1977**, *99*, 6332–6340.
- (134) Rodehorst, R. M.; Koch, T. H. Photochemical Reactivity of Keto Imino Ethers. VI. Type I Rearrangement and (2+2) Photocycloaddition to the Carbon-Nitrogen Double Bond of 2-Oxazolin-4-Ones. *J. Am. Chem. Soc.* **1975**, *97*, 7298–7304.
- (135) Koch, T. H.; Rodehorst, R. M. 2+2 Photocycloaddition to a Carbon Nitrogen Double Bond II. 2-Phenyl-2-Oxazolin-4-One. *Tetrahedron Lett.* **1972**, *13*, 4039–4042.
- (136) Howard, K. A.; Koch, T. H. Photochemical Reactivity of Keto Imino Ethers. V. (2+2) Photocycloaddition to the Carbon-Nitrogen Double Bond of 3-Ethoxyisoindolone. *J. Am. Chem. Soc.* **1975**, *97*, 7288–7298.
- (137) Koch, T. H.; Howard, K. H. 2+2 Photocycloaddition to a Carbon Nitrogen Double Bond I. 3-Ethoxyisoindolone. *Tetrahedron Lett.* **1972**, *13*, 4035–4038.
- (138) Swenton, J. S.; Balchunis, R. J. Photochemical Functionalization of 6-azauracils to 5-substituted-6-azauracils. *J. Heterocycl. Chem.* **1974**, *11*, 917–920.
- (139) Swenton, J. S.; Hyatt, J. A. Photosensitized Cycloadditions to 1,3-Dimethyl-6-Azauracil and 1,3-Dimethyl-6-Azathymine. An Imine Linkage Unusually Reactive toward Photocycloaddition. *J. Am. Chem. Soc.* **1974**, *96*, 4879–4885.

- (140) Hyatt, J. A.; Swenton, J. S. Photochemical Reactivity of 2,4-Dimethyl-1,2,4-Triazine-3,5-(2H)-Dione (1,3-Dimethyl-6-Azauracil). *J. Chem. Soc. Chem. Commun.* **1972**, 1144–1145.
- (141) Futamura, S.; Ohta, H.; Kamiya, Y. PHOTOCYCLOADDITION OF 6-CYANOPHENANTHRIDINE TO ELECTRON-RICH OLEFINS. *Chem. Lett.* **1980**, 9, 655–658.
- (142) Futamura, S.; Ohta, H.; Kamiya, Y. The Photocycloaddition of 6-Substituted Phenanthridines to Electron-Rich Olefins. *Bull. Chem. Soc. Jpn.* **1982**, 55, 2190–2194.
- (143) Nishio, T.; Kondo, M.; Omote, Y. Photochemical Reactions of Tetrahydroquinoxalin-2(1H)-ones and Related Compound. *Helv. Chim. Acta* **1991**, 74, 225–231.
- (144) Nishio, T.; Nishiyama, T.; Omote, Y. Photochemical [2+2] Cycloaddition of the C–N Bond of Pteridine-2,4,7-triones to Alkenes. *Liebigs Ann. Chem.* **1988**, 1988, 441–443.
- (145) Nishio, T.; Omote, Y. Photocycloaddition Reactions of 1,4-Benzoxazin-2-Ones and Electron-Poor Olefins. *J. Org. Chem.* **1985**, 50, 1370–1373.
- (146) Nishio, T. The (2+2) Photocycloaddition of the Carbon-Nitrogen Double Bond of Quinoxalin-2(1H)-Ones to Electron-Deficient Olefins. *J. Org. Chem.* **1984**, 49, 827–832.
- (147) Kawamura, Y.; Kumagai, T.; Mukai, T. PHOTOCYCLOADDITION REACTION OF 3-ARYL-2-ISOXAZOLINES WITH INDENE. GENERATION OF [2+2] CYCLOADDUCT STEREOISOMERS. *Chem. Lett.* **1985**, 14, 1937–1940.
- (148) Kumagai, T.; Kawamura, Y.; Mukai, T. PHOTOCYCLOADDITION OF 3-ARYL-2-ISOXAZOLINES WITH FIVE-MEMBERED HETEROCYCLES. *Chem. Lett.* **1983**, 12, 1357–1360.
- (149) Kumagai, T.; Shimizu, K.; Kawamura, Y.; Mukai, T. Photochemistry of 3-Aryl-2-Isoxazoline. *Tetrahedron* **1981**, 37, 3365–3376.

- (150) Sampedro, D.; Soldevilla, A.; Campos, P. J.; Ruiz, R.; Rodríguez, M. A. Regio- and Stereochemistry of [2+2] Photocycloadditions of Imines to Alkenes: A Computational and Experimental Study. *J. Org. Chem.* **2008**, *73*, 8331–8336.
- (151) Sampedro, D. Computational Exploration of the Photocycloaddition of Imines to Alkenes. *ChemPhysChem* **2006**, *7*, 2456–2459.
- (152) Sakamoto, R.; Inada, T.; Sakurai, S.; Maruoka, K. [2 + 2] Photocycloadditions between the Carbon-Nitrogen Double Bonds of Imines and Carbon-Carbon Double Bonds. *Org. Lett.* **2016**, *18*, 6252–6255.
- (153) Li, X.; Großkopf, J.; Jandl, C.; Bach, T. Enantioselective, Visible Light Mediated Aza Paternò–Büchi Reactions of Quinoxalinones. *Angew. Chem. Int. Ed.* **2021**, *60*, 2684–2688.
- (154) Fischer, G.; Fritz, H.; Prinzbach, H. An Intramolecular Imine/Ene - Photo-[2+2]-Cycloaddition Reaction. *Tetrahedron Lett.* **1986**, *27*, 1269–1272.
- (155) Kumarasamy, E.; Kandappa, S. K.; Raghunathan, R.; Jockusch, S.; Sivaguru, J. Realizing an Aza Paternò–Büchi Reaction. *Angew. Chem. Int. Ed.* **2017**, *56*, 7056–7061.
- (156) Kumarasamy, E.; Raghunathan, R.; Kandappa, S. K.; Sreenithya, A.; Jockusch, S.; Sunoj, R. B.; Sivaguru, J. Transposed Paternò–Büchi Reaction. *J. Am. Chem. Soc.* **2017**, *139*, 655–662.
- (157) Zhu, M.; Zhang, X.; Zheng, C.; You, S. L. Visible-Light-Induced Dearomatization via [2+2] Cycloaddition or 1,5-Hydrogen Atom Transfer: Divergent Reaction Pathways of Transient Diradicals. *ACS Catal.* **2020**, *10*, 12618–12626.
- (158) Stephenson, C. R. J.; Yoon, T. P.; MacMillan, D. W. C. *Visible Light Photocatalysis in Organic Chemistry*; Wiley-VCH: Weinheim, Germany, 2018.
- (159) Prier, C. K.; Rankic, D.; MacMillan, D. W. C. Visible Light Photoredox Catalysis with

- Transition Metal Complexes: Applications in Organic Synthesis. *Chem. Rev.* **2013**, *113*, 5322–5363.
- (160) Zhou, Q. Q.; Zou, Y. Q.; Lu, L. Q.; Xiao, W. J. Visible-Light-Induced Organic Photochemical Reactions through Energy-Transfer Pathways. *Angew. Chem. Int. Ed.* **2019**, *58*, 1586–1604.
- (161) Hammond, G. S.; Turro, N. J. Organic Photochemistry. *Science* **1963**, *142*, 1541–1553.
- (162) Strieth-Kalthoff, F.; James, M. J.; Teders, M.; Pitzer, L.; Glorius, F. Energy Transfer Catalysis Mediated by Visible Light: Principles, Applications, Directions. *Chem. Soc. Rev.* **2018**, *47*, 7190–7202.
- (163) Strieth-Kalthoff, F.; Glorius, F. Triplet Energy Transfer Photocatalysis: Unlocking the Next Level. *Chem* **2020**, *6*, 1888–1903.
- (164) Strieth-Kalthoff, F.; James, M. J.; Teders, M.; Pitzer, L.; Glorius, F. Energy Transfer Catalysis Mediated by Visible Light: Principles, Applications, Directions. *Chem. Soc. Rev.* **2018**, *47*, 7190–7202.
- (165) Teegardin, K.; Day, J. I.; Chan, J.; Weaver, J. Advances in Photocatalysis: A Microreview of Visible Light Mediated Ruthenium and Iridium Catalyzed Organic Transformations. *Org. Process Res. Dev.* **2016**, *20*, 1156–1163.
- (166) Ni, T.; Caldwell, R. A.; Melton, L. A. The Relaxed and Spectroscopic Energies of Olefin Triplets. *J. Am. Chem. Soc.* **1989**, *111*, 457–464.
- (167) Lu, Z.; Yoon, T. P. Visible Light Photocatalysis of [2+2] Styrene Cycloadditions by Energy Transfer. *Angew. Chem. Int. Ed.* **2012**, *51*, 10329–10332.
- (168) Hurlley, A. E.; Lu, Z.; Yoon, T. P. Cycloaddition of 1,3-Dienes by Visible Light Photocatalysis. *Angew. Chem. Int. Ed.* **2014**, *53*, 8991–8994.

- (169) Enders, D.; Gries, J. Asymmetric Synthesis of Substituted Azetidine Type α - and β -Amino Acids. *Synthesis* **2005**, 3508–3516.
- (170) Monos, T. M.; Sun, A. C.; McAtee, R. C.; Devery, J. J.; Stephenson, C. R. J. Microwave-Assisted Synthesis of Heteroleptic Ir(III)⁺ Polypyridyl Complexes. *J. Org. Chem.* **2016**, *81*, 6988–6994.
- (171) Frigerio, M.; Santagostino, M.; Sputore, S. A User-Friendly Entry to 2-Iodoxybenzoic Acid (IBX). *J. Org. Chem.* **1999**, *64*, 4537–4538.
- (172) Roth, H. G.; Romero, N. A.; Nicewicz, D. A. Experimental and Calculated Electrochemical Potentials of Common Organic Molecules for Applications to Single-Electron Redox Chemistry. *Synlett* **2016**, *27*, 714–723.
- (173) Huo, X.; He, R.; Fu, J.; Zhang, J.; Yang, G.; Zhang, W. Stereoselective and Site-Specific Allylic Alkylation of Amino Acids and Small Peptides via a Pd/Cu Dual Catalysis. *J. Am. Chem. Soc.* **2017**, *139*, 9819–9822.
- (174) Guo, R.; Yang, H.; Tang, P. Silver-Catalyzed Meerwein Arylation: Intermolecular and Intramolecular Fluoroarylation of Styrenes. *Chem. Commun.* **2015**, *51*, 8829–8832.
- (175) Venning, A. R. O.; Kwiatkowski, M. R.; Roque Peña, J. E.; Lainhart, B. C.; Guruparan, A. A.; Alexanian, E. J. Palladium-Catalyzed Carbocyclizations of Unactivated Alkyl Bromides with Alkenes Involving Auto-Tandem Catalysis. *J. Am. Chem. Soc.* **2017**, *139*, 11595–11600.
- (176) Tamura, O.; Mitsuya, T.; Huang, X.; Tsutsumi, Y.; Hattori, S.; Ishibashi, H. Intramolecular Cycloaddition of O-Tert-Butyldimethylsilyloximes in the Presence of BF₃-OEt₂. *J. Org. Chem.* **2005**, *70*, 10720–10725.
- (177) Musacchio, A. J.; Nguyen, L. Q.; Beard, G. H.; Knowles, R. R. Catalytic Olefin

- Hydroamination with Aminium Radical Cations: A Photoredox Method for Direct C-N Bond Formation. *J. Am. Chem. Soc.* **2014**, *136*, 12217–12220.
- (178) Miege, F.; Meyer, C.; Cossy, J. Rhodium-Catalyzed Cycloisomerization Involving Cyclopropenes: Efficient Stereoselective Synthesis of Medium-Sized Heterocyclic Scaffolds. *Angew. Chem. Int. Ed.* **2011**, *50*, 5932–5937.
- (179) Kimura, M.; Mori, M.; Tamaru, Y. Palladium-Catalyzed 1,3-Diol Fragmentation: Synthesis of ω -Dienyl Aldehydes. *Chem. Commun.* **2007**, 4504–4506.
- (180) Kablaoui, N. M.; Buchwald, S. L. Development of a Method for the Reductive Cyclization of Enones by a Titanium Catalyst. *J. Am. Chem. Soc.* **1996**, *118*, 3182–3191.
- (181) Miyata, O.; Muroya, K.; Kobayashi, T.; Yamanaka, R.; Kajisa, S.; Koide, J.; Naito, T. Radical Cyclization in Heterocycle Synthesis. Part 13: Sulfanyl Radical Addition-Cyclization of Oxime Ethers and Hydrazones Connected with Alkenes for Synthesis of Cyclic β -Amino Acids. *Tetrahedron* **2002**, *58*, 4459–4479.
- (182) Yu, Z.; Liu, L.; Zhang, J. Triflic Acid-Catalyzed Enynes Cyclization: A New Strategy beyond Electrophilic π -Activation. *Chem. Eur. J.* **2016**, *22*, 8488–8492.
- (183) West, T. H.; Daniels, D. S. B.; Slawin, A. M. Z.; Smith, A. D. An Isothiourea-Catalyzed Asymmetric [2,3]-Rearrangement of Allylic Ammonium Ylides. *J. Am. Chem. Soc.* **2014**, *136*, 4476–4479.
- (184) Chen, Z.; Sun, J. Enantio- and Diastereoselective Assembly of Tetrahydrofuran and Tetrahydropyran Skeletons with All-Carbon-Substituted Quaternary Stereocenters. *Angew. Chem. Int. Ed.* **2013**, *52*, 13593–13596.
- (185) Logan, A. W. J.; Parker, J. S.; Hallside, M. S.; Burton, J. W. Manganese(III) Acetate Mediated Oxidative Radical Cyclizations. Toward Vicinal All-Carbon Quaternary

- Stereocenters. *Org. Lett.* **2012**, *14*, 2940–2943.
- (186) Bosque, I.; Bagdatli, E.; Foubelo, F.; Gonzalez-Gomez, J. C. Regio- and Stereoselective Aminopentadienylation of Carbonyl Compounds. *J. Org. Chem.* **2014**, *79*, 1796–1804.
- (187) Li, G. Y.; Che, C. M. Highly Selective Intra- and Intermolecular Coupling Reactions of Diazo Compounds to Form Cis-Alkenes Using a Ruthenium Porphyrin Catalyst. *Org. Lett.* **2004**, *6*, 1621–1623.
- (188) Mahesh, M.; Murphy, J. A.; Wessel, H. P. Novel Deoxygenation Reaction of Epoxides by Indium. *J. Org. Chem.* **2005**, *70*, 4118–4123.
- (189) Desrat, S.; Van De Weghe, P. Intramolecular Imino Diels - Alder Reaction: Progress toward the Synthesis of Uncialamycin. *J. Org. Chem.* **2009**, *74*, 6728–6734.
- (190) Cremonesi, G.; Croce, P. D.; Fontana, F.; Fiorelli, C.; Rosa, C. La. Stereoselective Synthesis of β,ϵ -Dihydroxy- α -Amino Acids by Ring Opening of 4,5-Dihydroisoxazolyl Derivatives. *Tetrahedron Asymmetry* **2008**, *19*, 2850–2855.
- (191) D. Roth, H. Light-Induced Chemistry of Oximes and Derivatives. In *PATAI'S Chemistry of Functional Groups*; John Wiley & Sons, Ltd: Chichester, UK, 2010.
- (192) Kandappa, S. K.; Valloli, L. K.; Ahuja, S.; Parthiban, J.; Sivaguru, J. Taming the Excited State Reactivity of Imines – from Non-Radiative Decay to Aza Paternò-Büchi Reaction. *Chem. Soc. Rev.* **2021**, *50*, 1617–1641.
- (193) Padwa, A.; Albrecht, F. Concentration Effects in the Photochemical Syn-Anti Isomerization of an Oxime Ether. *J. Org. Chem.* **1974**, *39*, 2361–2366.
- (194) Padwa, A.; Albrecht, F. Excimer Involvement in the Photoisomerization of an Oxime Ether. *Tetrahedron Lett.* **1974**, *15*, 1083–1086.
- (195) Padwa, A.; Albrecht, F. Photoisomerization about the Carbon-Nitrogen Double Bond of an

- Oxime Ether. *J. Am. Chem. Soc.* **1972**, *94*, 1000–1002.
- (196) Padwa, A.; Albrecht, F. Photochemical Syn-Anti Isomerization About the Carbon-Nitrogen Double Bond. *J. Am. Chem. Soc.* **1974**, *96*, 4849–4857.
- (197) Amin, J. H.; de Mayo, P. The Irradiation of Aryl Aldoximes. *Tetrahedron Lett.* **1963**, *4*, 1585–1589.
- (198) Oine, T.; Mukai, T. Evidence for the Formation of Oxaziridines during the Irradiation of Oximes. *Tetrahedron Lett.* **1969**, *10*, 157–160.
- (199) Hasebe, M.; Tsuchiya, T. Photochemical Generation of Aliphatic Radicals from Benzophenone Oxime Esters: Simple Synthesis of Alkylbenzenes and Alkylpyridines. *Tetrahedron Lett.* **1986**, *27*, 3239–3242.
- (200) Hasebe, M.; Kogawa, K.; Tsuchiya, T. Photochemical Arylation by Oxime Esters in Benzene and Pyridine: Simple Synthesis of Biaryl Compounds. *Tetrahedron Lett.* **1984**, *25*, 3887–3890.
- (201) Stoermer, R. Über Die Umlagerung Der Stabilen Stereoisomeren in Labile Durch Ultraviolettes Licht. *Ber. Dtsch. Chem. Ges.* **1911**, *44*, 637–668.
- (202) Patra, T.; Mukherjee, S.; Ma, J.; Strieth-Kalthoff, F.; Glorius, F. Visible-Light-Photosensitized Aryl and Alkyl Decarboxylative Functionalization Reactions. *Angew. Chem. Int. Ed.* **2019**, *58*, 10514–10520.
- (203) Patra, T.; Bellotti, P.; Strieth-Kalthoff, F.; Glorius, F. Photosensitized Intermolecular Carboimination of Alkenes through the Persistent Radical Effect. *Angew. Chem. Int. Ed.* **2020**, *59*, 3172–3177.
- (204) Patra, T.; Das, M.; Daniliuc, C. G.; Glorius, F. Metal-Free Photosensitized Oxyimination of Unactivated Alkenes with Bifunctional Oxime Carbonates. *Nat. Catal.* **2021**, *4*, 54–61.

- (205) Soni, V. K.; Lee, S.; Kang, J.; Moon, Y. K.; Hwang, H. S.; You, Y.; Cho, E. J. Reactivity Tuning for Radical-Radical Cross-Coupling via Selective Photocatalytic Energy Transfer: Access to Amine Building Blocks. *ACS Catal.* **2019**, *9*, 10454–10463.
- (206) Nicastrì, M. C.; Lehnher, D.; Lam, Y. H.; Dirocco, D. A.; Rovis, T. Synthesis of Sterically Hindered Primary Amines by Concurrent Tandem Photoredox Catalysis. *J. Am. Chem. Soc.* **2020**, *142*, 987–998.
- (207) Prusinowski, A. F.; Twumasi, R. K.; Wappes, E. A.; Nagib, D. A. Vicinal, Double C-H Functionalization of Alcohols via an Imidate Radical-Polar Crossover Cascade. *J. Am. Chem. Soc.* **2020**, *142*, 5429–5438.
- (208) Nakafuku, K. M.; Twumasi, R. K.; Vanitcha, A.; Wappes, E. A.; Namitharan, K.; Bekkaye, M.; Nagib, D. A. Development of an Imine Chaperone for Selective C-H Functionalization of Alcohols via Radical Relay. *J. Org. Chem.* **2019**, *84*, 13065–13072.
- (209) Stateman, L. M.; Wappes, E. A.; Nakafuku, K. M.; Edwards, K. M.; Nagib, D. A. Catalytic β C-H Amination: Via an Imidate Radical Relay. *Chem. Sci.* **2019**, *10*, 2693–2699.
- (210) Nakafuku, K. M.; Fosu, S. C.; Nagib, D. A. Catalytic Alkene Difunctionalization via Imidate Radicals. *J. Am. Chem. Soc.* **2018**, *140*, 11202–11205.
- (211) Wappes, E. A.; Nakafuku, K. M.; Nagib, D. A. Directed β C-H Amination of Alcohols via Radical Relay Chaperones. *J. Am. Chem. Soc.* **2017**, *139*, 10204–10207.
- (212) Nakafuku, K. M.; Zhang, Z.; Wappes, E. A.; Stateman, L. M.; Chen, A. D.; Nagib, D. A. Enantioselective Radical C-H Amination for the Synthesis of β -Amino Alcohols. *Nat. Chem.* **2020**, *12*, 697–704.
- (213) Becker, M. R.; Richardson, A. D.; Schindler, C. S. Functionalized Azetidines via Visible Light-Enabled Aza Paternò-Büchi Reactions. *Nat. Commun.* **2019**, *10*, 5095.

- (214) Hopkinson, M. N.; Gómez-Suárez, A.; Teders, M.; Sahoo, B.; Glorius, F. Accelerated Discovery in Photocatalysis Using a Mechanism-Based Screening Method. *Angew. Chem. Int. Ed.* **2016**, *55*, 4361–4366.
- (215) Carreira, E. M.; Fessard, T. C. Four-Membered Ring-Containing Spirocycles: Synthetic Strategies and Opportunities. *Chem. Rev.* **2014**, *114*, 8257–8322.
- (216) Szostak, M.; Spain, M.; Procter, D. J. Recent Advances in the Chemoselective Reduction of Functional Groups Mediated by Samarium(Ii) Iodide: A Single Electron Transfer Approach. *Chem. Soc. Rev.* **2013**, *42*, 9155–9183.
- (217) Shi, J.; Manolikakes, G.; Yeh, C. H.; Guerrero, C. A.; Shenvi, R. A.; Shigehisa, H.; Baran, P. S. Scalable Synthesis of Cortistatin A and Related Structures. *J. Am. Chem. Soc.* **2011**, *133*, 8014–8027.
- (218) Shipet, W. D.; Sorensen, E. J. Convergent, Enantioselective Syntheses of Guanacastepenes A and E Featuring a Selective Cyclobutane Fragmentation. *J. Am. Chem. Soc.* **2006**, *128*, 7025–7035.
- (219) Hellmuth, T.; Frey, W.; Peters, R. Regioselective Catalytic Asymmetric C-Alkylation of Isoxazolinones by a Base-Free Palladacycle-Catalyzed Direct 1,4-Addition. *Angew. Chem. Int. Ed.* **2015**, *54*, 2788–2791.
- (220) Hu, X. Q.; Qi, X.; Chen, J. R.; Zhao, Q. Q.; Wei, Q.; Lan, Y.; Xiao, W. J. Catalytic N-Radical Cascade Reaction of Hydrazones by Oxidative Deprotonation Electron Transfer and TEMPO Mediation. *Nat. Commun.* **2016**, *7*, 11188.
- (221) Kalisiak, J.; Ralph, E. C.; Zhang, J.; Cashman, J. R. Amidine-Oximes: Reactivators for Organophosphate Exposure. *J. Med. Chem.* **2011**, *54*, 3319–3330.
- (222) Green, S. A.; Vásquez-Céspedes, S.; Shenvi, R. A. Iron-Nickel Dual-Catalysis: A New

- Engine for Olefin Functionalization and the Formation of Quaternary Centers. *J. Am. Chem. Soc.* **2018**, *140*, 11317–11324.
- (223) Simoni, D.; Rondanin, R.; Baruchello, R.; Rizzi, M.; Grisolia, G.; Eleopra, M.; Grimaudo, S.; Di Cristina, A.; Pipitone, M. R.; Bongiorno, M. R.; et al. Novel Terphenyls and 3,5-Diaryl Isoxazole Derivatives Endowed with Growth Supporting and Antiapoptotic Properties. *J. Med. Chem.* **2008**, *51*, 4796–4803.
- (224) Lempenauer, L.; Duñach, E.; Lemièrre, G. Tuning the Reactivity of Functionalized Diallylic Alcohols: Brønsted versus Lewis Acid Catalysis. *Chem. Eur. J.* **2017**, *23*, 10285–10288.
- (225) Zhu, X.; Wang, Y. F.; Ren, W.; Zhang, F. L.; Chiba, S. TEMPO-Mediated Aliphatic C-H Oxidation with Oximes and Hydrazones. *Org. Lett.* **2013**, *15*, 3214–3217.
- (226) Denton, R. M.; An, J.; Lindovska, P.; Lewis, W. Phosphonium Salt-Catalysed Synthesis of Nitriles from in Situ Activated Oximes. *Tetrahedron* **2012**, *68*, 2899–2905.
- (227) Howell, J. M.; Feng, K.; Clark, J. R.; Trzepakowski, L. J.; White, M. C. Remote Oxidation of Aliphatic C-H Bonds in Nitrogen-Containing Molecules. *J. Am. Chem. Soc.* **2015**, *137*, 14590–14593.
- (228) Kapat, A.; Nyfeler, E.; Giuffredi, G. T.; Renaud, P. Intramolecular Schmidt Reaction Involving Primary Azidoalcohols under Nonacidic Conditions: Synthesis of Indolizidine (-)-167B. *J. Am. Chem. Soc.* **2009**, *131*, 17746–17747.
- (229) Matos, J. L. M.; Vásquez-Céspedes, S.; Gu, J.; Oguma, T.; Shenvi, R. A. Branch-Selective Addition of Unactivated Olefins into Imines and Aldehydes. *J. Am. Chem. Soc.* **2018**, *140*, 16976–16981.
- (230) Du, Z.; Yanhui, L.; Dai, X.; Zhang-Negrerie, D.; Gao, Q. Synthesis of NO-NSAID Dendritic Prodrugs via Passerini Reaction: New Approach to the Design of Dendrimer-Drug

- Conjugates. *J. Chem. Res.* **2013**, *37*, 181–185.
- (231) Dallanoce, C.; Canovi, M.; Matera, C.; Mennini, T.; De Amici, M.; Gobbi, M.; De Micheli, C. A Novel Spirocyclic Tropanyl- Δ^2 -Isoxazoline Derivative Enhances Citalopram and Paroxetine Binding to Serotonin Transporters as Well as Serotonin Uptake. *Bioorg. Med. Chem.* **2012**, *20*, 6344–6355.
- (232) Green, S. A.; Huffman, T. R.; McCourt, R. O.; Van Der Puy, V.; Shenvi, R. A. Hydroalkylation of Olefins to Form Quaternary Carbons. *J. Am. Chem. Soc.* **2019**, *141*, 7709–7714.
- (233) Liu, Y.; Zhou, Y.; Zhao, Y.; Qu, J. Synthesis of Gem-Difluoroallylboronates via FeCl₂-Catalyzed Boration/ β -Fluorine Elimination of Trifluoromethyl Alkenes. *Org. Lett.* **2017**, *19*, 946–949.